MICROFICHED

MAR 31 1972

SD71-158

AN EXPERIMENTAL INVESTIGATION OF THE EFFECT OF REYNOLDS NUMBER ON THE LOW SPEED AERODYNAMIC CHARACTERISTICS OF A DELTA WING SPACE SHUTTLE ORBITER CONCEPT AT ANGLES OF ATTACK TO 45 DEGREES

(LTPT-57)

September 10, 1971

Prepared by

H. Parrell

W. E. Bornemann, Supervisor
Aerodynamics
Space Shuttle Program

N. F. Witte, Manager
Flight Technology
Space Shuttle Program

Space Division
North American Rockwell

NASA-CR-134266) AN EXPERIMENTAL INVESTIGATION OF THE EFFECT OF REYNOLDS NUMBER ON THE LOW SPEED AERODYNAMIC CHARACTERISTICS OF A DELTA WING SPACE (North American Rockwell Corp.) 307 p

N74-74018

Unclas
00/99 37497

SD71-158

AN EXPERIMENTAL INVESTIGATION OF THE EFFECT OF REYNOLDS NUMBER ON THE LOW SPEED AERODYNAMIC CHARACTERISTICS OF A DELTA WING SPACE SHUTTLE ORBITER CONCEPT AT ANGLES OF ATTACK TO 45 DEGREES

(LTPT-57)

September 10, 1971

Prepared by

H. Parrell

W. E. Bornemann, Supervisor
Aerodynamics
Space Shuttle Program

N. F. Witte, Manager
Flight Technology
Space Shuttle Program

Space Division
North American Rockwell

FOREWORD

This report presents the analysis of experimental data obtained in a low speed wind tunnel test of a high crossrange Space Shuttle Orbiter. The test was conducted at the NASA/Langley Research Center Low Turbulence Pressure Tunnel (LTPT 57) from February 2-11, 1971.

The NASA/LRC Engineers for the experimental investigation were Messrs. Bernard Spencer, Jr. and George Ware. Data preparation for this report was performed by Mrs. D. A. Jones (NR/SD).

The effort reported herein was performed under IR&D GO 05060, Subaccount 13362. This report was prepared by H. Parrell under the direction of T. E. Surber.

ABSTRACT

This report contains low speed longitudinal and lateral directional characteristics of a sting mounted 0.00763 scale full span development model of a Space Shuttle Delta Wing Orbiter. Test purposes were to determine the effect of Reynolds number on pitch and yaw stability, control effectiveness, induced drag, base drag, and boundary layer transition. In addition, the effects of wing tip geometry and wing position were determined. These data were obtained through -1 degree to 45 degrees angle-of-attack and 5 degrees angle-of-sideslip. The wind tunnel data is presented in the Appendix A.

The results of the analysis reveal that the vehicle is longitudinally stable up to wing stall and is directionally stable and has positive dihedral effectiveness beyond the operational angle-of-attack range of 17 degrees. The effect of Reynolds number variation on longitudinal stability, elevon and rudder effectiveness was negligible. Reynolds number had its most potent effects on induced drag and skin friction. Increasing Reynolds number decreased induced drag. Natural boundary layer transition (no transition strips) to turbulent skin friction was complete at a Reynolds number of 3.4×10^6 based on the MAC. The effect of wing tip geometry location was to decrease $C_{L\alpha}$ by 15%, the aerodynamic center by 5% of MAC or 2% body length, and $(L/D)_{max}$ by 10%. A total wing movement of 100 inches shifted the aerodynamic center 68 inches or 3% body length.

TABLE OF CONTENTS

	PAGE
FOREWORD	i
ABSTRACT	ii
TABLE OF CONTENTS	iii
LIST OF TABLES	iv
LIST OF FIGURES	v
1.0 INTRODUCTION	1
2.0 NOMENCLATURE	2
2.1 General	2
2.2 Coefficients	3
2.3 Subscripts	4
3.0 MODEL DESCRIPTION	5
4.0 TEST CONDITIONS	6
5.0 DISCUSSION	7
5.1 Longitudinal Characteristics	7
5.1.1 Effect of Fixed Transition	7
5.1.2 Effect of Wing Tip Geometry	9
5.1.3 Effect of Wing Location	10
5.1.4 Elevon Effectiveness	10
5.2 Lateral Directional Characteristics	11
2.2.1 Directional Control	11
5.2.2 Lateral-Directional Stability	11
6.0 CONCLUSIONS	12
7.0 REFERENCES	13
APPENDIX A - WIND TUNNEL DATA	64
General	64
Run Index	65
Index of Figures - Appendix A	67

LIST OF TABLES

		PAGE
I	MODEL DESCRIPTION	14
II	TEST CONDITIONS	24
III	TRANSITION GRIT DESCRIPTION.	25

LIST OF FIGURES

FIGURE NO.	TITLE	PAGE
1	Alternate Wing Position and Wing Tips	26
2	3-View Sketch - Delta Wing Orbiter	27
3	Installation Photographs	28
4	Effect of Reynolds Number in Pitch	29
5	Effect of Reynolds Number on L/D	30
6a, 6b	Effect of Reynolds Number and Transition on the Aerodynamic Characteristics	31, 32
7	Effect of Reynolds Number and Transition on Base Pressure Measurements	33
8	Effect of Reynolds Number and Transition on the Zero Lift Drag	34
9a, b, c	Effect of Reynolds Number on Induced Drag, $B_4ZW_{16}V_{26}$, $B_4ZW_{16}V_{26}tr_6$ and $B_4ZW_{16}V_{26}tr$, Configurations Respectively	35, 36, 37
10	Effect of Reynolds Number and Transition on Induced Drag Efficiency	38
11a, b	Effect of Wing Tip Geometry and Reynolds Number on the Aerodynamic Characteristics	39, 40
12a, b, c	Effect of Wing Tip Geometry on Drag Due to Lift, RN/FT = 6, 8, 10 x 10^6 Respectively	41, 42, 43
13	Effect of Wing Tip Geometry and Reynolds Number on Induced Drag Efficiency	44
14a, b	Effect of Wing Location and Reynolds Number on the Aerodynamic Characteristics	45, 46
15a, b, c	Effect of Wing Location on Induced Drag, RN/FT = 6, 8, 10 x 10^6, Respectively	47, 48, 49
16a, b, c	Elevon Effectiveness in Pitch, 134-D RN/FT = 6, 8, 10 x 10^6, Respectively	50, 51, 52
17	Effect of Reynolds Number on Elevon Effectiveness Derivatives in Pitch -134-D	53
18	Effect of Reynolds Number on Elevon Effectiveness at -30° Elevon Deflection	54
19	Effect of Elevon Deflection and Reynolds Number on Base Pressure Measurements	55

FIGURE NO.	TITLE	PAGE
20a, b, c	Rudder Effectiveness, 134D, RN/FT = 6, 8, 10 x 10^6 Respectively	56, 57, 58
21	Effect of Reynolds Number on Rudder Effectiveness Derivatives	59
22	Effect of Reynolds Number on Rudder Effectiveness for -30° Rudder Deflection	60
23	Effect of Reynolds Number on the Lateral Directional Derivatives, Tail-on, -134D	61
24	Effect of Reynolds Number on the Lateral Directional Stability Derivatives, Tail-off, 134D	62
25	Effect of Reynolds Number on the Vertical Tail Input Stability Derivatives	63

1.0 INTRODUCTION

North American Rockwell is conducting a preliminary design study of a reusable delta wing Space Shuttle Orbiter capable of high crossrange during entry followed by a conventional aircraft landing. To develop the aerodynamic configuration NR is performing a wind tunnel program on a development model to investigate the general stability and control characteristics throughout the flight envelope.

This report presents the analysis of experimental data obtained during a low speed test of a sting mounted 0.00763 scale full span model of the delta wing orbiter conducted at NASA Langley Research Center's Low Turbulence Pressure Tunnel (LTPT No. 57).

The primary objectives of the test were to determine the effect of Reynolds number on pitch and yaw stability, control effectiveness, induced drag, base drag, and boundary layer transition. In addition, the effects of wing tip geometry and wing position were determined.

2.0 NOMENCLATURE

2.1 GENERAL

ITEM	DESCRIPTION
a.c.	Aerodynamic center, $X/\bar{c}$, measured from leading edge of $\bar{c}$.
AR	Aspect ratio, b^2/S
b_{ref}	Reference wing span (noted on plots)
B.P.	Buttock plane, in.
$\bar{c}$, M.A.C.	Reference wing mean aerodynamic chord (noted on plots)
c.g.	Center-of-gravity
F.S.	Fuselage station, in.
FRL	Fuselage reference line
L	Rolling moment, in. lbs.
S_{ref}	Reference wing area, ft^2, (noted on plots)
SW	Wing area, ft^2
W.P.	Water plane, in.
C	Chord force, lbs.
D	Drag force, lbs.
L	Lift Force, lbs. or length of fuselage, in.
m	Pitching moment, in. lbs.
n	Yawing moment, in. lbs.
Y	Side force, lbs., or buttocks plane, in.
q	Dynamic pressure, lbs/ft^2
P_t	Total pressure, lbs/ft^2
RN	Reynolds number
α	Alpha, angle of attack of the FRL corrected for sting deflection; deg.
β	Angle of sideslip, deg.
δ	Control surface deflection denoted by subscript, deg.
Δ	Increment

2.2 COEFFICIENTS

C_C	Chord force coefficient, $\frac{C}{qS_{ref}}$
C_D	Drag coefficient, $\frac{D}{qS_{ref}}$
C_L	Lift coefficient, $\frac{L}{qS_{ref}}$
C_{L_α}	Lift curve slope, $dC_L/d\alpha$, per degree
$C_{L_{\delta_e}}$	Elevon effectiveness in lift, $dC_L/d\delta_e$, per degree
C_l	Rolling moment coefficient, $\frac{l}{qS_{ref}b_{ref}}$
C_{l_β}	Roll due to sideslip, $dC_l/d\beta$, per degree
$C_{l_{\delta_a}}$	Elevon effectiveness in roll, $dC_l/d\delta_a$, per degree
$C_{l_{\delta_r}}$	Rudder effectiveness in roll, $dC_l/d\delta_r$, per degree
C_m	Pitching moment coefficient, $\frac{m}{qS_{ref}\bar{c}}$
$C_{m_{\delta_e}}$	Elevon effectiveness in pitch, $dC_m/d\delta_e$, per degree
$C_{m_{C_L}}$	Pitch stability, dCm/dC_L
C_{m_α}	Pitch stability, $dCm/d\alpha$, per degree
C_N	Normal force coefficient, $\frac{N}{qS_{ref}}$
C_{N_α}	Normal force slope, $dC_N/d\alpha$, per degree
C_n	Yawing moment, coefficient, $\frac{n}{qS_{ref}b_{ref}}$
C_{n_β}	Yaw due to sideslip, $dCn/d\beta$, per degree
$C_{n_{\delta_a}}$	Yawing moment due to elevon, $dCn/d\delta a$, per degree

2.2 COEFFICIENTS (continued)

$C_{n_{\delta_r}}$	Yawing moment due to rudder, $dCn/d\delta r$, per degree
C_Y	Side force coefficient, $\frac{Y}{qS_{ref}}$
C_{Y_β}	Side force due to sideslip, $dC_Y/d\beta$, per degree
$C_{Y_{\delta_a}}$	Side force due to elevons, $dC_Y/d\delta_a$, per degree
$C_{Y_{\delta_r}}$	Side force due to rudder, $dC_Y/d\delta_r$, per degree

2.3 SUBSCRIPTS

s	stability axes
b	body axes
o	zero lift
L	lift
R	Rudder
st	sting
u	uncorrected
v	vertical tail
W	Wing
max	maximum

3.0 MODEL DESCRIPTION

The model is an 0.00763 scale simulation of the North American Rockwell 134D configuration, Reference 1, except for the elevon which simulates the more advanced 161C, Rev. A, Reference 1. The 161C, Rev. A elevon hinge line is unswept to reduce roll-yaw coupling. Reference 2 presents the basic model drawings.

The 134D configuration consists of a flat bottom moderate bluntness ogival nose fuselage, delta planform wing with streamlined tips and a leading edge cuff which blends into the fuselage, and a fuselage centerline vertical tail. Pitch and roll control are provided by full span elevons located at the trailing edge of the wing. Yaw control at low angles of attack is furnished by a full span rudder in the vertical fin. Additionally, the rudder may be deflected trailing edge outboard to provide incremental directional stability and drag.

The 161C, Rev. A vehicle is slightly larger than the 134D (the body length and total wing area of the 161C, Rev. A vehicle are 2165 inches and 6474 ft^2, respectively, compared to 2120 inches and 6084 ft^2 for the 134D). Configuration characteristics are very nearly identical, slight differences occurring in the fuselage side-bottom chine radius (slightly larger or "softer" for the 134D), the wing location (the 134D wing is approximately 15 inches full scale forward on the fuselage as compared to the 161C, Rev. A wing) and in the nominal center of gravity (.671L for the 134D and .676L for the 161C, Rev. A vehicle) and wing tip geometry.

Model geometry is shown in Figures 1 and 2 and tabulated in Table 1. Photographs of the model are presented in Figure 3.

The model allows for component buildup testing (body, body-wing, body-wing-tail) and elevon and rudder deflections, wing location, and wing tip geometry.

Wing twist varies from 0° at the exposed root (BP 240) to -5° at the tip (B.P. 542). The elevon is an integral part of the wing. The elevon spanwise incidence may therefore be determined from wing twist for a particular spanwise station.

Control surface deflection angles are measured in a plane located perpendicular to the control surface hinge axis.

4.0 TEST CONDITIONS

The test was conducted in the NASA Langley Research Center Low Turbulence Pressure Tunnel. The tunnel is a closed circuit type which has the capability of varying the Reynolds number range from 2.5 to 15 x 10^6 per foot at constant Mach number by pressurizing the test medium of air. Nominal test conditions are presented in Table II. Data was obtained from -1 to 45 degrees angle-of-attack with a 1.0 inch diameter sting exiting from the base. The angle of attack test range of -1 to 25 degrees and 18 to 45 degrees was accomplished by changing a knuckle that was connected from the pitch mechanism to the sting. Yaw angle of 5 degrees was achieved by utilizing a 5-degree offset knuckle connected to the pitch mechanism.

Two transition grit sizes were used on the model in order to determine:

1. The drag directly attributed to the grit itself

2. The Reynolds number where natural transition to turbulent skin friction occurs

Once the natural transition Reynolds number was determined, the remainding test program was conducted without the transition grit on the model. The transition grit is described in Table III.

5.0 DISCUSSION

The results of the analyses are discussed in this section. All coefficients are presented in the stability axis except where noted. All drag data presented herein has been corrected to freestream base and cavity pressures. All coefficients are referenced to the theoretical delta wing reference area of 6084 ft^2, mean aerodynamic chord of 821.2 inches and wing span of 1422.8 inches. The moments were taken about the full scale fuselage station of 1422.5 at water plane 130 inches. This reference center of gravity location is at 67.1% of the fuselage length corresponding to 14.9 percent of the mean aerodynamic chord of the reference wing. Detail information on data reduction can be found in the pre-test report, Reference 3.

5.1 LONGITUDINAL CHARACTERISTICS

The wind tunnel data from which the longitudinal analysis was obtained can be found on Figures A-1 through A-13 of Appendix A.

5.1.1 Effect of Fixed Transition

The purpose of transition grit is to assure turbulent flow at a fixed and known location, thereby allowing one to correlate and extrapolate skin friction estimated on the model to full scale flight conditions. For example, the highest test Reynolds number based on the MAC of the model was 7.8×10^6, approximately 1/16 the flight Reynolds number of 127×10^6 at Mach = 0.26 sea level. Two different grit dimensions were sized, Reference 4, for model Reynolds numbers per foot of 2.5 and 6×10^6 in order to determine the drag directly attributed to the grit itself. However, the grit sized for 6×10^6 RN/FT was unfortunately not held in the same location as that sized for 2.5×10^6, thereby negating an exact data correlation. However, data trends can be established. Detail description of the transition strips can be found in Table II.

The transition-free configuration 134D longitudinal stability characteristics and L/D for the small angle-of-attack range are presented on Figures 4 and 5. Lift data, Figure 4, is insensitive to Reynolds number and agrees with test data from Reference 6. Stability characteristics, Figure 4, have a Cm shift at the low Reynolds number and show fair agreement with test data of Reference 6. Also notice in Figure 4 that over a very small angle of attack range, near 18°, there appears to be a temporary pitchup probably due to interactions and interferences of the vortex shed from the body with the vortex generated by the wing. The resulting interference temporarally stalled the wing aft of the moment center resulting in a positive nose-up pitching moment. A similar phenomena occurs on the lateral directional characteristics at the same angle-of-attack (Section 5.2.2). The most significant effect of Reynolds

number is on the lift to drag ratio, Figure 5.

A summary of the effect of Reynolds number and transition is found on Figures 6(a) and (b). Of all the variables presented, L/Dmax was the only one that exhibited a significant variation with Reynolds number and transition. Without transition strips, (L/D)max of the 134D configuration with the orbiter maneuvering system engine cover (Z) increased 8 percent from 9.0 to 9.63 due to increasing Reynolds number. The effect of the applied transition strips was to decrease (L/D)max indicating that considerable laminar flow existed on the clean model.

The aerodynamic center was at 24% of the MAC or at 70.3% of the body length and the lift curve slope was .037 per degree. The slopes were taken as an average through the low lift range. Comparison of the 134D configuration with test data of Reference 6 is also shown on Figure 6. Excellent agreement is noted with the exception of $C_{L_{max}}$ and α @ $C_{L_{max}}$. The $C_{L_{max}}$ from Reference 6 was 13% higher and α @ $C_{L_{max}}$ was 26% higher than the LTPT data. This phenomena could be attributed to different tunnel characteristics, blockage effects, etc. Further investigations with larger models are required to determine the actual $C_{L_{max}}$. However, it is not considered a serious problem since wing stall is considerably above the normal operating range. For example, 17 degrees is the maximum design touchdown angle of attack and α @ $C_{L_{max}}$ from the LTPT data occurs at 29 degrees.

The influence of Reynolds number and transition on L/D is due to a change in skin friction and induced drag. Base drag is not considered since this term has already been isolated and removed. However, for our own erudition, examples of measured pressure coefficients and the resulting base drag are presented on Figure 7. There is no significant variation shown with Reynolds number and just a small change due to transition strips.

Minimum drag coefficient as a function of Reynolds number with and without transition strips is presented with the estimated laminar and turbulent skin friction variation on Figure 8. Several interesting trends are noted. The addition of the transition strip at RN/FT = 2.5×10^6 increases $C_{D_{min}}$ by 33%, and the variation with Reynolds number follows the estimated trend up to a RN/FT of 8×10^6. Beyond 8×10^6 there is a slight increase rather than a decrease. This, in all probability, is caused by decreasing boundary layer thickness with increasing Reynolds No., and thus the grit originally sized for 2.5×10^6 becomes too large and causes excessive grit drag. The transition free configuration shows an increase in drag as the Reynolds number increases due to the natural transition point moving forward. Beyond RN/FT of 6×10^6 the transition free configuration once again follows the estimated variation. Thus it can be concluded that at RN/FT $\approx 6 \times 10^6$ the model, transition free, has nearly as much turbulent skin friction, (within 4 drag counts) as the model with fixed transition. This also agrees with the results in Reference 5, where R_x crit = 3.2×10^5 for a flat plate. Thus at RN/FT = 6×10^6 natural transition should occur at approximately 0.6 inch aft of the leading edge. At the highest Reynolds number the actual skin friction level is 30 drag counts higher

than the estimate. It is possible that this discrepancy represents an interference level or separated flow region not accounted for in the estimate.

Drag due to lift is presented on Figures 9 (a) through (c) which show that induced drag decreases with increasing Reynolds number. Further investigation allows one to extract the Oswald efficiency factor, ε, which is a measure of induced drag efficiency. This is shown on Figure 10 for C_L of .3, .4, and .5, transition strips on and off. The efficiency factor, ε, was estimated from the expression $\varepsilon = \frac{C_L^2 \frac{Sref}{Sw}}{\pi AR\ C_{D_i}}$. The ratio Sref/Sw accounts for the fact that the delta wing with zero taper was used as reference area rather than the actual wing area. The effect of transition was negligible at the higher Reynolds number. The efficiency factor, ε, increased from .80 to .98 with increasing Reynolds number at $C_L = 0.3$; .74 to .92 at $C_L = 0.4$; and .67 to .81 at $C_L = 0.5$. If the expression $\varepsilon = \frac{(C_L - C_{LK})^2}{\pi\ AR\ C_D} \times Sref/Sw$ is used, where C_{L_K} is the lift coefficient where minimum drag occurs, say .035, the variation of ε at $C_L = .3$ would be decreased by a factor $\left(\frac{C_L - C_{LK}}{C_L}\right)^2 \approx .78$. It is difficult to select the precise C_L where minimum drag occurs (see Figures 9(a) - (c)) and since ε is very sensitive to this parameter, it can be concluded that the Reynolds number where ε reaches a maximum may not have been reached. In other words, further increases in induced drag efficiency may still be expected with increasing Reynolds number. This means that further investigation on a larger model is required to solve this problem.

5.1.2 Effect of Wing Tip Geometry

The purpose for testing various wing tip geometries was to obtain the effect on the aerodynamic center movement and thereby support data substantiation for trade studies to match subsonic and hypersonic stability requirements. Results are presented in terms of a wing tip location parameter, η, defined as the ratio of the semi-span of the wing to the semi-span of the delta wing with zero taper ratio. Three values of η were investigated, 1.0, 0.93 for the 134D wing tip, and 0.875 for simulation of the 161C wing tip. These wing tips are shown on Figure 1.

As η decreased the aspect ratio and wing area were also decreased, however the reference system of W_9 and $\eta = 1.0$ remained the same. A summary of the aerodynamic characteristics is presented on Figures 11(a) and (b), as a function of η and Reynolds number. A noticeable effect of wing tip geometry is on L/D. The $(L/D)_{max}$ decreased 10% from 10 to 9 at RN/FT = 10×10^6 due to decreased aspect ratio. As η decreased, the area of the wing which was at a negative 5 degrees incidence outboard of B.P. 542 decreased, resulting in a smaller down-loading at the tips. This effect is seen on the $CL_{\alpha = 0}$ and $CM_{CL = 0}$ variation with η. The linear twist should be changed when modifying the wing tips to retain a positive $(CM)_{C_L = 0}$ required for good trim and stability characteristics.

The lift curve slope is observed to decrease 15% from .042 to .036 and the static margin decreased 5% MAC or 2% body length due to decreasing η.

Figures 12(a)-(c) present the influence of wing tip geometry on induced drag. The Oswald efficienty, ε, is presented on Figure 13. Decreasing η increased the induced drag due to the decrease in geometric wing aspect ratio, Figures 12(a) through (c). However, the Oswald efficiency factor, ε increased with decreasing η, Figure 13. It can be concluded from the aforementioned results that wing tip geometry can be an effective means to control the static margin and thus trim losses, and L/D which has direct implication on wing size and Air Breathing Engine System (ABES) requirements for landing and ferry performance.

5.1.3 Effect of Wing Location

Two wings of the 134D type, η = .93, were moved 50 inches forward and aft for a total 100 inch movement as shown on Figure 1. The purpose of this phase of the test was to obtain the effect of wing location on the aerodynamic center movement and thereby support trade studies to match subsonic and hypersonic stability requirements. Summary analysis of the aerodynamic characteristics are presented on Figures 14(a) and (b) as a function of wing movement and Reynolds number. A wing shift aft of 100 inches from the forward wing position moved the a.c. aft by 68 inches or 3% body length, Figure 14(a). Wing location has some influence on C_D min., Figure 14(b), due to skin friction interference emanating from the different leading edge cuffs for each wing location. This type of interference usually can be reduced with proper cuff design. (L/D)max and induced drag, Figures 15(a) through (c), are also influenced by wing location, however, the most significant effect of wing location is on the aerodynamic center.

5.1.4 Elevon Effectiveness

Elevon effectiveness in pitch for the 134D configuration, η = .93, is presented on Figures 16(a) through (c) for RN/FT of 6, 8, 10 x 10^6 respectively. These data show a linear variation in lift and moment with elevon deflections through 20 degrees. The pitch effectiveness derivatives, Figure 17, show a 42% loss in $C_{m_{\delta_e}}$ going from zero to 40 degrees angle of attack. The Reynolds number variation had 8% scatter in $C_{m_{\delta_e}}$ and negligible effect on $C_{L_{\delta_e}}$. Comparison with data obtained from NAAL 633 (Reference 6) for the 134D configuration is also presented and shows fair agreement with the trends and levels of the LTPT data. The effect of Reynolds number might be expected to be more prevelant at the maximum elevon deflection due to a possible effect on elevon stall, however, Figure 18 shows that this is not the case for the Reynolds numbers tested. Elevon deflection does affect the base and cavity pressure measurements which is insensitive to Reynolds number variation as shown on Figure 19. This result indicates a need to simulate, in a future test, the base with rocket engine housing to determine accurately not only the level of base drag, but also the effect due to elevon deflection.

5.2 LATERAL DIRECTIONAL CHARACTERISTICS

The wind tunnel data from which the lateral-directional analysis was obtained can be found on Figures A-14 through A-21 of Appendix A.

5.2.1 Directional Control

Rudder effectiveness, for the 134D configuration with the double wedge vertical, is presented on Figures 20(a) through (c) for RN/FT of 6, 8, 10 x 10^6 respectively. These data show the side force and yawing moment to be rather insensitive to the angle of attack over the range from 0 through 25 degrees. However, the rolling moment is very sensitive to angle of attack, a result not unexpected when remembering the data shown is in the stability axis system. The effectiveness derivatives, Figure 21, show the derivatives to be insensitive to angle of attack, except for $C_{L_{\delta_R}}$, and insensitive to Reynolds number variation. The data from Reference 6, NAAL 633, is also presented and excellent agreement is noted. The effect of Reynolds number on the maximum deflection of minus 30 degrees, Figure 22, reveals negligible sensitivity due to Reynolds number and good agreement with the data of Reference 6.

5.2.2 Lateral-Directional Stability

Lateral-directional stability derivatives for the 134D configuration are shown on Figure 23. The configuration exhibits positive static weathercock stability through 31 degrees angle of attack and static positive dihedral effectiveness through 24 degrees angle of attack. The derivatives are rather insensitive to Reynolds number. Fair agreement with data from Reference 6 is noted. Above the stall, say $\alpha = 40°$, increasing Reynolds number decreased C_{n_β} to about -.0065 per degree and increased C_{l_β} to -.0025 degree. However, it should be remembered that the slope was taken through a positive 5 degrees sideslip and does not account for unknown non-linearities with sideslip. At approximately 17 degrees angle of attack, a sharp discontinuity in C_{n_β} and C_{l_β} variations occur over a small angle of attack range. At the same angle of attack a slight temporary pitchup was noted in Section 5.1.1. This is due to interference of the body vortex with the vortex shed by the wing. This effect is seen also in the derivatives with the vertical tail off, Figure 24, but is not present in the vertical tail input, Figure 25, and therefore is not caused by the vertical tail. This characteristic is not considered serious since static stability in the stability axis system is still present. Further investigation is required to determine the exact cause and the correction required to eliminate this characteristic. The effect of Reynolds number on the vertical tail input, Figure 24, is most pronounced above the wing stall where increasing Reynolds number causes C_{Y_β} to become positive, and C_{n_β} more negative due to adverse sidewash.

6.0 CONCLUSIONS

Based on the data presented herein the following conclusions are evident:

1. The 134D configuration is longitudinally stable up to wing stall and all the aerodynamic characteristics except for drag were rather insensitive to Reynolds number variation.

2. Transition grit is required at low Reynolds number to assure turbulent skin friction and natural turbulent skin friction without the transition grit occurs at RN/FT = 6×10^6.

3. Induced drag is reduced with increasing Reynolds number (Oswald efficiency factor increases).

4. Decreasing wing tip geometry location decreases C_{L_α} by 15%, aerodynamic center by 5% (MAC) or 2% body length, and (L/D)max by 10% due to decreased aspect ratio. Altering the wing tip geometry can be utilized as a device for controlling subsonic static margin and L/D.

5. Moving the wing aft moved the a.c. aft by 68% of the total wing shift of 100 inches or 3% body length. Wing shift data can be used to support trade studies to match subsonic-hypersonic stability requirements.

6. Effect of Reynolds number was negligible on elevon effectiveness in pitch and rudder effectiveness.

7. Elevon deflections affect the pressures measured on the base and balance cavity. It is required in a future test to simulate the base with rocket engine housing to determine accurately not only the level of base drag, but also the effect due to elevon deflections.

8. 134D configuration has positive static weathercock stability to 30° and positive dihedral effect to 24 degrees angle of attack.

9. Increasing Reynolds number decreased weathercock stability and decreased the dihedral effect above 20 degrees angle ofaattack.

10. The vertical tail input due to sideslip remained effective to 31 degrees angle of attack.

7.0 REFERENCES

1. Space Division Drawings 9992-129 dated 23 December 1969, 9992-134B dated 14 May 1970, 9992-134D dated 1 September 1970, and 9992-161C Rev. A, dated 3 March 1971.

2. Wind Tunnel Model Drawings S-828 dated 8 May 1970, S-863 dated 8 May 1970, and S-877 dated 2 July 1970.

3. NA-70-723, "Pretest Information for Test of the .0076 Scale Force Models of the North American Rockwell Space Shuttle Vehicles in the LRC, LTPT, 8 FT, TPT, and 31 Inch Wind Tunnels."

4. NACA TN 4363, "Simplified Method for Determination of Critical Height of Distributed Roughness Particles for Boundary Layer Transition at Mach Numbers from 0 to 5," dated September 1958.

5. Schlichting, Hermann, "Boundary Layer Theory," Fourth Edition

6. SD 70-604, "An Experimental Investigation of the Low Speed Aerodynamic Characteristics of a Delta Wing Space Shuttle Orbiter Concept - Third Test (NAAL-633)," dated 2 February 1971.

TABLE I. MODEL DESCRIPTION

MODEL DESCRIPTION & FULL SCALE DIMENSIONS

Model configuration description symbols, and full scale dimensions, are presented below.

BODY-B4

Description: Basic delta wing orbiter fuselage contour including canopy and body-wing fairings.

Dimensions	Full Scale	Model Scale
Length, in.	2120.00	16.176
Max. Width, in.	465.27	3.550
Max. depth, in.	271.95	2.075
Max. X-sectional area, ft^2	641.65	0.03735
Fineness Ratio	6.181	6.181

WING - W9

Description: Delta wing with 5° twist.

Dimensions	Full Scale	Model Scale
TOTAL DATA		
Area, ft^2	6084.	0.354
Planform		
Span (equivalent), in.	1422.80	10.856
Aspect Ratio	2.293	2.293
Rate of Taper	1.719	1.719
Taper Ratio	0.0	0.0
Dihedral Angle, degrees	7.0	7.0
Incidence Angle, degrees	0.0	0.0
Aerodynamic Twist, degrees (about T.E.)	-5.0	-5.0
Incidence, Root (B.P. 240.00)	0.0	0.0
Incidence, Tip (B.P. 542.00)	-5.0	-5.0
Sweep Back Angles, degrees		
Leading Edge	60.0	60.0
Trailing Edge	0.0	0.0
0.25 Element Line	52.20	52.20
Chords: in.		
Root (Wing Sta. 0.0)	1231.85	9.399
Tip, (equivalent) (W.S. 716.74)	0.00	0.000
MAC (W.S. 238.91)	821.33	6.266
Fus. Sta. of .25 MAC	1504.13	11.477
W.P. of .25 MAC	66.49	0.507
B.L. of .25 MAC	237.13	1.809
Airfoil Section		
Root (Wing Sta. 241.77)	NACA 0009-64	
Tip (Wing Sta. 546.01)	NACA 0012-64	
EXPOSED DATA		
Area, ft^2	2871.3	0.167
Span (equivalent), in.	846.27	6.457
Aspect Ratio	1.719	1.719
Taper Ratio	0.00	0.000
Chords, in.		
Root, (Equiv.) (W.S. 224.41)	846.17	6.456
Tip, (Equiv.) (W.S. 7161.74)	0.00	0.000
MAC (W.S. 388.52)	564.11	4.304
Fus. Sta. of .25 MAC	1696.97	12.948
W.P. of .25 MAC	84.73	0.646
B.L. of .25 MAC	385.62	2.942
Leading Edge Cuff		
Planform Area, ft^2	53.39	0.00311
Leading edge intersects Fus.M@Sta.In.	1019.27	7.777
Leading edge intersects Wing L.E. @ Sta., in.	1425.29	10.875

WING - W16

Description: Delta wing with -5° twist and rounded wing tips. Wing blends into body. Follows NR lines 9992-134D.

Dimensions	Full Scale	Model Scale
TOTAL DATA		
Area ft^2		
Planform	6020.	0.35050
Span (equivalent), in.	1275.61	9.733
Aspect Ratio	1.863	1.863
Rate of Taper	1.719	1.719
Taper Ratio	0.103	0.103
Dihedral Angle, degrees	7.000	7.000
Incidence Angle, degrees	0.000	0.000
Aerodynamic Twist, degrees (about T.E.)	-5.000	-5.000
Incidence, Root (B.P. 240.00)	0.000	0.000
Incidence, Tip (B.P. 542.00)	-5.000	-5.000
Sweep Back Angles, degrees		
Leading Edge	60.00	60.00
Trailing Edge	0.000	0.000
0.25 Element Line	52.20	52.20
Chords: in		
Root (Wing Sta. 0.0)	1231.85	9.399
Tip, (equivalent) (W.S. 642.60)	127.44	0.972
MAC (W.S. 234.28)	829.20	6.327
Fus. Sta. of .25 MAC	1498.15	11.431
W.P. of .25 MAC	65.93	0.503
B.L. of .25 MAC	232.53	1.774
Airfoil Section		
Root (Wing Sta. 241.77)	NACA009-64	NACA009-64
Tip (Wing Sta. 546.01)	NACA 0012-64	NACA 0012-64
EXPOSED DATA		
Area, ft^2	2806.0	0.16335
Span (equivalent), in.	830.14	6.334
Aspect Ratio	1.693	1.693
Taper Ratio	0.151	0.151
Chords: in.		
Root (Equiv.) (W.S. 224.41)	846.17	6.456
Tip (Equiv.) (W.S. 642.60)	127.44	0.972
MAC (W.S. 38205	575.23	4.389
Fus. Sta. of .25 MAC	1688.63	12.884
W.P. of .25 MAC	83.94	0.640
B.L. of .25 MAC	379.20	2.893
Leading Edge Cuff		
Planform Area, Ft^2	53.39	0.00311
Leading Edge intersects ML sta., in.	1019.27	7.777
Leading Edge intersects wing L.E. @ Sta. in.	1425.29	10.875

WING - W18

Description: Delta wing with -5° twist and rounded wing tips. Follows NR lines 9992-134D except modified outboard of B.P. 541.94 to simulate the -161B configuration, wing tip.

Dimensions	Full Scale	Model Scale
TOTAL DATA		
Area, ft^2		
Planform	5968.20	0.34747
Span (equivalent), in.	1225.36	9.350
Aspect Ratio	1.734	1.734
Rate of Taper	1.719	1.719
Taper Ratio	0.139	0.139
Dihedral Angle, degrees	7.000	7.000
Incidence Angle, degrees	0.000	0.000
Aerodynamic Twist, degrees (about T.E.)	-5.000	-5.000
Incidence, Root (B.P. 240.00)	0.000	0.000
Incidence, Tip (B.P. 542.00)	-5.000	-5.000
Sweep Back Angles, degrees		
Leading Edge	60.000	60.000
Trailing Edge	0.000	0.000
0.25 Element Line	52.200	52.200
Chords:, in.		
Root (Wing Sta. 0.0)	1231.85	9.399
Tip, (Equivaoent) (W.S. 617.28)	170.95	1.304
MAC (W.S. 230.83)	835.12	6.372
Fus. Sta. of .25 MAC	1493.71	11.397
W.P. of .25 MAC	65.51	0.500
B.L. of .25 MAC	229.11	1.748
Airfoil Section		
Root (Wing Sta. 241.77)	NACA 009-64	
Tip (Wing Sta. 546.01)	NACA 0012-64	
EXPOSED DATA		
Area, ft^2	2754.15	0.16035
Span (equivalent), in.	779.89	5.951
Aspect Ratio	1.522	1.522
Taper Ratio	0.202	0.202
Chords: in.		
Root (Equiv.) (W.S. 224.41)	846.17	6.456
Tip (Equiv.) (W.S. 617.28)	170.95	1.304
MAC (W.S. 377.37)	583.26	4.450
Fus. Sta. of .25 MAC	1682.60	12.838
W.P. of .25 MAC	83.37	0.636
B.L. of .25 MAC	374.56	2.858
Leading Edge Cuff		
Planform Area, ft^2	53.39	0.00311
L.E. Intersects Fus. ML at Sta., In.	1019.27	7.777
L.E. Intersects Wing L.E. @ Sta., In.	1425.29	10.875

WING - W19

Description: Delta wing with -5° twist and rounded wing tips. Follows NR lines 9992-134D except wing is moved aft 50.00 in.

Dimensions	Full Scale	Model Scale
TOTAL DATA		
Area (Planform), ft^2	6020.	0.35050
Void Area (Incl. above;	134.88	0.00785
Area Aft. of Fus. T.E.)	-	-
Span (equivalent), in.	1275.61	9.733
Aspect Ratio	1.863	1.863
Rate of Taper	1.719	1.719
Taper Ratio	0.103	0.103
Dihedral Angle, degrees	7.000	7.000
Incidence Angle, degrees	0.000	0.000
Aerodynamic Twist, degrees (about T.E.)	-5.000	-5.000
Incidence, Root (B.P. 240.00)	0.000	0.000
Incidence, Tip (B.P. 542.00)	-5.000	-5.000
Sweep Back Angles, degrees		
Leading Edge	60.000	60.000
Trailing Edge	0.000	0.000
0.25 Element Line	52.200	52.200
Chords: in		
Root (Wing Sta. 0.0)	1231.85	9.3999
Tip (equivalent) (W.S. 642.60)	127.44	0.972
MAC (W.S. 234.28)	829.20	6.327
Fus. Sta. of .25 MAC	1548.22	11.813
W.P. of .25 MAC	65.93	0.503
B.L. of .25 MAC	232.53	1.774
Airfoil Section		
Root (W.S. 241.77)	NACA 0009-64	
Tip (W.S. 546.01)	NACA 0012-64	
EXPOSED DATA		
Area (Void Area Not Incl.), ft^2	2781.46	0.161.94
Span, (equivalent), in.	825.92	6.302
Aspect Ratio	1.690	1.690
Taper Ratio	0.151	0.151
Chords: in.		
Root (Equiv.) (W.S. 226.53)	842.51	6.428
Tip (Equiv.) (W.S. 642.60)	127.44	0.972
MAC (W.S. 383.44)	572.84	4.371
Fus. Sta. of .25 MAC	1740.49	13.280
W.P. of .25 MAC	84.11	0.642
B.L. of .25 MAC	380.59	2.904
Leading Edge Cuff		
Planform area, ft^2	63.10	0.00367
L.E. Intersects Fus. ML at Sta., in.	1019.27	7.777
L.E. Intersects Wing L.E. @ Sta. in.	1475.36	11.257

WING - W20

Description: Delta wing with -5° twist and rounded wing tips. Follows NR lines 9992-134D except wing is moved forward 50.00 in.

Dimensions	Full Scale	Model Scale
TOTAL DATA		
Area, ft^2		
Planform	6020.	0.35050
Span (equivalent), in.	1275.61	9.733
Aspect Ratio	1.863	1.863
Rate of Taper	1.719	1.719
Taper Ratio	0.103	0.103
Dihedral Angle, degrees	7.000	7.000
Incidence Angle, degrees	0.000	0.000
Aerodynamic Twist, degrees (About T.E.)	-5.000	-5.000
Incidence, Root (B.P. 240.00)	0.000	0.000
Incidence, Tip (B.P. 542.00)	-5.00	-5.00
Sweep Back Angles, degrees		
Leading Edge	60.000	60.000
Trailing Edge	0.000	0.000
0.25 Element Line	52.200	52.200
Chords: in.		
Root (Wing Sta. 0.0)	1231.85	9.399
Tip, (equivalent) (W.S. 642.60)	127.44	0.972
MAC (W.S. 234.28)	829.20	6.327
Fus. Sta. of .25 MAC	1448.09	11.049
W.P. of .25 MAC	65.93	0.503
B.L. of .25 MAC	232.53	1.774
Airfoil Section		
Root (W.S. 241.77)	NACA 0009-64	
Tip (W.S. 546.01)	NACA 0012-64	
EXPOSED DATA		
Area, ft^2	2778.00	0.16173
Span (equivalent), in.	825.33	6.297
Aspect Ratio	1.690	1.690
Taper Ratio	0.151	0.151
Chords: in.		
Root (equiv.) (W.S. 226.83)	842.00	6.424
Tip (Equiv.) (W.S. 642.60)	127.44	0.972
MAC (W.S. 383.64)	572.50	4.368
Fus. Sta. of .25 MAC	1640.61	12.518
W.P. of .25 MAC	84.13	0.642
B.L. of .25 MAC	380.78	2.905
Leading Edge Cuff		
Planform Area, ft^2	24.27	0.00141
L.E. Intersects Fus. ML at Sta. In.	1019.27	7.777
L.E. Intersects Wing L.E. @ Sta. In.	1316.25	10.043

ELEVON - E7 (Data for one of two sides)

Description: Full span, constant chord elevon located on wing W16. Deflection noted as left side/right side.

Dimensions	Full Scale	Model Scale
Area, (true), ft^2	392.83	0.02287
Span (equivalent), in.	428.61	3.270
Inb'd equivalent chord, in. (W.S. 220.14)	132.00	1.007
Outb'd equivalent chord, in. (W.S. 648.75)	132.00	1.007
Ratio movable surface chord/ total surface chord		
At Inb'd equiv. chord	0.155	0.155
At Outb'd equiv. chord	1.129	1.129
Sweep Back Angles, degrees		
Leading Edge	0.000	0.000
Trailing Edge	0.000	0.000
Hingeline	0.000	0.000
Area Moment (Normal to hinge line) ft^3 (Product of area and mean chord)	4320.43	0.00192

ORBITER MANEUVERING SYSTEM ENGINE COVER - Z

Description: OMS engine cover located at aft top of fuselage below centerline vertical tail. Per NR lines 9992-161B except where modified for the 9992-129 delta wing fuselage.

Dimensions	Full Scale	Model Scale
Length, in.	321.10	2.450
Max. Width, in.	150.72	1.150
Max. Depth, in.	39.32	0.300
Fineness Ratio	DNA	DNA
Area, ft^2		
Max. Cross-Sectional	38.85	0.00226
Planform	DNA	DNA
Wetted	DNA	DNA
Base	38.85	0.00226
Fuse. Sta. of Trailing Edge, in.	2203.91	16.816
Water Plane Upper Surface, in.	262.12	2.000
Buttock Plane Cover , in.	0.00	0.000

VERTICAL TAIL - V26

Description: Centerline vertical tail on delta wing configuration with double wedge airfoil and rounded leading edge. The total data includes the void area listed below.

Dimensions	Full Scale	Model Scale
TOTAL DATA		
Area, ft^2	669.78	0.3899
*(Void (included above))	5.67	0.00033
Blanketed (included above)	1.21	0.00007
Span (equivalent), in.	377.46	2.880
Aspect Ratio	1.480	1.480
Rate of Taper	0.718	0.718
Taper Ratio	0.306	0.306
Toe-In Angle, Degrees	0.000	0.000
Cant Angle, Degrees	0.000	0.000
Sweep Back Angles, degrees		
Leading Edge	45.000	45.000
Trailing Edge	15.750	15.750
0.25 Element Line	39.369	39.369
Chords: in.		
Root (W.P. 269.99)	390.56	2.980
Tip (equivaoent) (W.P. 647.45)	119.56	0.912
MAC (W.P. 425.29)	279.06	2.129
Fus. Sta. of .25 MAC	2034.25	15.521
W.P. of .25 MAC	425.29	3.245
B.L. of .25 MAC	0.00	0.000
Airfoil Section		
Root	5° Half Angle Double Wedge with	
Tip	Leading Edge	
L.E. Radius, % Chord	1.60	1.600
Thickness, % Chord	10.50	10.500

*This area is the void area located at the lower aft portion of the surface.

RUDDER - R10

Description: Rudder used with delta wing orbiter vehicle centerline vertical tail - V26

Dimensions	Full Scale	Model Scale
Area, (Aft of Hingeline), ft^2	262.67	0.01529
Span (equivalent), in.	374.95	2.861
Inb'd equivalent chord, in. (W.P. 275.24)	154.72	1.180
Outb'd equivalent chord, in. (W.P. 650.20)	47.03	0.359
Ratio movable surface chord/ total surface chord		
At Inb'd equiv. chord	0.400	0.400
At Outb'd equiv. chord	0.400	0.400
Sweep Back Angles, degrees		
Leading Edge	29.650	29.650
Trailing Edge	15.750	15.750
Hingeline	29.650	29.650
Area Moment (Normal to hinge line), ft^3 (Product of area & mean chord)	2328.37	0.00103

TABLE II. TEST CONDITIONS

RN/FT x 10^{-6}	MACH NO.	$q_{(16/FT^2)}$	$P_{total\ psi}$	RN BASED ON $\bar{C}$
2.8	.26	136	22	1.46
4.5	.26	227	36	2.35
6.4	.25	317	55	3.35
8.6	.26	453	72	4.50
10.1	.26	543	86	5.30
12.0	.23	590	110	6.28
15.0	.22	682	150	7.85

Flight RN based on $\bar{C}$ at M = 0.26

Sea Level = 127 x 10^6

TABLE III. TRANSITION GRIT DESCRIPTION

TRANSITION GRIT - t_r6	
Dimensions (In model scale only)	
FUSELAGE	
Mean Diameter, in.	0.0049
Distance of L.E. Aft of Nose, in.	1.500
Width of Strip, in.	0.050 - 0.100
WING AND TAILS (Both Sides)	
Mean Diameter, in.	0.0049
*Distance of Strip L.E. from Airfoil	0.500
Width of Strip, in.	0.050 - 0.100
TRANSITION GRIT - t_r7	
FUSELAGE	
Mean Diameter, in.	0.0029
Distance of L.E. Aft of Nose, in.	1.500
Width of Strip, in.	0.050 - 0.100
WING AND TAILS (both sides)	
Mean Diameter, in.	0.0029
*Distance of Strip L.E. from Airfoil L.E., in.	0.35
Width of strip, in.	0.050 - 0.100

* Measured parallel to FRL

WING	$\bar{c}_{W/4}$	$\bar{c}$
W_9	1504.13 IN.	821.23 IN.
W_{16}	1498.15 IN.	829.20 IN.
W_{18}	1493.71 IN.	835.12 IN.
W_{19}	1548.22 IN.	829.20 IN.
W_{20}	1448.09 IN.	829.20 IN.

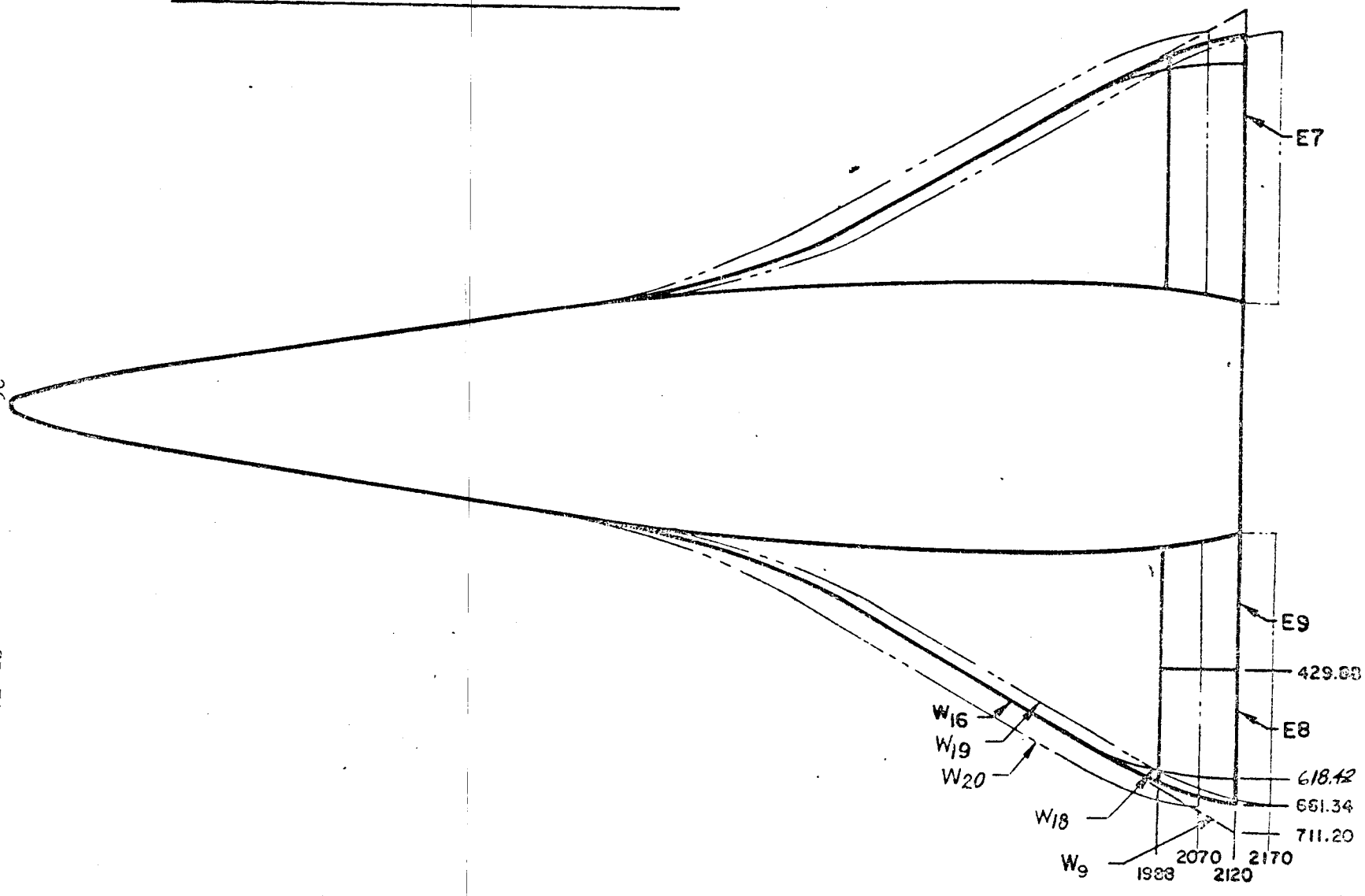

FIGURE I. ALTERNATE WING POSITIONS AND WING TIPS

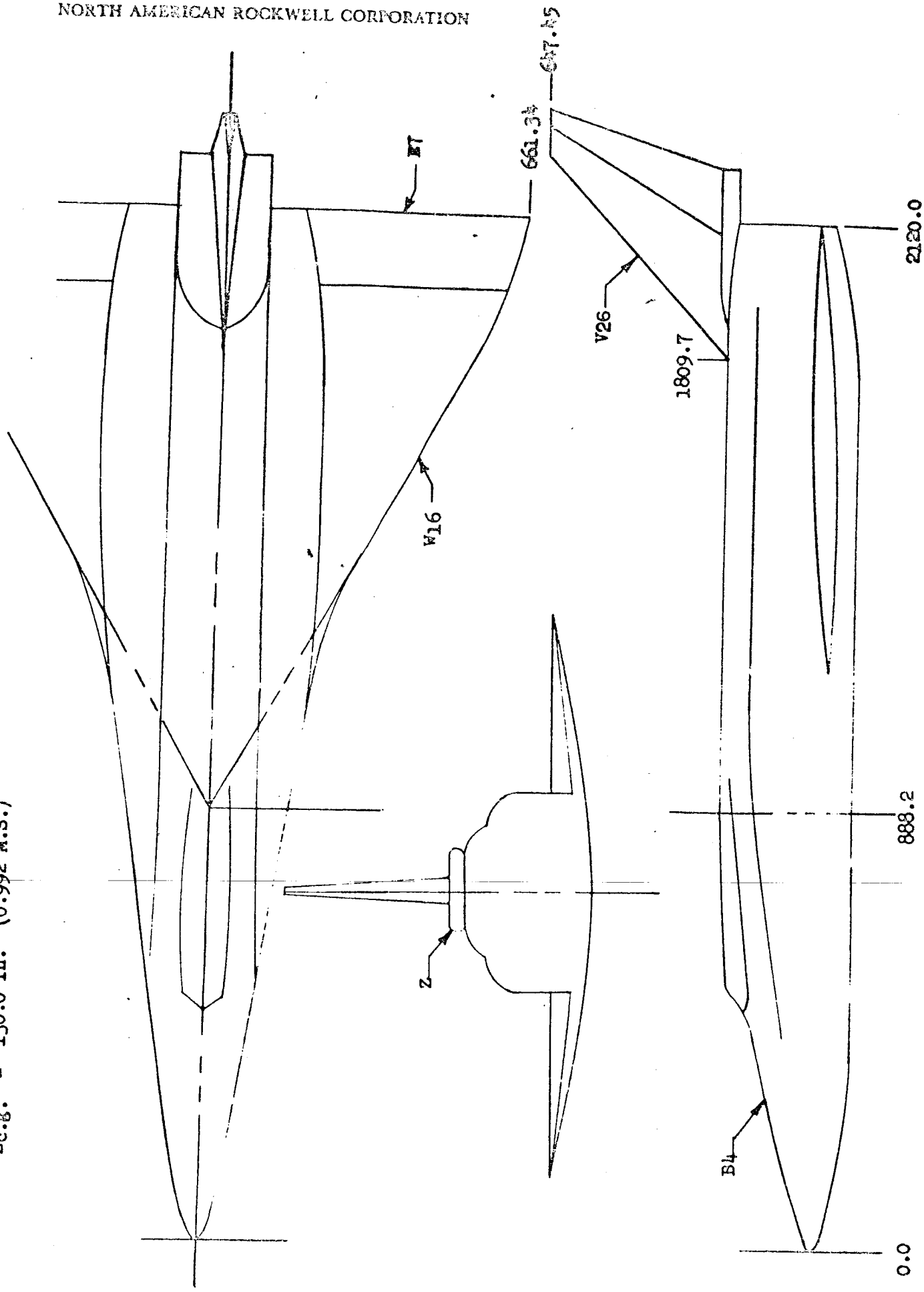

FIGURE 2. 3 VIEW SKETCH-DELTA WING ORBITER

SIDE VIEW

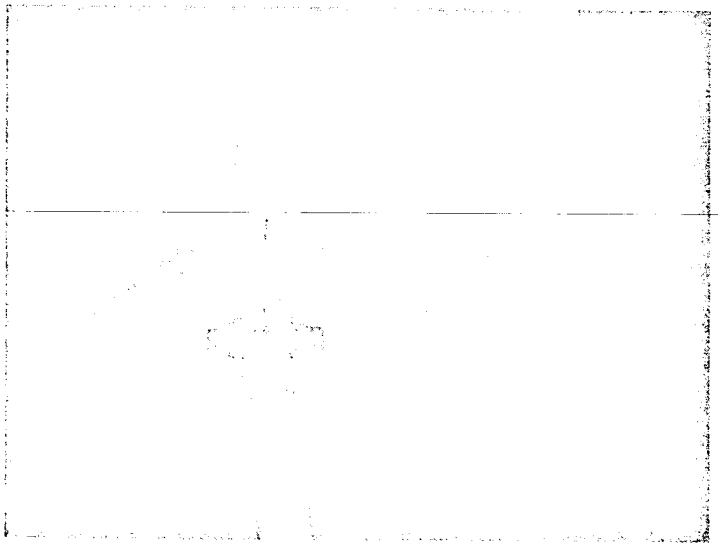

REAR TOP VIEW

Figure 3 - INSTALLATION PHOTOGRAPHS

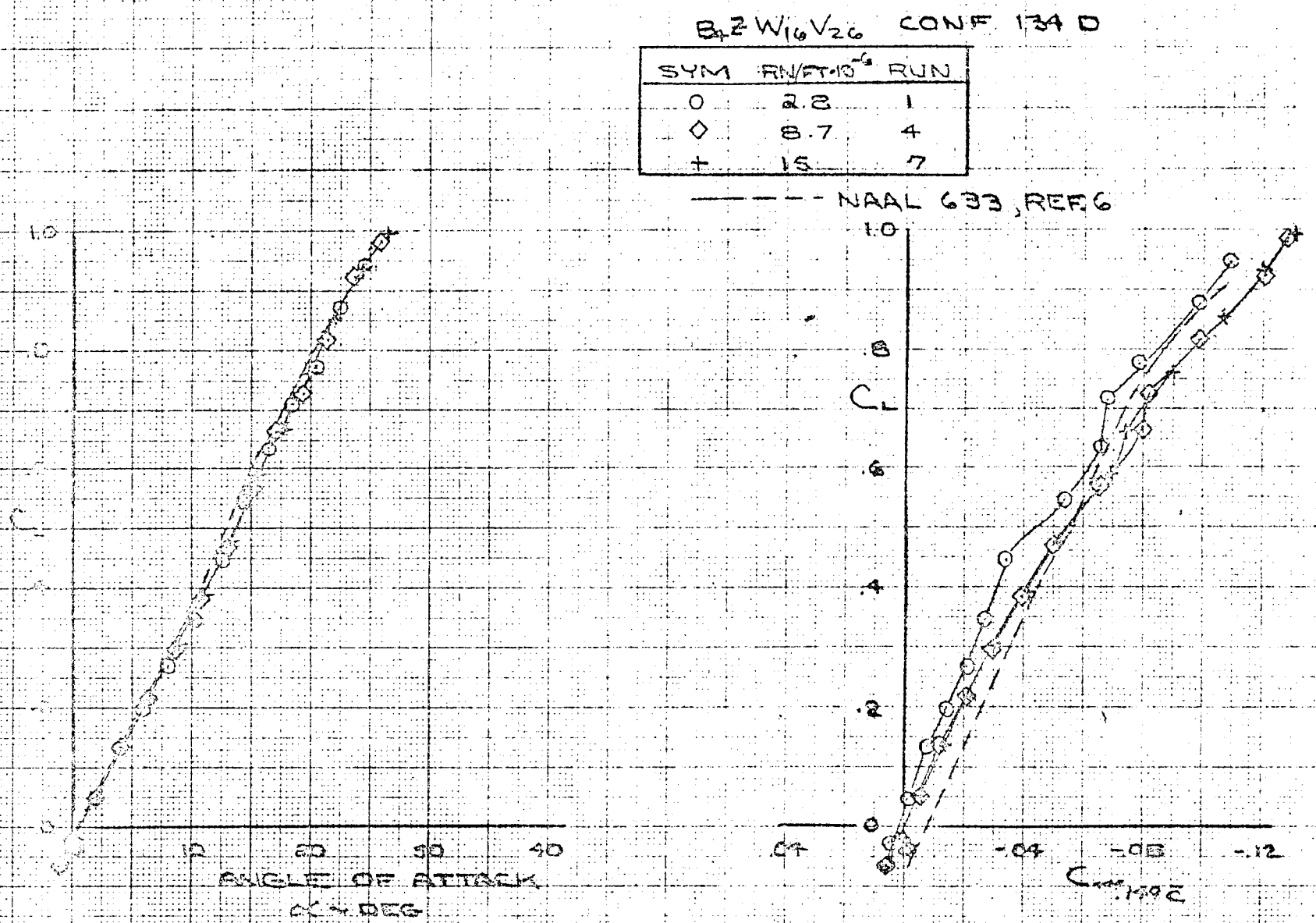

FIGURE 4. EFFECT OF REYNOLDS NUMBER IN PITCH

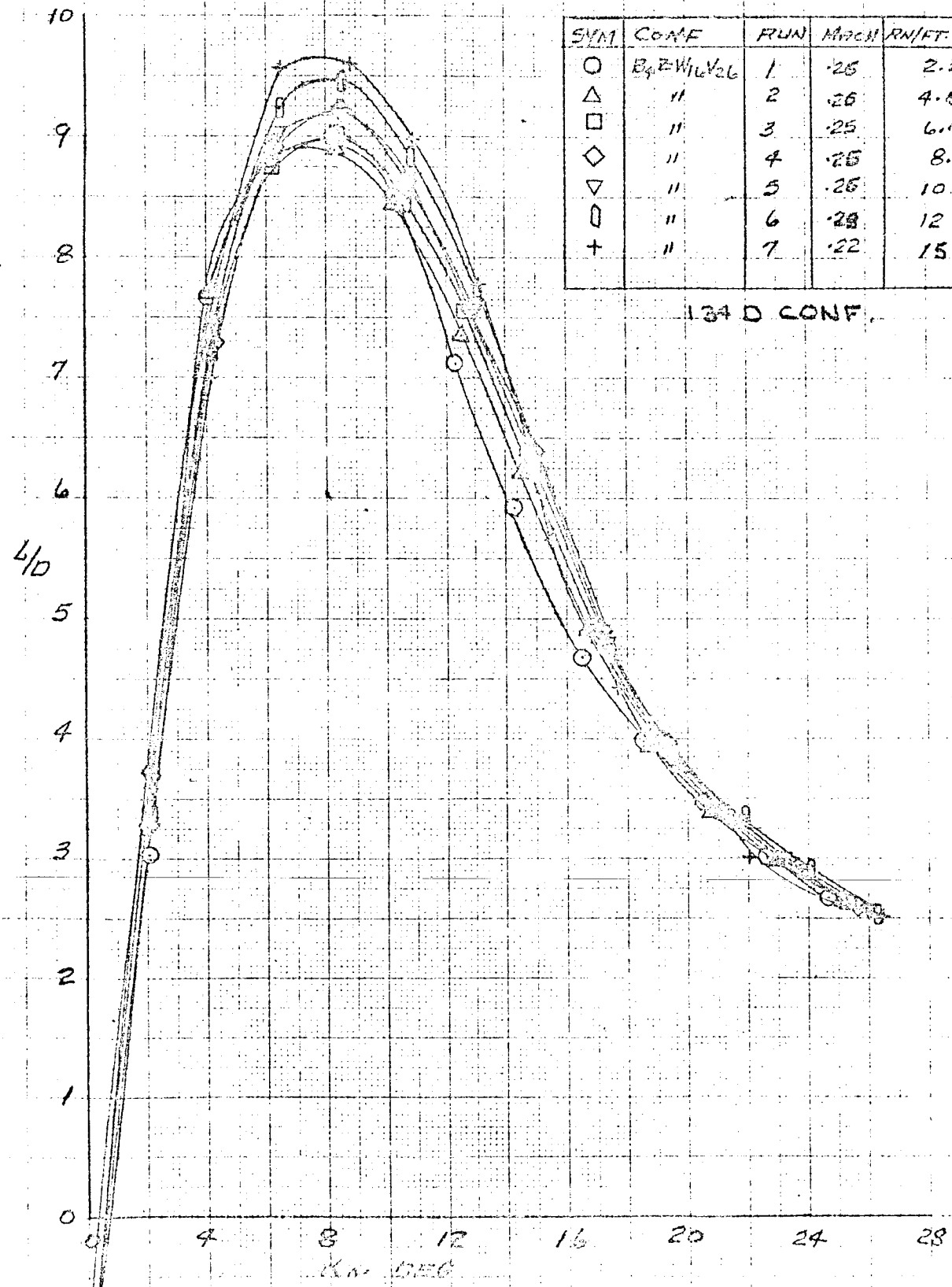

SYM	CONF	RUN	MACH	RN/FT x10^-6
○	$B_4E_2W_{16}V_{26}$	1	.26	2.8
△	"	2	.26	4.5
□	"	3	.25	6.4
◇	"	4	.26	8.7
▽	"	5	.26	10
▯	"	6	.28	12
+	"	7	.22	15

134 D CONF.

FIGURE 6. EFFECT OF REYNOLDS ON L/D

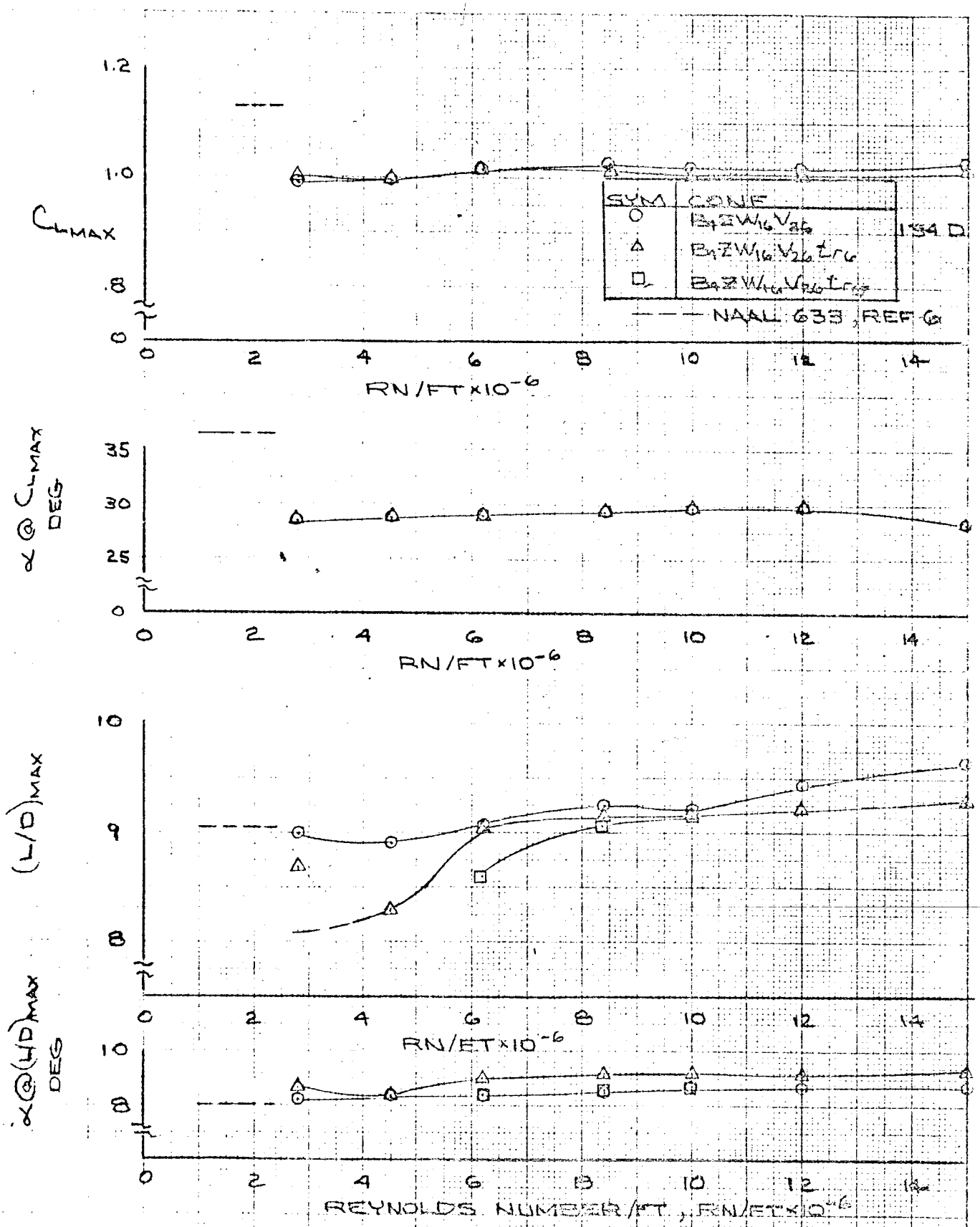

FIGURE 6a. EFFECT OF REYNOLDS NUMBER AND TRANSITION ON THE AERODYNAMIC CHARACTERISTICS

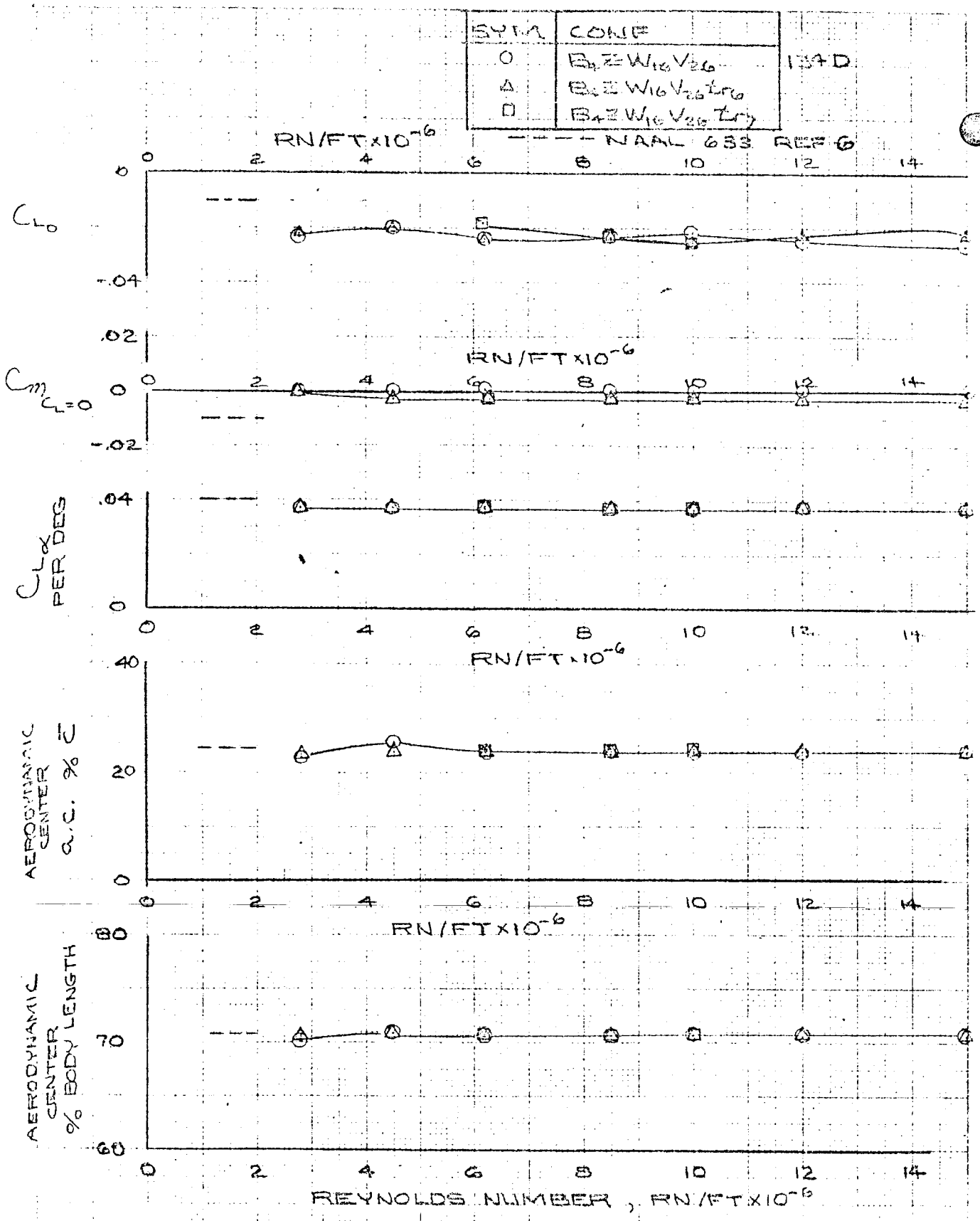

FIGURE 66. EFFECT OF REYNOLDS NUMBER AND TRANSITION ON THE AERODYNAMIC CHARACTERISTICS

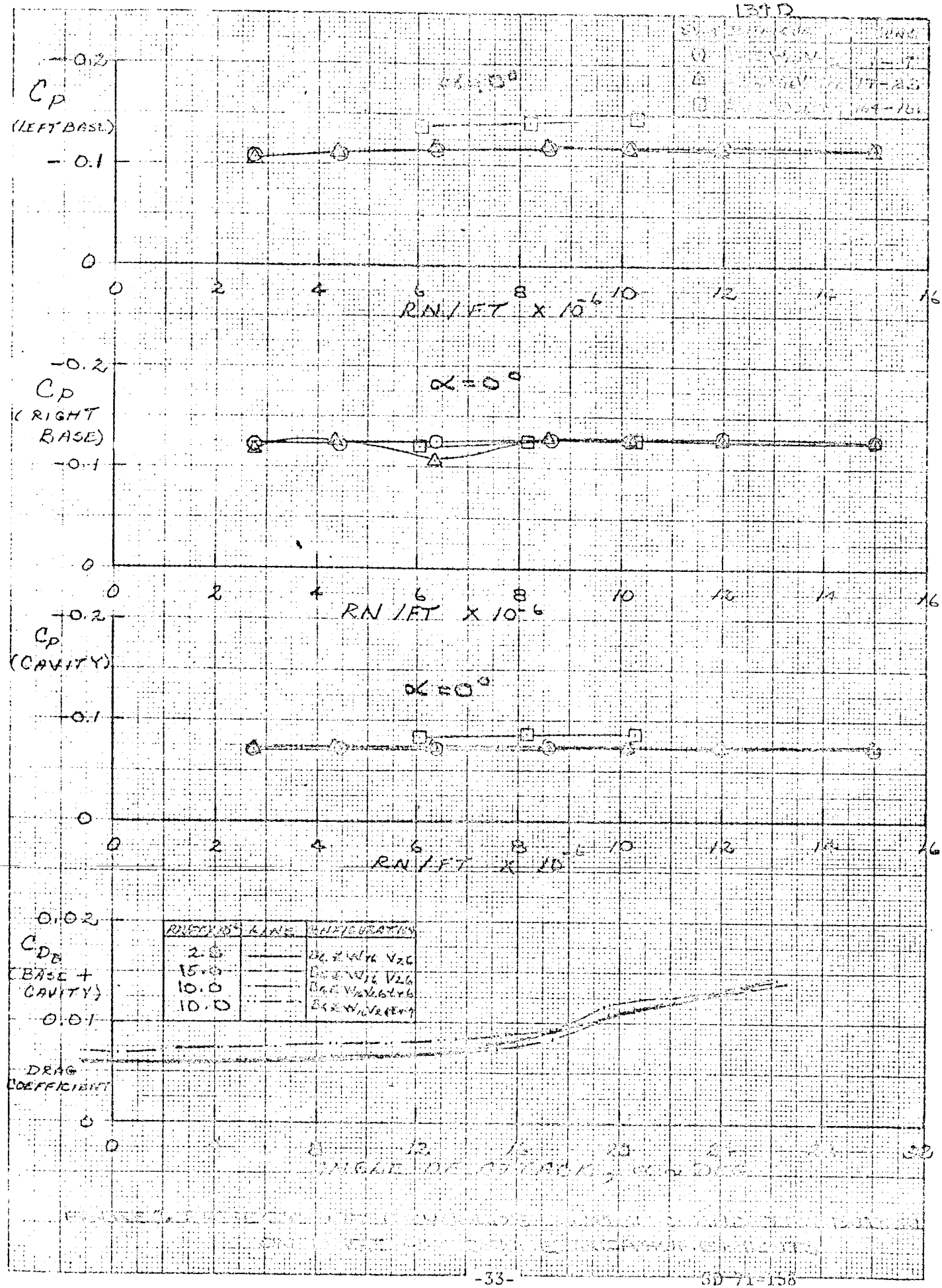
C_p (LEFT BASE)
$\alpha = 0°$
RN/FT X 10^{-6}
C_p (RIGHT BASE)
$\alpha = 0°$
RN/FT X 10^{-6}
C_p (CAVITY)
$\alpha = 0°$
RN/FT X 10^{-6}
C_{D_B} (BASE + CAVITY)
DRAG COEFFICIENT
RN/FT X 10^{-6}

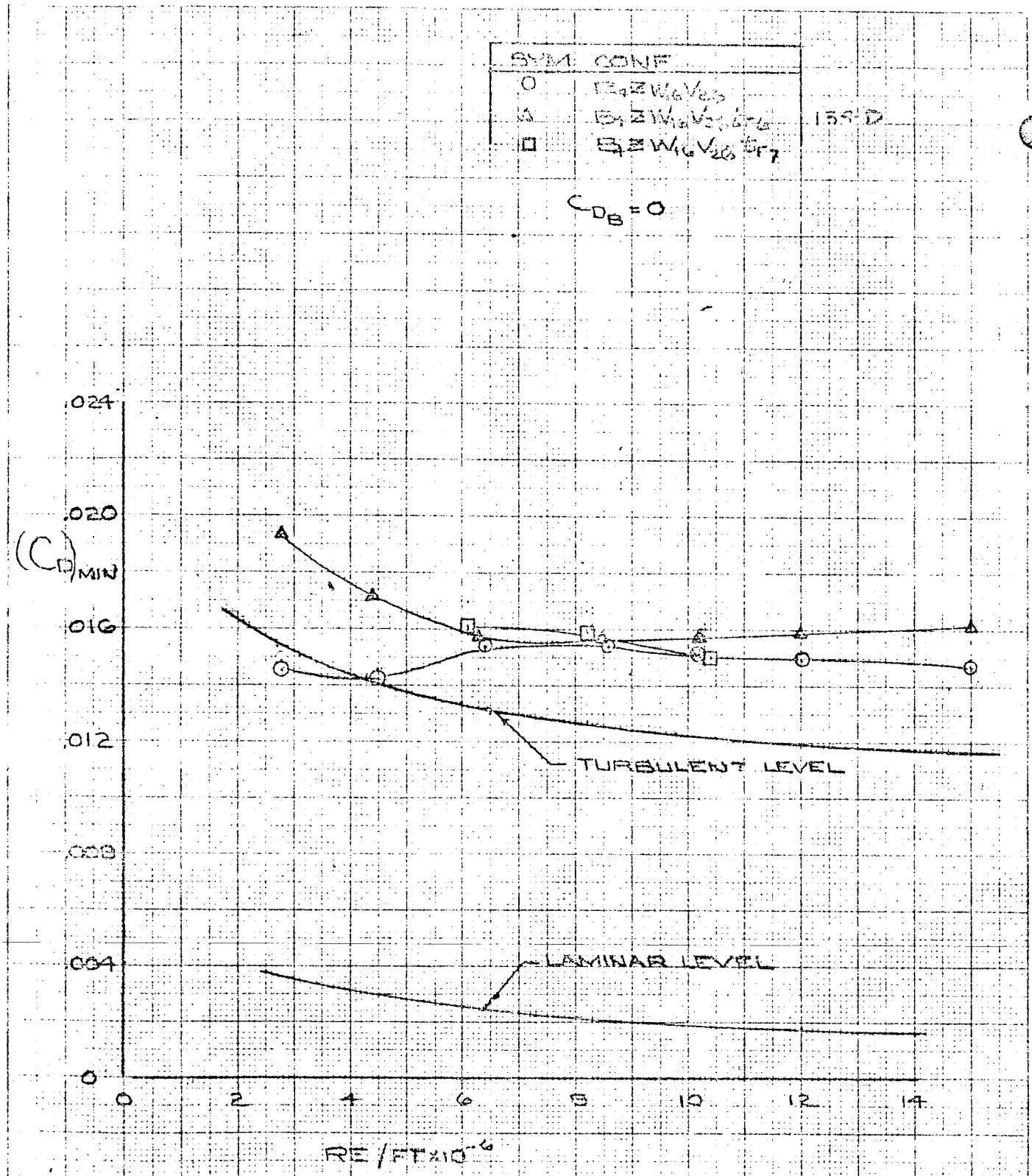

FIGURE 9. EFFECT OF REYNOLDS NUMBER AND TRANSITION ON THE METRO LIFT DRAG

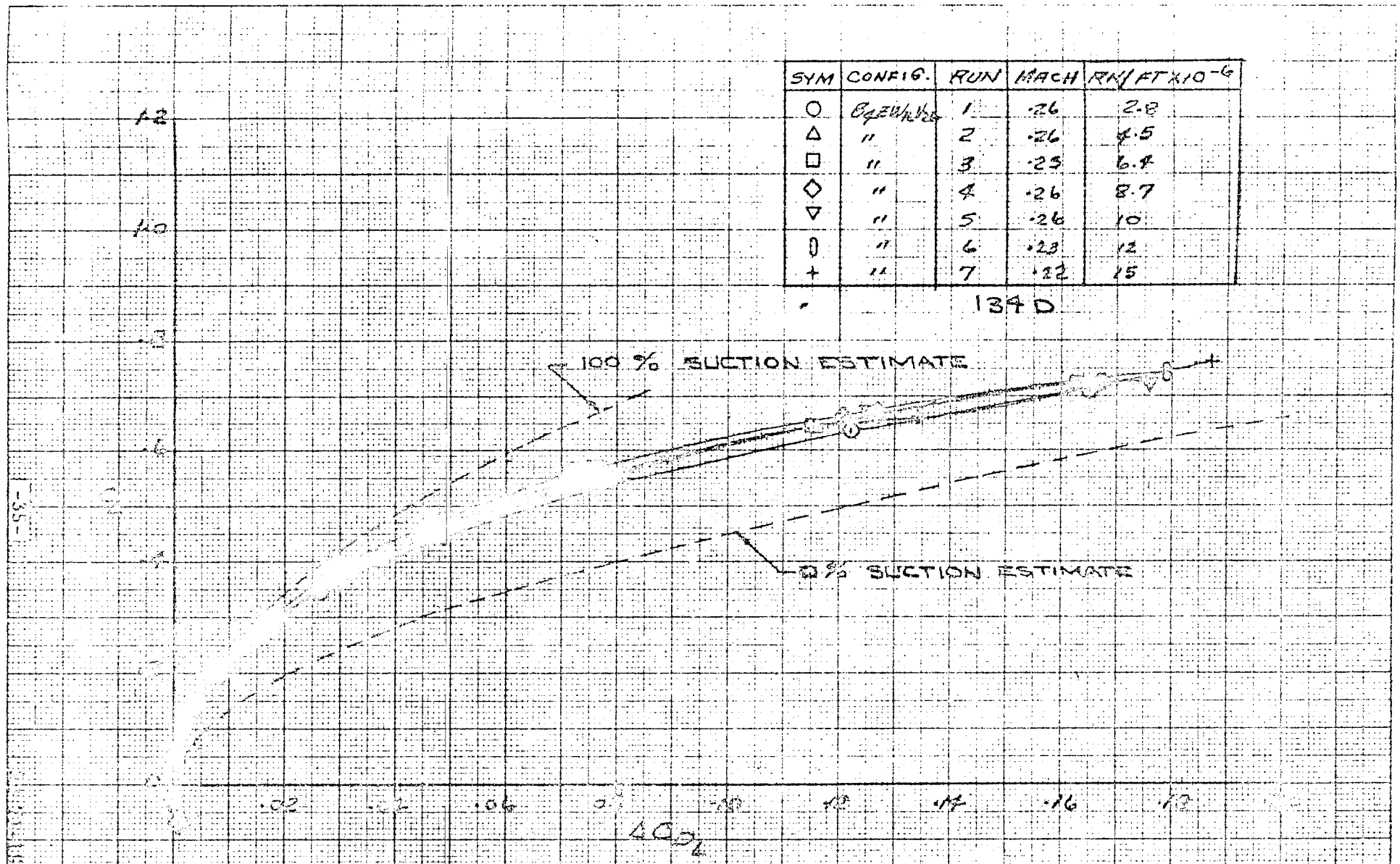

FIGURE 8a, EFFECT OF REYNOLDS NUMBER ON INDUCED DRAG, $B_{q2}W_1V_2$ CONFIG.

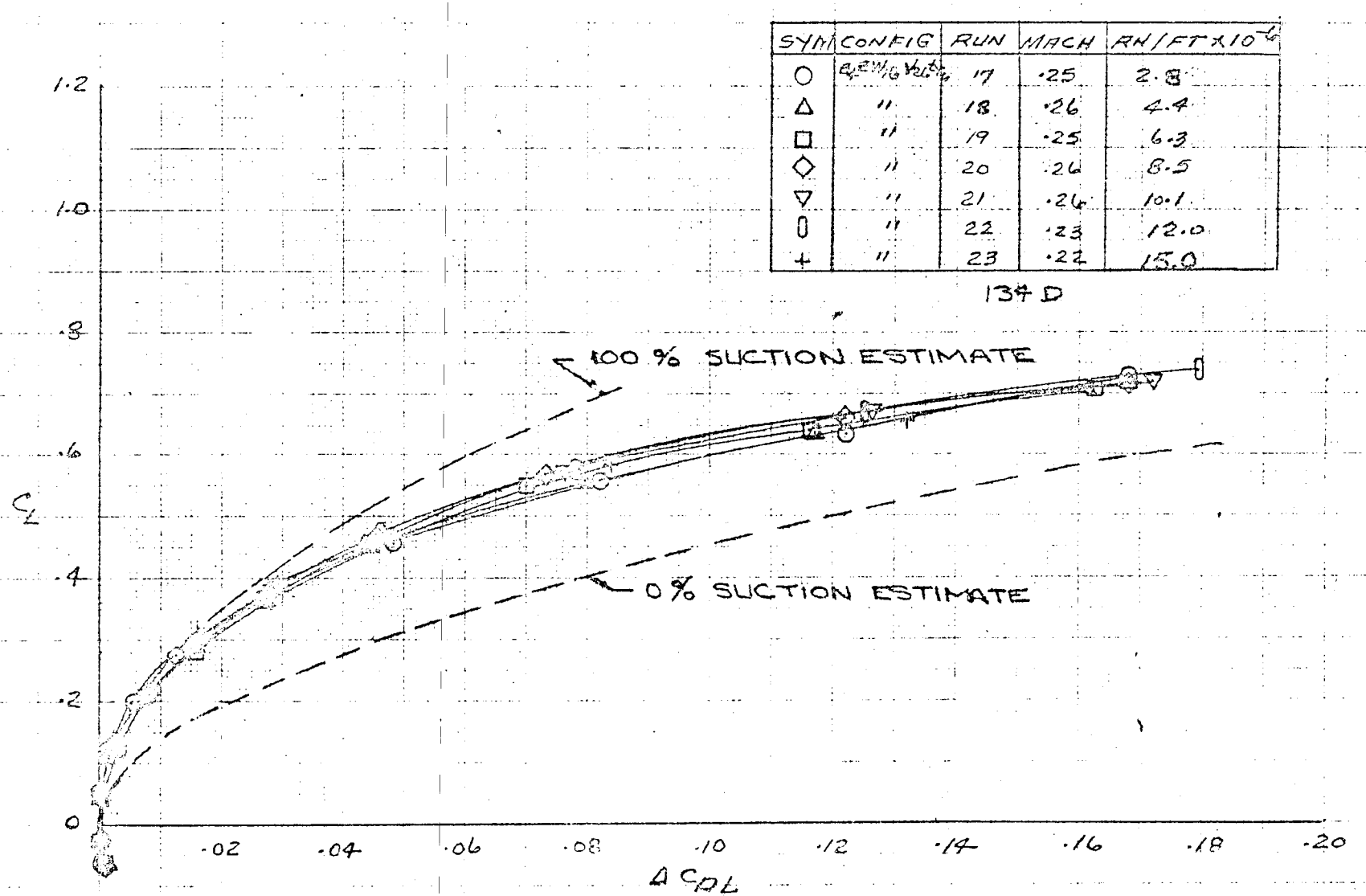

FIGURE 96. EFFECT OF REYNOLD'S NUMBER ON INDUCED DRAG-$B_4ZW_{16}V_{26}t_6$ CONT.

SYM	CONFIG.	RUN	MACH	RN/FT X 10^{-6}
□	$B_4 \bar{X} W_1 V_{2L} t_r 7$	104	0.26	6
◇	"	105	0.26	8
▽	"	106	0.26	10

139-D

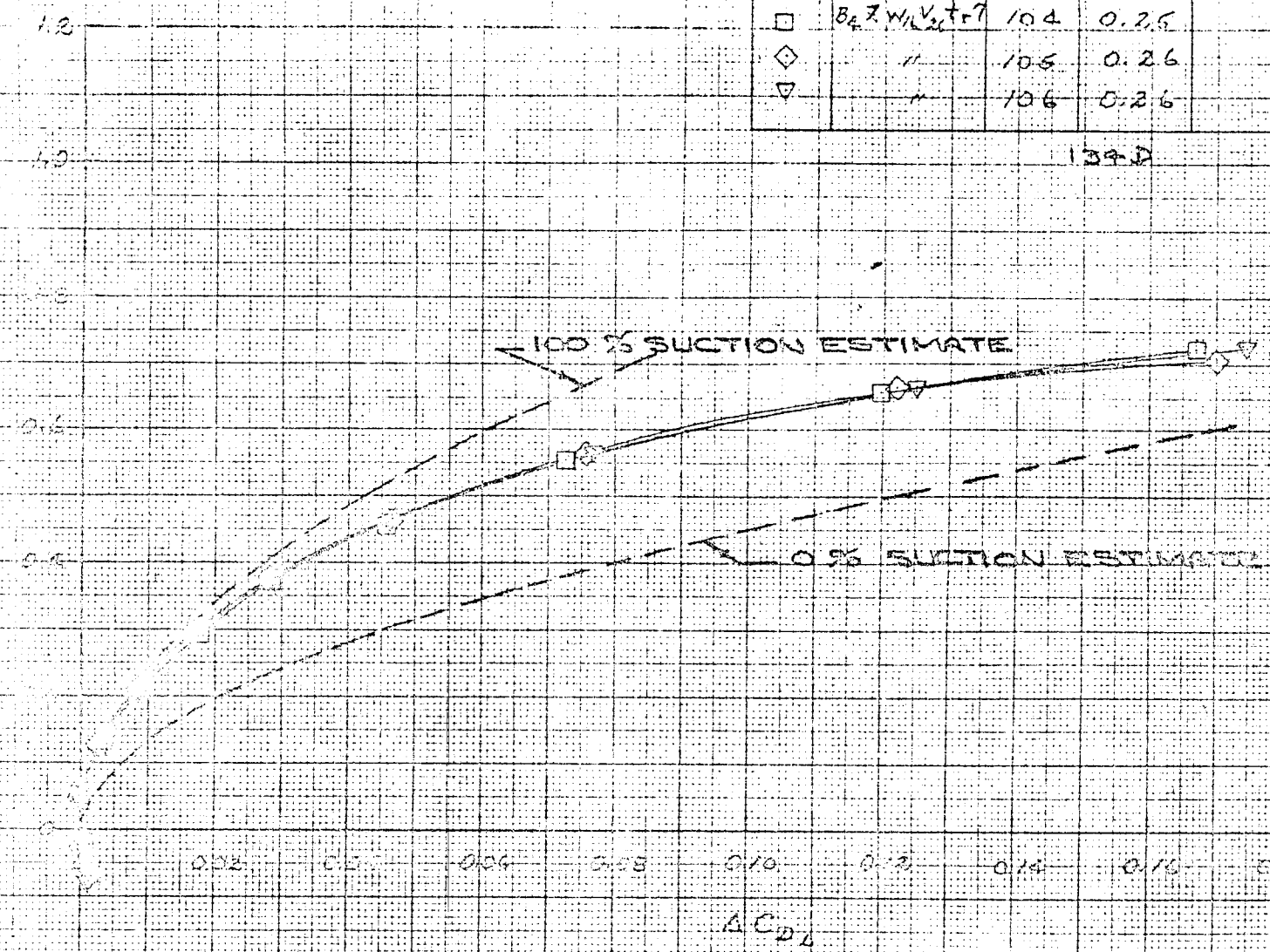

[illegible] PROFILE DRAG COEFFICIENT [illegible] INDUCED DRAG, $B_4 \bar{X} W_1 V_{2L} t_r 7$ CONFIGURATION

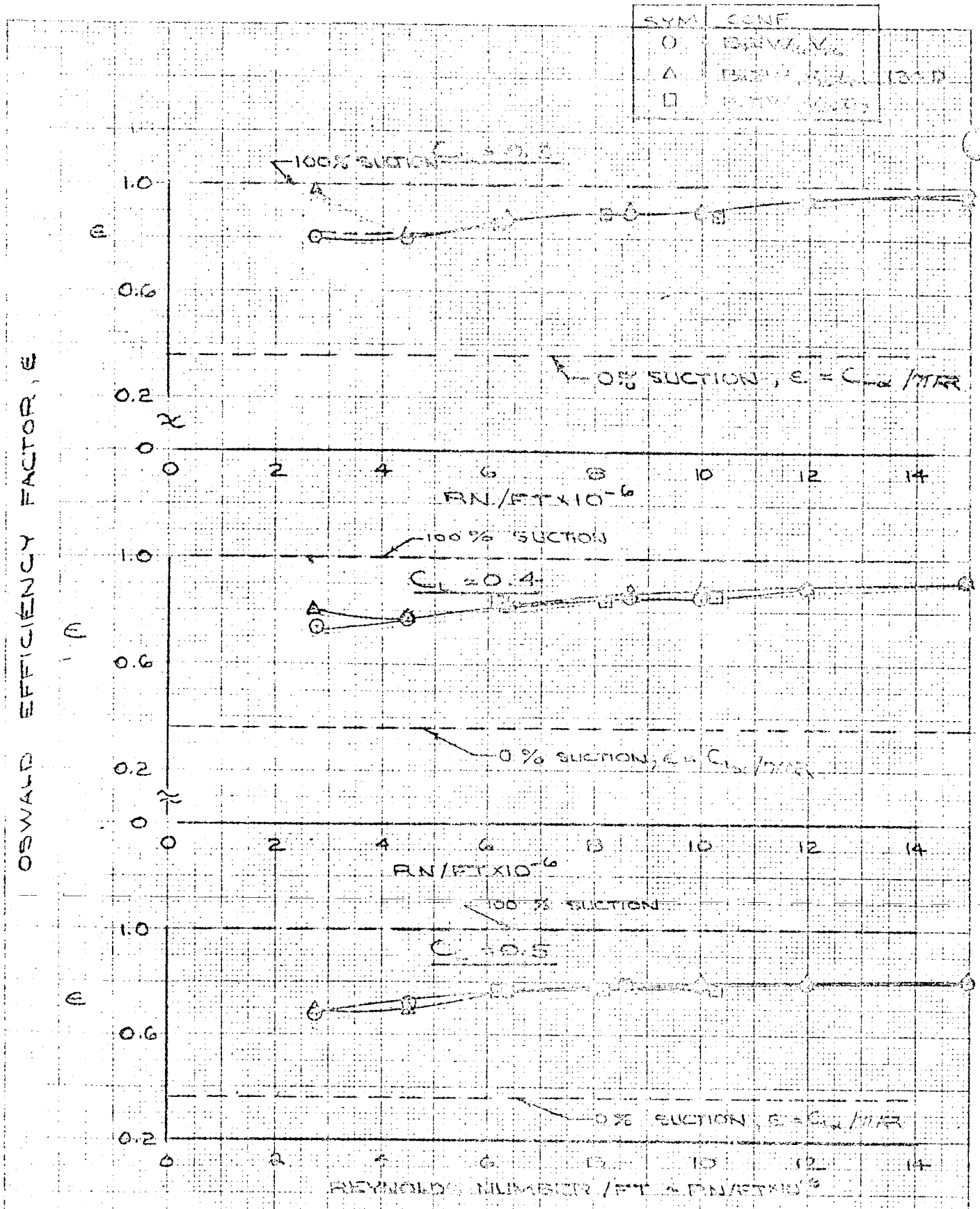

FIGURE 10. EFFECT OF REYNOLDS NUMBER AND SUCTION ON INDUCED DRAG EFFICIENCY

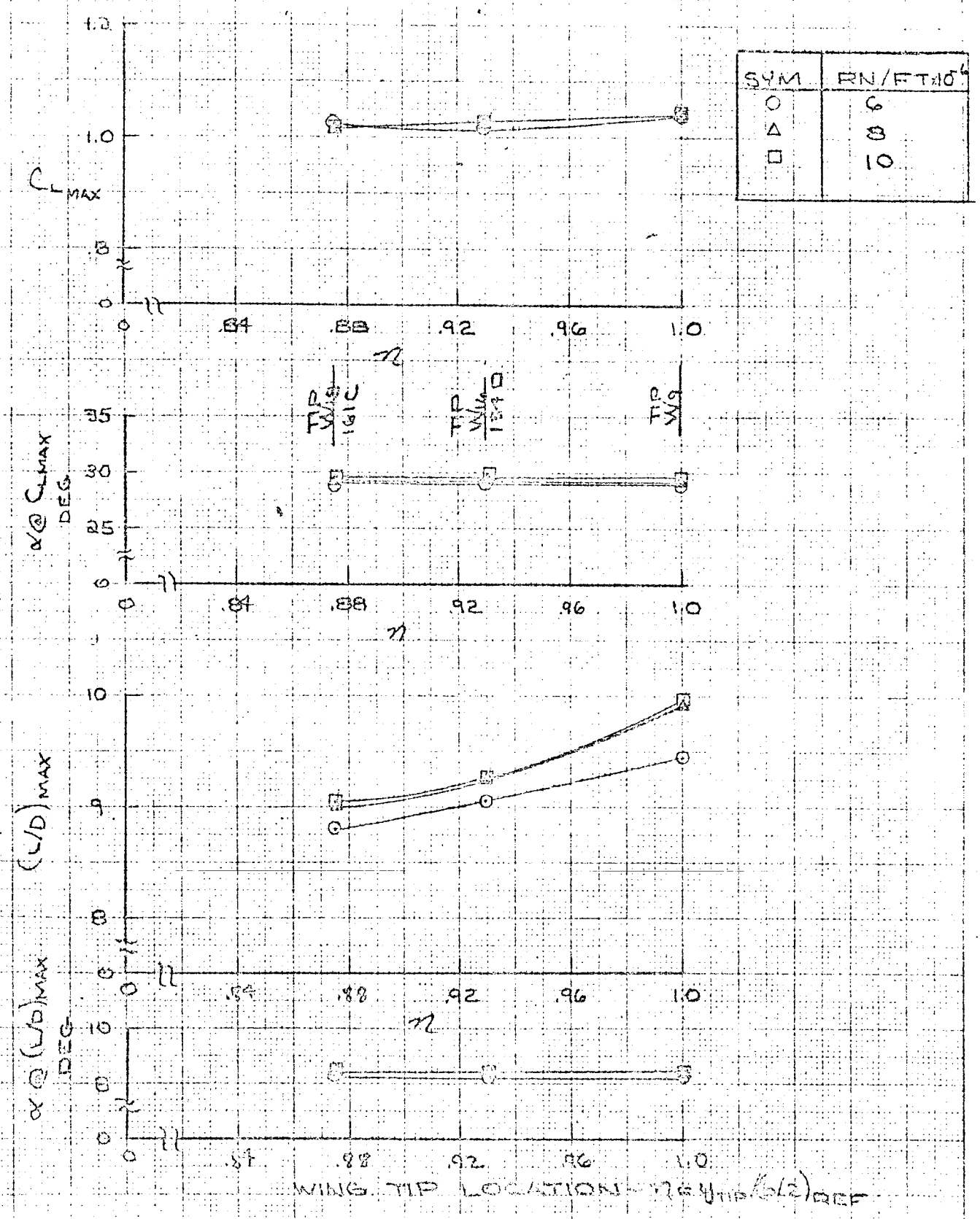

FIGURE 11 [illegible] EFFECT OF WING TIP [illegible] AND REYNOLDS NUMBER ON RELATIVE AERODYNAMIC CHARACTERISTICS

C_{L_0}
$C_{m_{C_L=0}}$
C_{L_α} PER DEG
AERODYNAMIC CENTER
AERODYNAMIC CENTER IN BODY LENGTH
M
.01
.02
.04
.10
.20
.70
.80
.88
.92
.96
1.0

SYM	CONFIG.	RUN	MACH	RN/FT x10^6	η WING
⊙	B4Z W9 V26	90	0.25	6	1.000
△	B4Z W16 V26	3	0.25	6	0.930
□	B4Z W18 V26	95	0.25	6	0.875

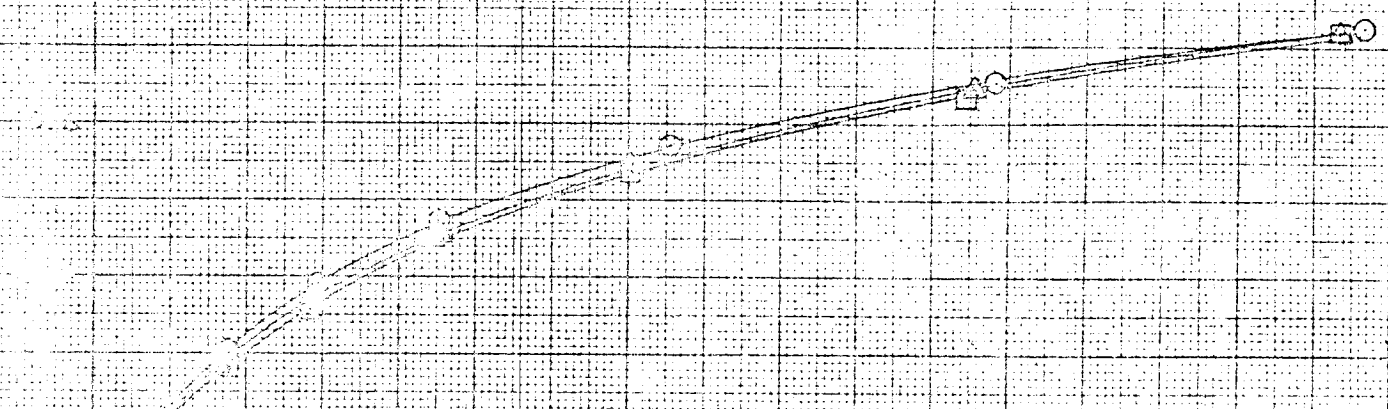

SYM	CONFIG.	RUN	MACH	RN/FT x10⁶	M WING
⊙	$B_6 Z W_9 V_{26}$	91	0.26	8	1.000
△	$B_4 Z W_{16} V_{26}$	4	0.26	8	0.930
□	$B_4 Z W_{18} V_{26}$	94	0.26	8	0.875

134 D

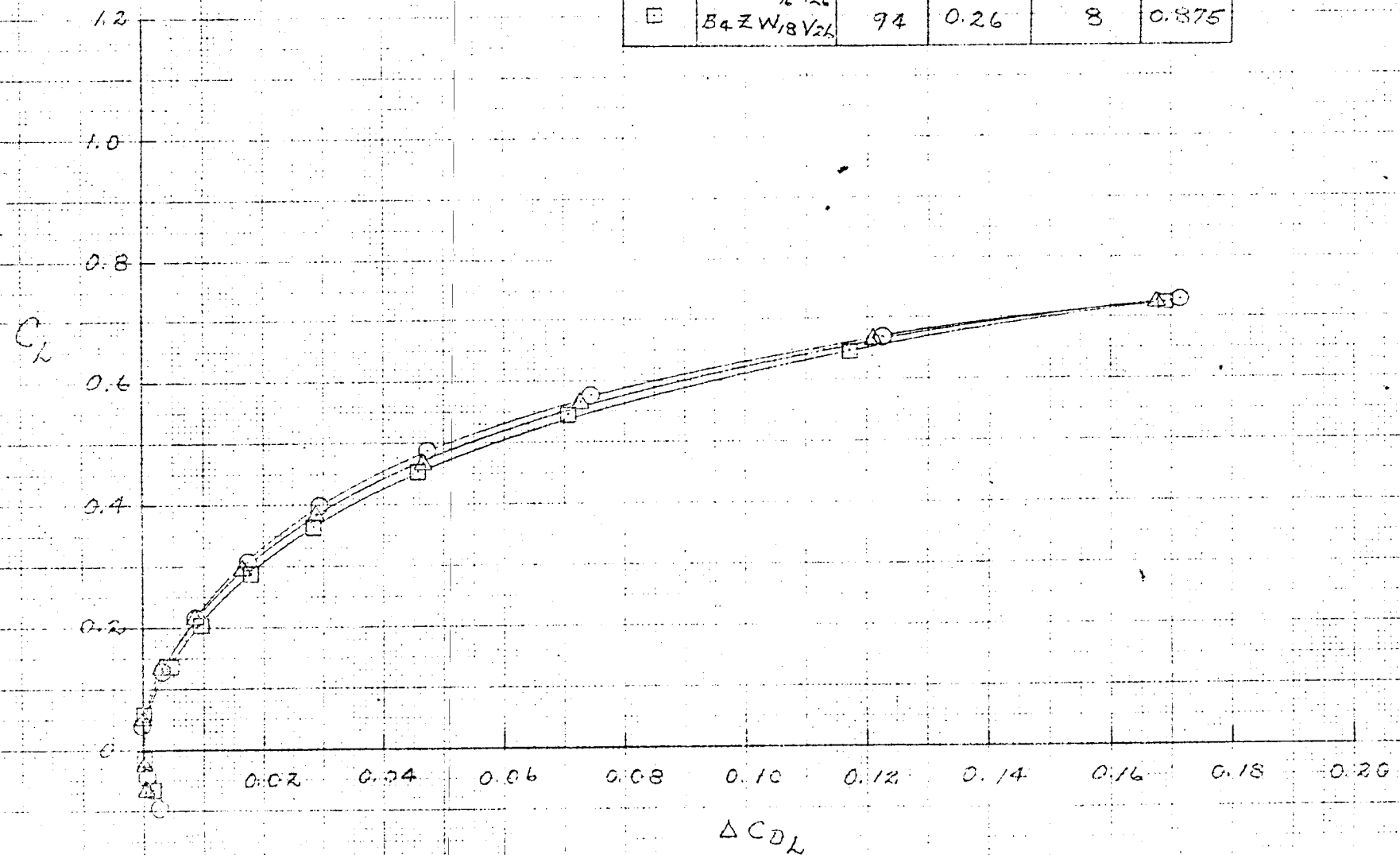

FIGURE 126 EFFECT OF WING TIP GEOMETRY ON DRAG DUE TO LIFT, RN/FT = 8 X 10⁶

SYM	CONFIG.	RUN	MACH	RN/FT $\times 10^6$	η_{WING}
⊙	$B_4 E W_7 V_{26}$	92	0.26	10	1.000
△	$B_4 E W_{16} V_{26}$	6	0.26	10	0.930
⊡	$B_4 E W_{18} V_{26}$	95	0.26	10	0.875

134 D

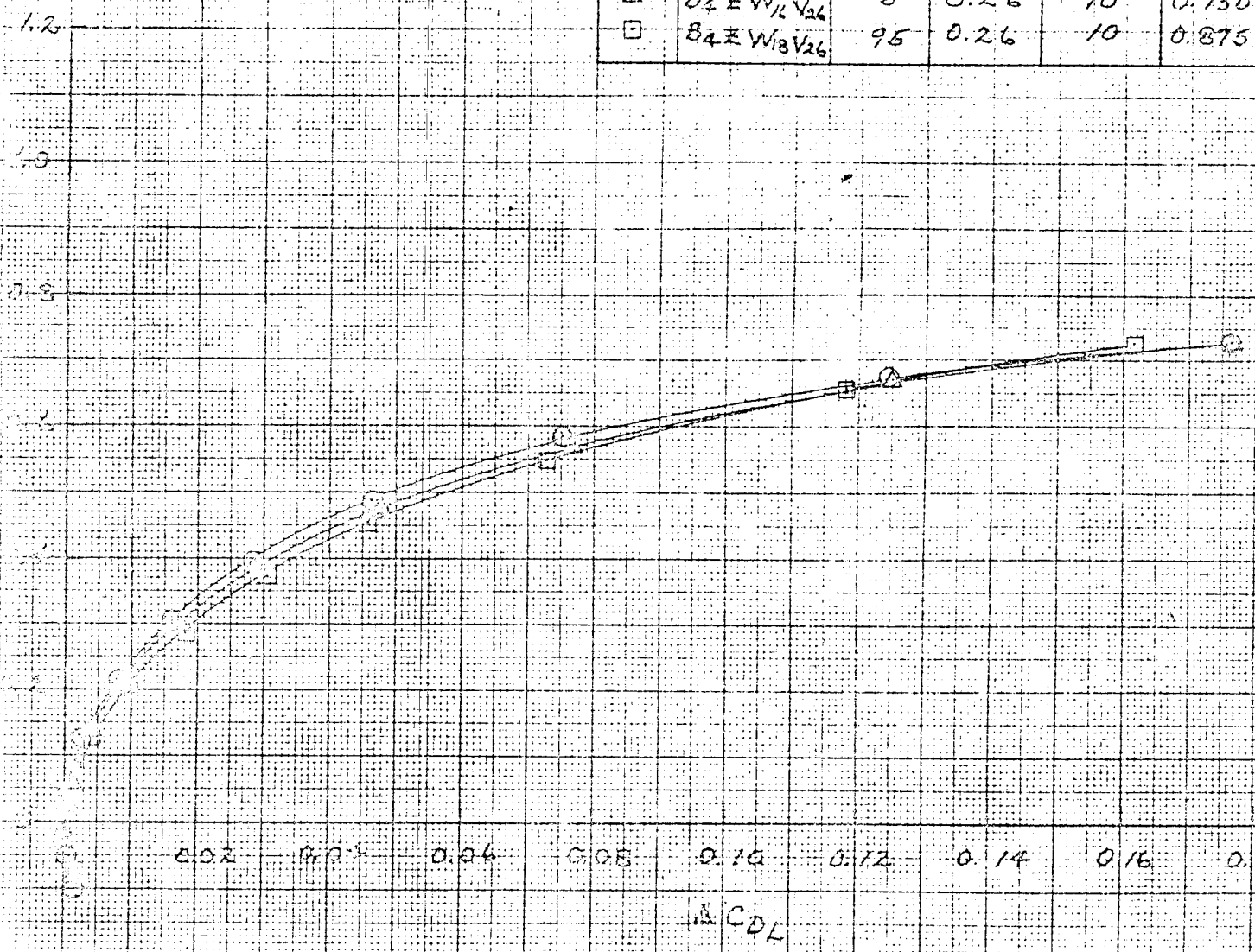

EFFECT OF WING TIP GEOMETRY ON DRAG DUE TO LIFT, RN/FT = 10

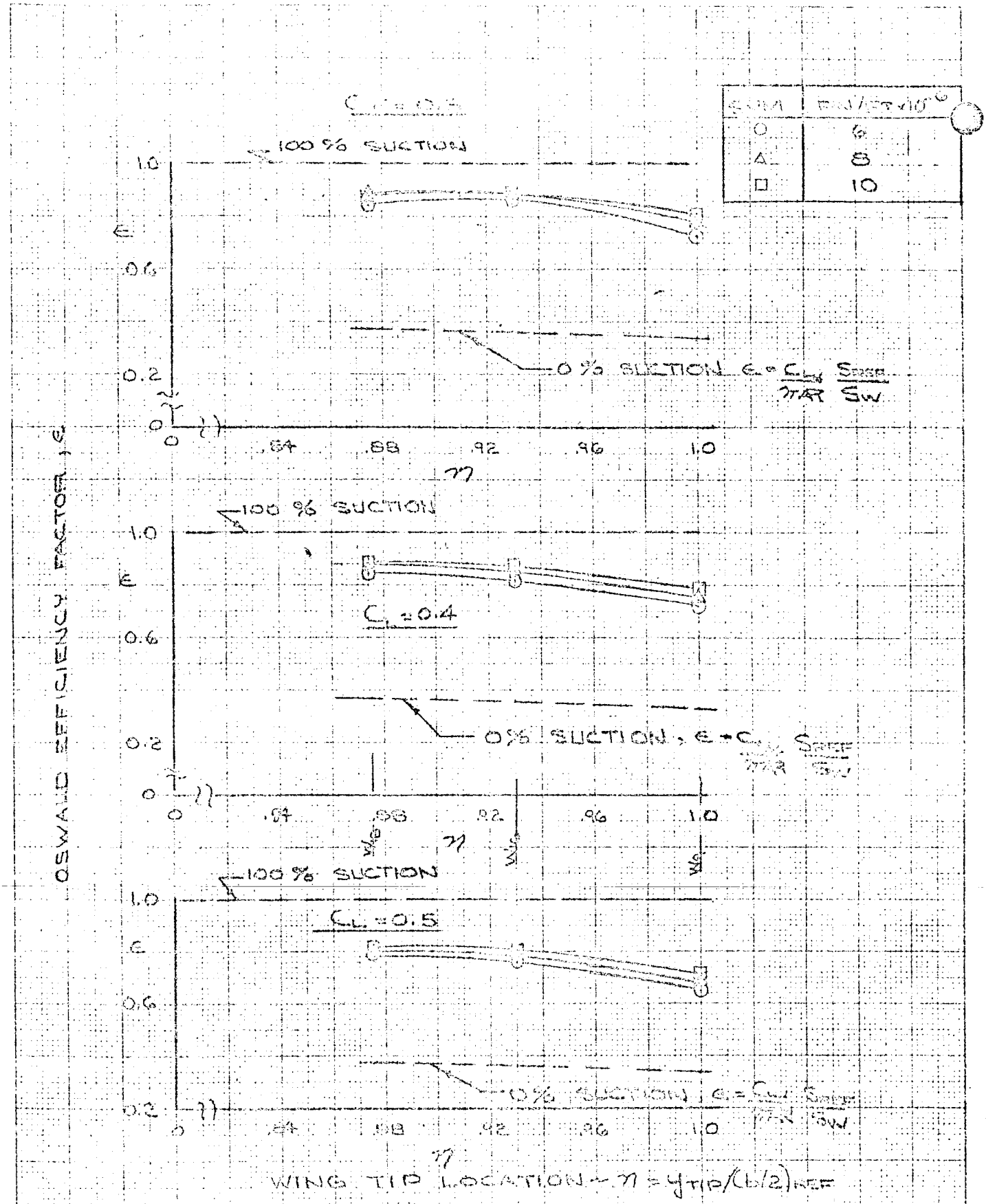

INFLUENCE OF WING TIP SUCTION AND DRAG ON NUMBER OF INDUCED DRAG EFFICIENCY

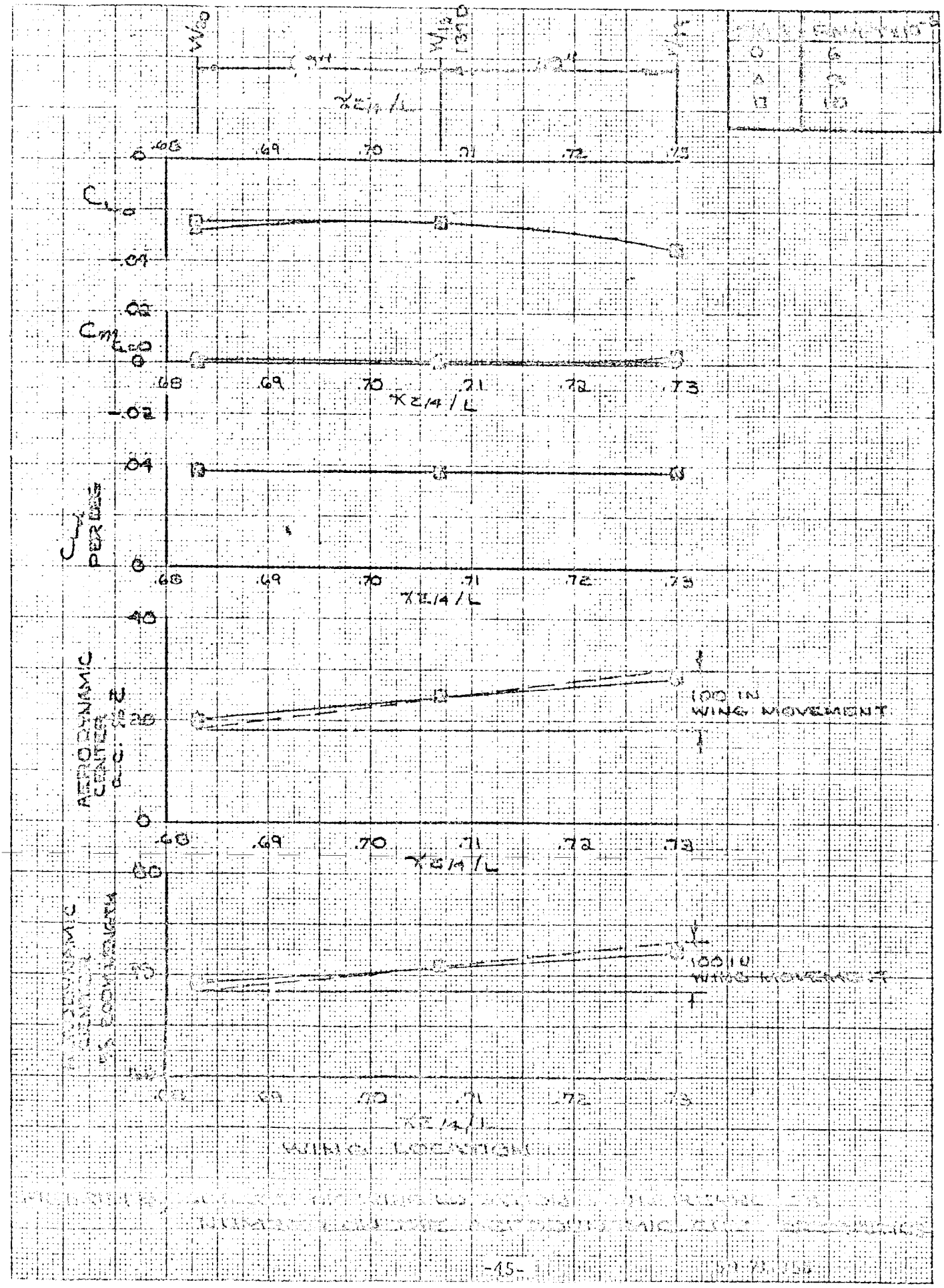
.68
.69
.70
.71
.72
.73
C_{L_0}
$C_{m_{L=0}}$
C_{m_L} PER DEG
AERODYNAMIC CENTER
100 IN WING MOVEMENT
AERODYNAMIC CENTER
100 IN WING MOVEMENT

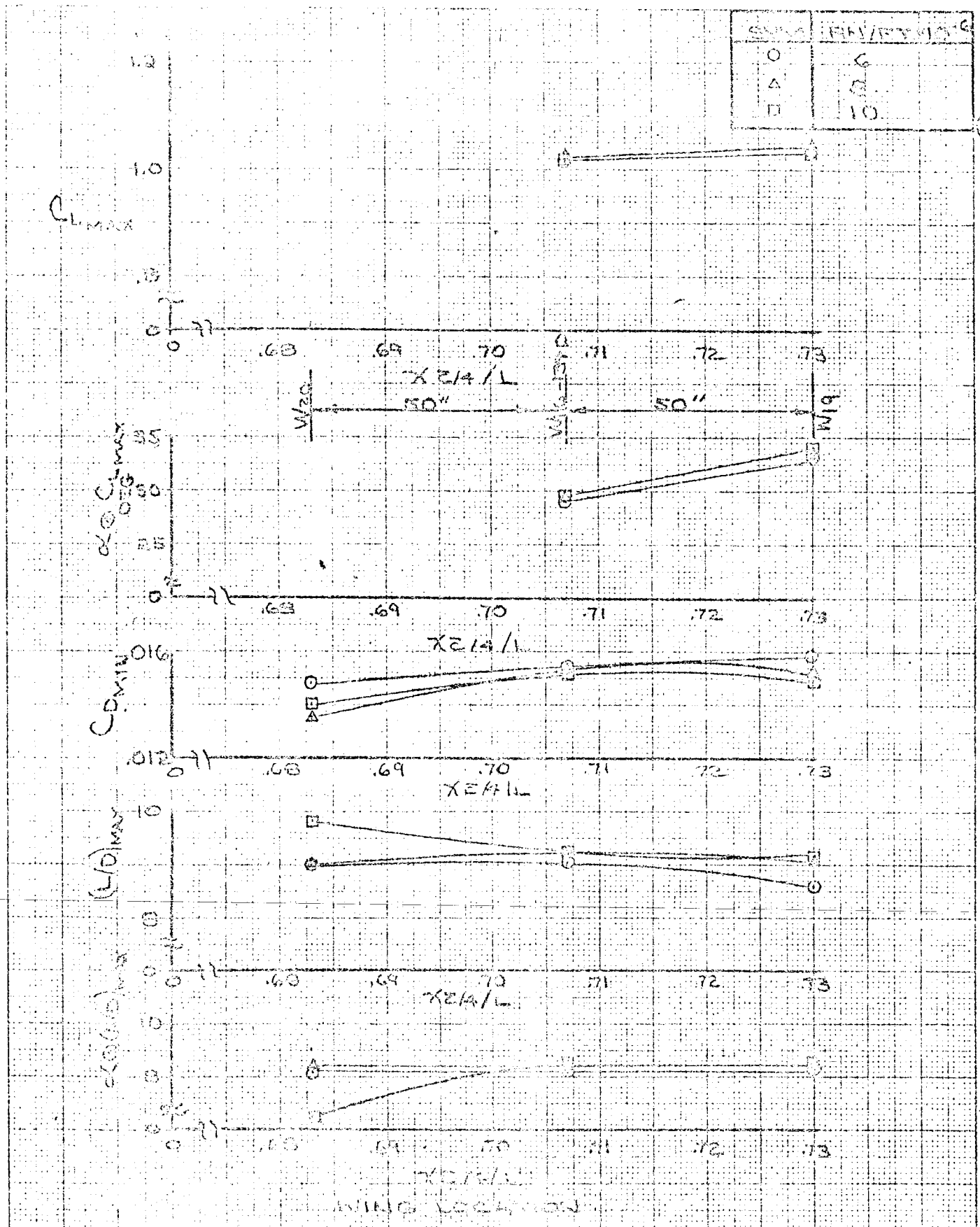

FIGURE [illegible] WING LOCATION [illegible]

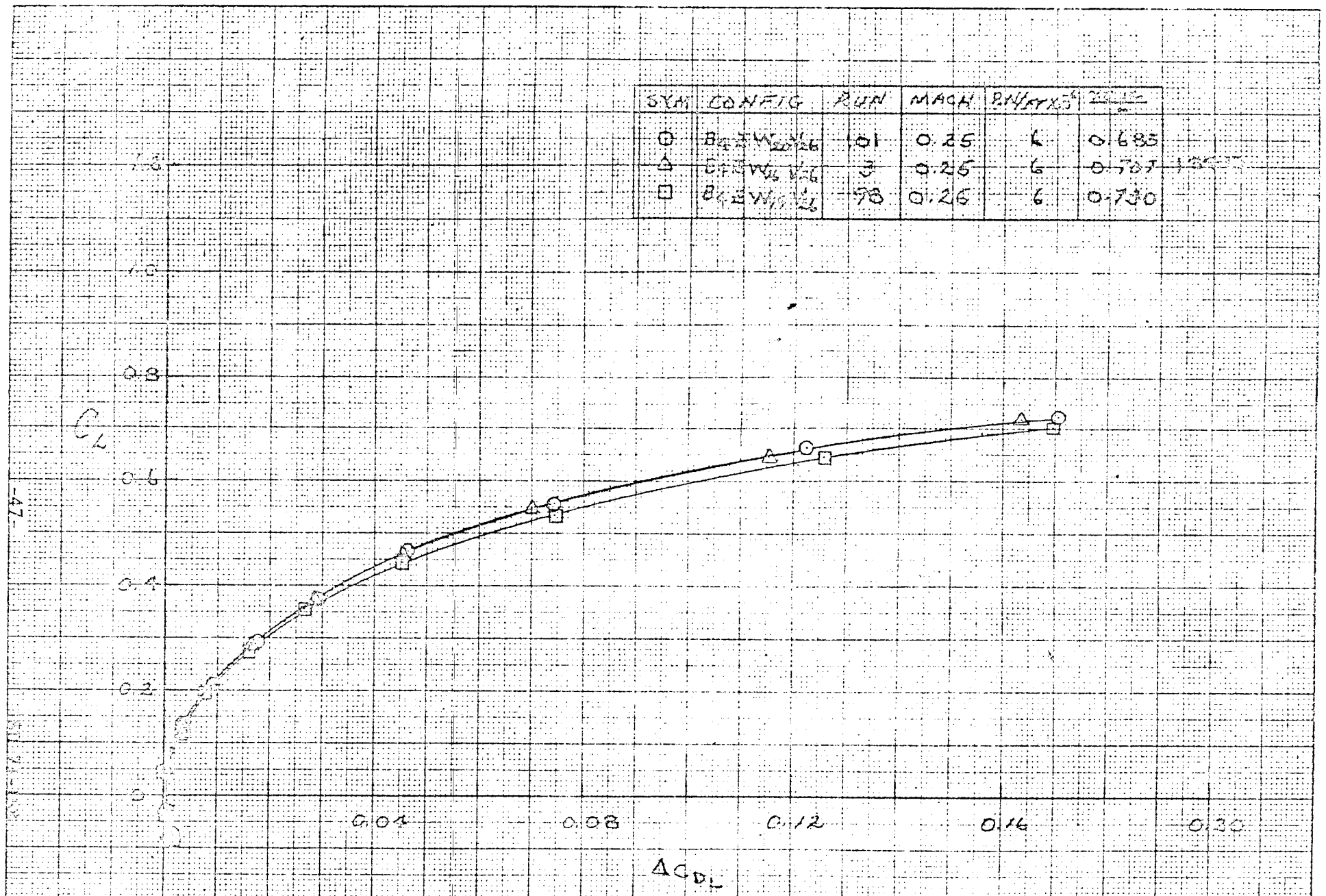

FIGURE 15a, EFFECT OF WING LOCATION ON INDUCED DRAG
RN/FT = 6×10^6

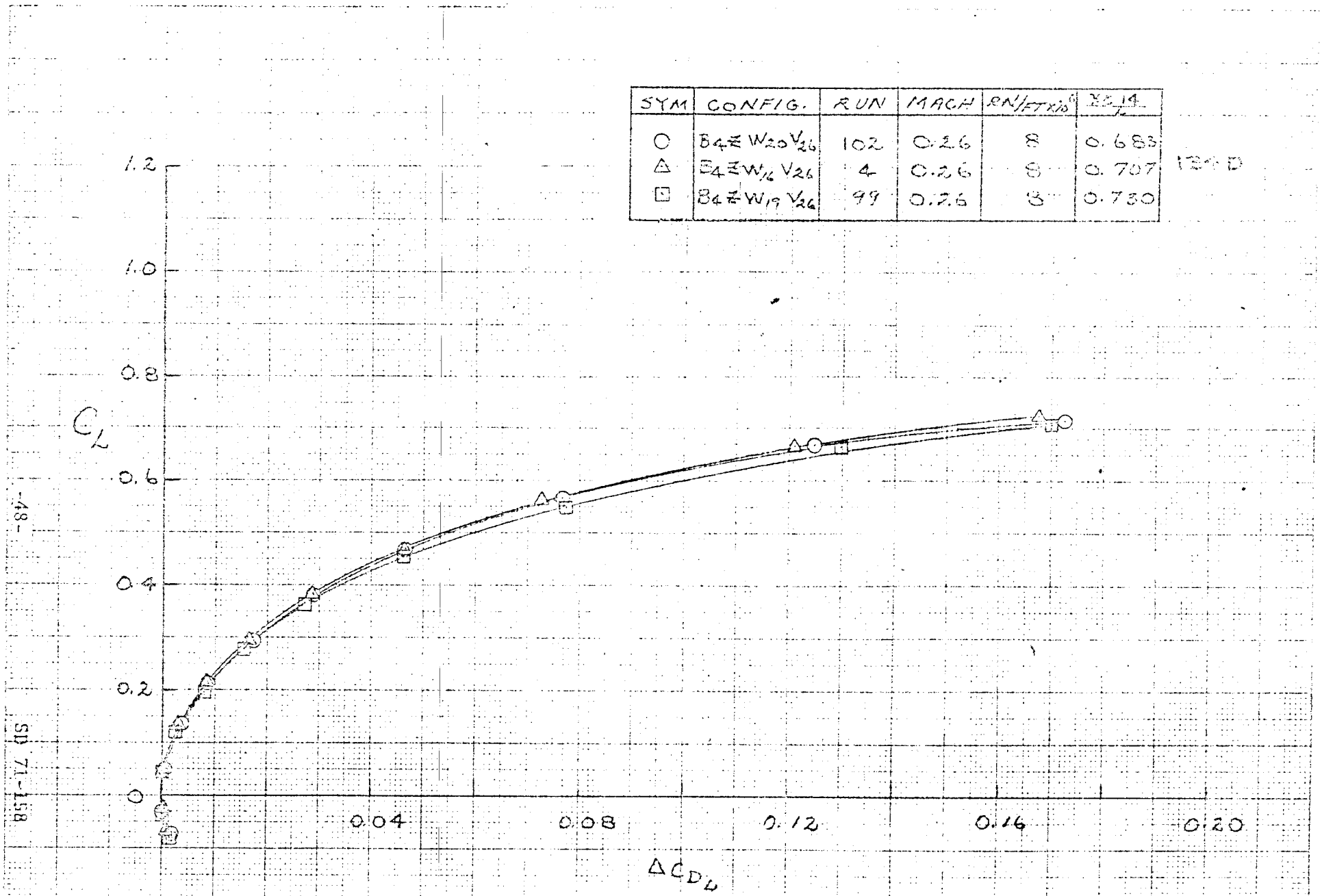

FIGURE 15b, EFFECT OF WING LOCATION ON INDUCED DRAG
RN/FT = 8 X 10^6

SYM	CONFIG.	RUN	MACH	$RN/FT \times 10^6$	$\frac{Z_E}{L}$
⊙	$B_4 Z W_{20} V_{26}$	103	0.26	10	0.683
△	$B_4 Z W_{16} V_{26}$	5	0.26	10	0.707
⊡	$B_4 Z W_{19} V_{26}$	100	0.26	10	0.730

134-D

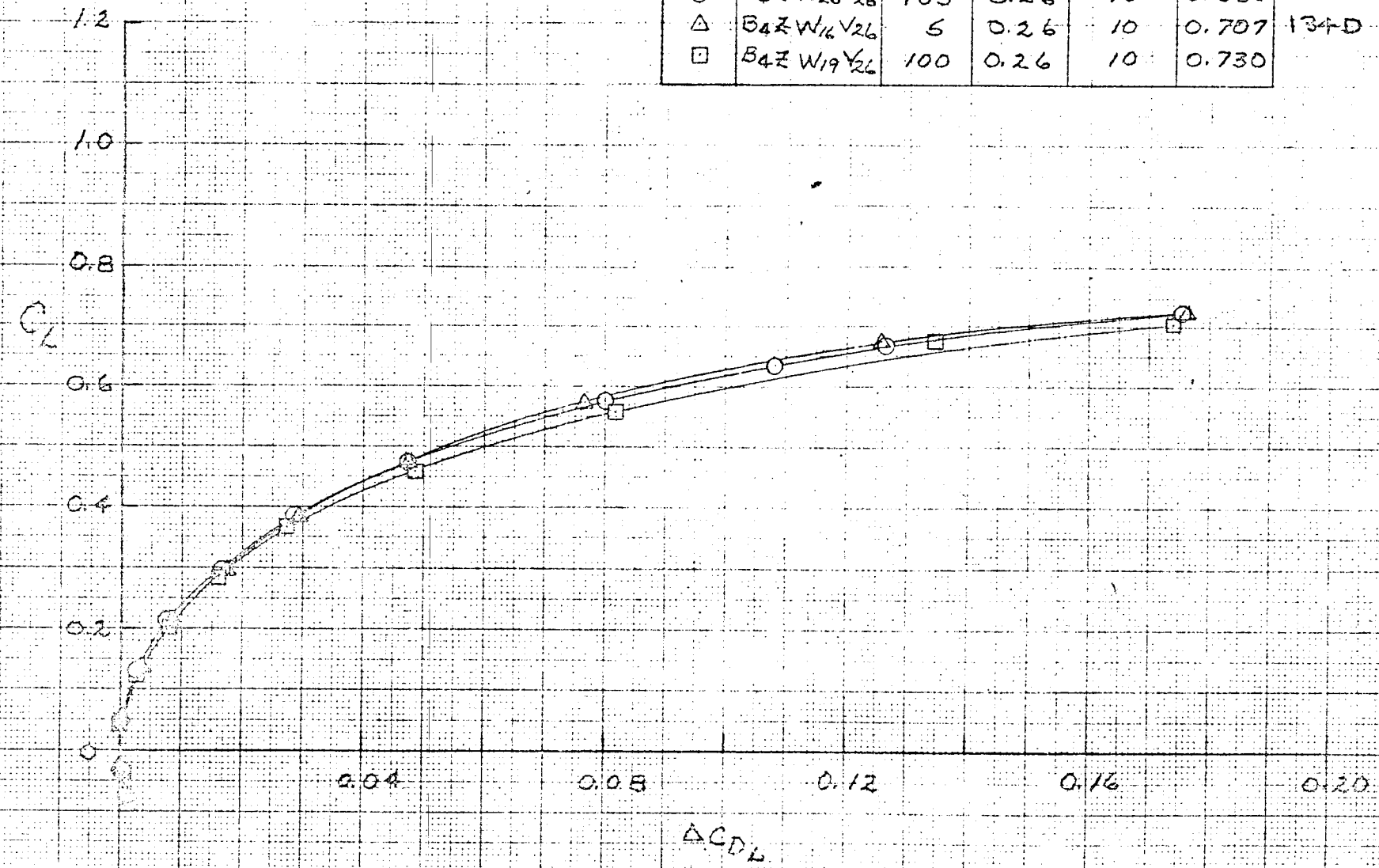

FIGURE 15. EFFECT OF WING LOCATION ON INDUCED DRAG
$RN/FT = 10 \times 10^6$

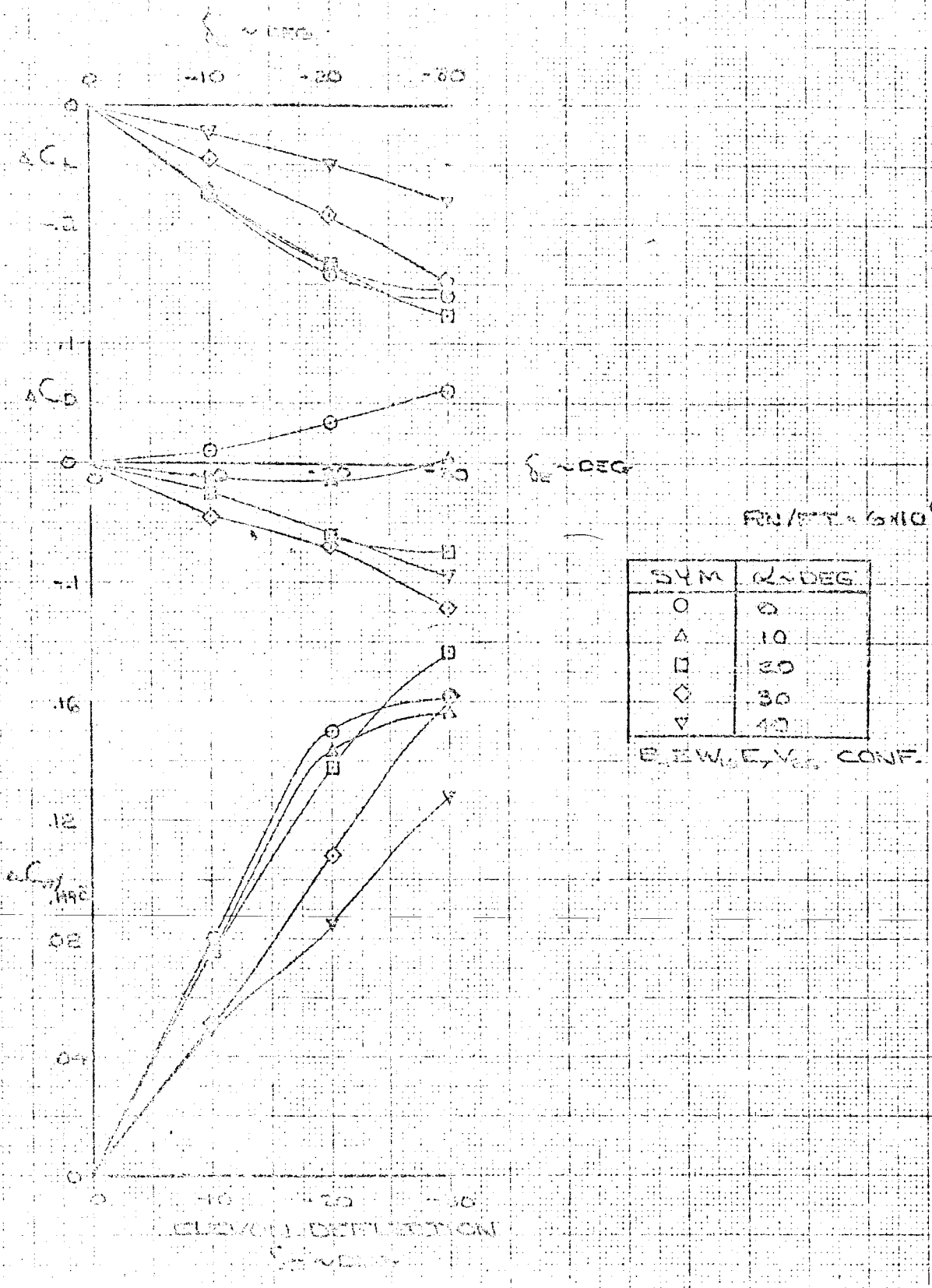
δe ~ DEG
0
-10
-20
-30
ΔCL
-.1
ΔCD
-.1
.16
.12
ΔCm/ΔαB
.08
.04
0
-10
-20
-30
ELEVON DEFLECTION
δe ~ DEG
δe ~ DEG
RN/FT ~ 6×10^6
SYM
α ~ DEG
0
10
20
30
40
B, EW, E, VS, CONF.

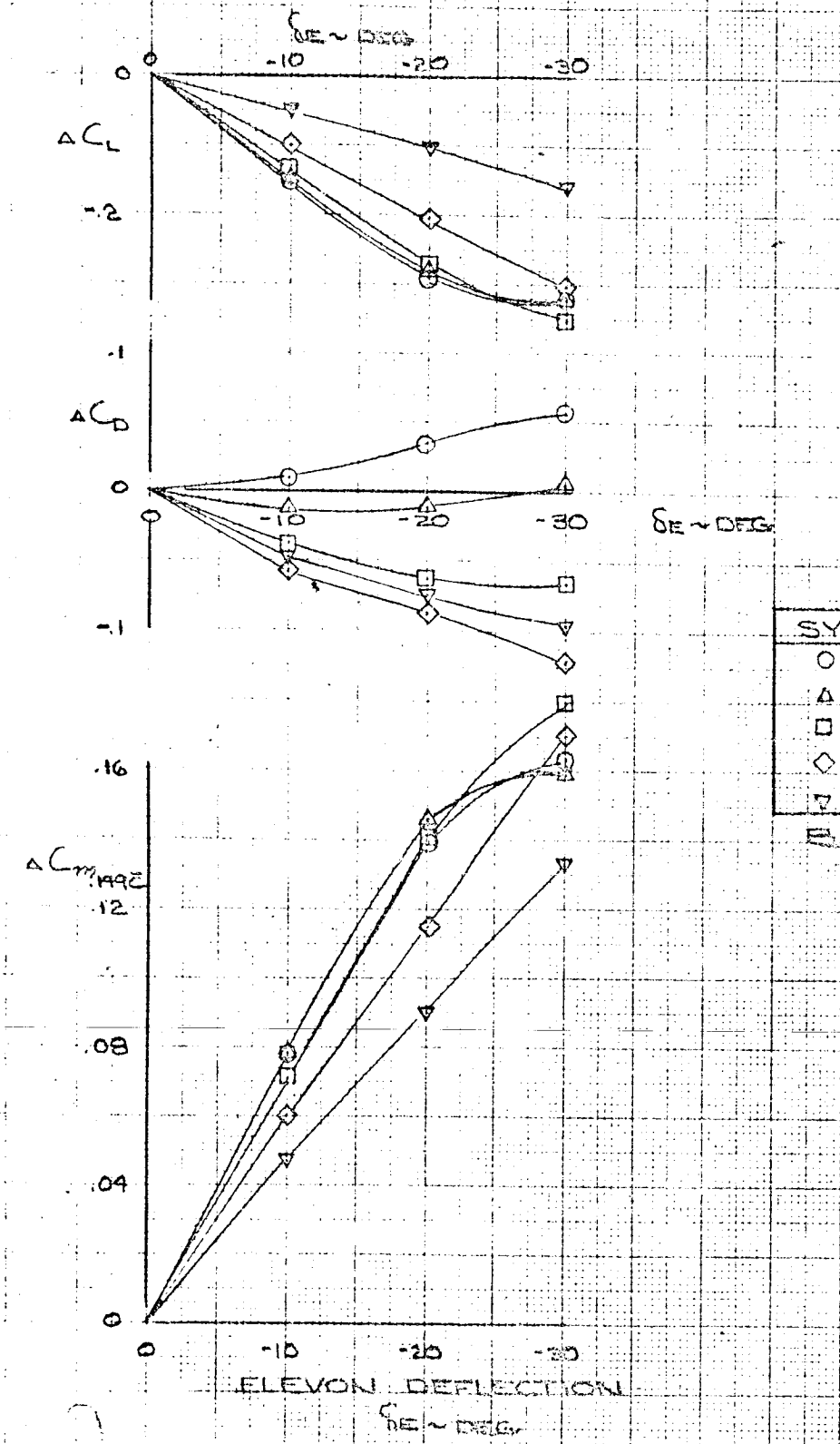

SYM	α ~ DEG
○	0
△	10
□	20
◇	30
▽	40

$R_{e_{JET}} = 8 \times 10^4$

$E_1 V_{1_0}$ $E_2 V_{2_0}$ CONF

FIGURE 16 b, ELEVON EFFECTIVENESS IN PITCH, $R_{e_{JET}} = 8 \times 10^4$, 1970

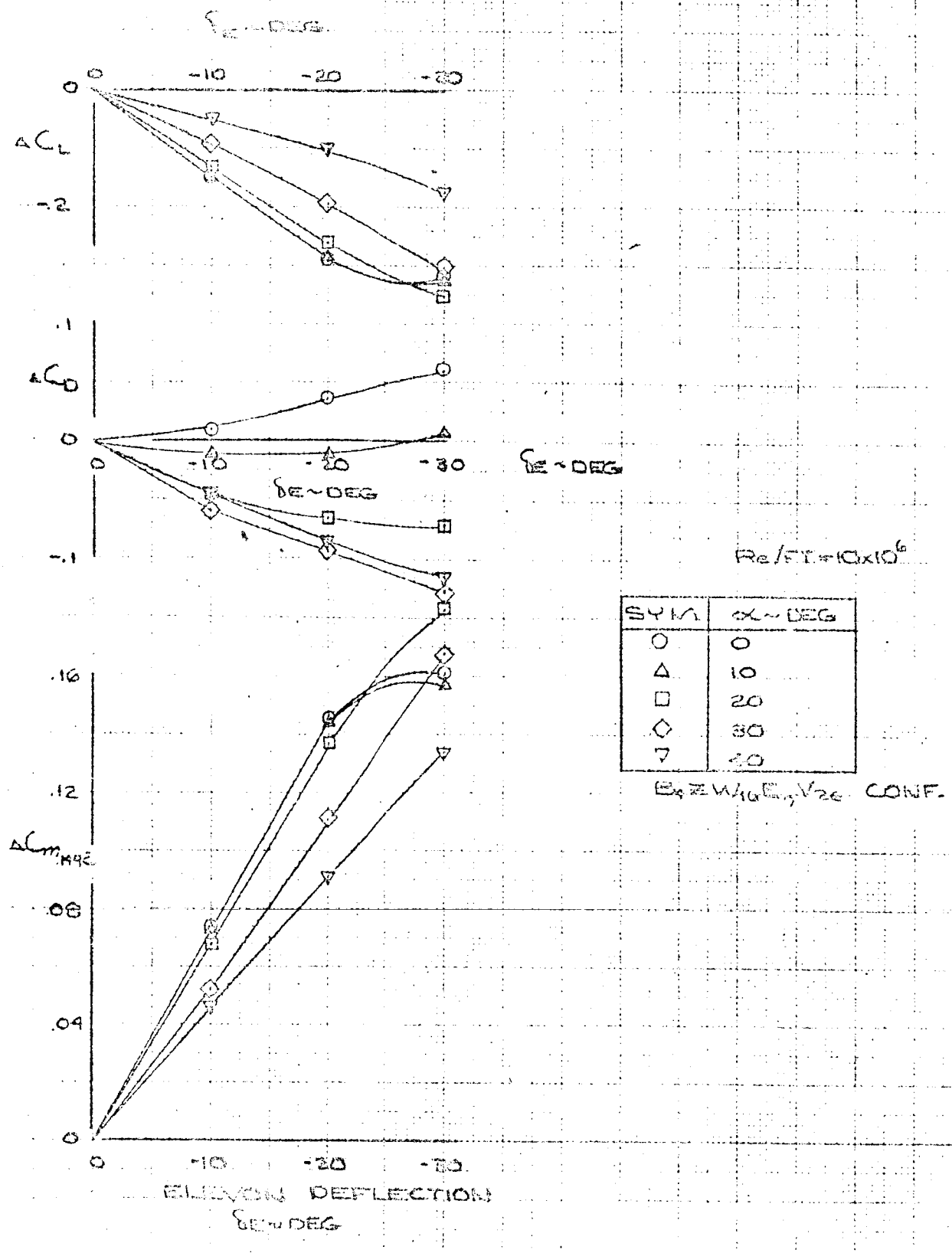

FIGURE 15. ELEVON EFFECTIVENESS IN PITCH, Re/FT = 10x10^6 (CONT.)

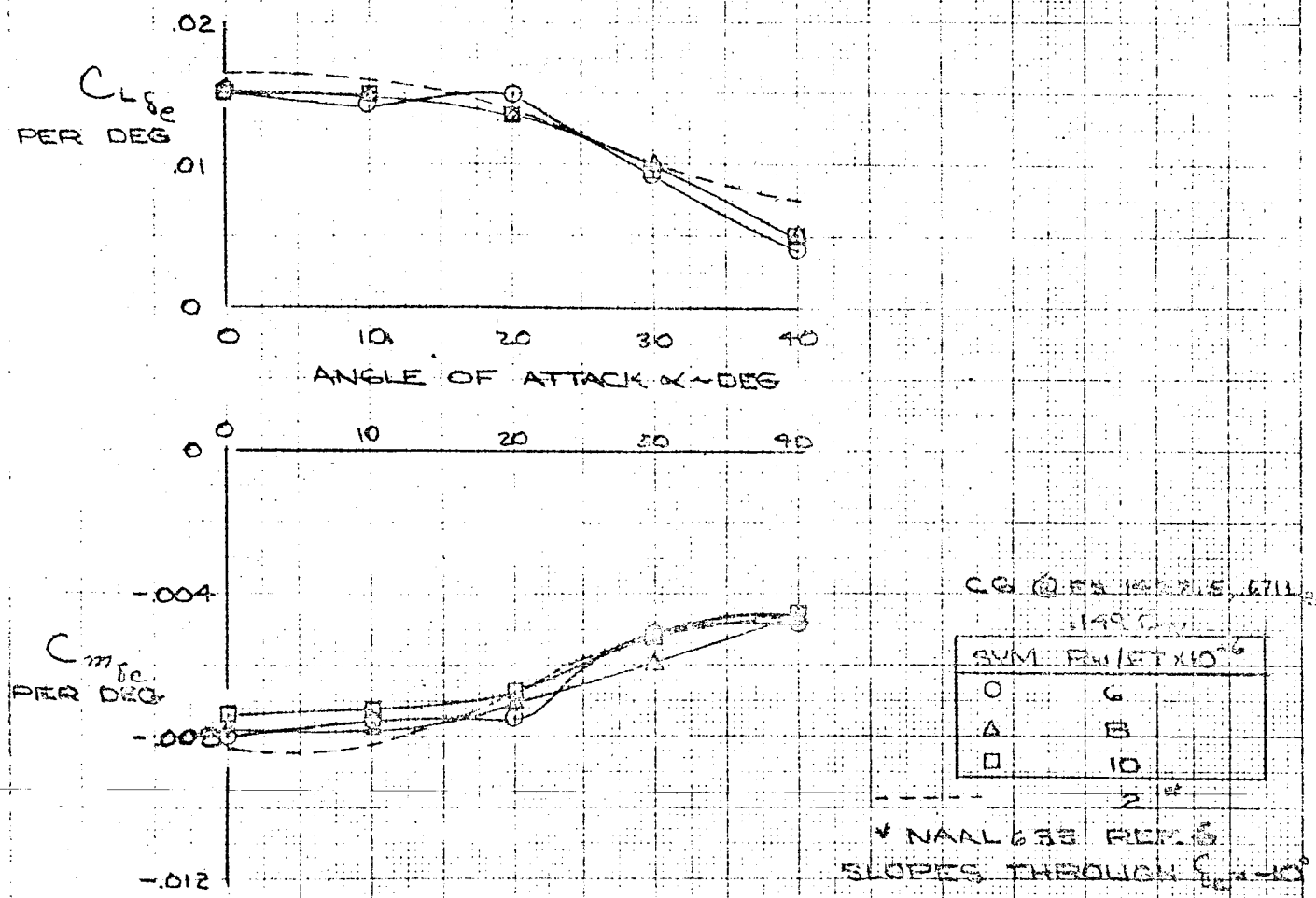

FIGURE 17. EFFECT OF REYNOLD'S NUMBER ON ELEVON EFFECTIVENESS DERIVATIVES IN PITCH - 3M. D

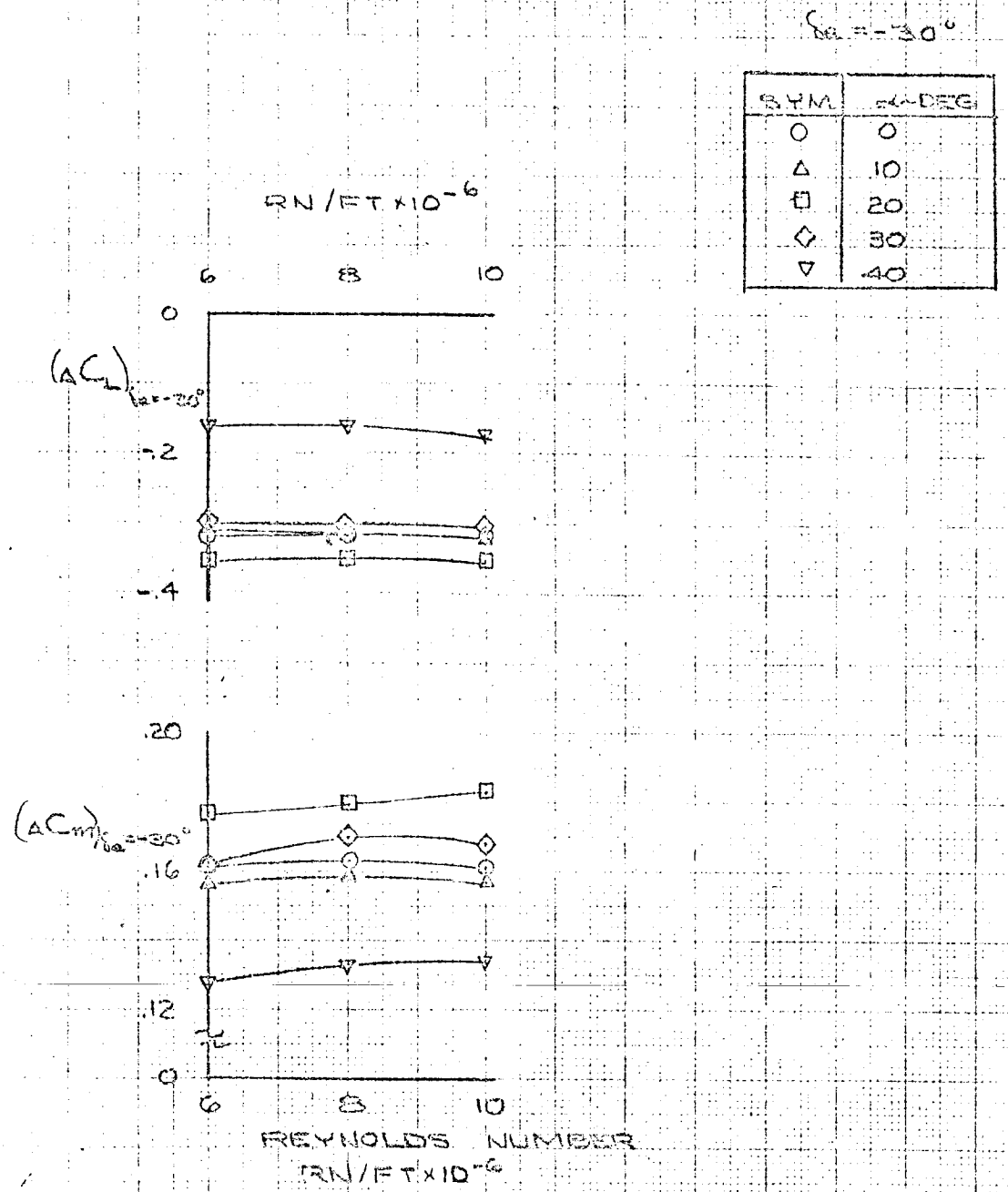

FIGURE 18. EFFECT OF REYNOLDS NUMBER ON ELEVON EFFECTIVENESS AT -30° ELEVON DEFLECTION

D.A.J.
6-2-1971

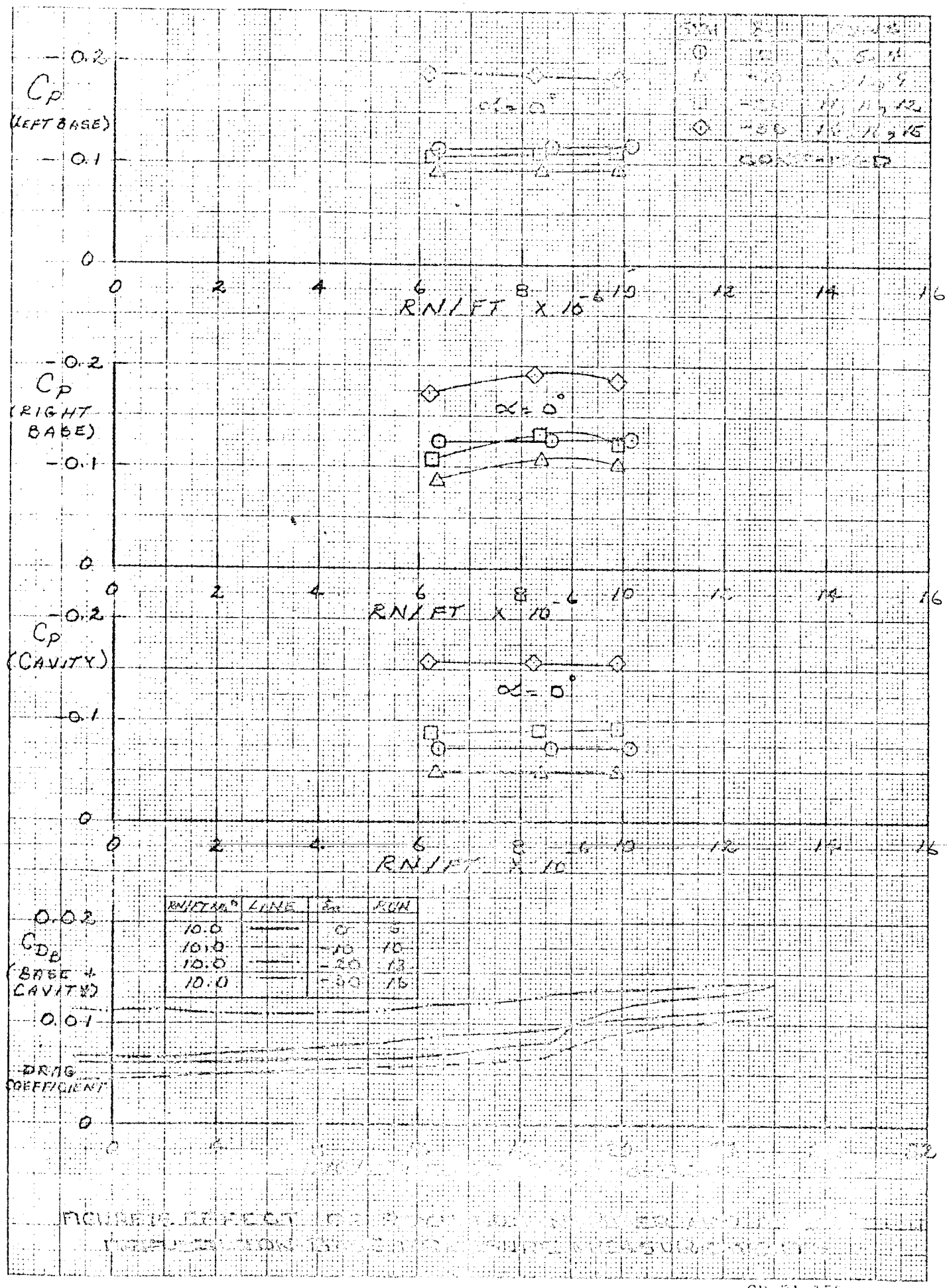
C_p (LEFT BASE)
C_p (RIGHT BASE)
C_p (CAVITY)
C_{D_B} (BASE + CAVITY)
DRAG COEFFICIENT
RNLFT X 10^{-6}
$\alpha = 0°$
RNLFT X 10^{-6}
RNLFT X 10^{-6}
RNLFT X 10^{-6}
RUN
5
10
13
16

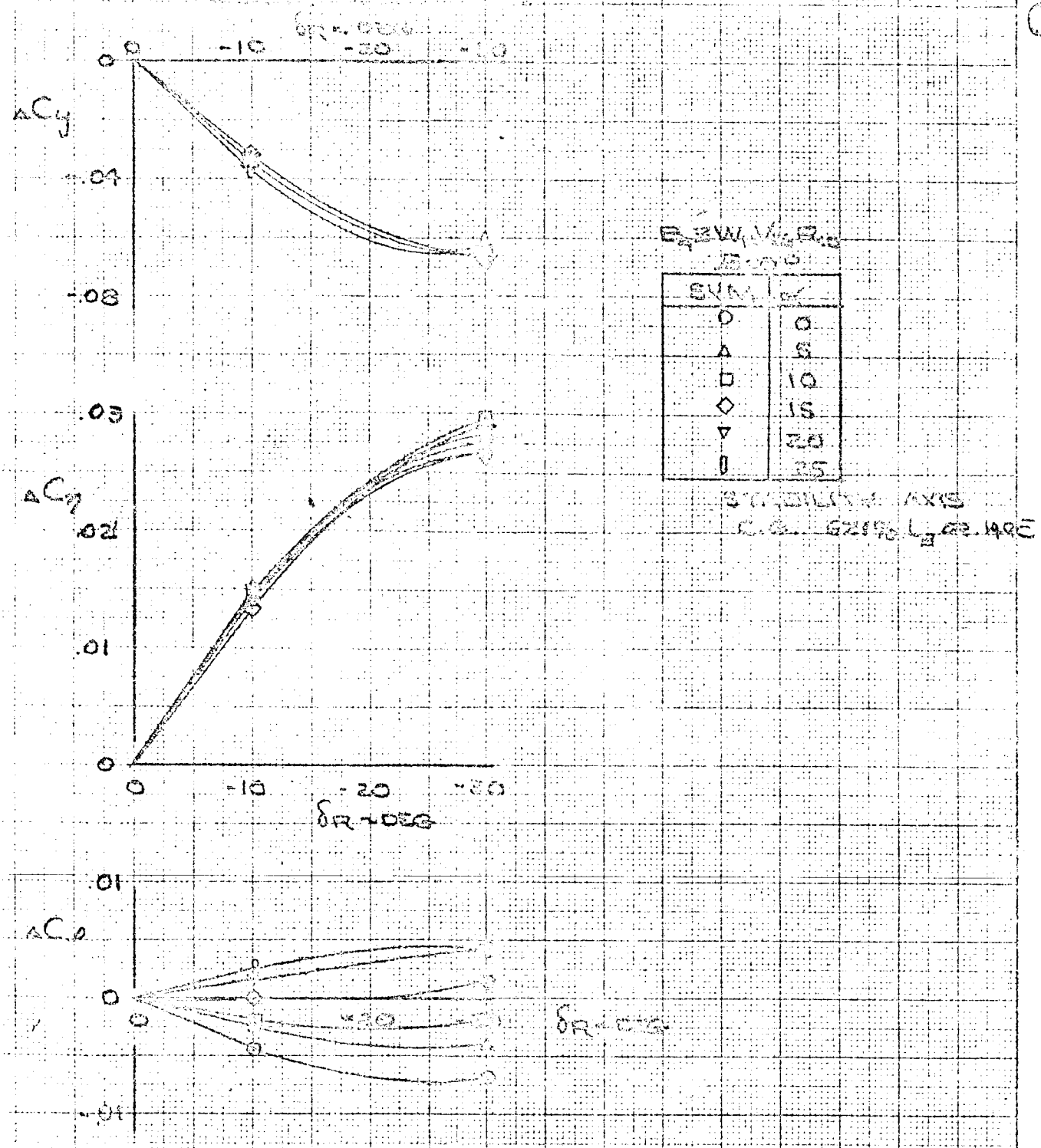

FIGURE [illegible] RUDDER [illegible]

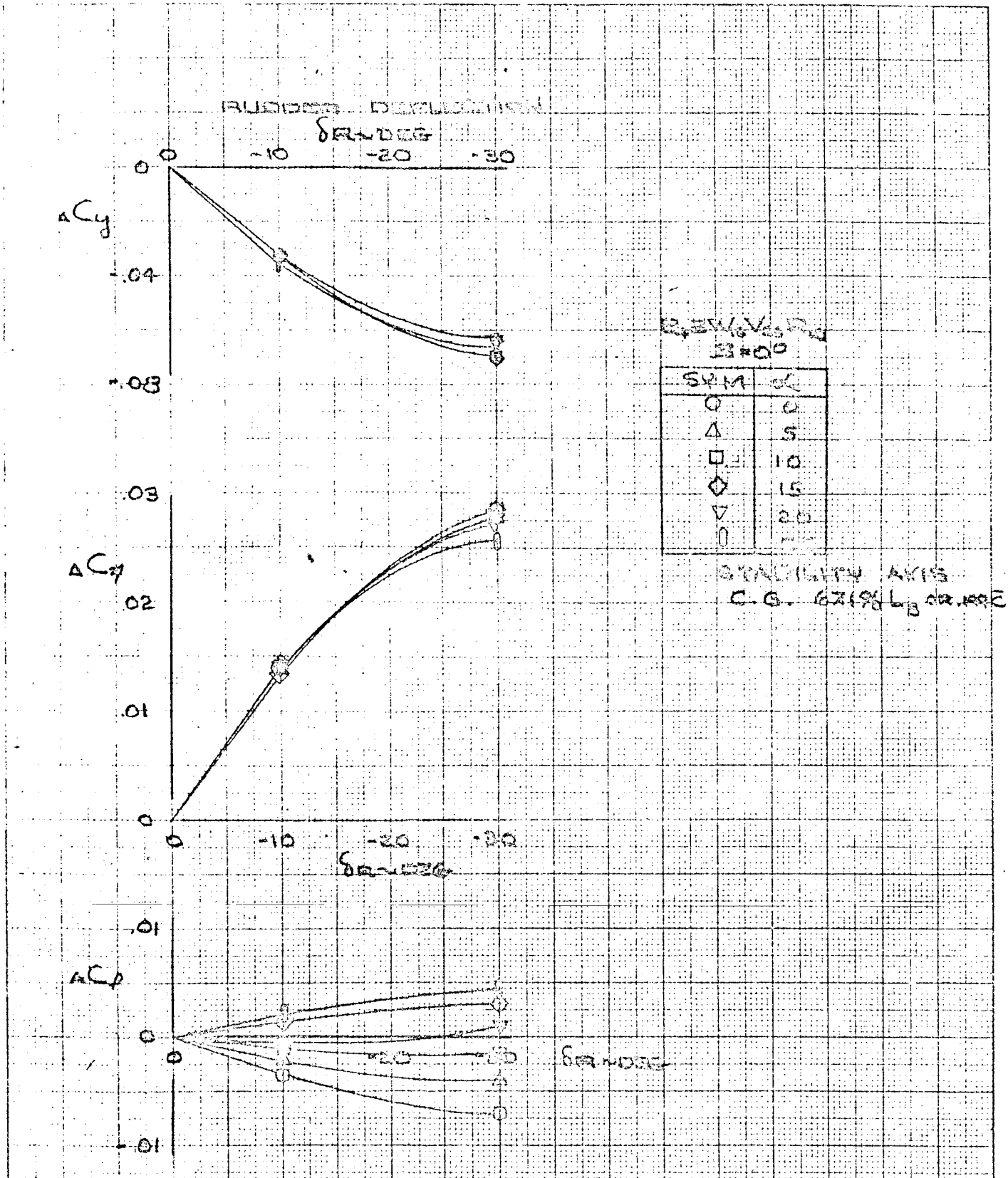
RUDDER DEFLECTION
δR~DEG
0
-10
-20
-30
ΔCy
0
-.04
-.08
.03
ΔCy
.02
.01
0
0
-10
-20
-30
δR~DEG
-.01
ΔCp
0
0
-20
-30
δR~DEG
-.01
β=0°
SYM
α
0
Δ
5
□
10
◇
15
∇
20
STABILITY AXIS
C.G. 62.9% LB

FIGURE [illegible]

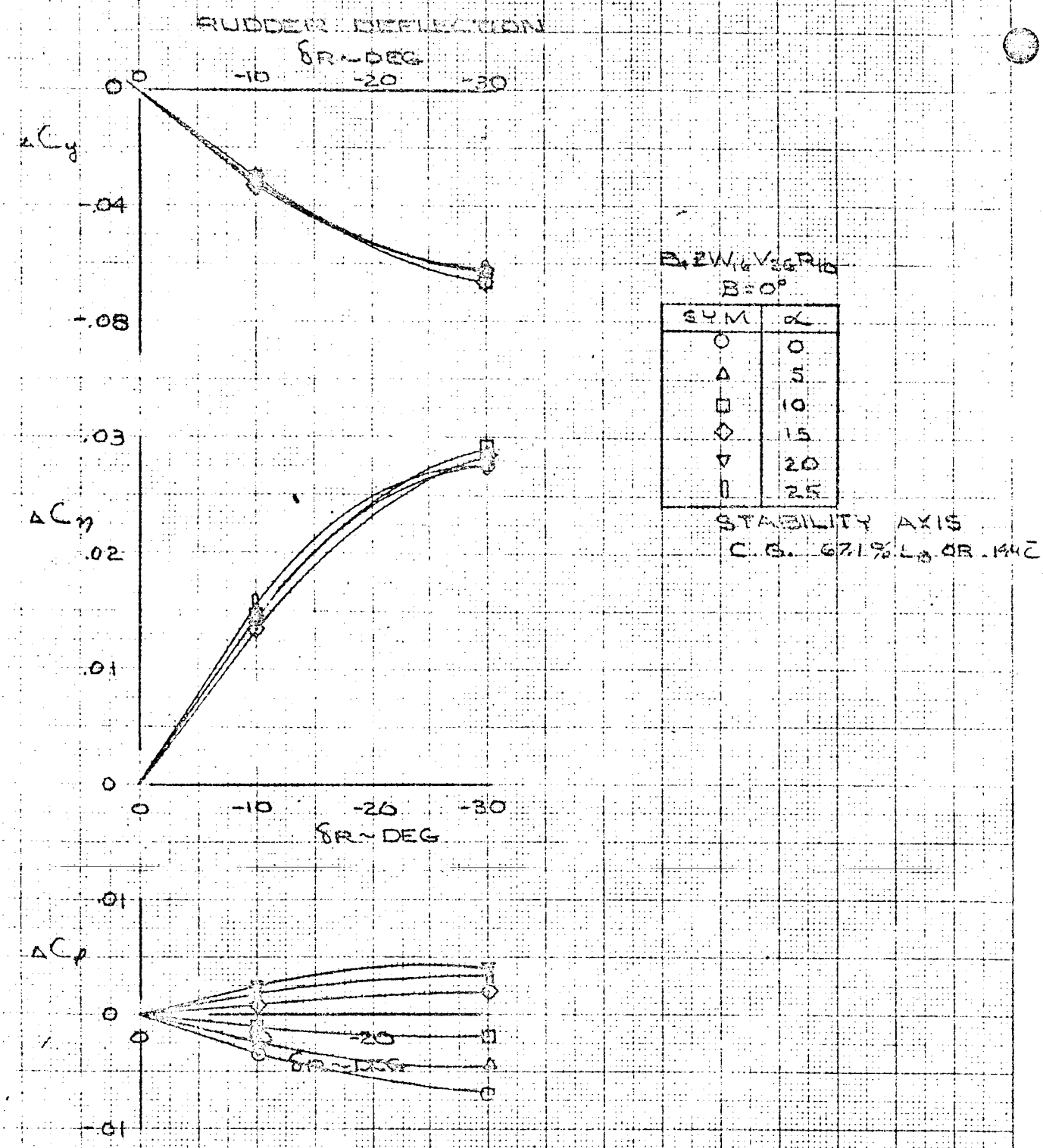

FIGURE 8.0.4. RUDDER EFFECTIVENESS, LAND
PRIMARY 10 KTS

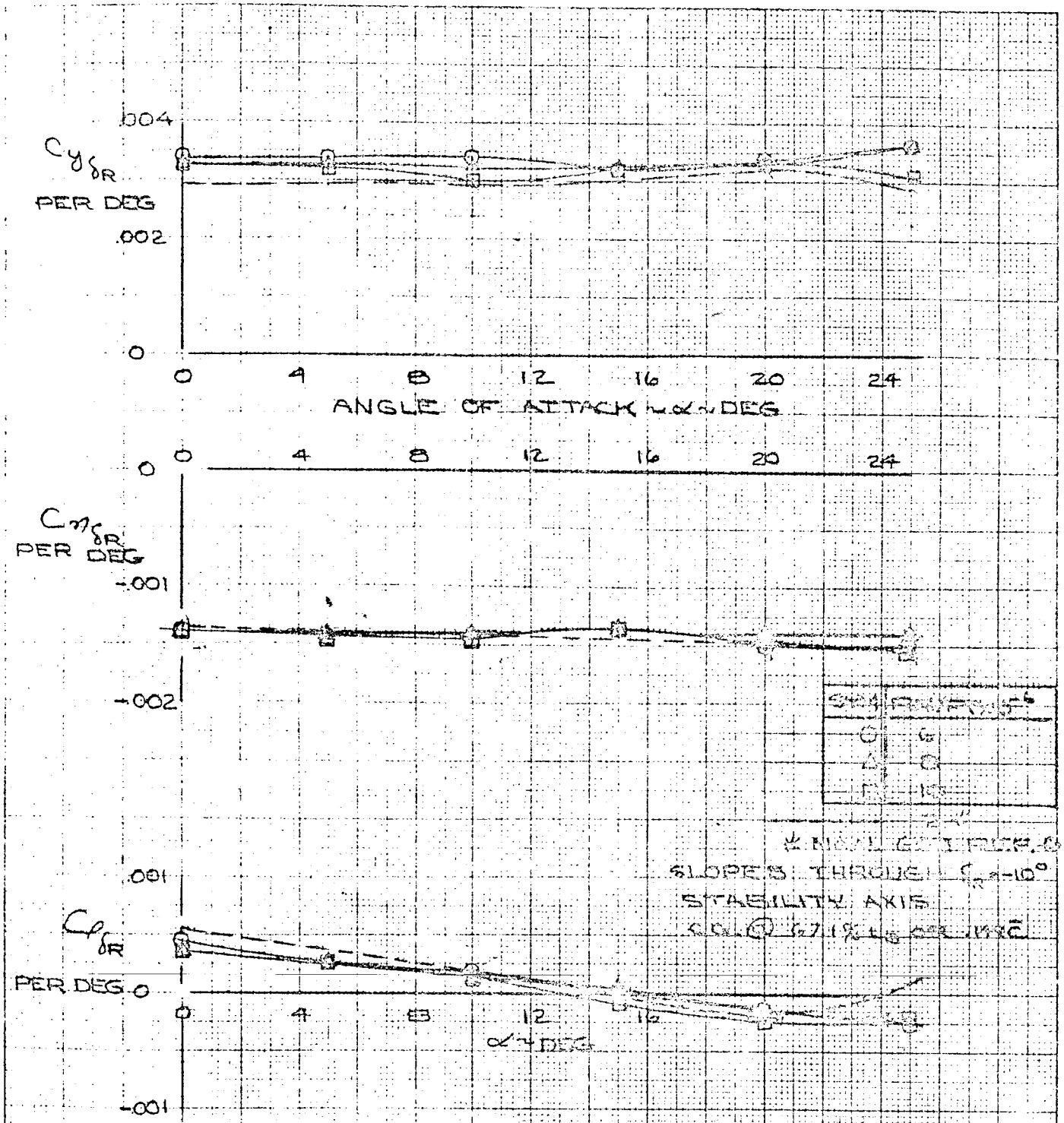

FIGURE 21. EFFECT OF REYNOLDS NUMBER ON RUDDER EFFECTIVENESS

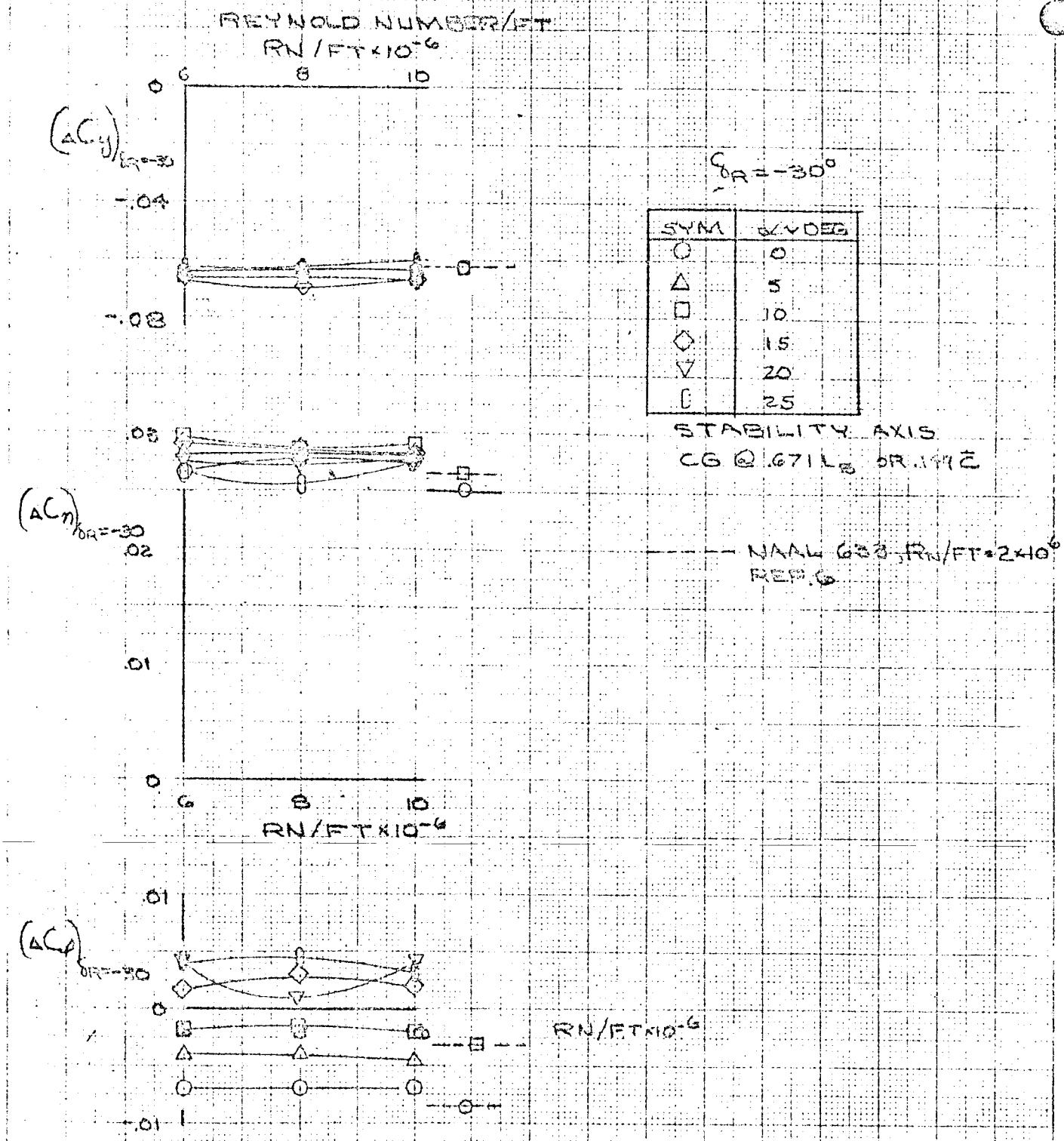

FIGURE 20. EFFECT OF REYNOLDS NUMBER ON RUDDER EFFECTIVENESS FOR -30 DEGREE RUDDER DEFLECTION

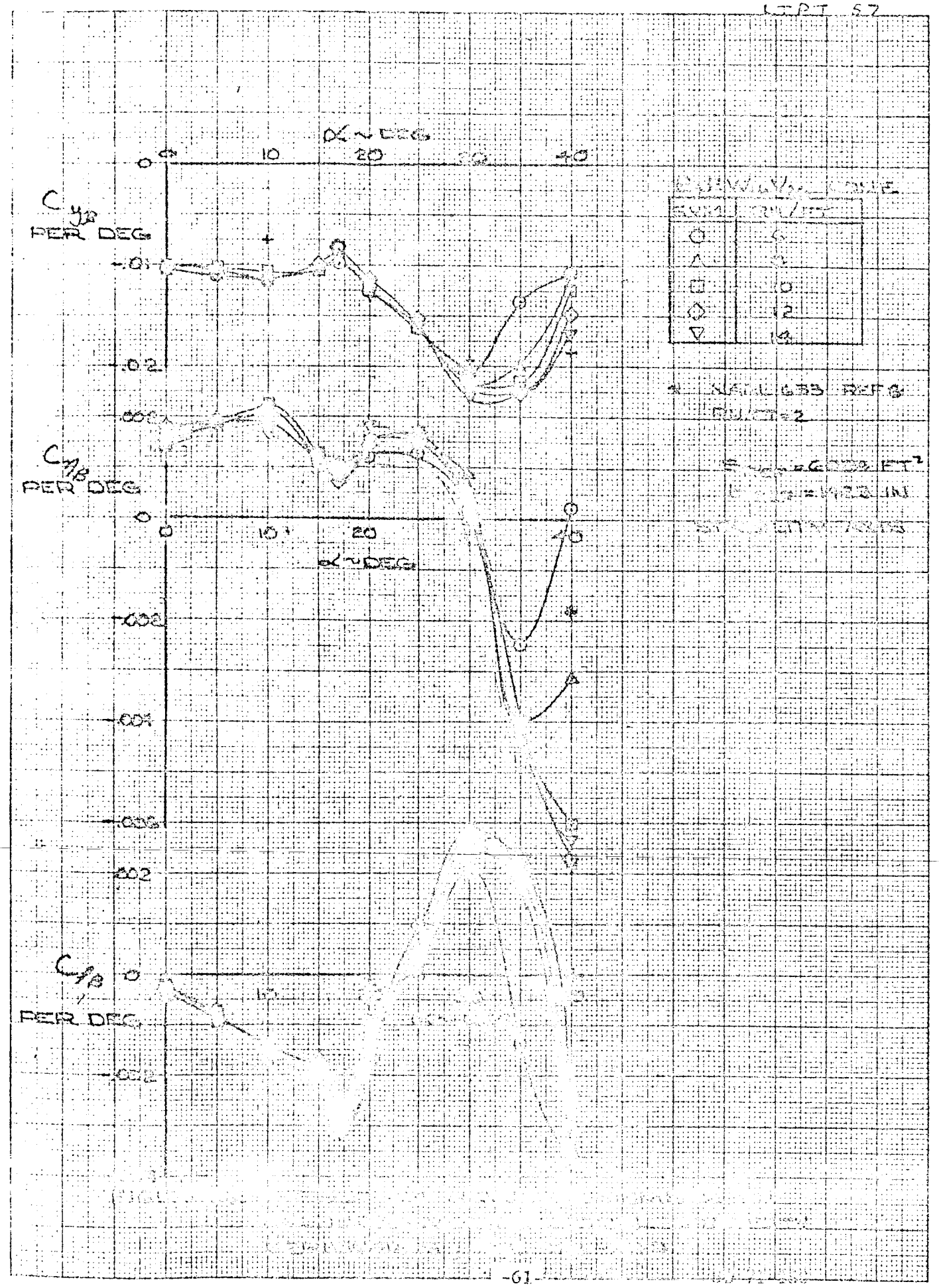
α ~ DEG
0
10
20
30
40
C_{y_β}
PER DEG
.01
.02
.003
C_{n_β}
PER DEG
.002
.001
.003
.002
C_{l_β}
PER DEG
.002

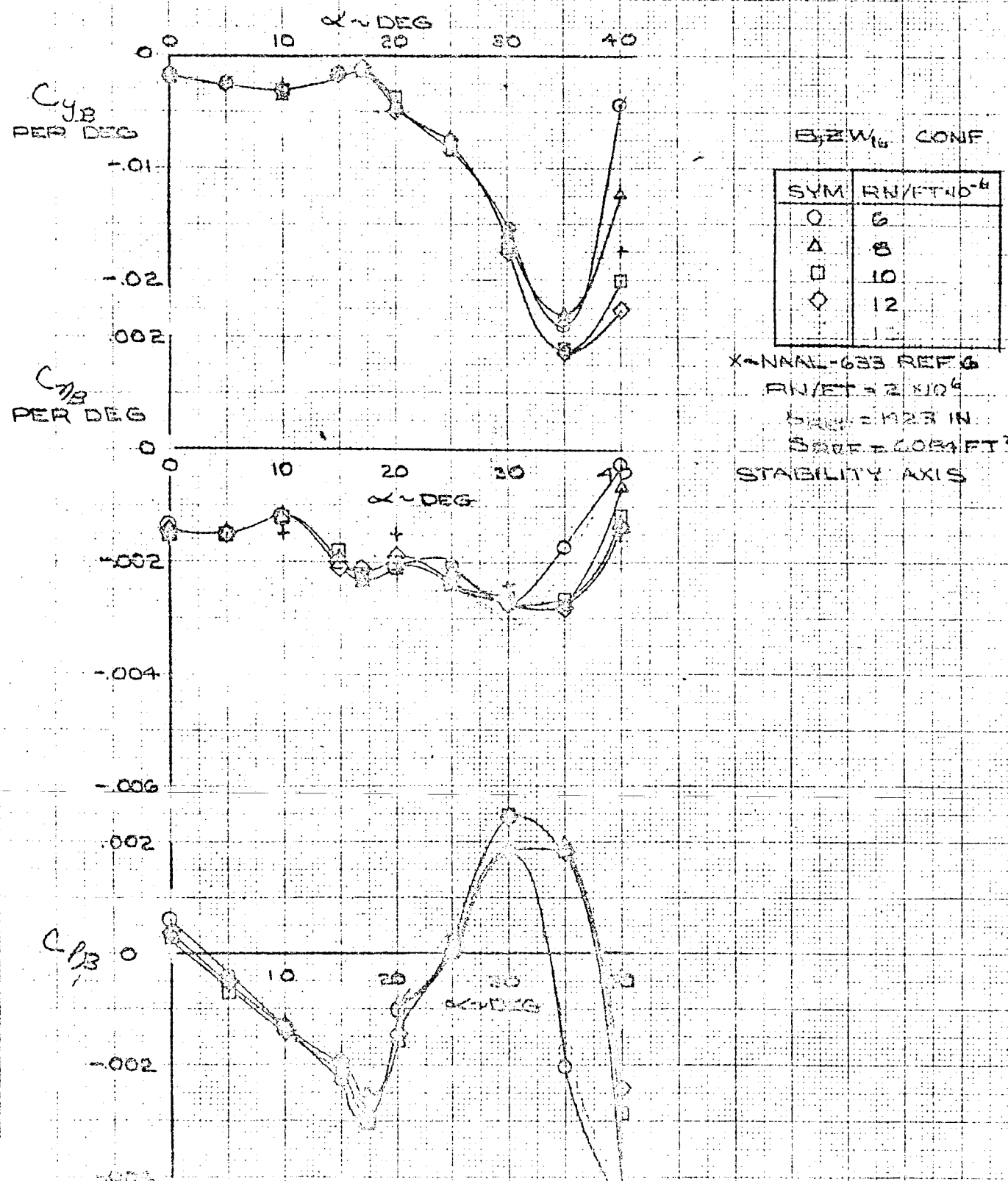

FIGURE 44. EFFECT OF REYNOLDS NUMBER ON THE LATERAL DIRECTIONAL STABILITY DERIVATIVES, TAIL OFF, [illegible]

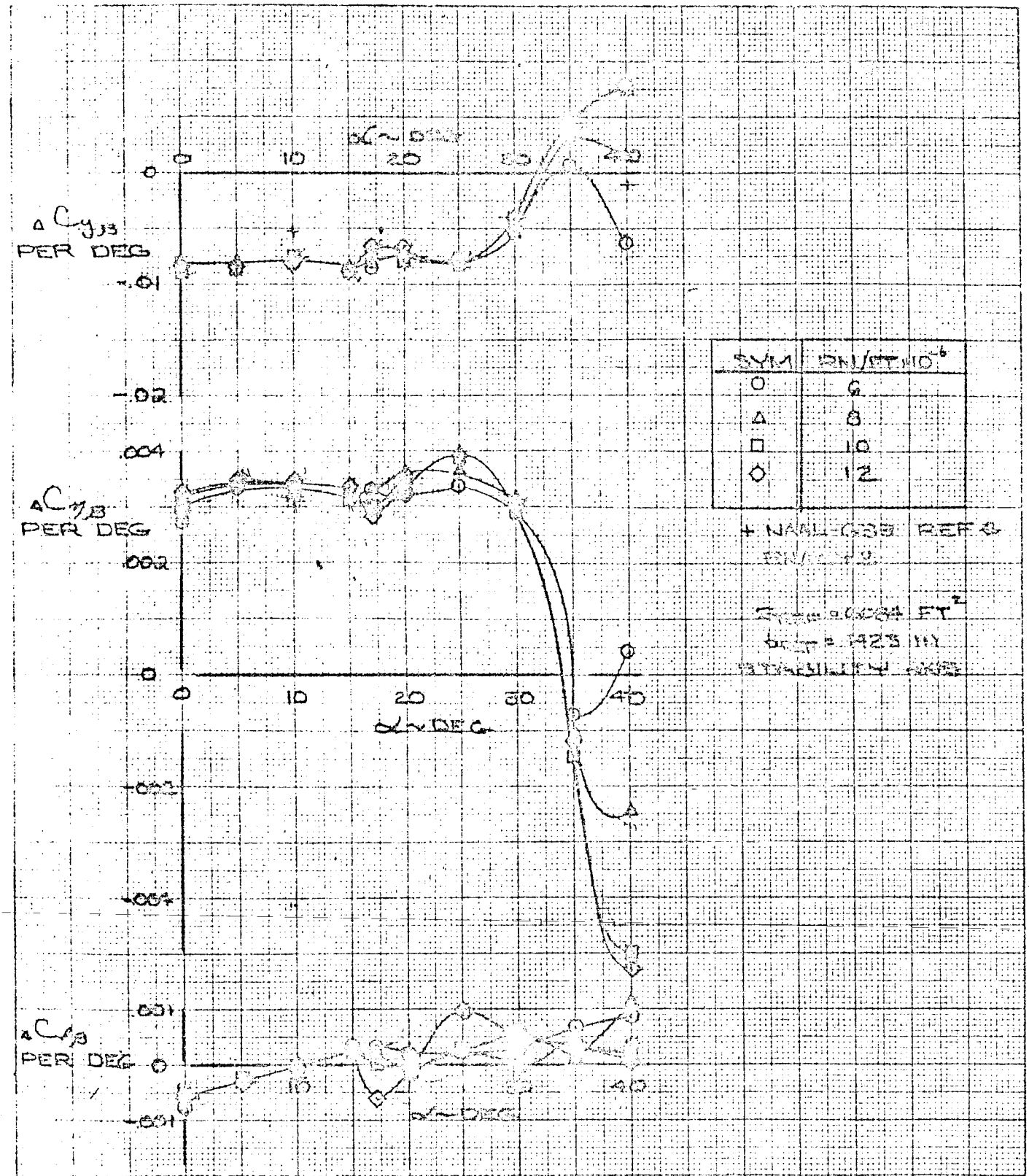

FIGURE 26. EFFECT OF REYNOLDS NUMBER ON THE VERTICAL TAIL IN PITCH STATIC WIND TUNNEL

APPENDIX A

WIND TUNNEL DATA

GENERAL

The wind tunnel data presented herein was obtained at NASA/LRC Low Turbulence Pressure Tunnel. The 0.00763 scale full span model of the delta wing orbiter was mounted on a 1 in. diameter sting exiting from the base.

The balance data were reduced to coefficient form using S_W = 6084 ft^2, $\bar{c}_W$ = 821.2 in., and b_W = 1422.4 in. The reference c.g. was taken at 67.1% of the fuselage length (F.S. 1422.5) and W.P. 130.

Nominal test conditions are given below:

RN/FT x 10^{-6}	MACH NO.	q (lb/FT)^2	P_{total} psi	RN BASED ON $\bar{C}$
2.8	.26	136	22	1.46
4.5	.26	227	36	2.35
6.4	.25	317	55	3.35
3.6	.26	453	72	4.50
10.1	.26	543	86	5.30
12.0	.23	590	110	6.28
15.0	.22	682	150	7.85

Flight RN based on $\bar{c}$ at M = 0.26

sea level = 127 x 10^6

All drag data presented herein has been corrected to ambient base and cavity pressure. Three pressures were measured, one on the left and right hand base each, and one in the cavity. The pressure transducers were referenced to the ambient tunnel pressure and the pressure applied to the base and cavity area for drag corrections. Problems arose after Run 39 when the pressure line leading to the ambient tunnel pressure probe was accidently jarred loose, the model pressures then became automatically referenced to the chamber area pressure. The accident was not noticed until completion of test at which time the chamber area pressure was calibrated so that the new reference pressure was known relative to the ambient tunnel pressure and the data so corrected.

RUN INDEX

CONFIGURATION	RN/FT x 10^{-6} 2.5	4	6	8	10	12	14	α	β	δ_e	δ_r
$B_4ZW_{16}V_{26}$	1	2	3	4	5	6	7	-1°→24°	0°	0°	0°
$B_4ZW_{16}E_7V_{26}$			8	9	10					-10°	
			11	12	13					-20°	
			14	15	16					-30°	
$B_4ZW_{16}V_{26}tr_{26}$	17	18	19	20	21	22	23			0°	0°
							24	24→1°		0°	0°
	25	26	27	28	29	30	31	14°→41°		0°	0°
$B_4ZW_{16}V_{26}$	32	33	34	35	36	37	38	17°→41°		0°	0°
$B_4ZW_{16}E_7V_{26}$			39	40	41					-10°	
			42	43	44					-20°	
			45	46	47					-30°	
$B_4ZW_9V_{26}$			48	49	50	51	52			0°	
$B_4ZW_{18}V_{26}$			53	54	55					0°	
$B_4ZW_{19}V_{26}$			56	57	58					0°	
B_4ZW_{16}			59	60	61	62				0°	-
B_4ZW_{16}			63	64	65	66			5°	0°	-
$B_4ZW_{16}V_{26}$			67	68	69	70	71		5°	0°	0°
			72	73	74	75		-1°→24°	5°	0°	0°
B_4ZW_{16}			76	77	78	79		-1°→24°	5°	0°	0°
B_4ZW_{16}			80	81	82	83			0°	0°	0°
$B_4ZW_{16}V_{26}R_{10}$			84	85	86				0°	0°	-10°

1/2 dental plaster in rudder joint missing

Dental plaster missing from upper RT. elevon wing joint

Hysterisis effect

Run 39 and on pressure transducer referenced to chamber pressure.

Space Division
North American Rockwell

RUN INDEX (CONTINUED)

CONFIGURATION	RN/FT x 10^{-6} 2.5	4	6	8	10	12	15	α	β	δ_e	δ_r
$B_4ZW_{16}V_{26}R_{10}$			87	88	89			-1° 24°	0°	0°	-30°
$B_4ZW_9V_{26}$			90	91	92						0°
$B_4ZW_{18}V_{26}$			93	94	95	96	97				
$B_4ZW_{19}V_{26}$			98	99	100						
$B_4ZW_{20}V_{26}$			101	102	103						
$B_4ZW_{16}V_{26}tr_7$			104	105	106						

Space Division
North American Rockwell

APPENDIX A

INDEX OF FIGURES

LONGITUDINAL DATA, STABILITY AND CONTROL

FIGURE NO.	TITLE	PAGE
A-1a - A-1r	Effect of Reynolds Number $B_4ZW_{16}V_{26}$ Configuration	69 - 86
A-2a - A-2r	Effect of Reynolds Number $B_4ZW_{16}V_{26}t_{r6}$ Configuration	87 - 104
A-3a - A-3i	Effect of Reynolds Number $B_4ZW_{16}V_{26}t_{r7}$ Configuration	105 - 113
A-4a - A-4i	Sting Support Hysteresis Effects, RN/FT = 14×10^6	114 - 122
A-5a - A-5i	Elevon Effectiveness, RN/FT = 6×10^6, 134D	123 - 131
A-6a - A-6i	Elevon Effectiveness, RN/FT = 8×10^6, 134D	132 - 140
A-7a - A-7i	Elevon Effectiveness, RN/FT = 10×10^6, 134D	141 - 149
A-8a - A-8i	Effect of Wing Tip Geometry, RN/FT - 6×10^6	150 - 158
A-9a - A-9i	Effect of Wing Tip Geometry, RN/FT - 8×10^6	159 - 167
A-10a - A-10i	Effect of Wing Tip Geometry, RN/FT = 10×10^6	168 - 176
A-11a - A-11i	Effect of Wing Position, RN/FT = 6×10^6	177 - 185
A-12a - A-12i	Effect of Wing Position, RN/FT = 8×10^6	186 - 194
A-13a - A-13i	Effect of Wing Position, RN/FT - 10×10^6	195 - 203

APPENDIX A (cont)

LATERAL-DIRECTIONAL DATA - STABILITY AND CONTROL

FIGURE NO.	TITLE	PAGE
A-14a - A-141	Rudder Effectiveness, RN/FT = 6×10^6, 134D	204 - 215
A-15a - A-151	Rudder Effectiveness, RN/FT = 8×10^6, 134D	216 - 227
A-16a - A-161	Rudder Effectiveness, RN/FT = 10×10^6, 134D	228 - 239
A-17a - A-171	Effect of Vertical Tail, RN/FT = 6×10^6, 134D	240 - 251
A-18a - A-181	Effect of Vertical Tail, RN/FT = 8×10^6, 134D	252 - 263
A-19a - A-191	Effect of Vertical Tail, RN/FT = 10×10^6, 134D	264 - 275
A-20a - A-201	Effect of Vertical Tail, RN/FT = 12×10^6, 134D	276 - 287
A-21a - A-211	Effect of Vertical Tail, RN/FT = 14×10^6, 134D	288 - 299

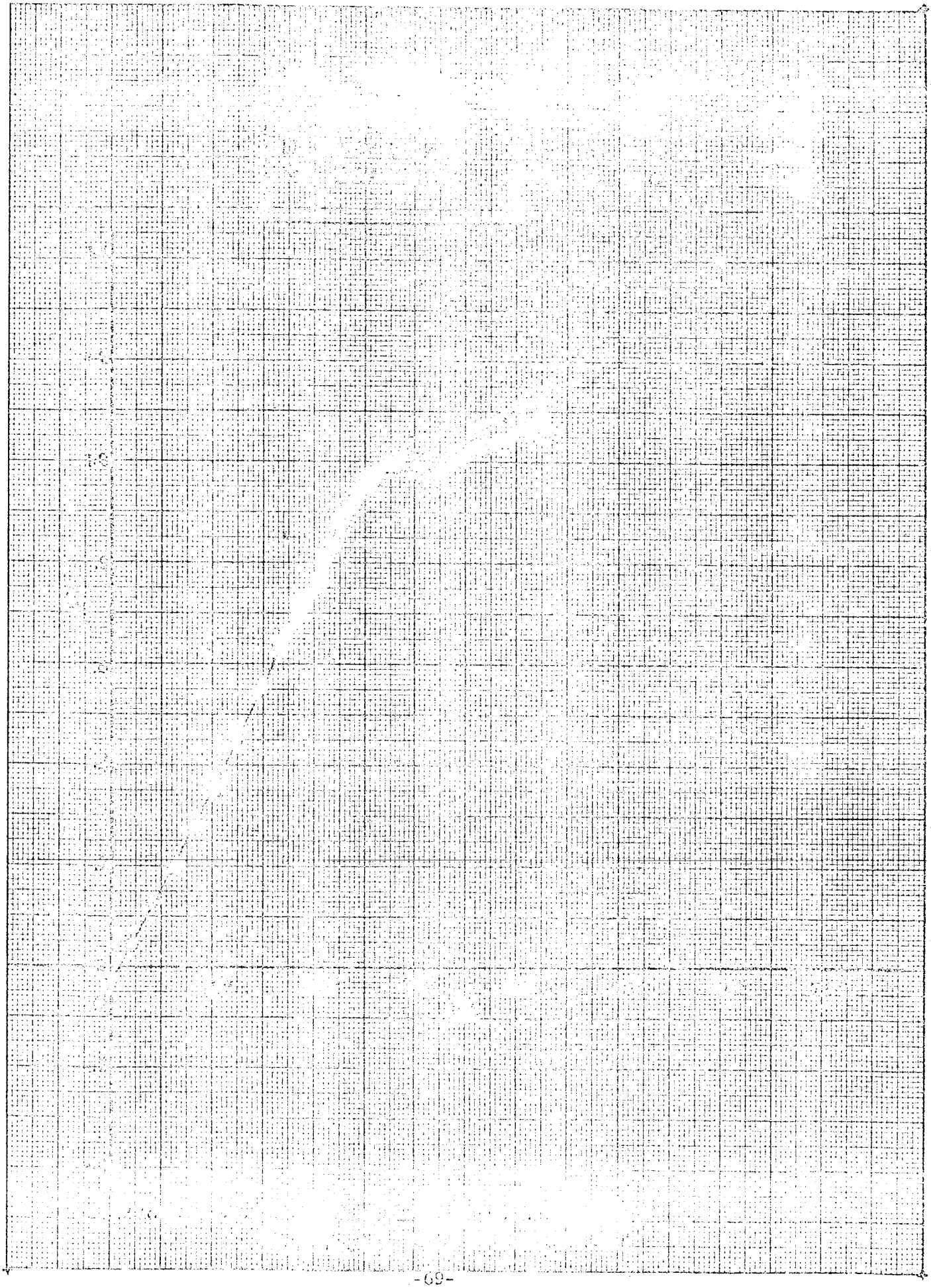

KEUFFEL & ESSER CO.

19 X 25 CM. • ALPANENE 3
KEUFFEL & ESSER CO.

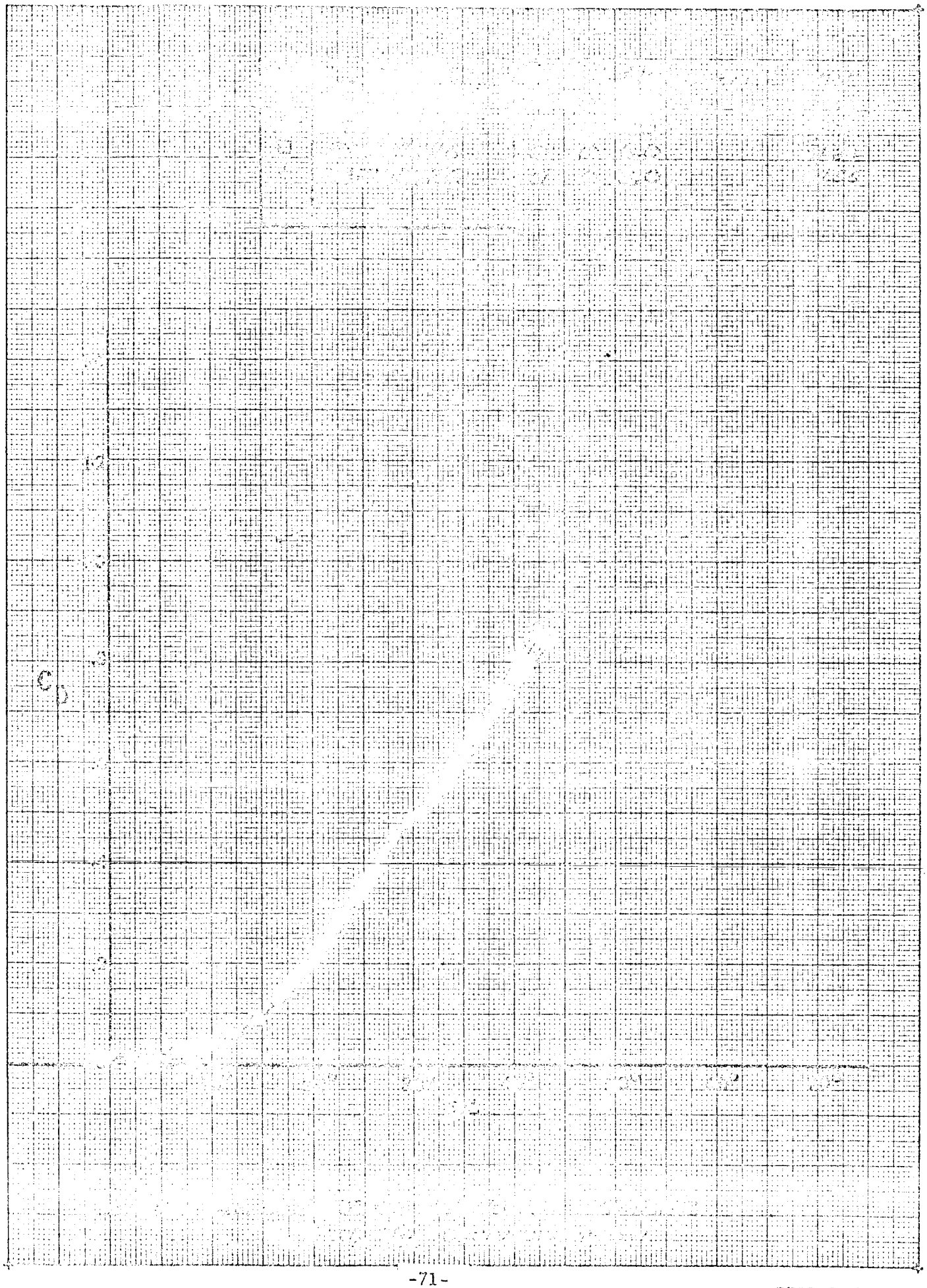

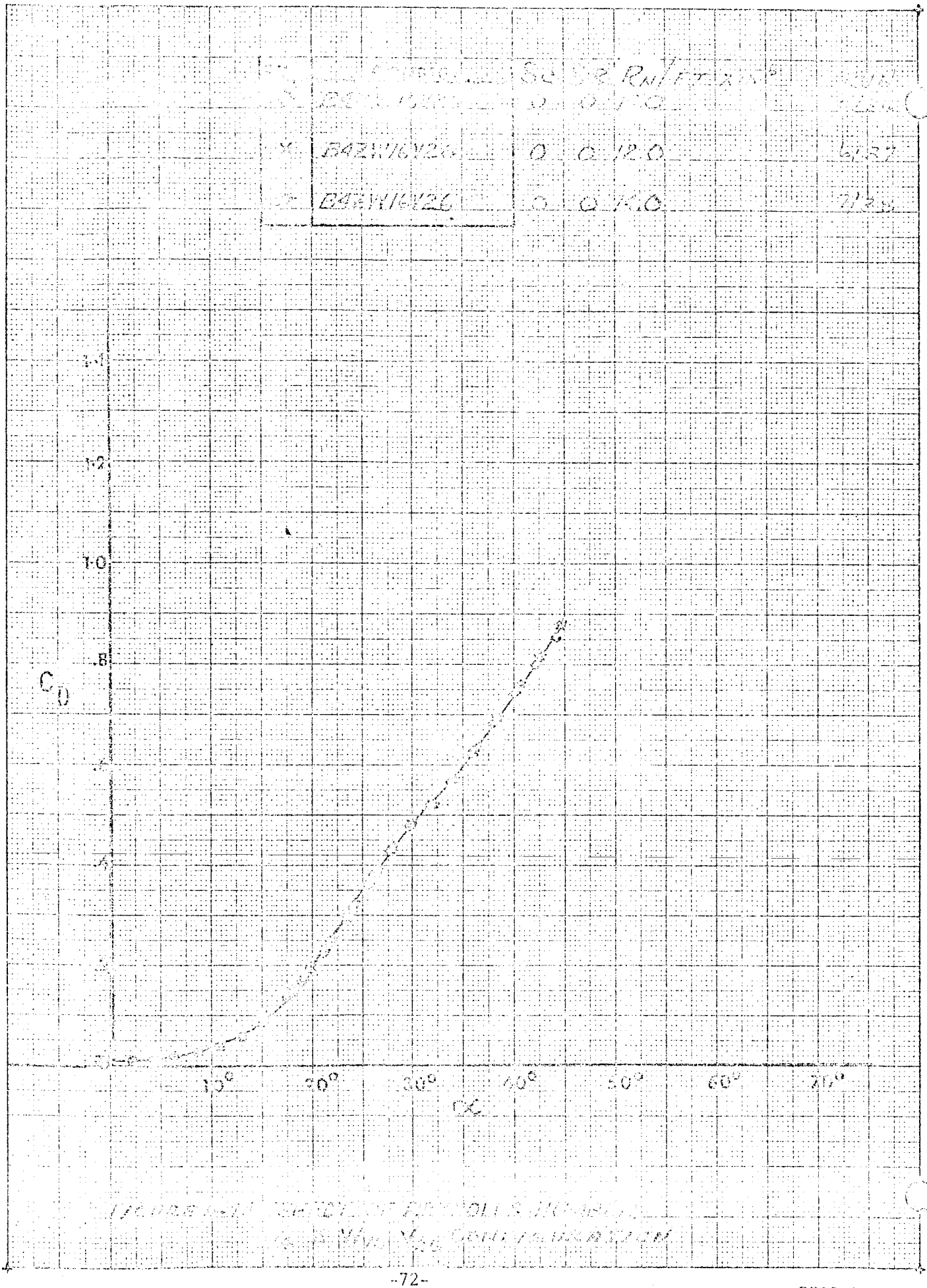
1.2
1.0
.8
C_D
10°
20°
30°
40°
50°
60°
70°
α

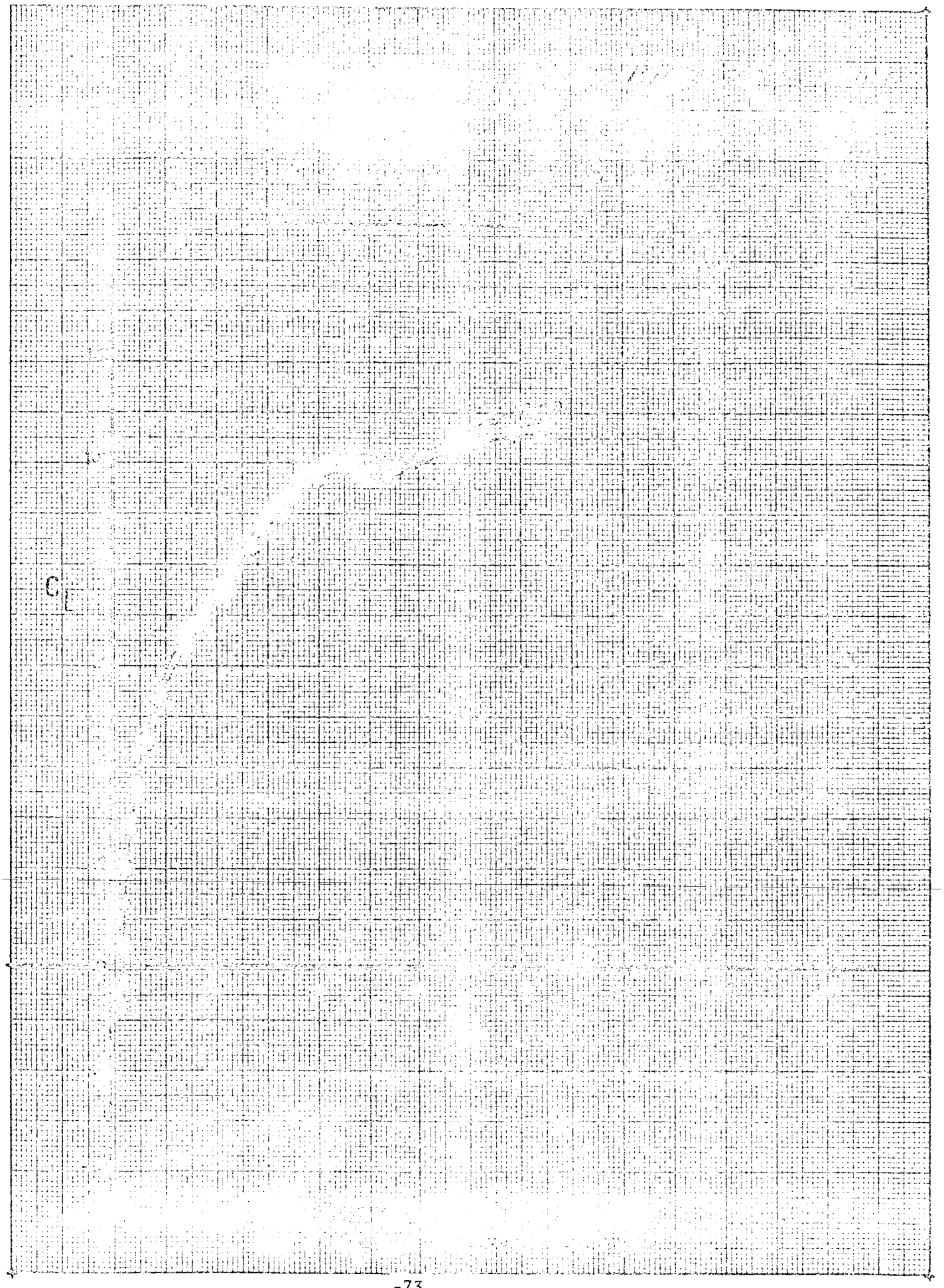

10 X 10 TO THE CENTIMETER 46 1517
18 X 25 CM. • ALBANENE
KEUFFEL & ESSER CO.

273

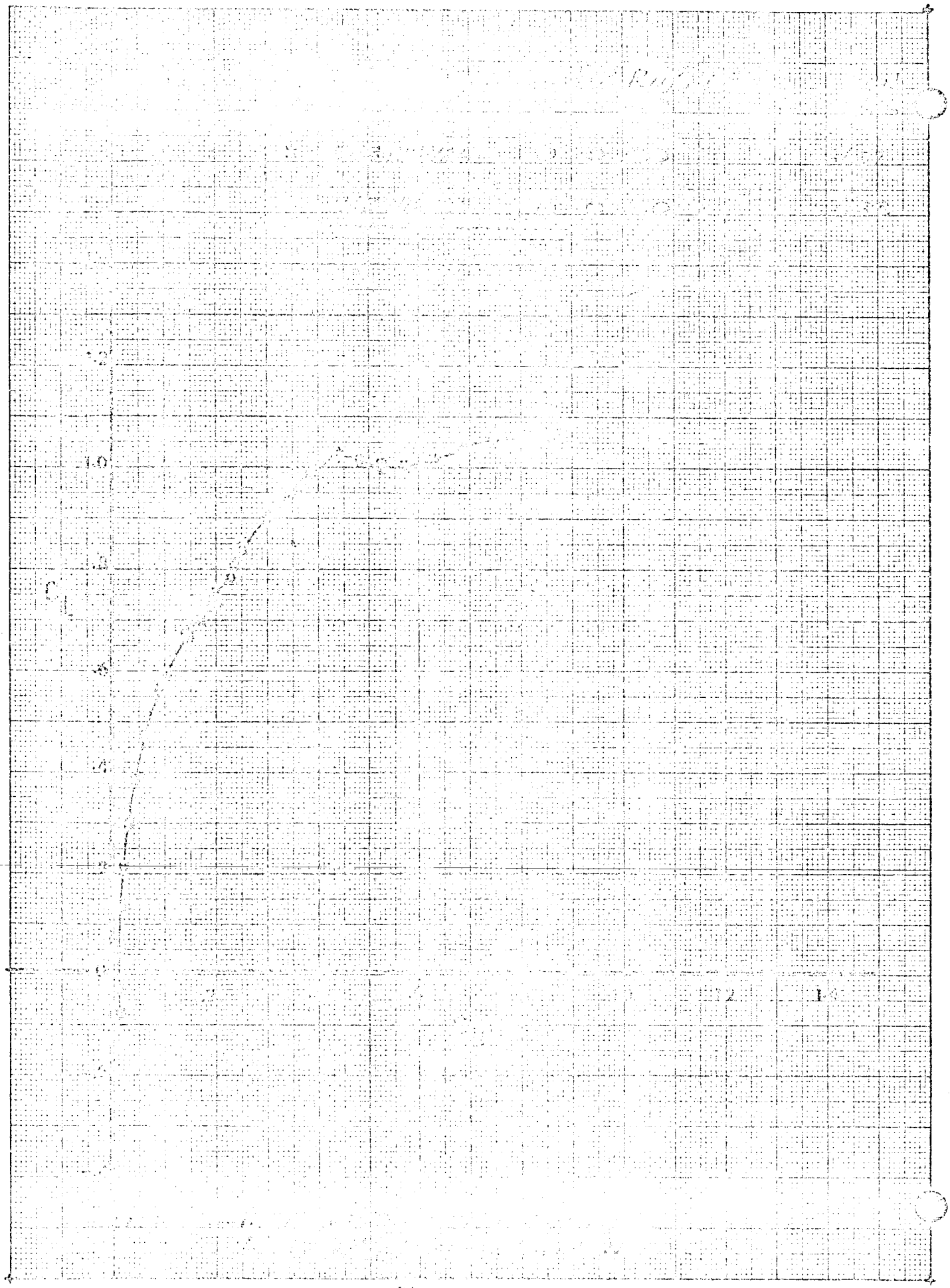

KEUFFEL & ESSER CO.

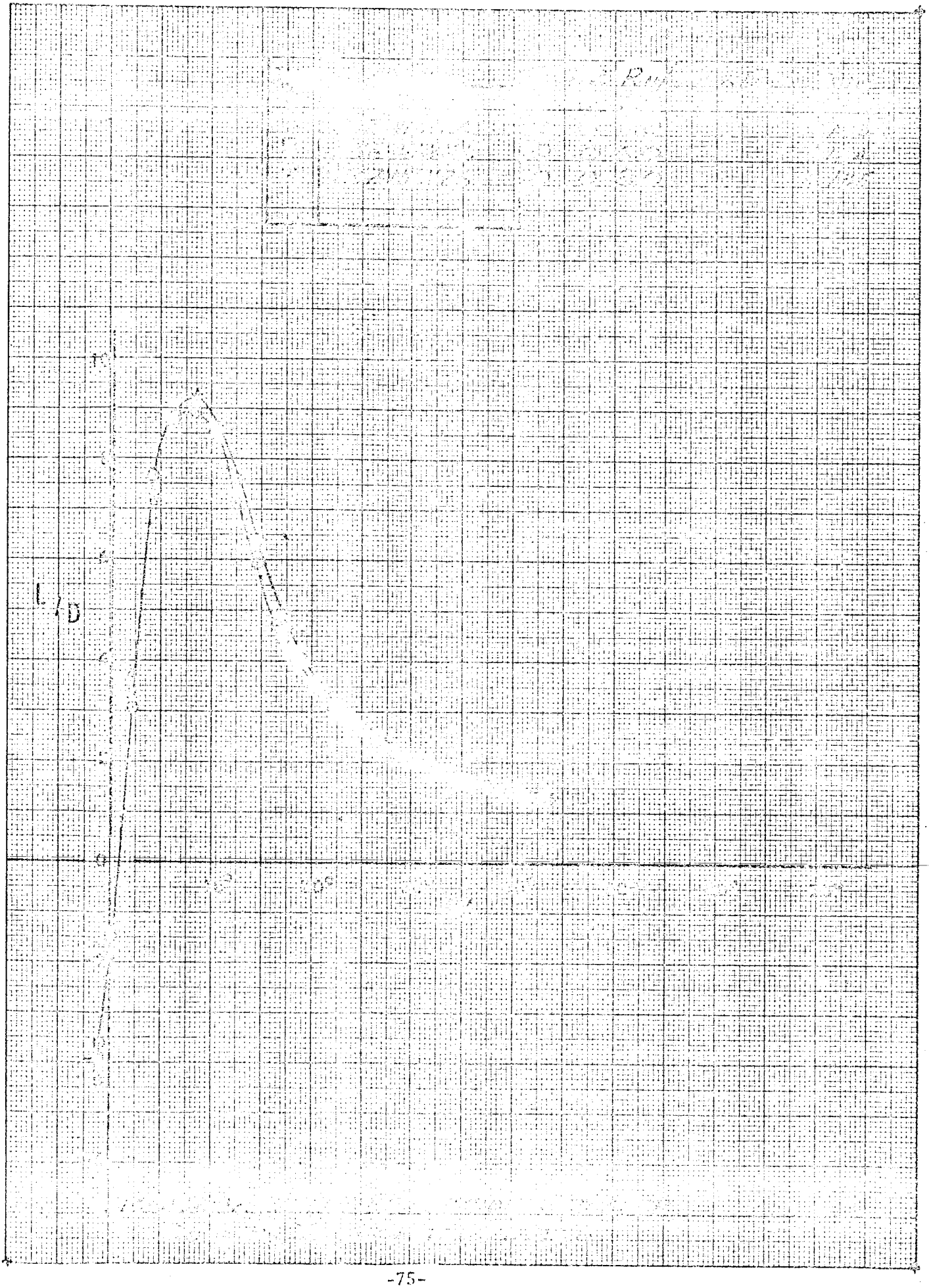

10 X 10 TO THE CENTIMETER 46 1517
16 X 25 CM • ALBANENE
MADE IN U.S.A.
KEUFFEL & ESSER CO.

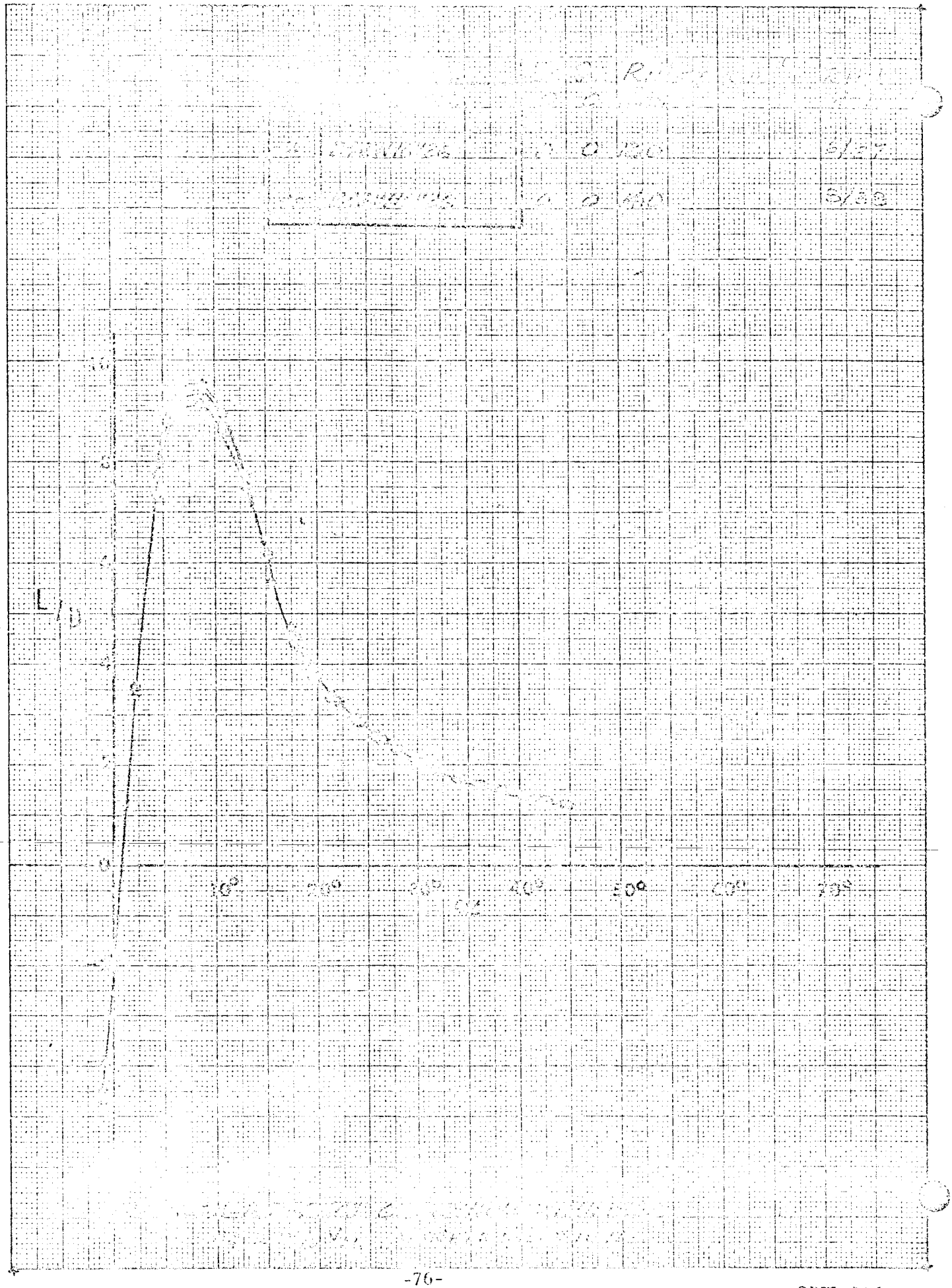
L/D
10°
20°
30°
40°
50°
60°
70°

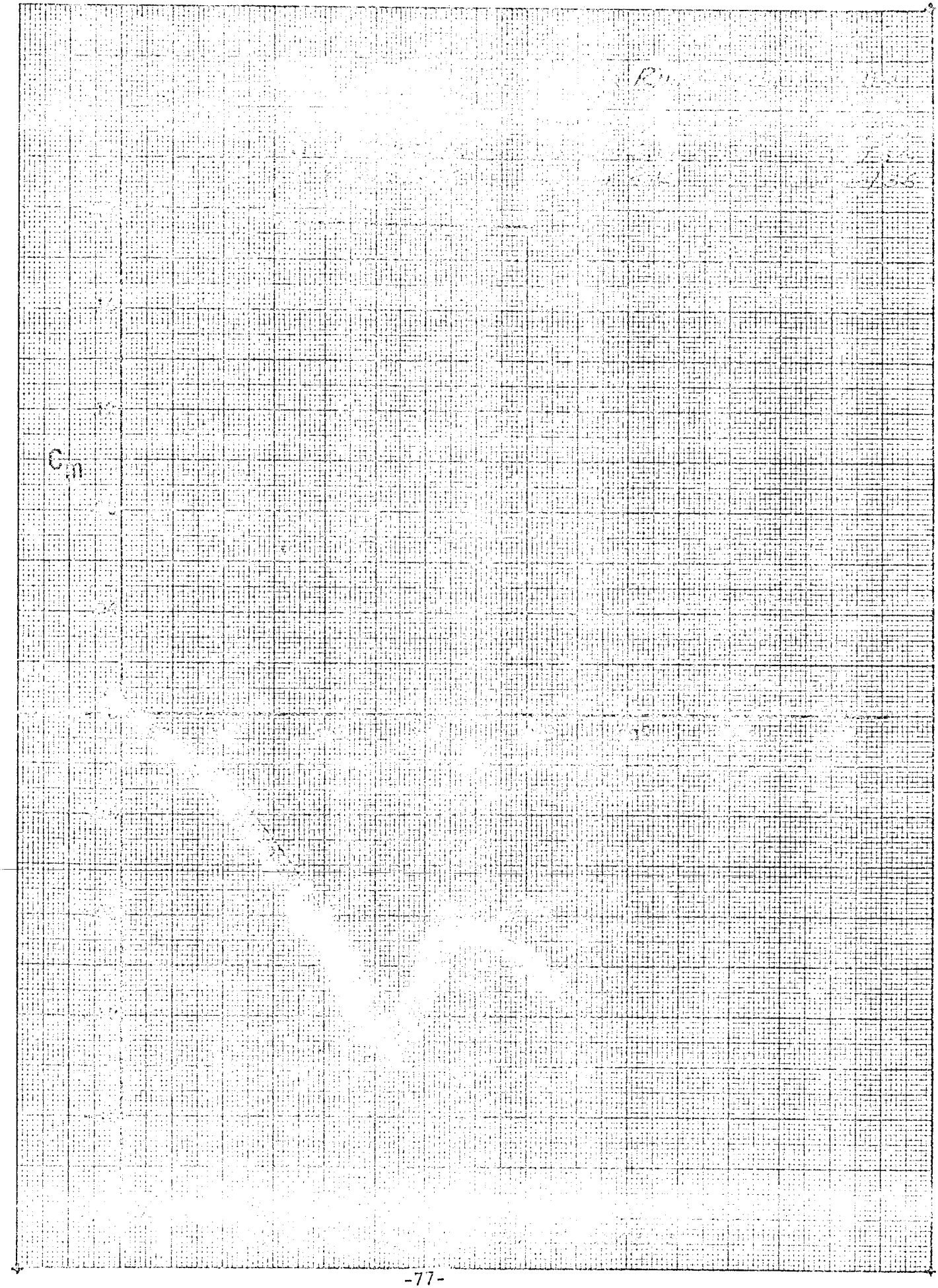

10 X 10 TO THE CENTIMETER 46 1517
18 X 25 CM. • ALBANENE®
KEUFFEL & ESSER CO.

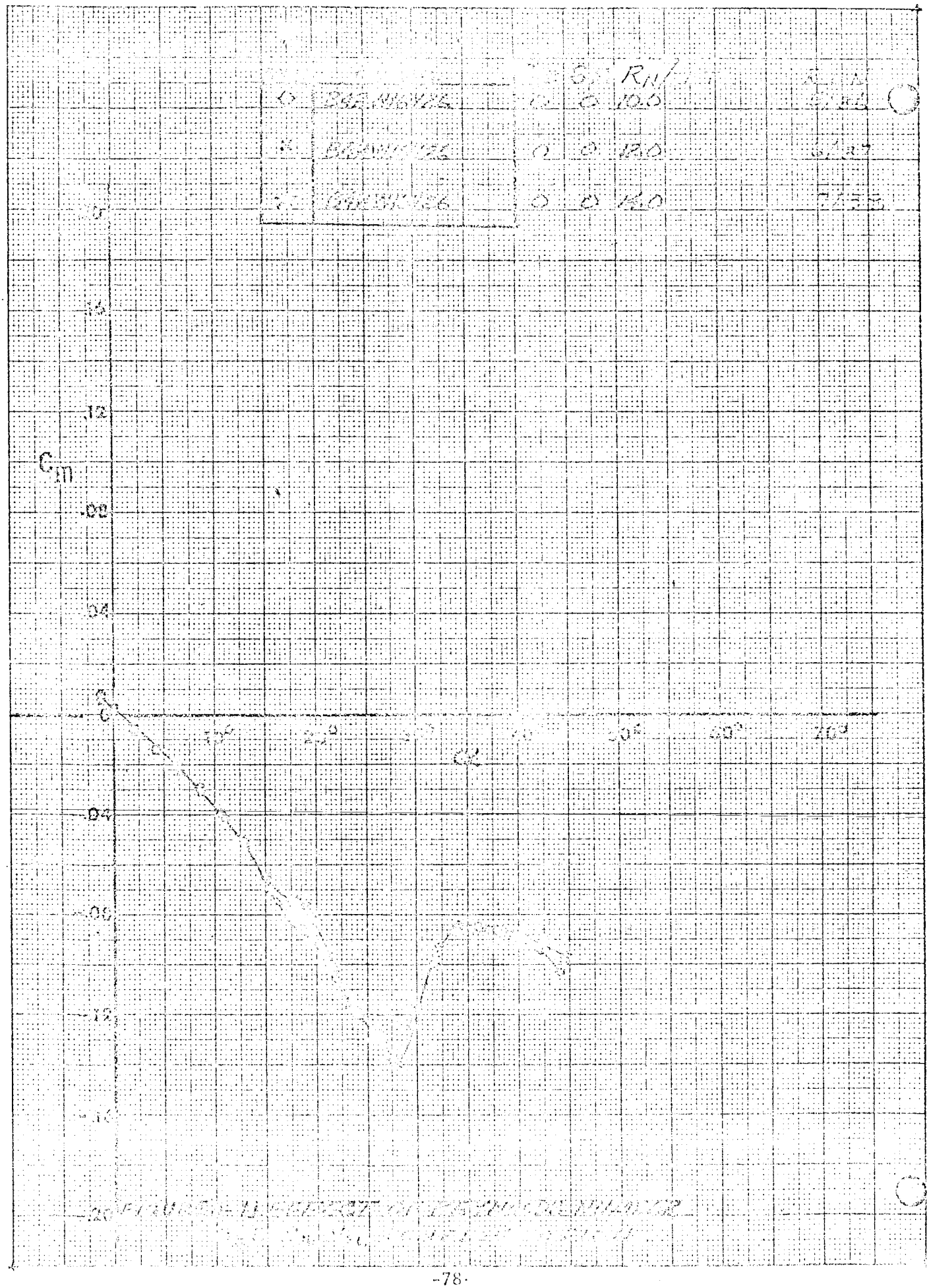
R_N
C_m
.08
.04
0
-.04
-.08
-.12
-.16
-.20
α

260

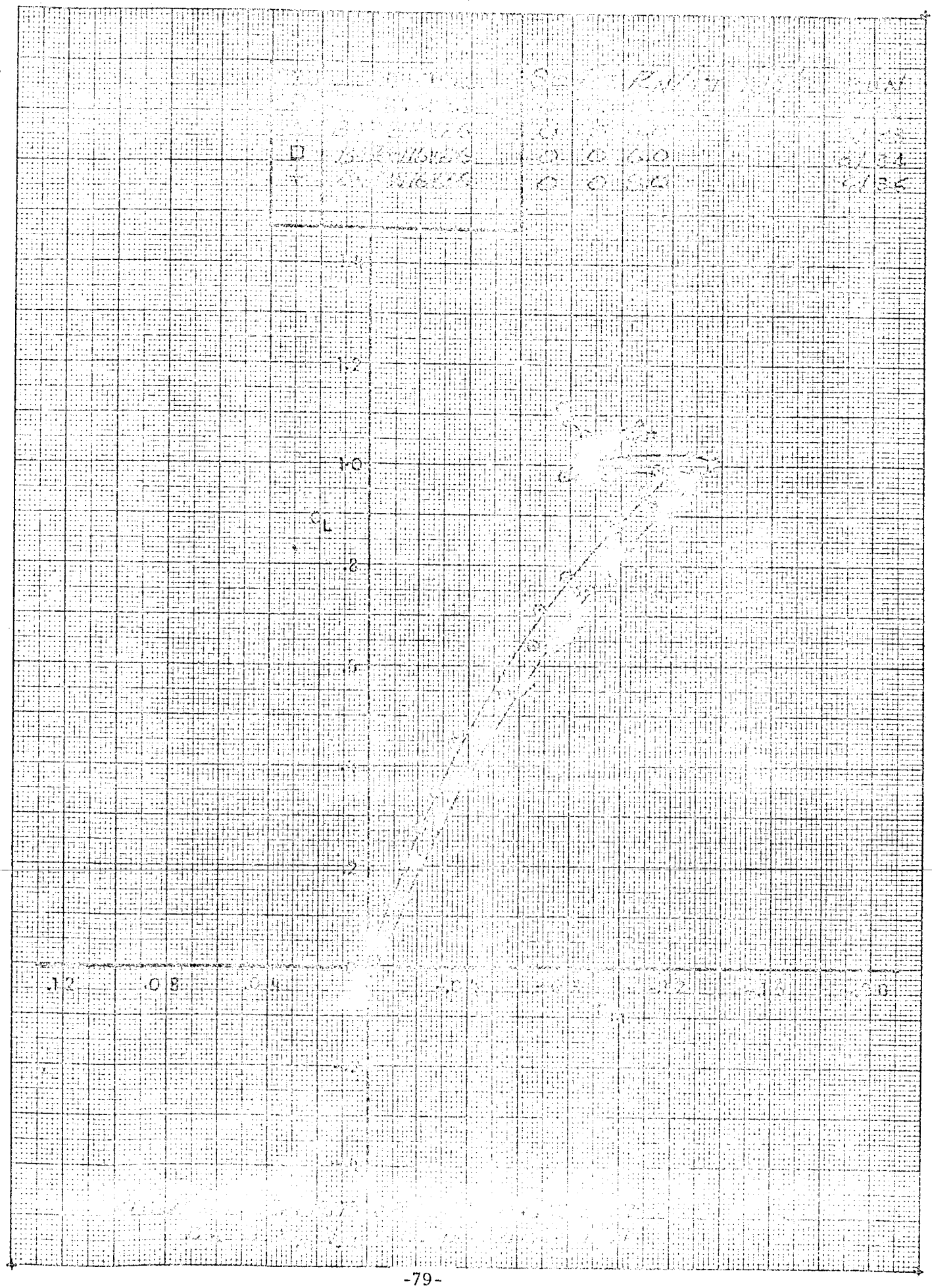

10 X 10 TO THE CENTIMETER 46 1517
18 X 25 CM • ALBANENE
KEUFFEL & ESSER CO.

260

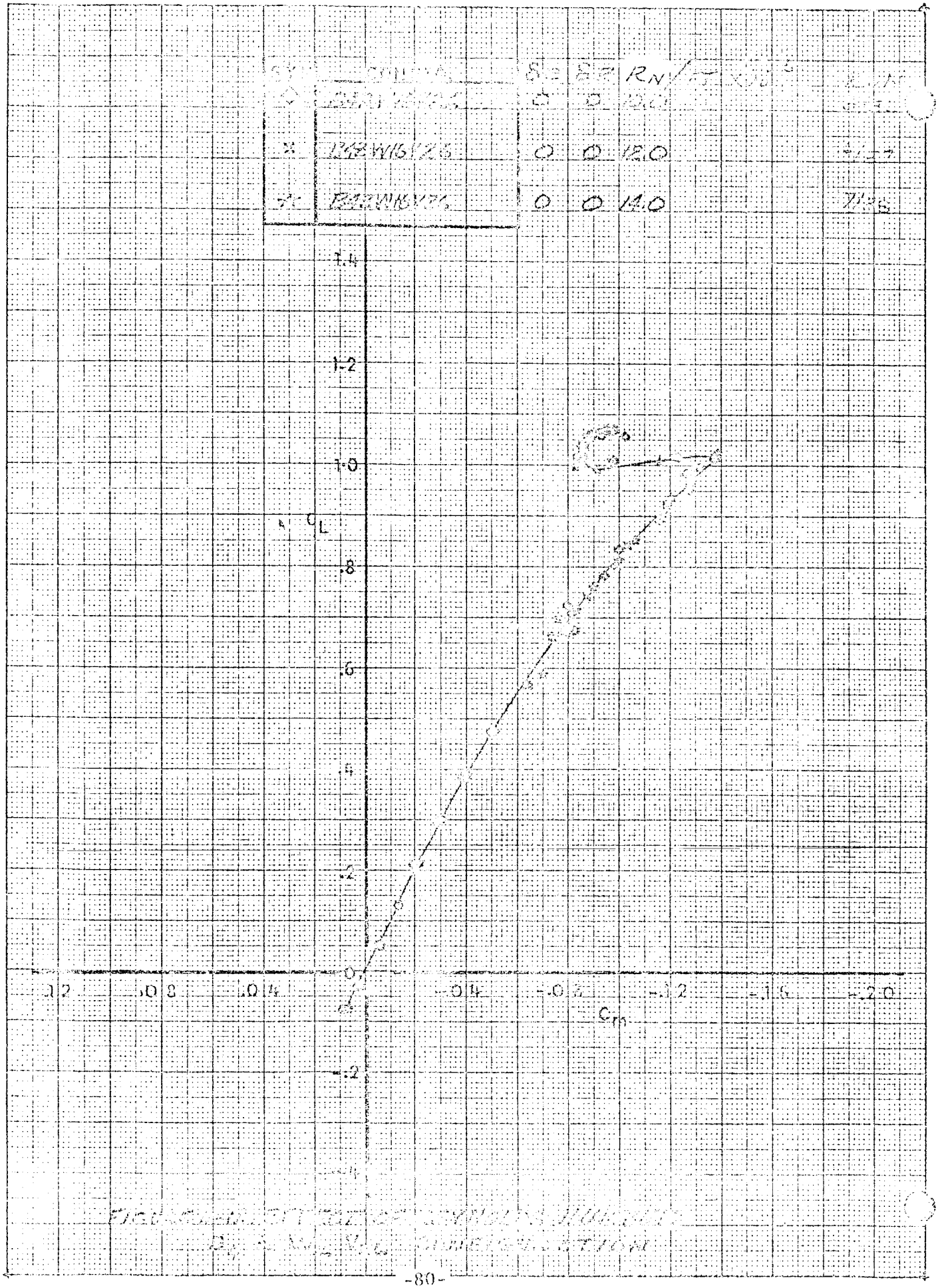

10 X 10 TO THE CENTIMETER 46 1517
18 X 25 CM. • ALBANENE®
KEUFFEL & ESSER CO.

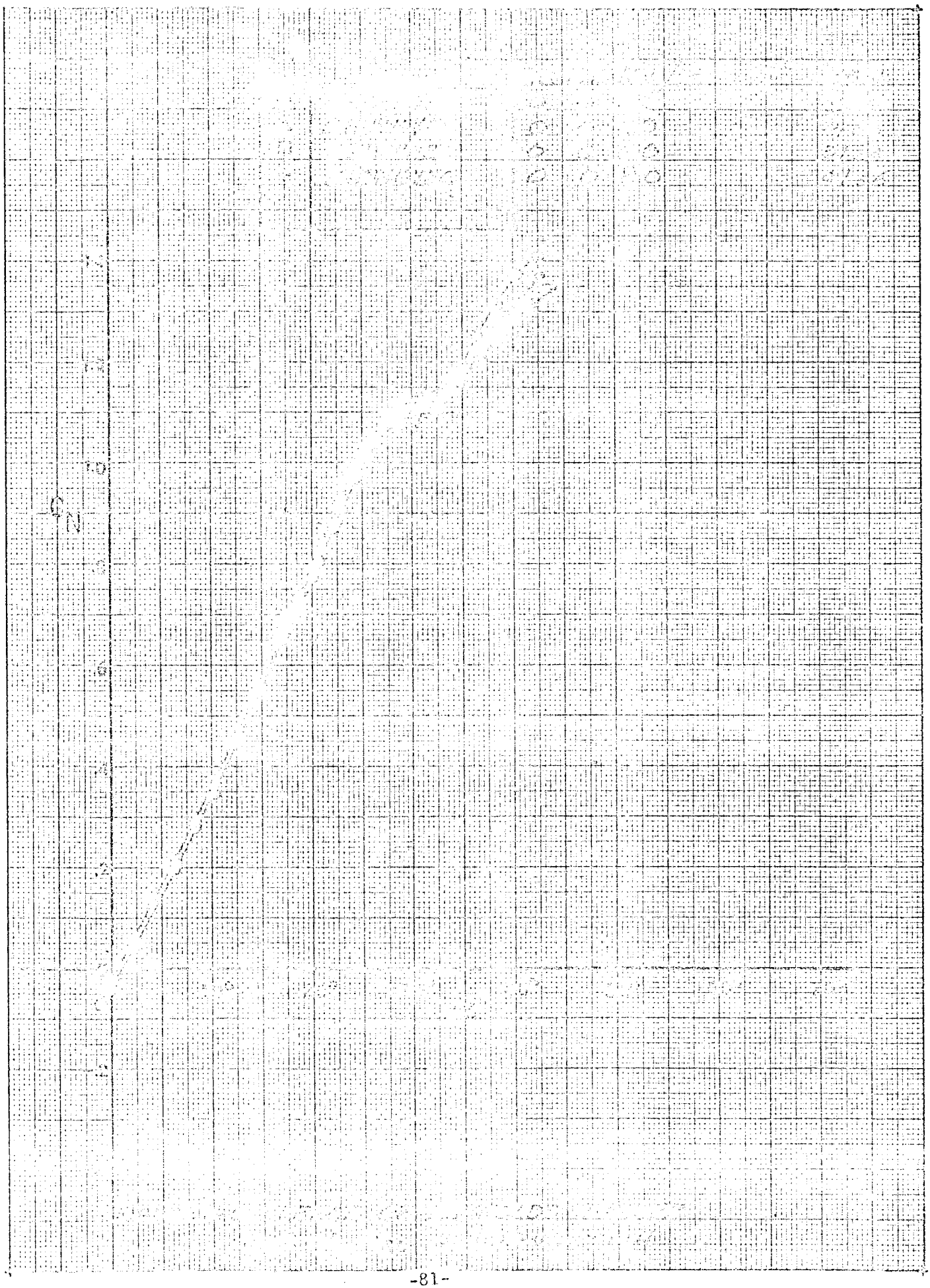

10 X 10 TO THE CENTIMETER 46 1511
18 X 25 CM. • ALBANENE
MADE IN U.S.A.
KEUFFEL & ESSER CO.

3

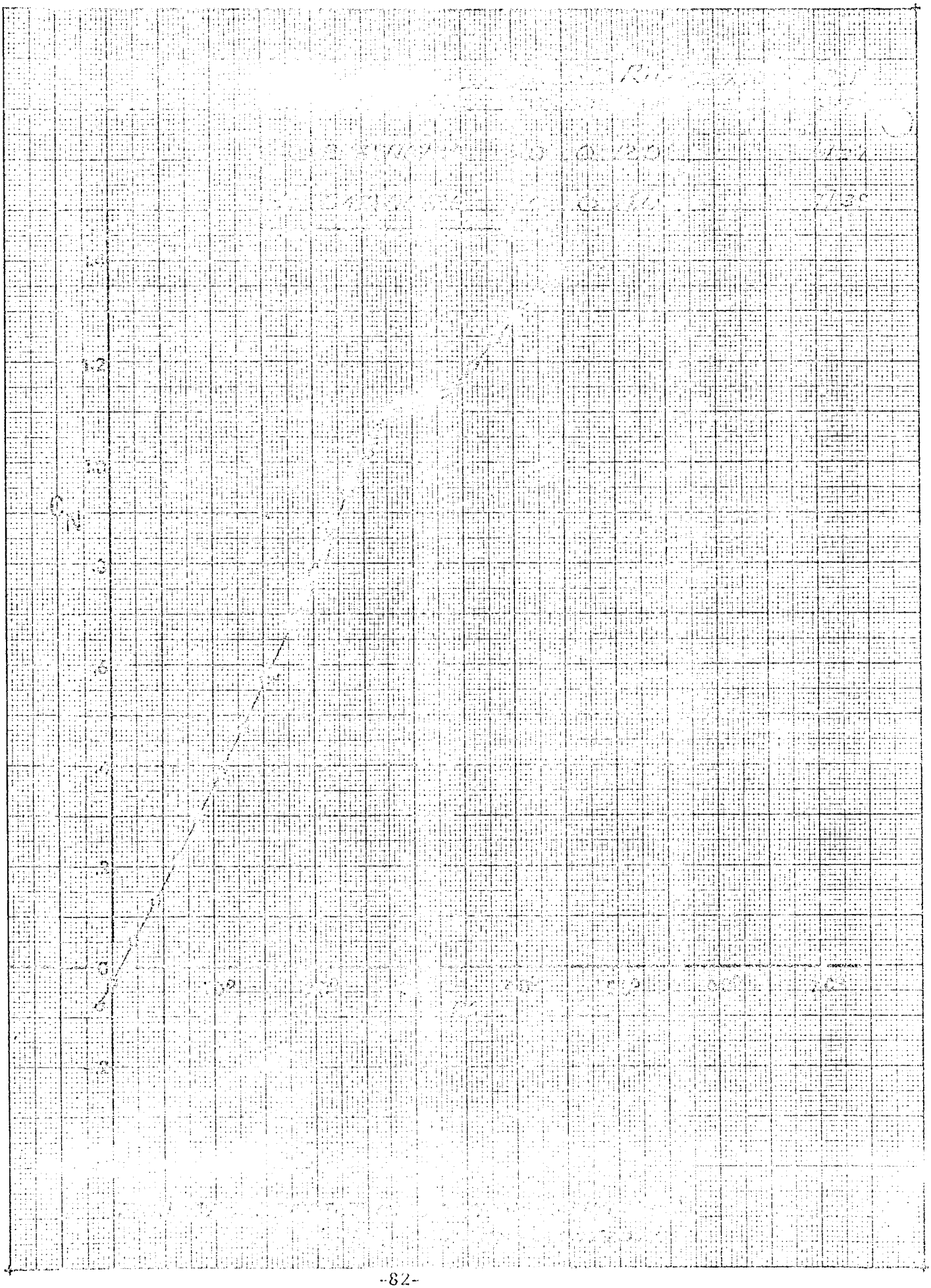

K&E 10 X 10 TO THE CENTIMETER 46 1517
18 X 25 CM. • ALBANENE MADE IN U.S.A.
KEUFFEL & ESSER CO.

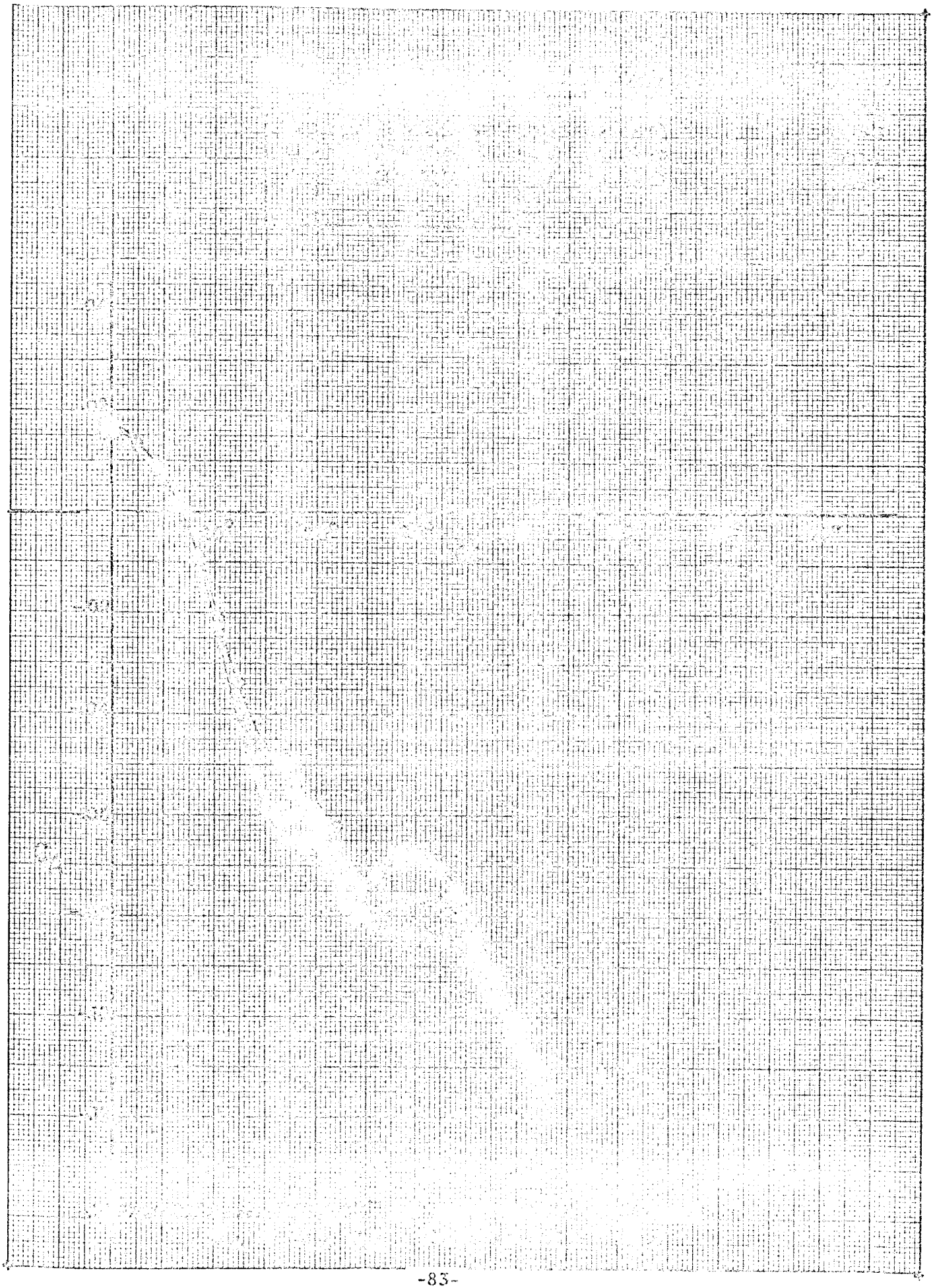

KEUFFEL & ESSER CO.

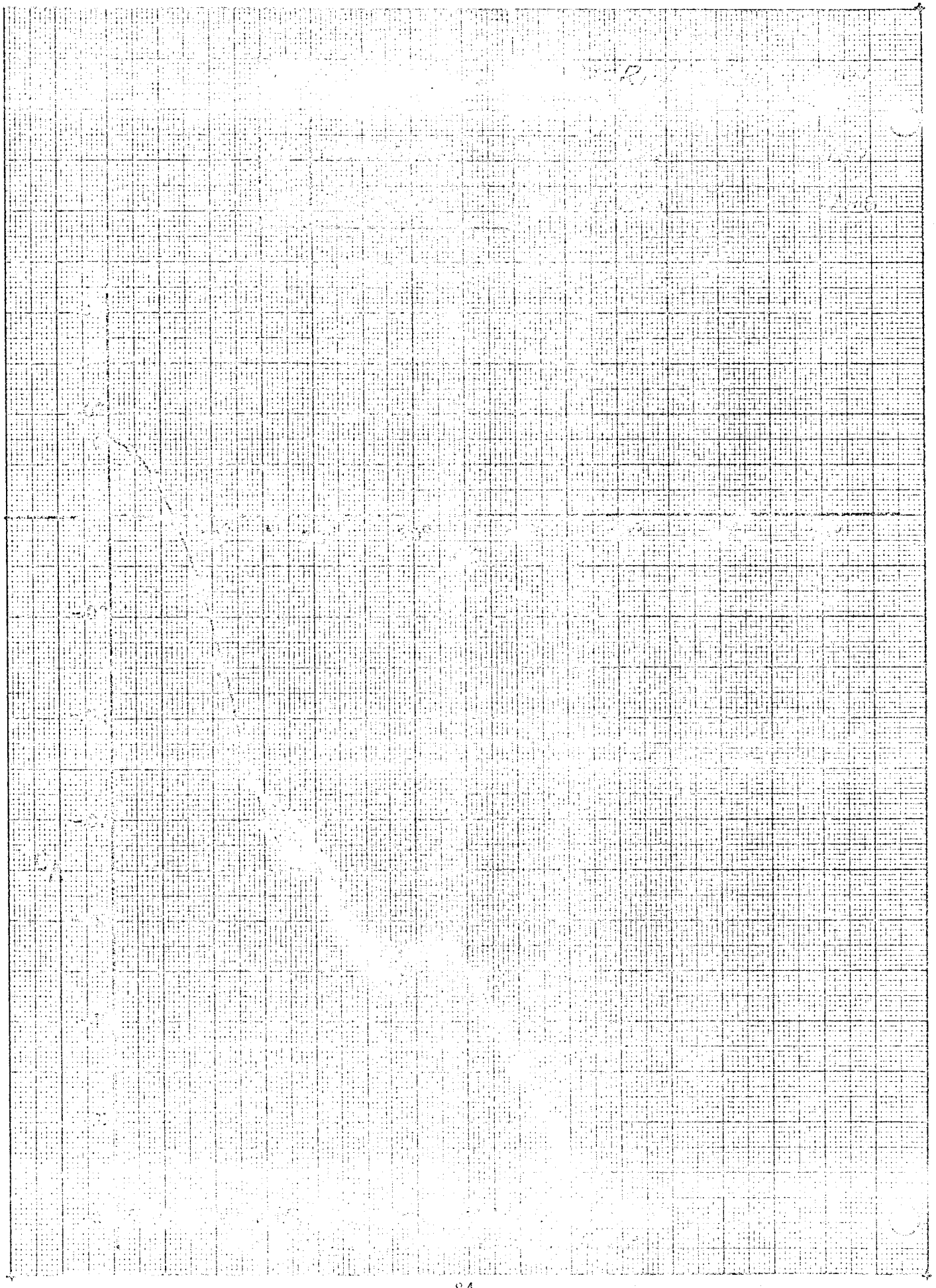

10 X 10 TO THE CENTIMETER 46 1517
18 X 25 CM. • ALBANENE
KEUFFEL & ESSER CO.

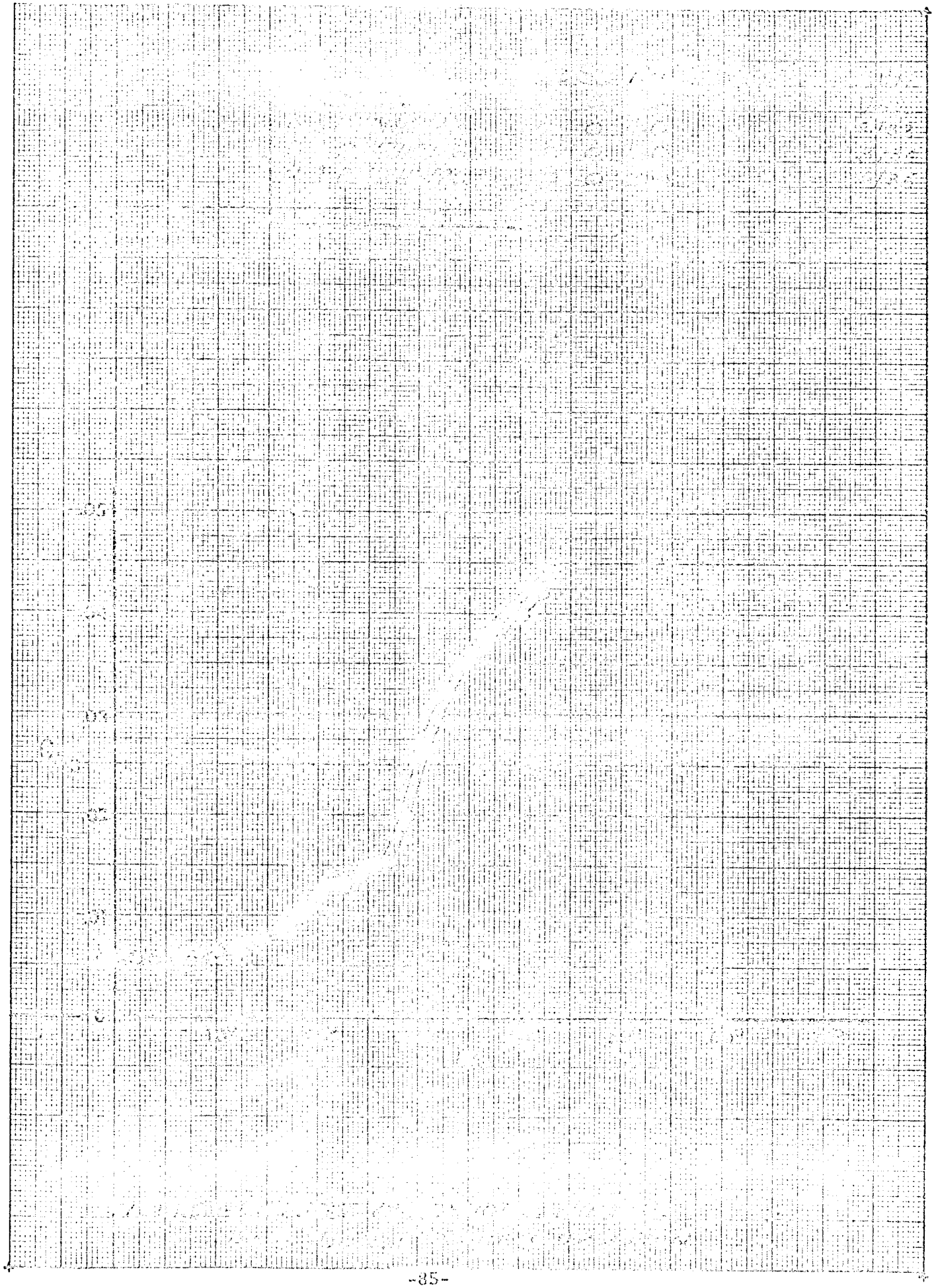

10 X 10 TO THE CENTIMETER 46 1517
10 X 25 CM. • ALBANY, N.Y. U.S.A.
KEUFFEL & ESSER CO.

276

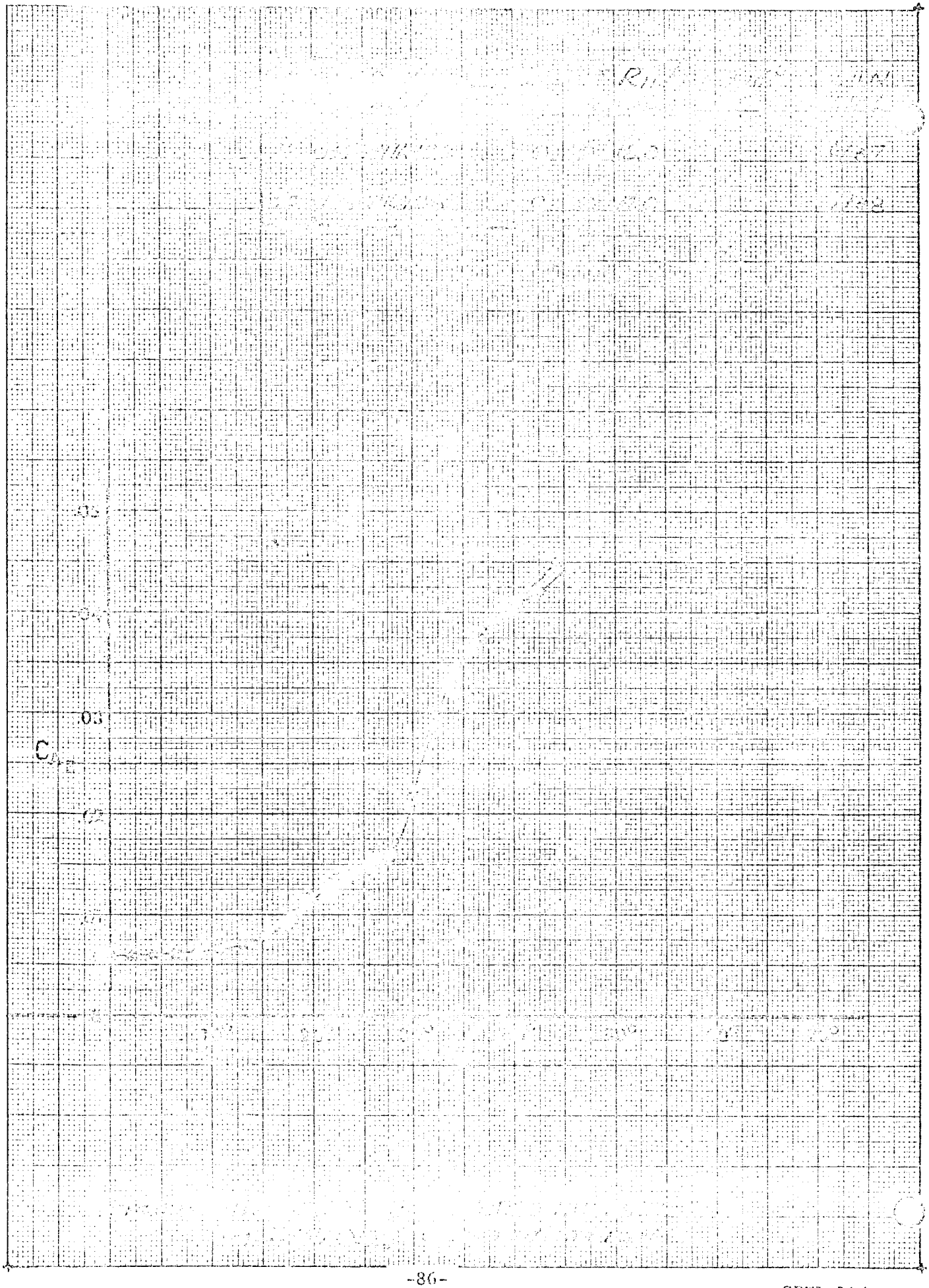
10 X 10 TO THE CENTIMETER 46 1517
10 X 25 CM. • ALBANENE
KEUFFEL & ESSER CO.

K&E 10 X 10 TO THE CENTIMETER 46 1517
18 X 25 CM. • ALBANENE®
KEUFFEL & ESSER CO.

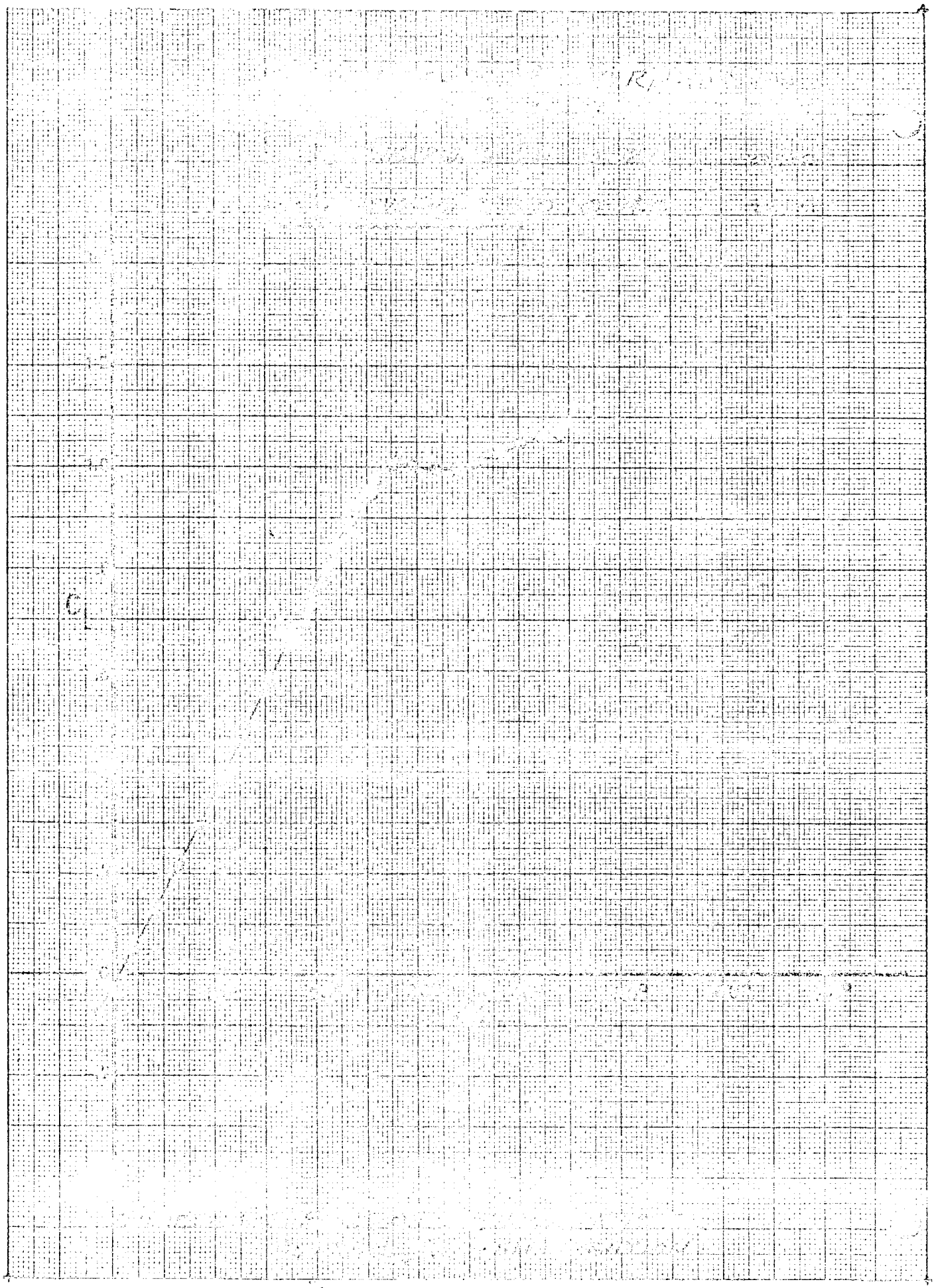

10 X 10 TO THE CENTIMETER 46 1517
18 X 25 CM. • ALBANENE
KEUFFEL & ESSER CO.

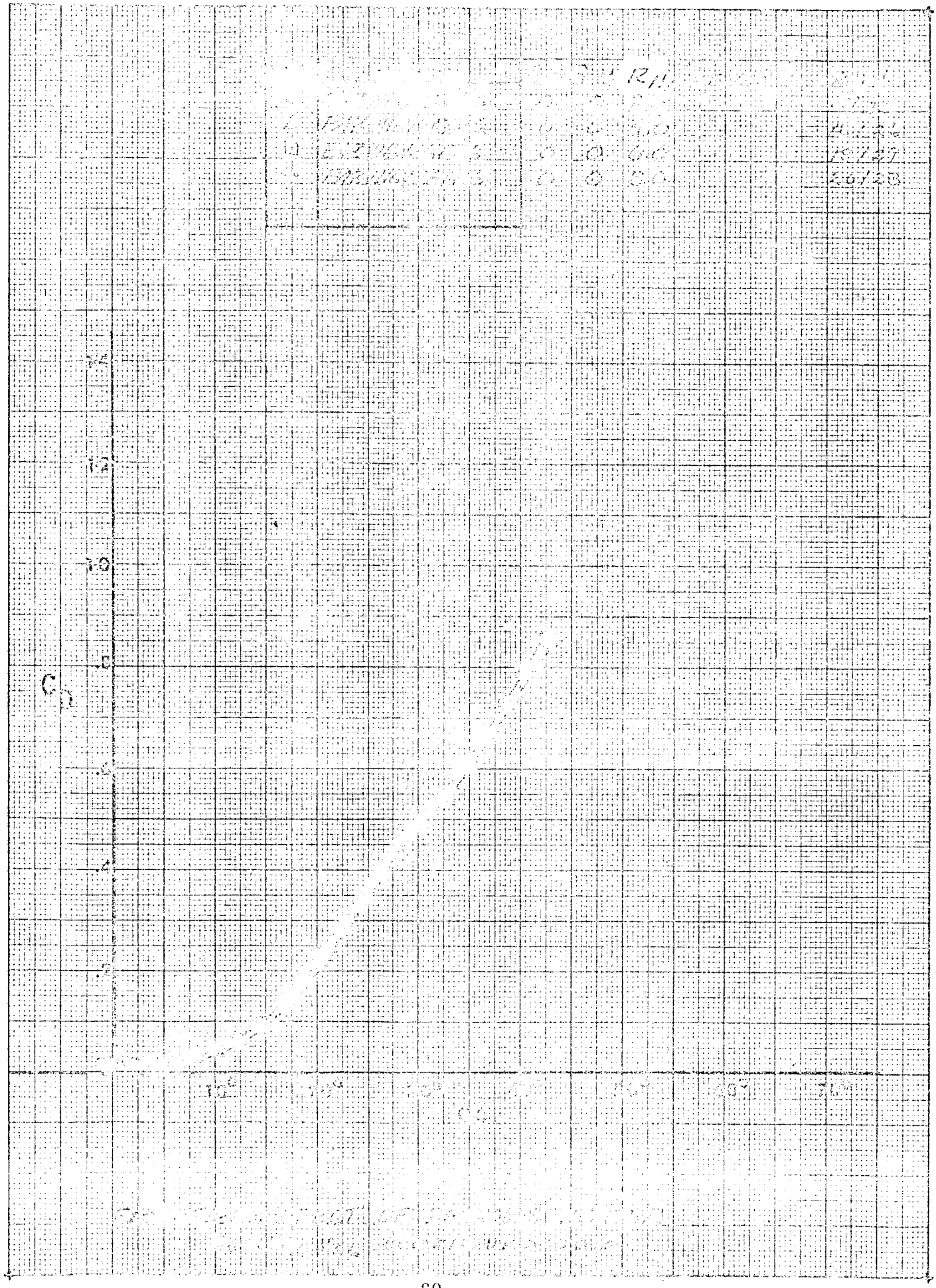

10 X 10 TO THE CENTIMETER · 46 1517
18 X 25 CM. · ALBANENE
KEUFFEL & ESSER CO.

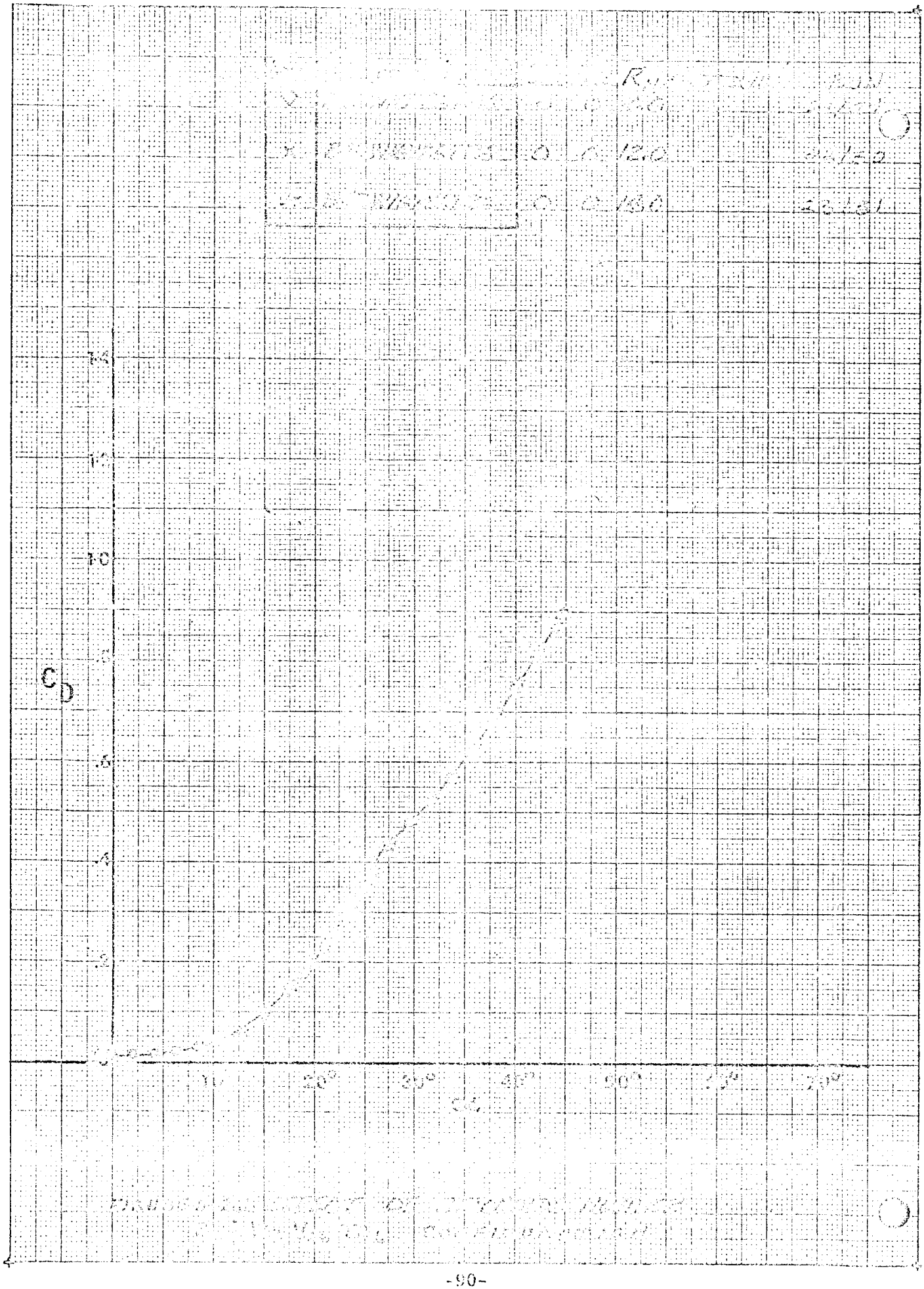

10 X 10 TO THE CENTIMETER 46 1517
KEUFFEL & ESSER CO.

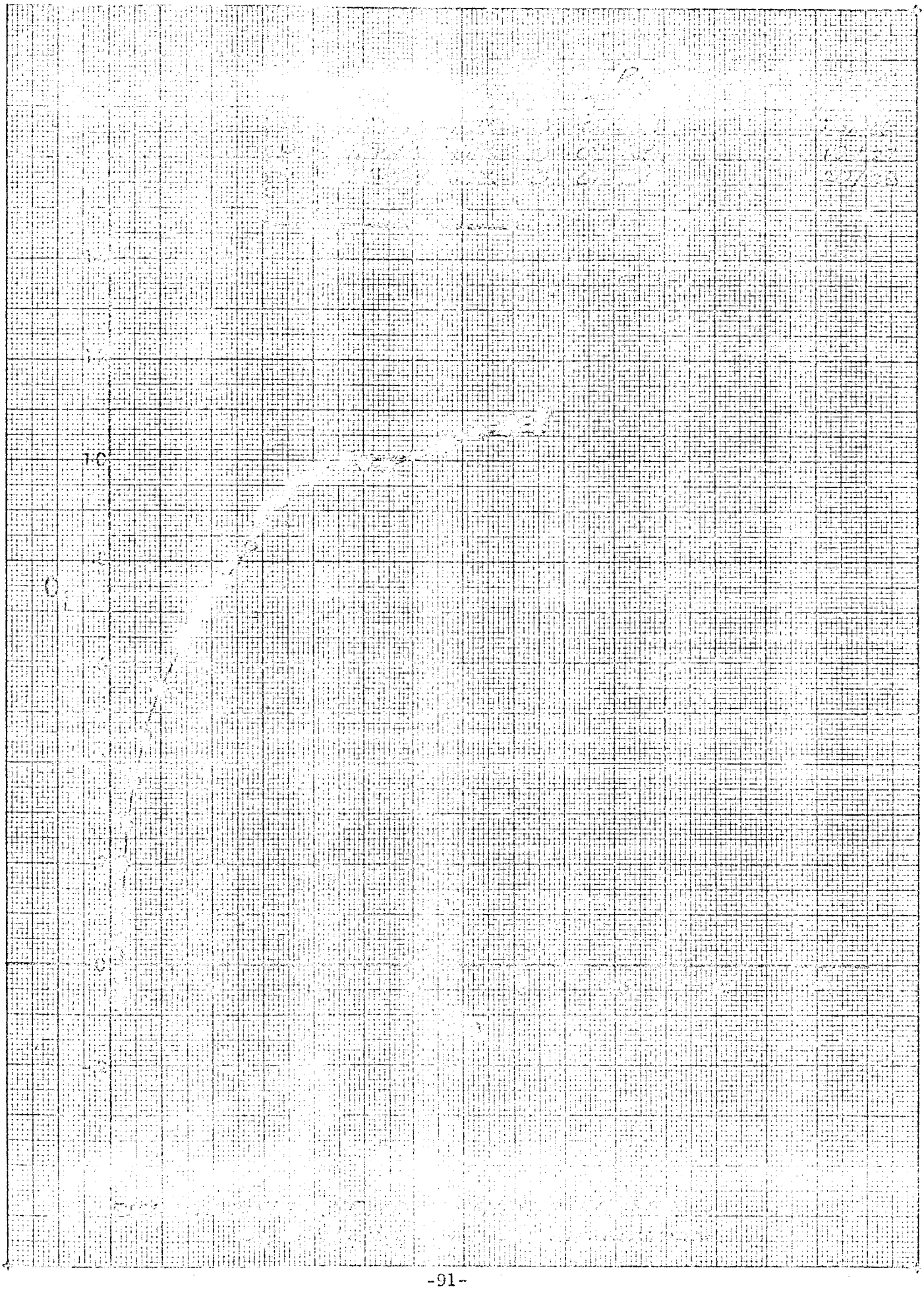

10 X 10 TO THE CENTIMETER 46 1517
19 X 25 CM. • ALBANENE
KEUFFEL & ESSER CO.

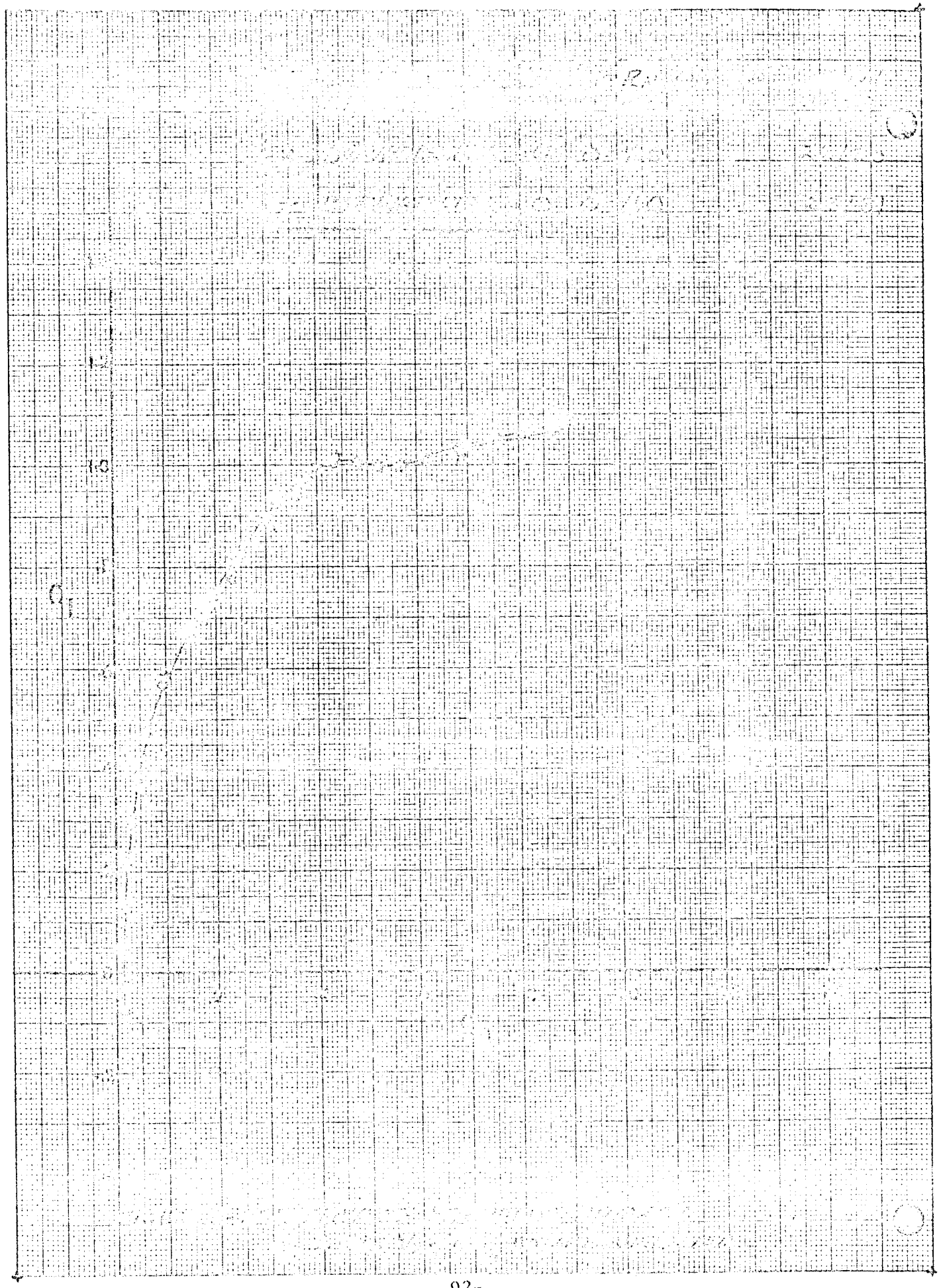

10 X 10 TO THE CENTIMETER 46 1517
18 X 25 CM. • ALPANEMA
KEUFFEL & ESSER CO.

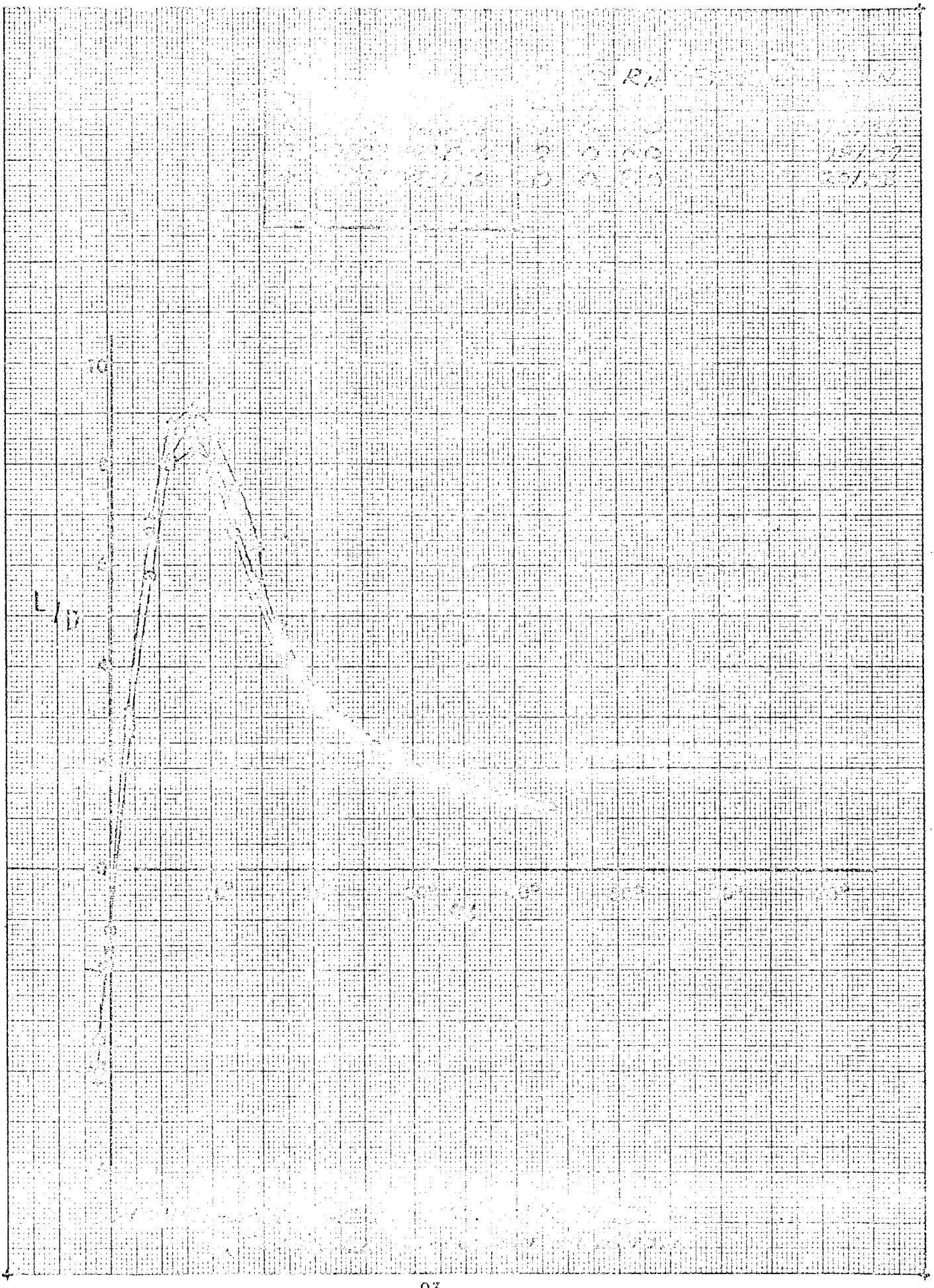

10 X 10 TO THE CENTIMETER 46 1517
18 X 25 CM • ALBANENE
MADE IN U.S.A.
KEUFFEL & ESSER CO.

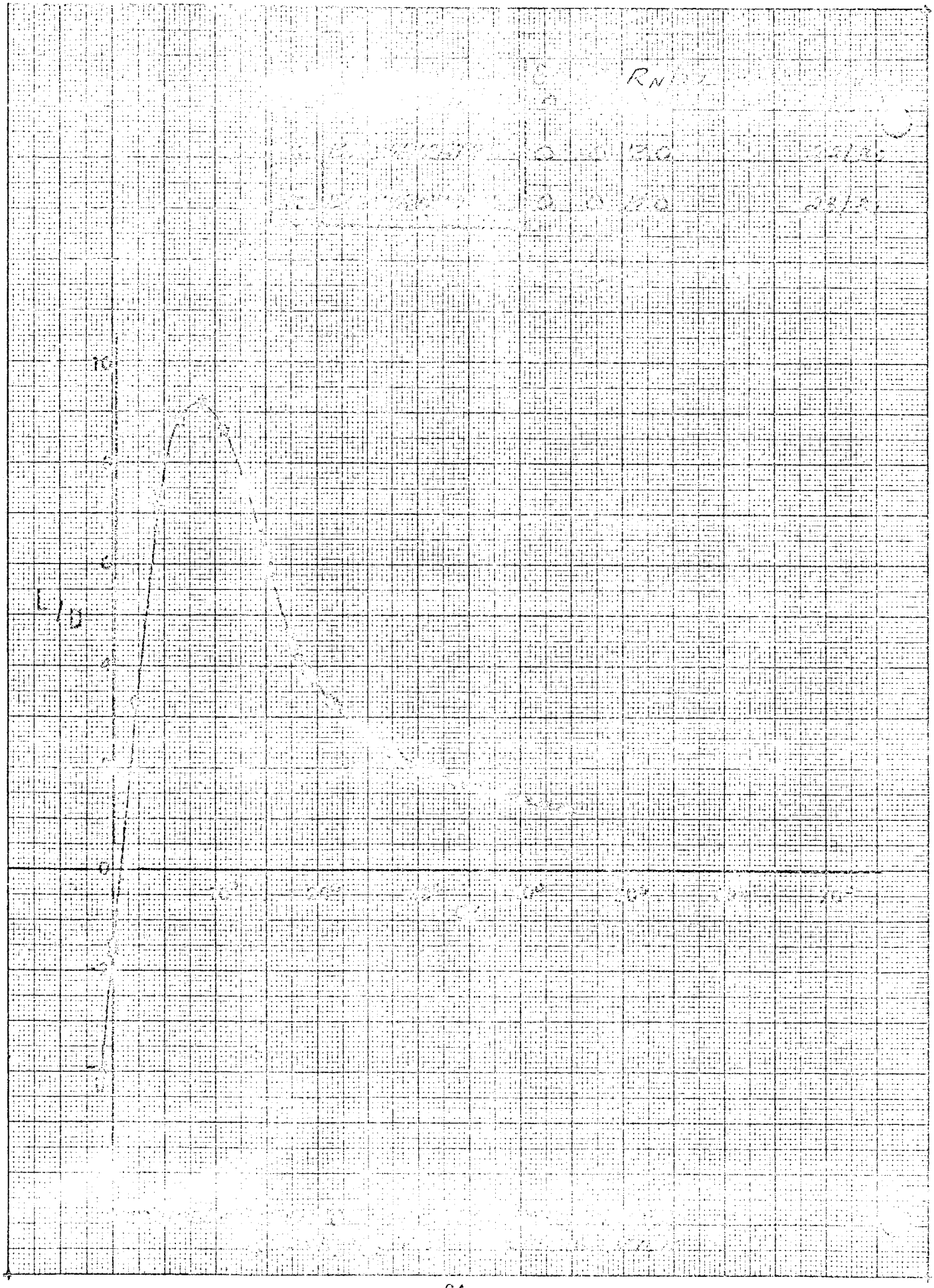

K+E 10 X 10 TO THE CENTIMETER 46 1517
18 X 25 CM. • ALBANENE™ MADE IN U.S.A.
KEUFFEL & ESSER CO.

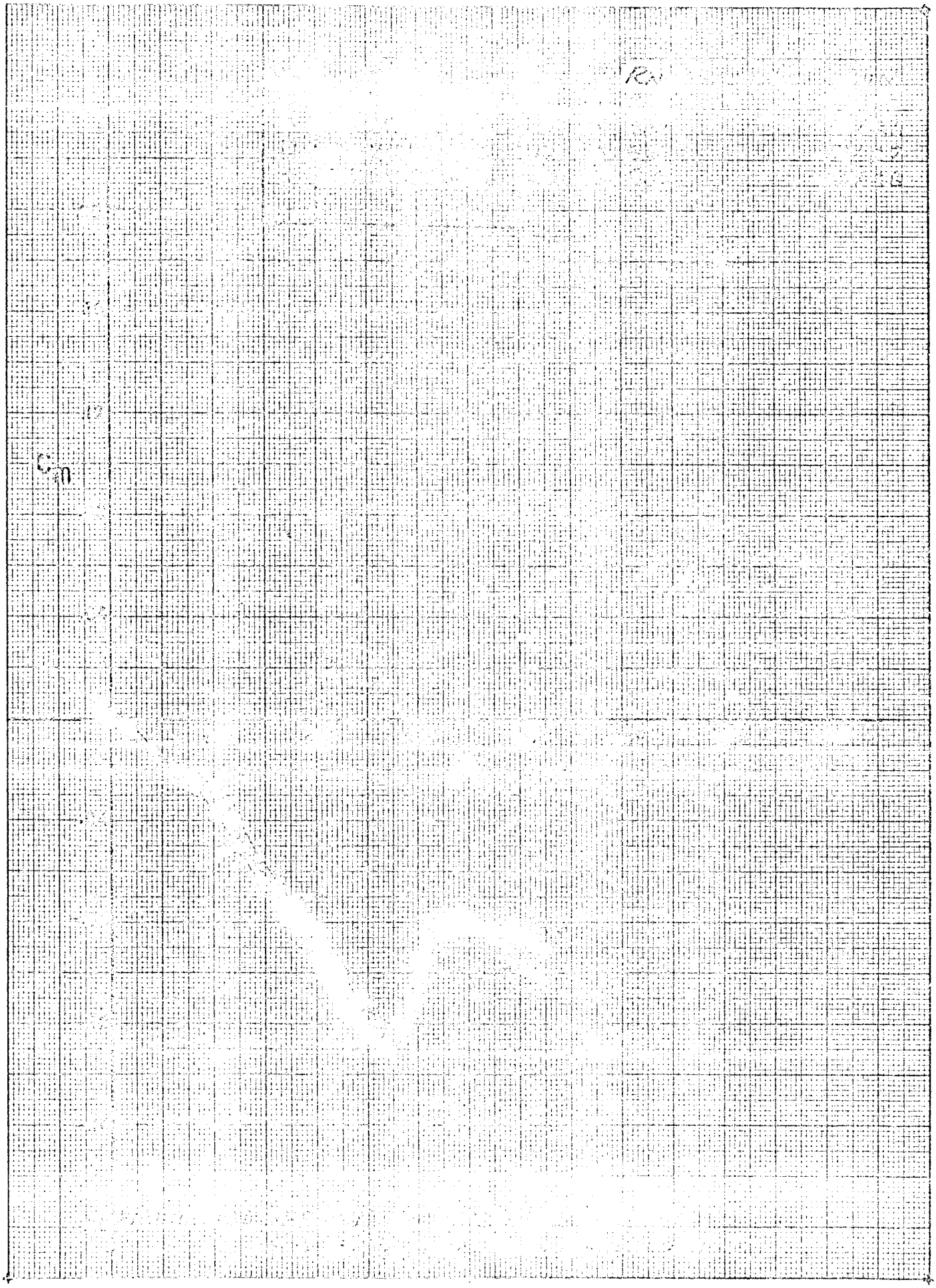

K&E 10 X 10 TO THE CENTIMETER 46 1517
18 X 25 CM. • ALBANENE
KEUFFEL & ESSER CO.

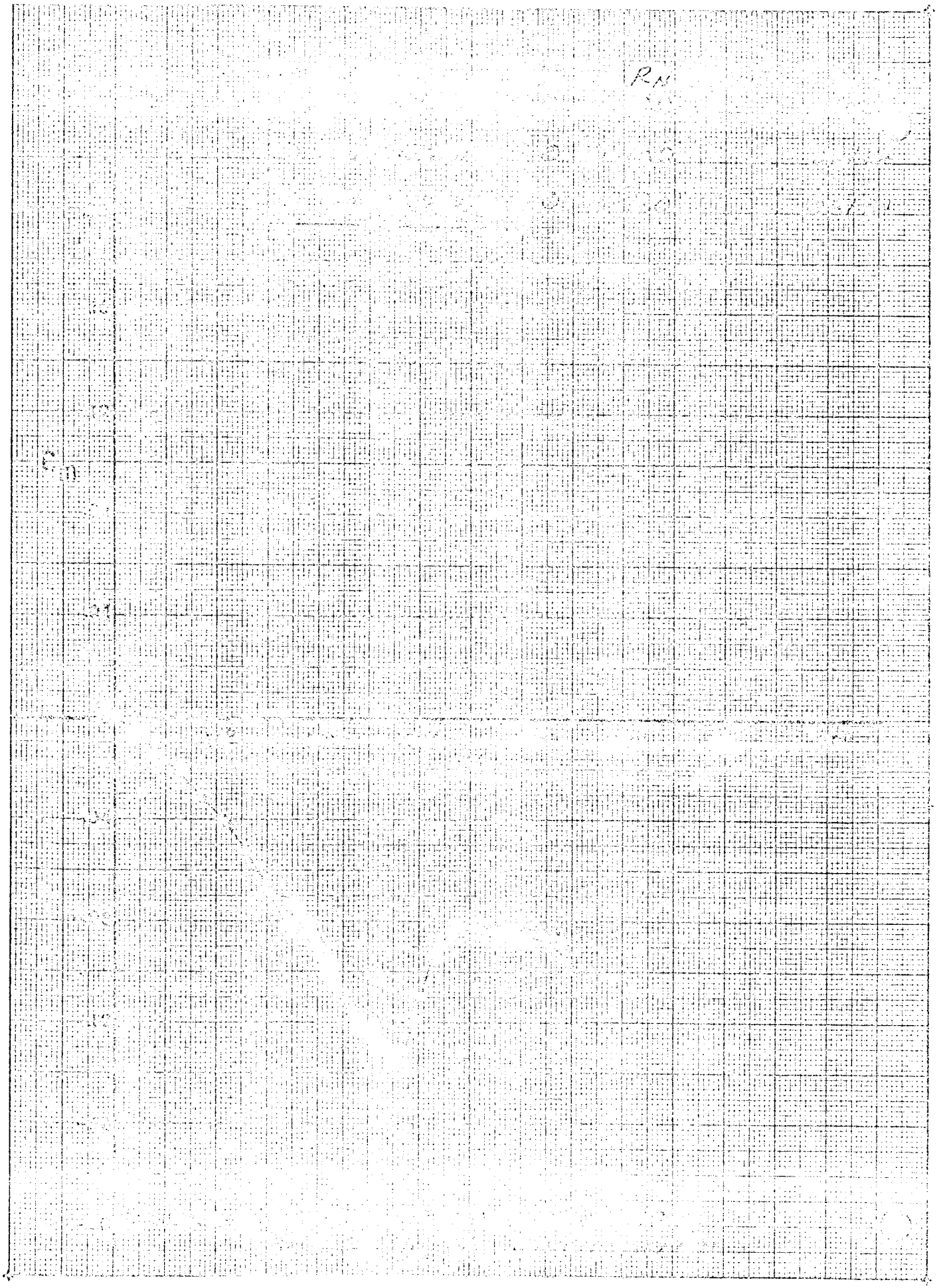

10 X 10 TO THE CENTIMETER 46 1517
18 X 25 CM. • ALBANENE
KEUFFEL & ESSER CO.

260

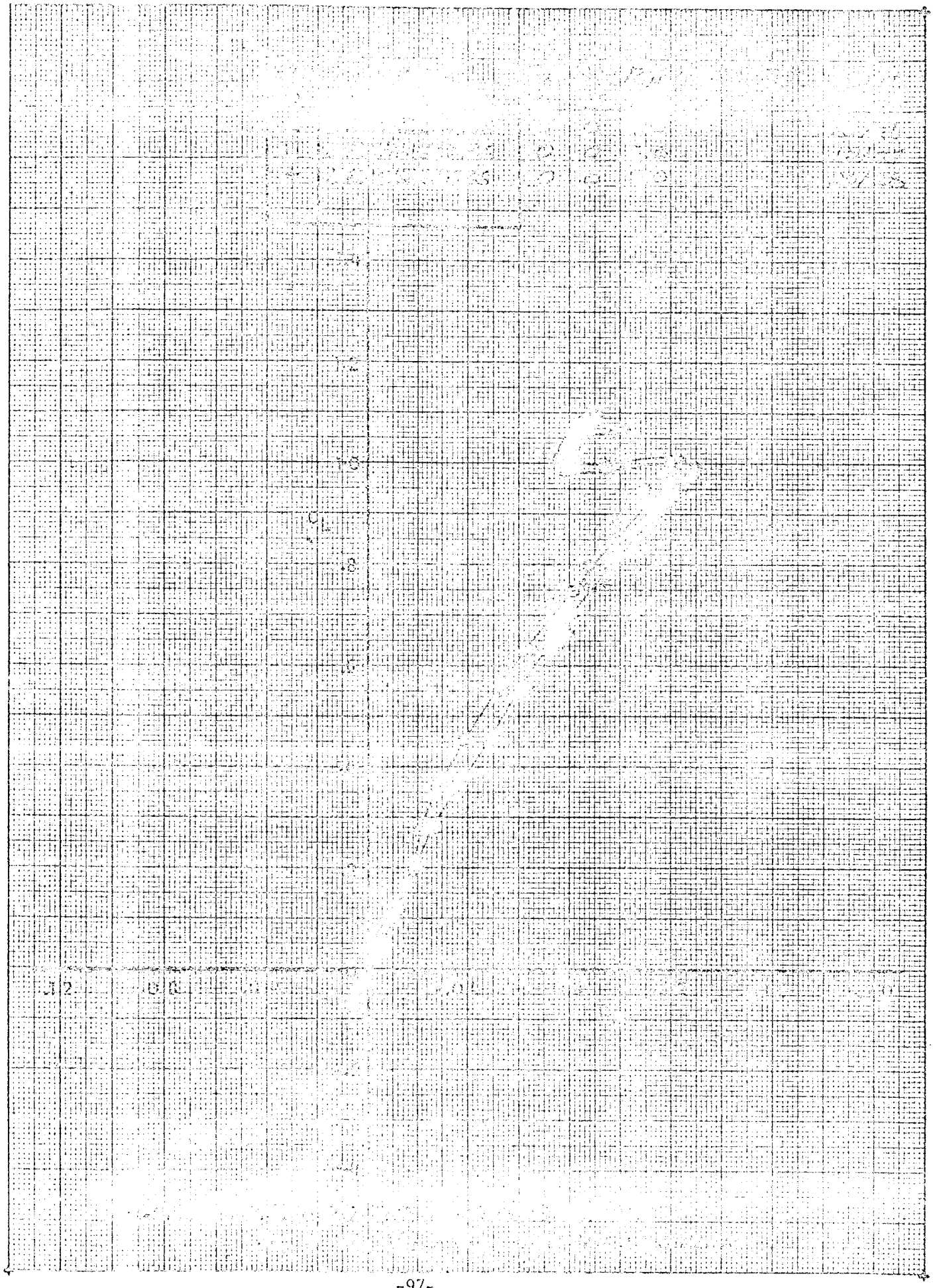

KEUFFEL & ESSER CO.

260

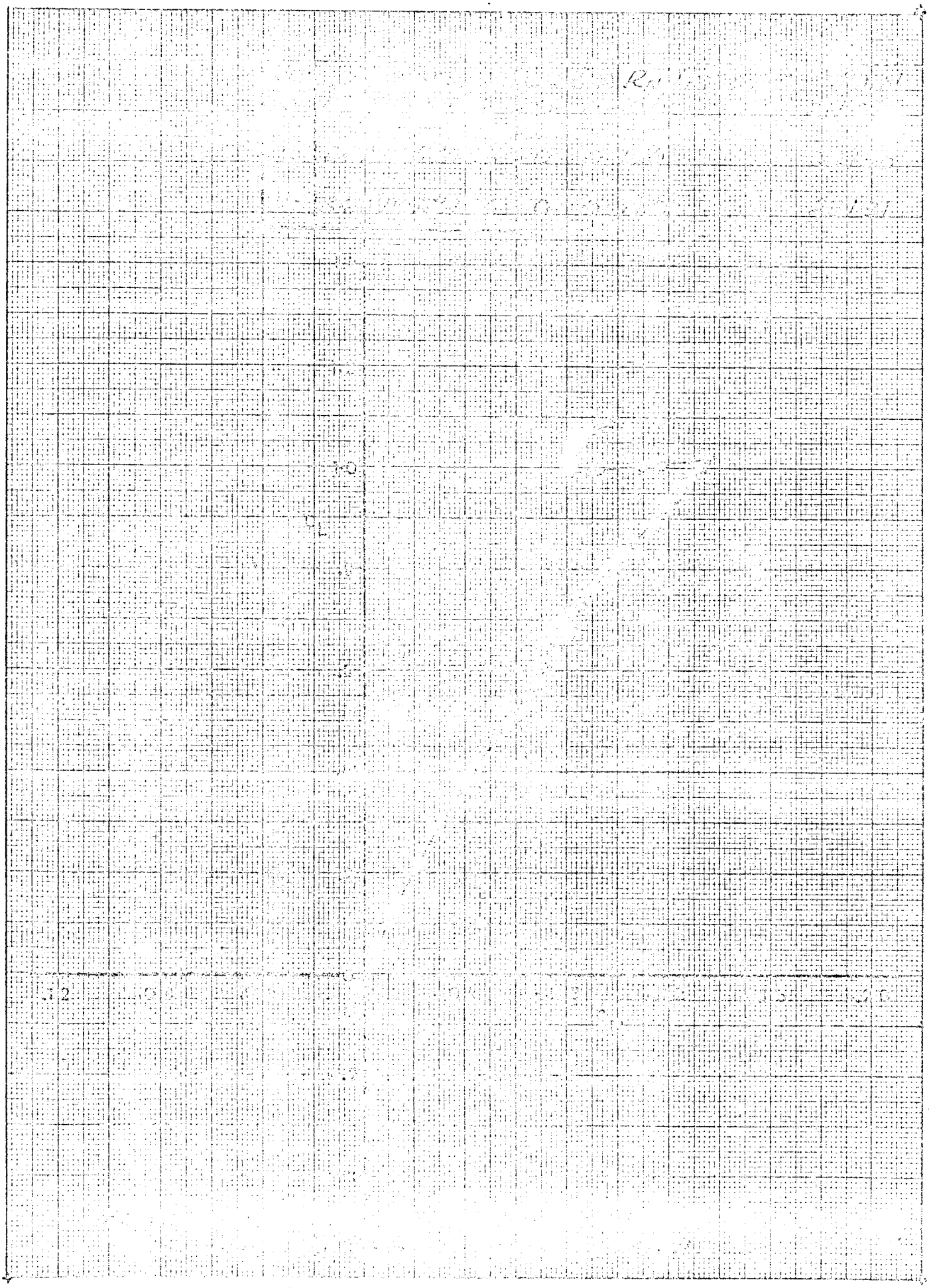

10 X 10 TO THE CENTIMETER 46 1517
18 X 25 CM. • ALBANENE®
MADE IN U.S.A.
KEUFFEL & ESSER CO.

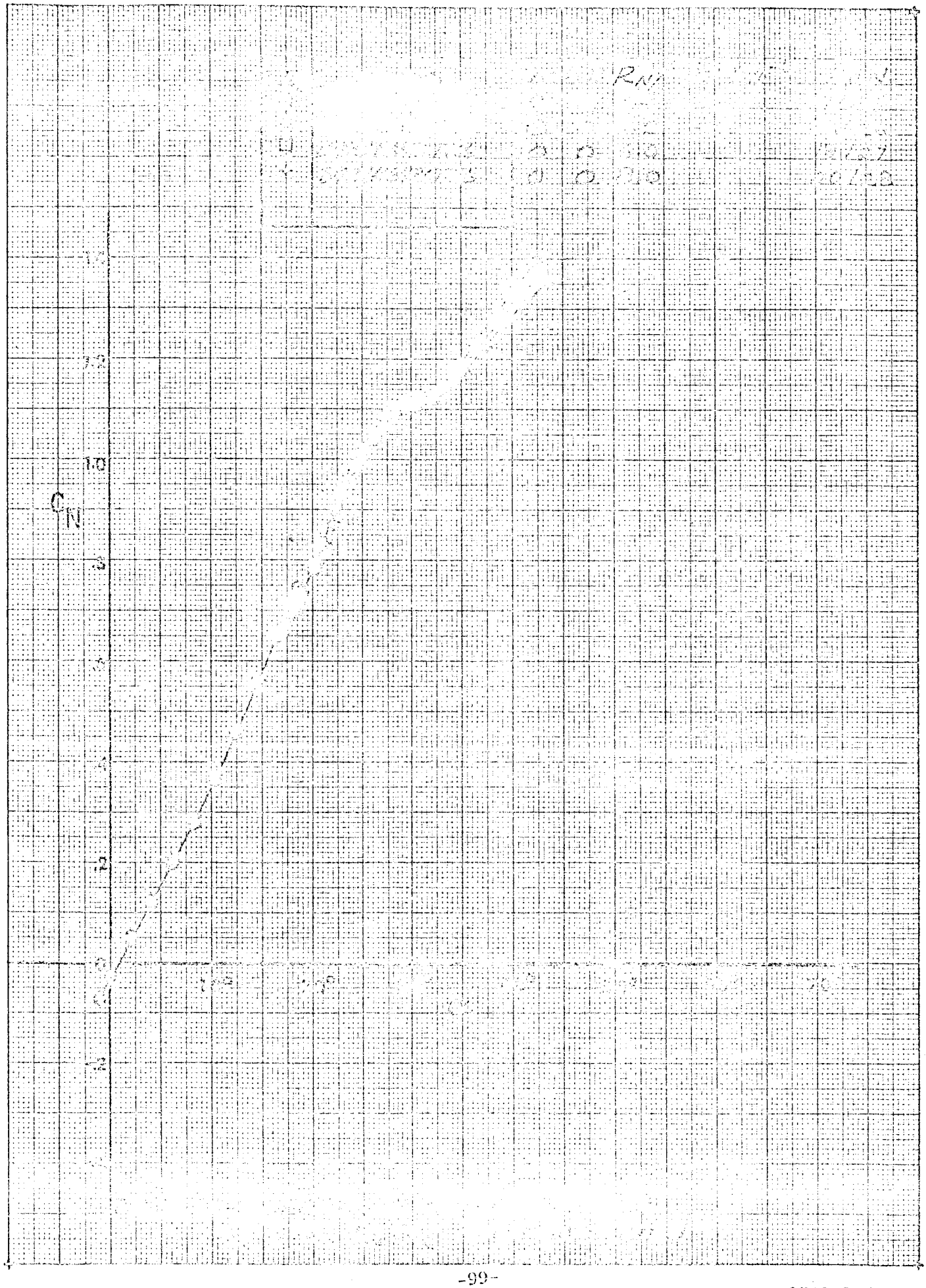
KEUFFEL & ESSER CO.

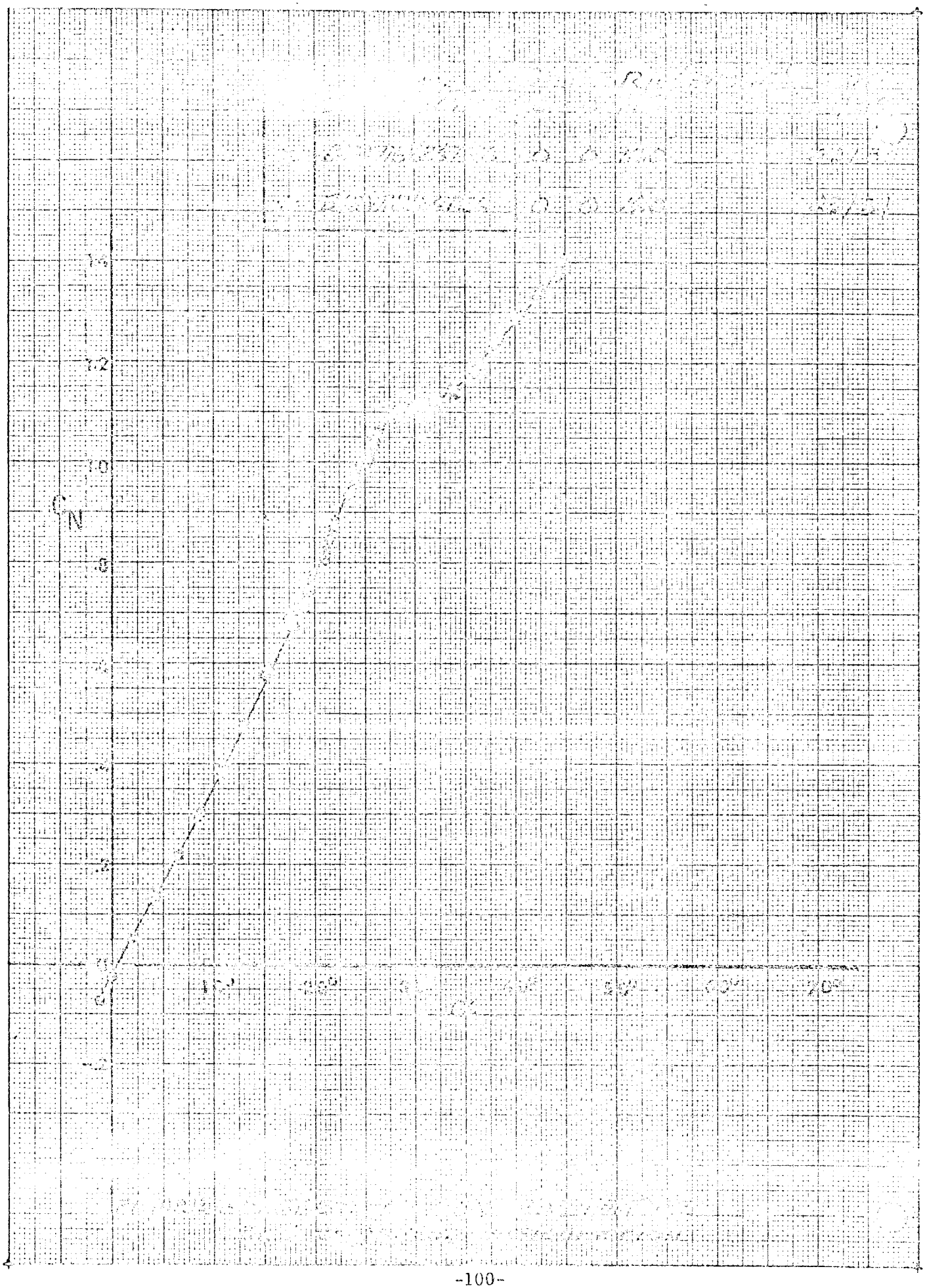

10 X 10 TO THE CENTIMETER 46 1517
18 X 25 CM. • ALBANENSE
KEUFFEL & ESSER CO.

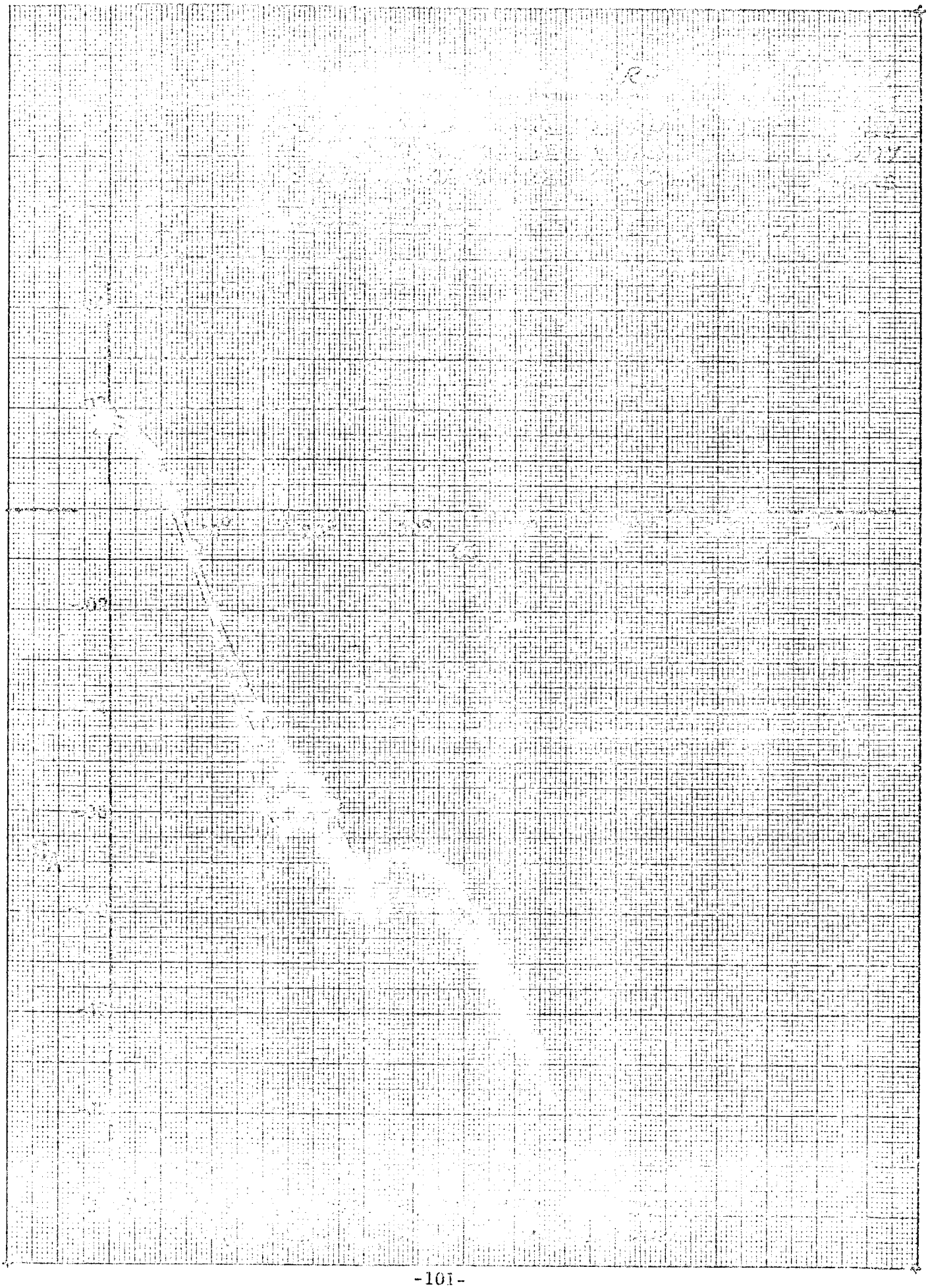

KEUFFEL & ESSER CO.

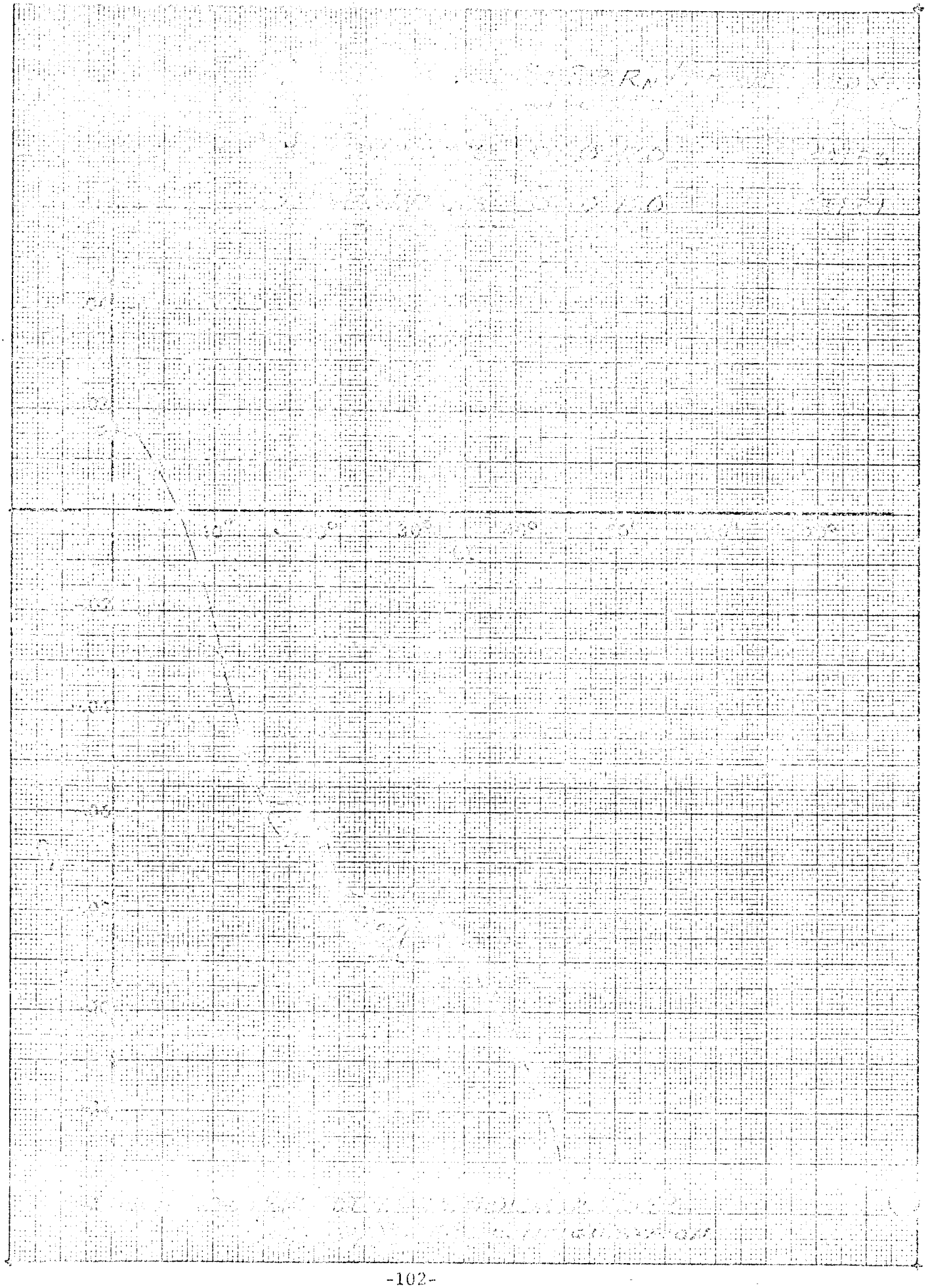

10 X 10 TO THE CENTIMETER 46 1517
18 X 25 CM. • ALBANENE
KEUFFEL & ESSER CO.

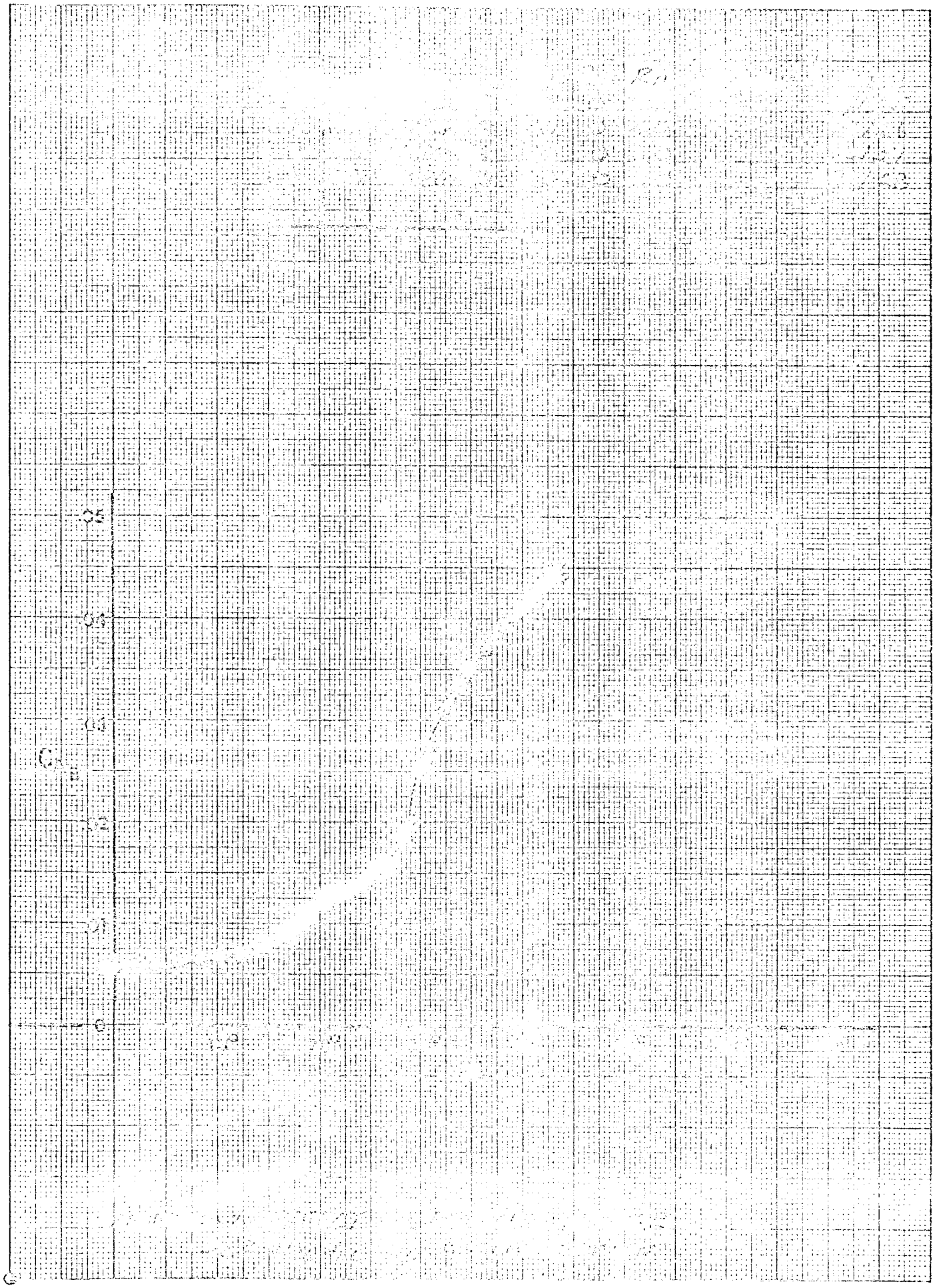
KEUFFEL & ESSER CO.

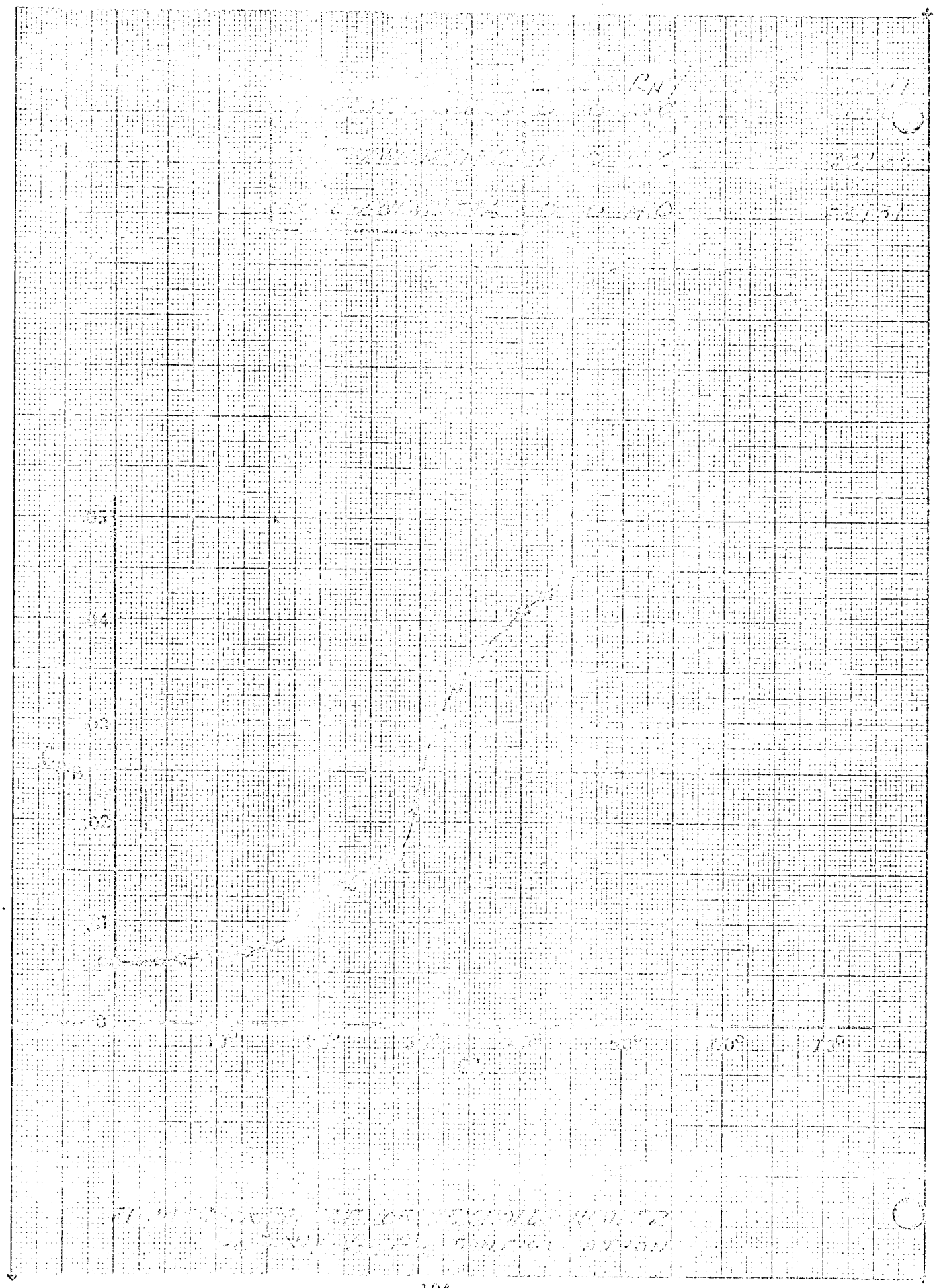

10 X 10 TO THE CENTIMETER 46 1517
18 X 25 CM. • ALBANENE
KEUFFEL & ESSER CO.

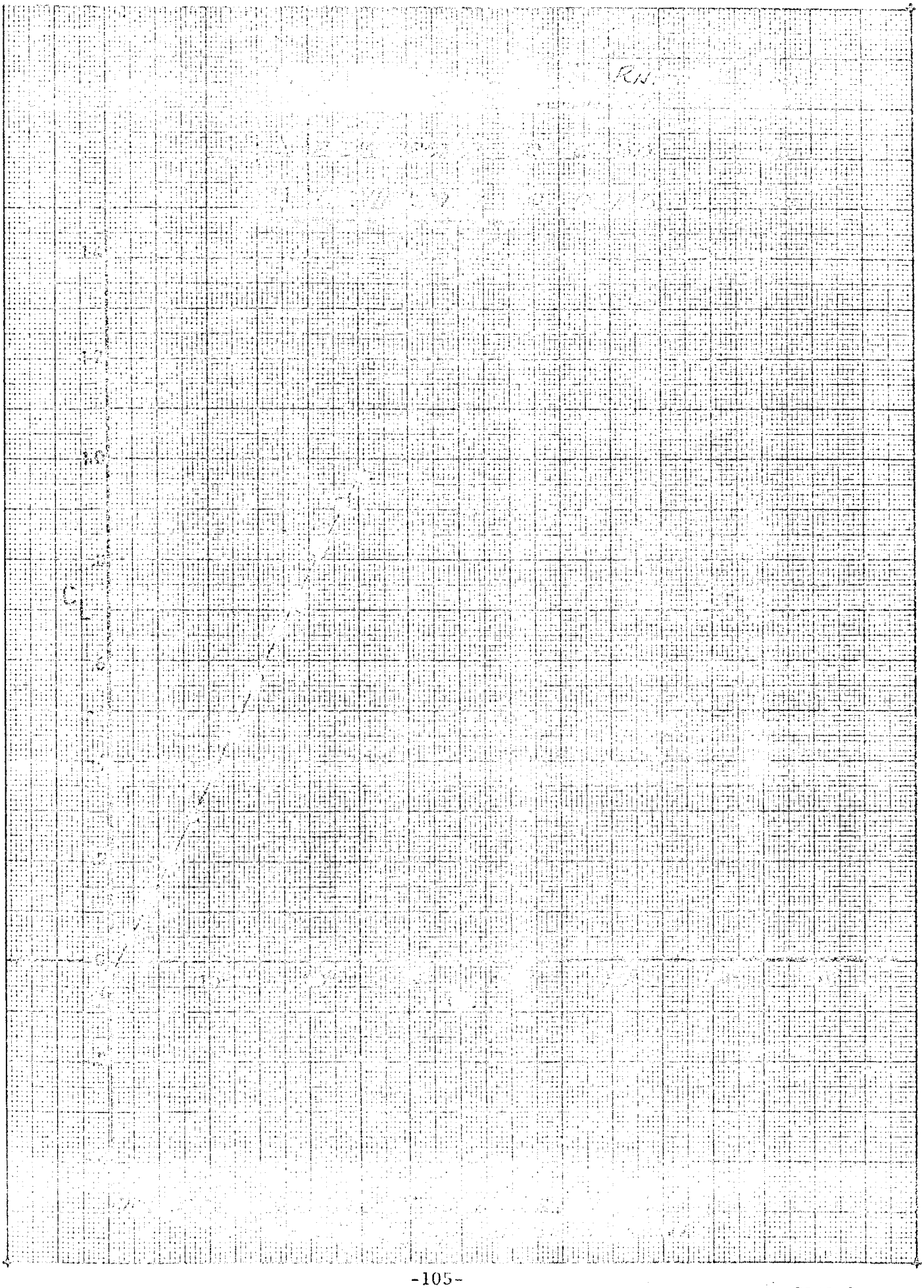
RN.

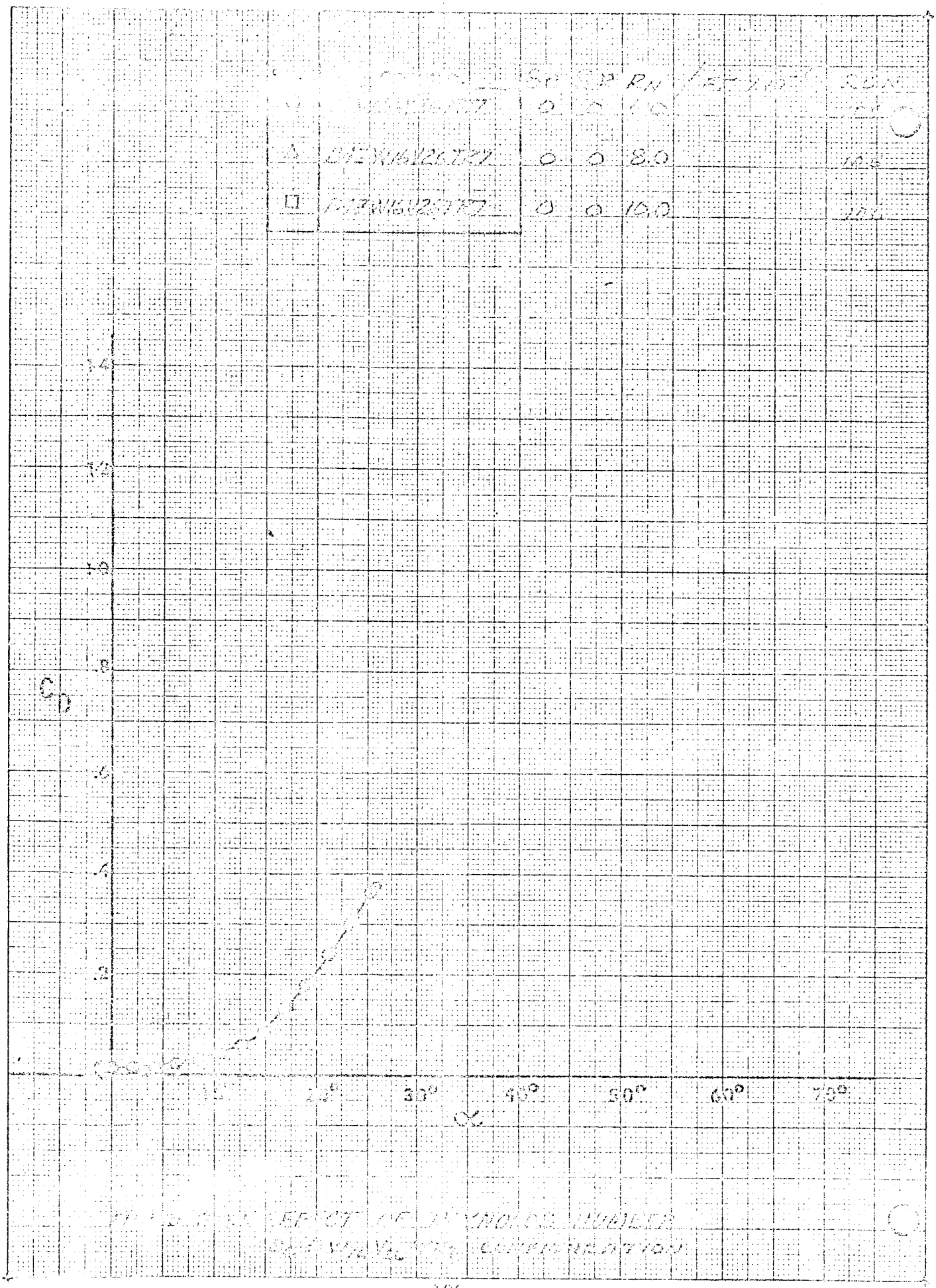
Sp
Dp
RN
0
0
8.0
0
0
10.0
.4
.2
.8
.6
.4
.2
30°
45°
60°
75°
α

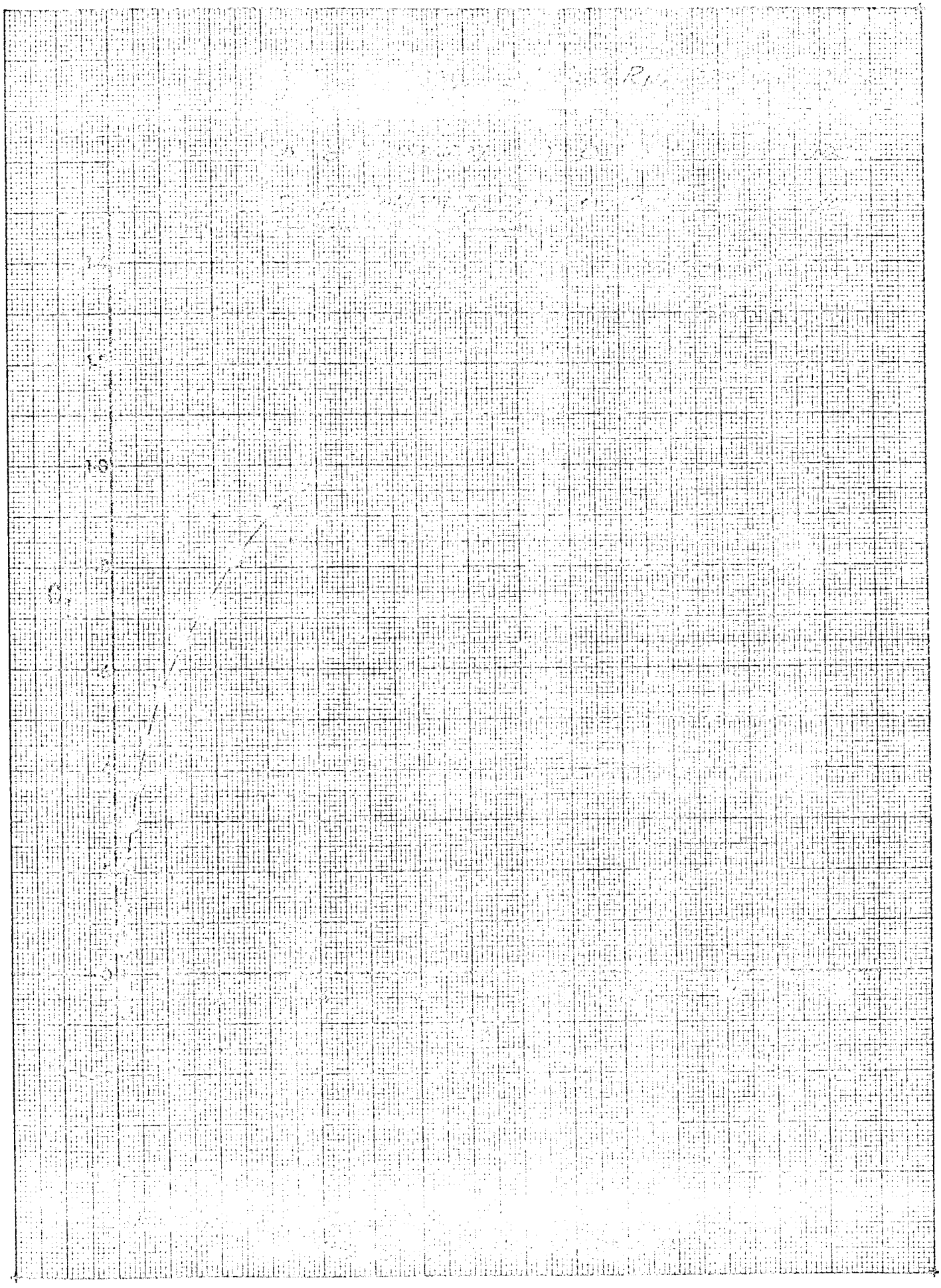

10 X 10 TO THE CENTIMETER 46 1517
18 X 25 CM • ALBANENE
KEUFFEL & ESSER CO.

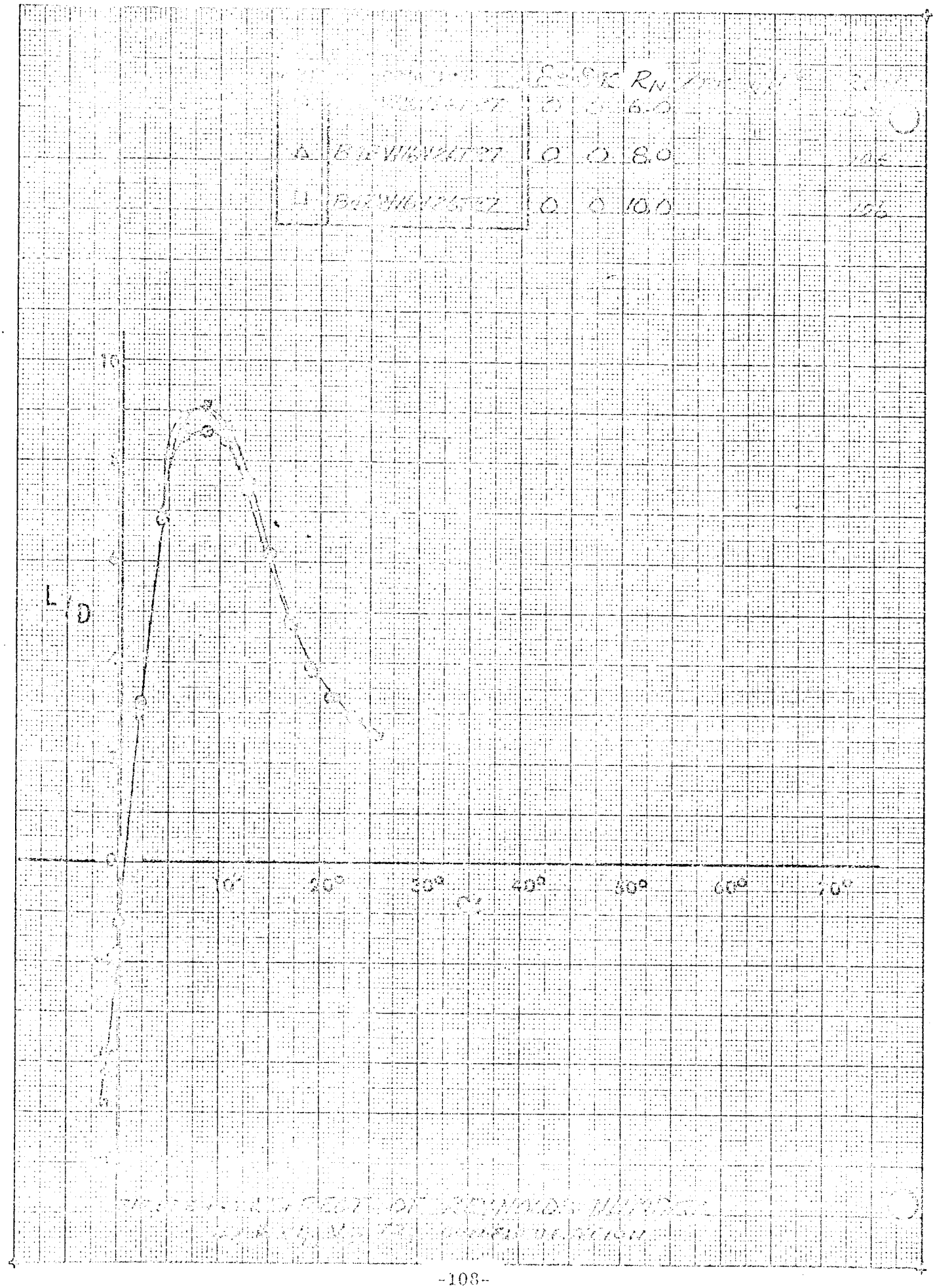
L/D
10°
20°
30°
40°
50°
60°
70°
α

10 X 10 TO THE CENTIMETER 46 1517
10 X 25 CM. • ALBANENE
KEUFFEL & ESSER CO.

260

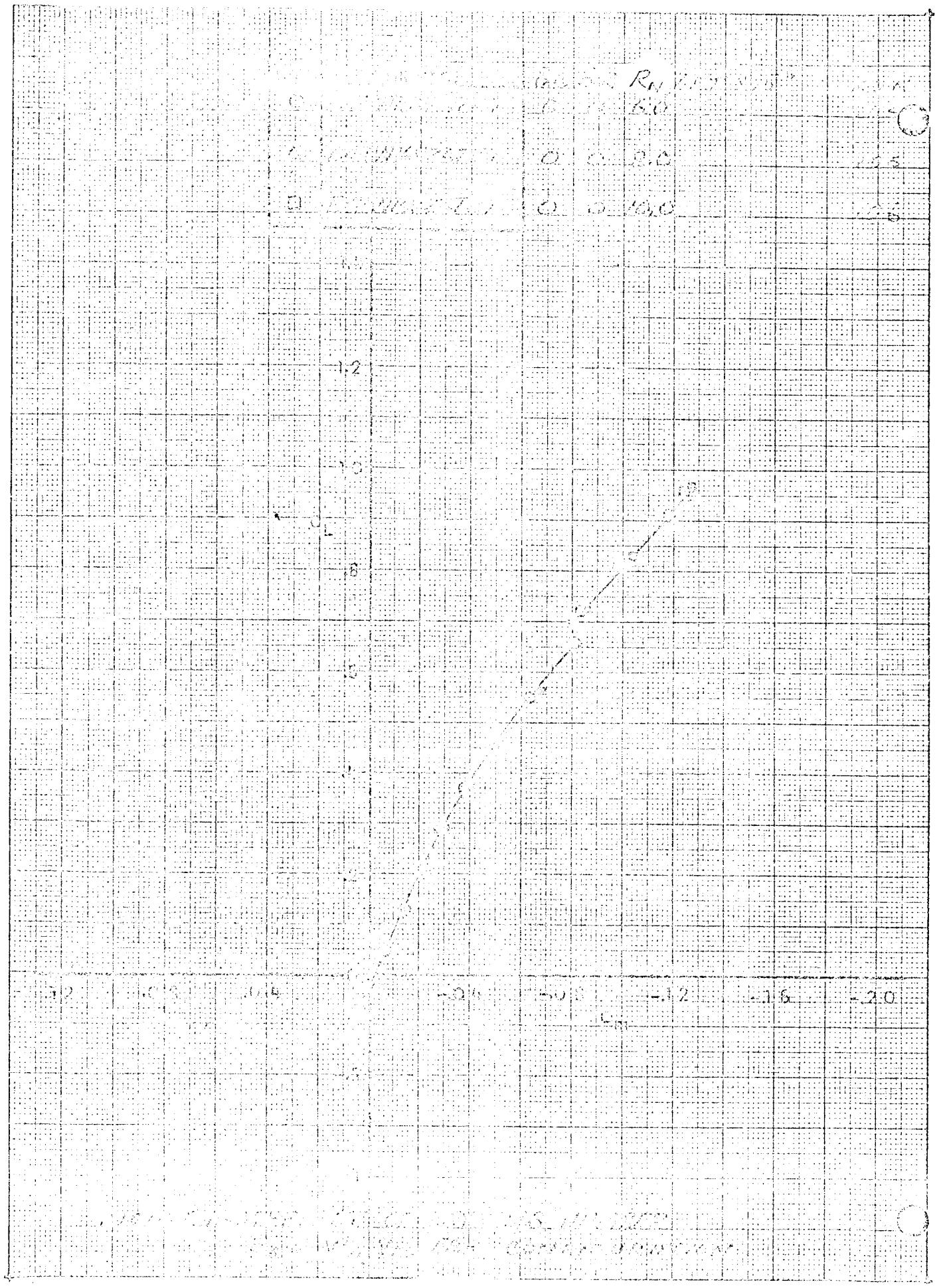

10 X 10 TO THE CENTIMETER 46 1517
25 X 25 CM. • ALBANENE
KEUFFEL & ESSER CO.

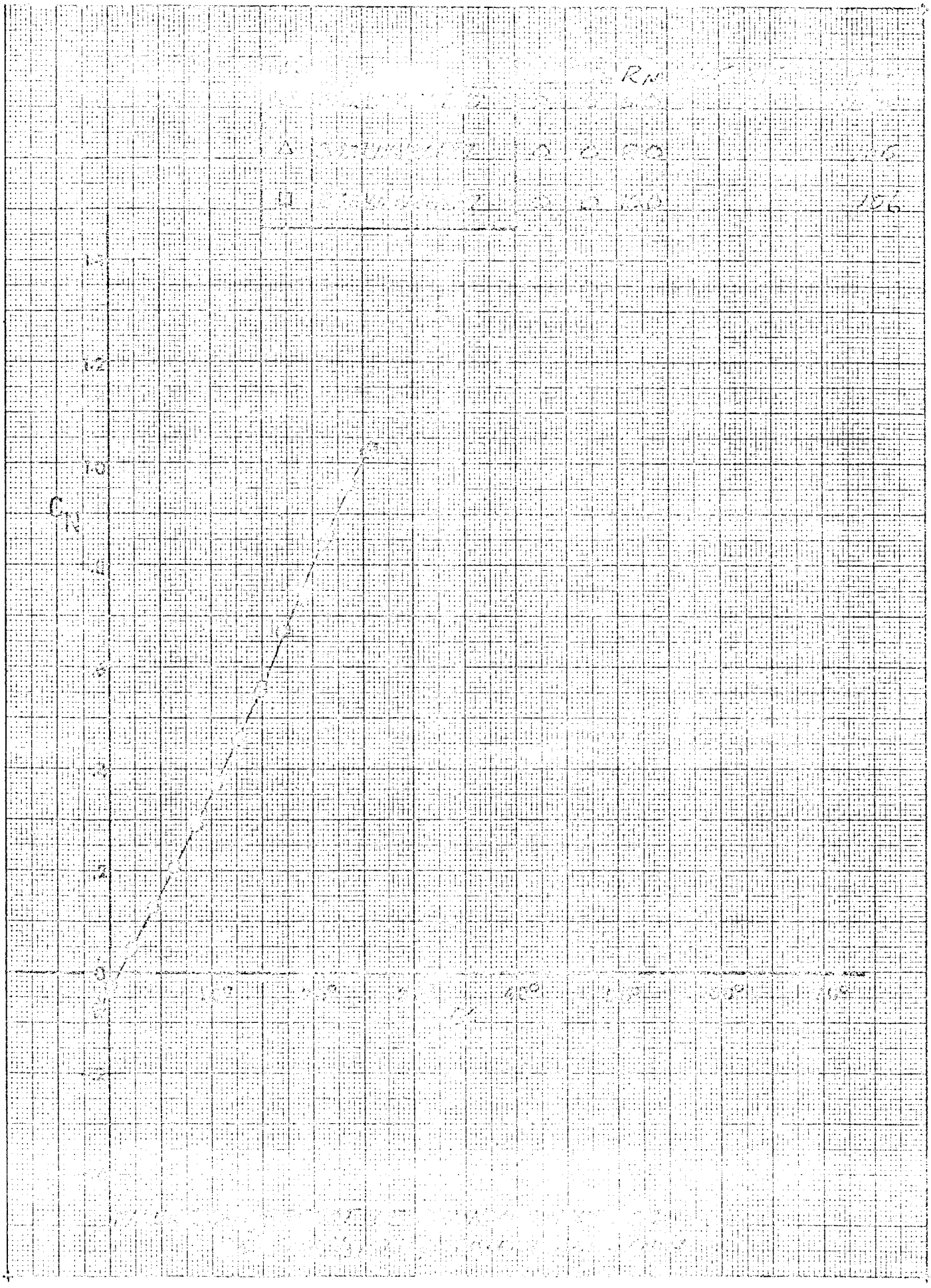

10 X 10 TO THE CENTIMETER 46 1517
KEUFFEL & ESSER CO.

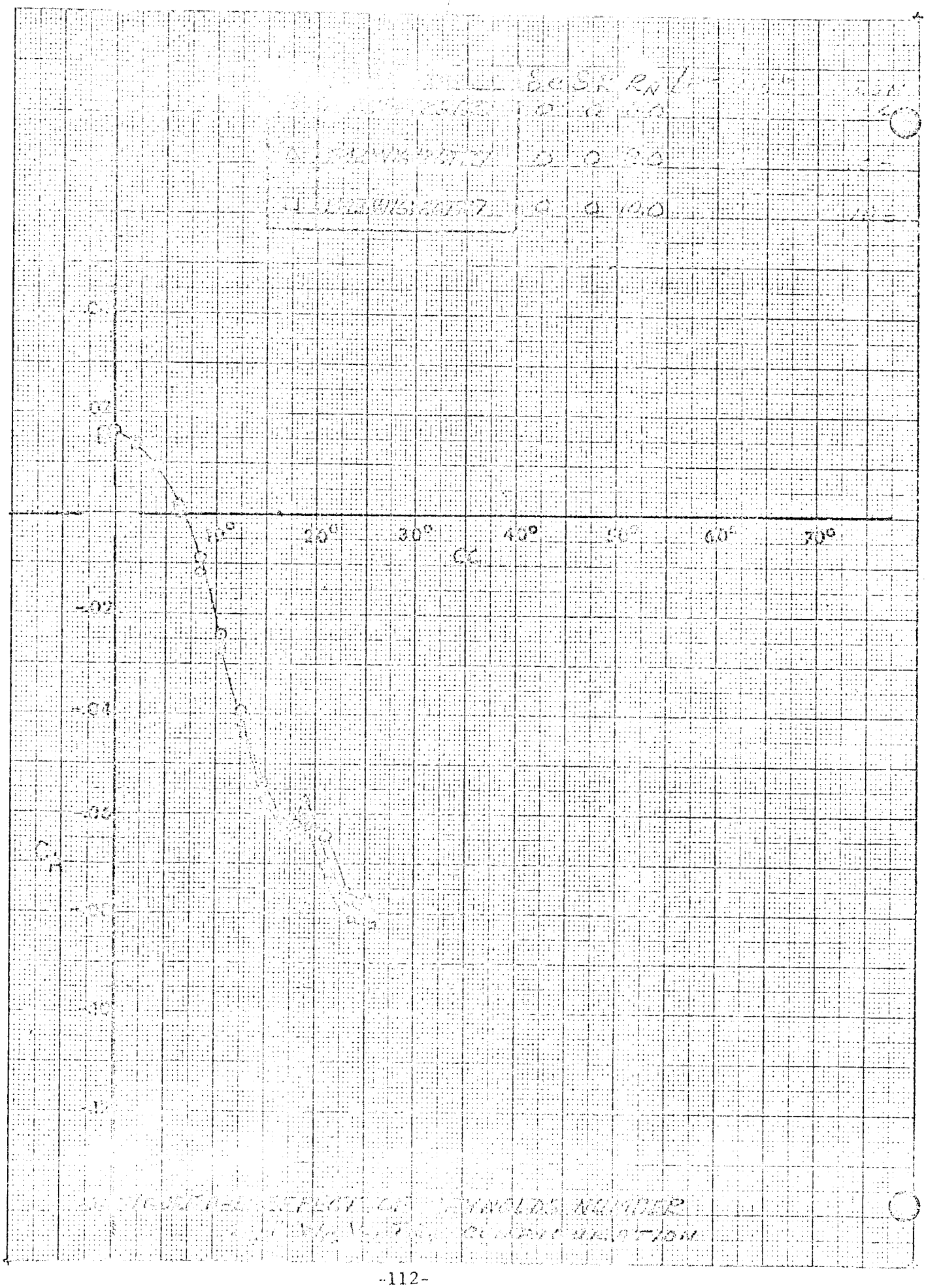
10°
20°
30°
40°
50°
60°
70°
α

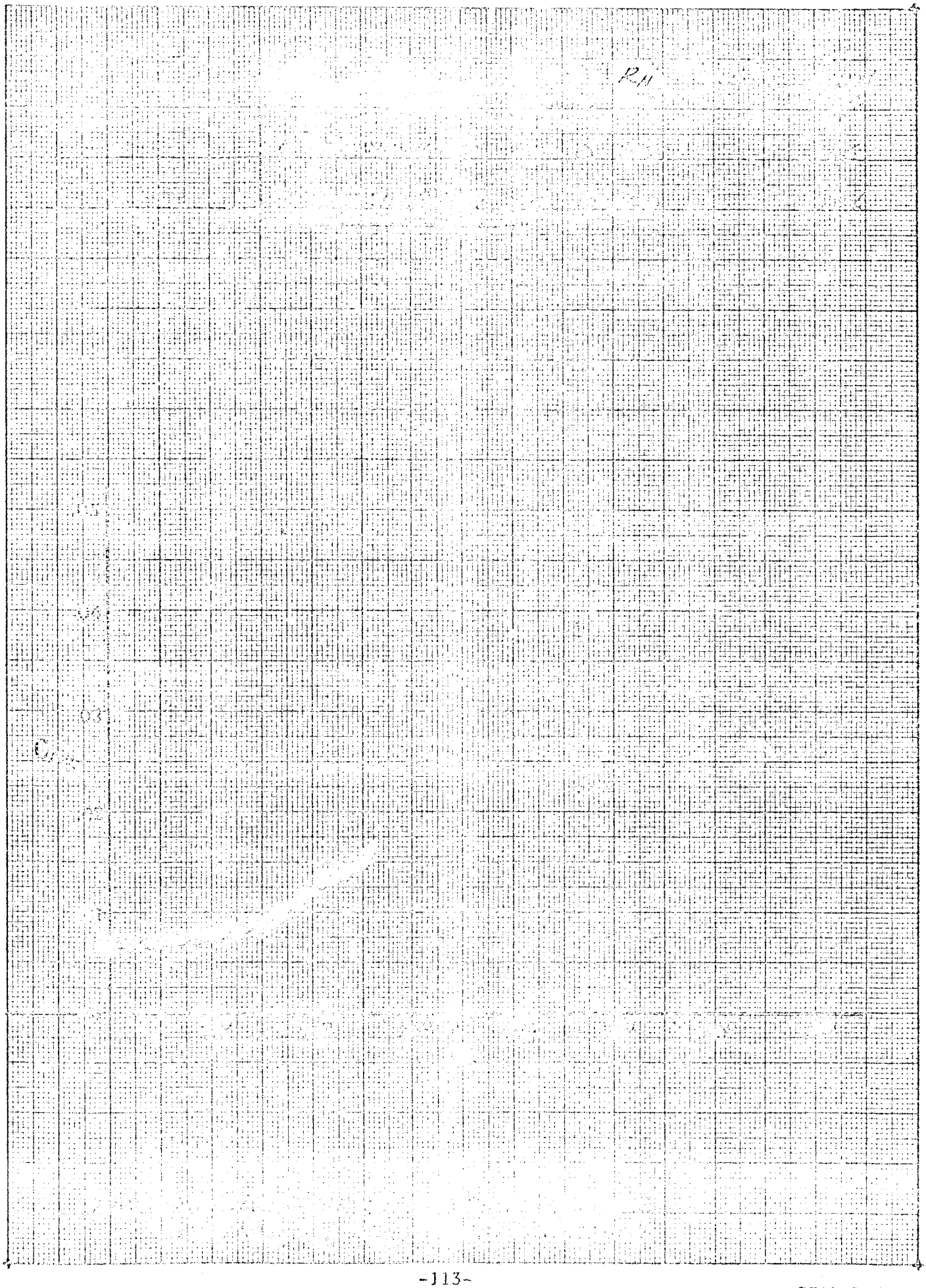

10 X 10 TO THE CENTIMETER 46 1517
10 X 25 CM. • ALBANENE
KEUFFEL & ESSER CO.

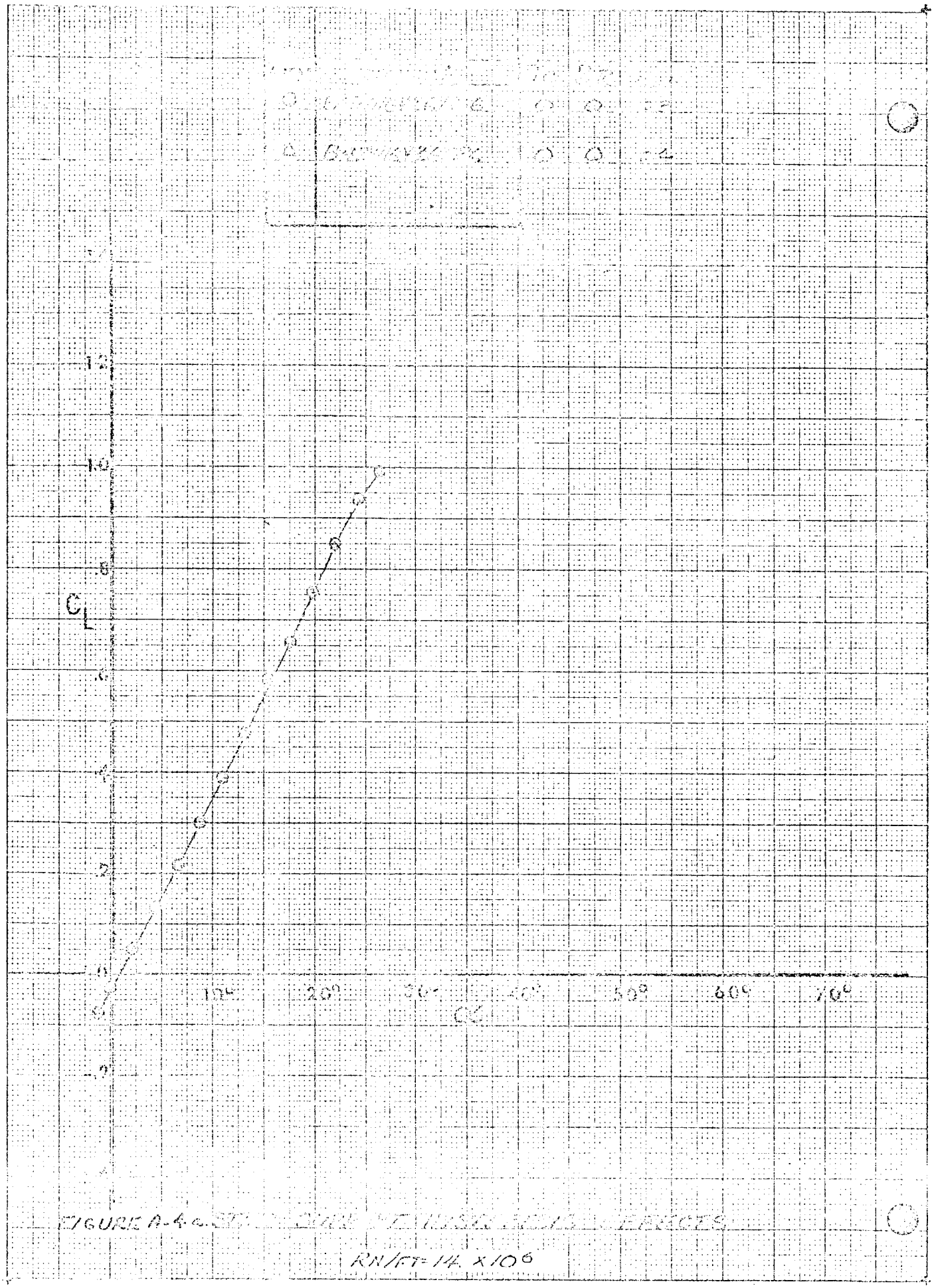

FIGURE A-4a. [illegible] EFFECTS

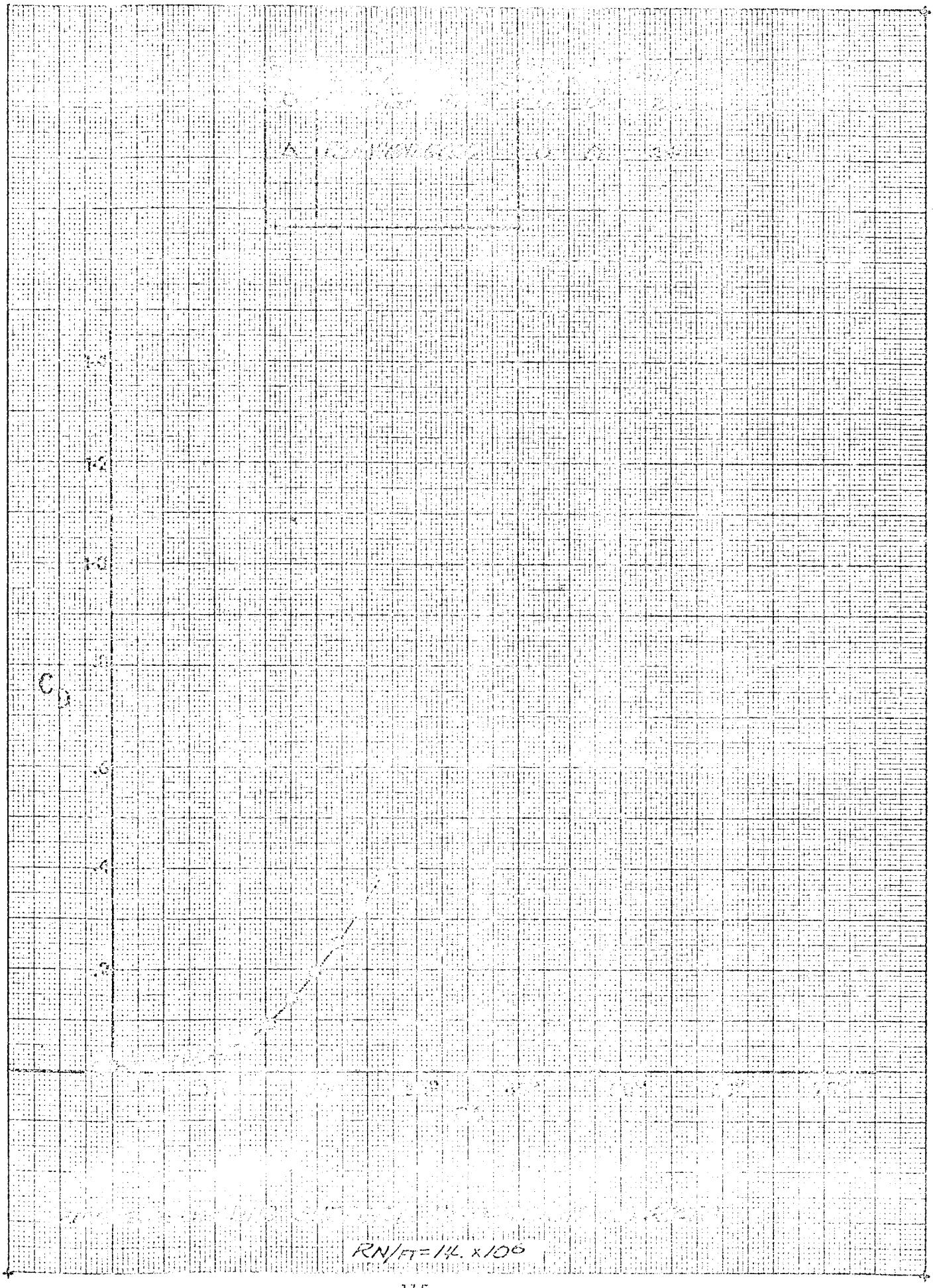
C_D
RN/FT = 14. x 10^6

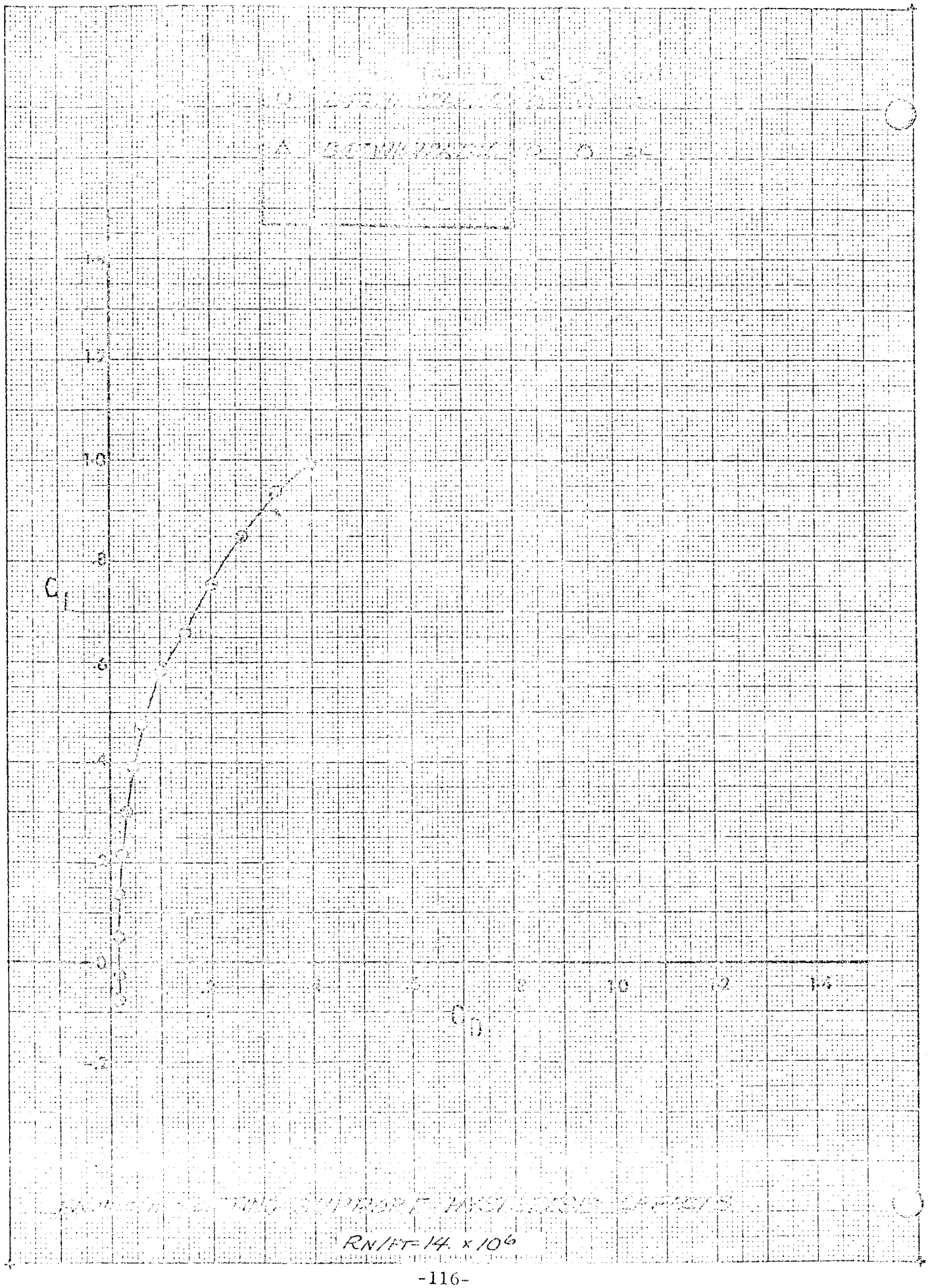
C_L
C_D
RN/FT = 14 x 10^6

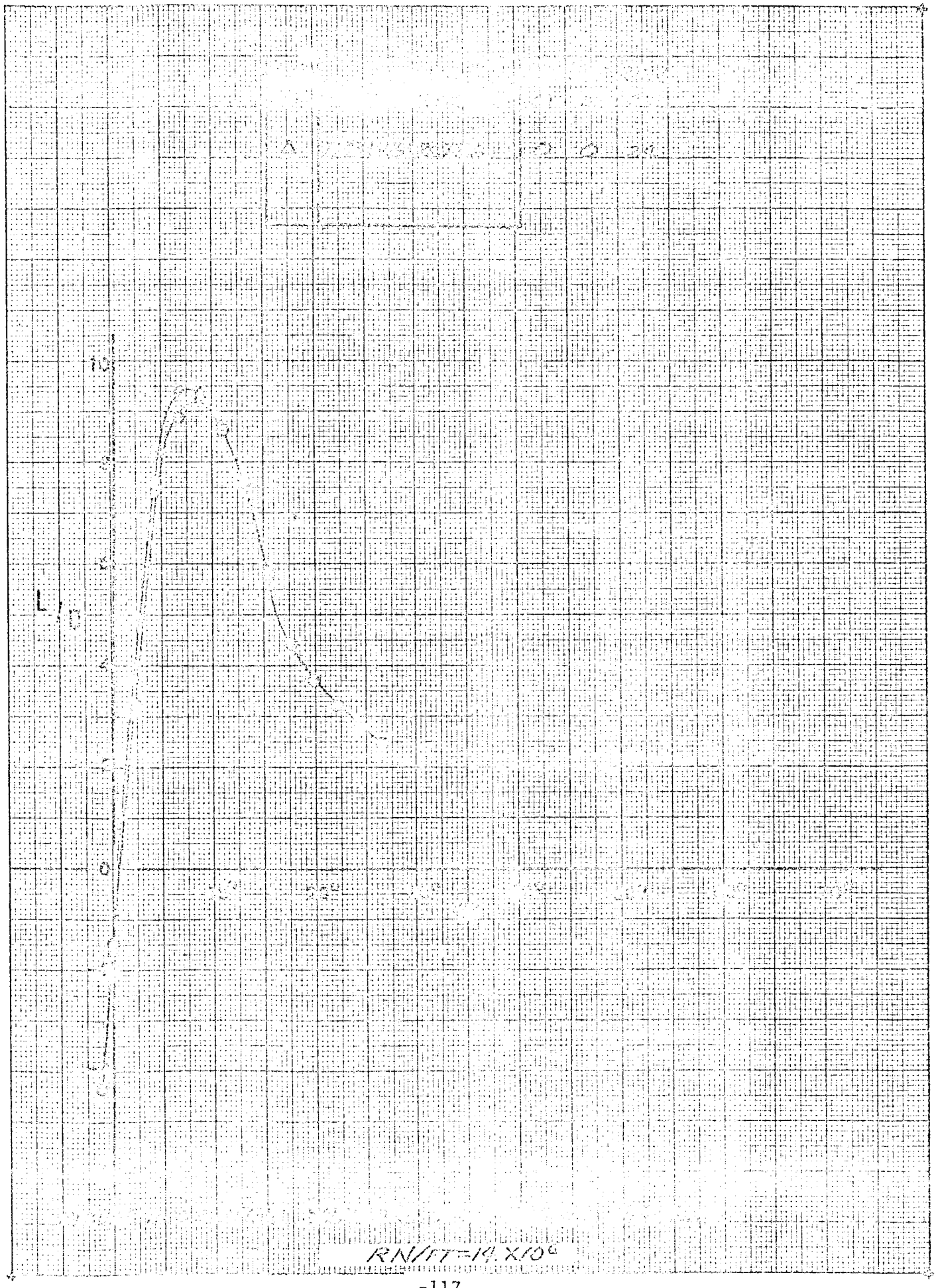
RN/FT=19 X10^6

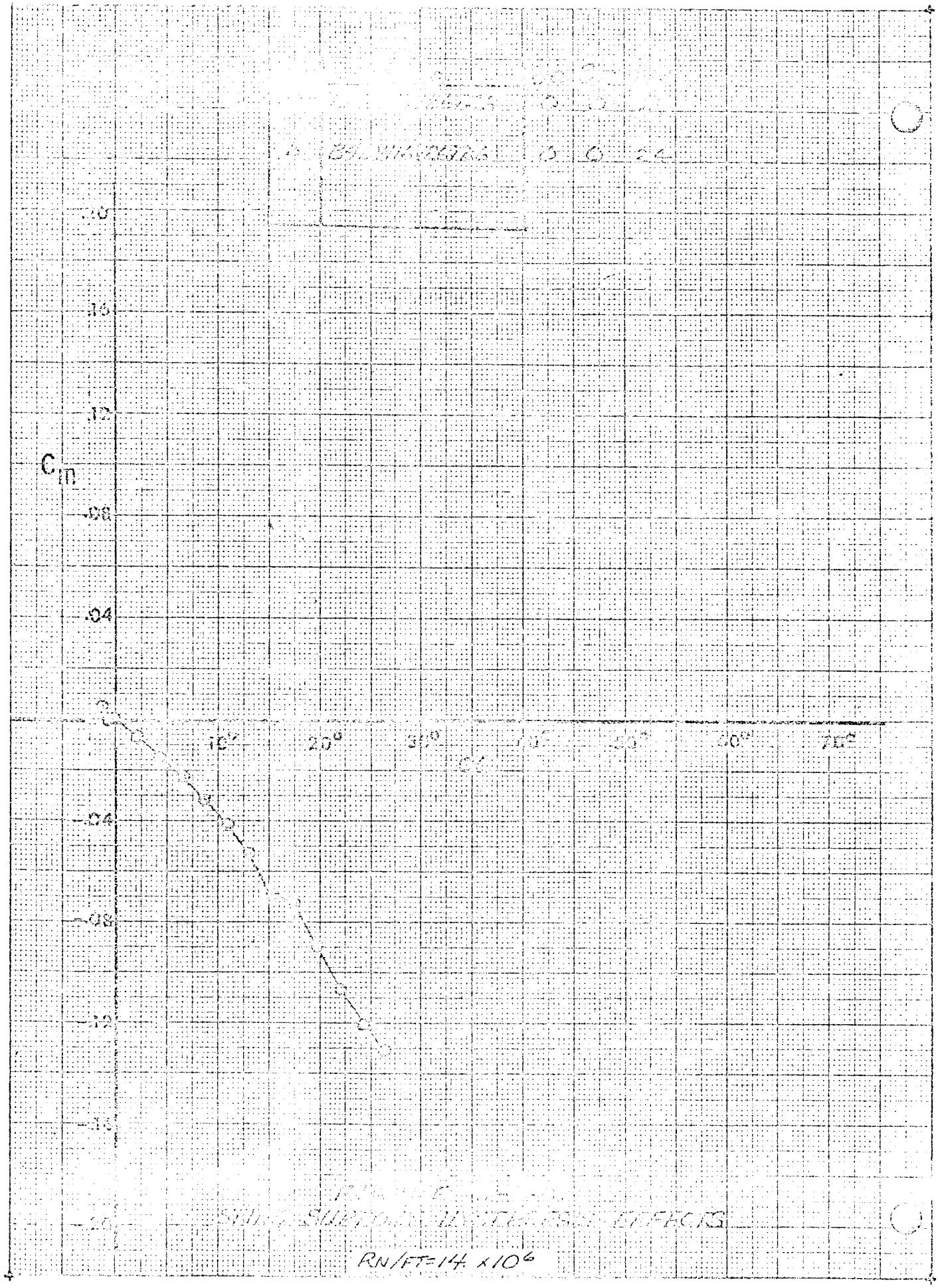
.20
.16
.12
C_m
.08
.04
0
10°
20°
30°
40°
50°
60°
70°
-.04
-.08
-.12
-.16
-.20
RN/FT=14 x10^6

260

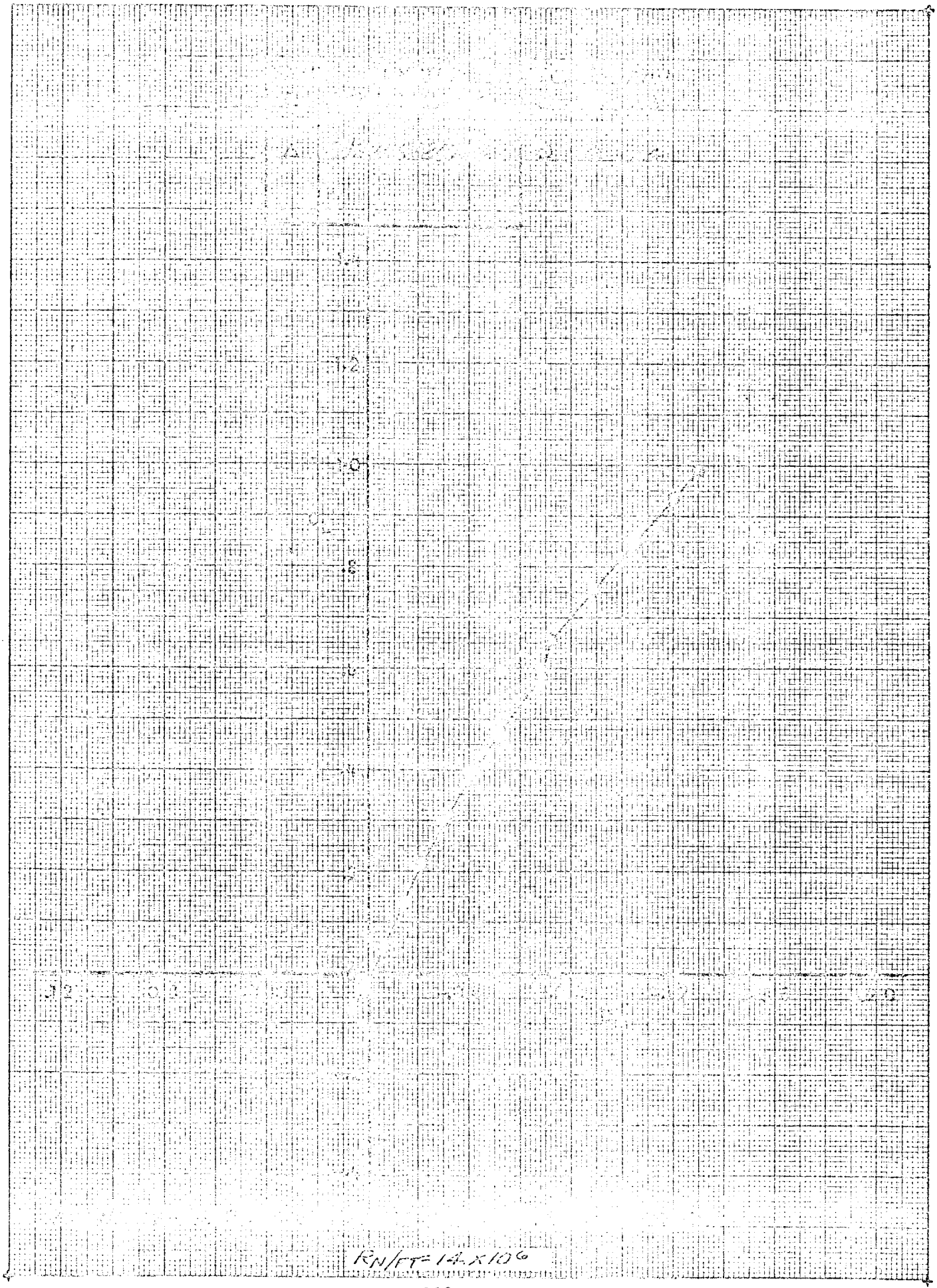

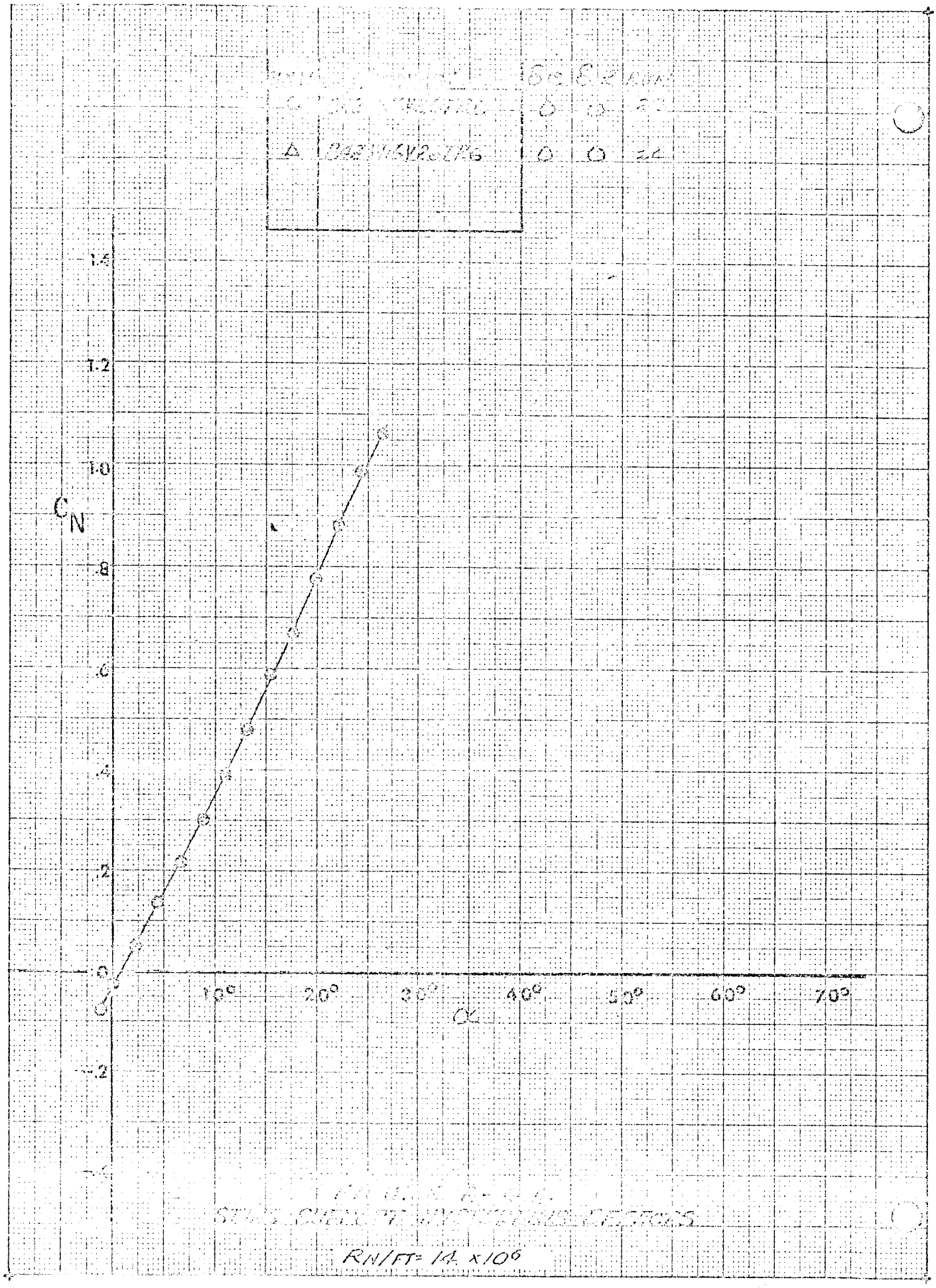
1.4
1.2
1.0
C_N
.8
.6
.4
.2
0
-.2
10°
20°
30°
40°
50°
60°
70°
α
RN/FT = 14 x 10^6

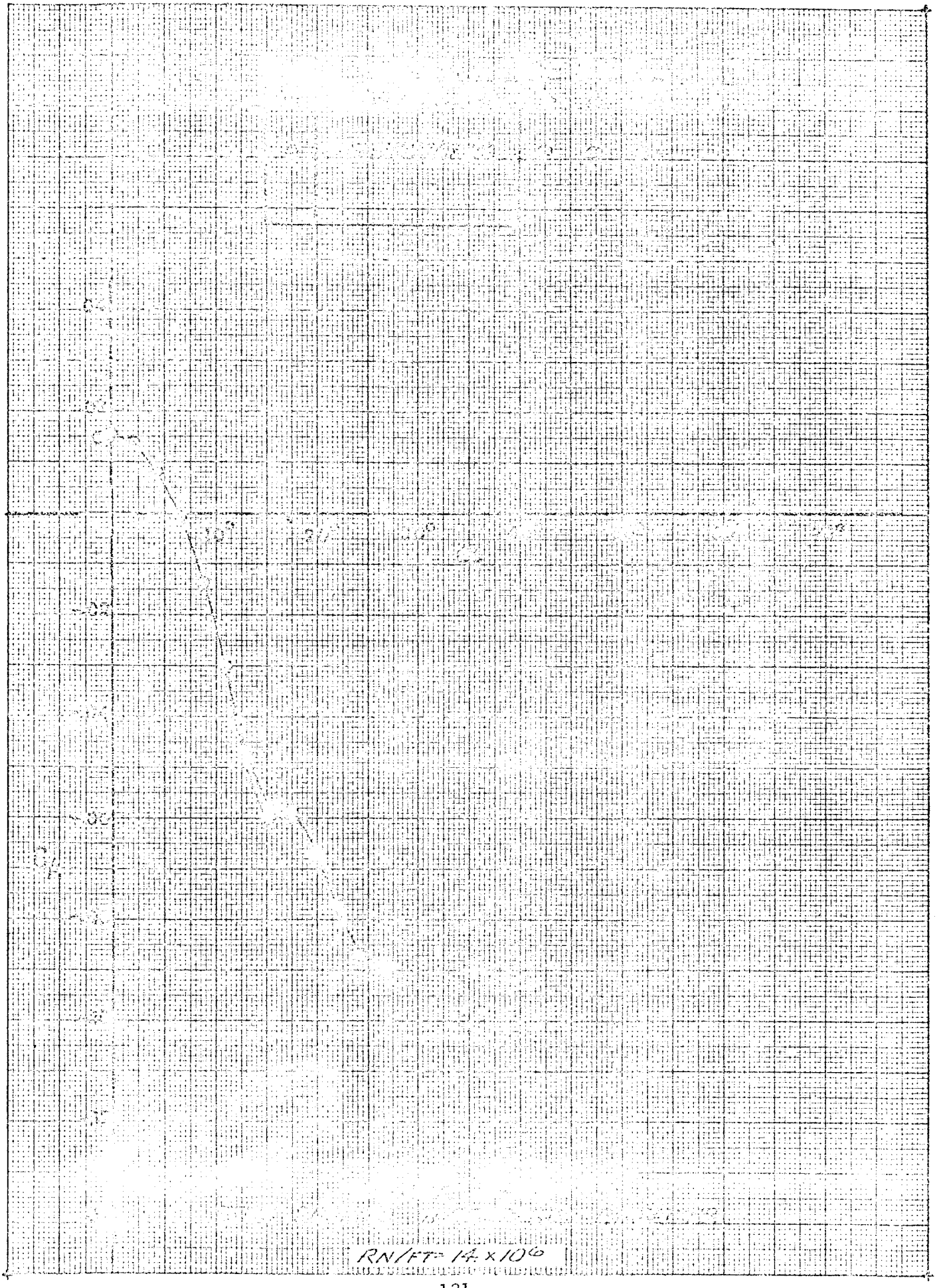

10 X 10 TO THE CENTIMETER 46 1517
18 X 25 CM. • ALBANENE
KEUFFEL & ESSER CO.

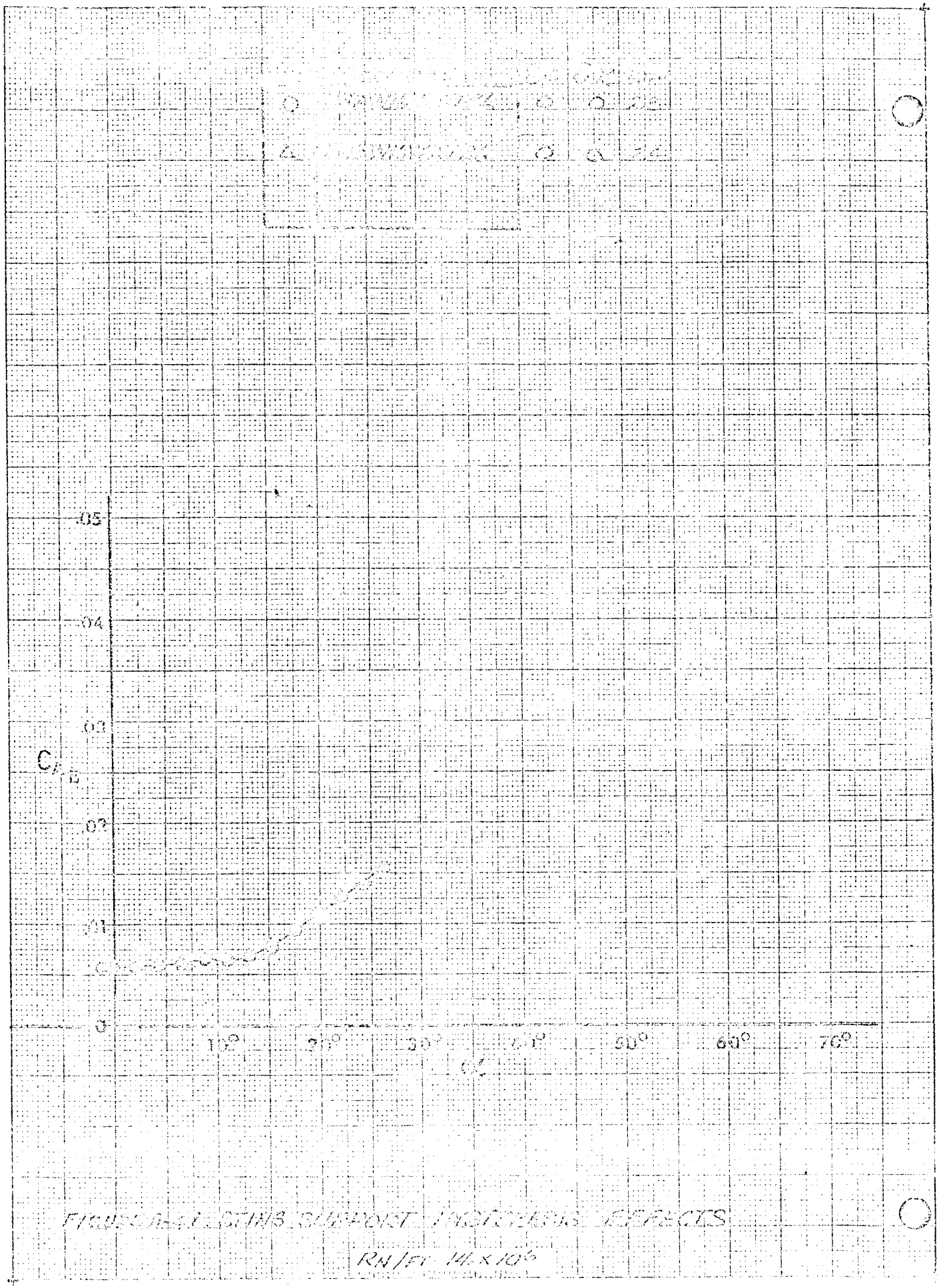

FIGURE A-11 STING SUPPORT INTERFERENCE EFFECTS

RN/FT 14 × 10⁶

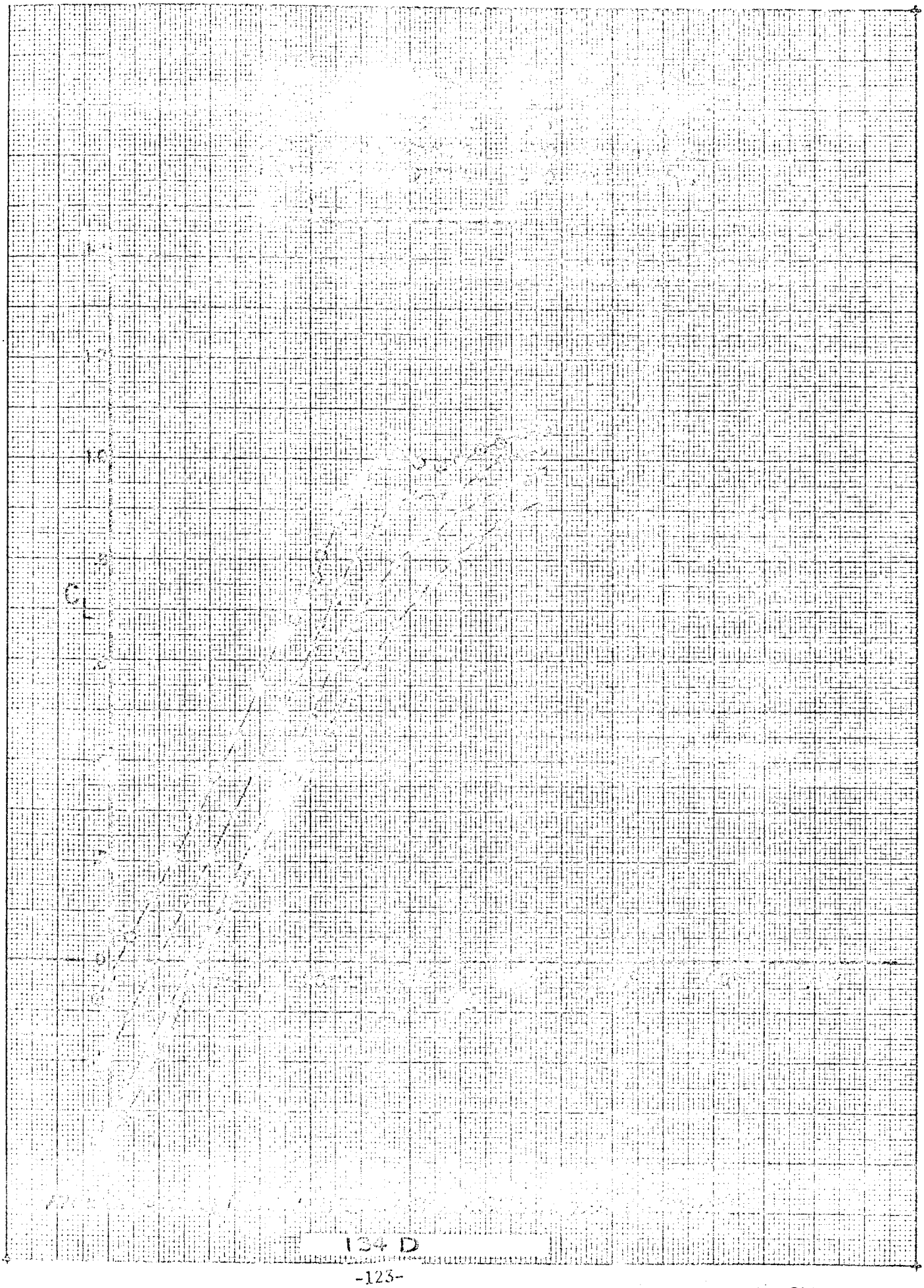
134 D

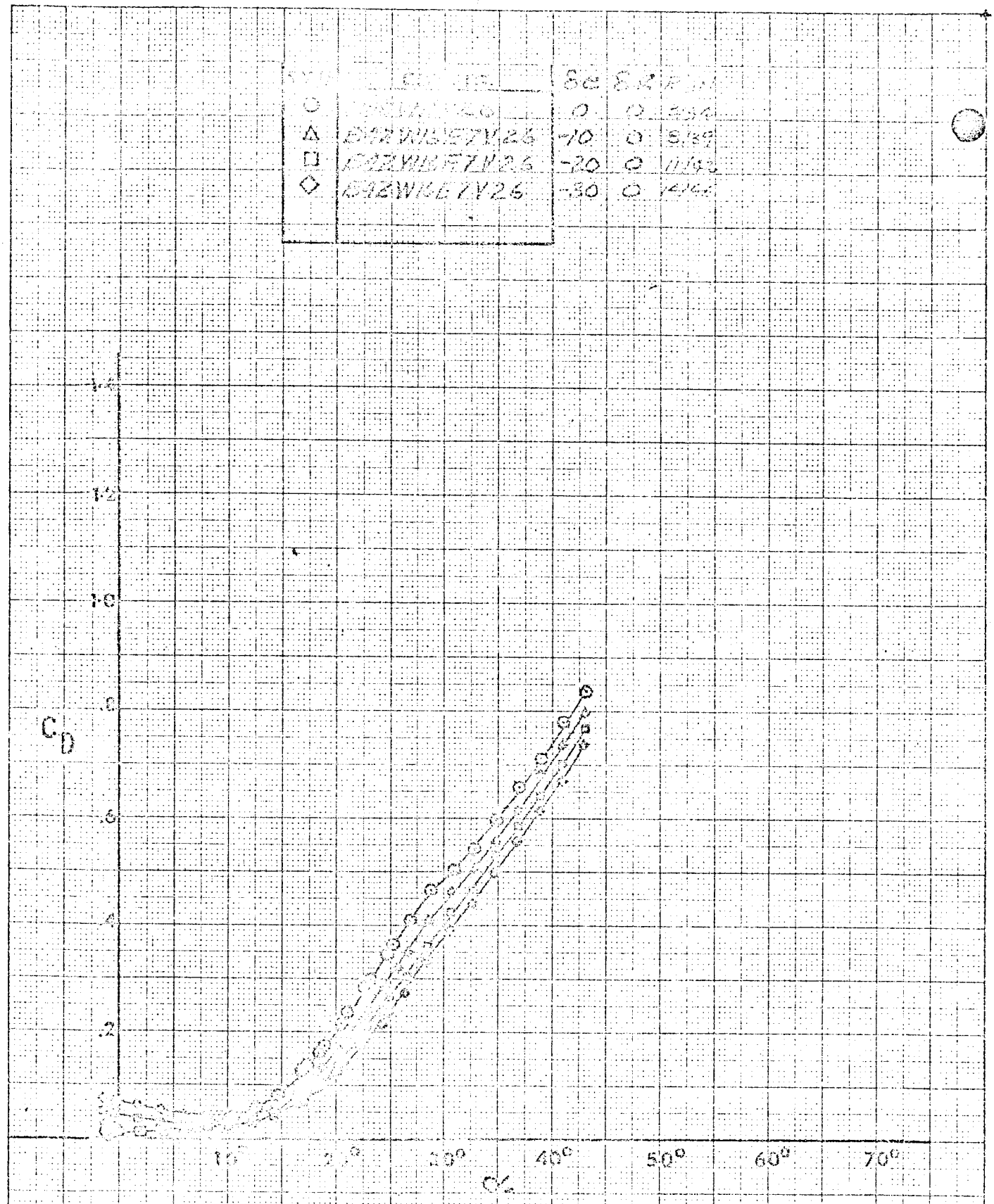

FIGURE 3. SPL ELEVON EFFECTIVENESS $RN/l = 6.0 \times 10^6$

134-D

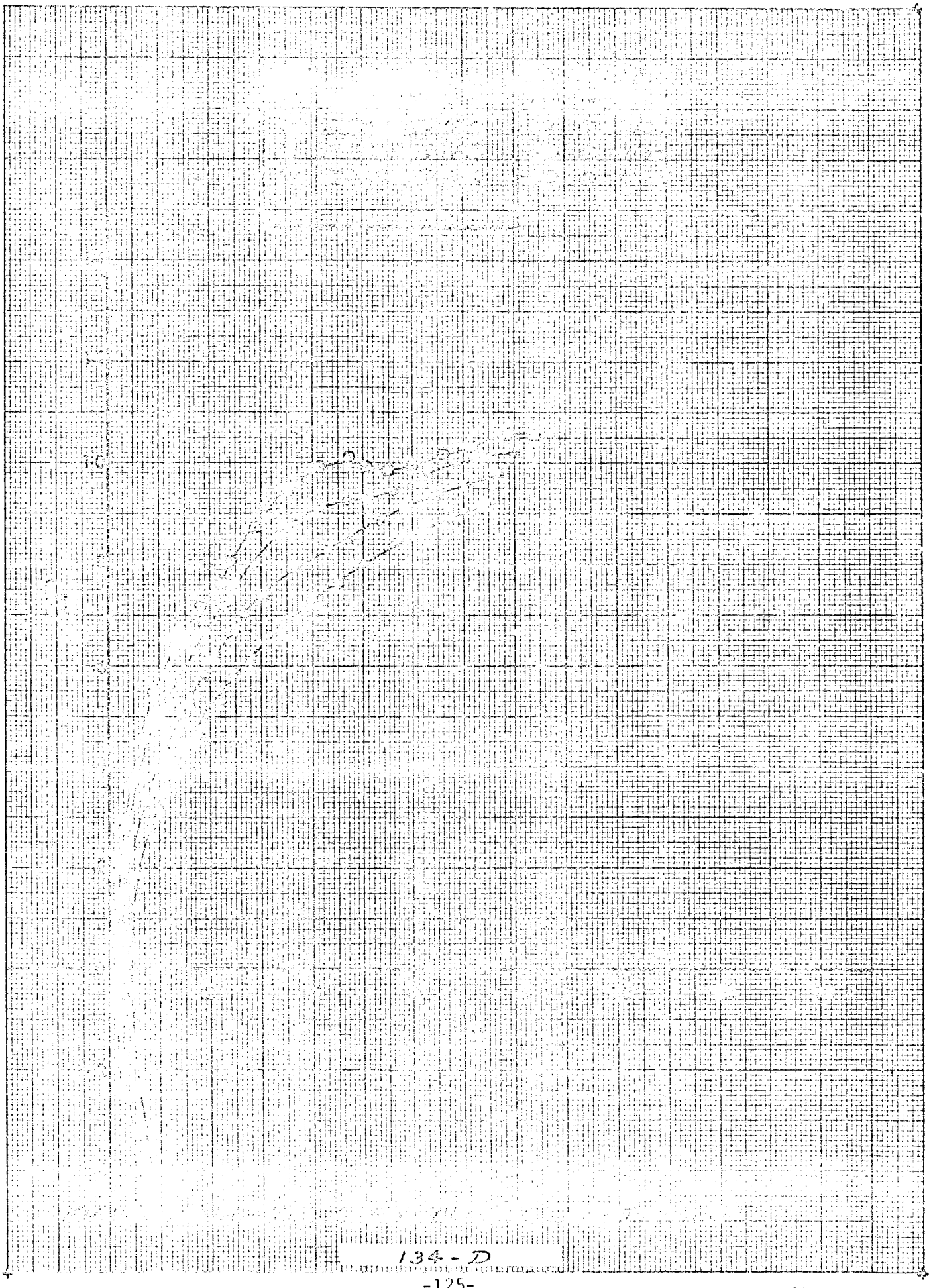

134-D

10 X 10 TO THE CENTIMETER 46 1517
18 X 25 CM • ALBANENE
KEUFFEL & ESSER CO.

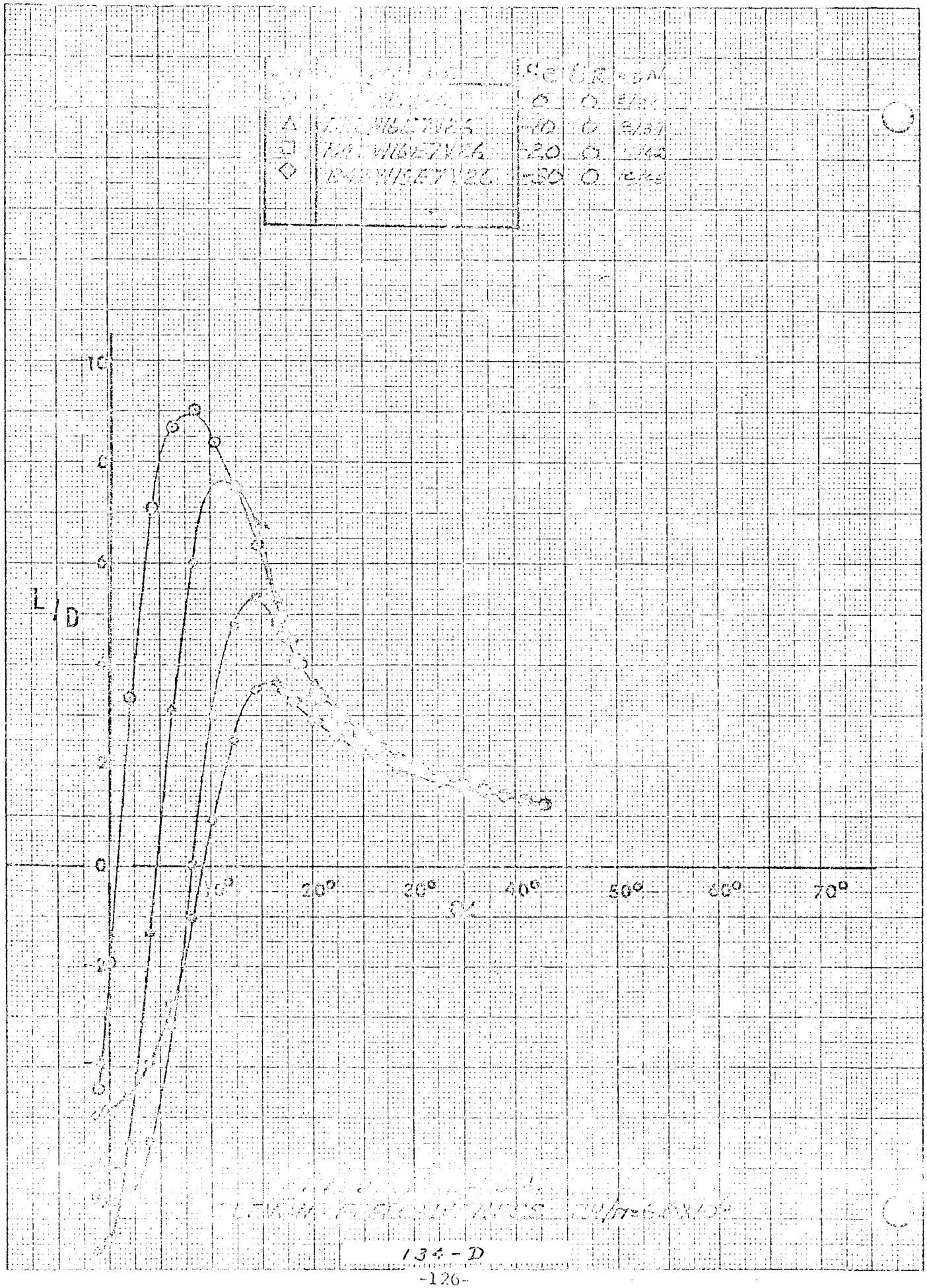

134 - D

10 X 10 TO THE CENTIMETER 46 1517
KEUFFEL & ESSER CO.

SD71-168

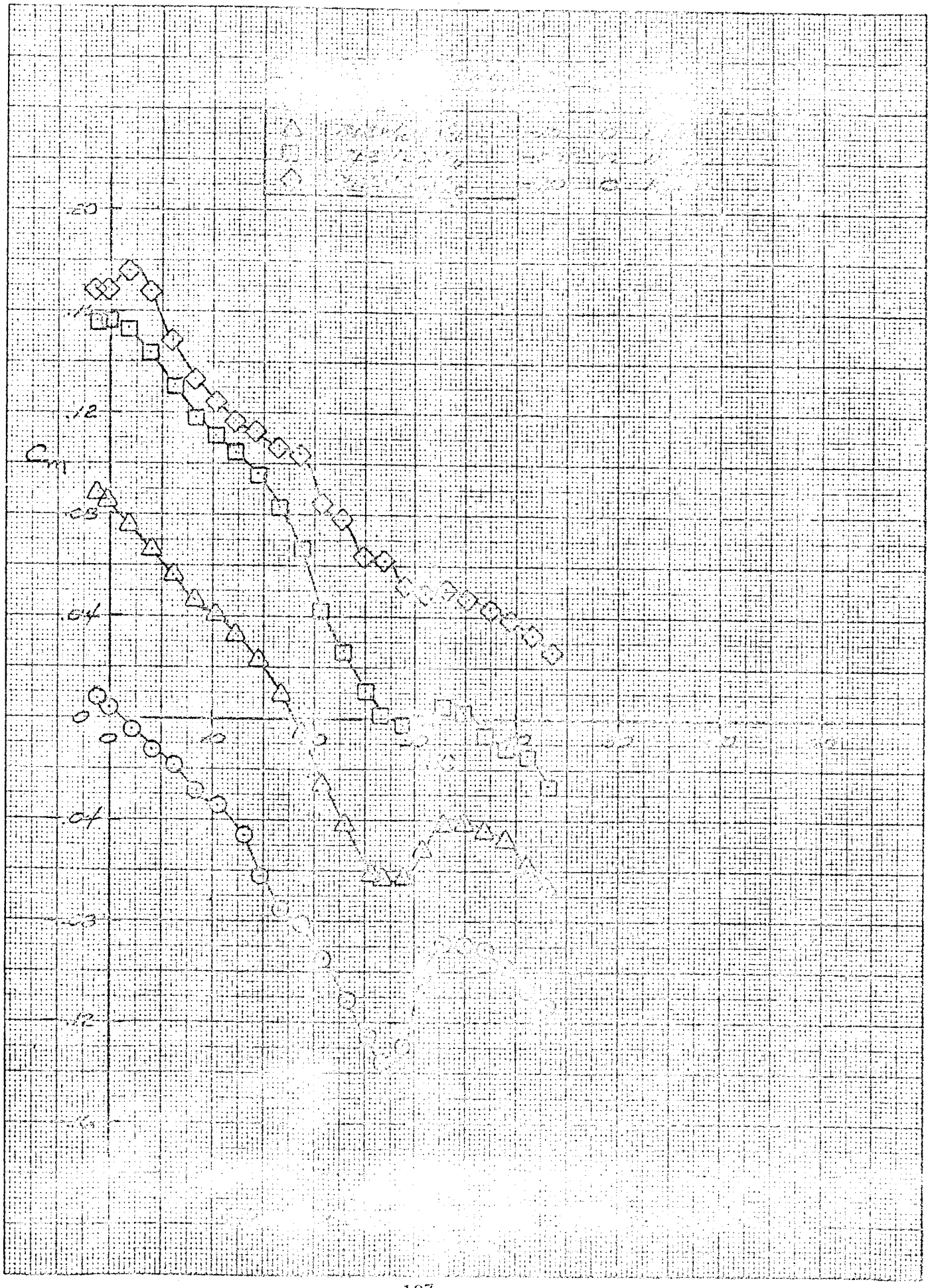
.20
.12
C_m
.03
.04
0
0
.04
.03
.12

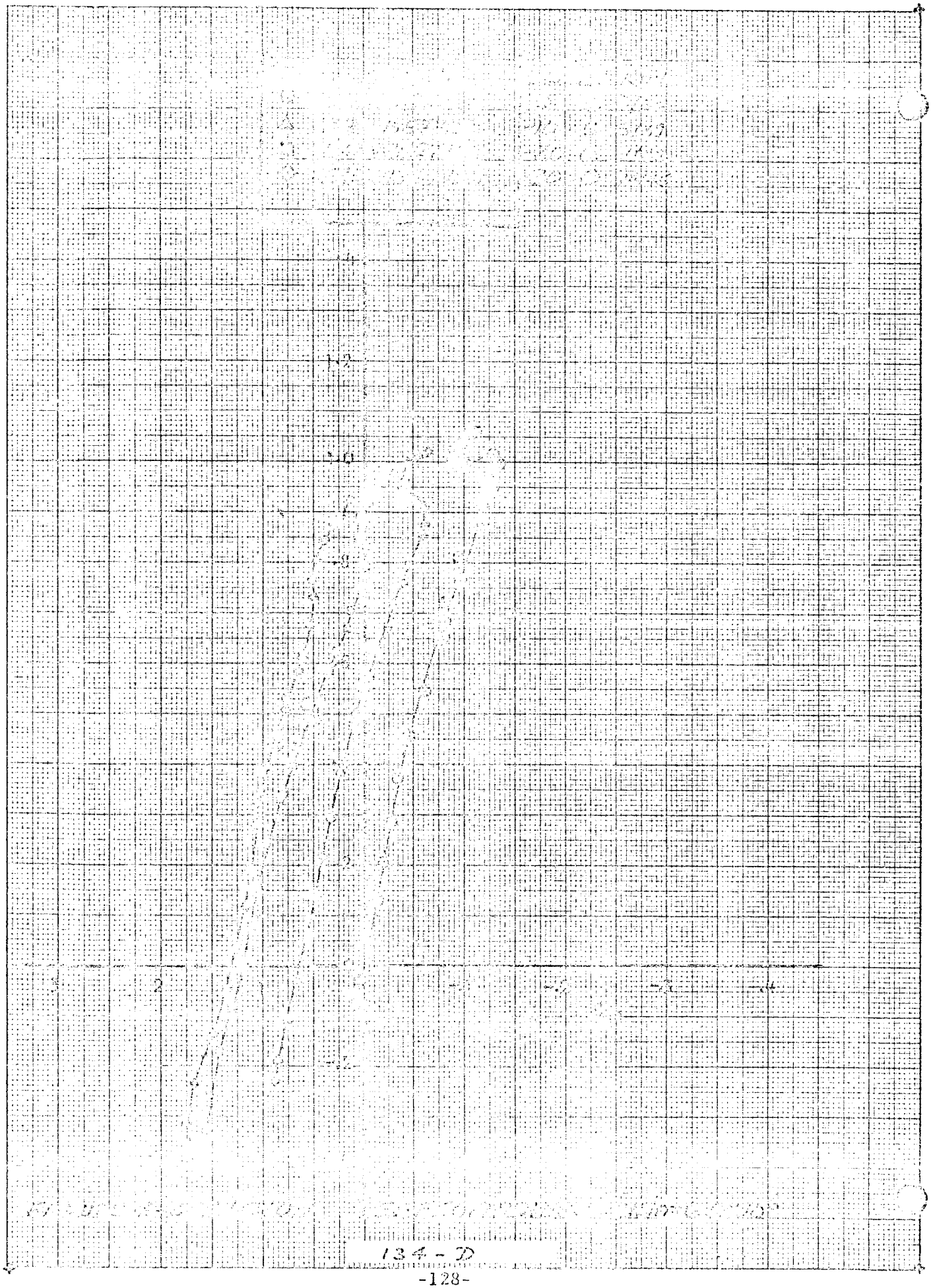

10 X 10 TO THE CENTIMETER • 46 1517
10 X 25 CM. • ALBANENE
KEUFFEL & ESSER CO.

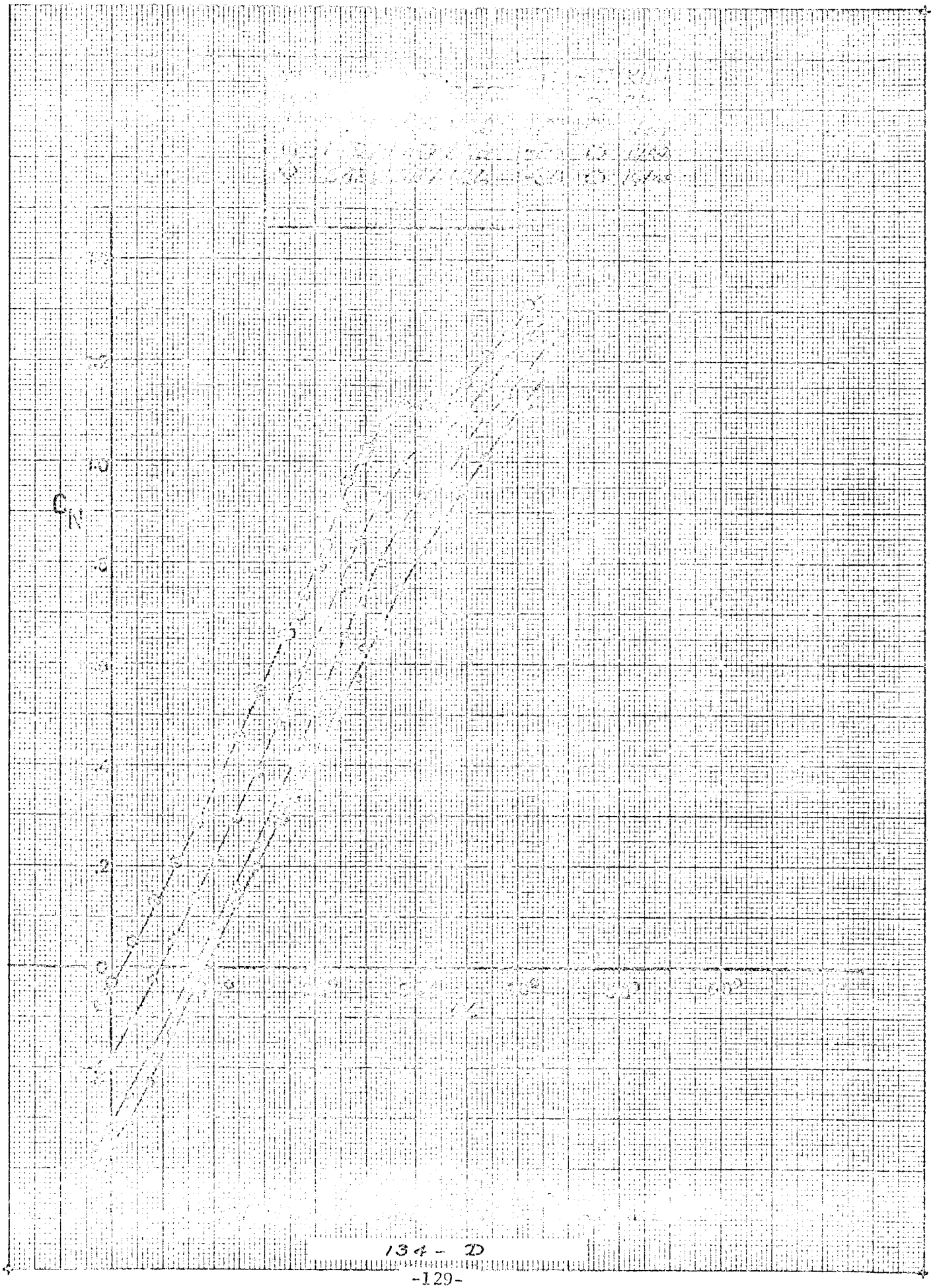

K&E 10 X 10 TO THE CENTIMETER 46 1517
13 X 25 CM. • ALBANENE®
KEUFFEL & ESSER CO.
MADE IN U.S.A.

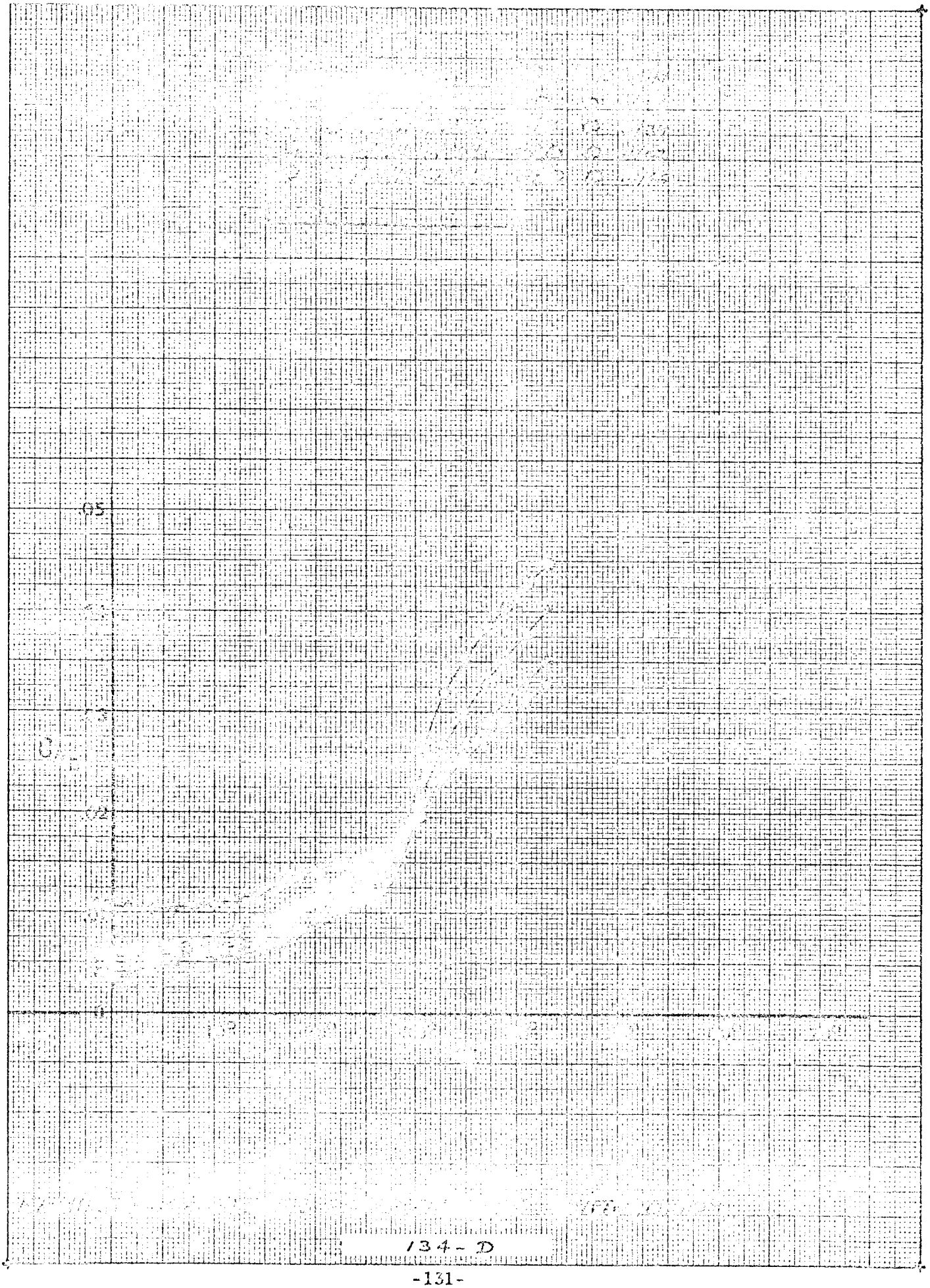

10 X 10 TO THE CENTIMETER 46 1517
18 X 25 CM. • ALBANENE®
KEUFFEL & ESSER CO.

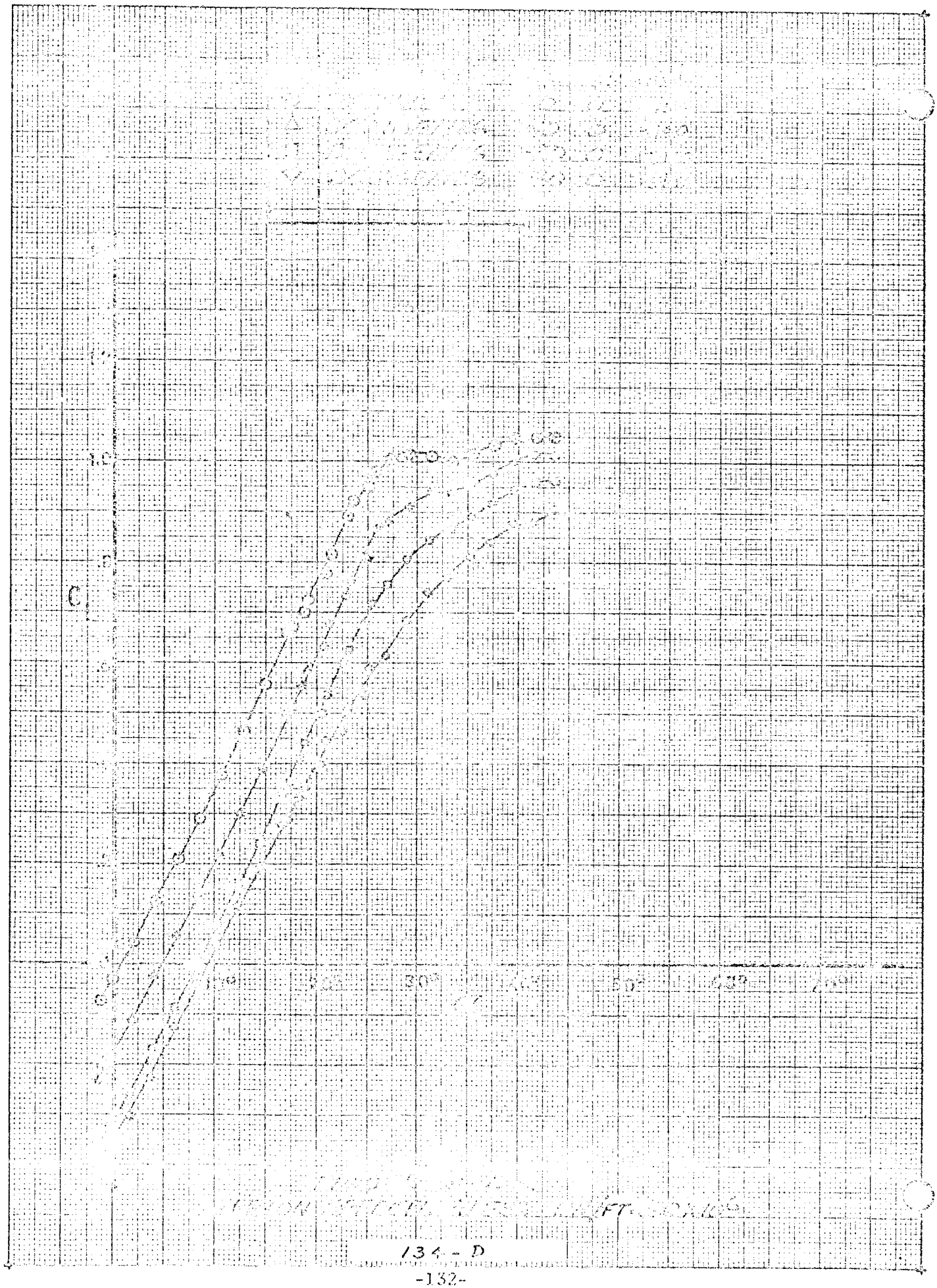

10 X 10 TO THE CENTIMETER. 46 1517
18 X 25 CM. • ALBANENE®
KEUFFEL & ESSER CO.

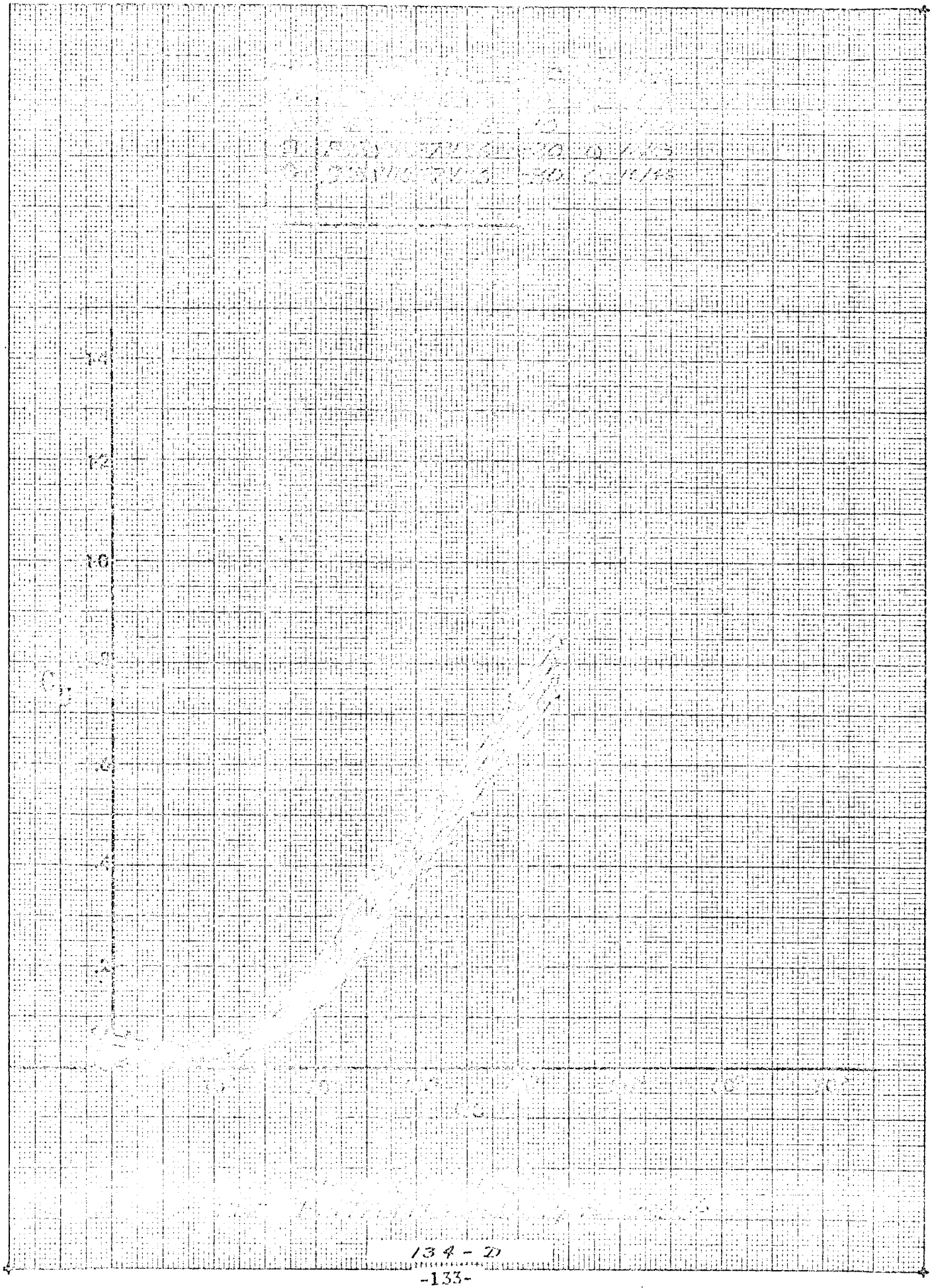

K&E 10 X 10 TO THE CENTIMETER 46 1517
19 X 25 CM. • ALBANENE
KEUFFEL & ESSER CO.

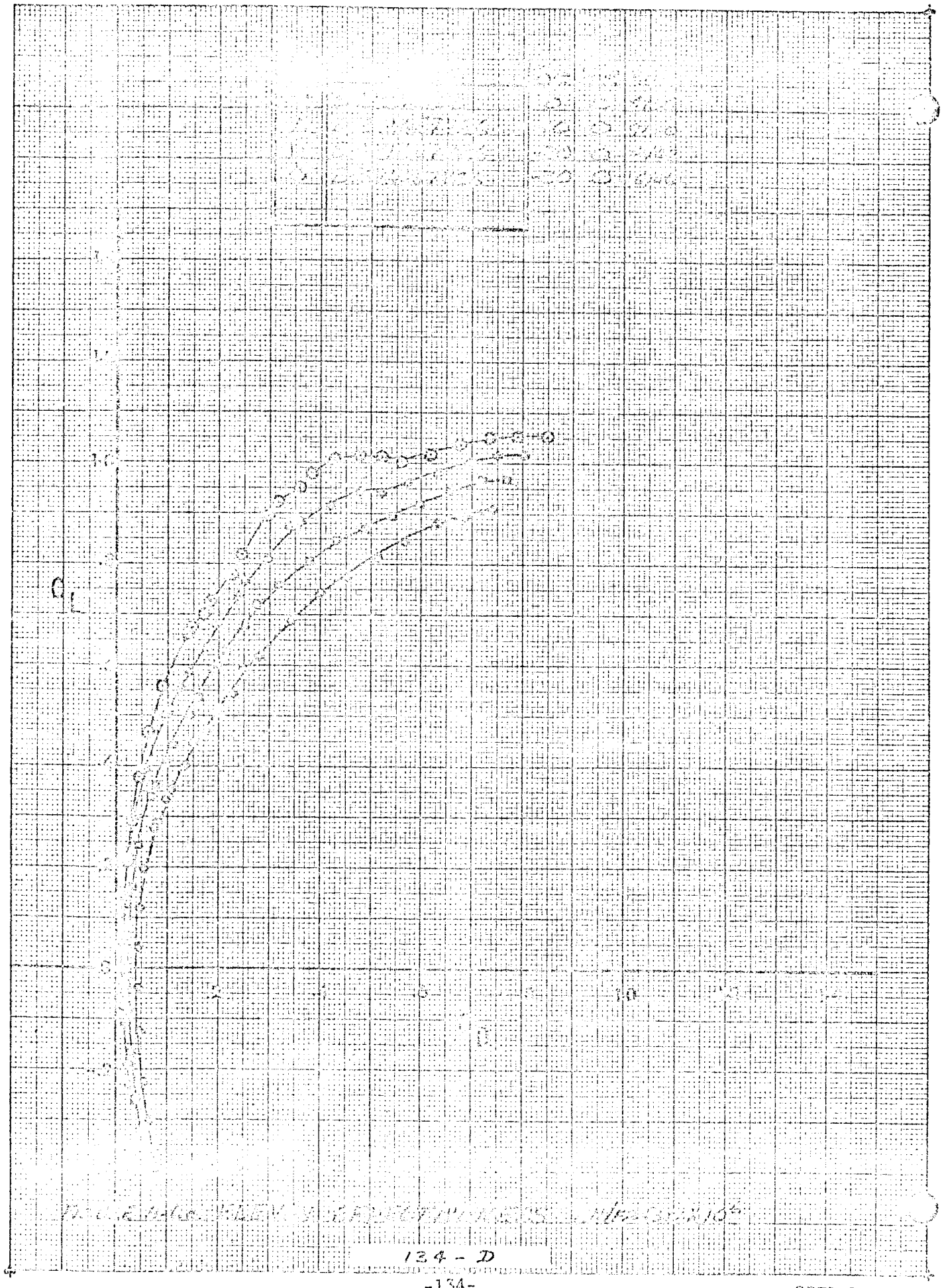

134 - D

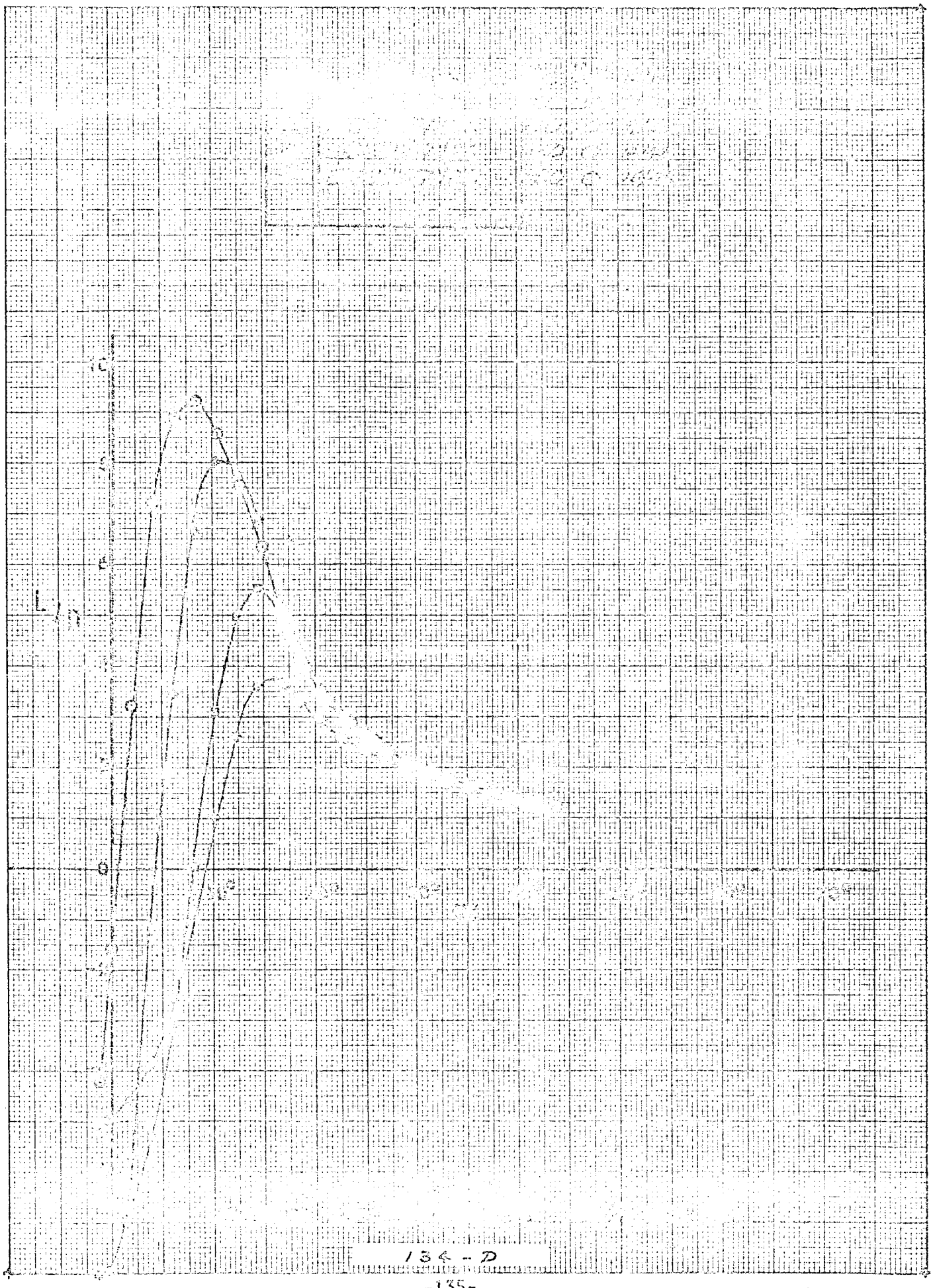
KEUFFEL & ESSER CO.
13 4 - D

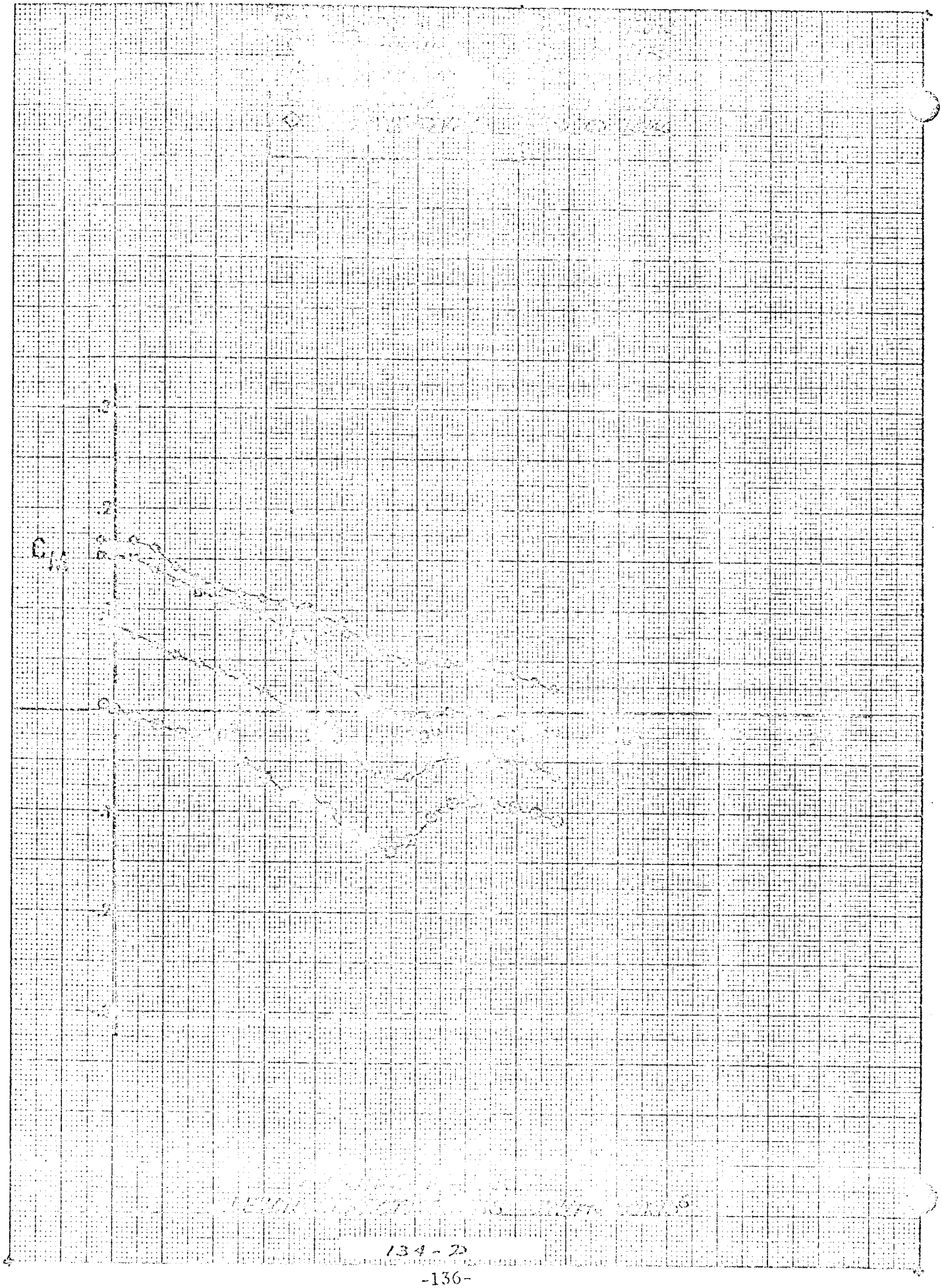

KEUFFEL & ESSER CO.

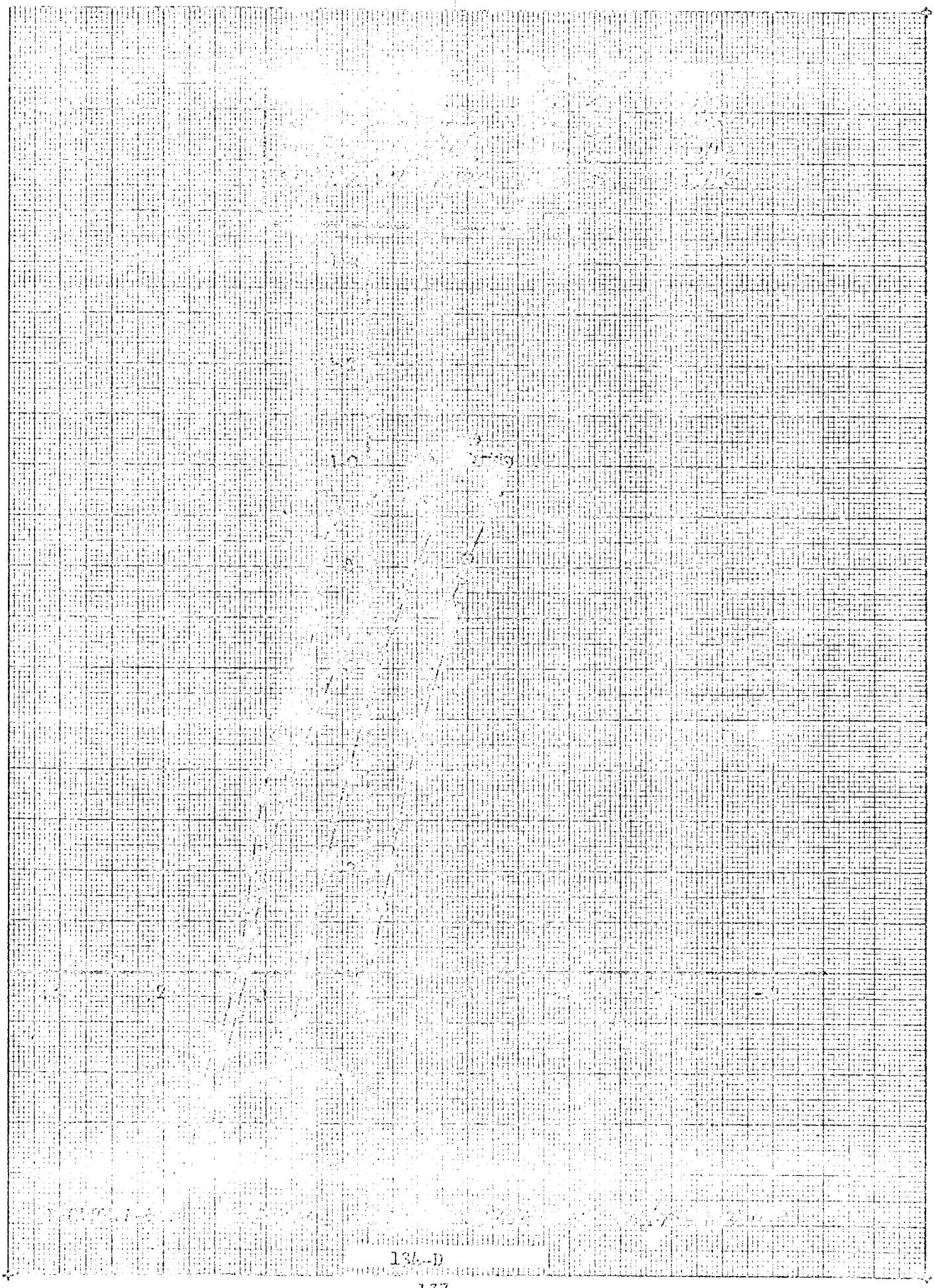

10 X 10 TO THE CENTIMETER 46 1517
18 X 25 CM. • ALBANENE®
KEUFFEL & ESSER CO.

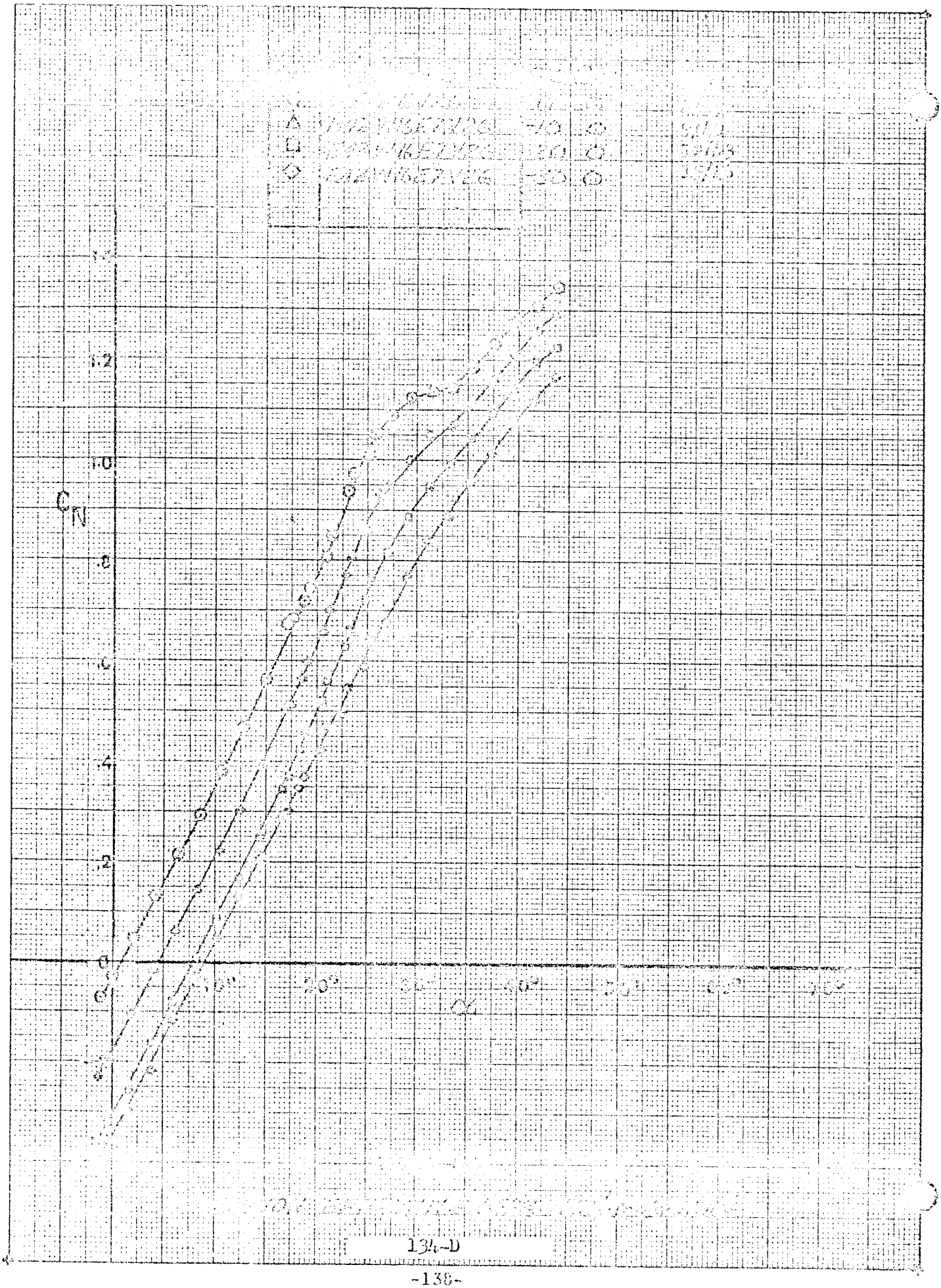

134-D

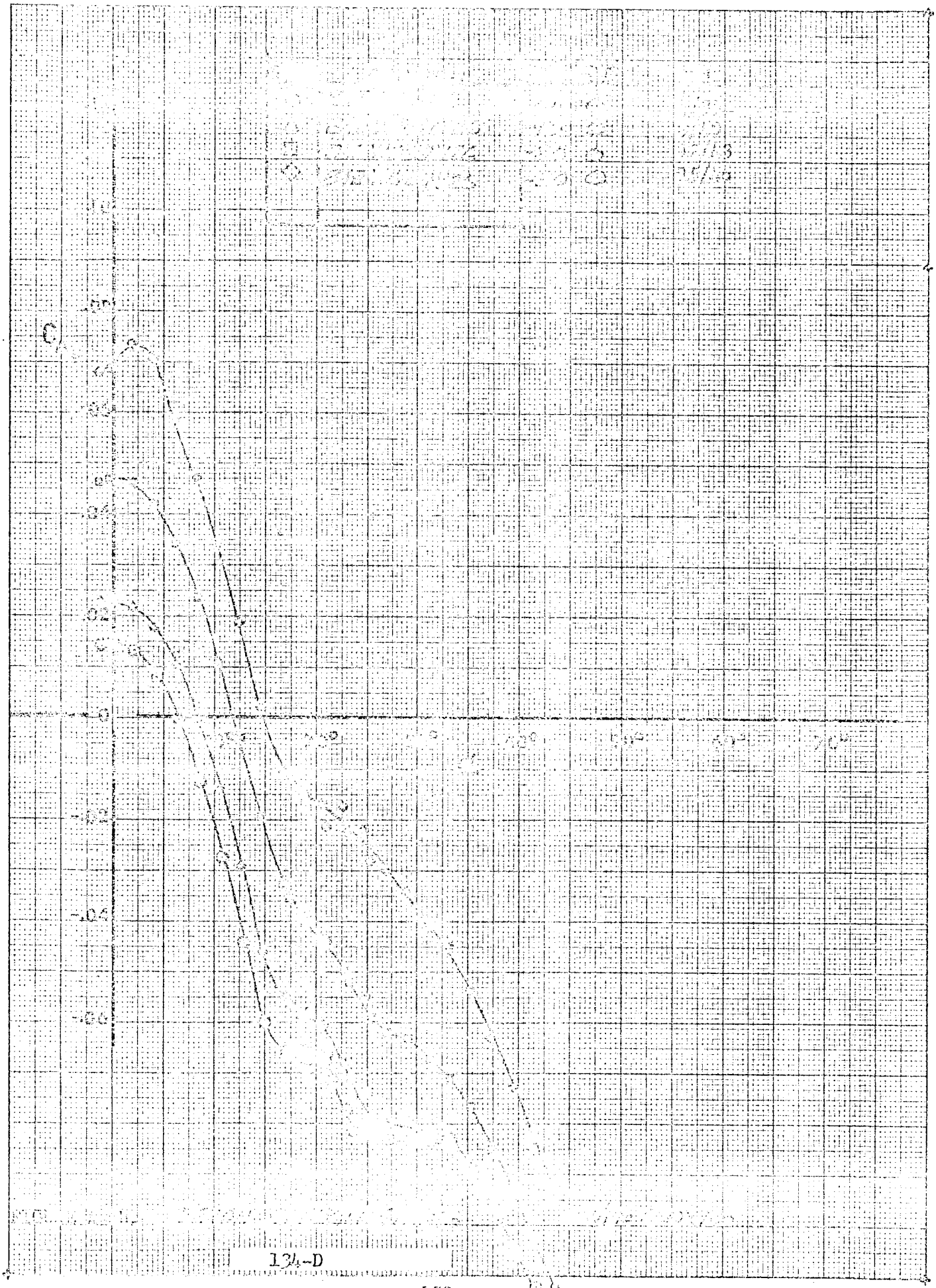

134-D

10 X 10 TO THE CENTIMETER 46 1517
18 X 25 CM. • ALBANY, N.Y.
KEUFFEL & ESSER CO.

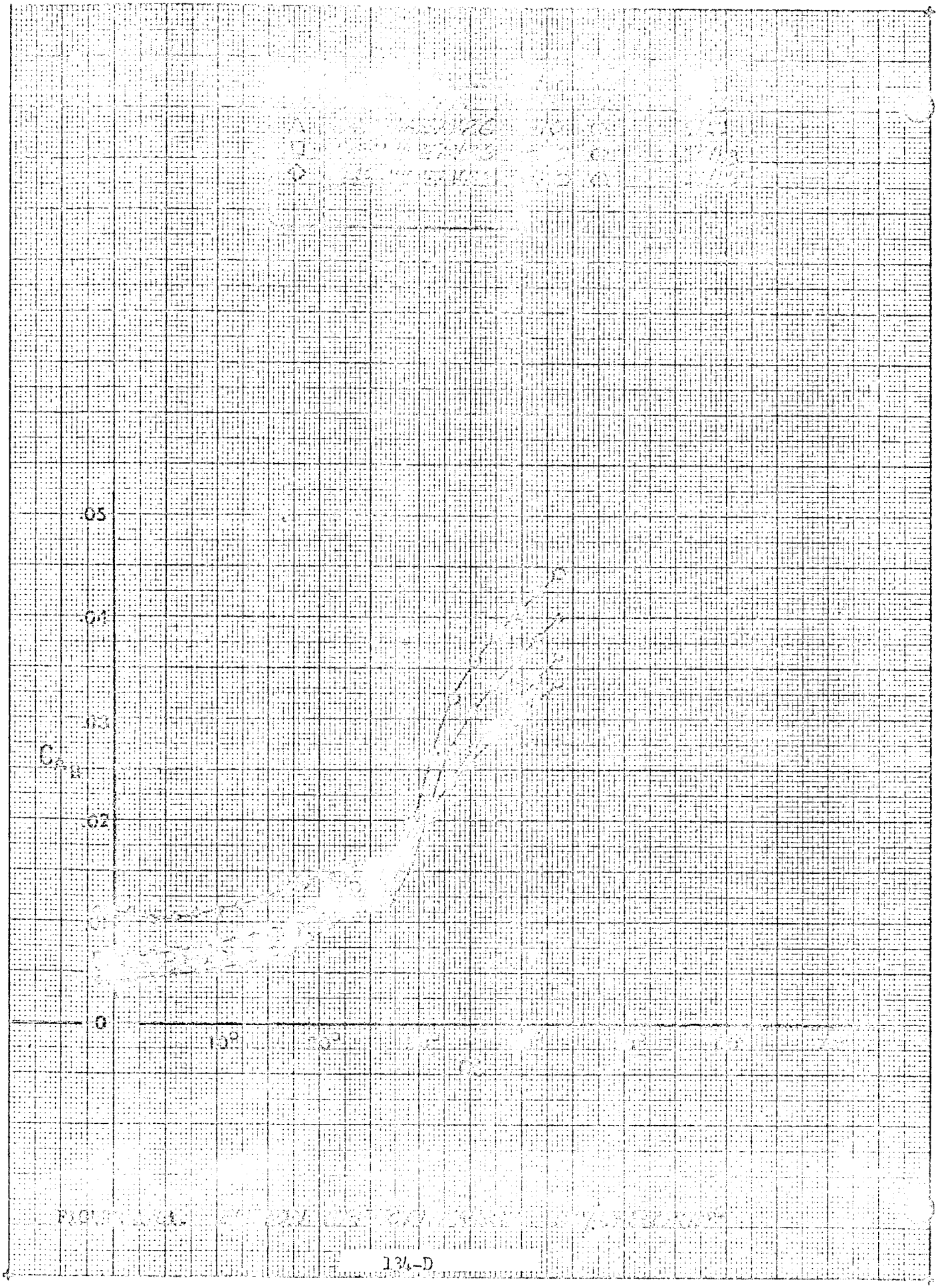

134-D

10 Y 10 TO THE CENTIMETER 46 1517
10 X 25 CM. • ALBANENE
KEUFFEL & ESSER CO.

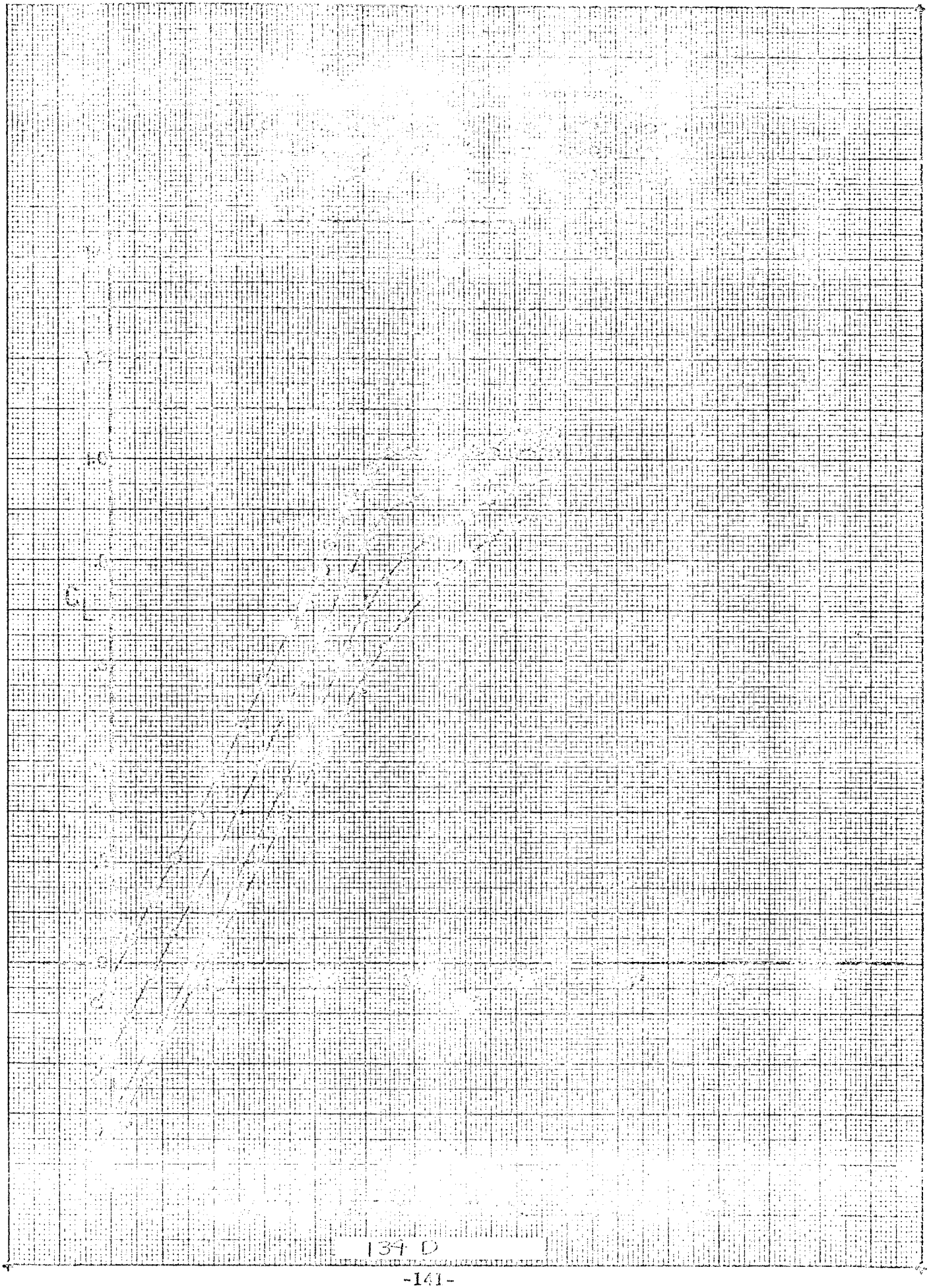

10 X 10 TO THE CENTIMETER 46 1517
11 X 25 CM. • ALBANENE
KEUFFEL & ESSER CO.

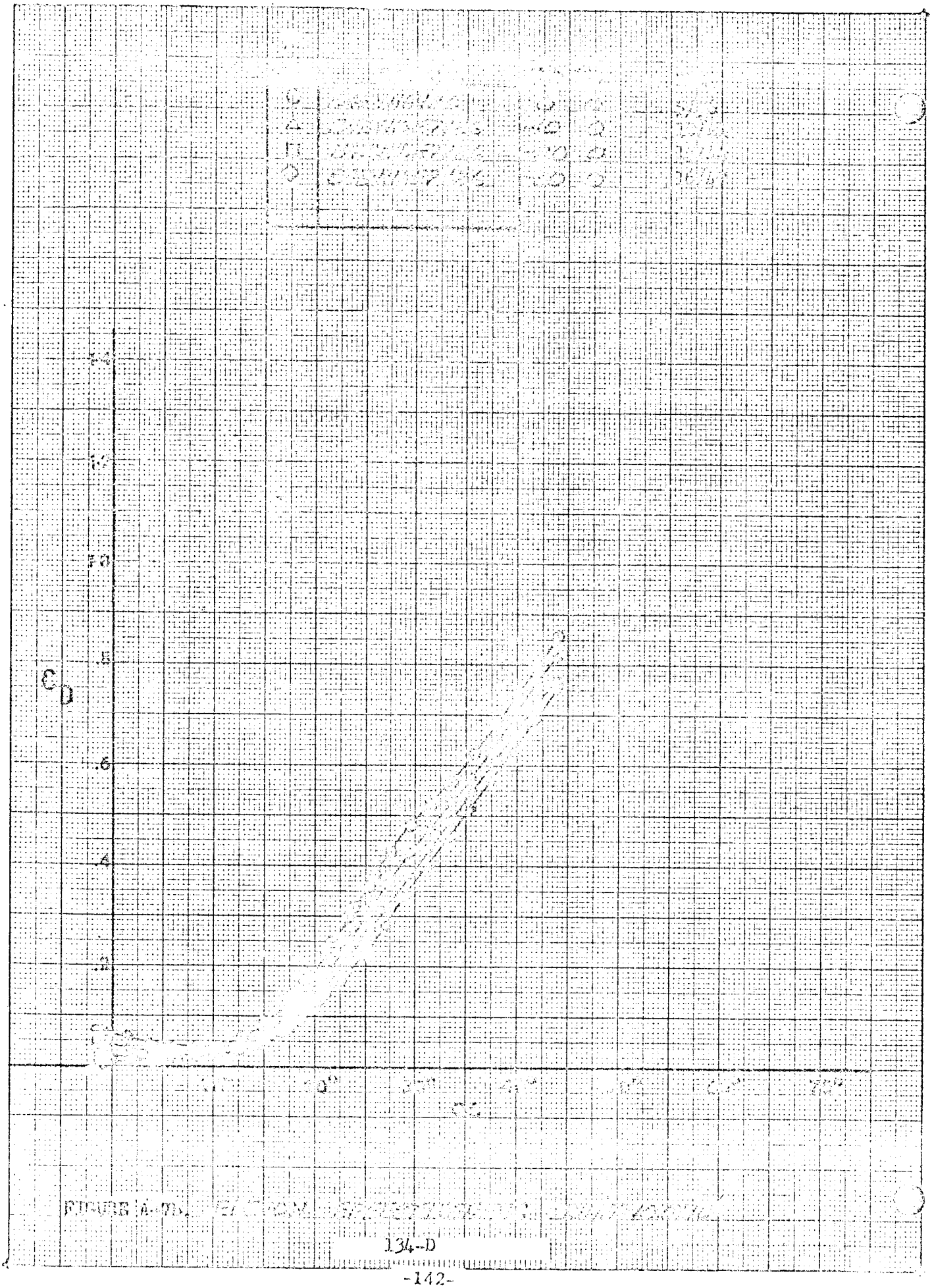

FIGURE A-7b

134-D

10 X 10 TO THE CENTIMETER 46 1517
KEUFFEL & ESSER CO.

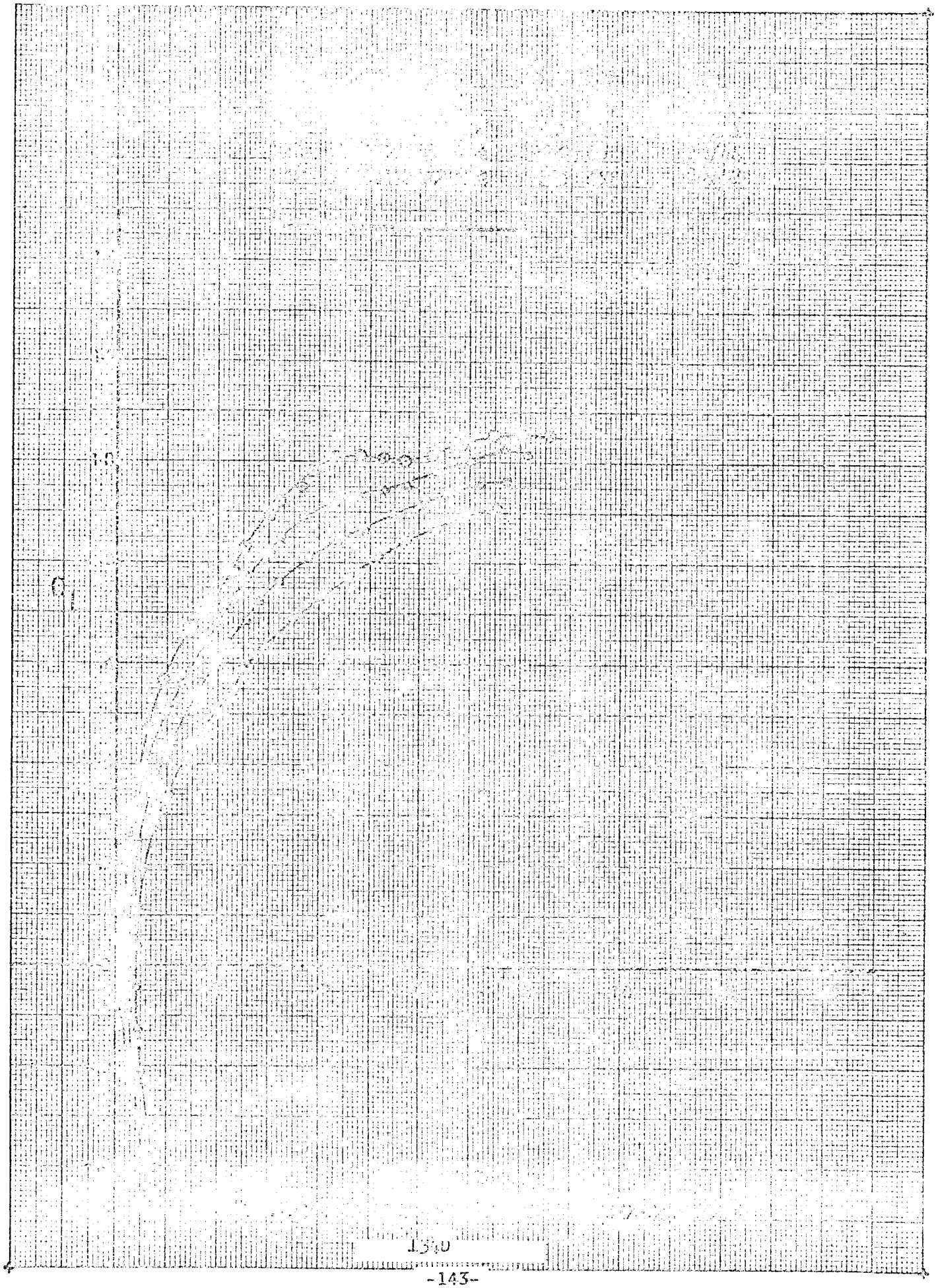

10 X 10 TO THE CENTIMETER 46 1517
18 X 25 CM. • ALBANENE
MADE IN U.S.A.
KEUFFEL & ESSER CO.

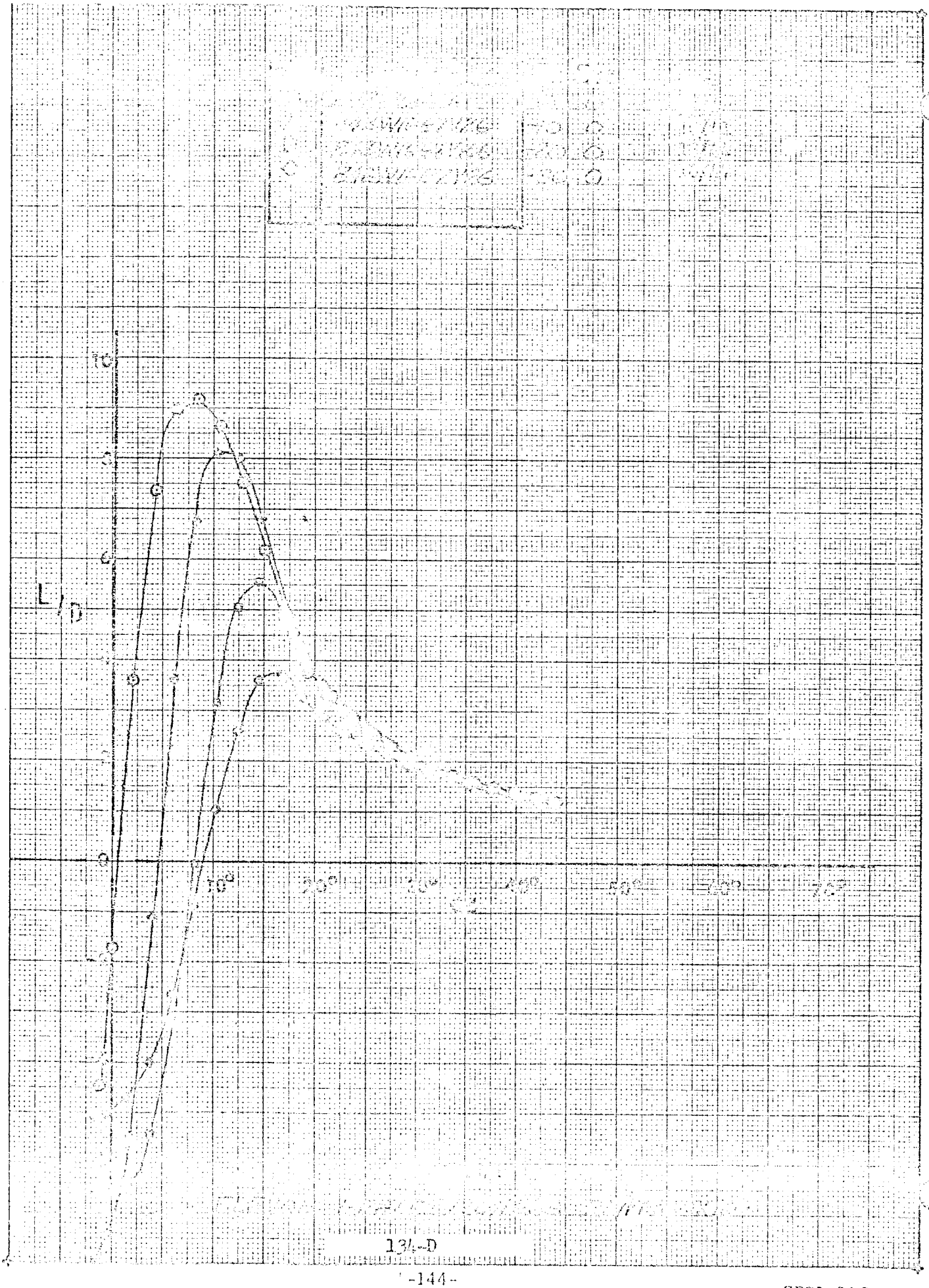

13½-D

KEUFFEL & ESSER CO.

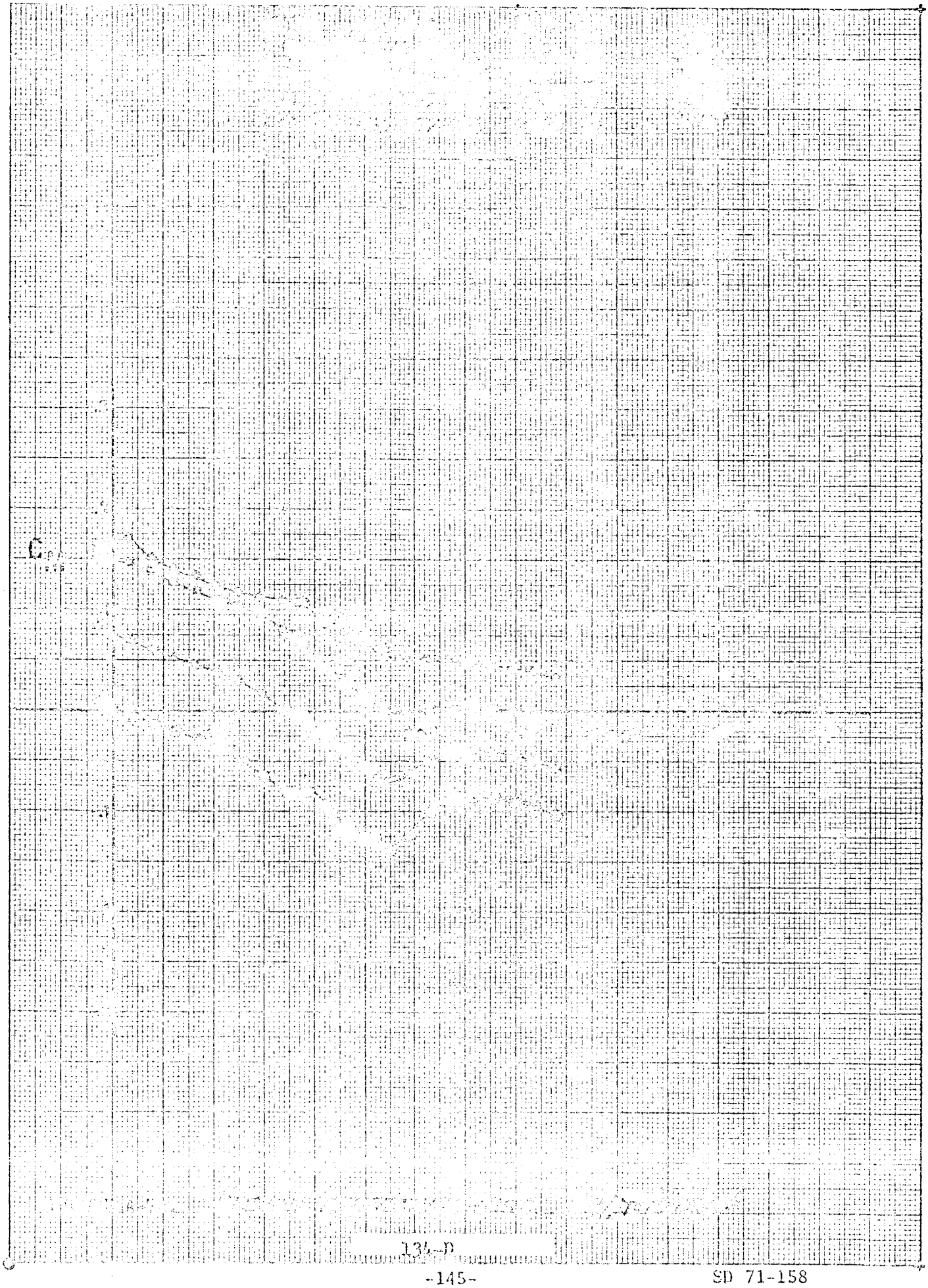

10 X 10 TO THE CENTIMETER 46 1517
18 X 25 CM. • ALBANENE
KEUFFEL & ESSER CO.

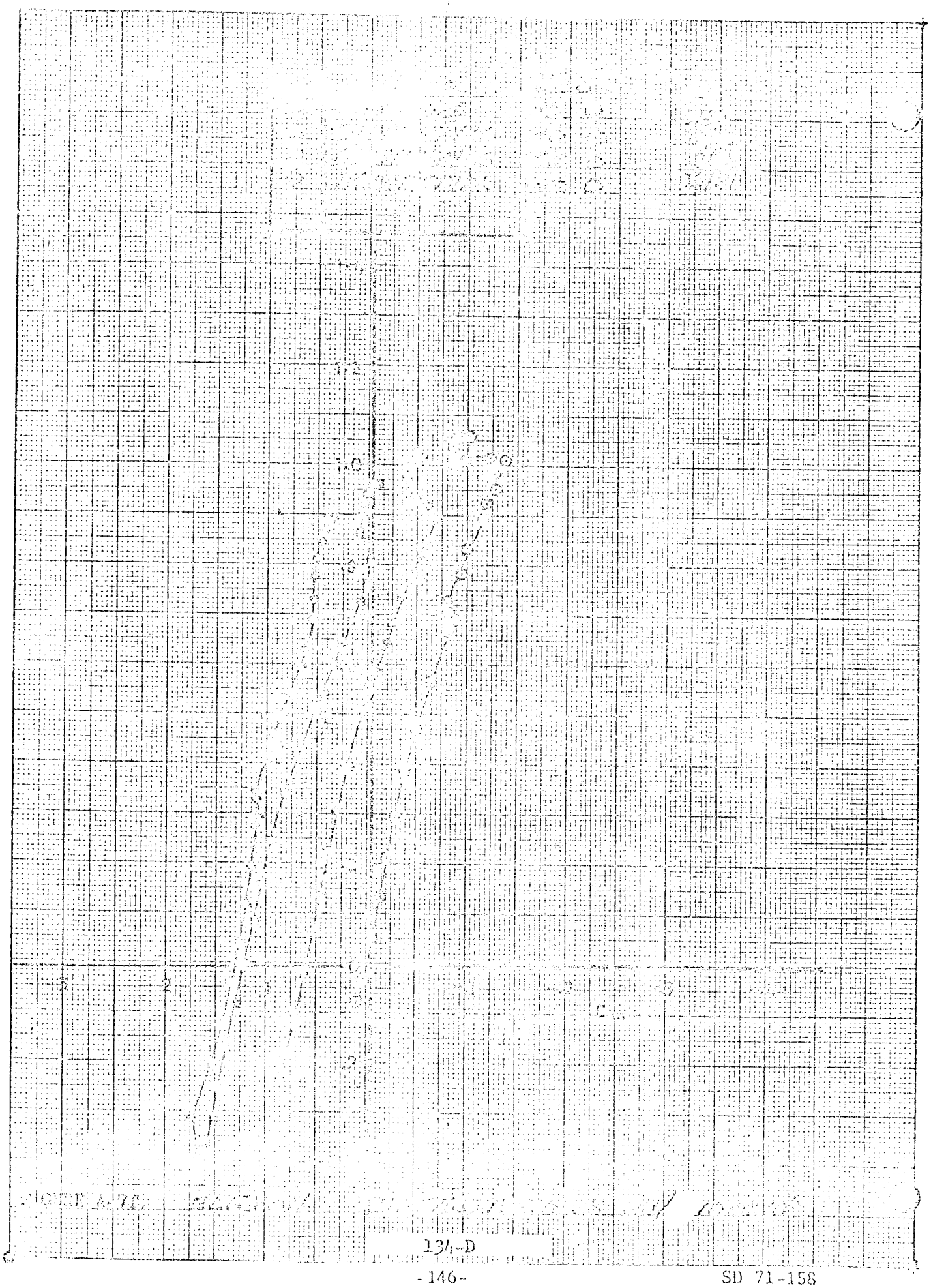

134-D

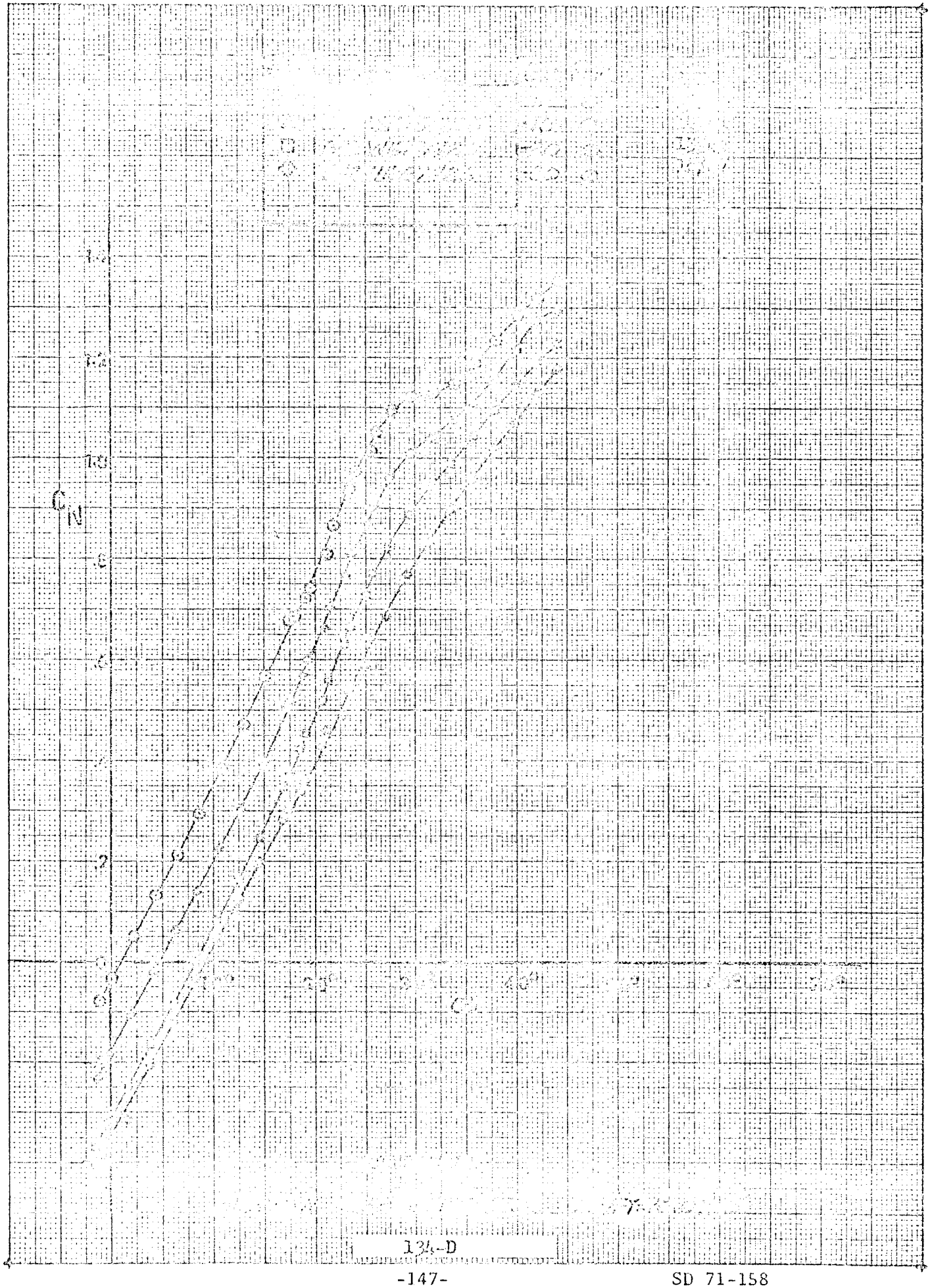
C_N
.2
.4
.6
.8
1.0
1.2
1.4
1.6
1.8
2.0
2.2
2.4
2.6
2.8
3.0
3.2
3.4
3.6
3.8
4.0
4.2
4.4
4.6
4.8
5.0
5.2
5.4
5.6
5.8
6.0
6.2
6.4
6.6
6.8
7.0
7.2
7.4
7.6
7.8
8.0
8.2
8.4
8.6
8.8

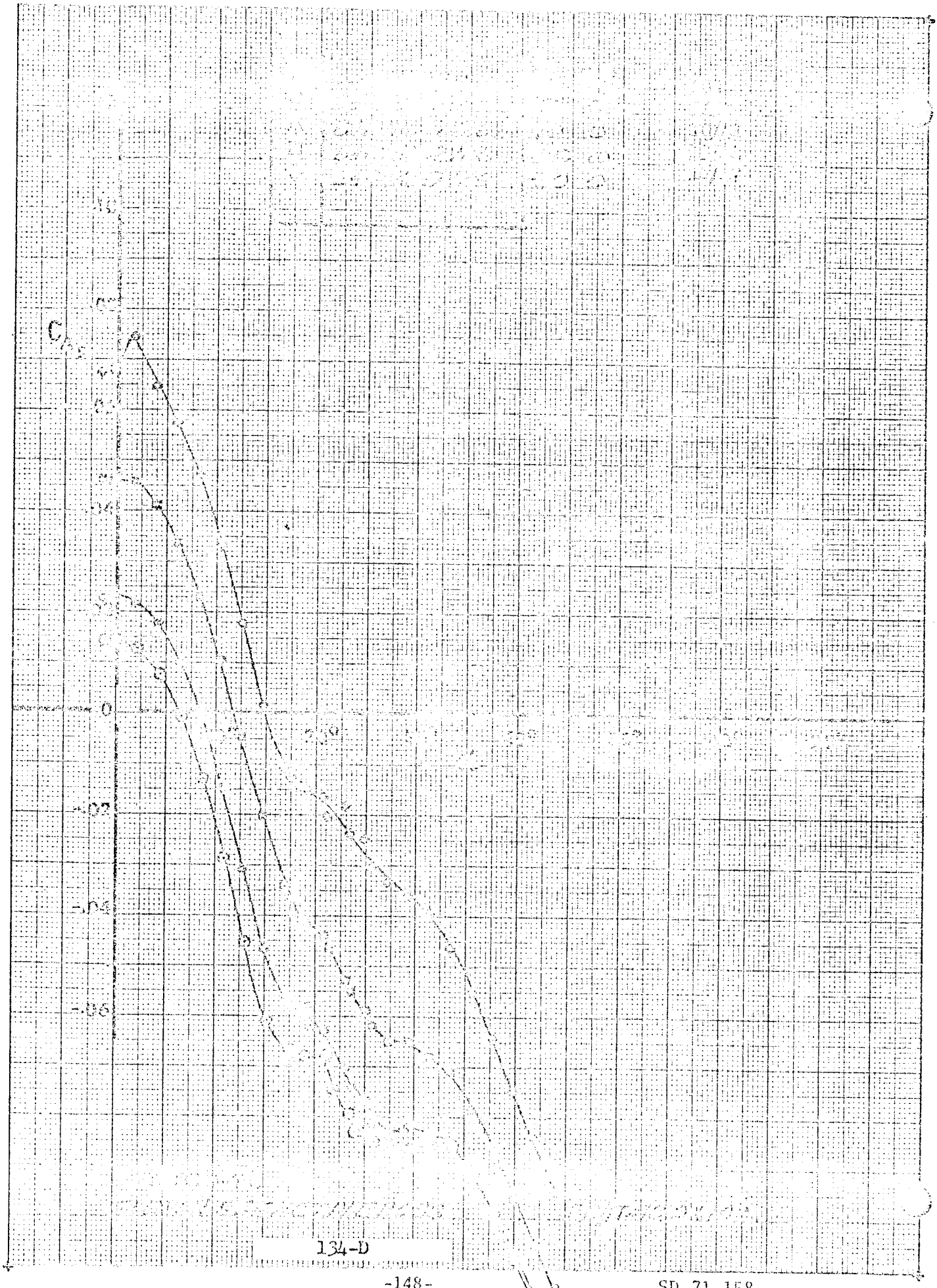
C_{L_α}
.10
.08
.06
.04
.02
0
-.02
-.04
-.06
134-D

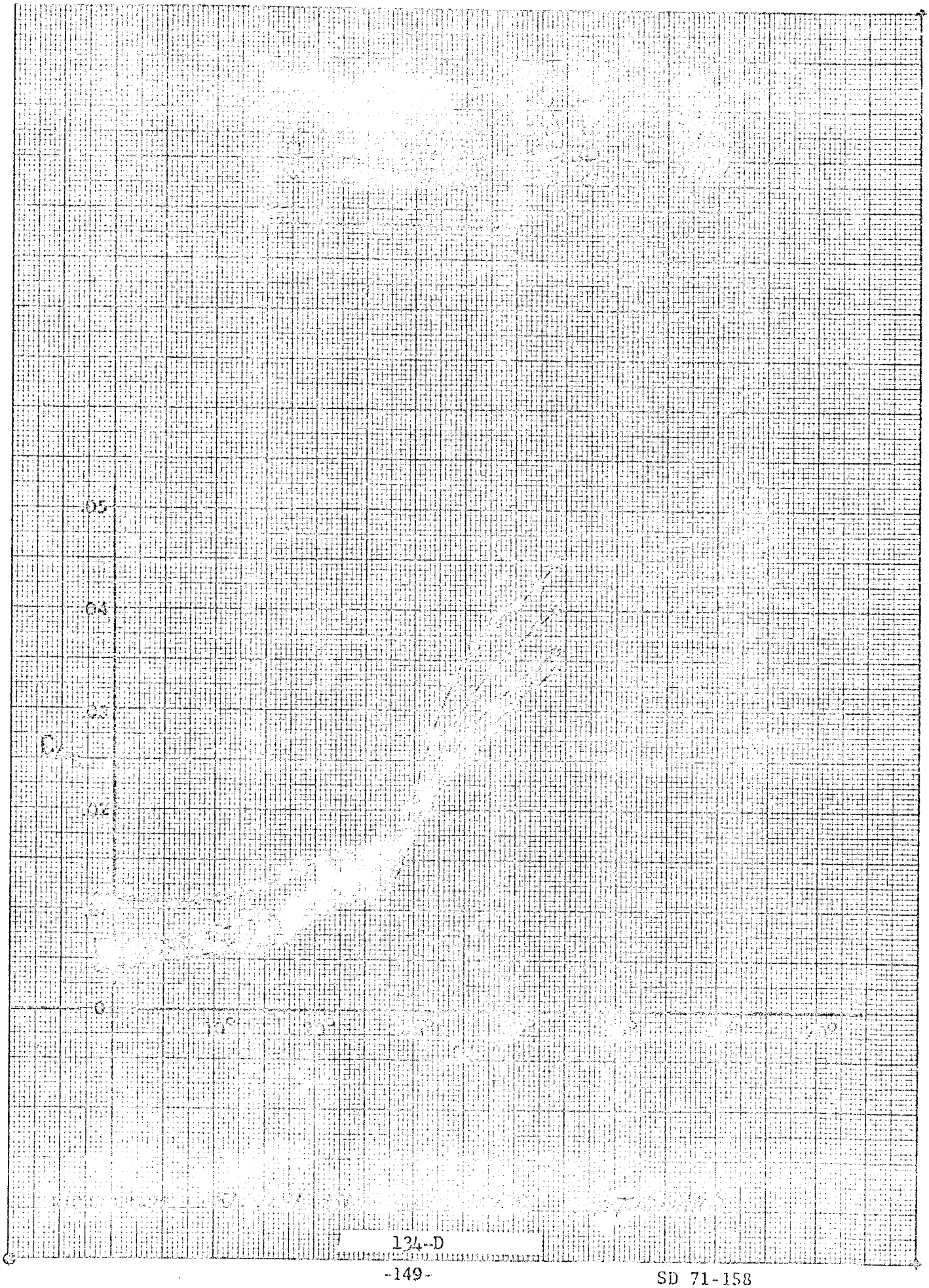

K&E 10 X 10 TO THE CENTIMETER 46 1517
18 X 25 CM. • ALBANENE®
KEUFFEL & ESSER CO.

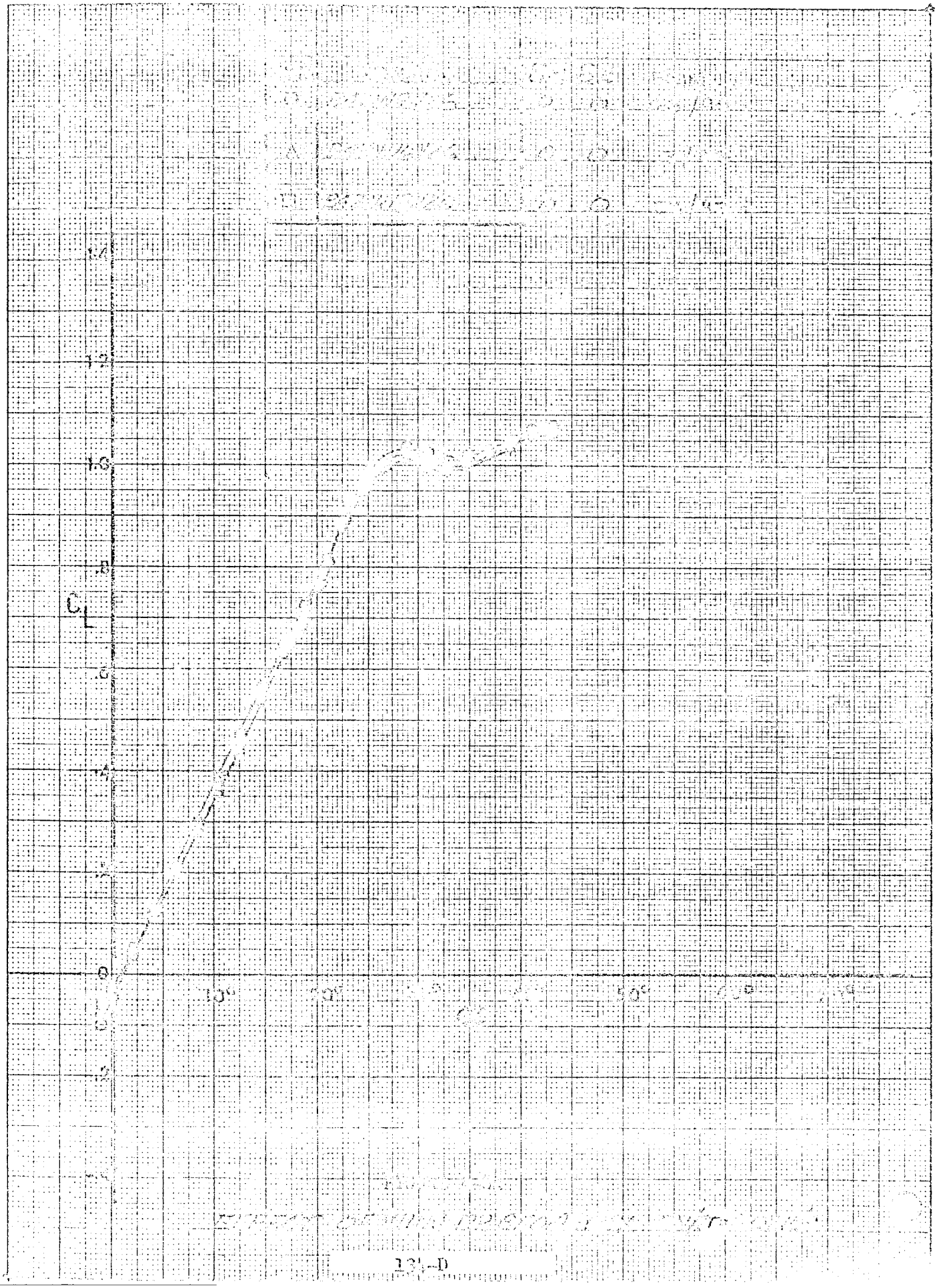
C_L
1.6
1.4
1.2
1.0
.8
.6
.4
.2
0
-.2
-.4
10°
20°
30°
40°
50°
60°
70°
80°

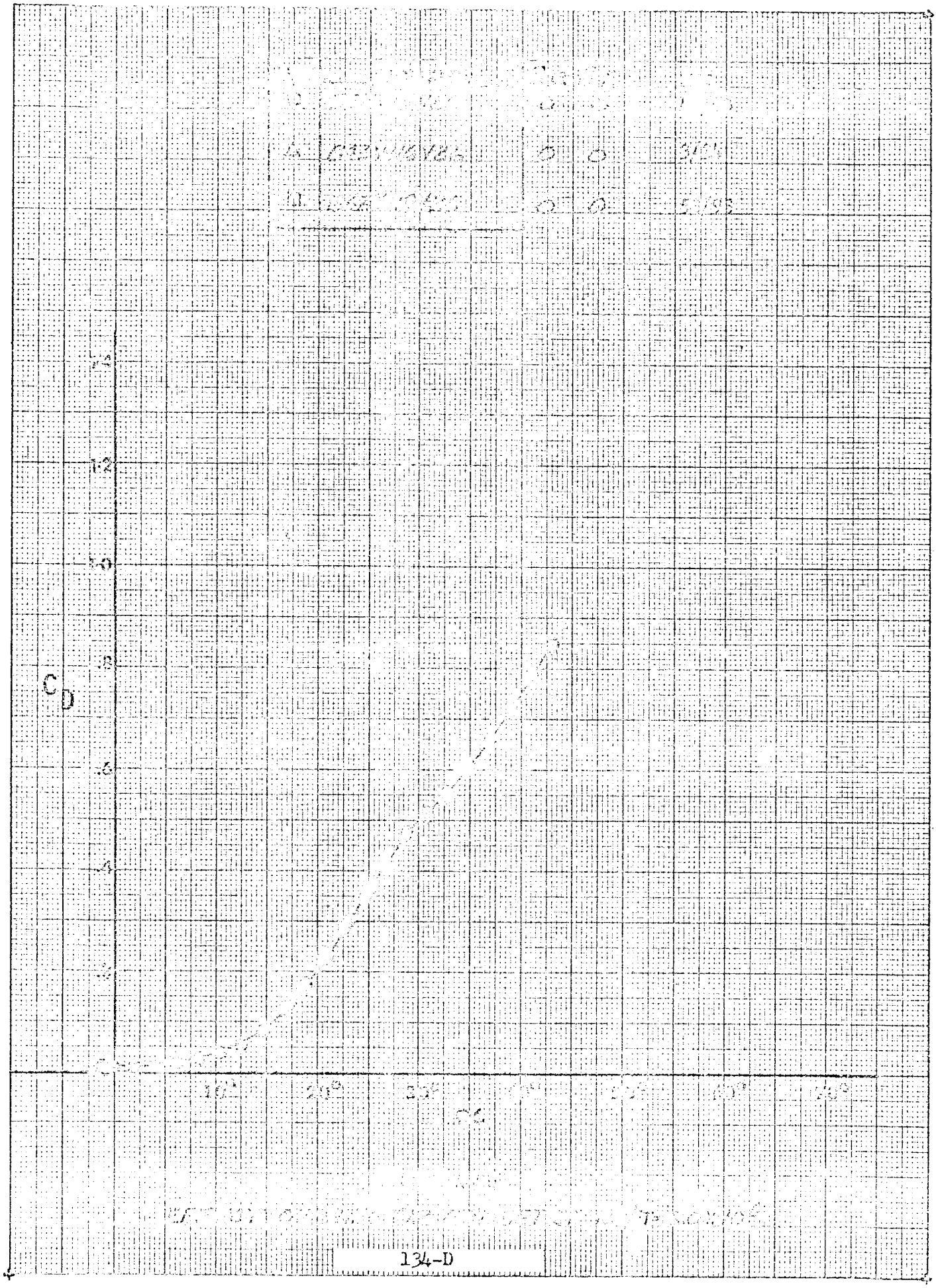
1.2
1.0
0.8
0.6
0.4
0.2
C_D
100°
200°
300°
400°
500°
C_L
134-D

273

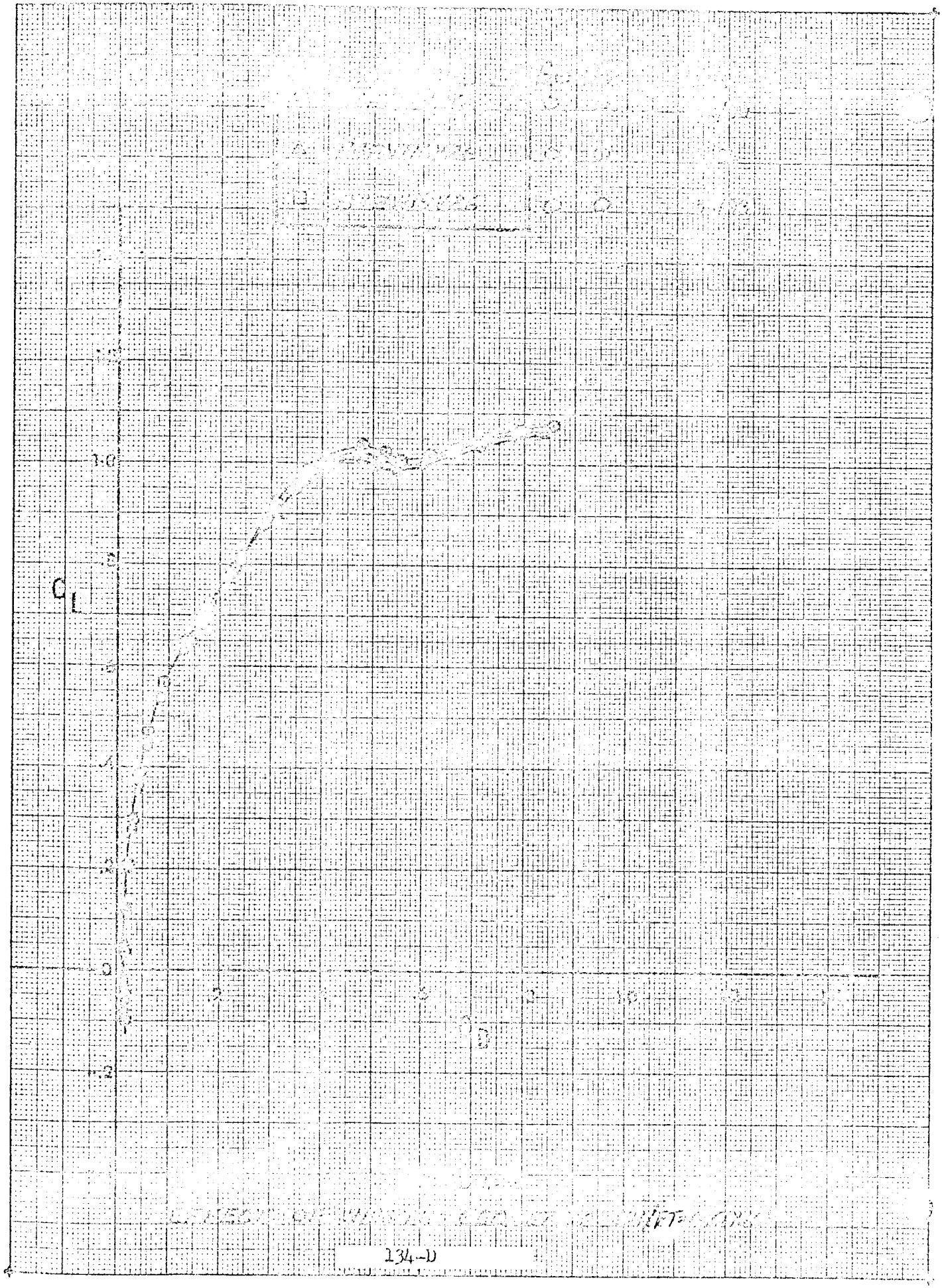

10 X 10 TO THE CENTIMETER 46 1517
KEUFFEL & ESSER CO.

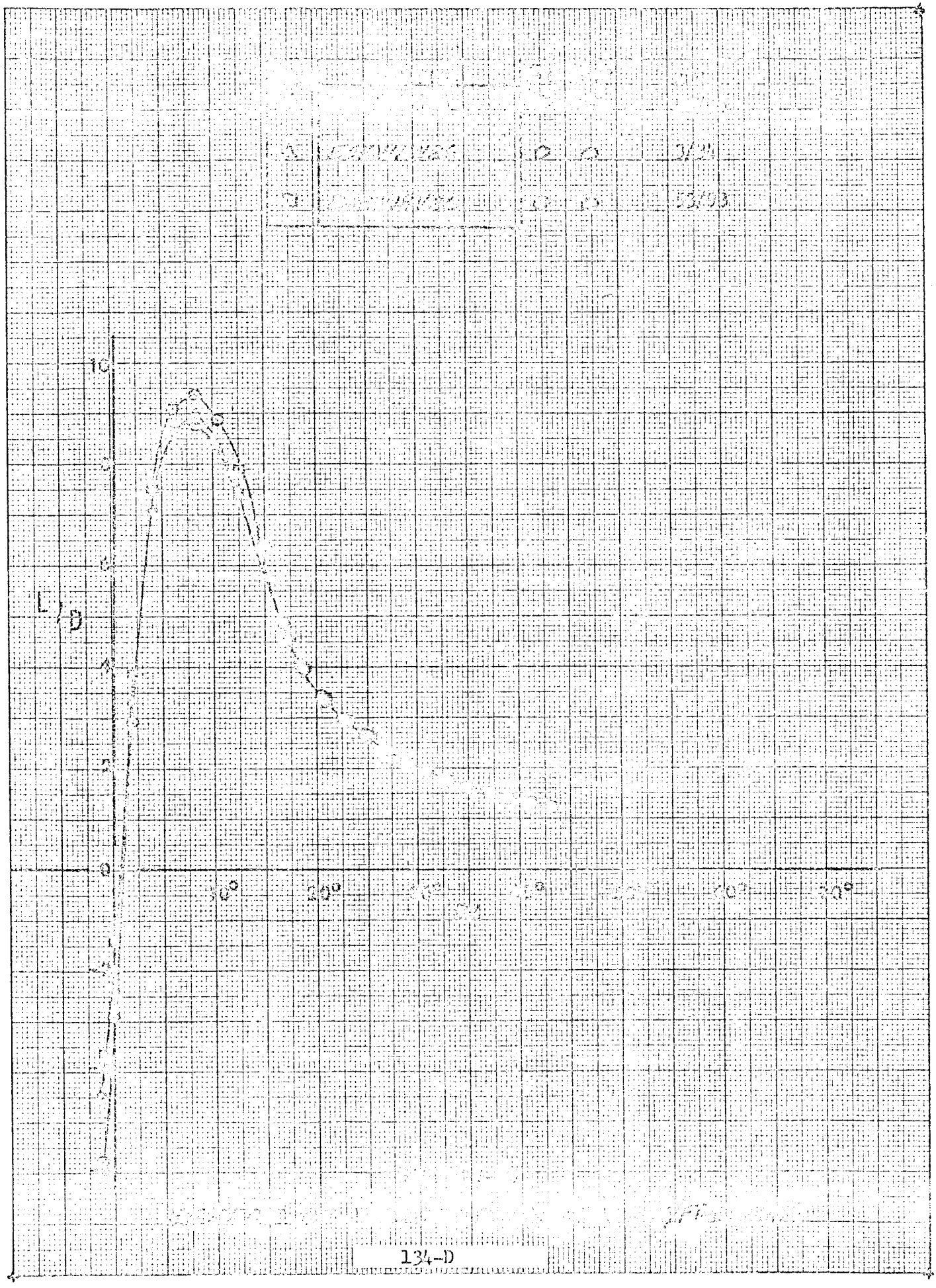

134-D

K&E 10 X 10 TO THE CENTIMETER 46 1517
18 X 25 CM. • ALBANENE W
KEUFFEL & ESSER CO.

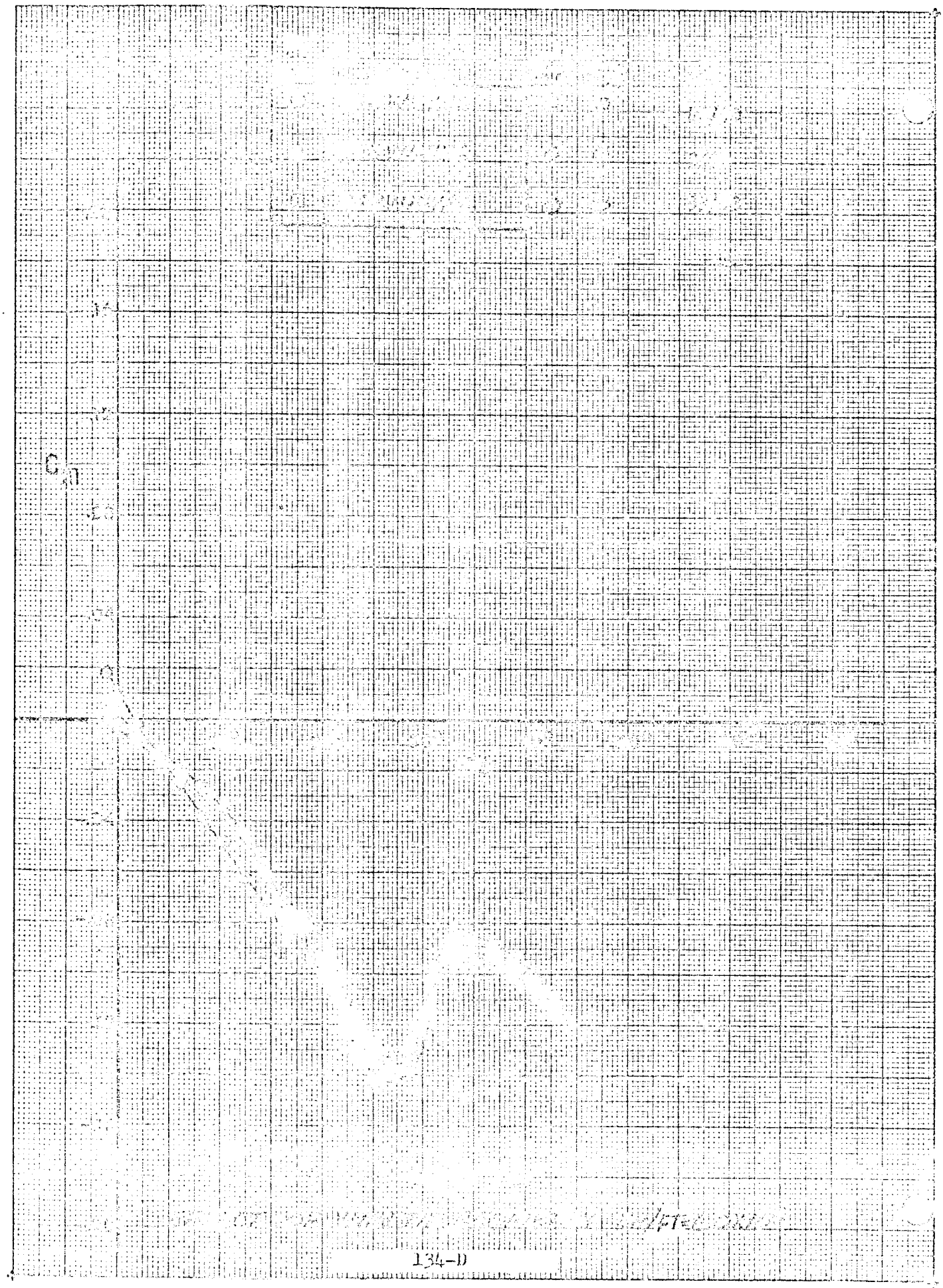

134-D

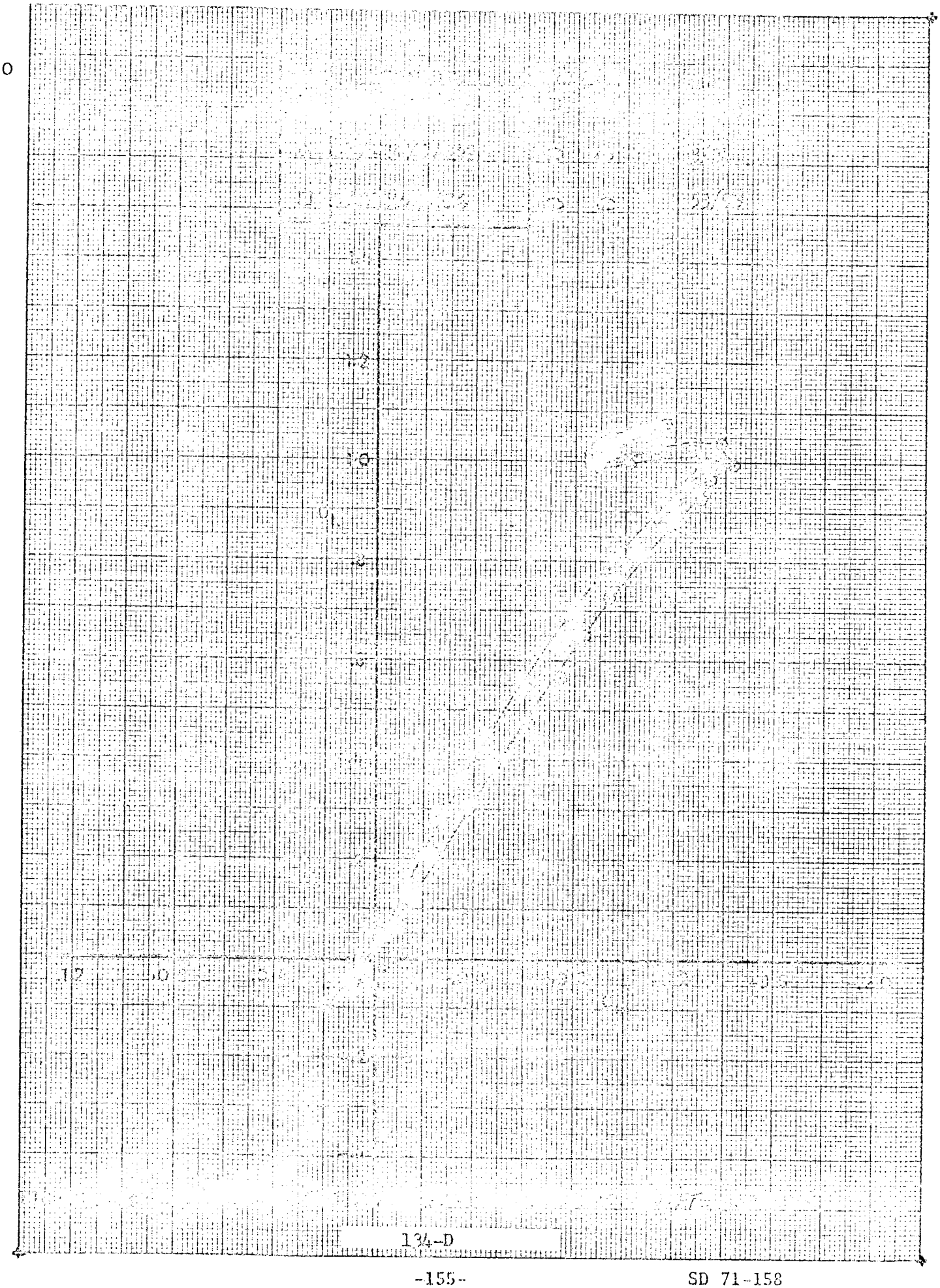

K+E 10 X 10 TO THE CENTIMETER 46 1517
18 X 25 CM. • ALBANENEM MADE IN U.S.A.
KEUFFEL & ESSER CO.

284

14

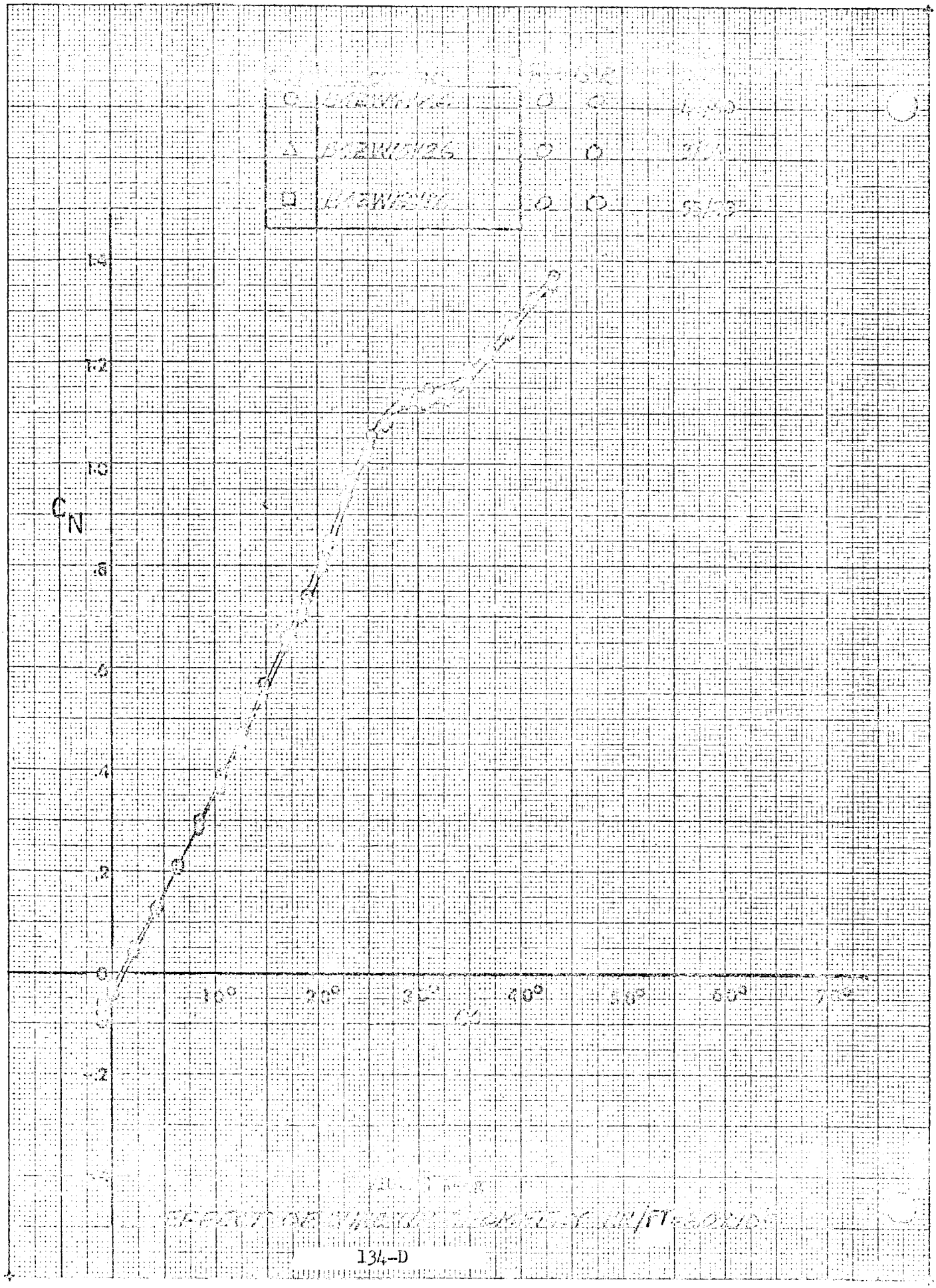

134-D

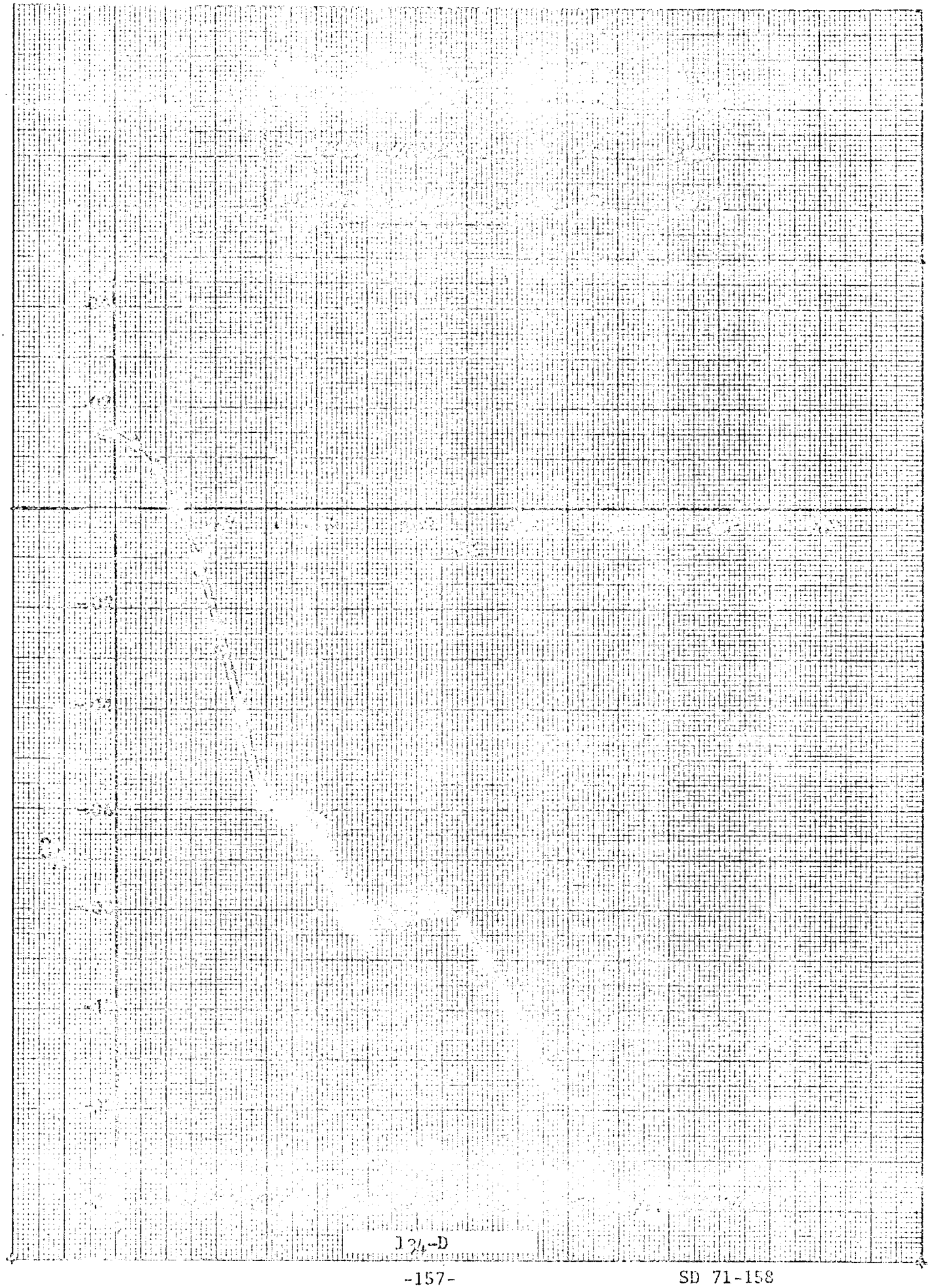

K+E 10 X 10 TO THE CENTIMETER 46 1517
18 X 25 CM. • ALBANENE®
KEUFFEL & ESSER CO.

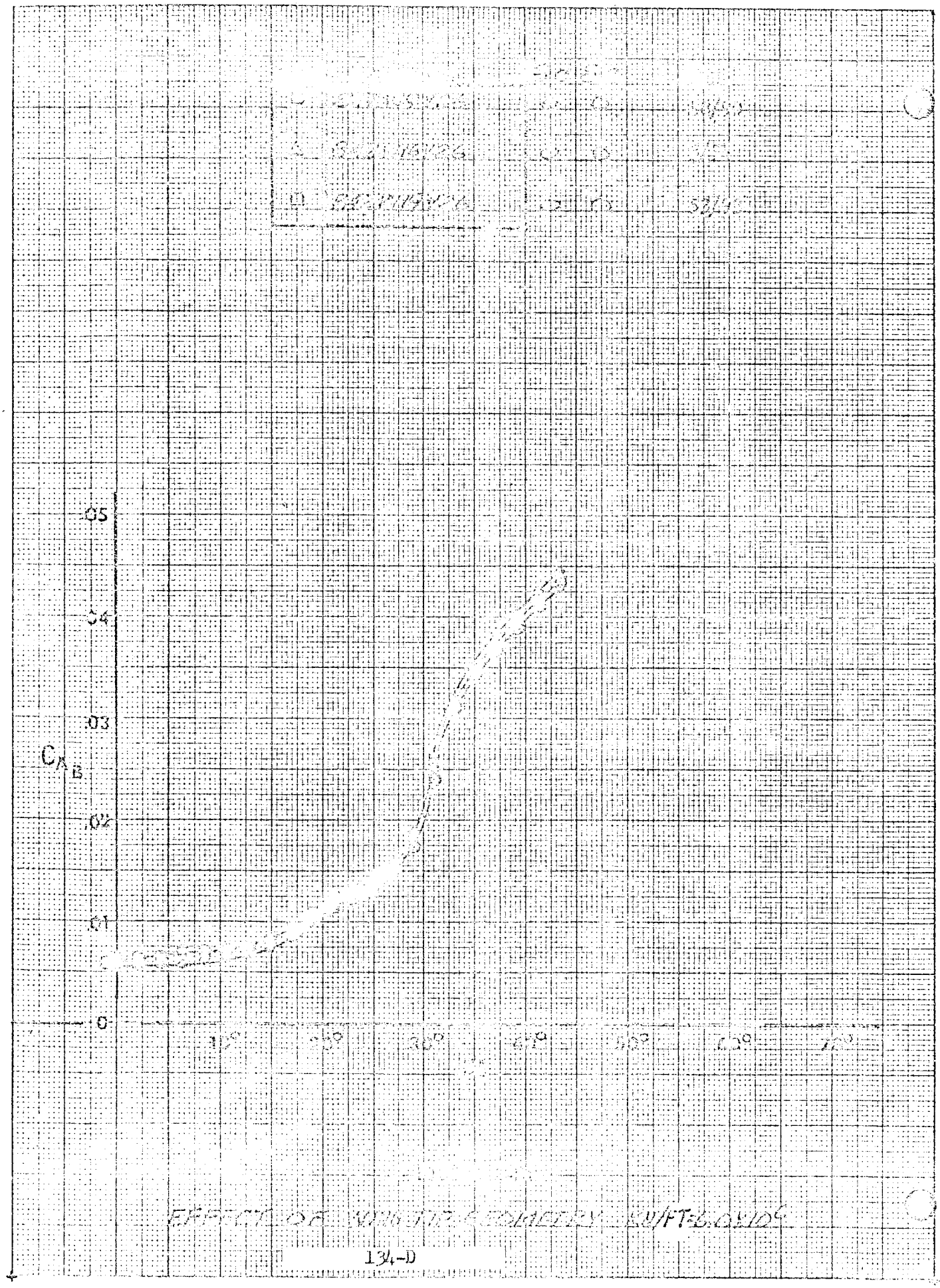

134-D

10 X 10 TO THE CENTIMETER 46 1217
18 X 25 CM. • ALBANENA
KEUFFEL & ESSER CO.

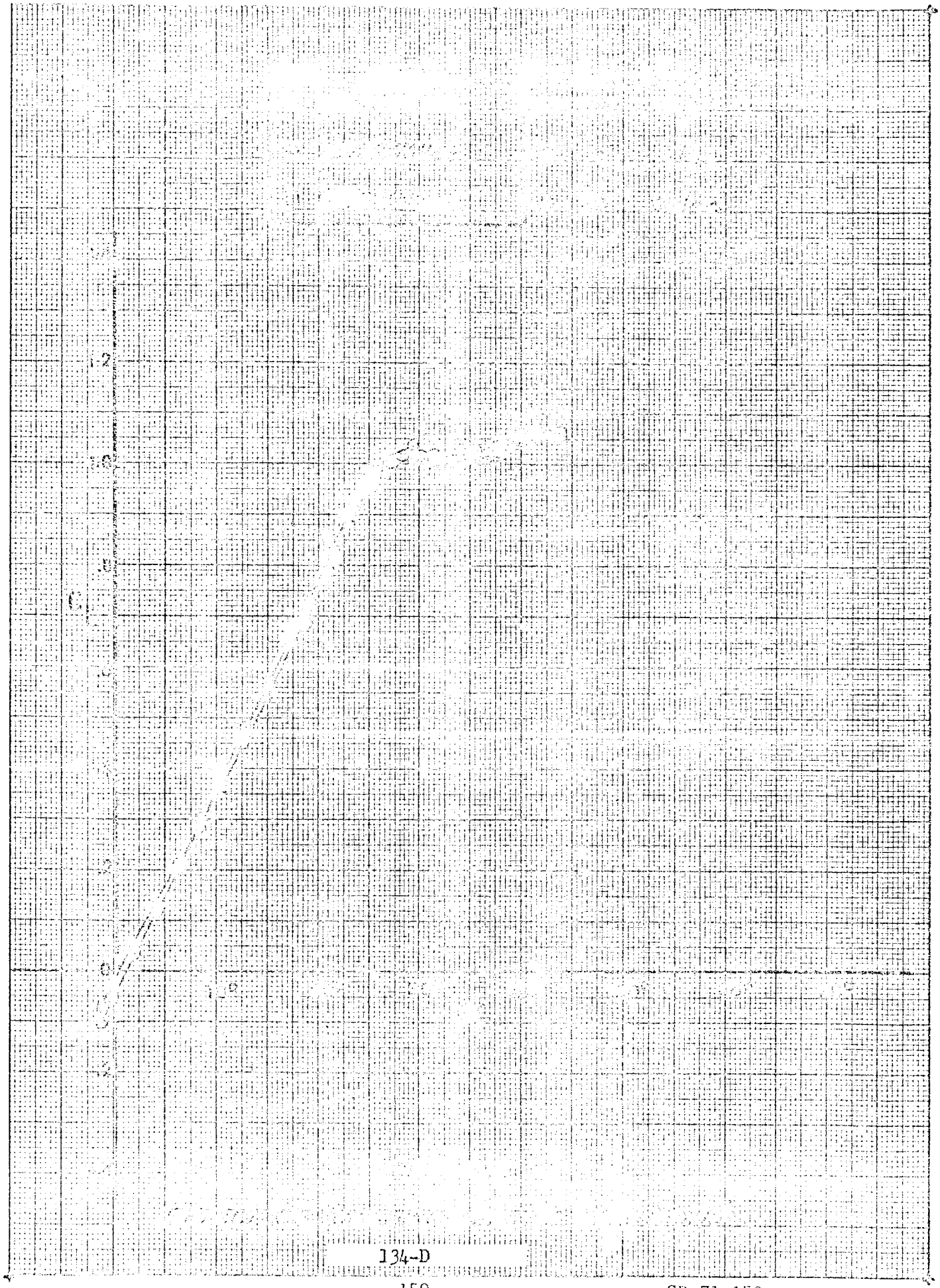

134-D

10 X 25 CM. • ALBANENE®
KEUFFEL & ESSER CO.

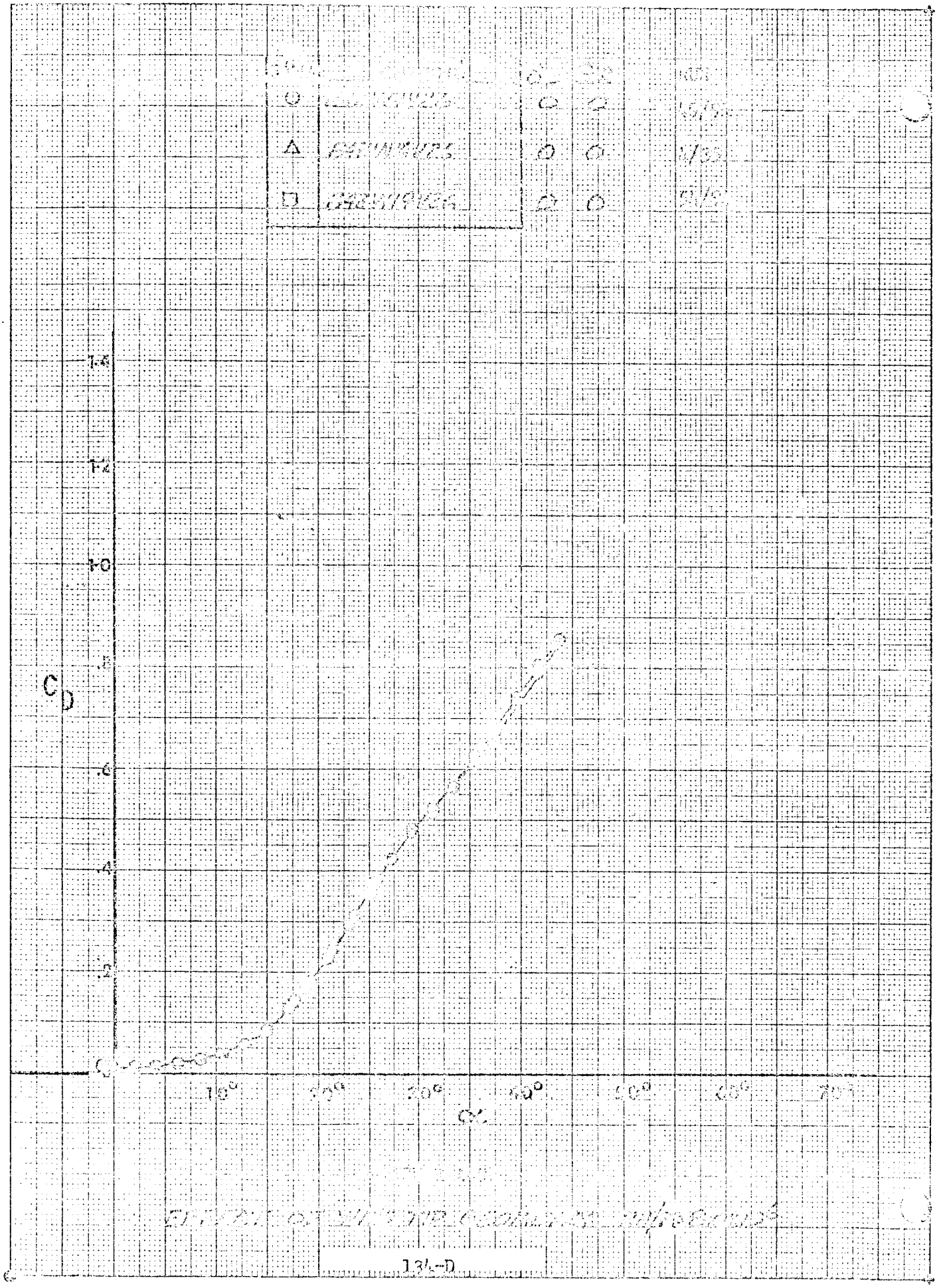

13½-D

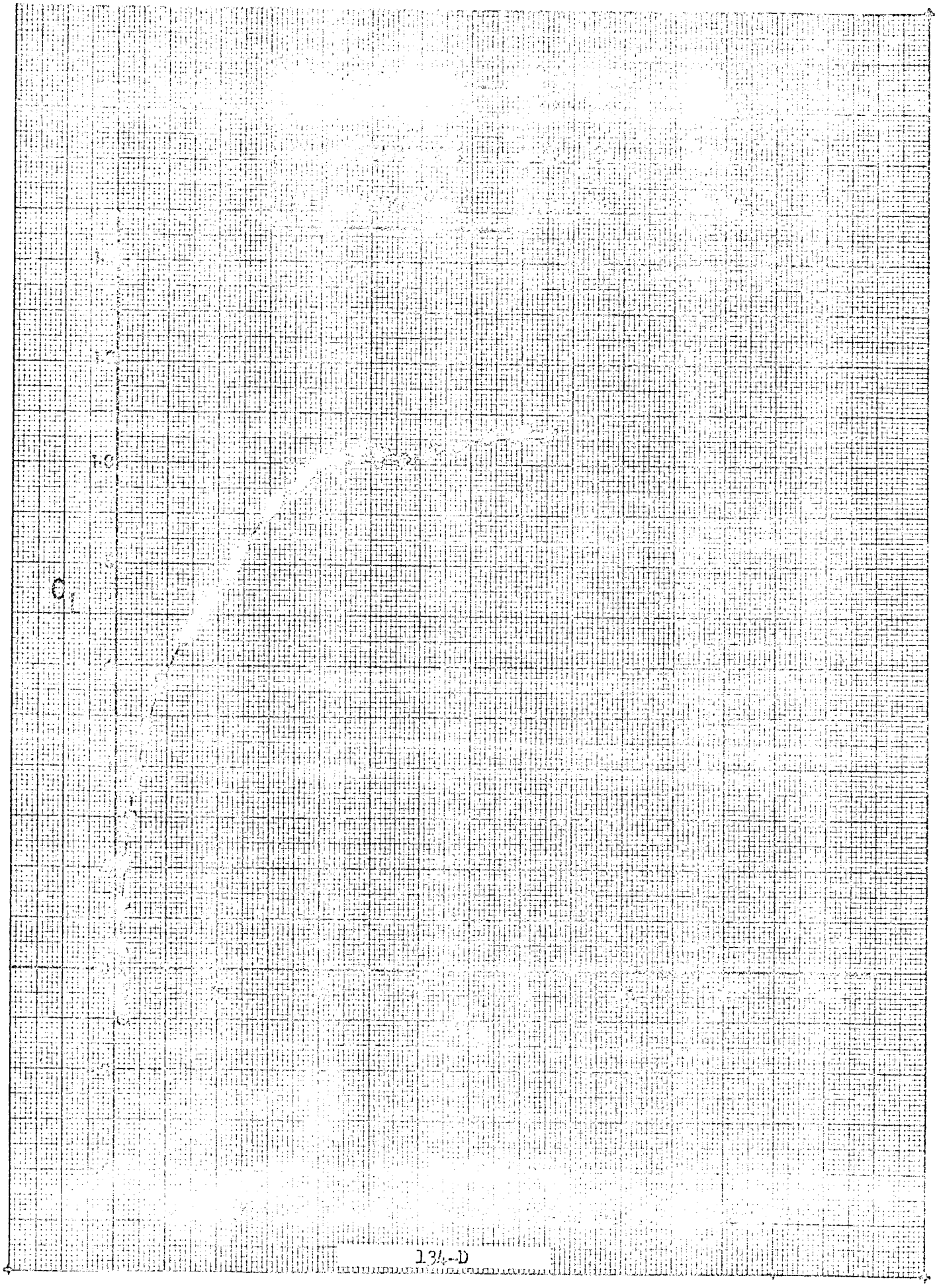

K&E 10 X 10 TO THE CENTIMETER 46 1517
18 X 25 CM. • ALBANENE
MADE IN U.S.A.
KEUFFEL & ESSER CO.

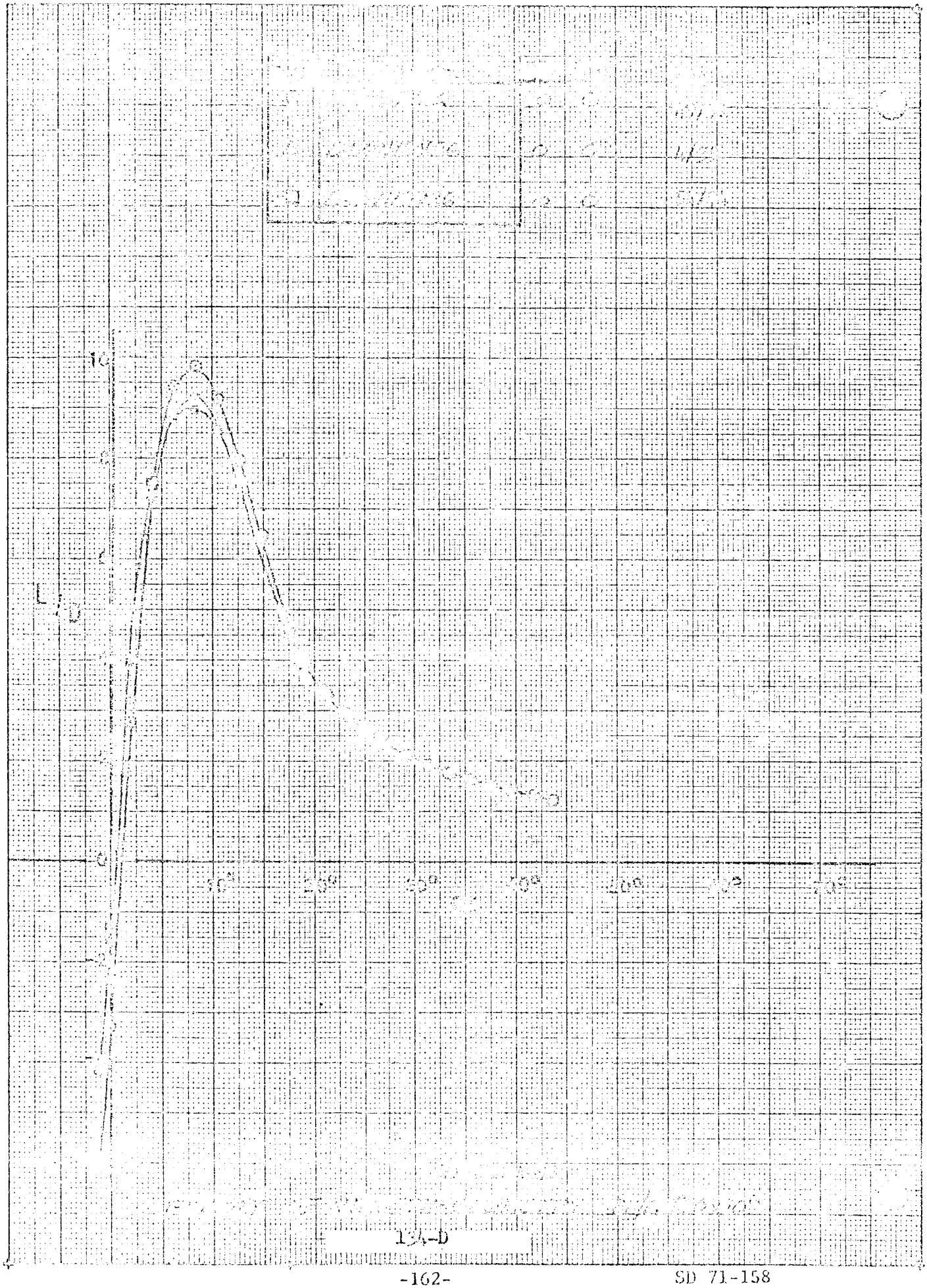
10
50
100
150
200
250
300
350
400
450
500
550
600
650
700
750
10 X 10 TO THE CENTIMETER 45 1517
18 X 25 CM • ALBANENE
KEUFFEL & ESSER CO.

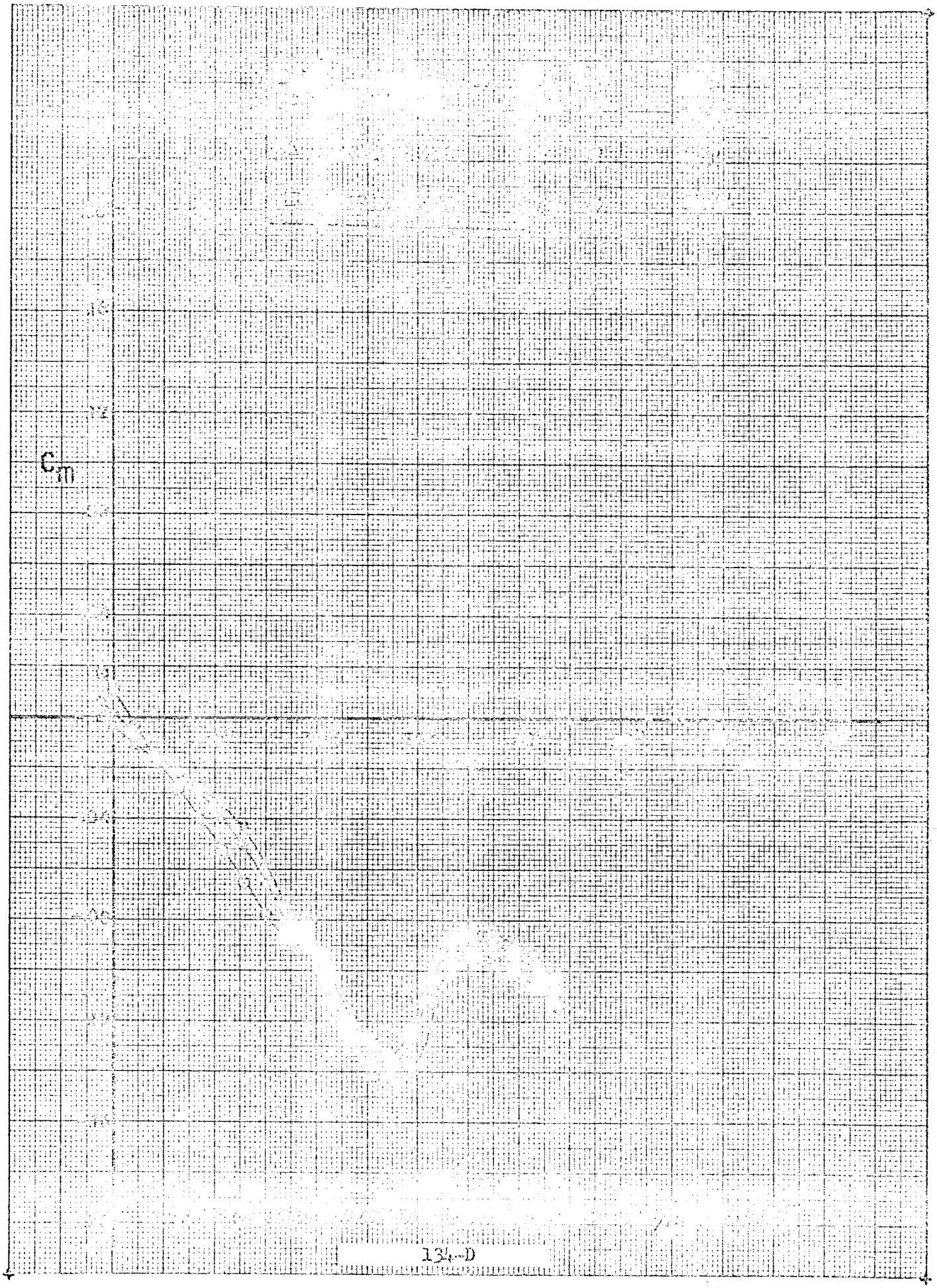

K+E 10 Y 10 TO THE CENTIMETER 46 1517
19 X 25 CM. • ALBANENE
KEUFFEL & ESSER CO.

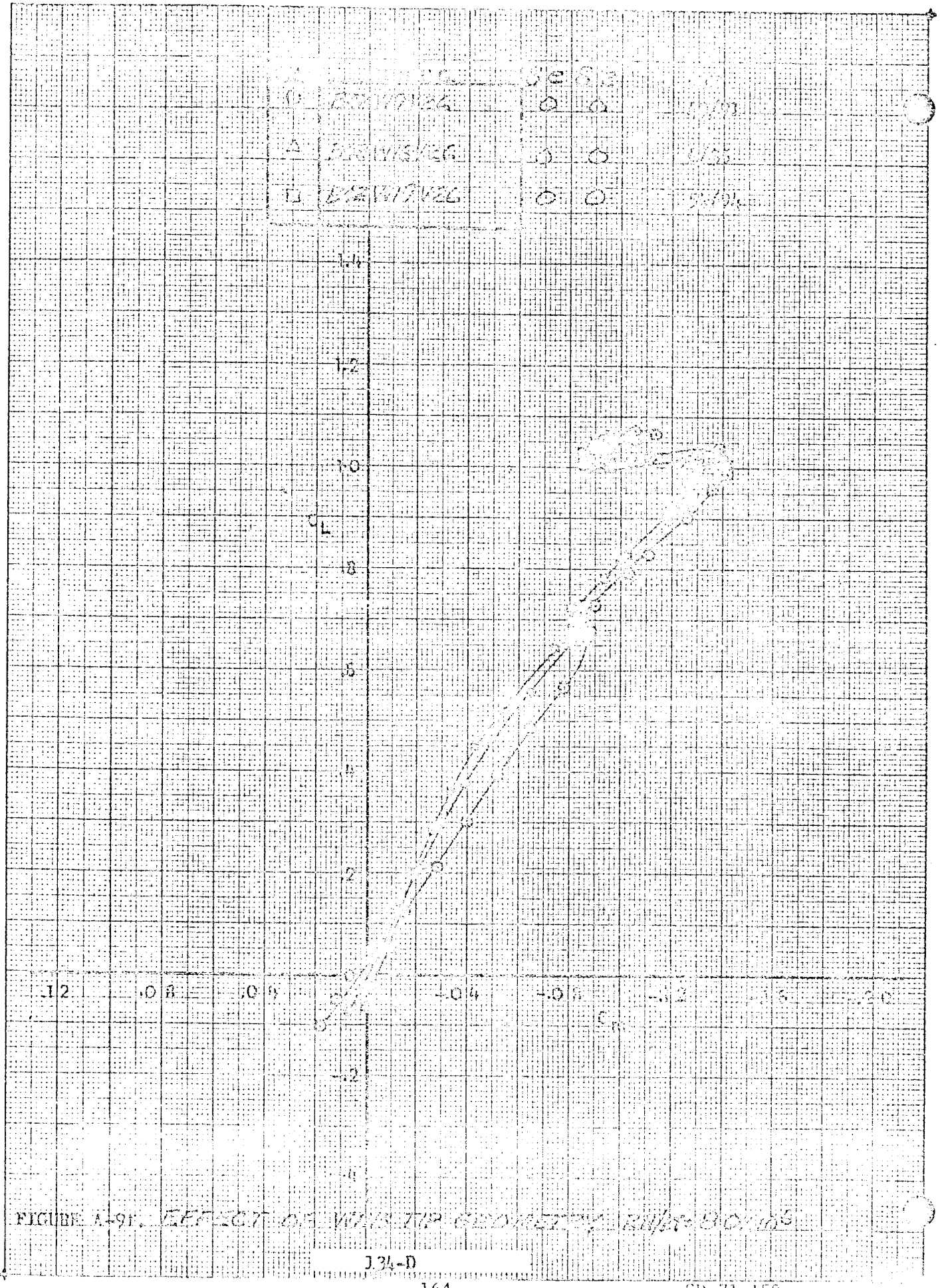

FIGURE A-91. EFFECT OF WEAK TIP CONVERGENCE ON RUDDER BOXES

J34-D

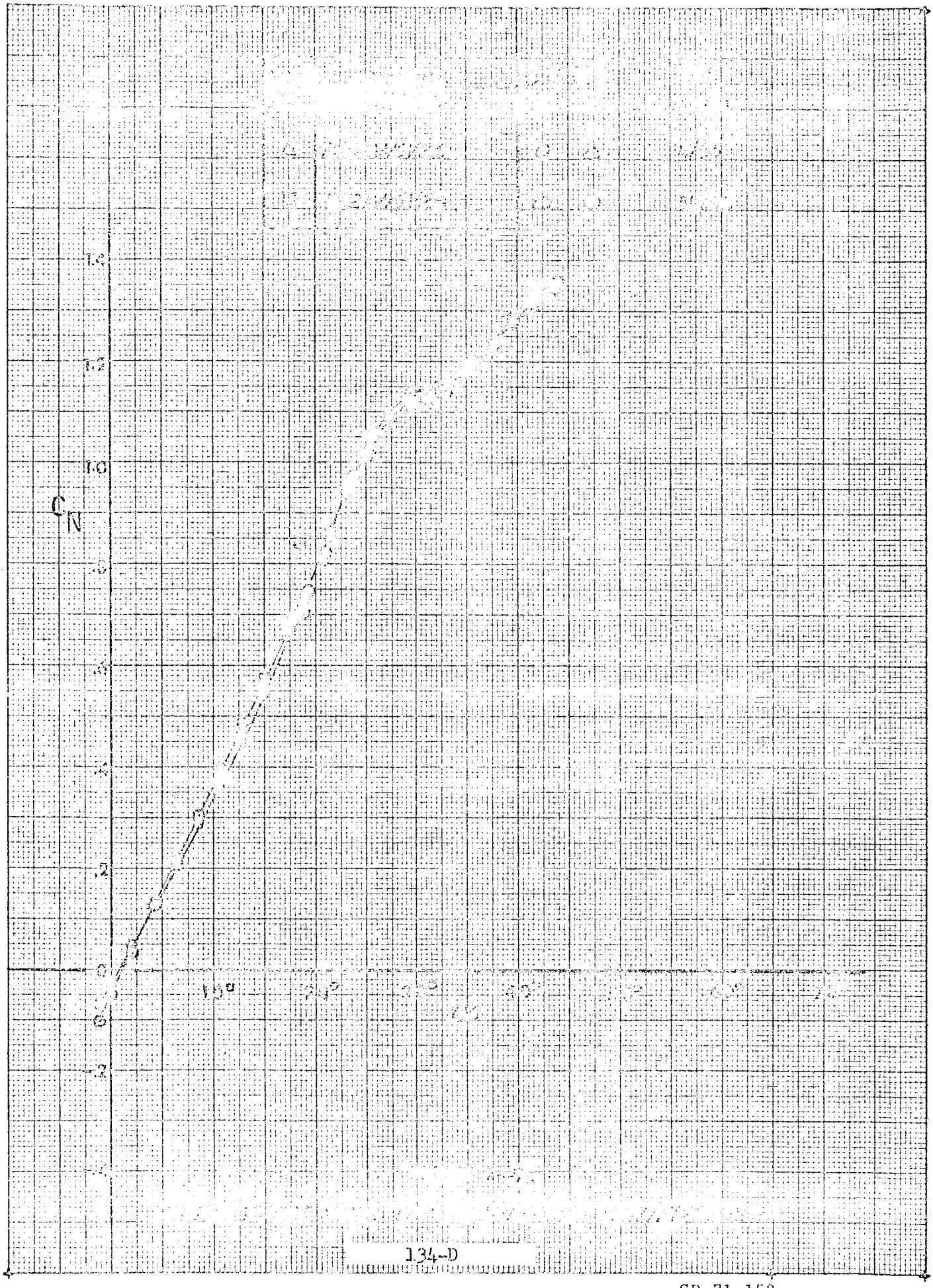

134-D

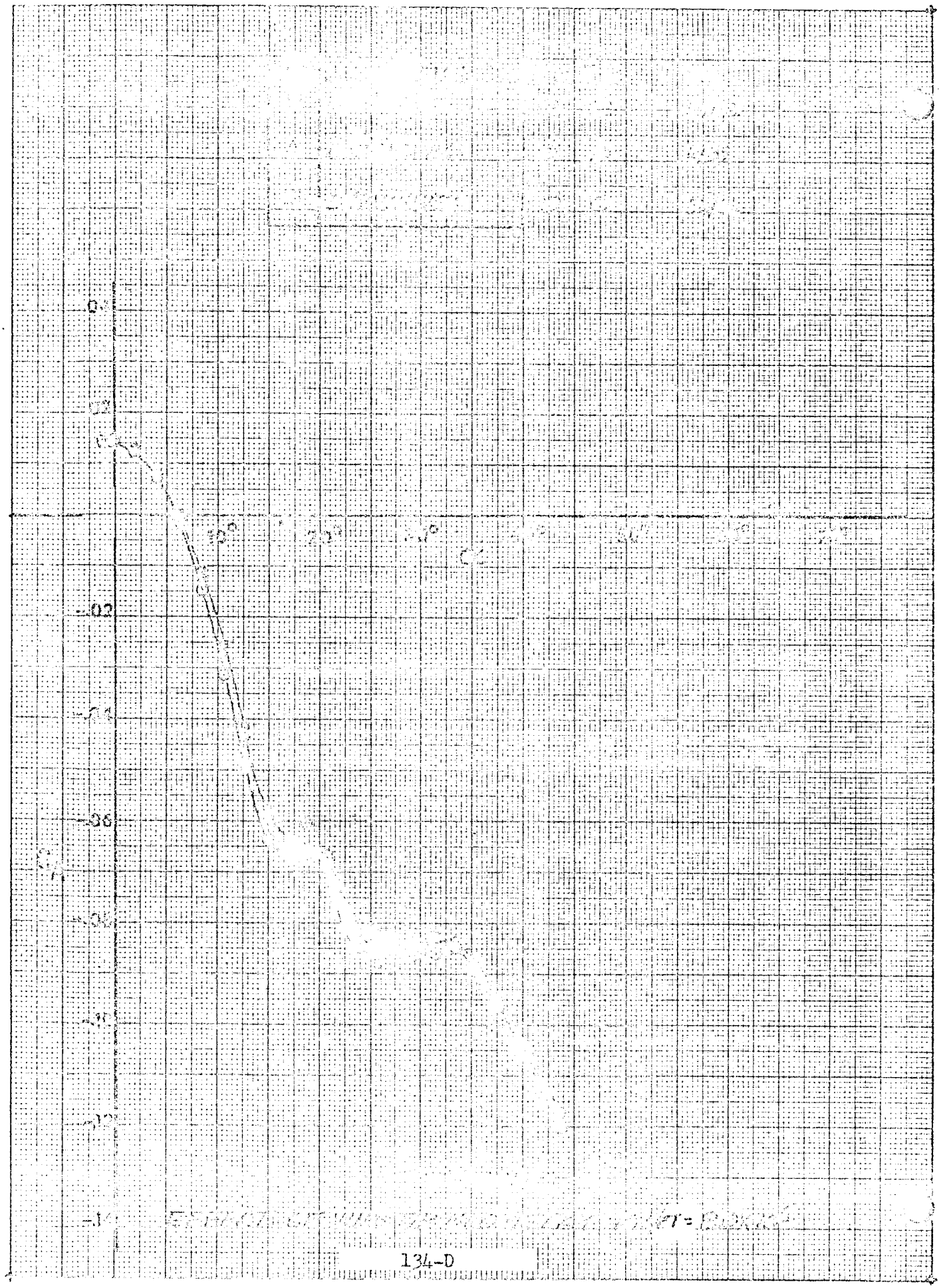

134-D

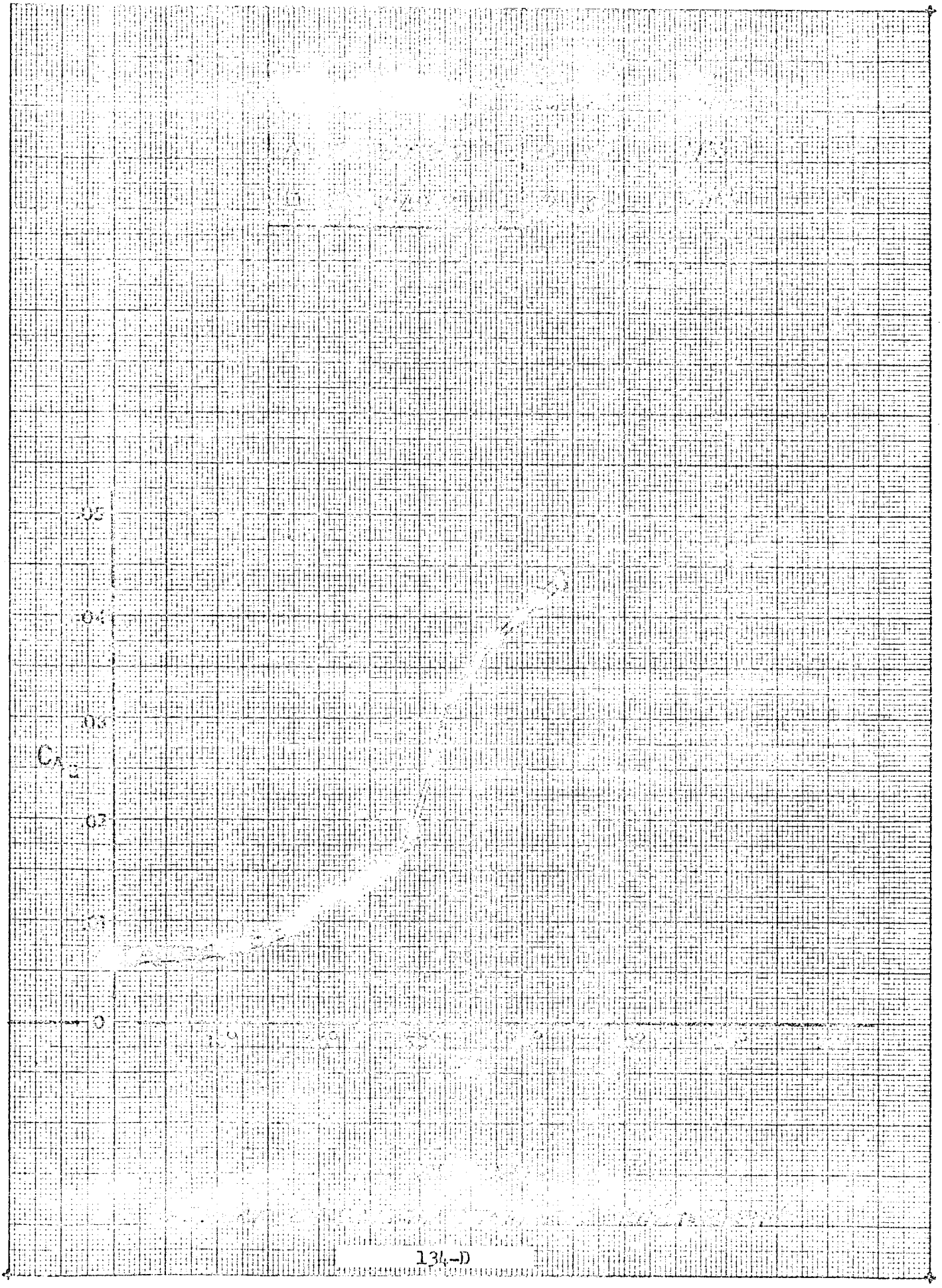
134-D

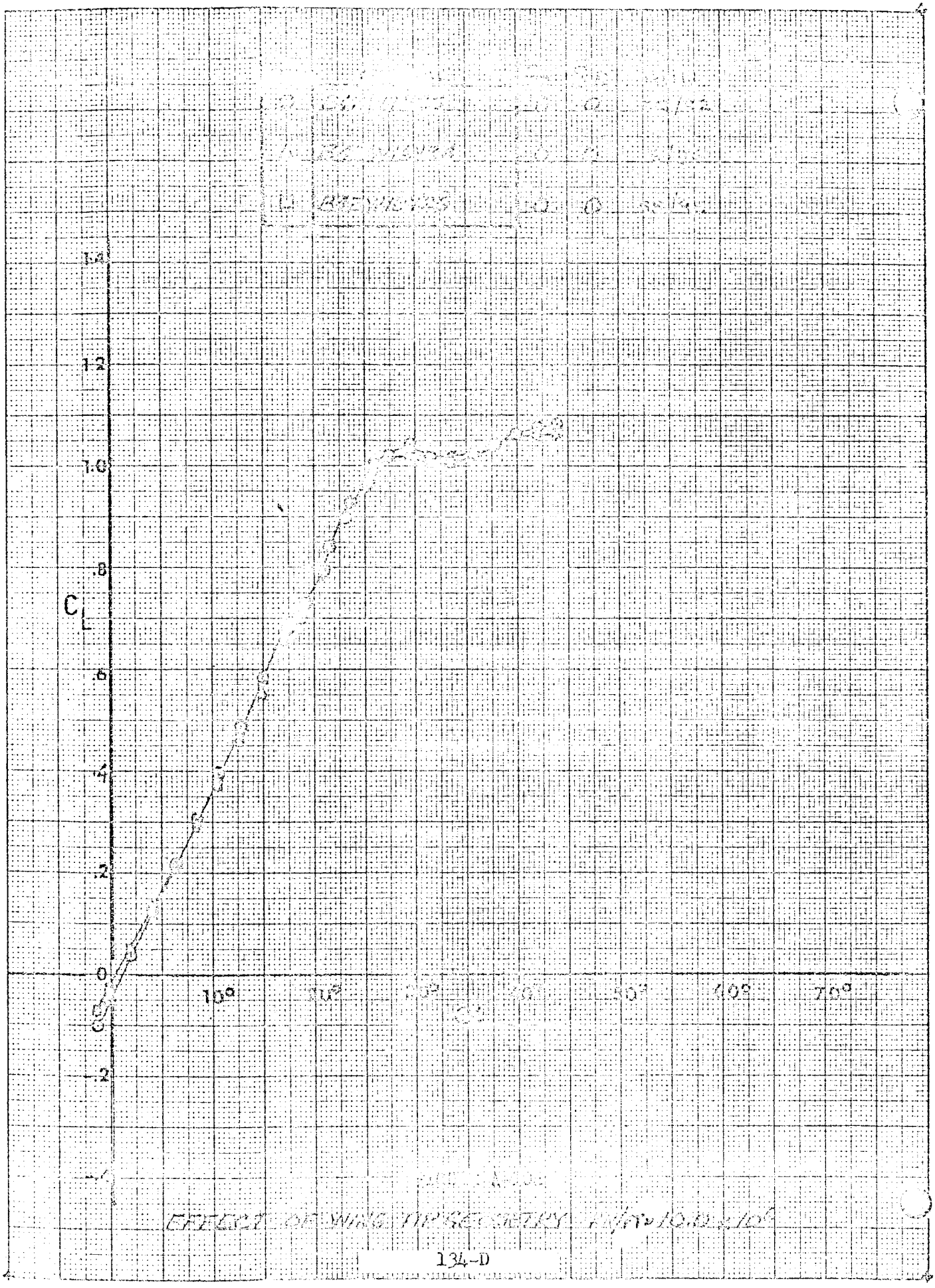

134-D

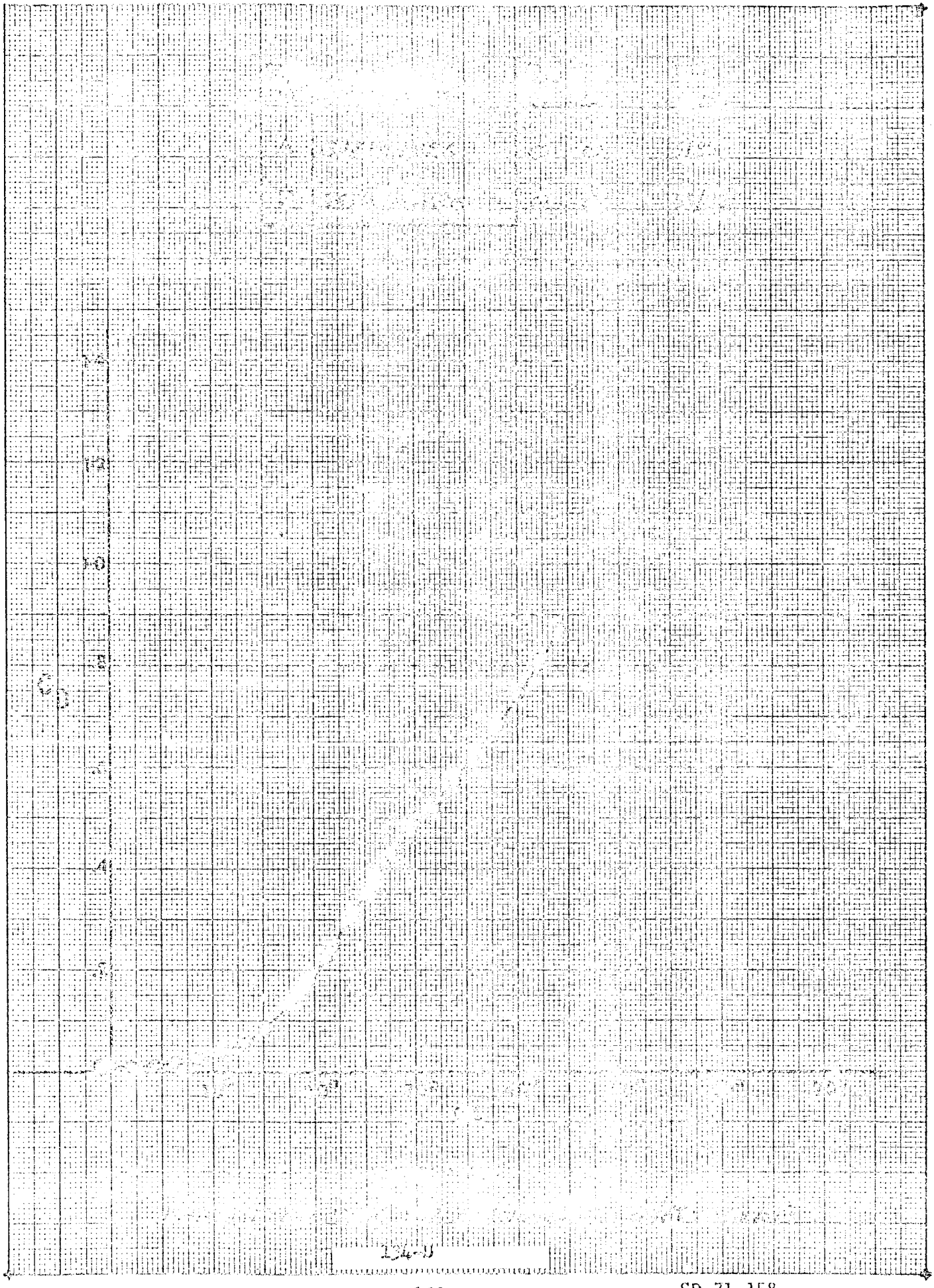

K+E 10 X 10 TO THE CENTIMETER 46 5137
18 X 25 CM. • ALBANENE
MADE IN U.S.A.
KEUFFEL & ESSER CO.

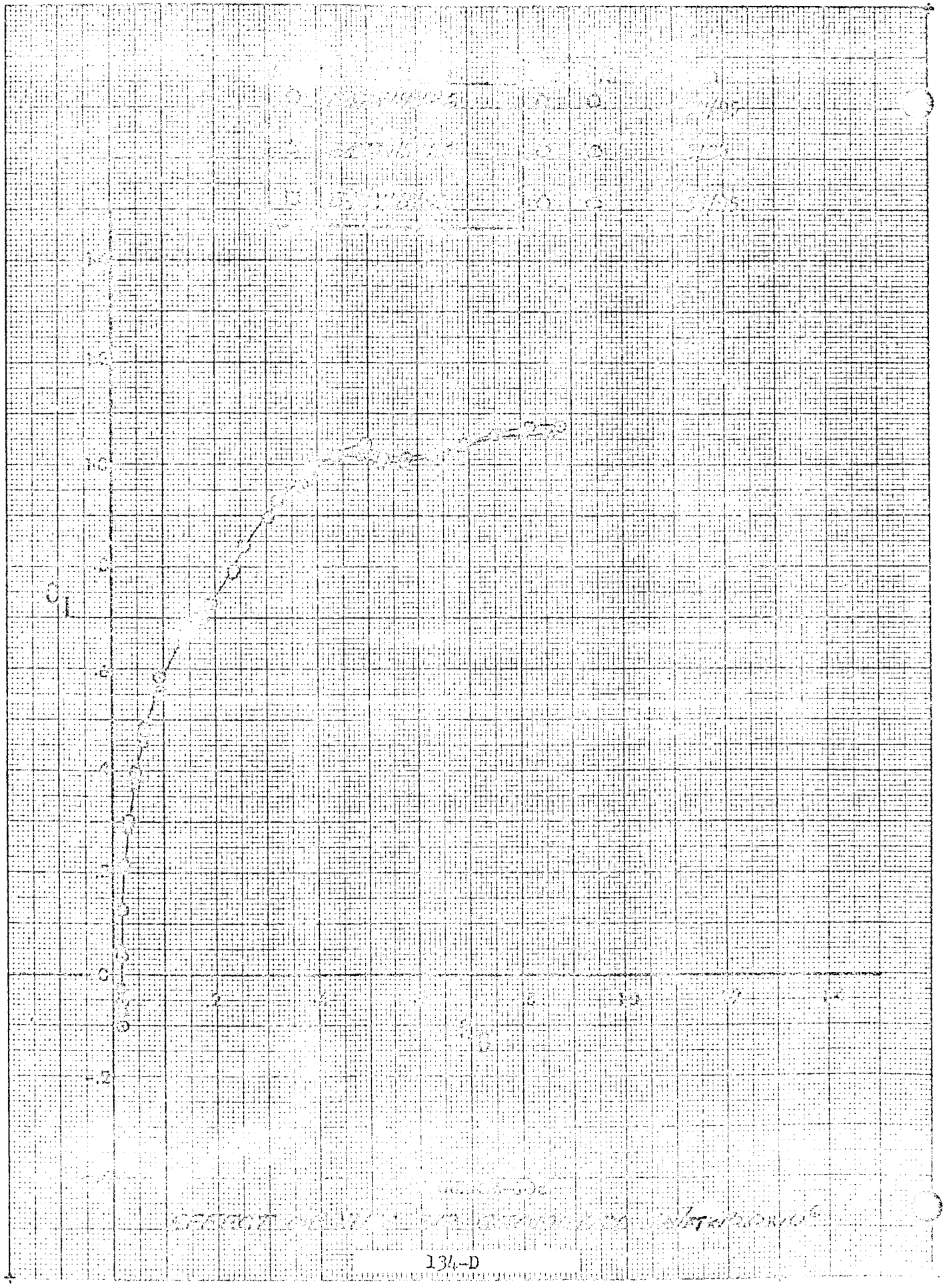

10 X 10 TO THE CENTIMETER 46 1517
KEUFFEL & ESSER CO.

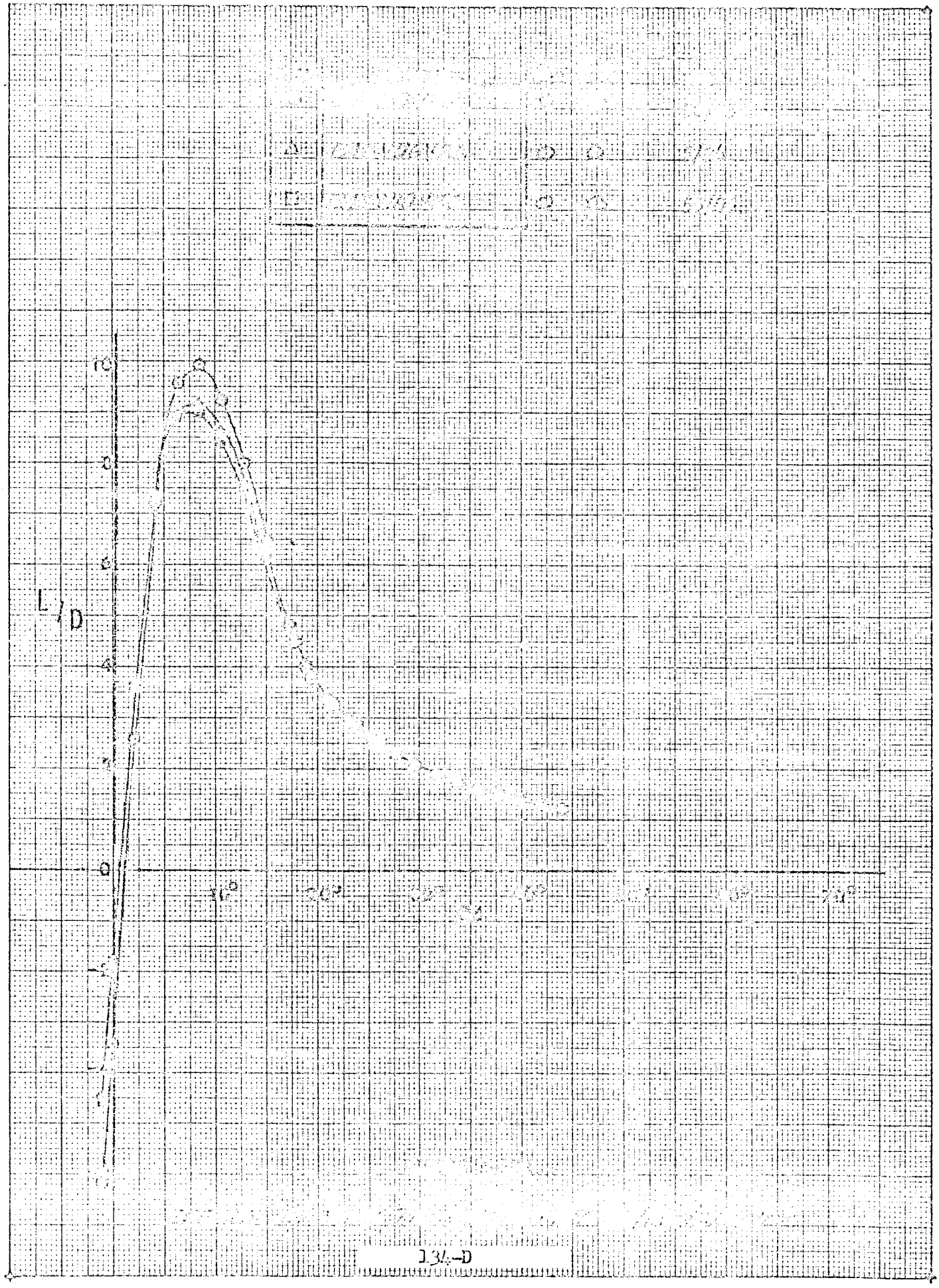

KEUFFEL & ESSER CO.

K&E 10 X 10 TO THE CENTIMETER 46 1517
18 X 25 CM. • ALBANENE®
KEUFFEL & ESSER CO.

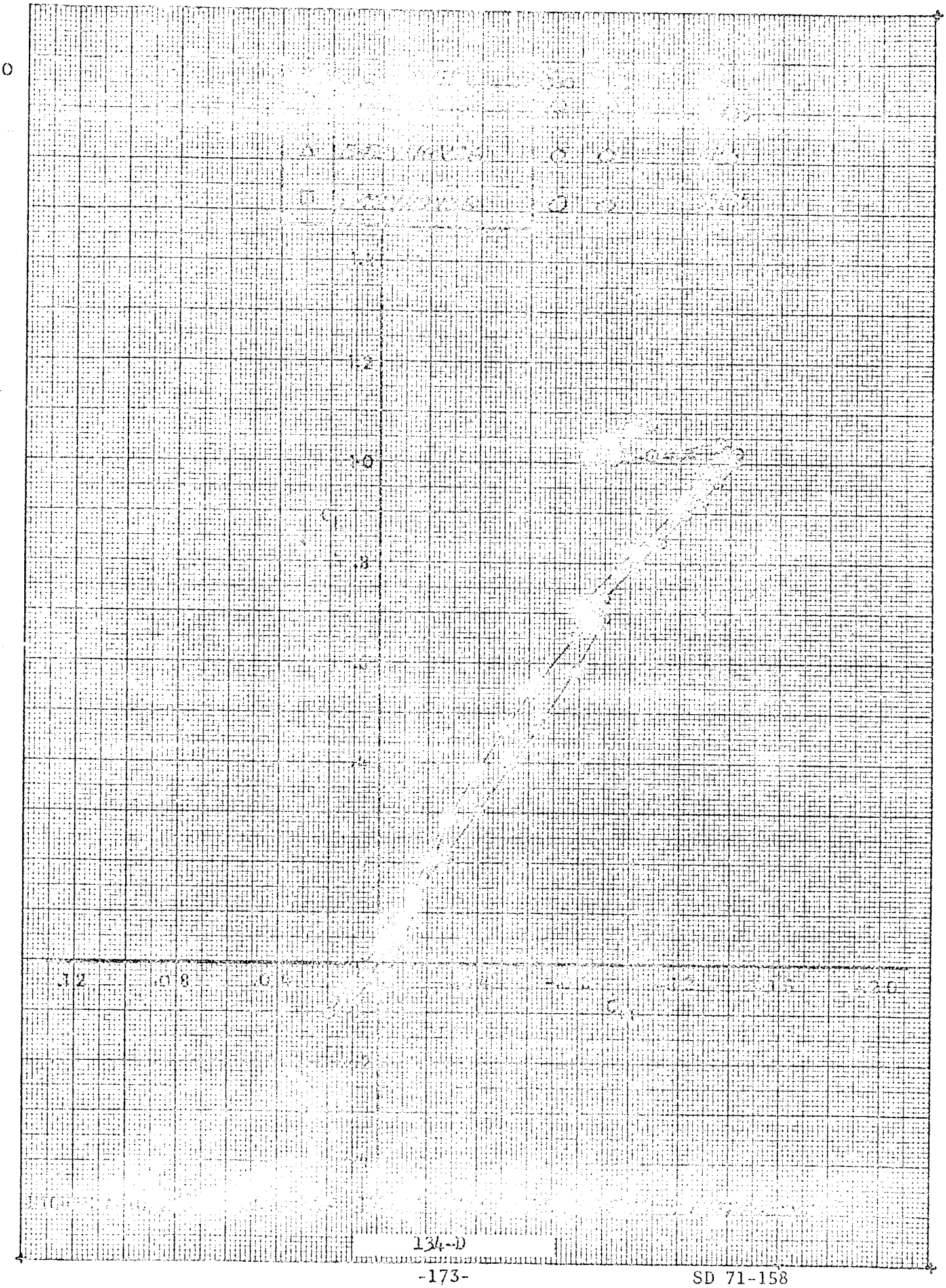

K&E 10 X 10 TO THE CENTIMETER 46 1517
18 X 25 CM. • ALBANENE®
MADE IN U.S.A.
KEUFFEL & ESSER CO.

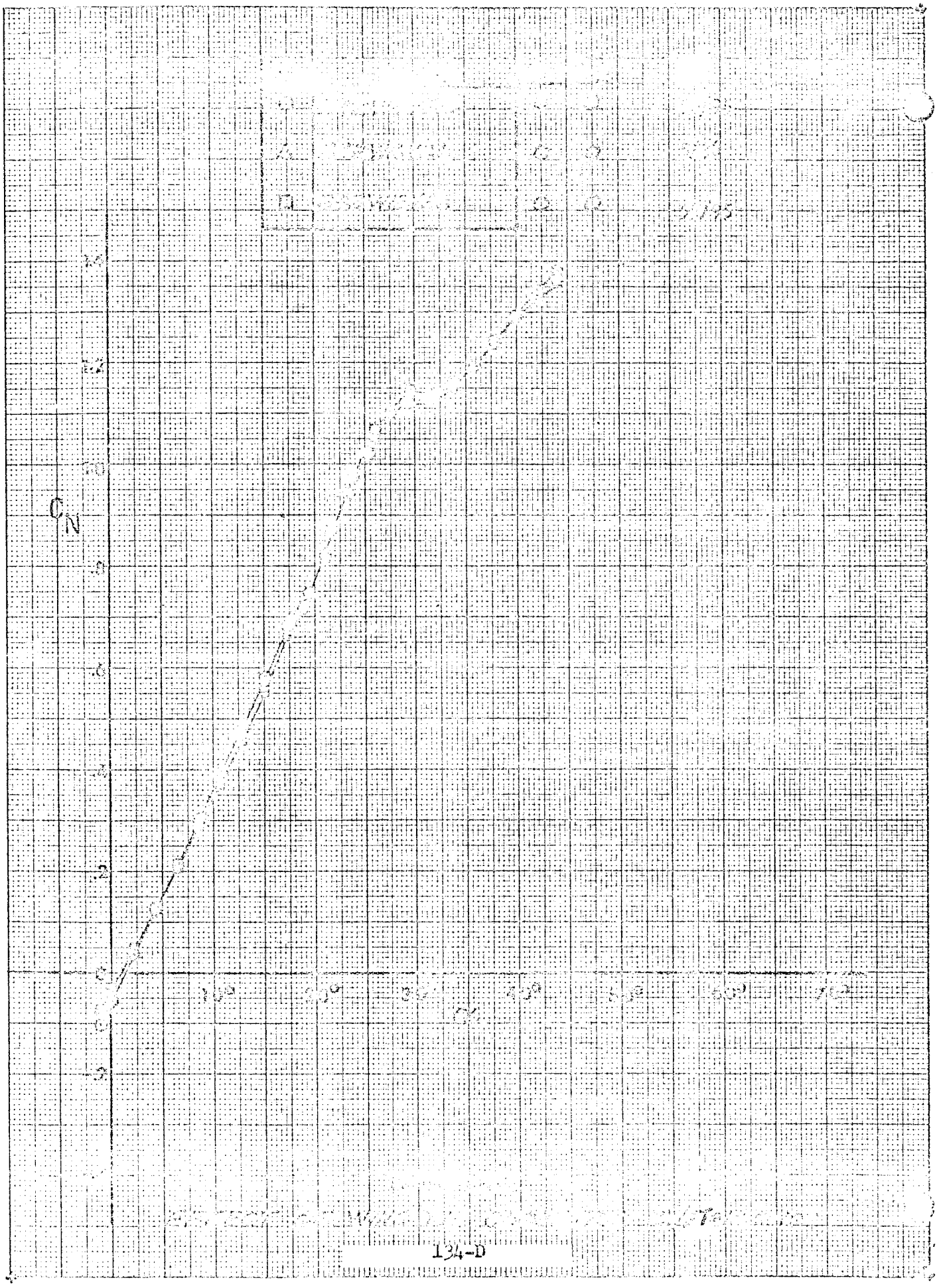
C_N
134-D

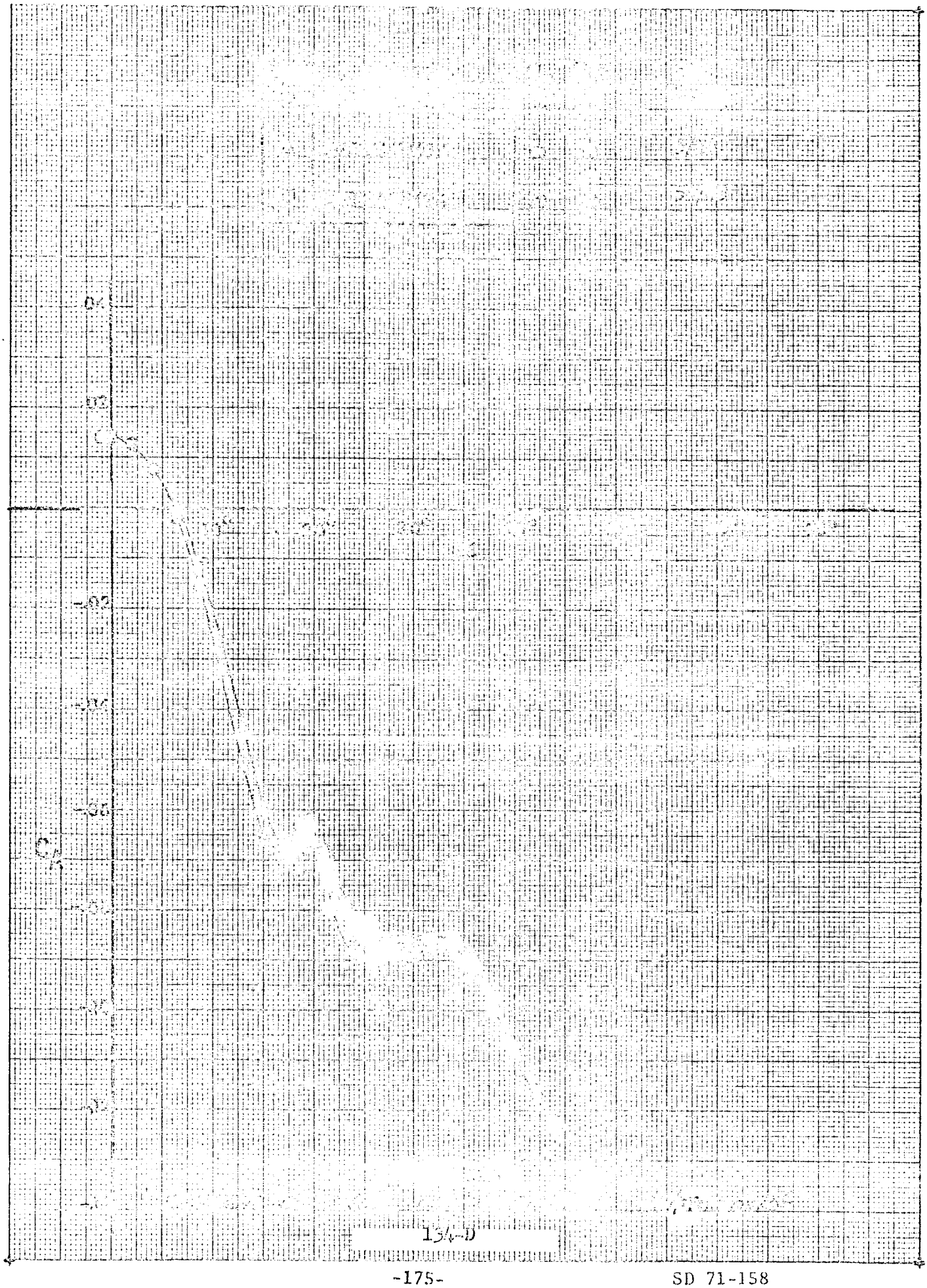

K&E 10 X 10 TO THE CENTIMETER 46 1517
18 X 25 CM. • ALBANENE®
KEUFFEL & ESSER CO.
MADE IN U.S.A.

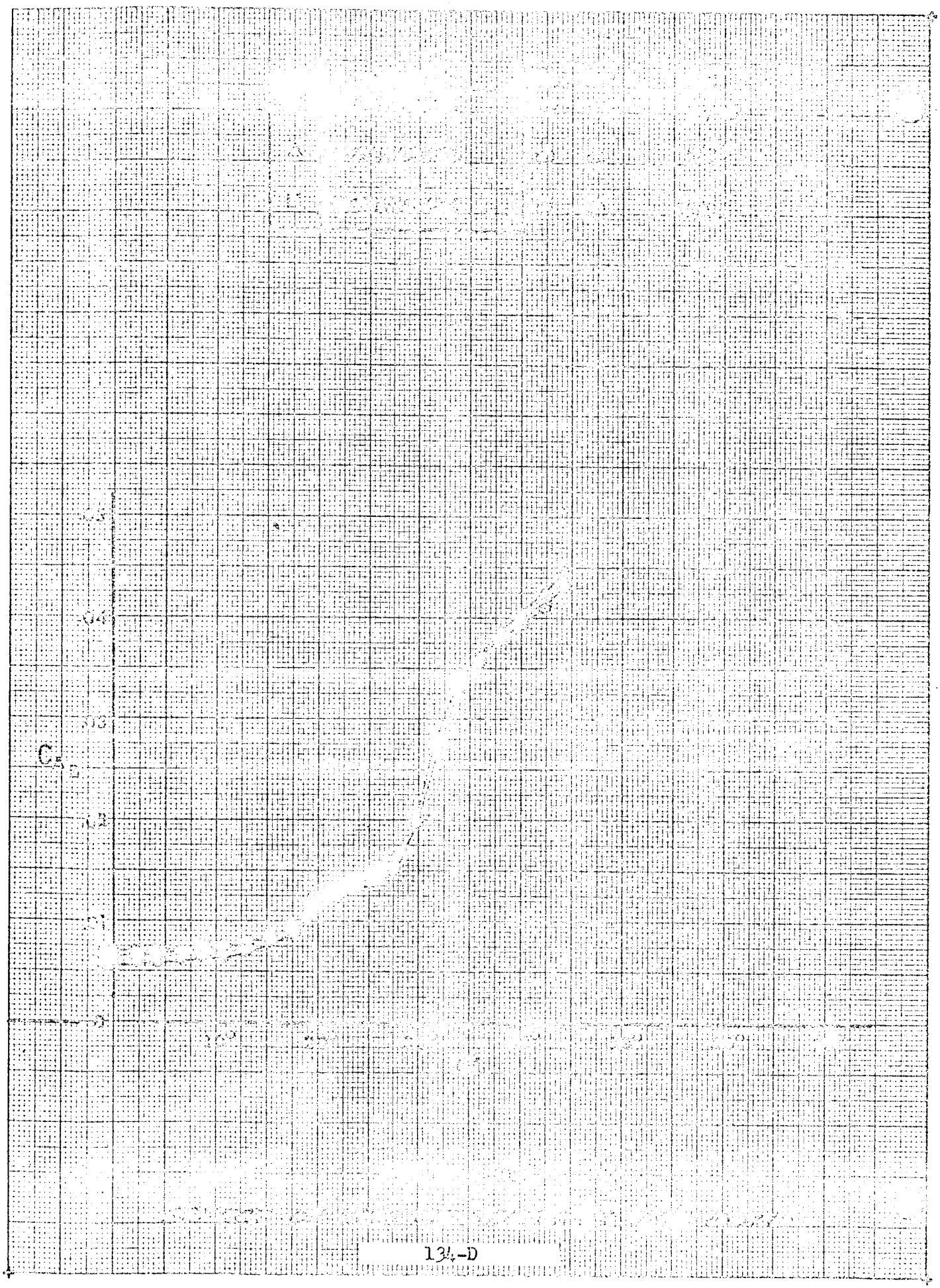

10 X 10 TO THE CENTIMETER 46 1517
10 X 25 CM. • ALBANENE
KEUFFEL & ESSER CO.

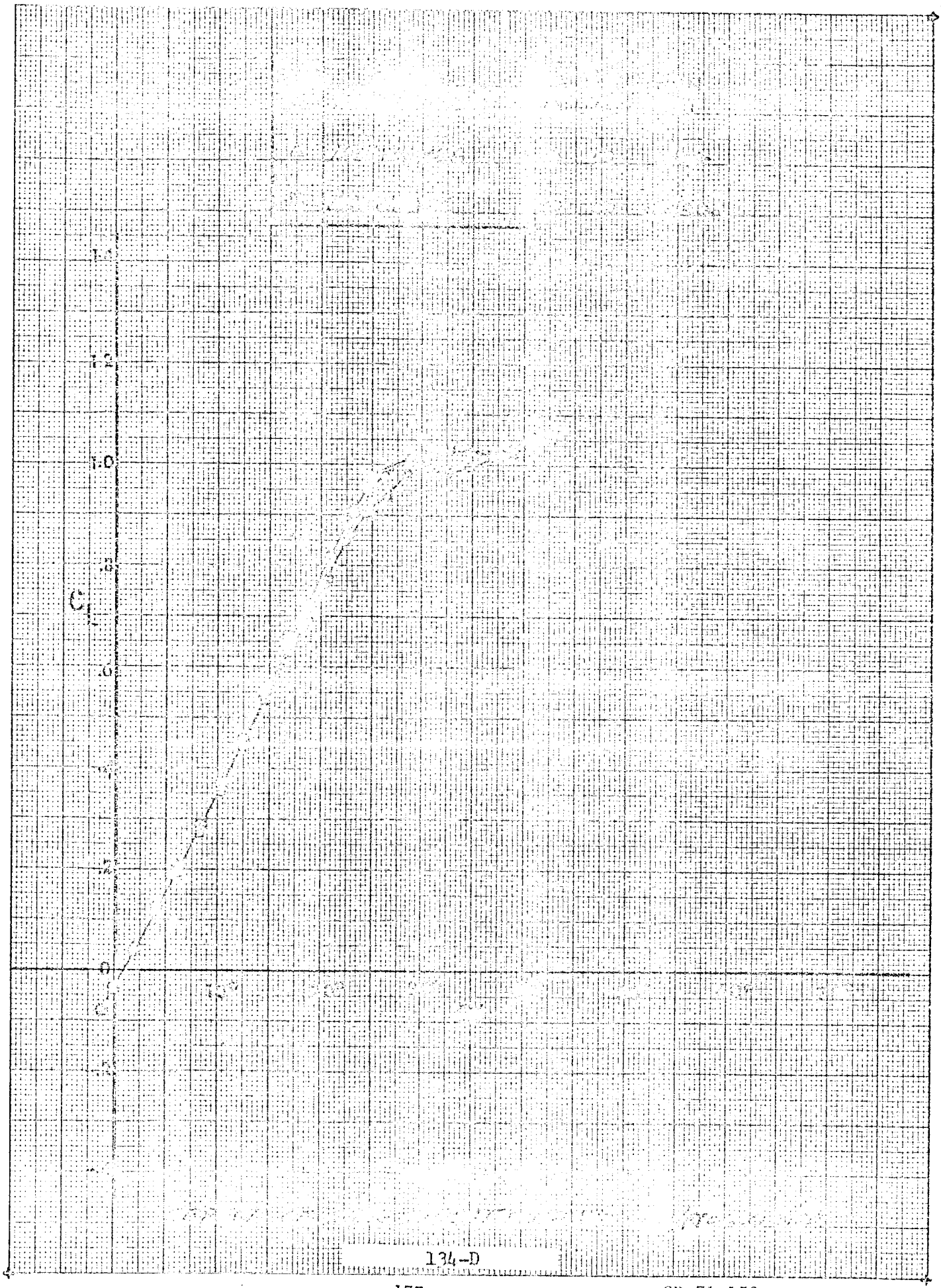

KEUFFEL & ESSER CO.
19 X 25 CM • ALBANENE

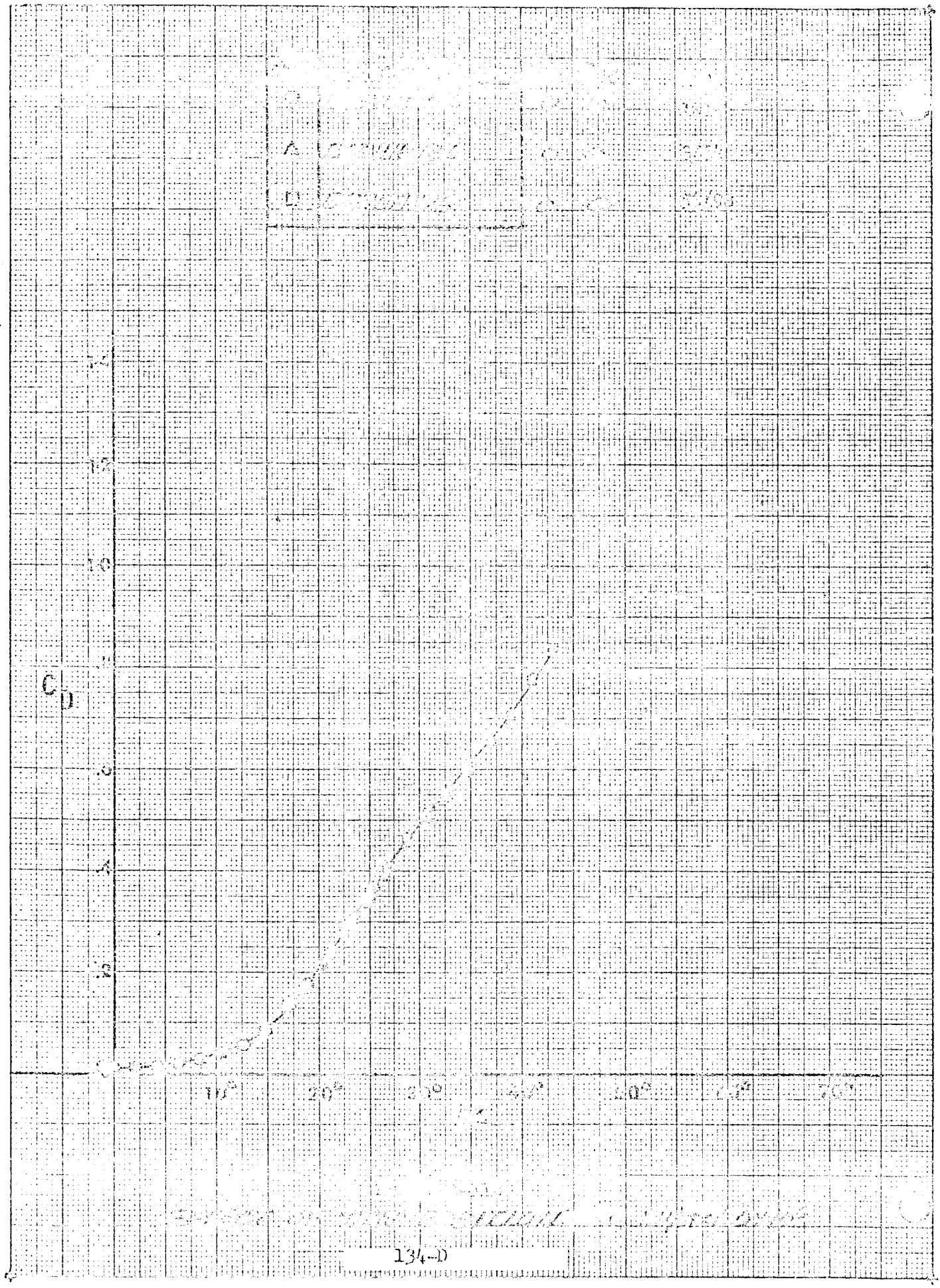
C_D
.2
.4
.6
.8
1.0
1.2
10°
20°
30°
40°
50°
60°
70°
134-D

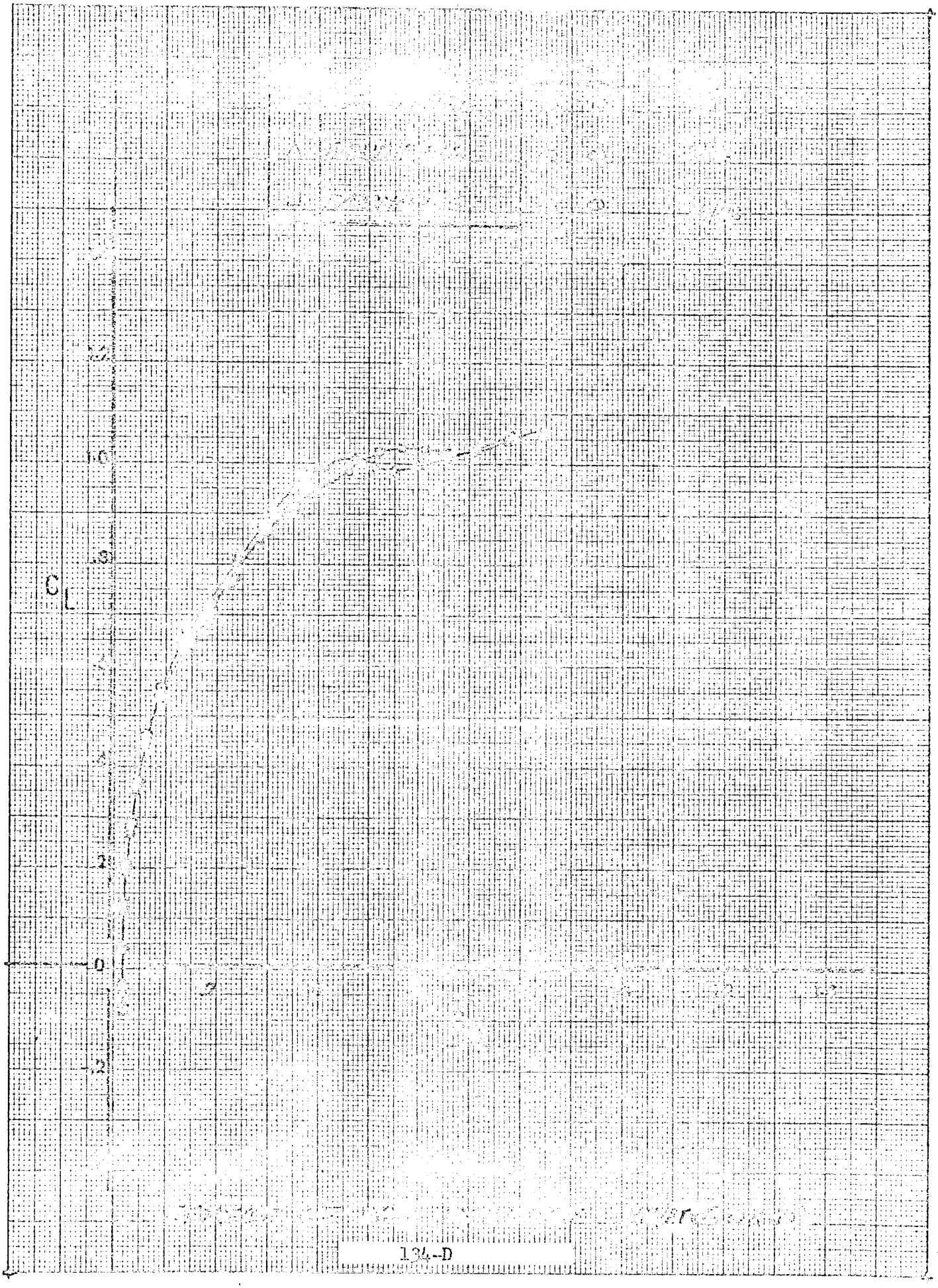

K+E 10 X 10 TO THE CENTIMETER 46 1517
18 X 25 CM. • ALBANENE® MADE IN U.S.A.
KEUFFEL & ESSER CO.

17

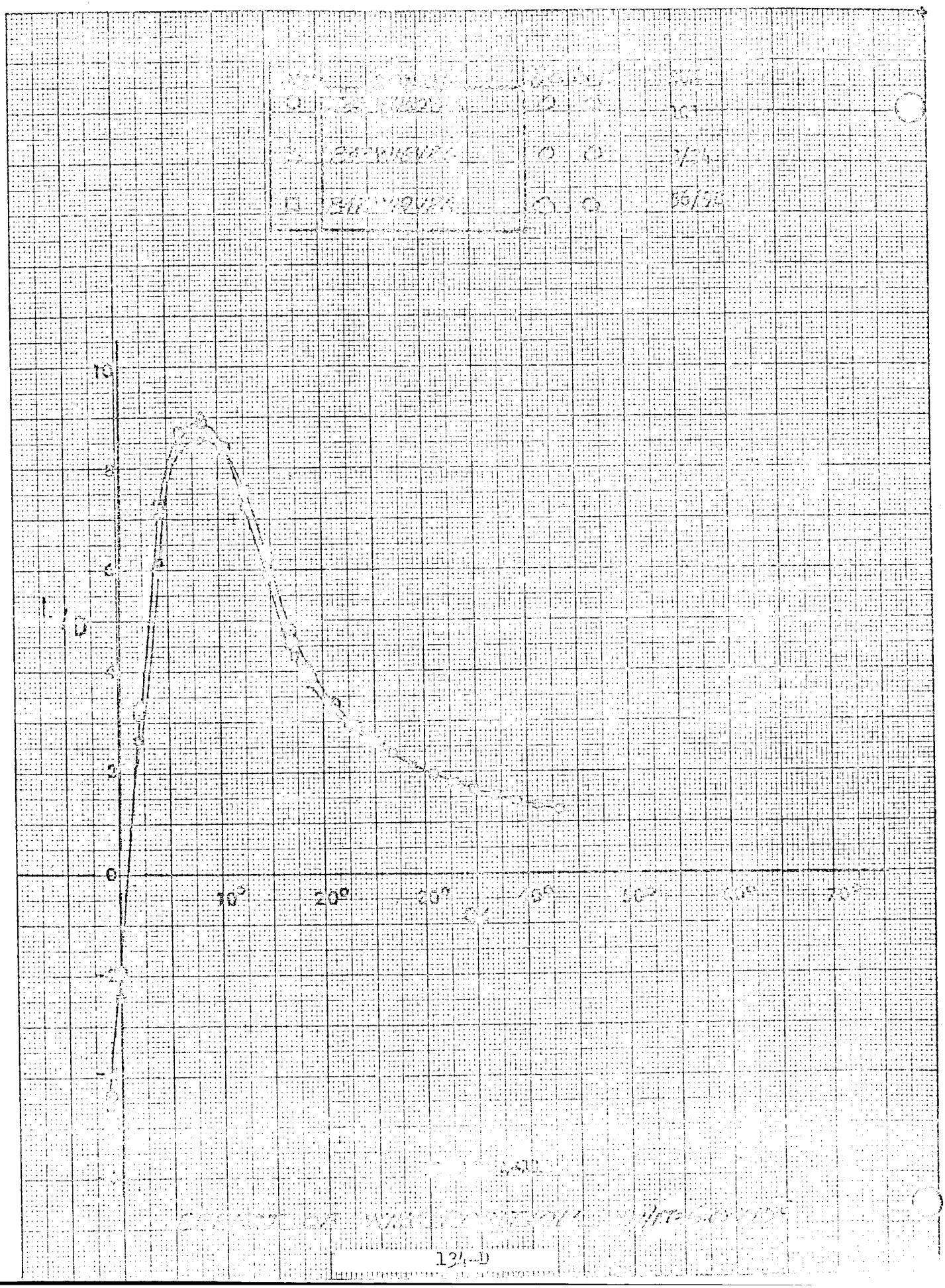

10 X 10 TO THE CENTIMETER 46 1517
KEUFFEL & ESSER CO.

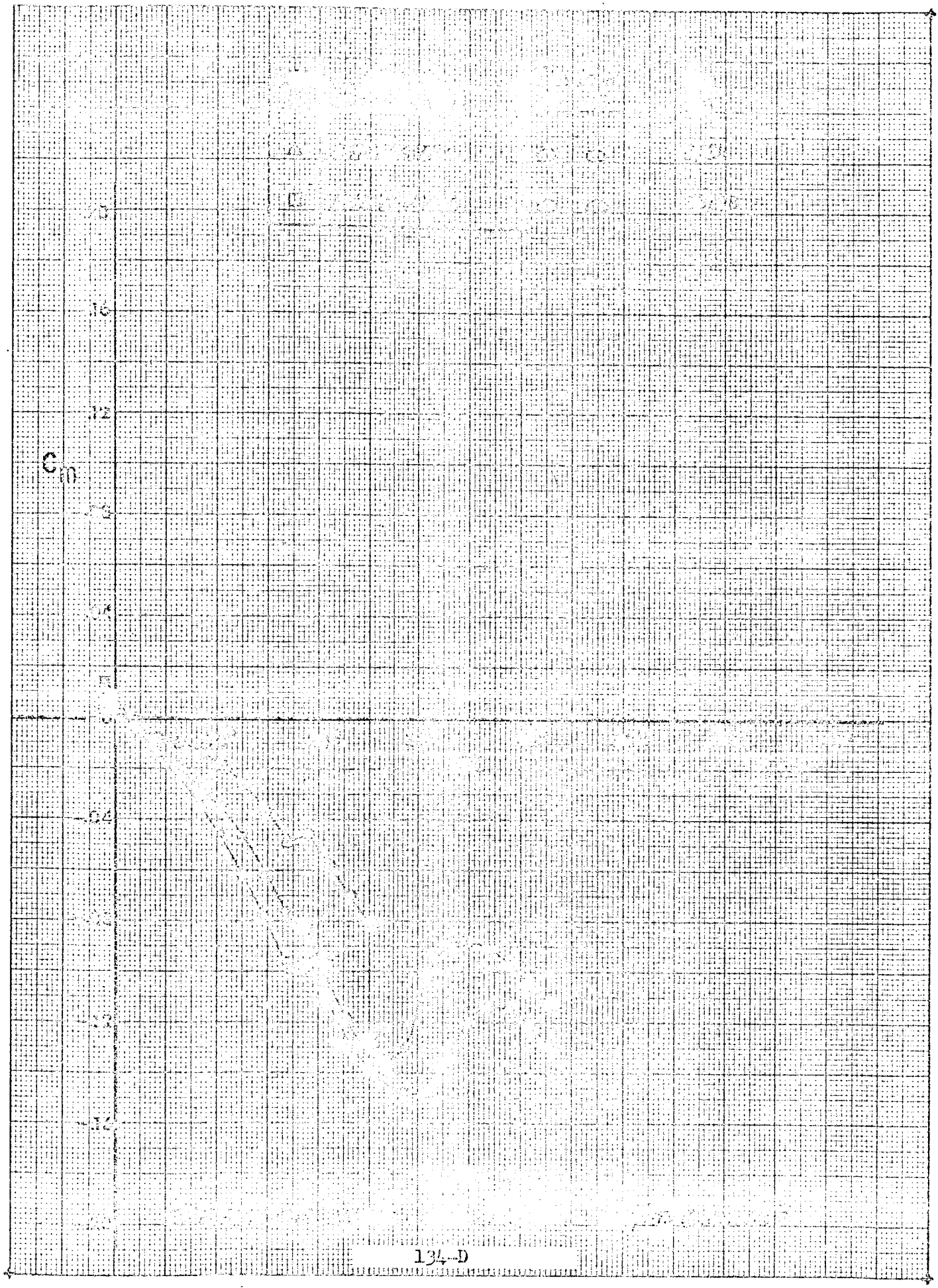

K&E 10 X 10 TO THE CENTIMETER 46 1517
18 X 25 CM. • ALBANENE
KEUFFEL & ESSER CO.

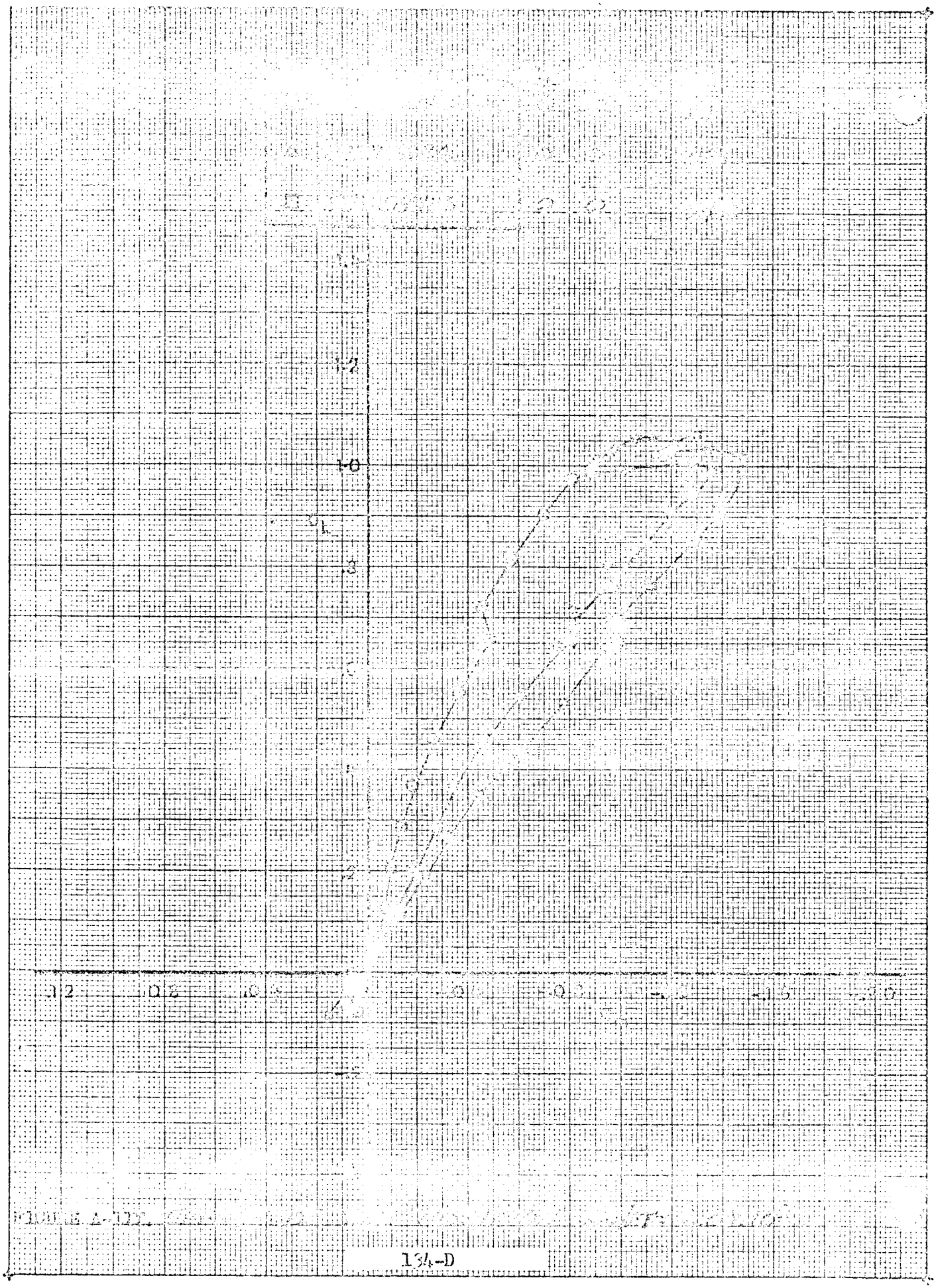

K&E 10 X 10 TO THE CENTIMETER 46 1517
18 X 25 CM • ALBANY, N.Y.
KEUFFEL & ESSER CO.

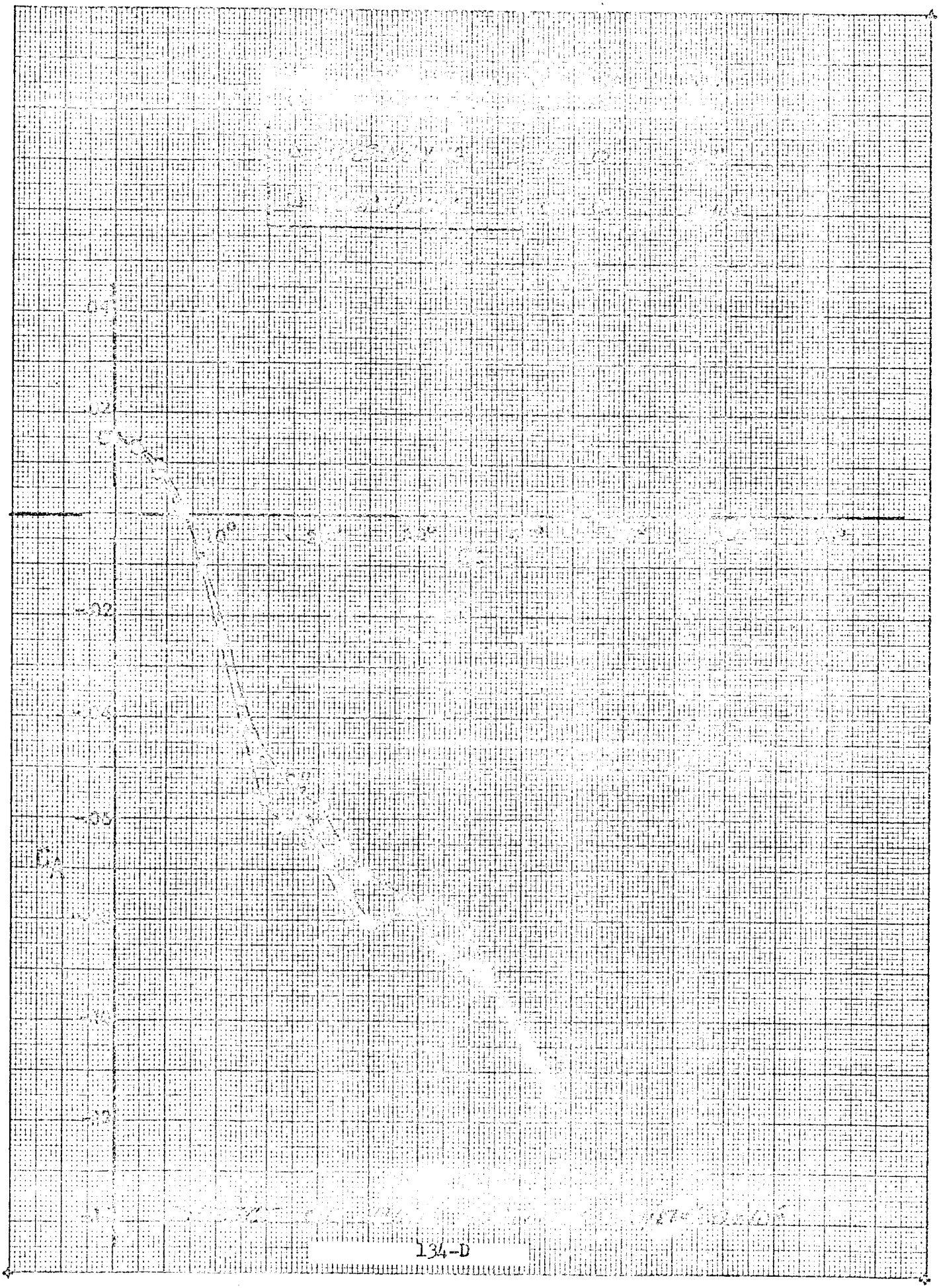

10 X 10 TO THE CENTIMETER 46 1317
18 X 25 CM. • ALBANENE®
KEUFFEL & ESSER CO.

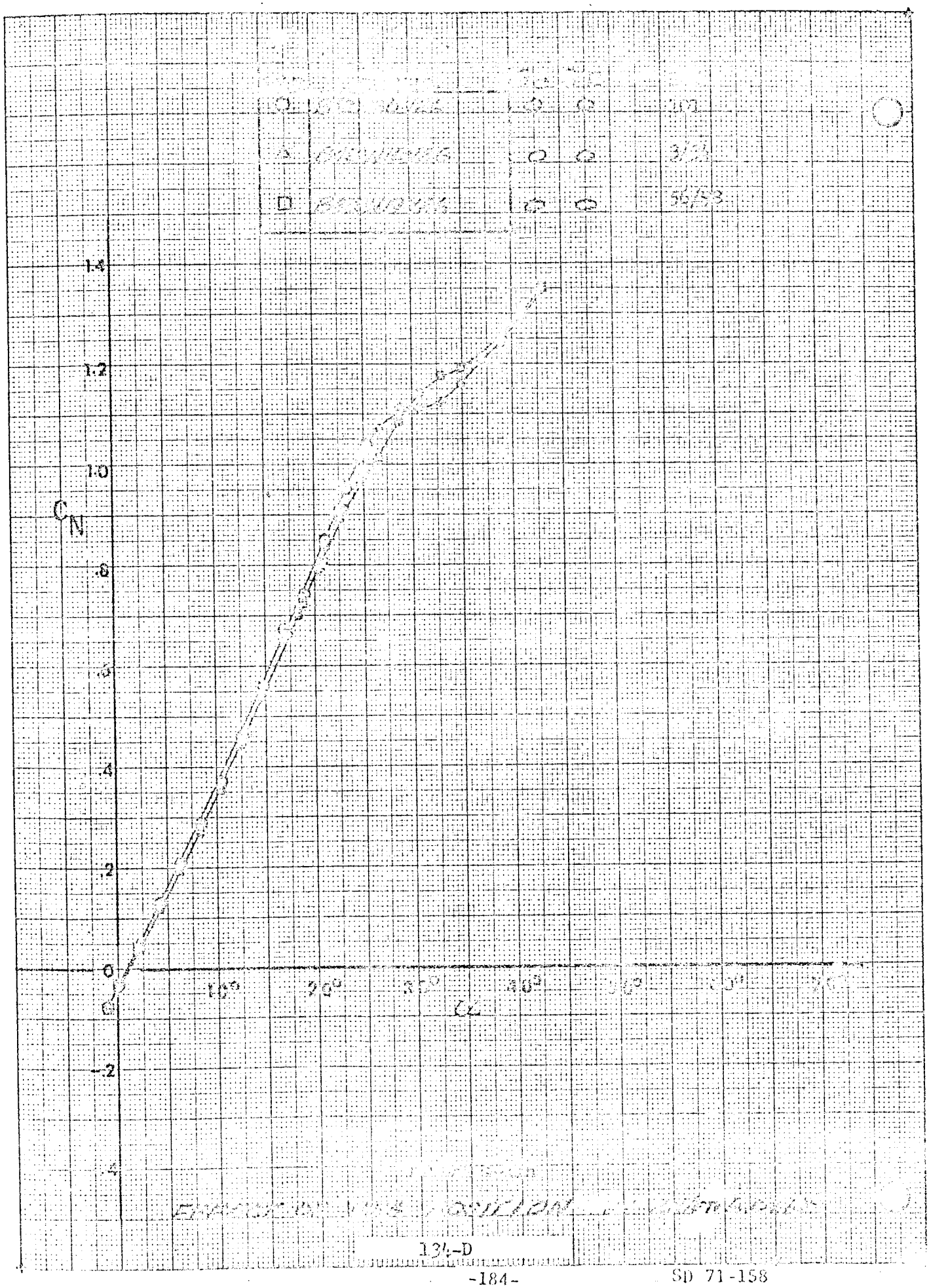

134-D

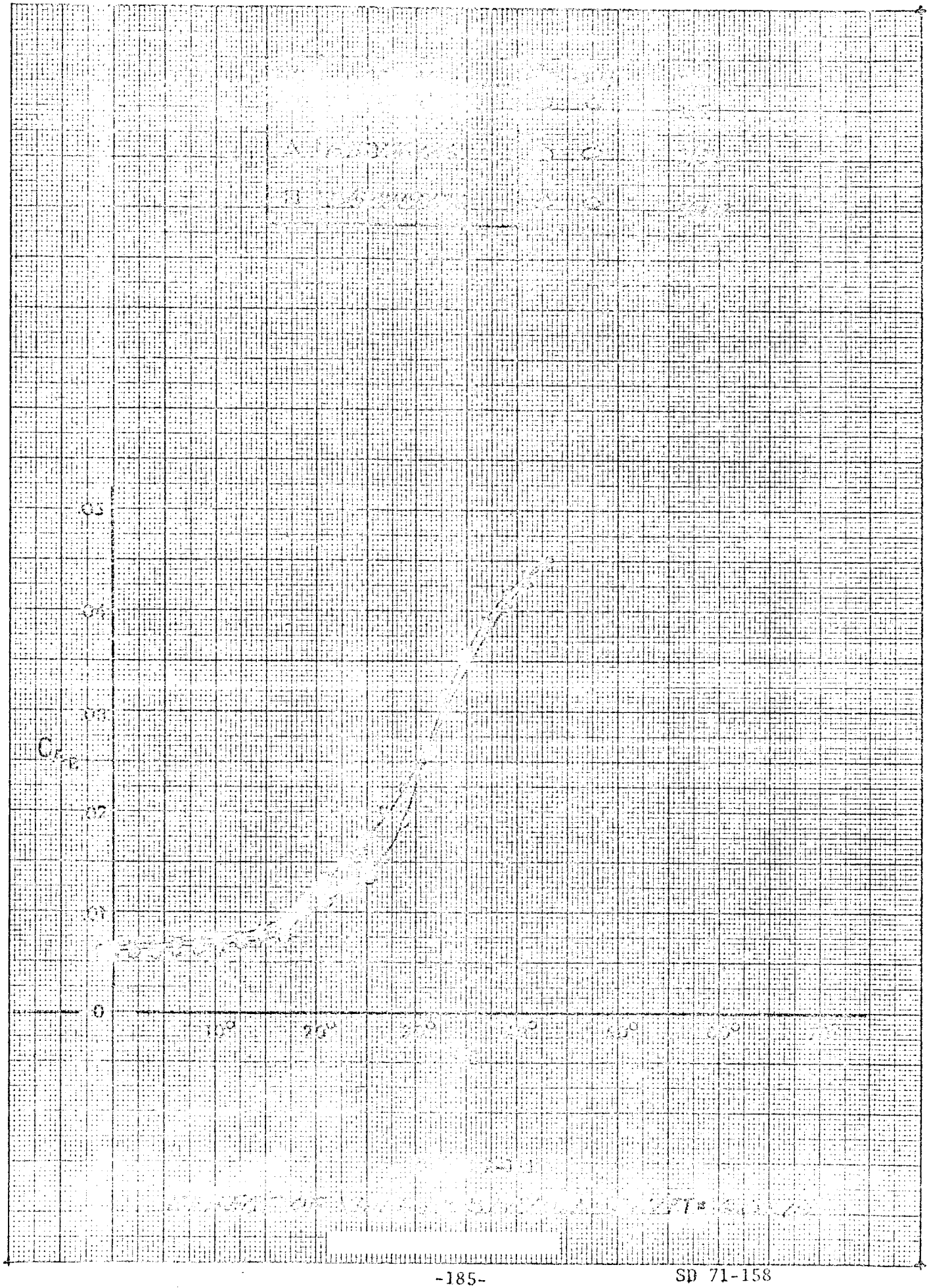

10 X 10 TO THE CENTIMETER 46 1517
18 X 25 CM. • ALBANENE
KEUFFEL & ESSER CO.

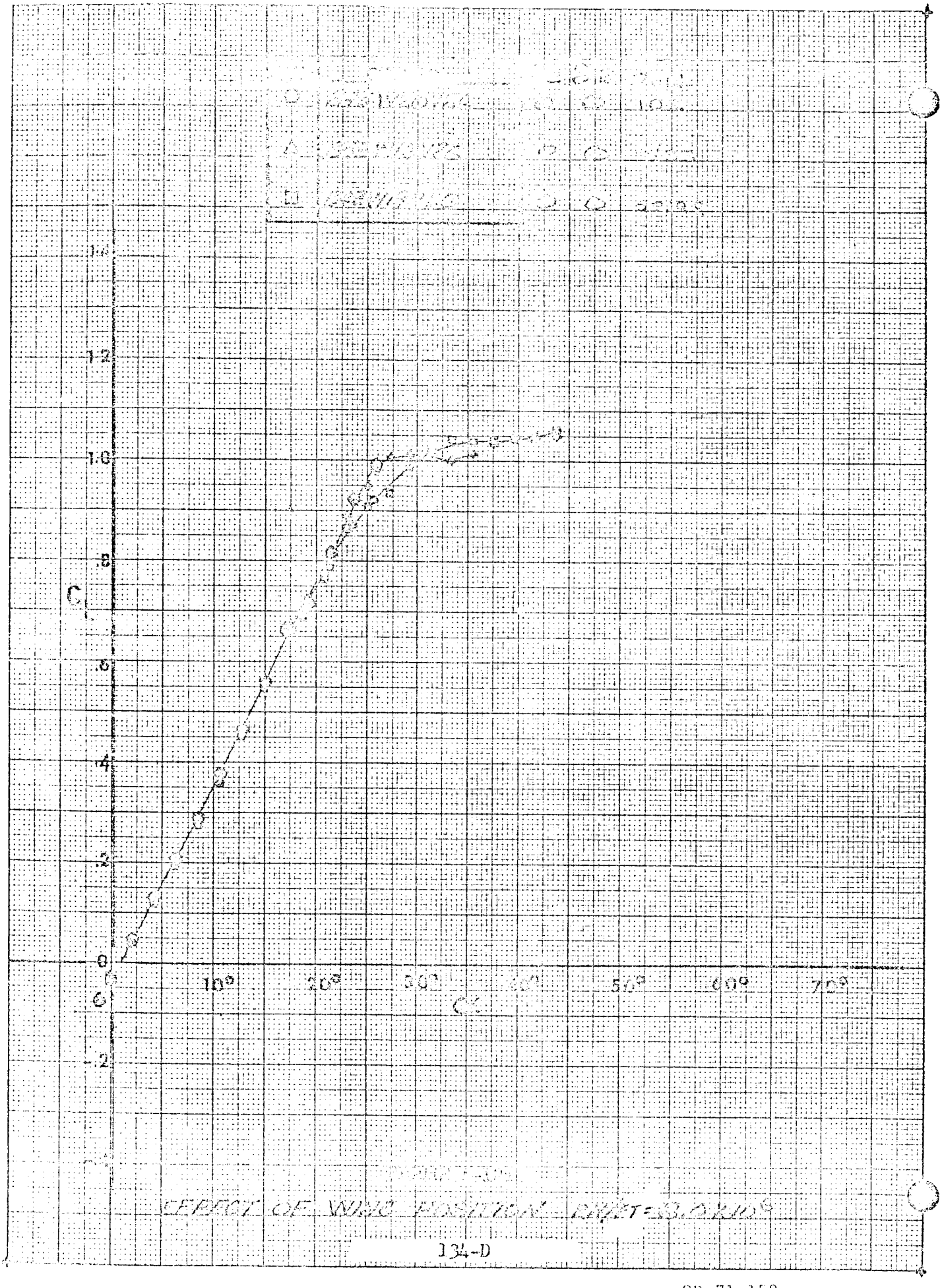
1.4
1.2
1.0
.8
C_L
.6
.4
.2
0
-.2
10°
20°
30°
40°
50°
60°
70°
C_D
EFFECT OF WING POSITION

134-D

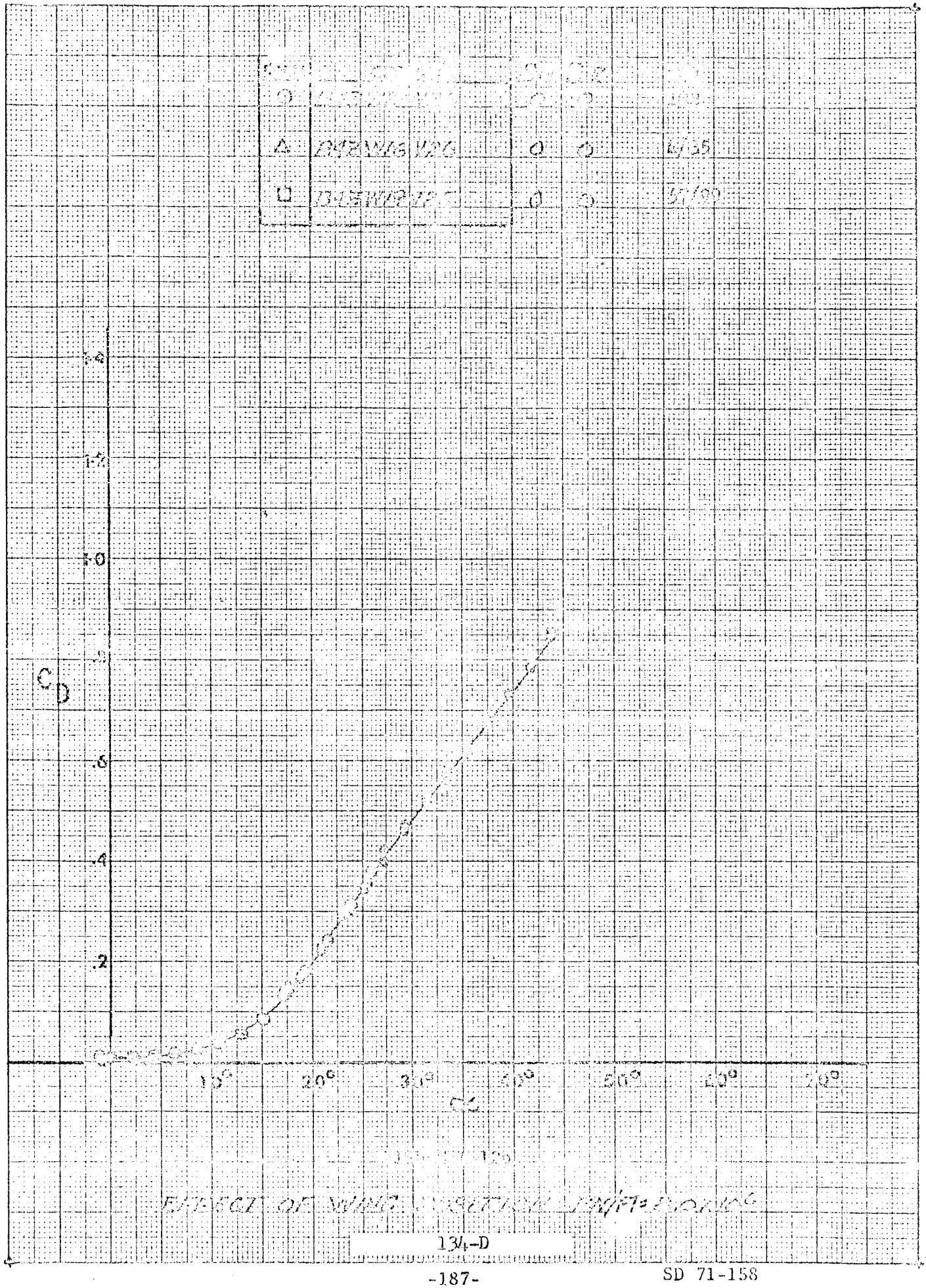

EFFECT OF WING INCIDENCE ON DRAG

13¼-D

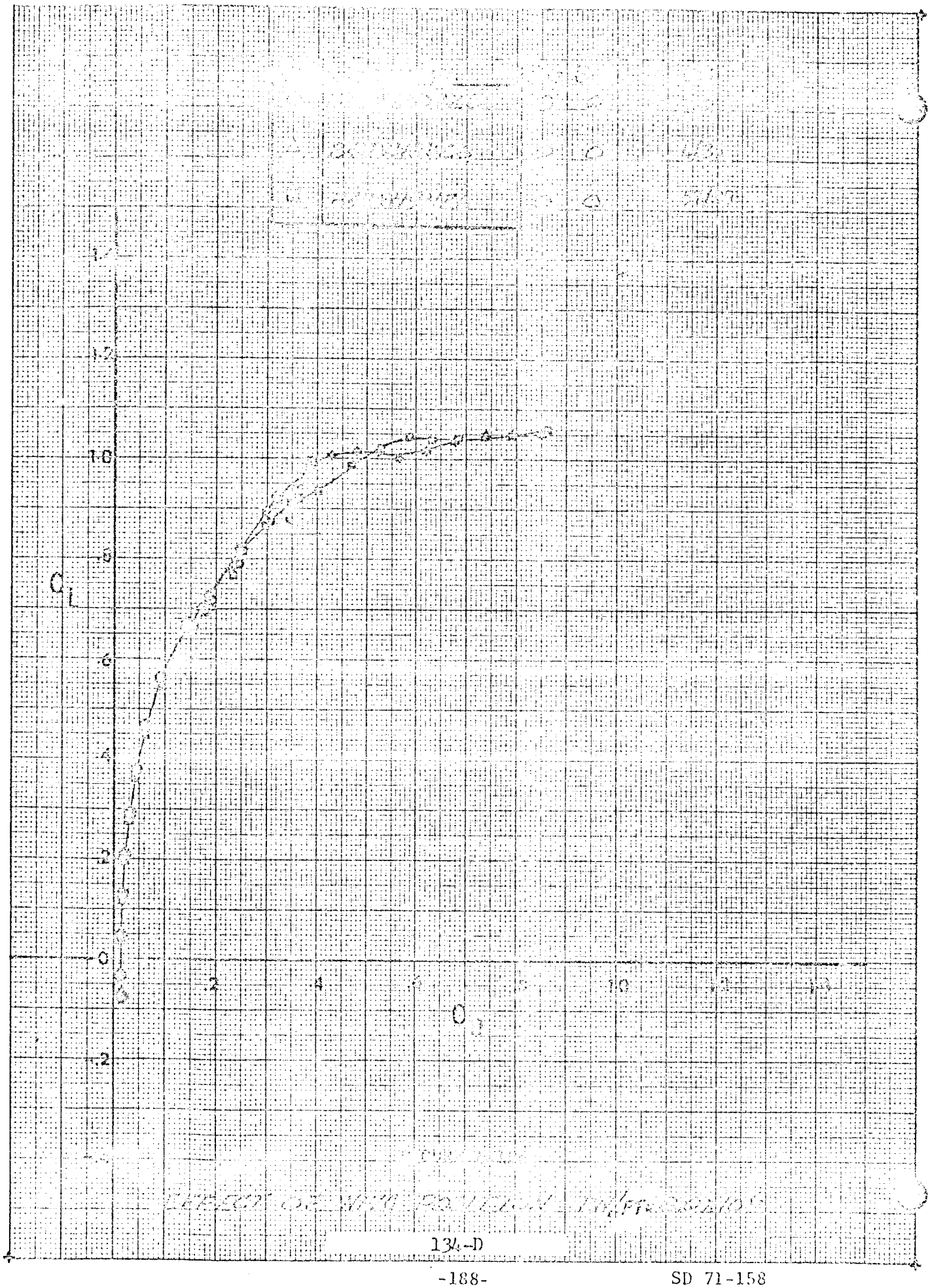

134-D

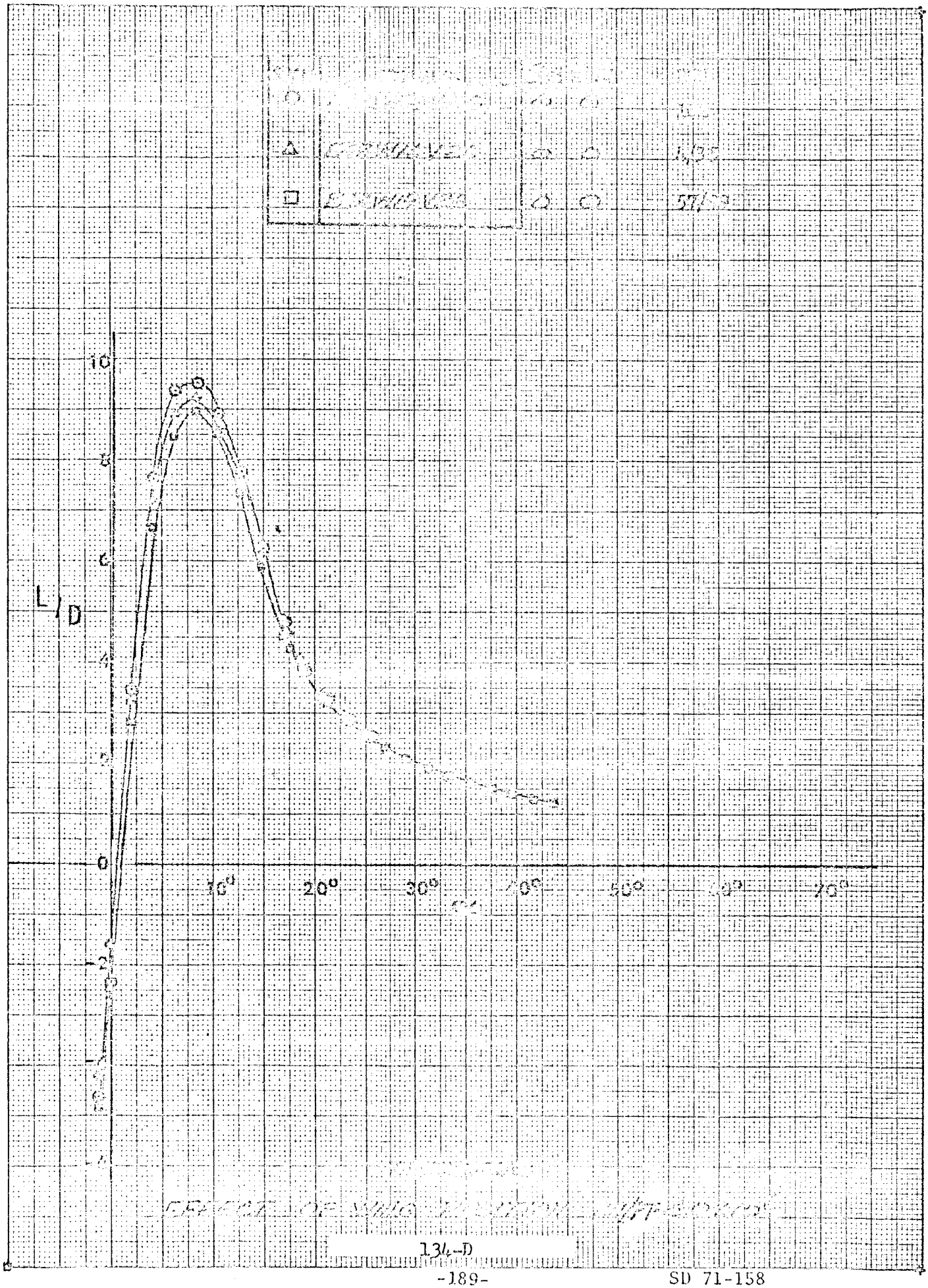

136-D

10 X 10 TO THE CENTIMETER 46 1517
18 X 25 CM • ALBANENE
KEUFFEL & ESSER CO.

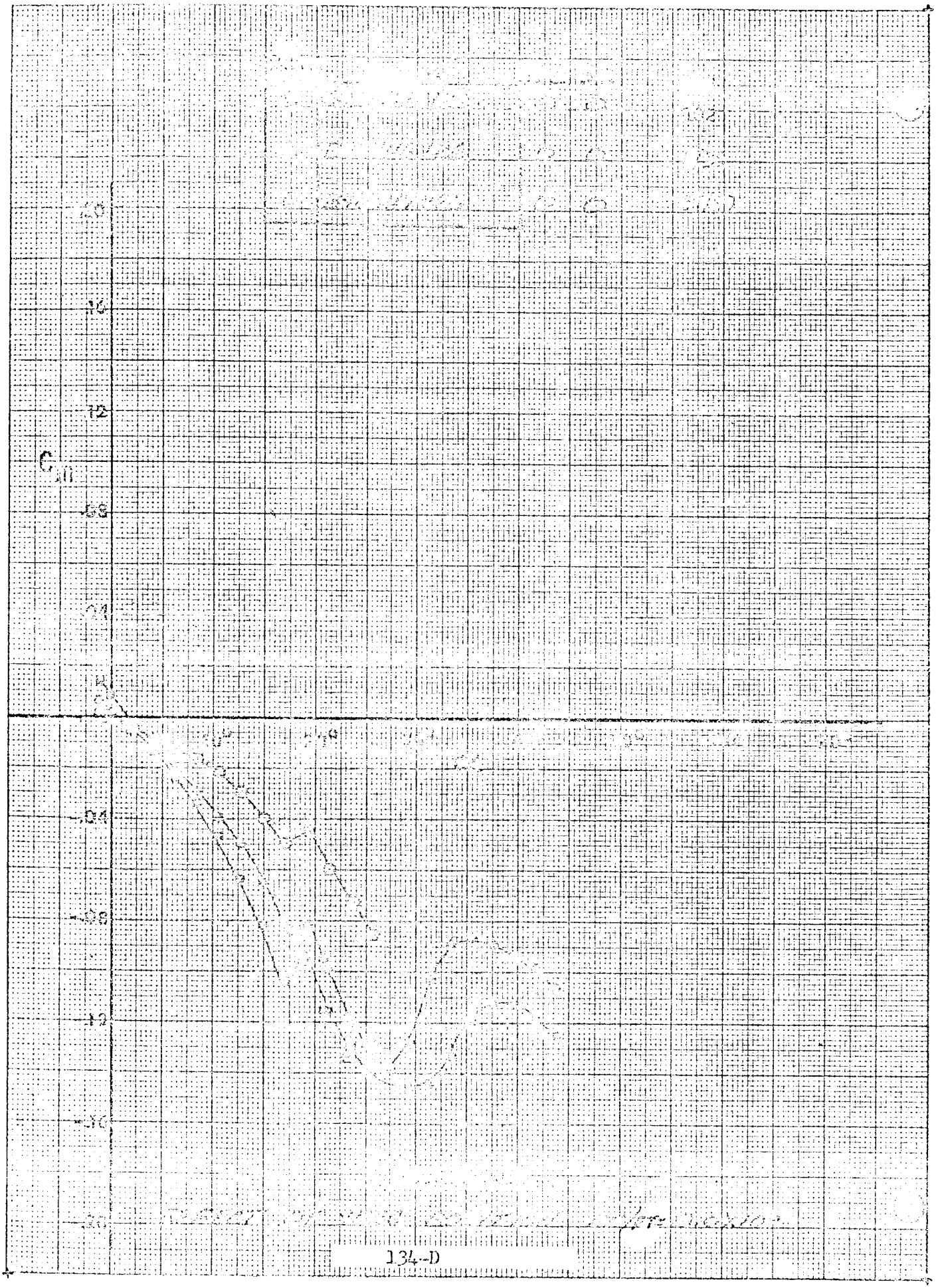

134-D

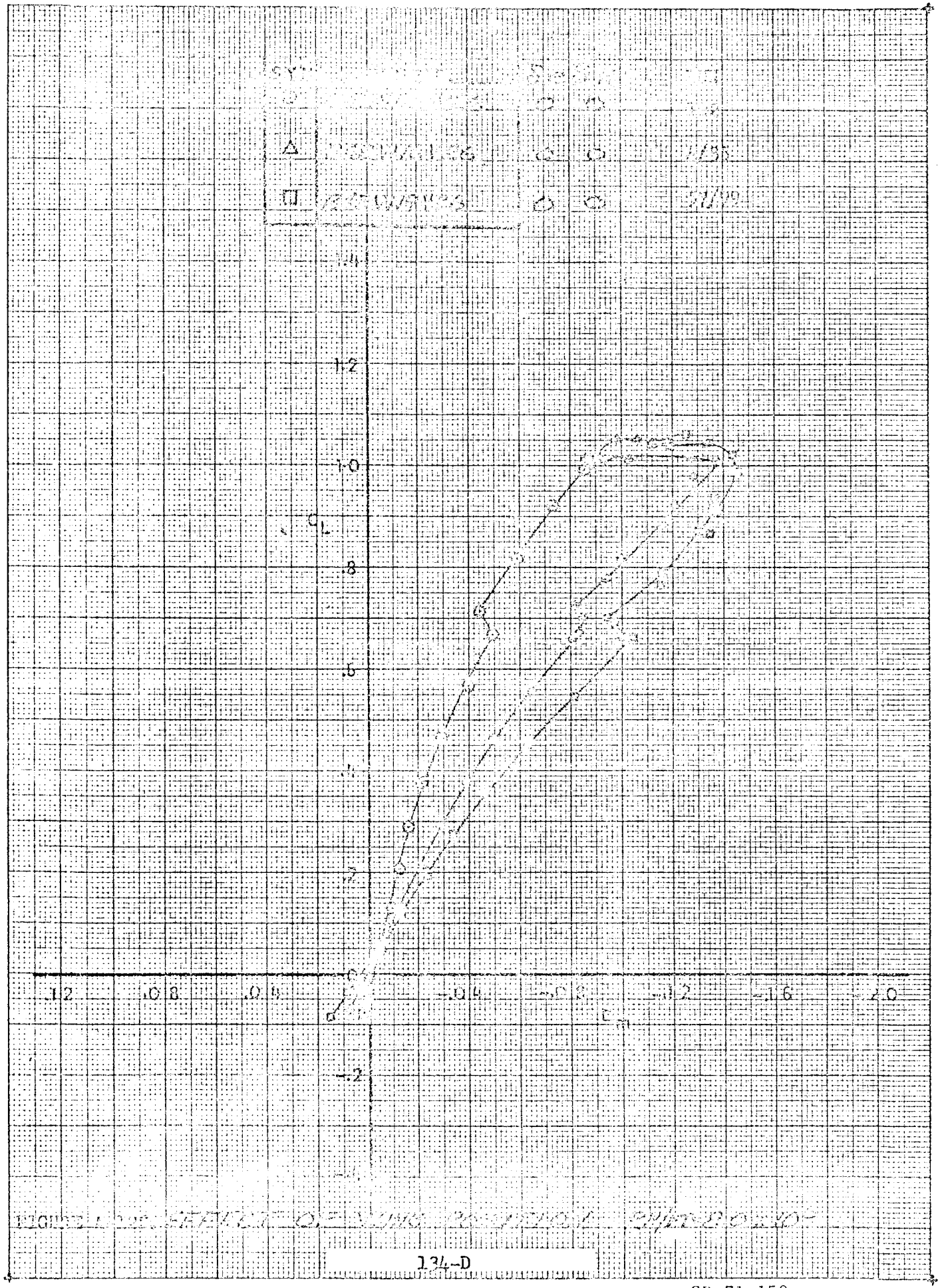

134-D

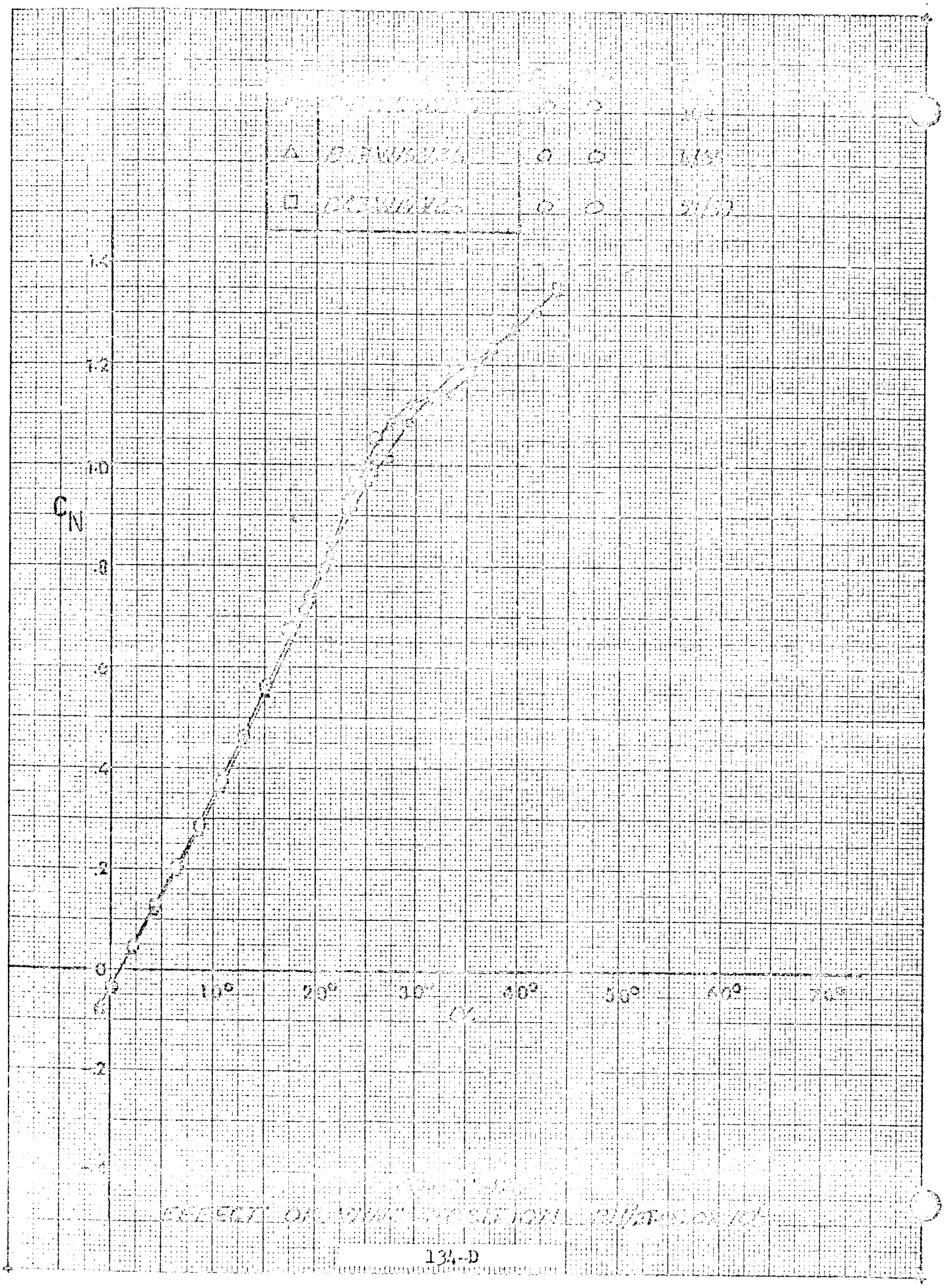

134-D

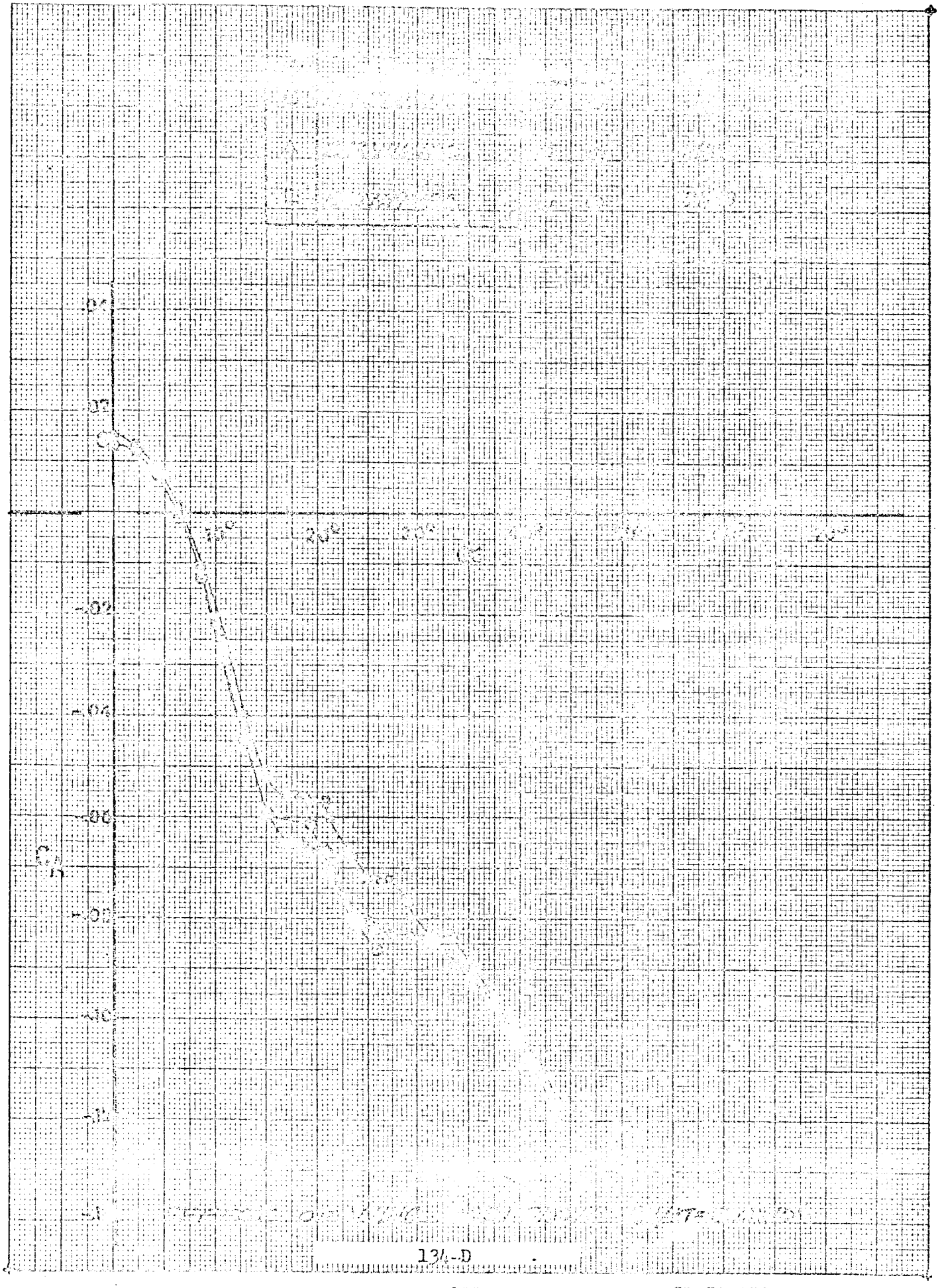

134-D

10 X 10 TO THE CENTIMETER 46 1517
10 X 25 CM. • ALBANY, N.Y.
KEUFFEL & ESSER CO.

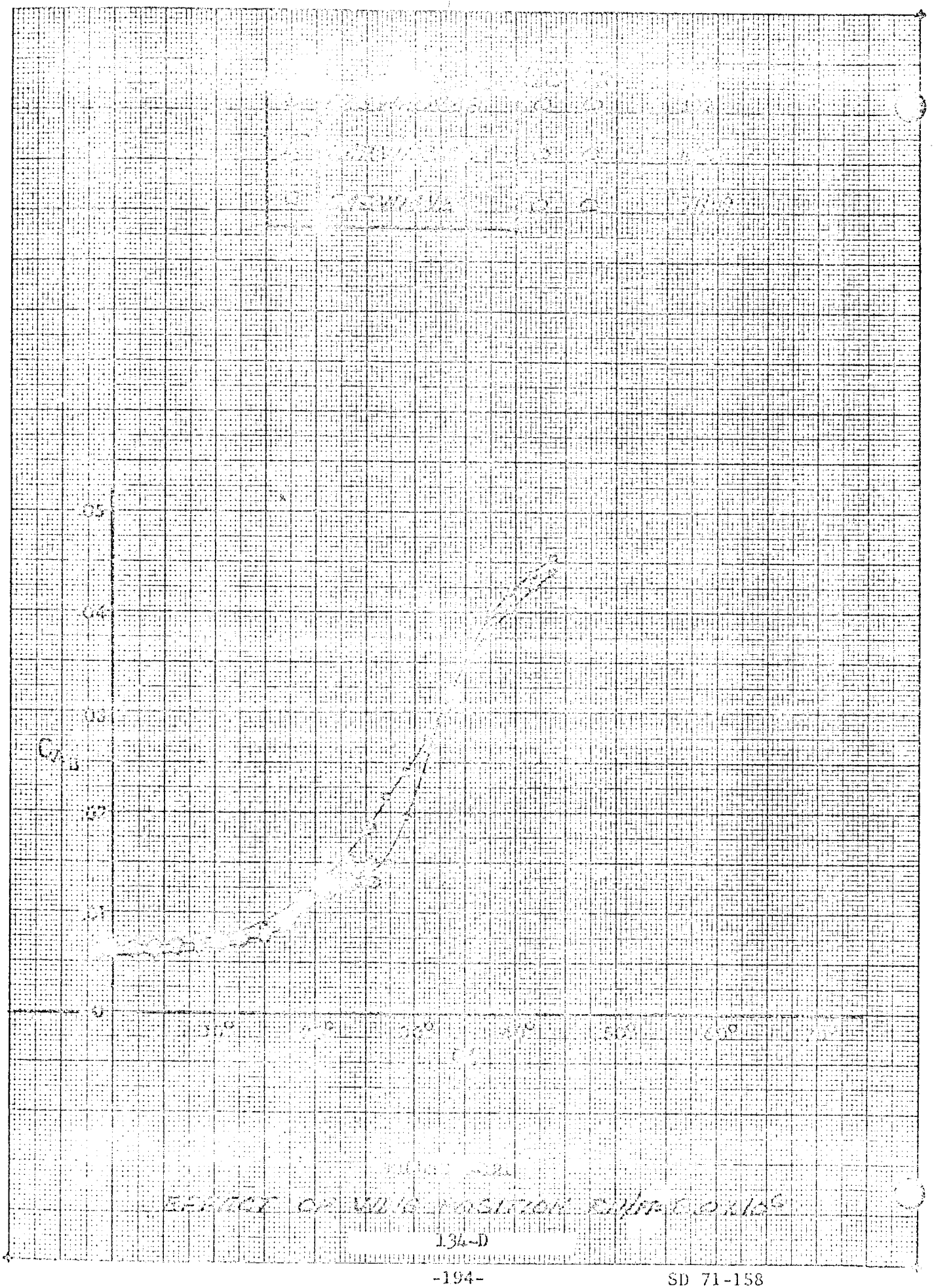
.05
.04
.03
.02
.01
0
300
200
100
0
100
200
300
400
500
600
700
800
Effect of Wall Position Eccentricity

134-D

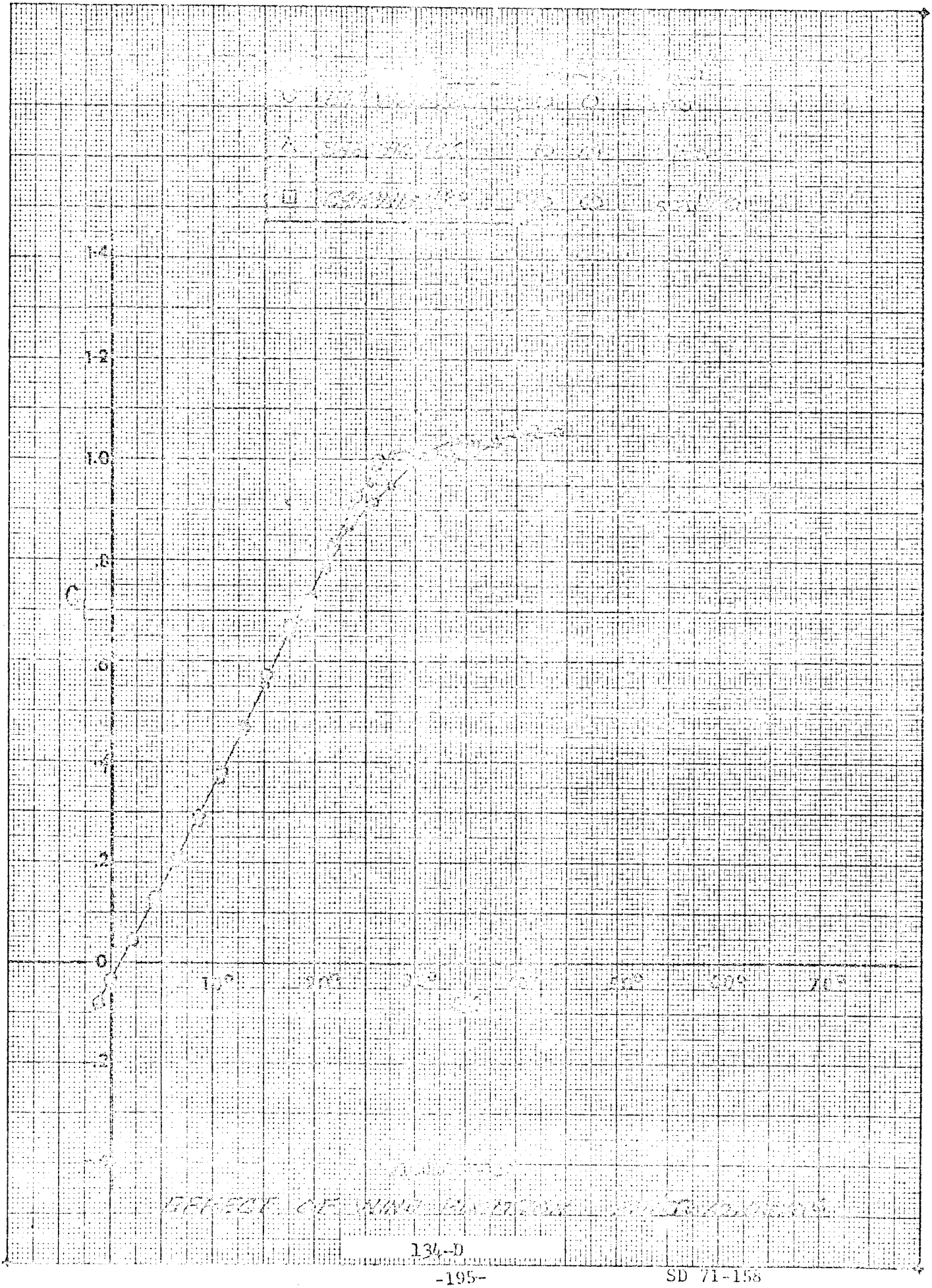

134-D

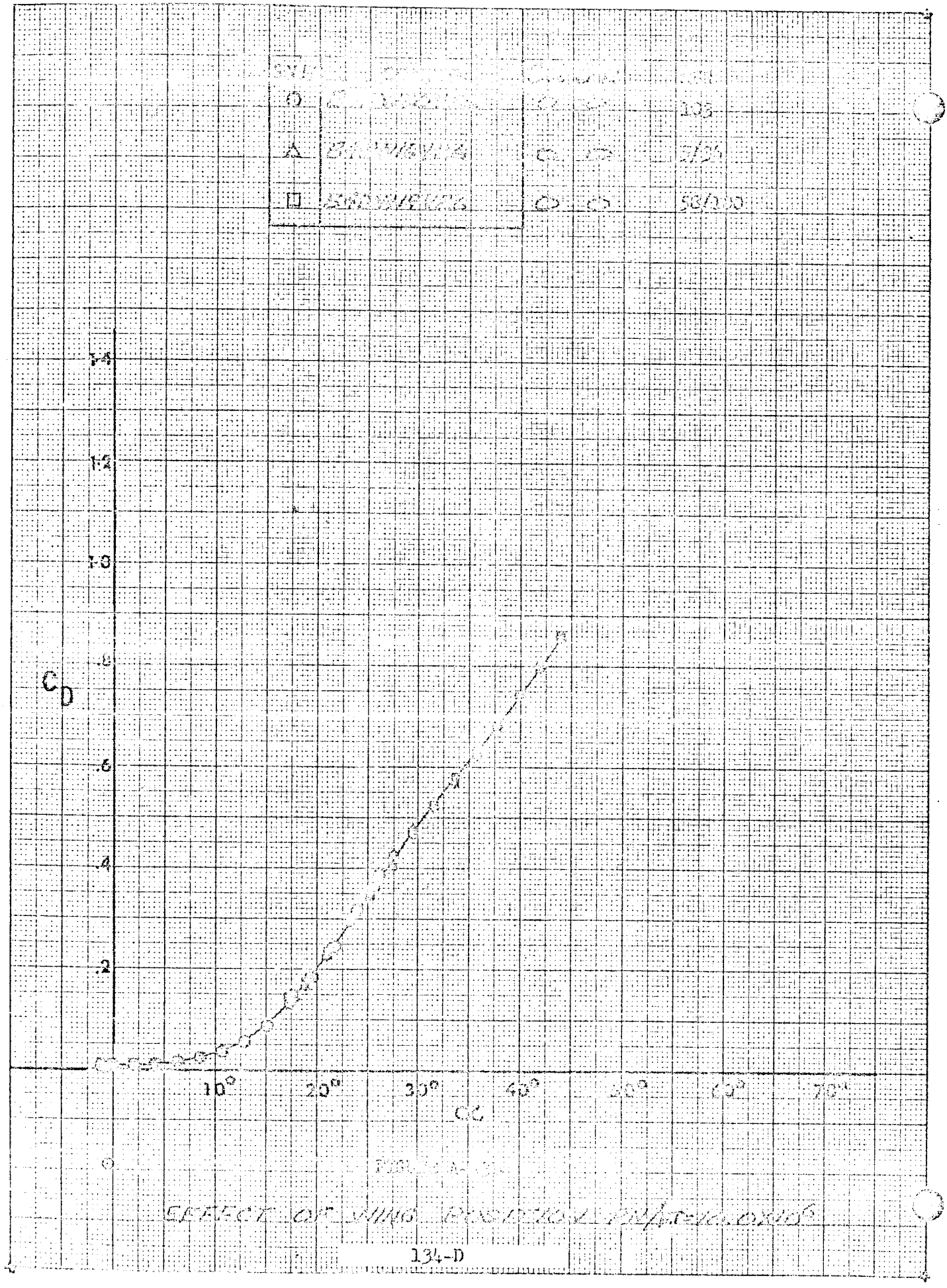
1.4
1.2
1.0
.8
.6
.4
.2
C_D
10°
20°
30°
40°
50°
60°
70°
α
134-D

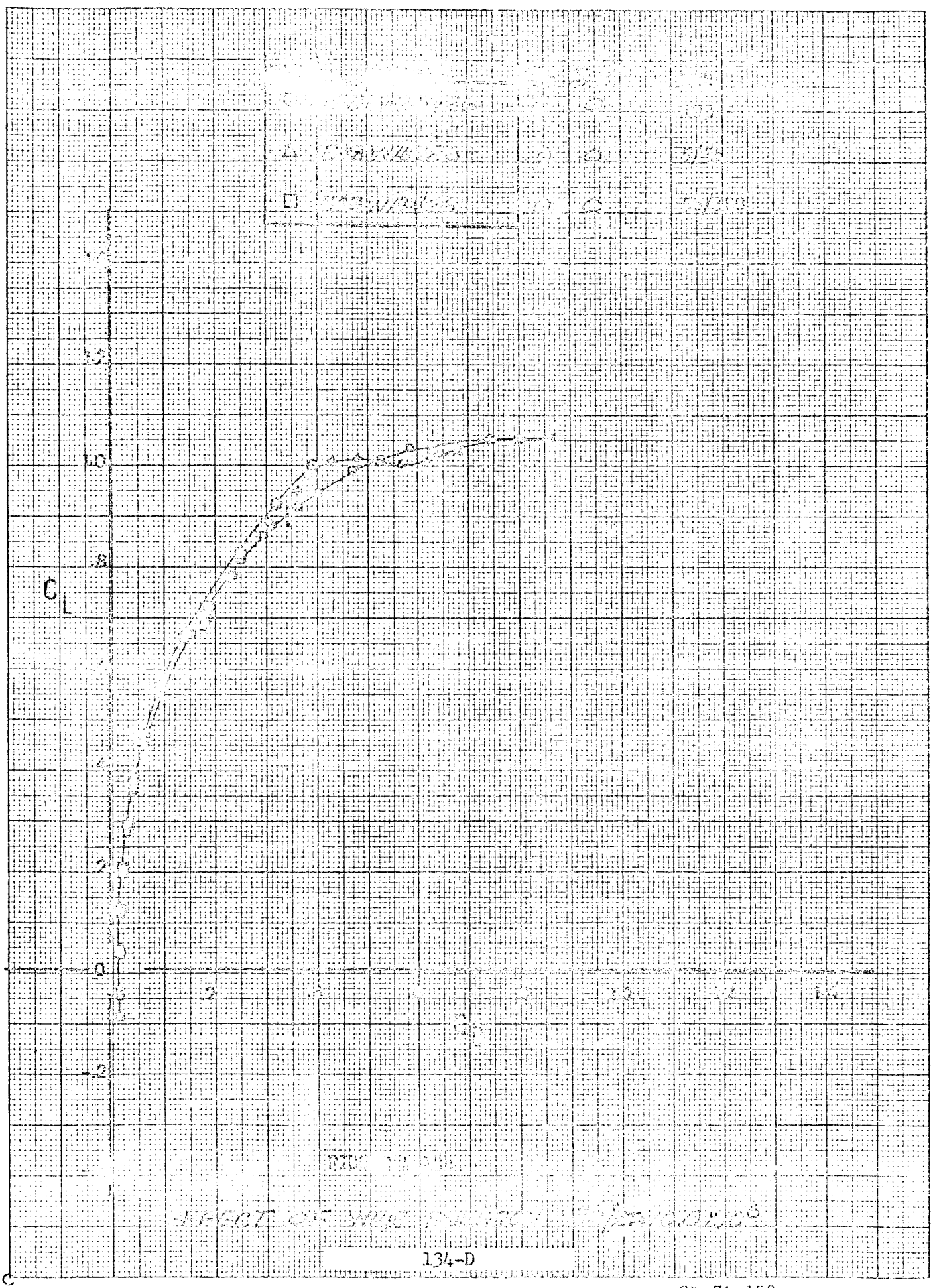

134-D

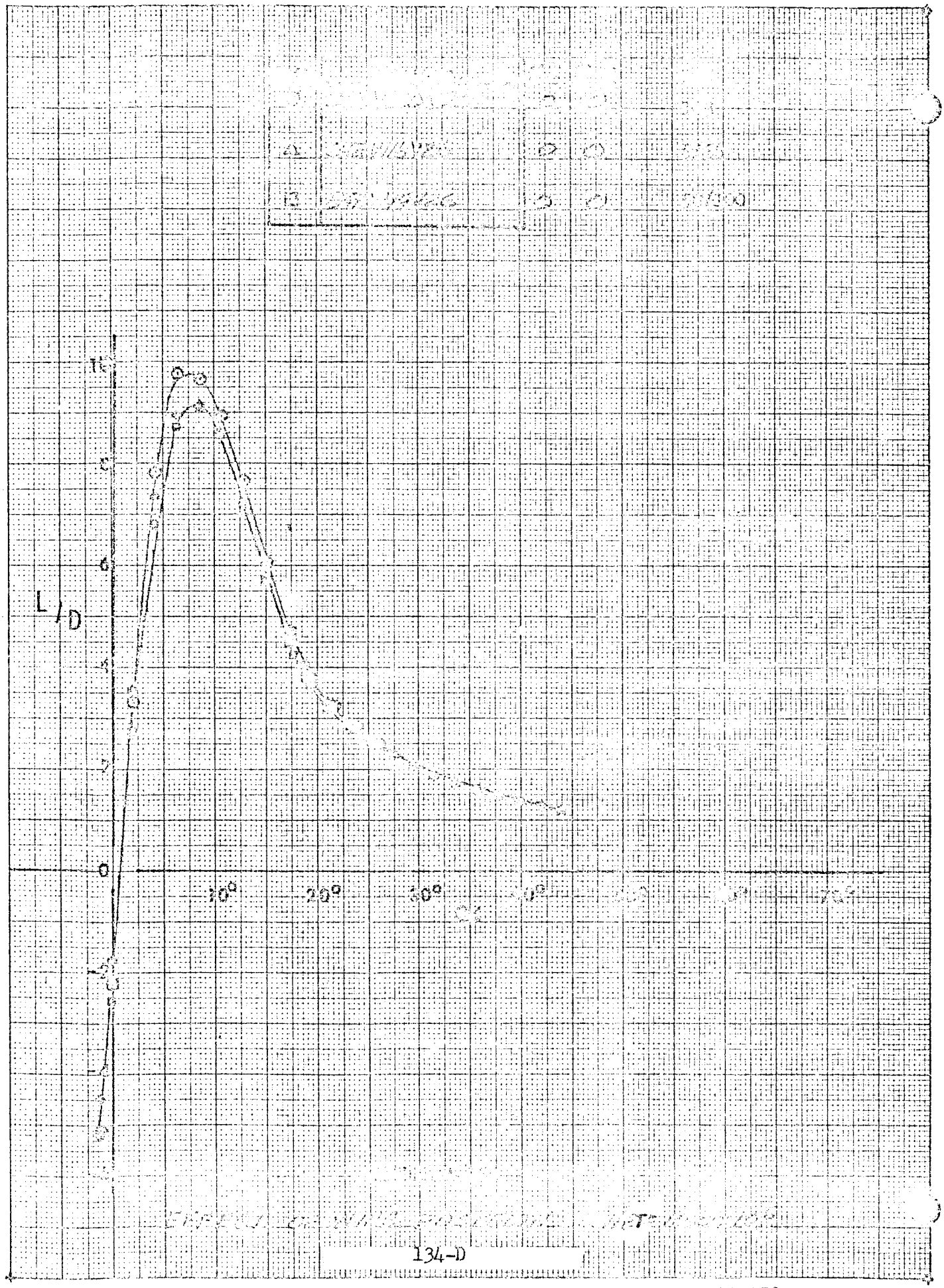
L/D
10
8
6
4
2
0
10°
20°
30°
134-D

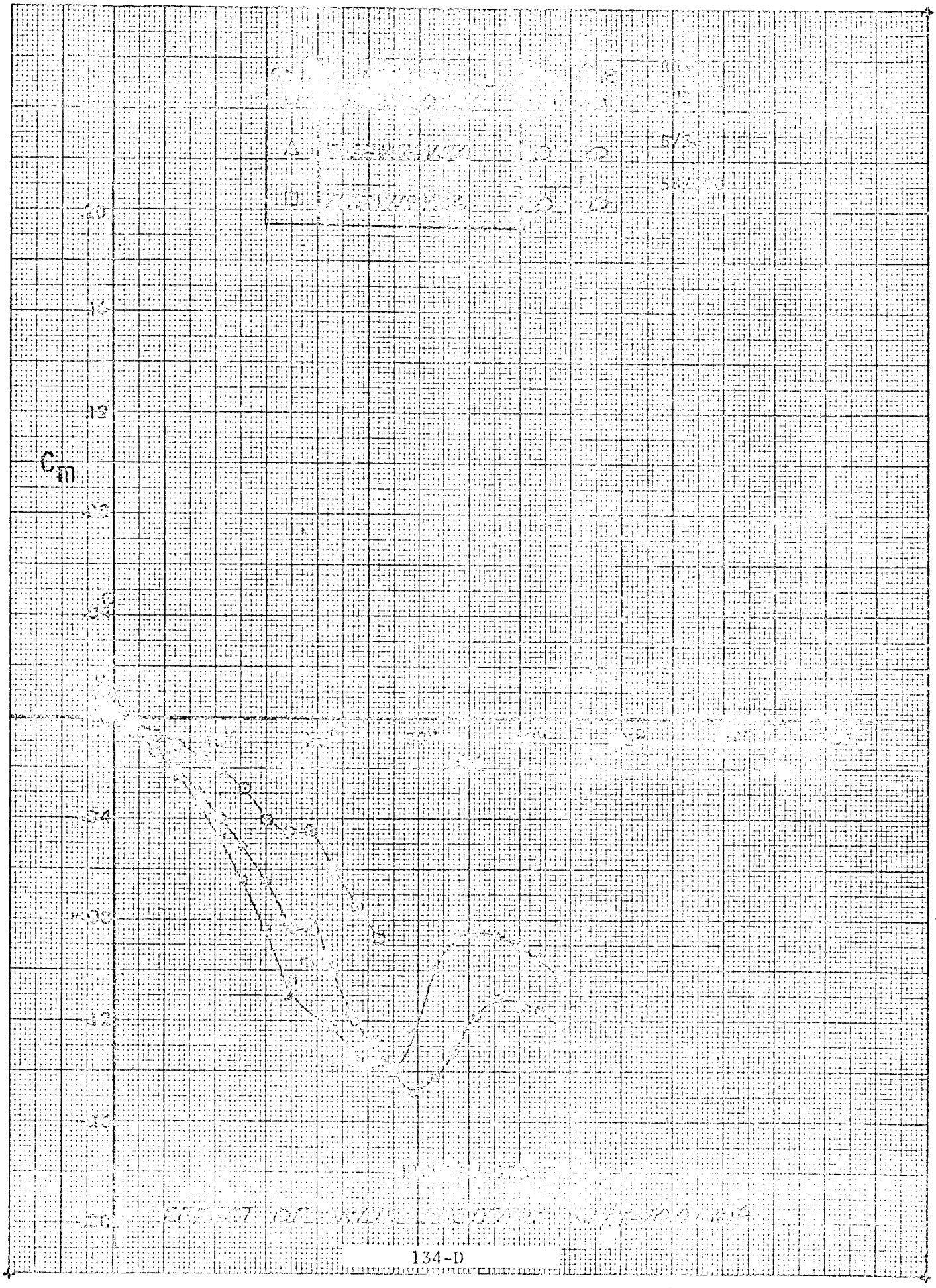
C_m
134-D

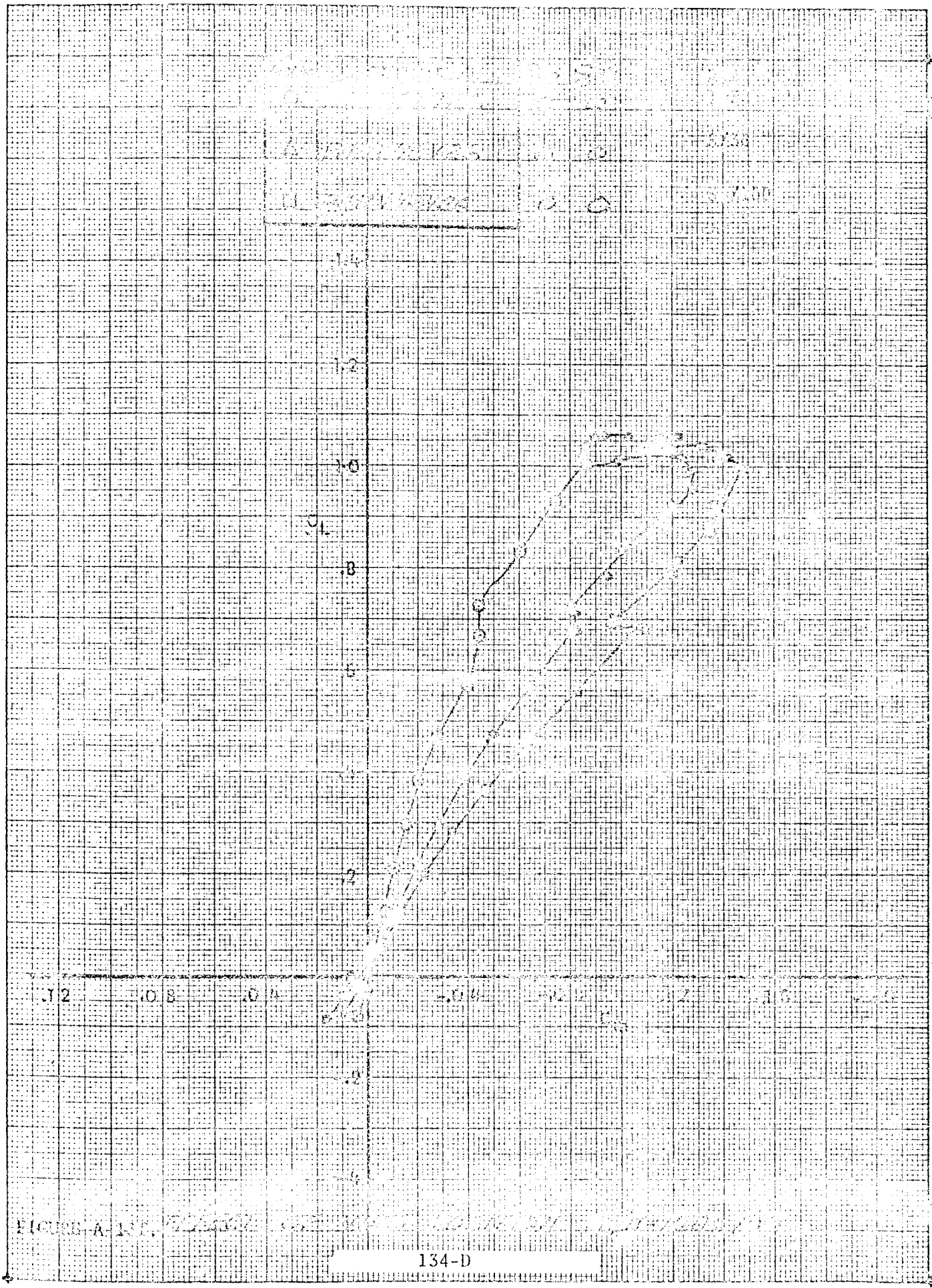

FIGURE A-13[illegible]

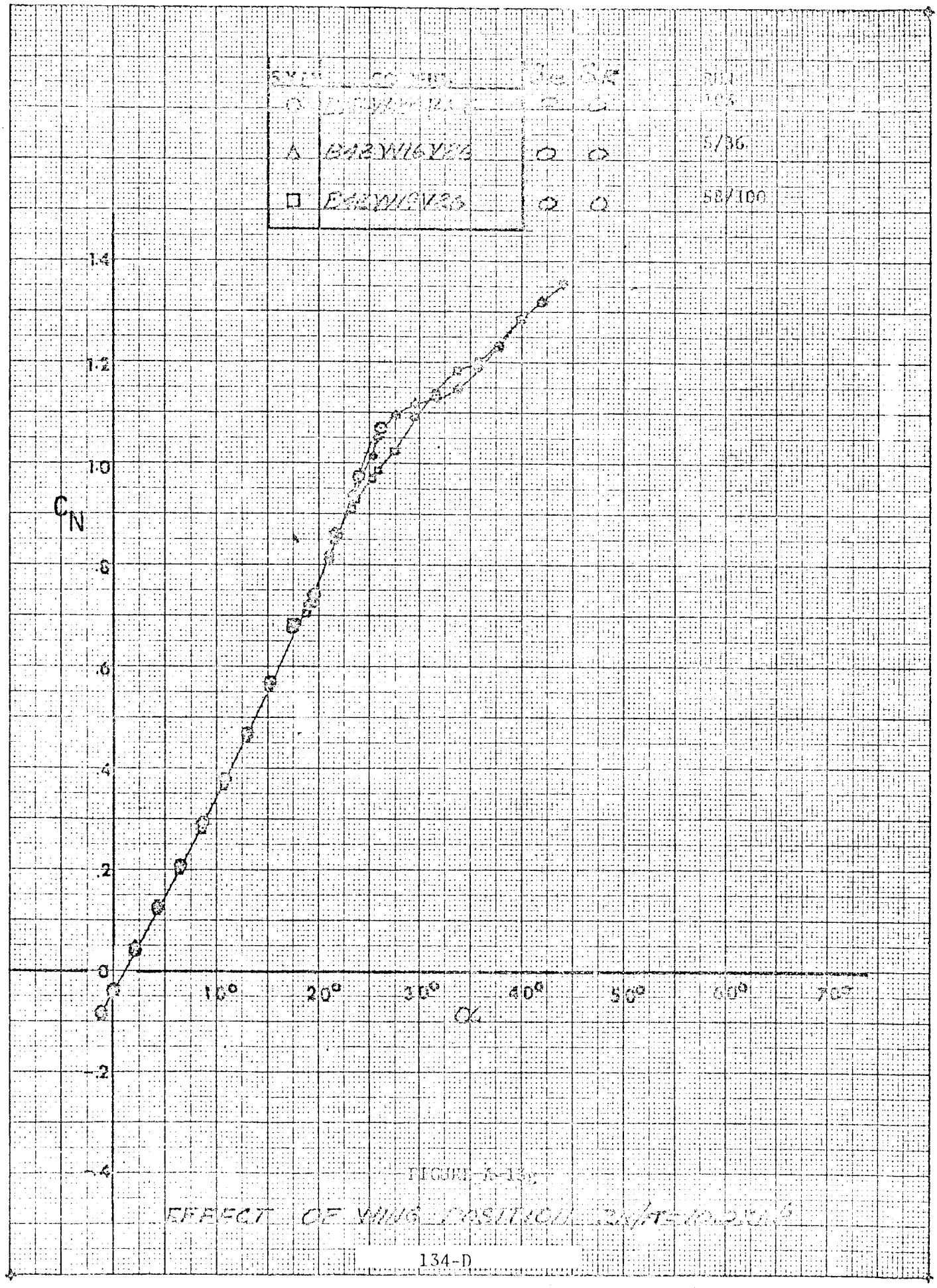

FIGURE A-13

EFFECT OF WING POSITION ON LIFT-DRAG

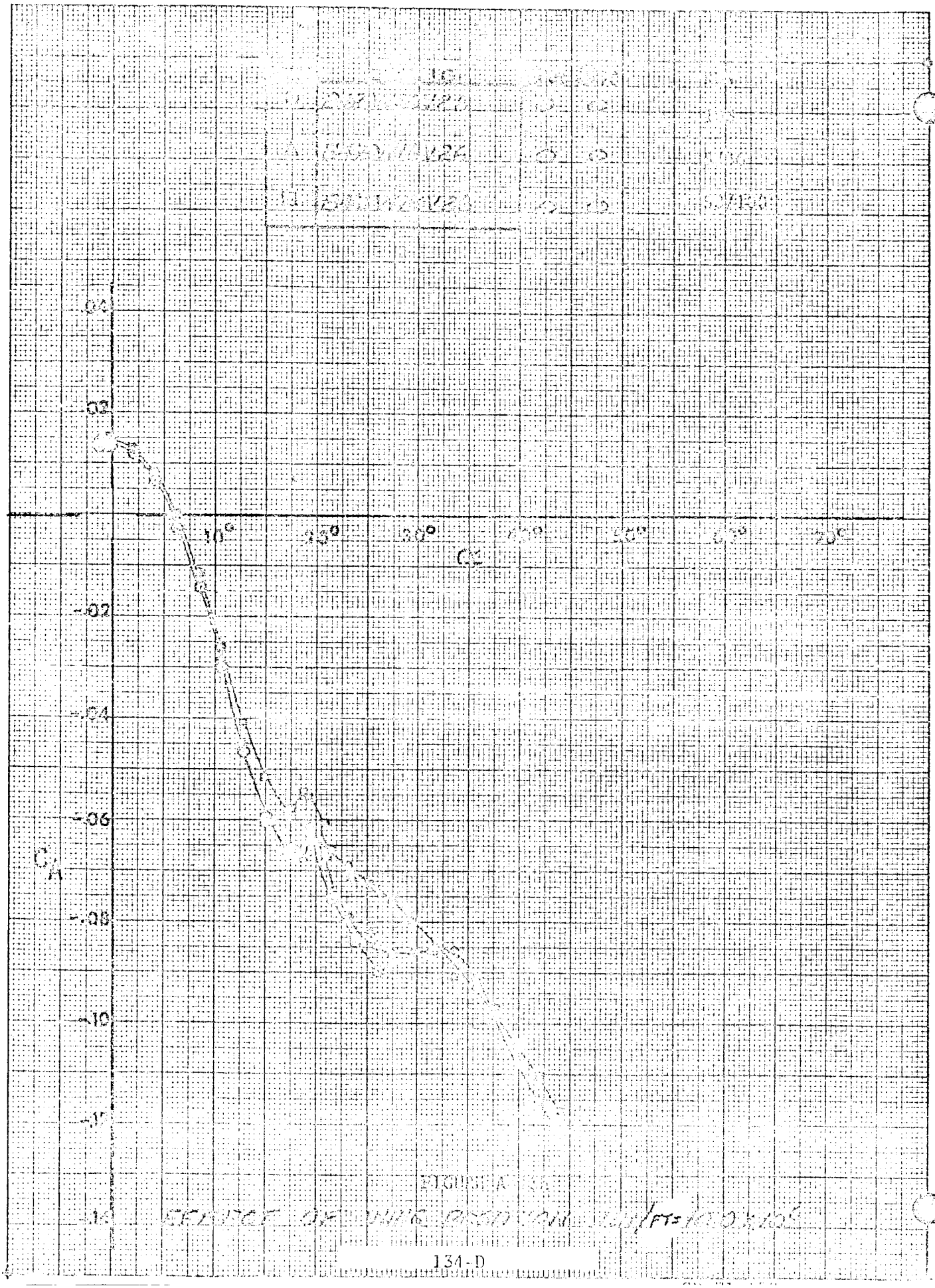

FIGURE A

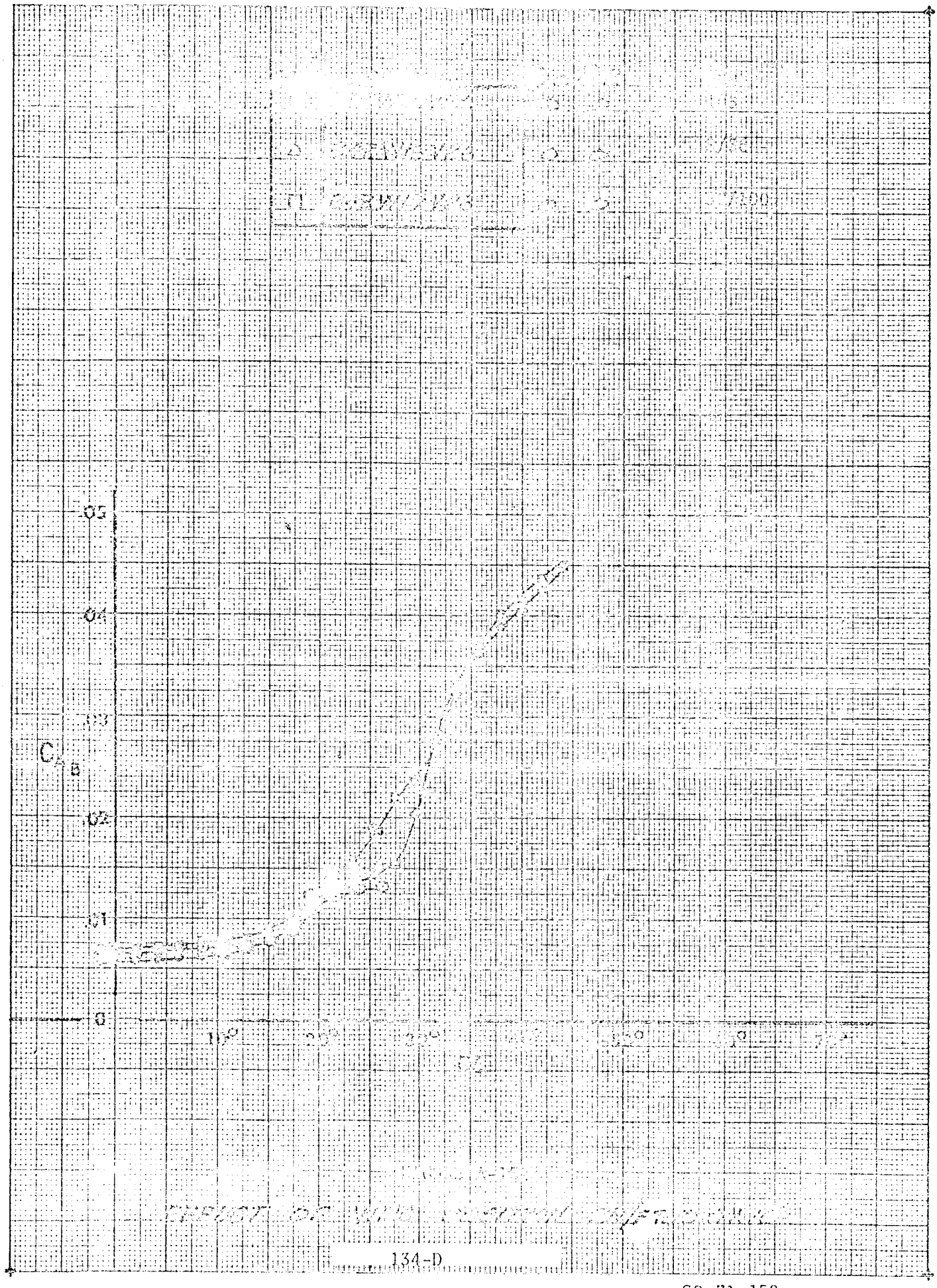

134-D

10 X 10 TO THE CENTIMETER 46 1517
10 X 25 CM. • ALBANENE
KEUFFEL & ESSER CO.

30

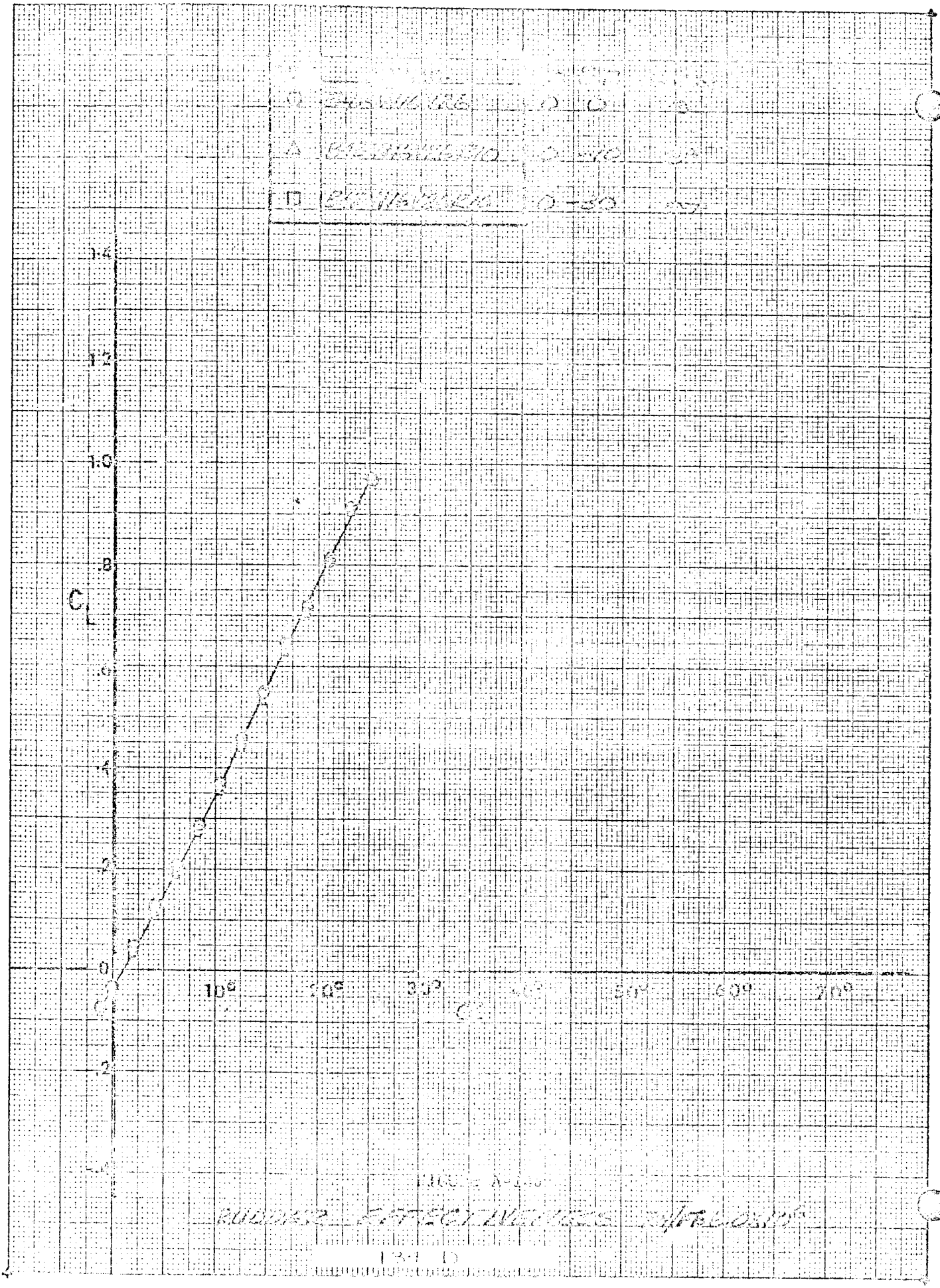

FIGURE A-[illegible]

AUDIBLE EFFECTIVENESS [illegible]

20

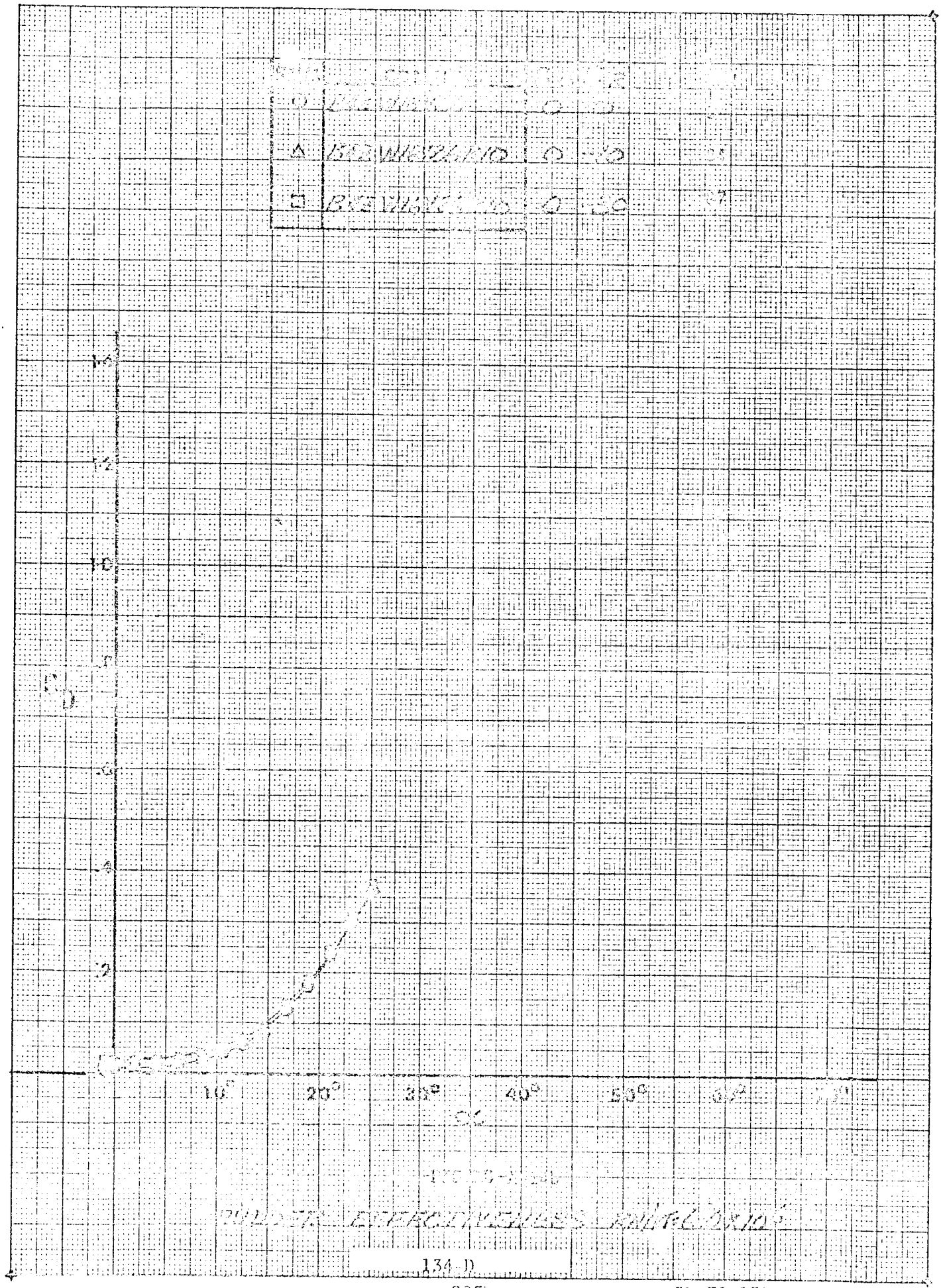

10 X 10 TO THE CENTIMETER 46 1517
18 X 25 CM. • ALBANENE
KEUFFEL & ESSER CO.

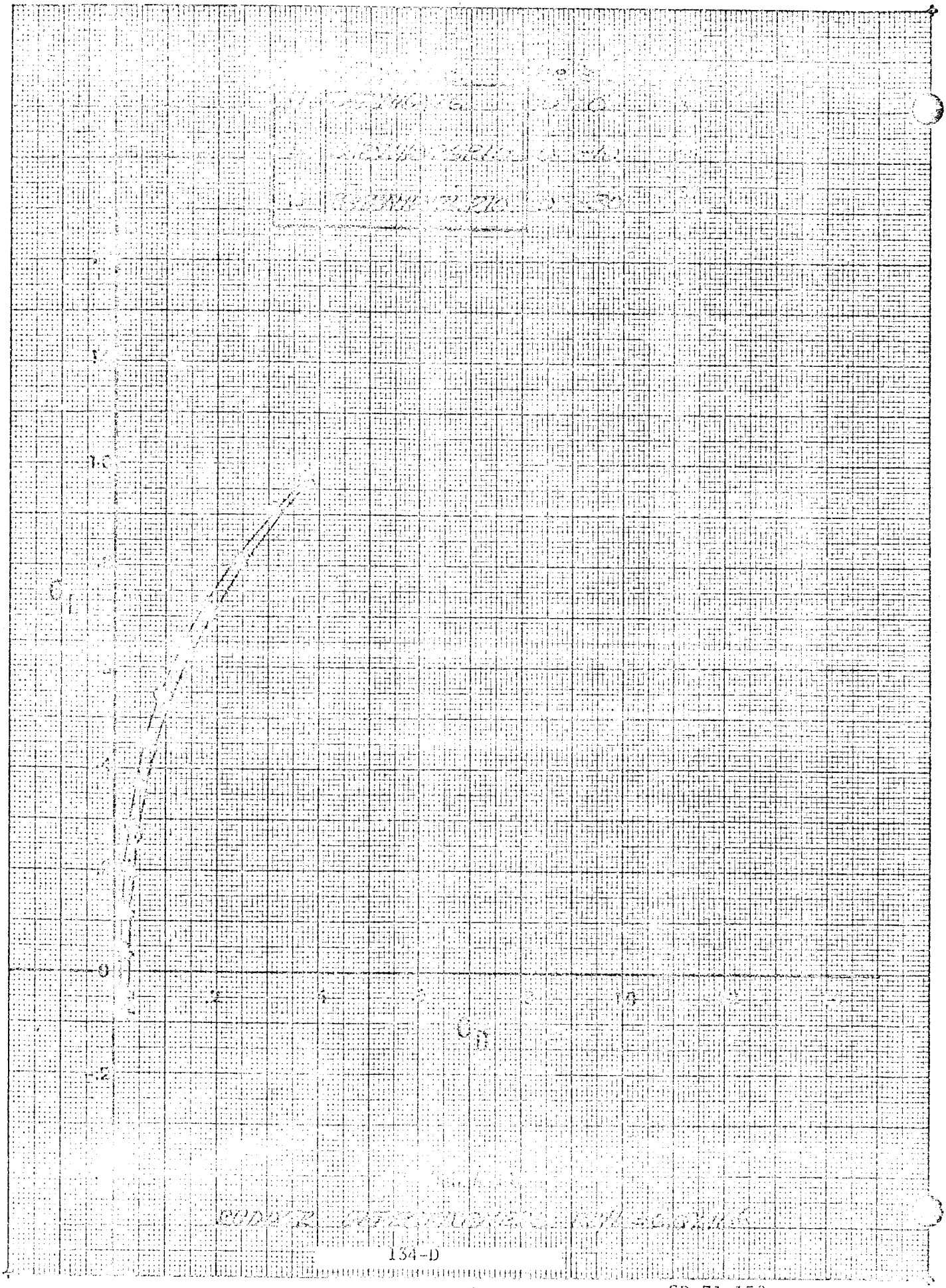

134-D

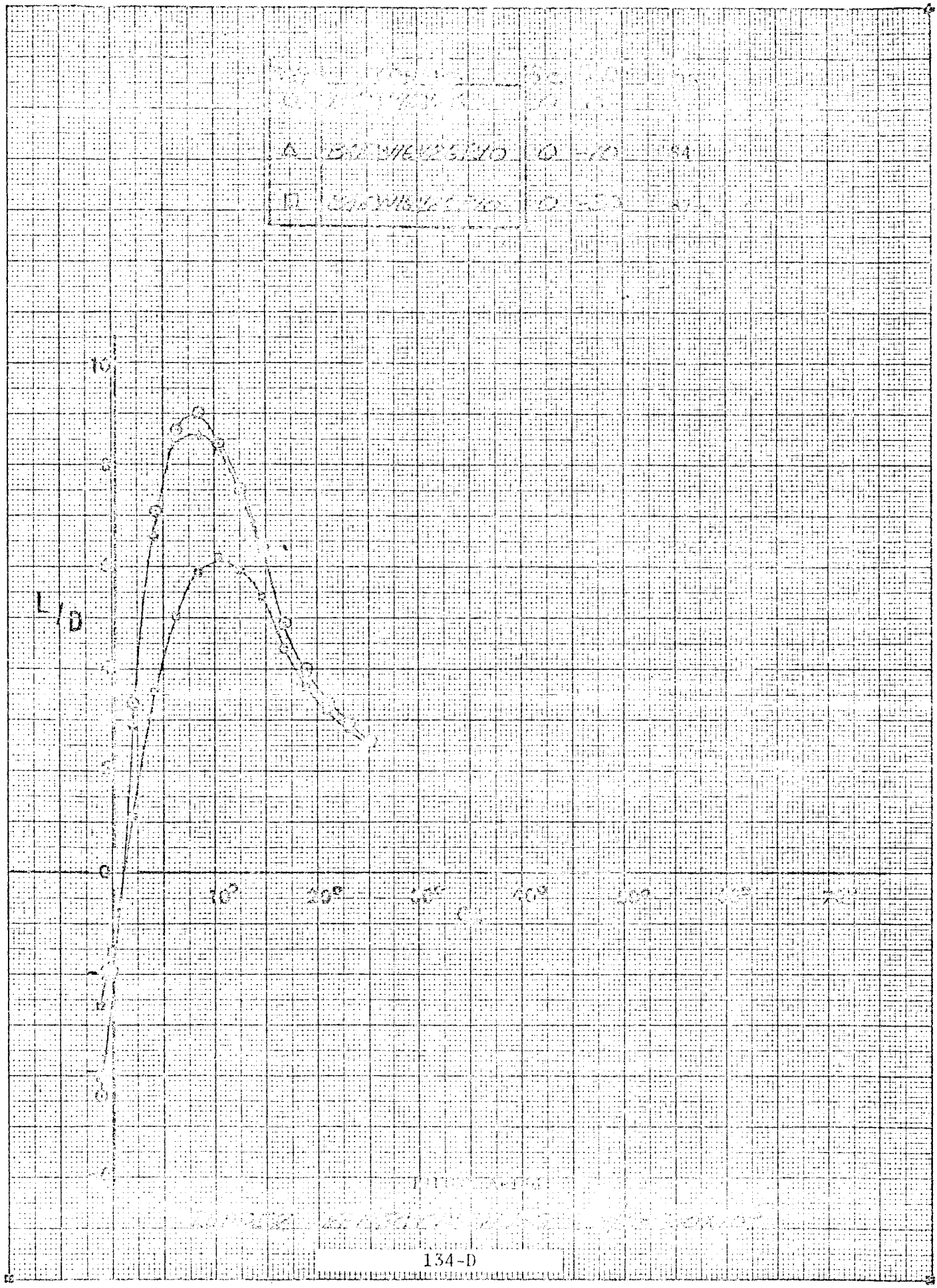
L/D
10
0
-1
-2
-3
-4
-5
-6
-7
-8
-9
-10
-20
-30
-40
-50
-60
-70
-80
-90
-100
-110
-120
-130
-140
-150
-160
-170
-180
-190
-200
-210
-220
-230
-240
-250
-260
-270
-280
-290
-300
-310
-320
-330
-340
-350
-360
-370
-380
-390
-400

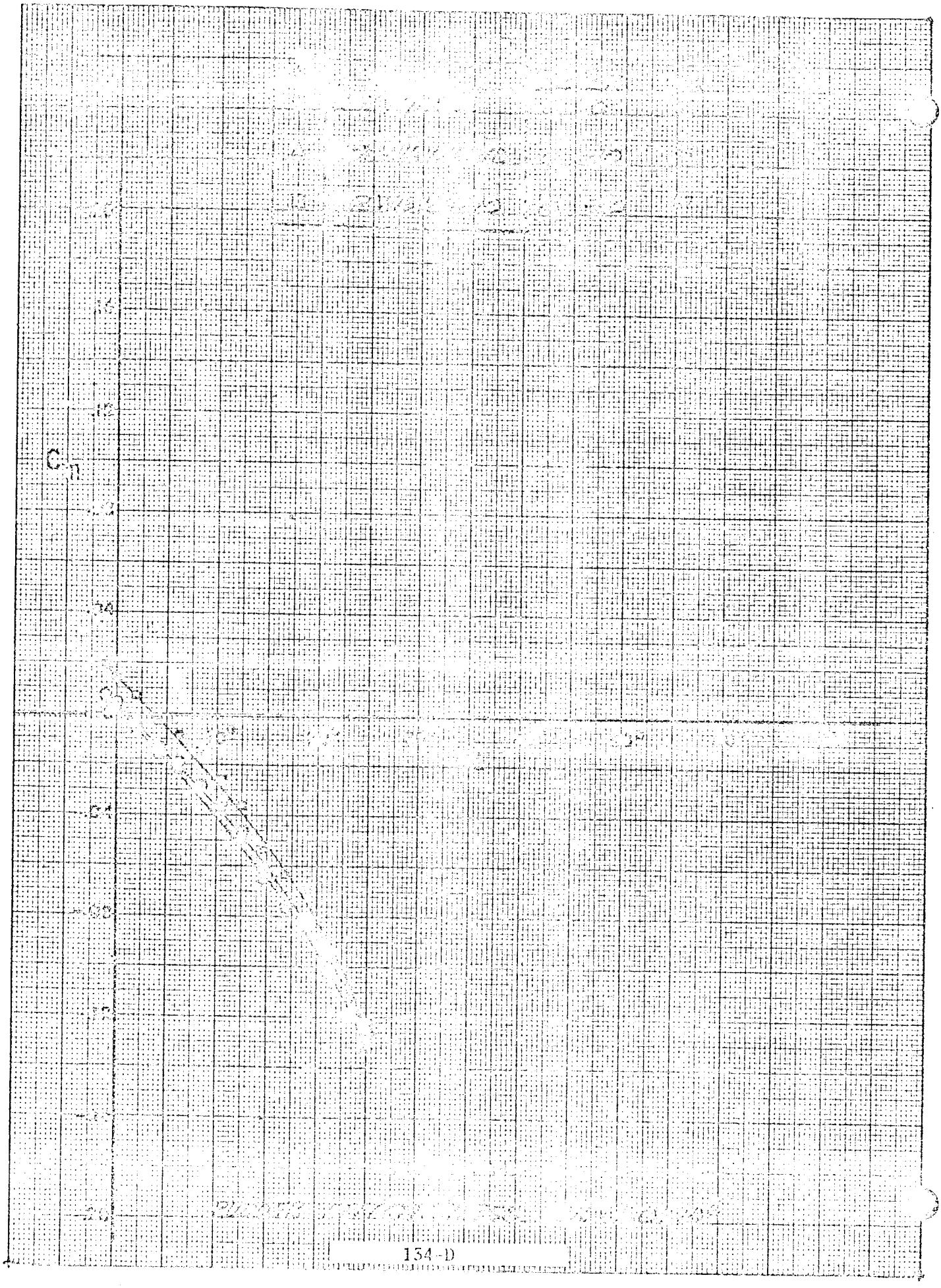

134-D

10 X 25 CM. • ALBANENE
KEUFFEL & ESSER CO.

260

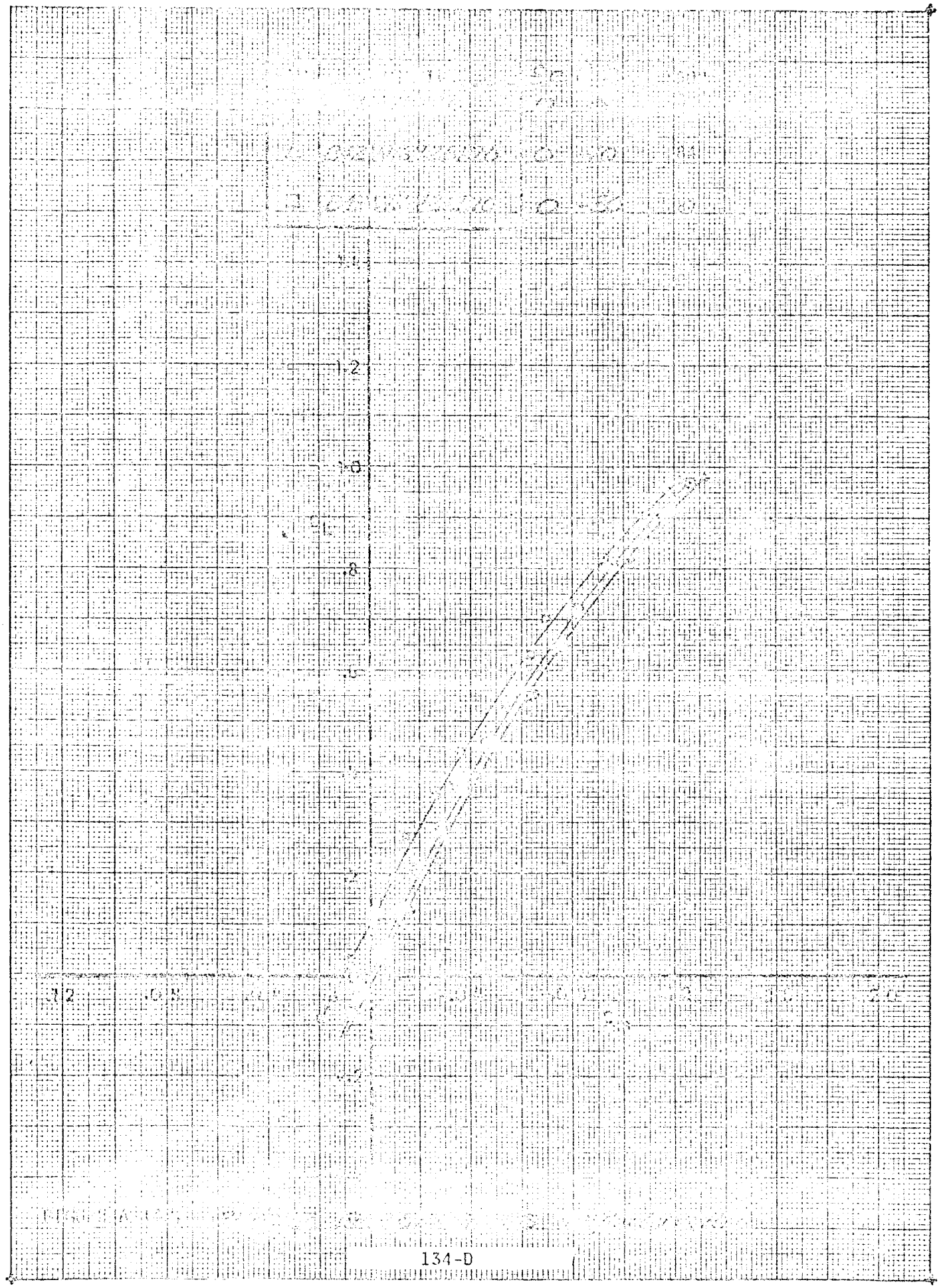

K&E 10 X 10 TO THE CENTIMETER 46 1517
18 X 25 CM. • ALBANENE
MADE IN U.S.A.
KEUFFEL & ESSER CO.

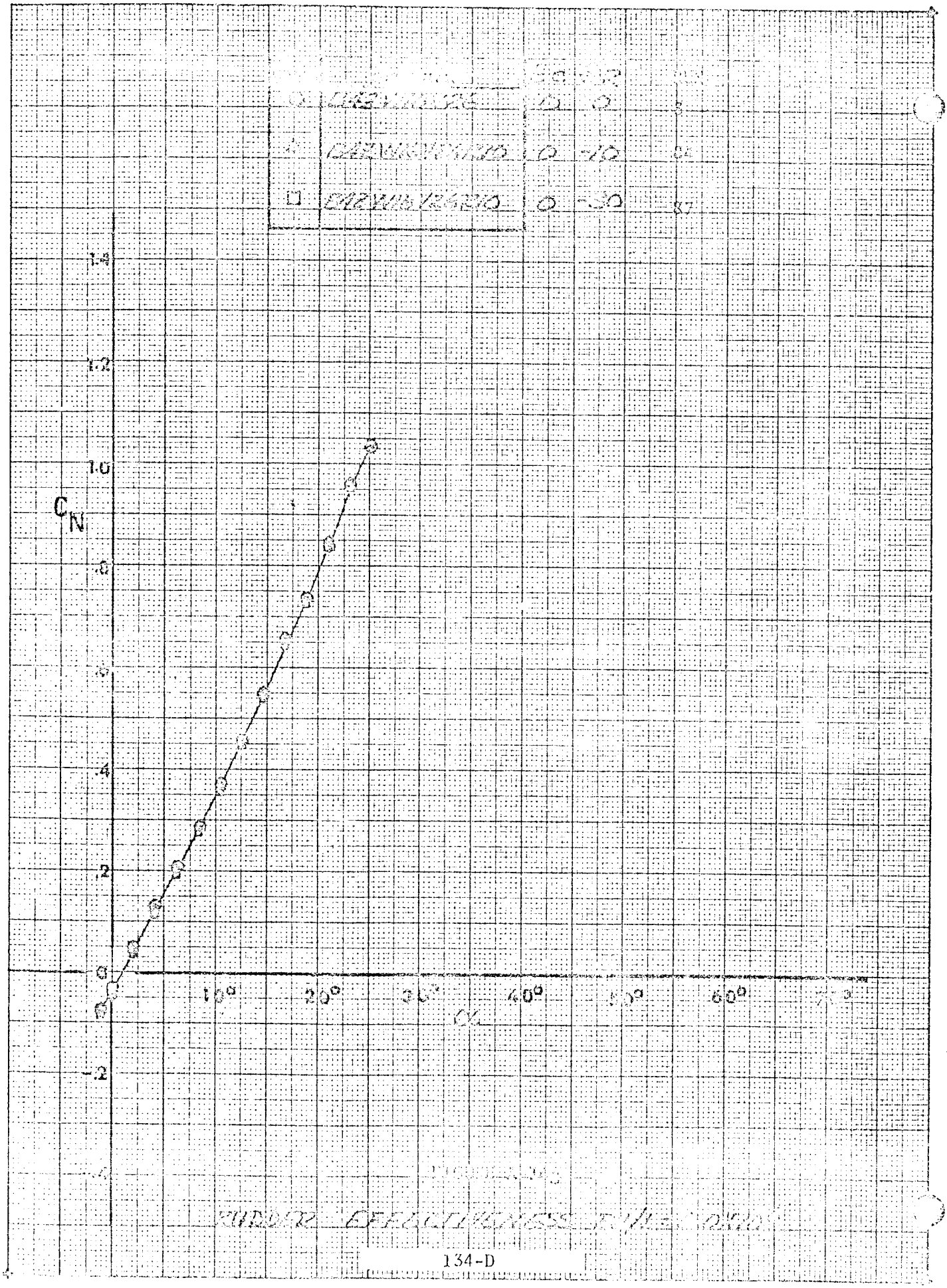

134-D

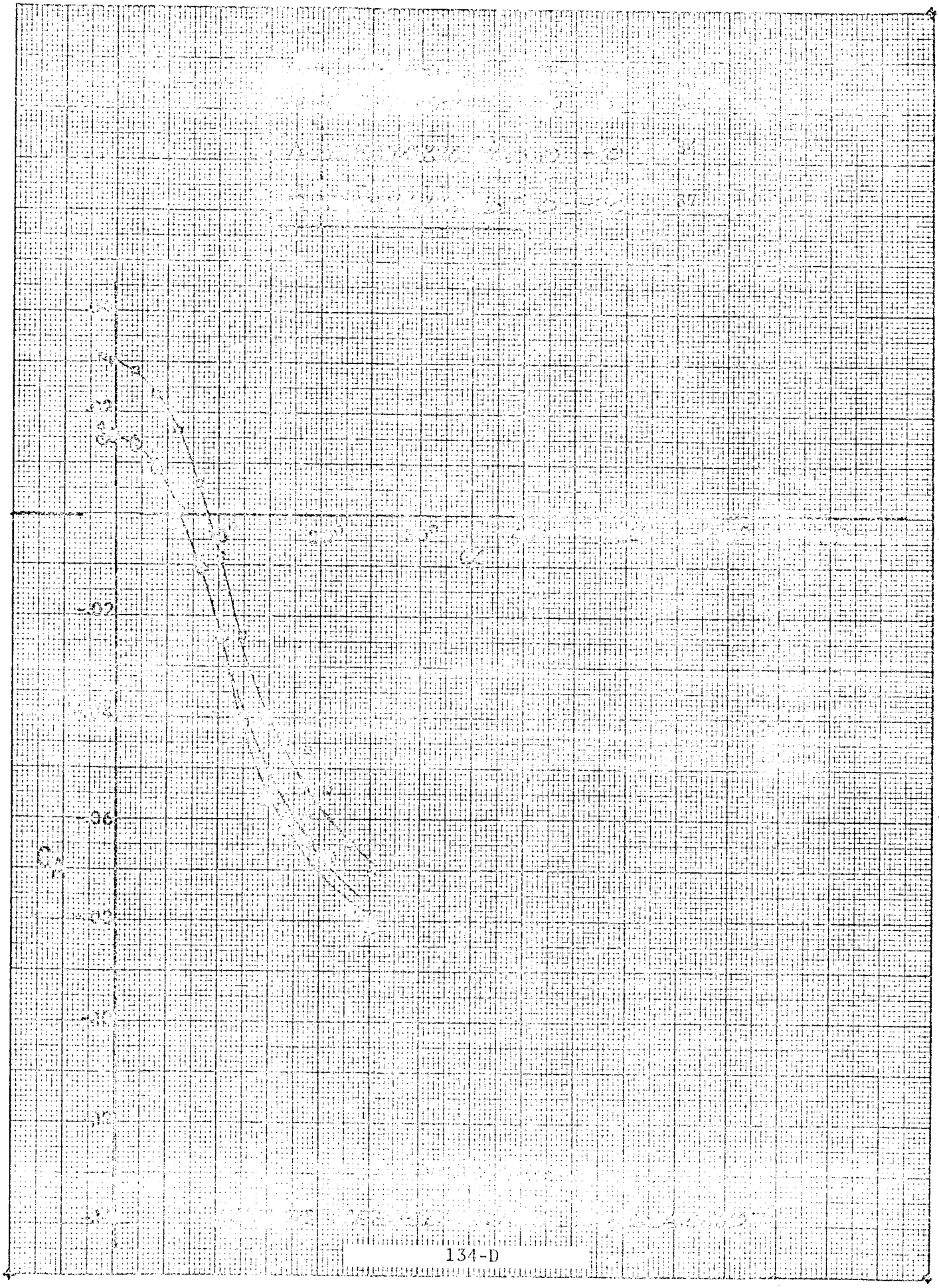

10 X 25 CM. • ALBANENE
KEUFFEL & ESSER CO.

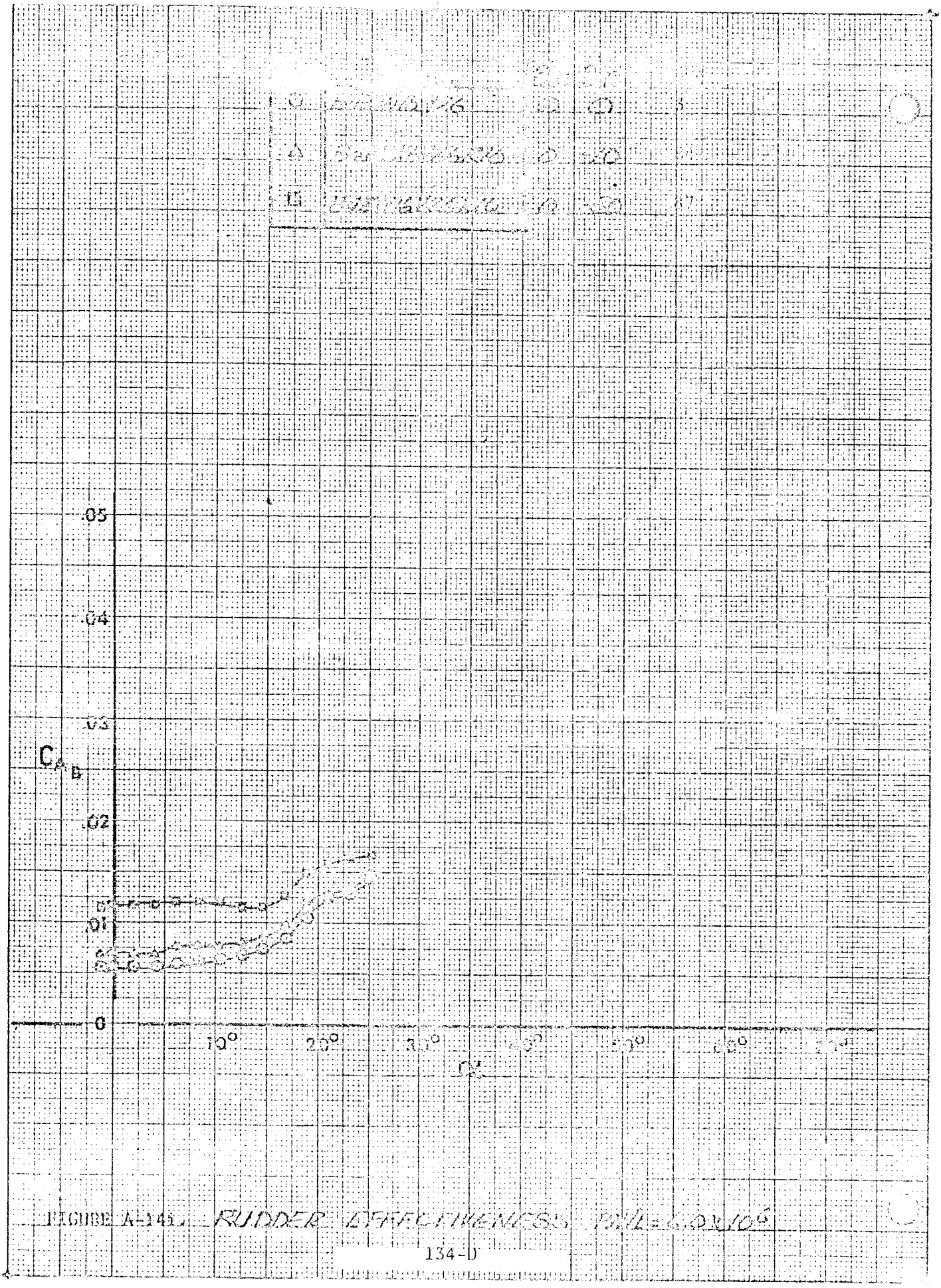

FIGURE A-145 RUDDER EFFECTIVENESS

10 X 10 TO THE CENTIMETER 46 1517
18 X 25 CM. • ALBANENE
KEUFFEL & ESSER CO.

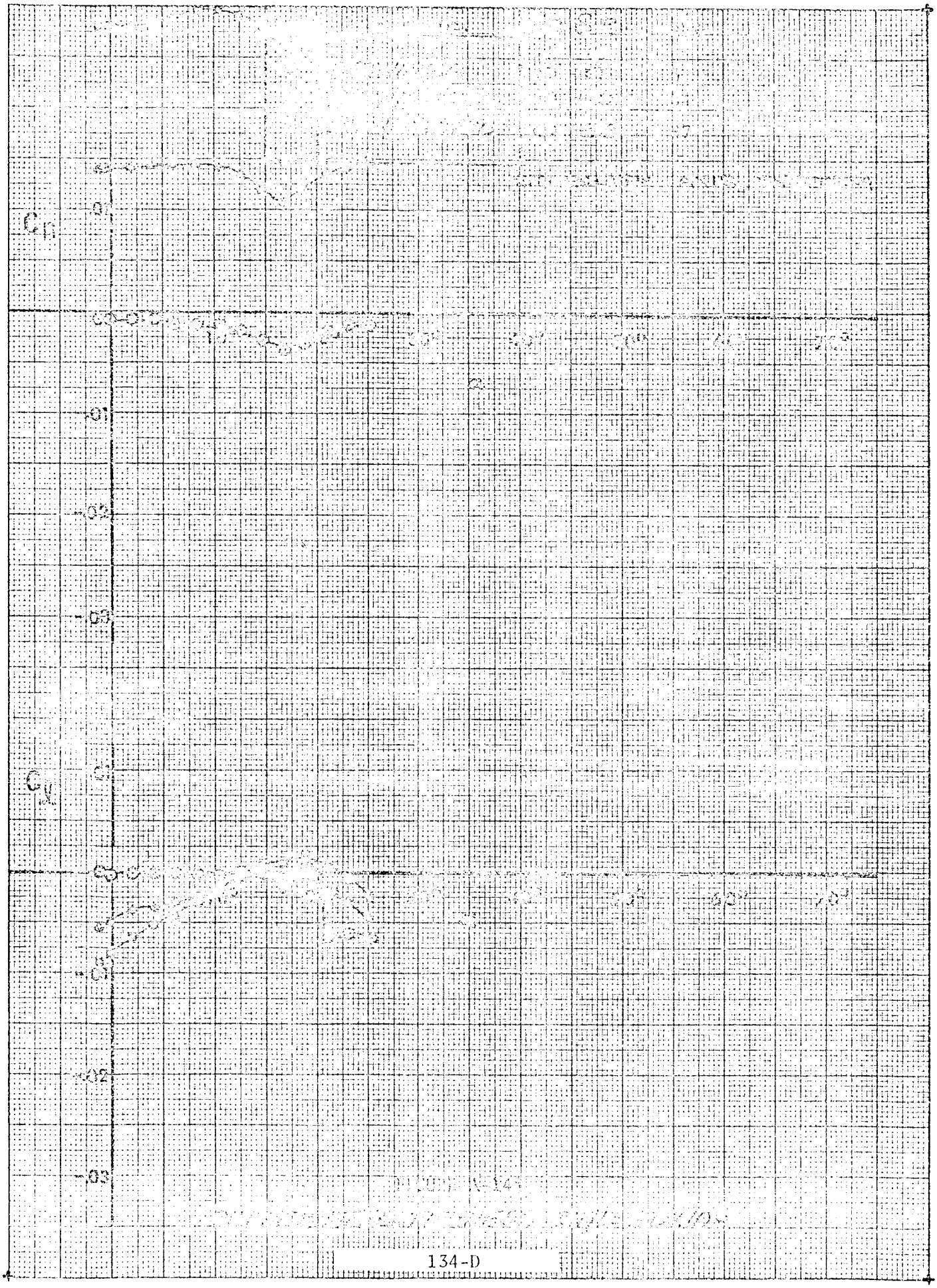
134-D

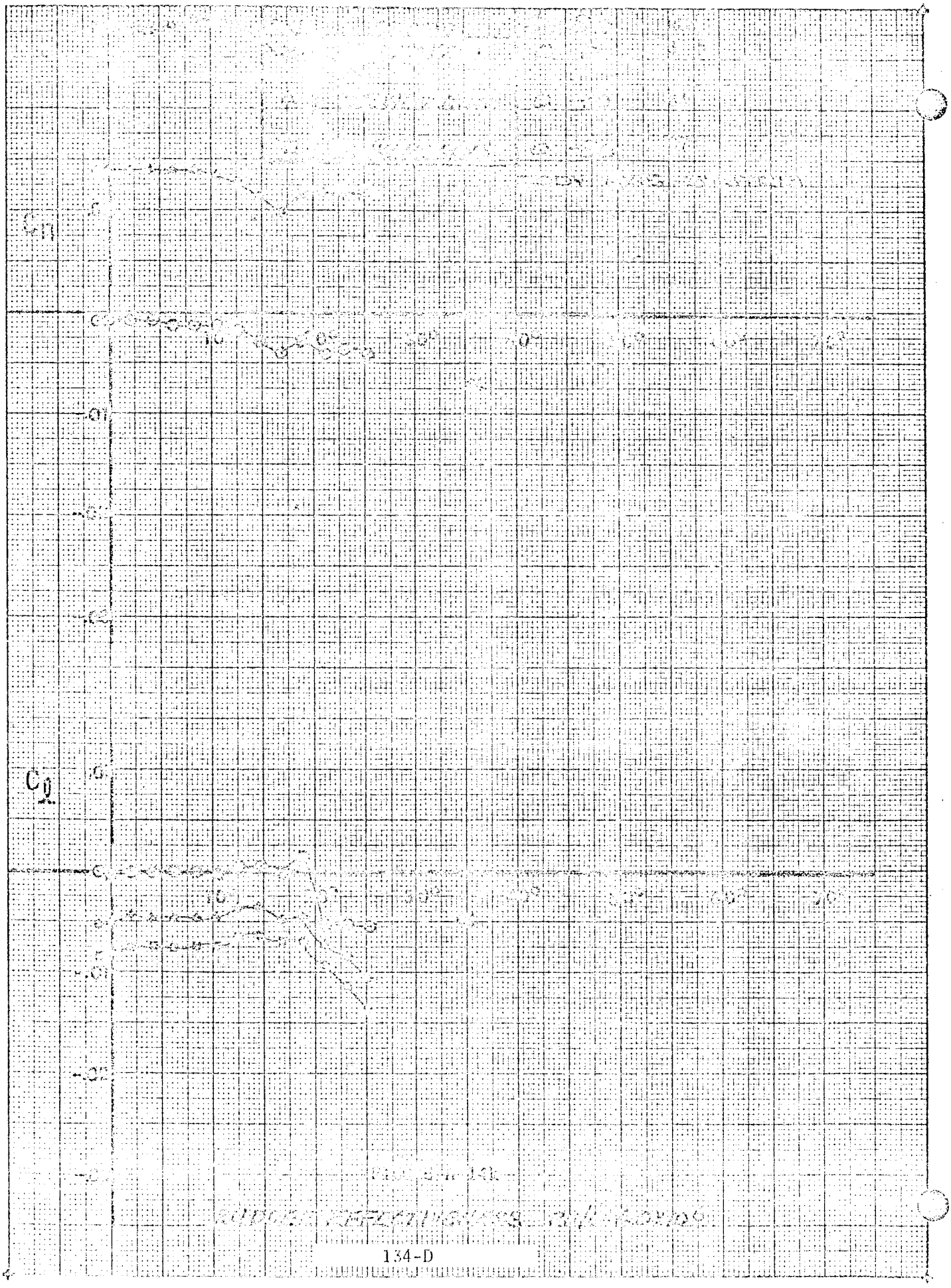

134-D

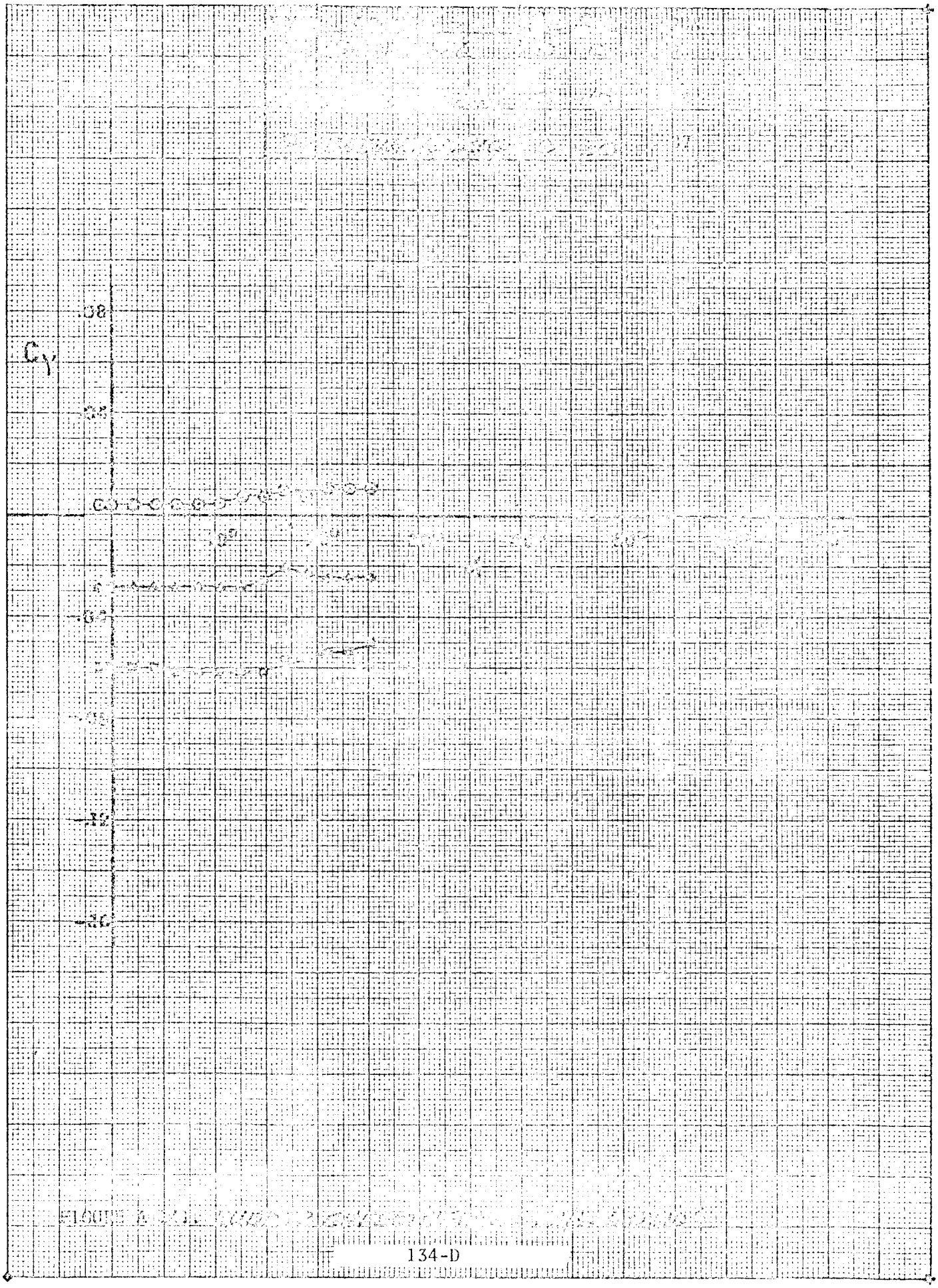

134-D

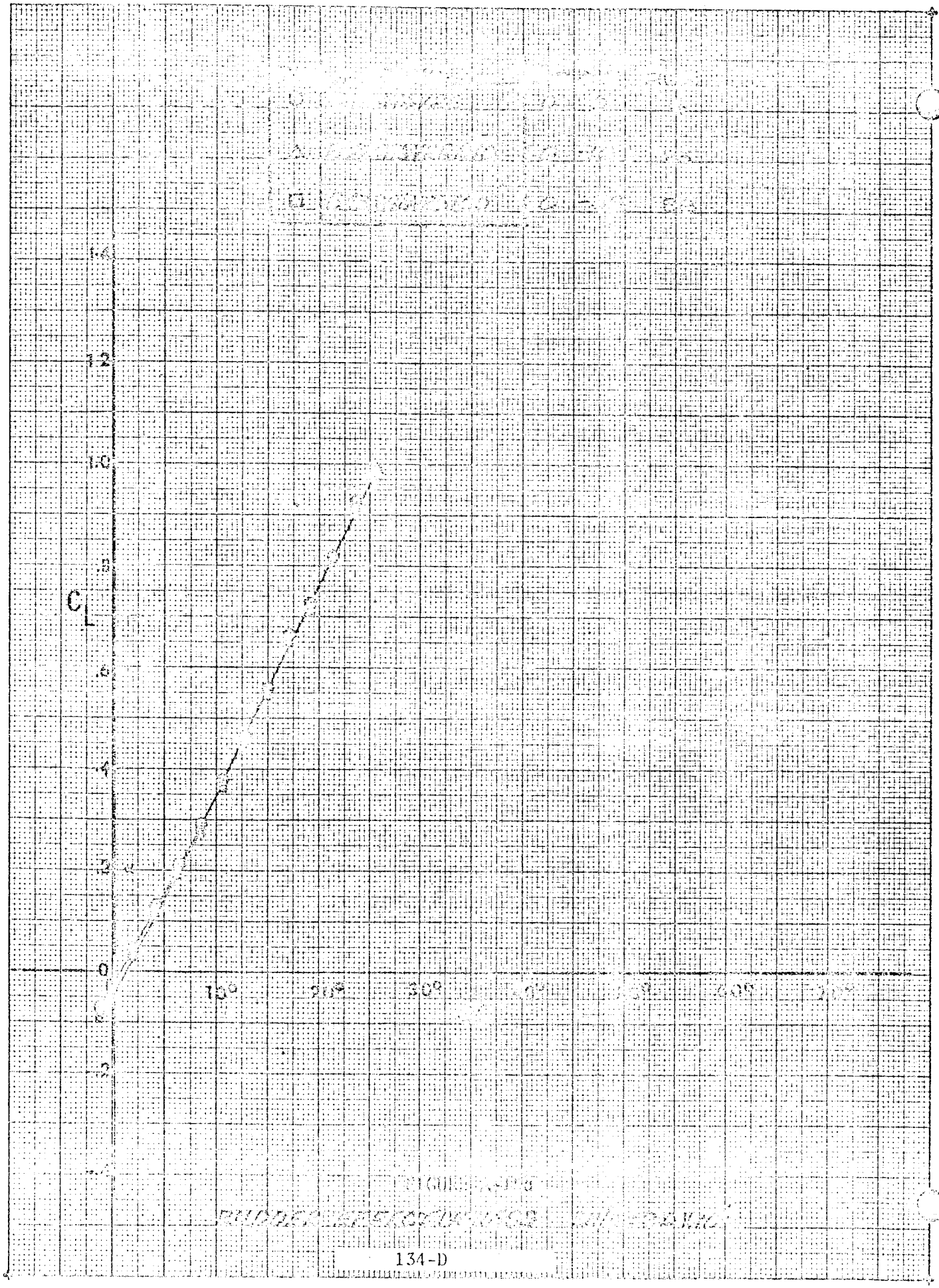

134-D

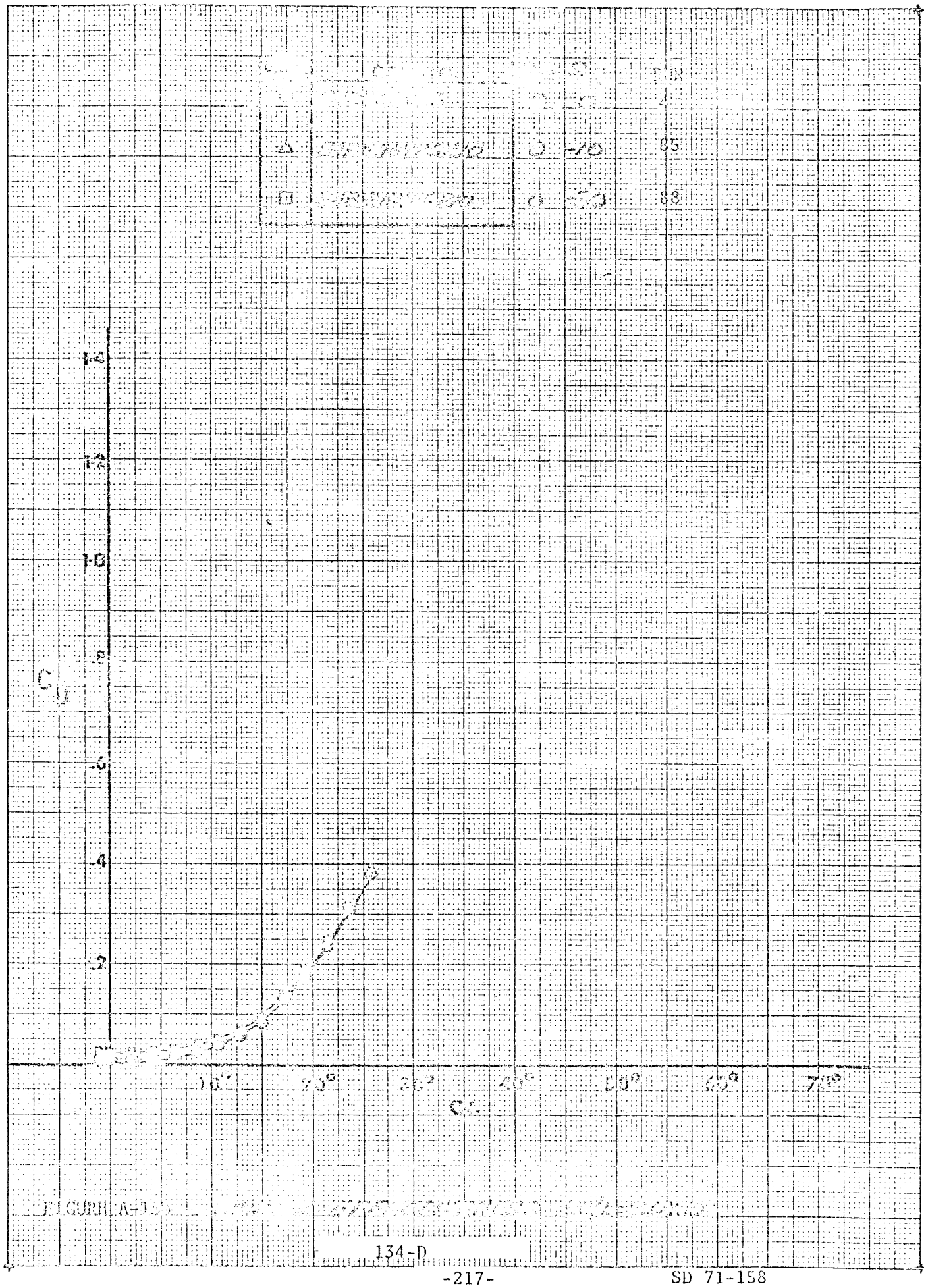

FIGURE A-15

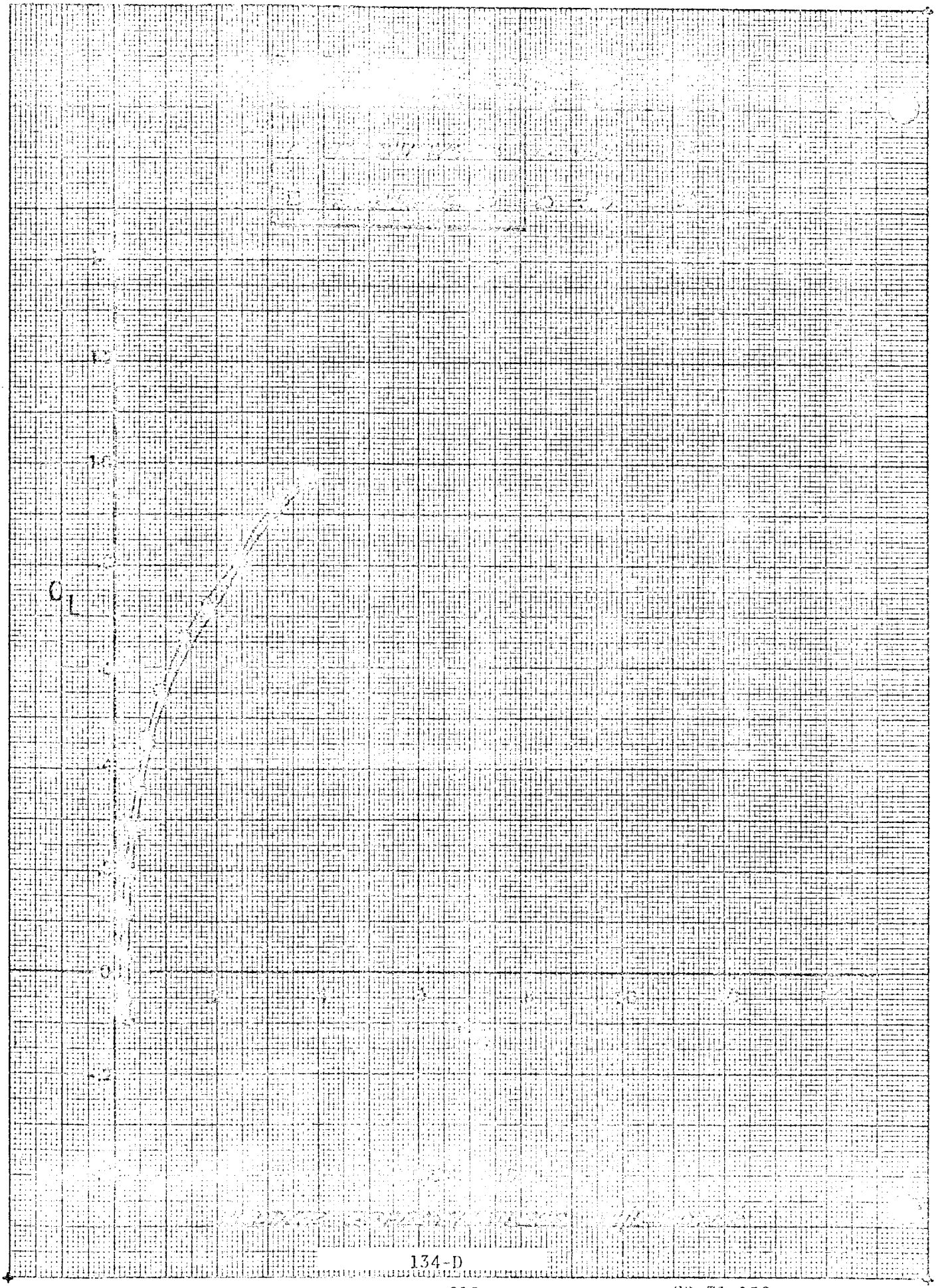

K&E 10 X 10 TO THE CENTIMETER 46 1517
18 X 25 CM • ALBANENE
KEUFFEL & ESSER CO.

134-D

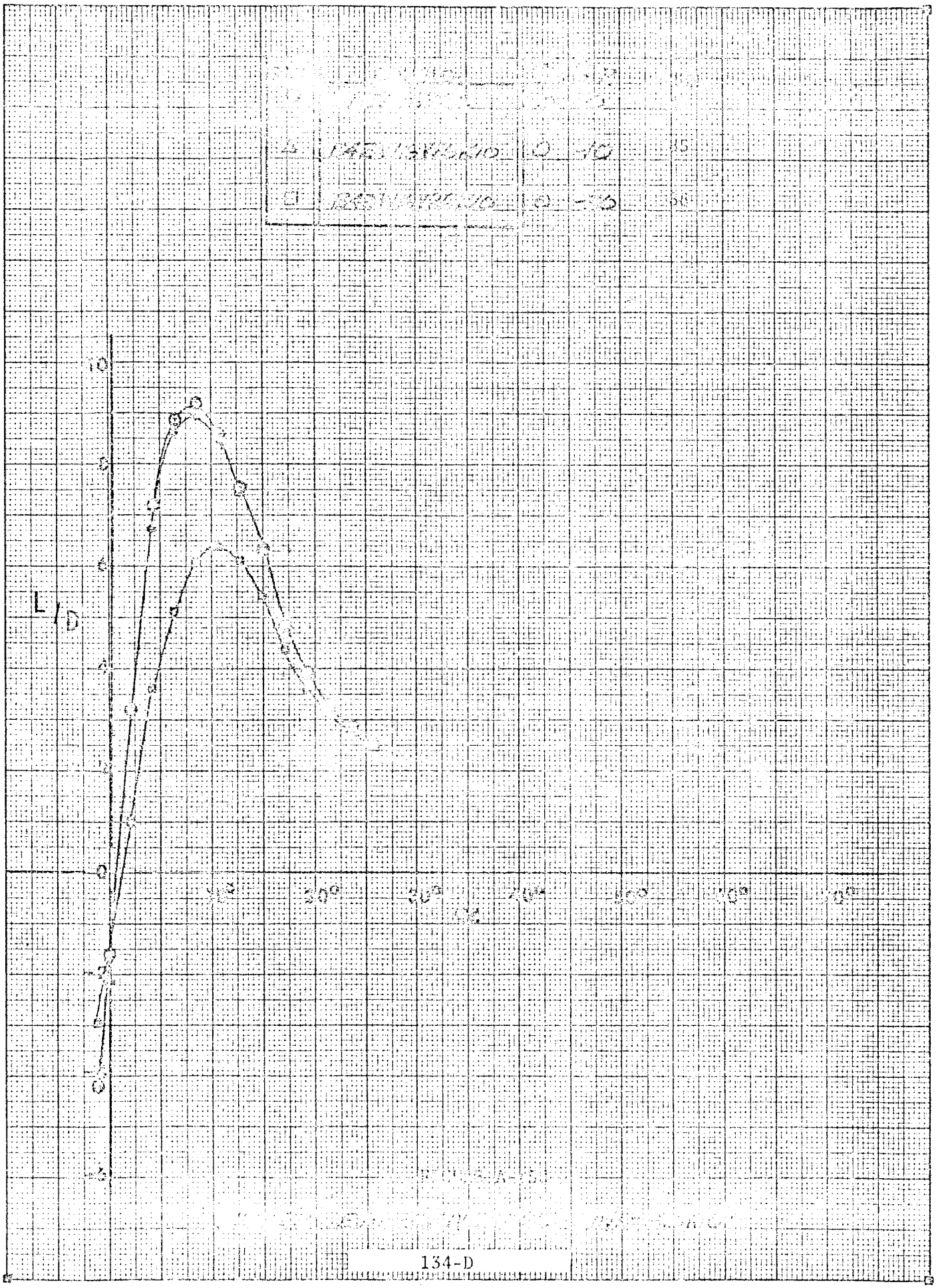

134-D

Sym	Configuration	δ_E	δ_R	Run
○	$B_4 E W_{16} V_{26}$	0	0	4
△	$B_4 E W_{16} V_{26} R_{10}$	0	-10	85
□	$B_4 E W_{16} V_{26} R_{10}$	0	-30	88

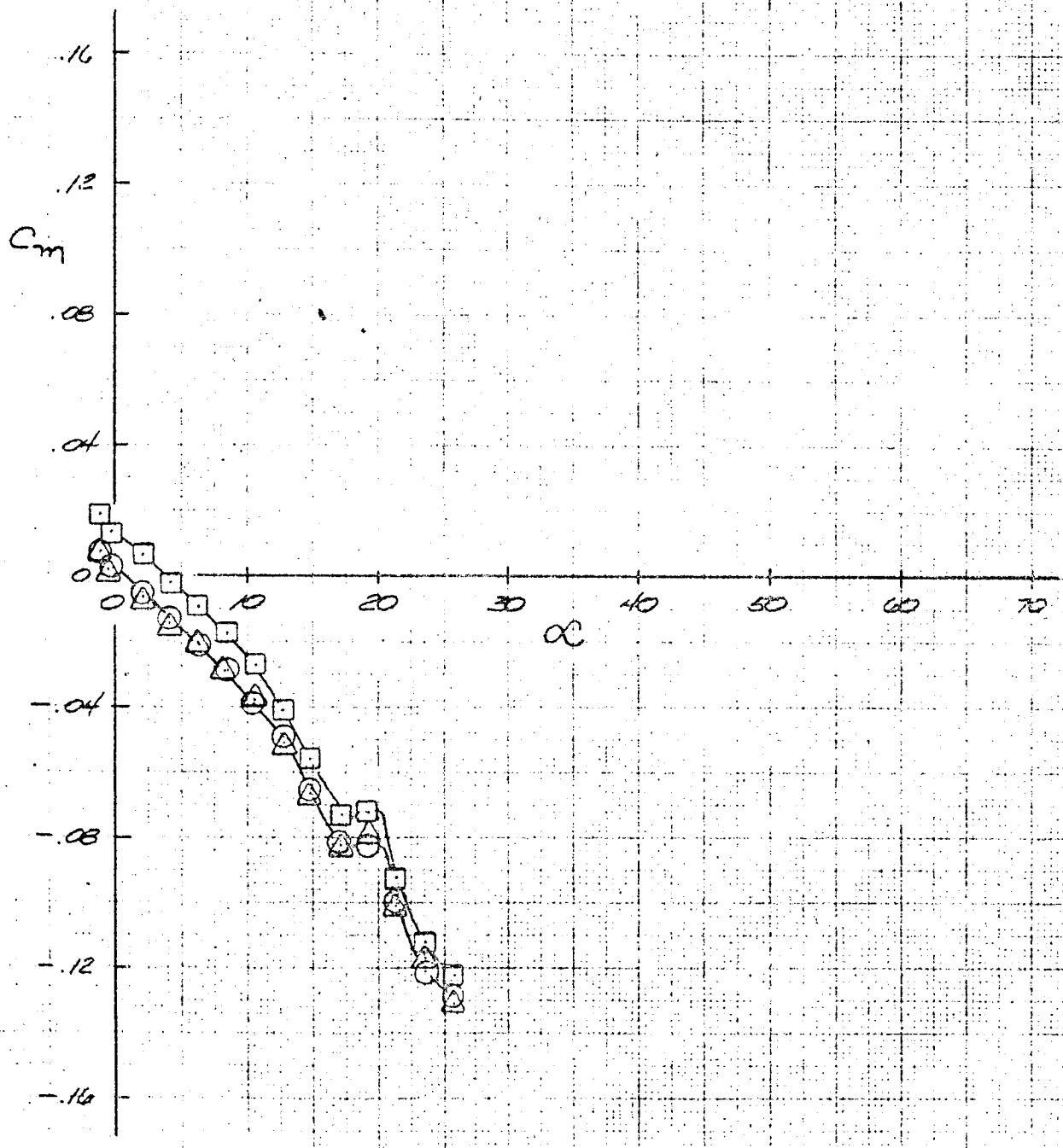

FIGURE A-15 e
RUDDER EFFECTIVENESS $R_N/L = 8.0 \times 10^6$
B4D

260

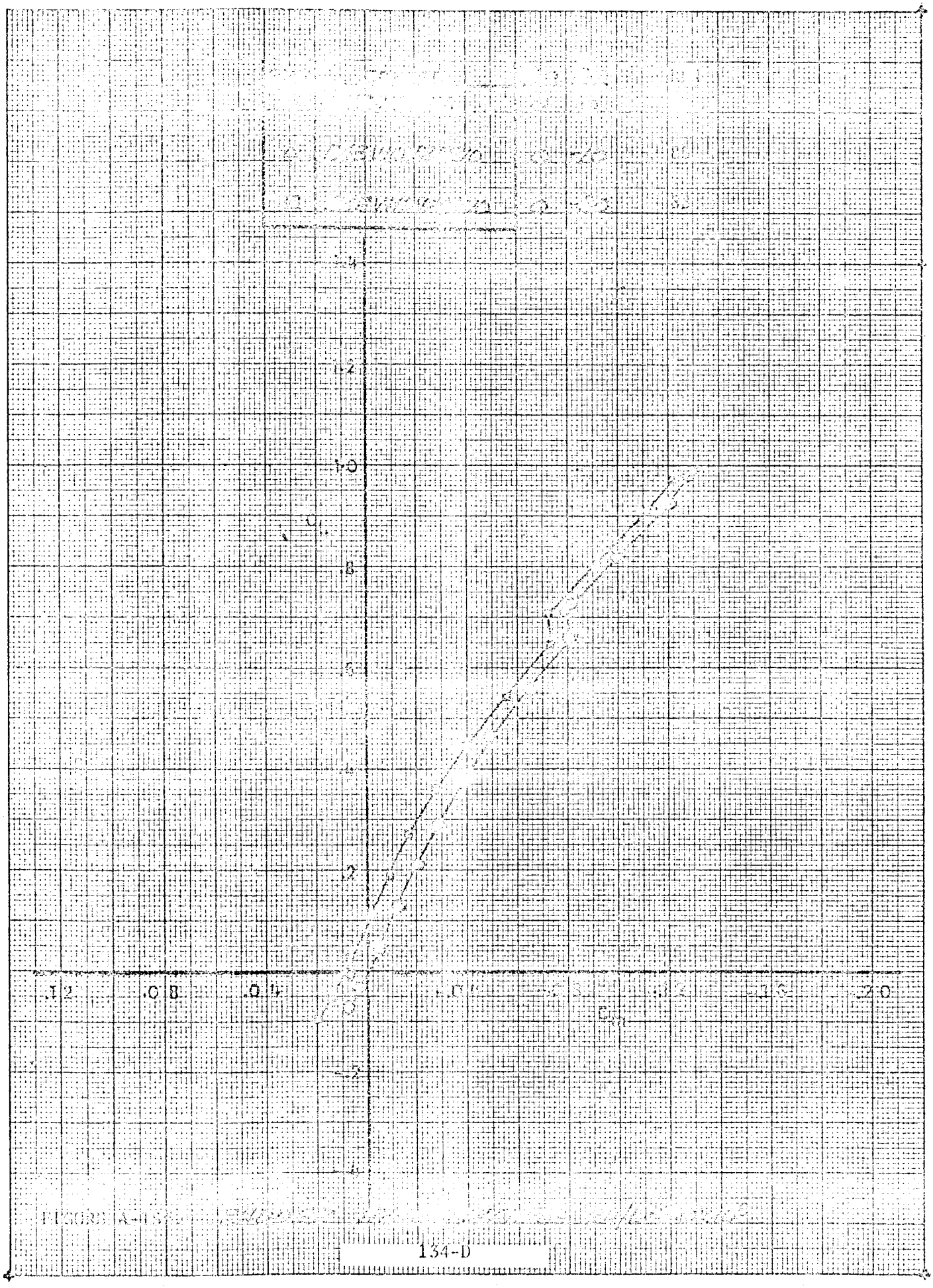

K&E 10 X 10 TO THE CENTIMETER 46 1517
18 X 25 CM. • ALBANENE
MADE IN U.S.A.
KEUFFEL & ESSER CO.

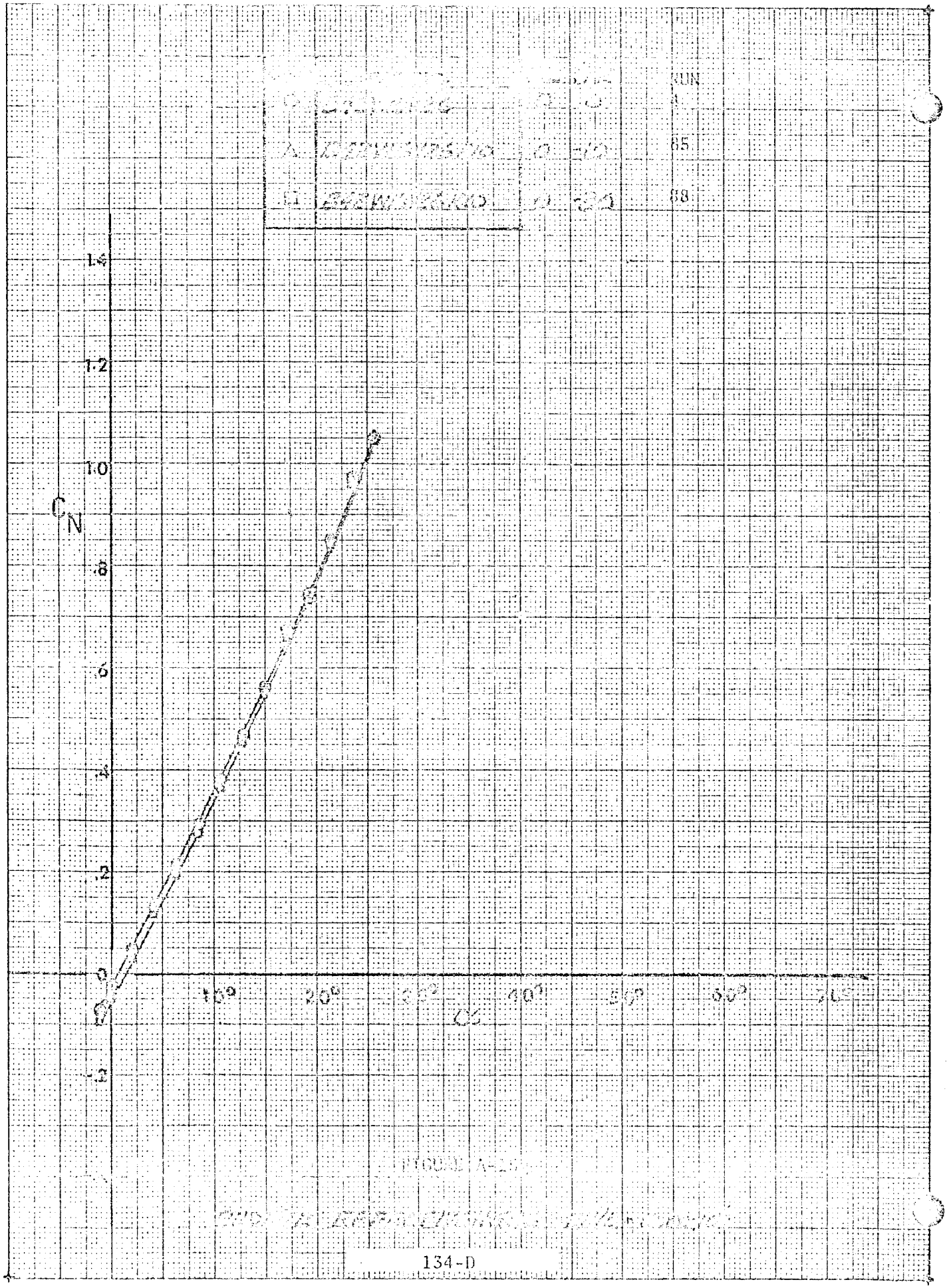

FIGURE A-20

134-D

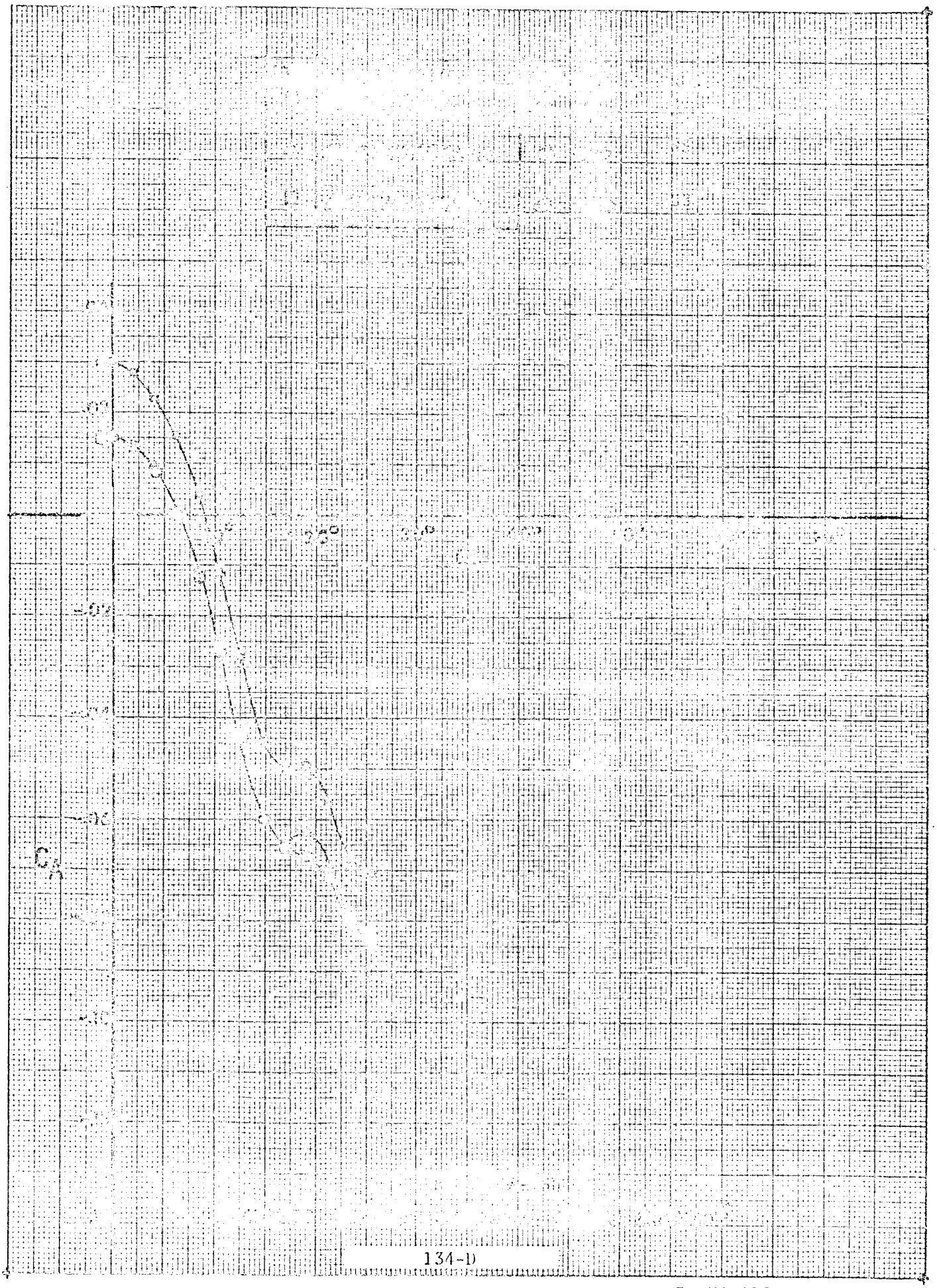

16 X 25 CM. • ALBANENE
KEUFFEL & ESSER CO.

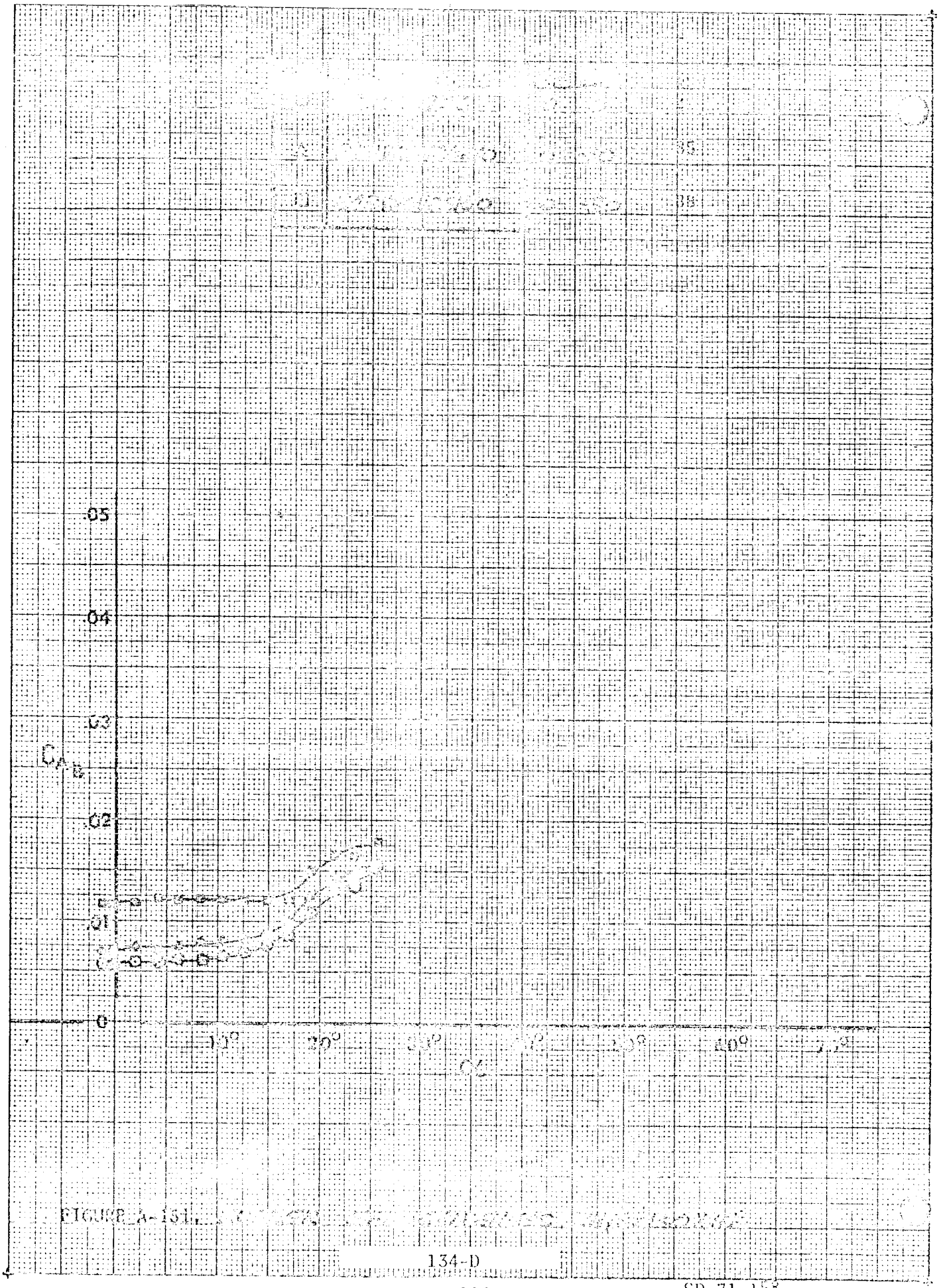

FIGURE A-151

134-D

10 X 10 TO THE CENTIMETER 46 1517
18 X 25 CM. • ALBANENE®
KEUFFEL & ESSER CO.

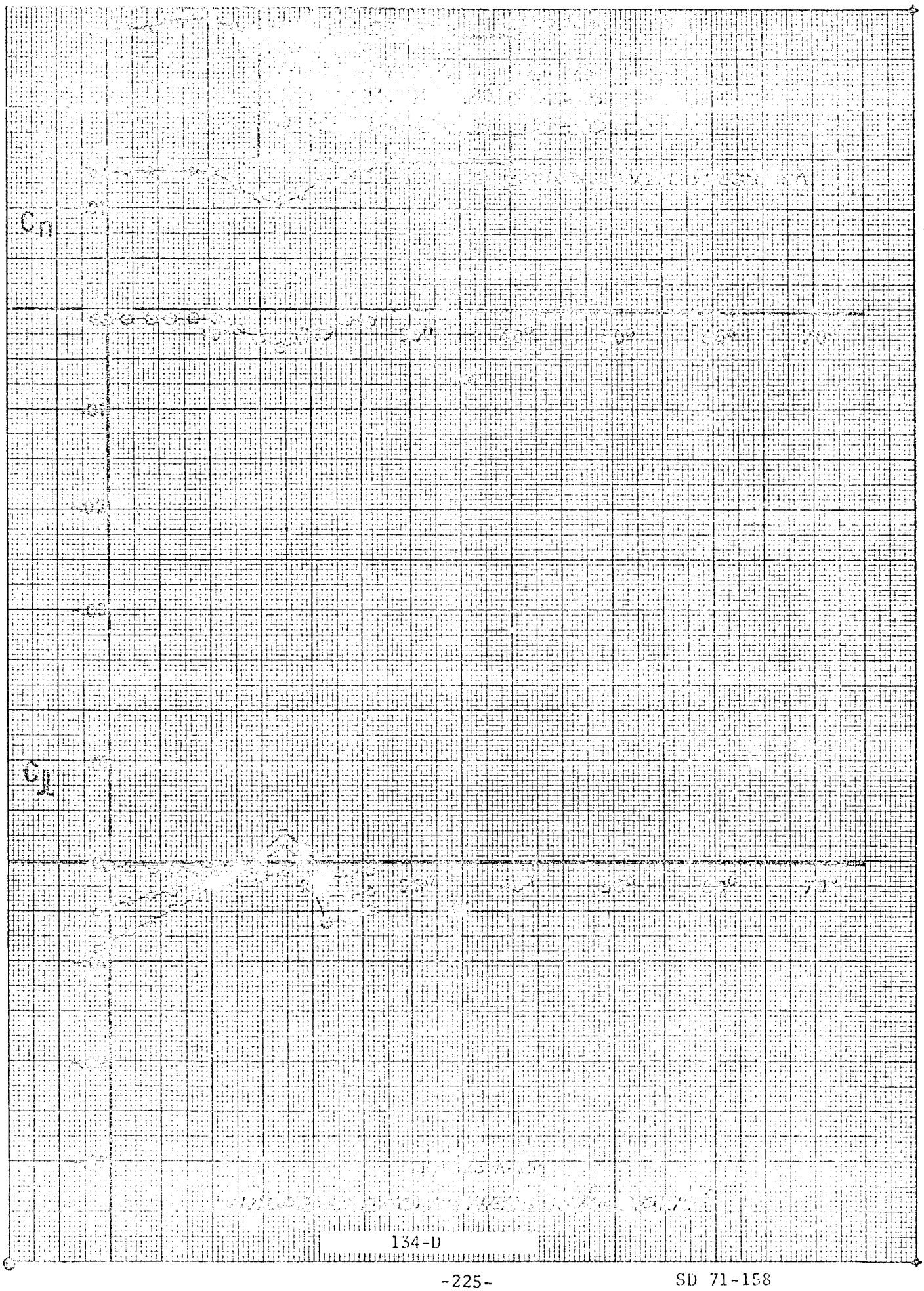

KEUFFEL & ESSER CO.

277

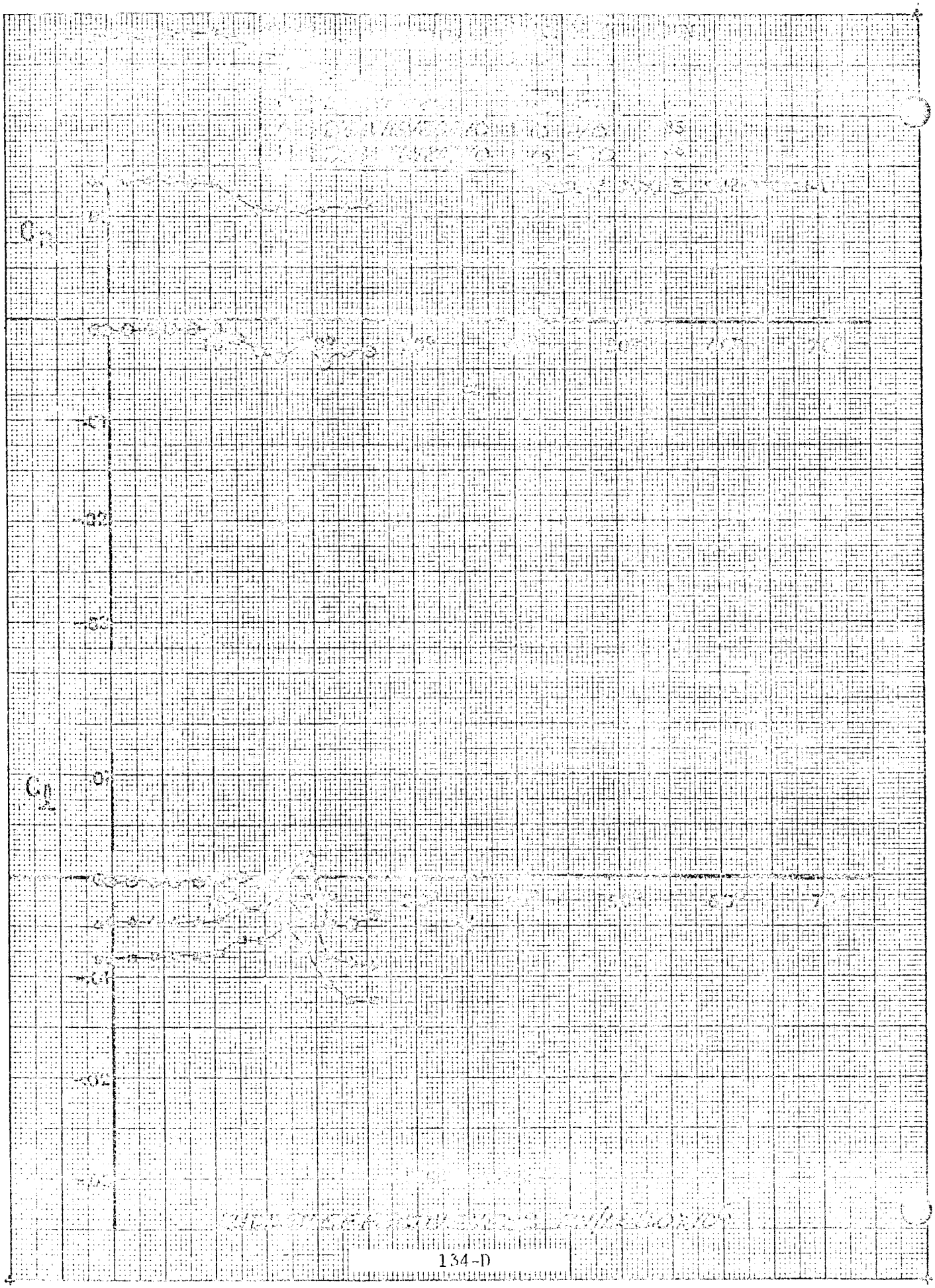

134-D

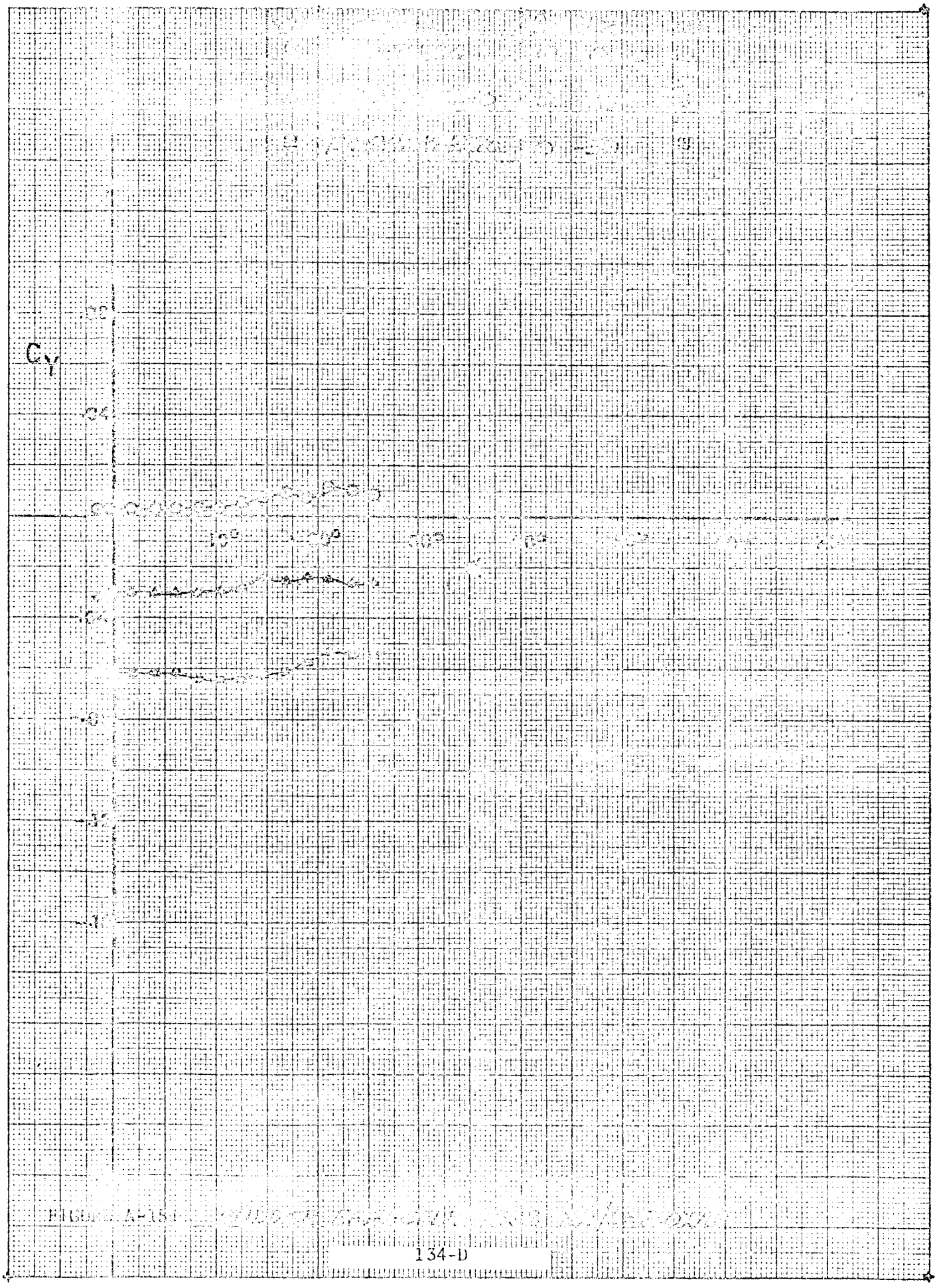
C_Y
.25
.20
.15
.10
.05
0
-.05
-.10
-.15
-.20
-.25
100
200
300
400
500
600
700
800
900
1000
1100
1200
1300
1400
1500
1600
1700
1800
1900
2000
2100
2200
2300
2400
2500
2600
2700
2800
2900
3000
3100
3200
3300
3400
3500
3600
3700
3800
3900
4000

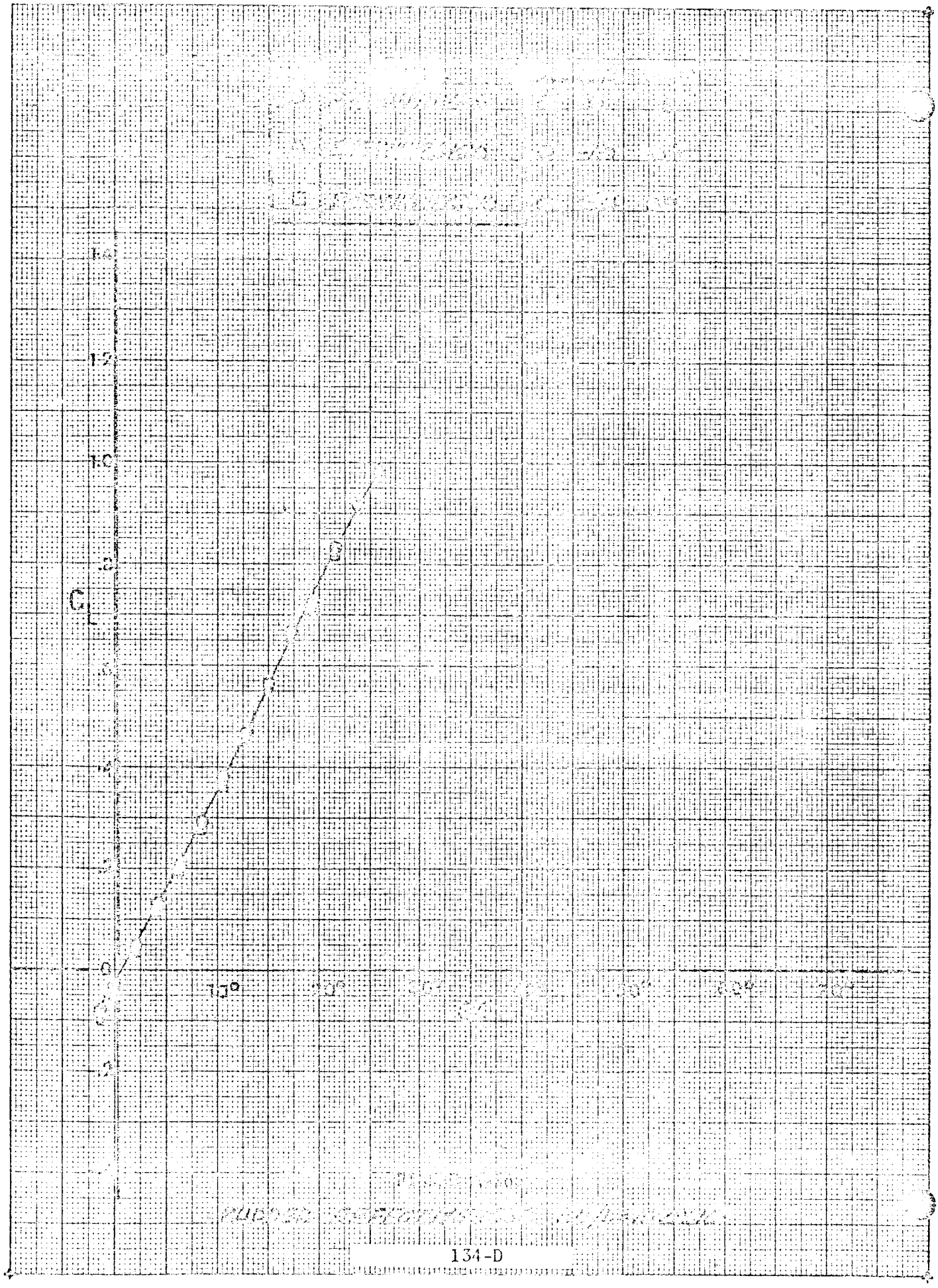

134-D

10 X 10 TO THE CENTIMETER • 46 1517
10 X 25 CM. • ALBANENE
KEUFFEL & ESSER CO.

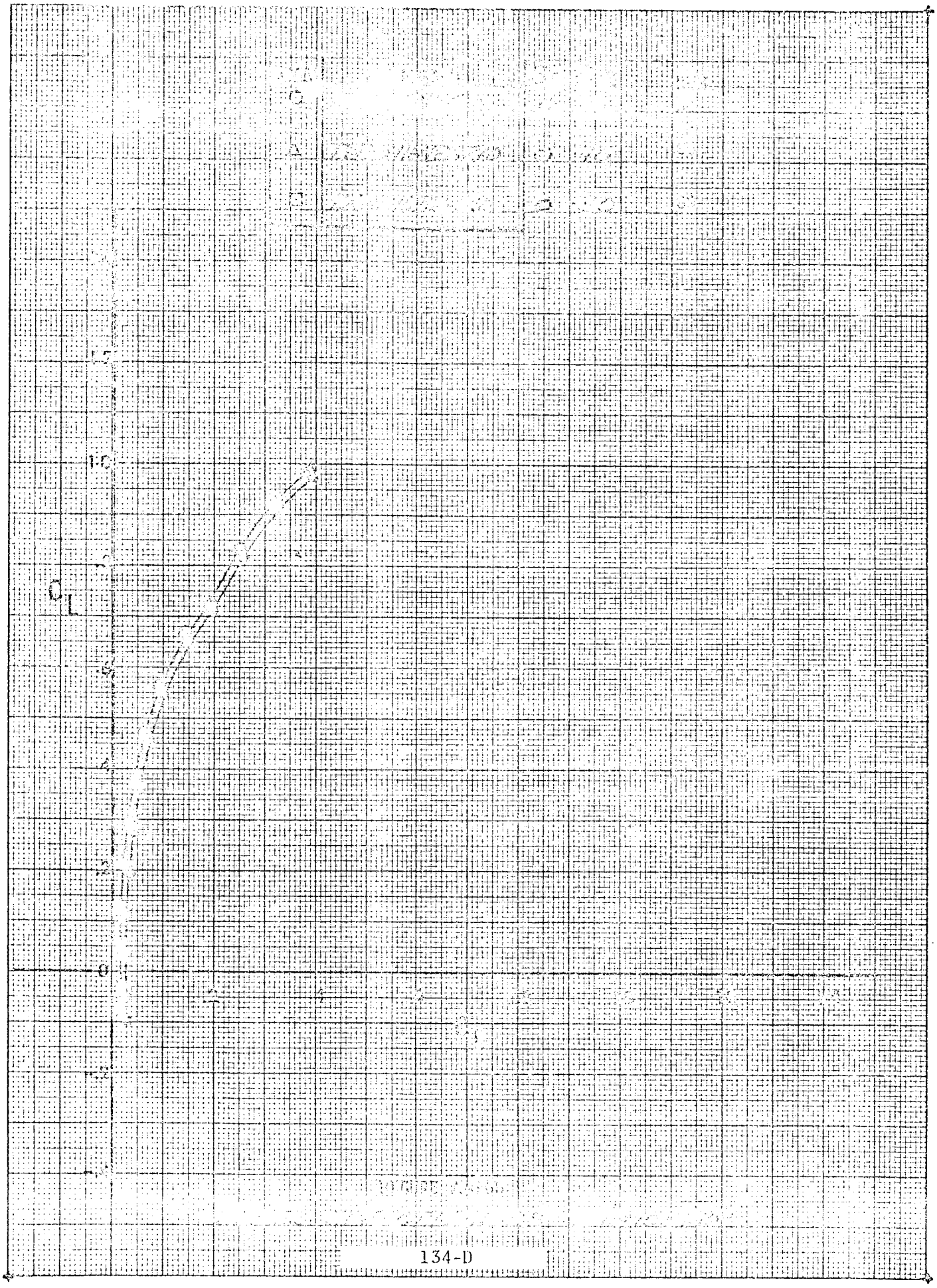

KEUFFEL & ESSER CO.

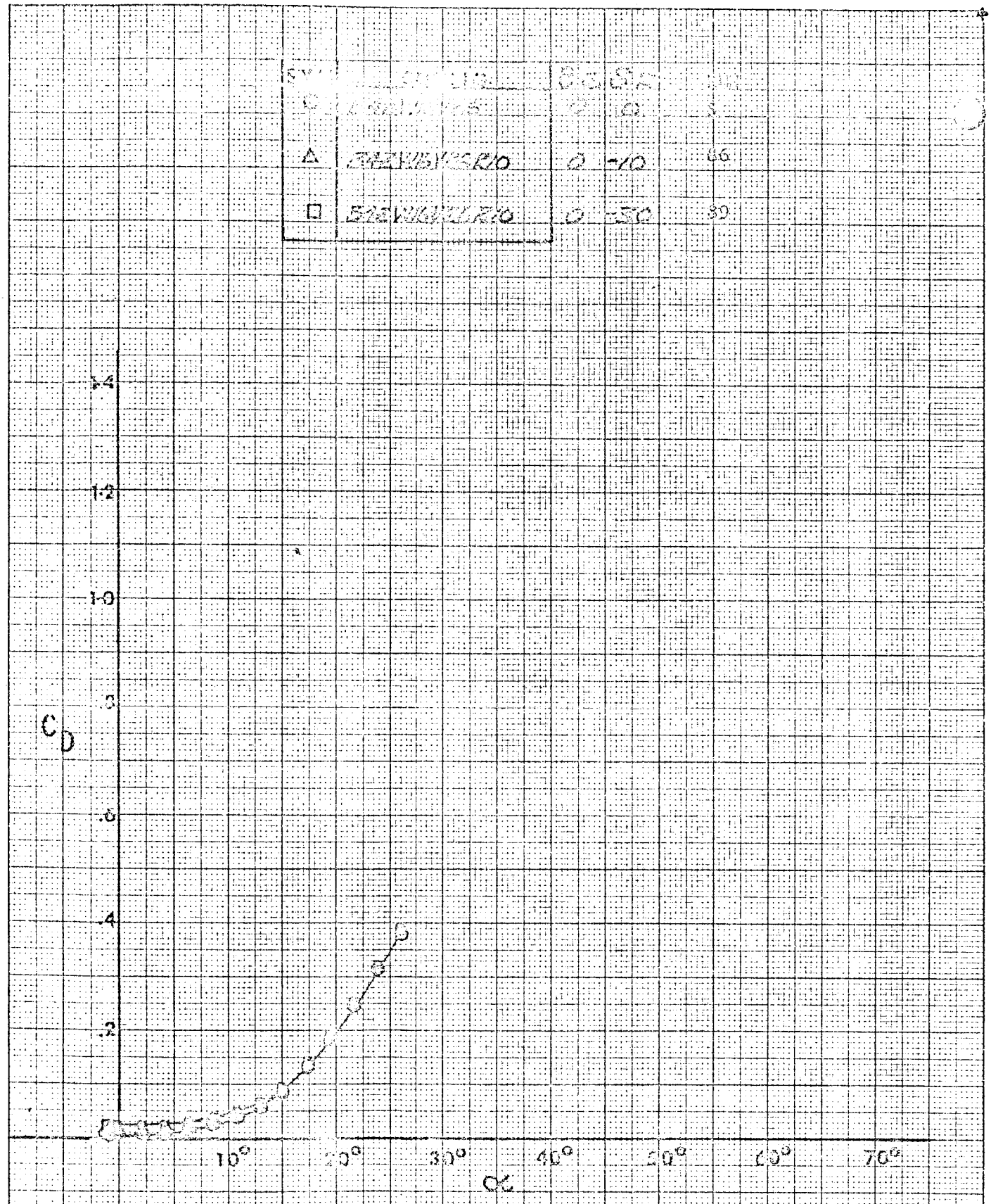

FIGURE A-16: RUDDER EFFECTIVENESS BULLROOKS

134-D

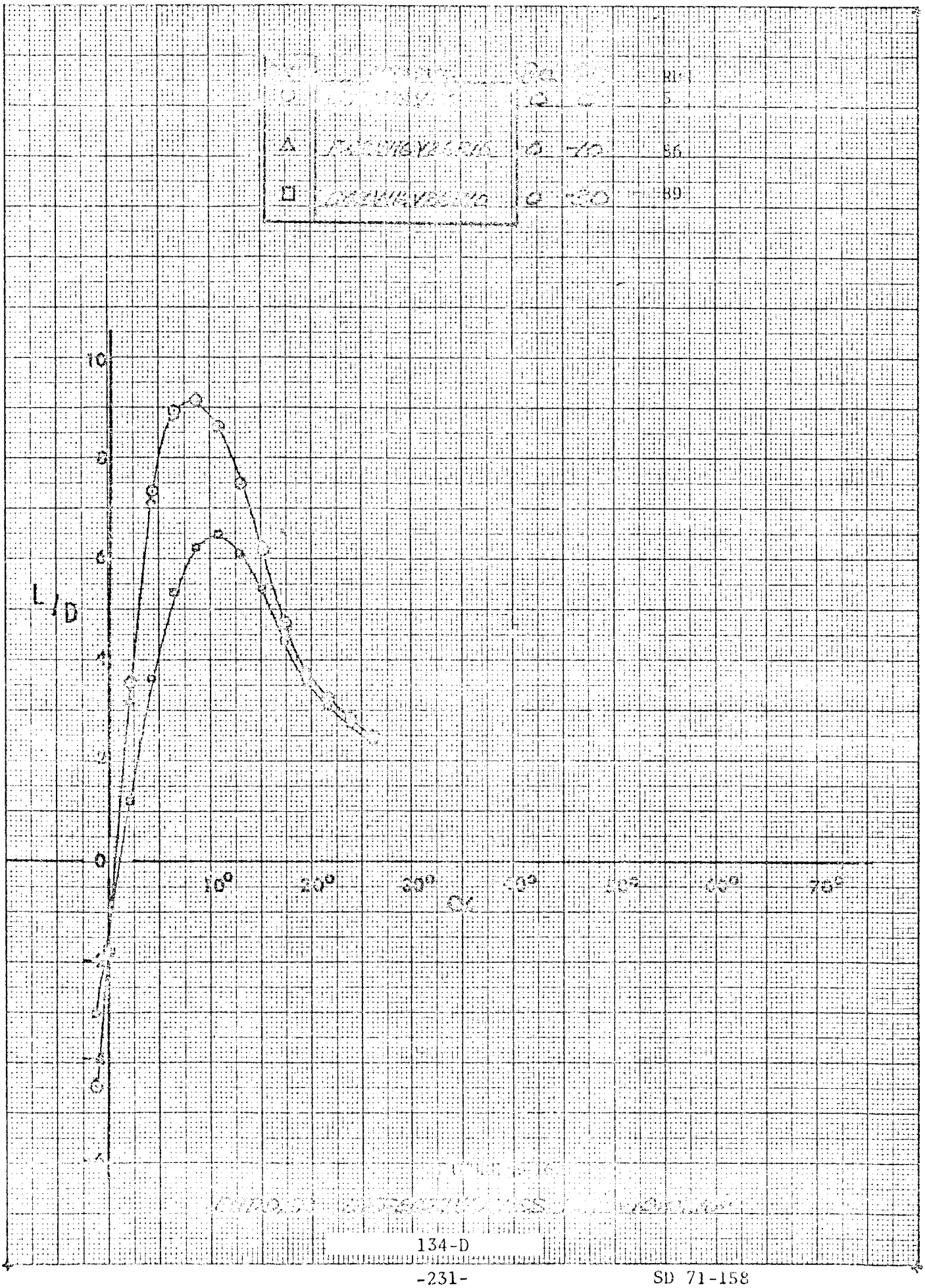

134-D

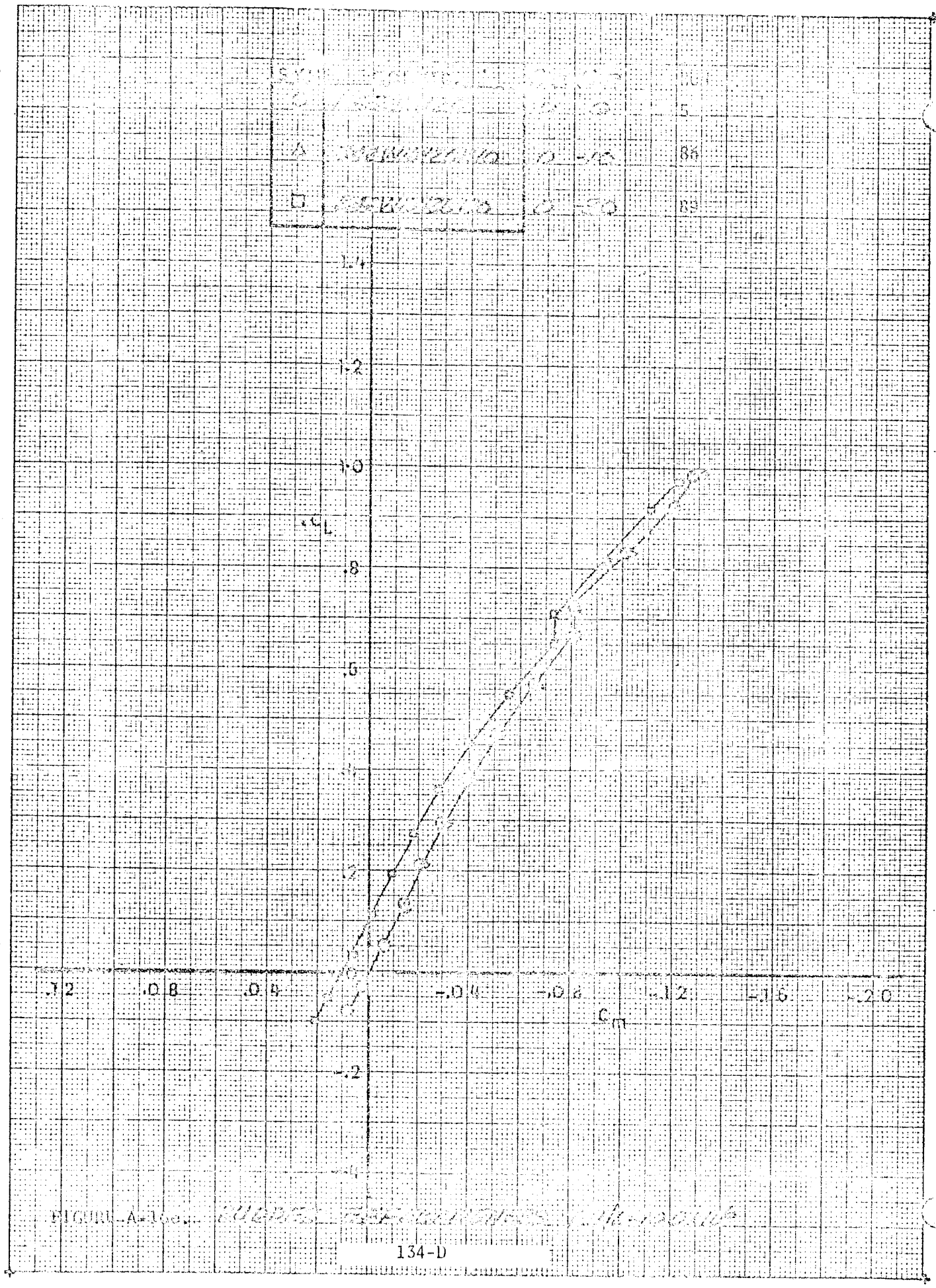

FIGURE A-100. [illegible]

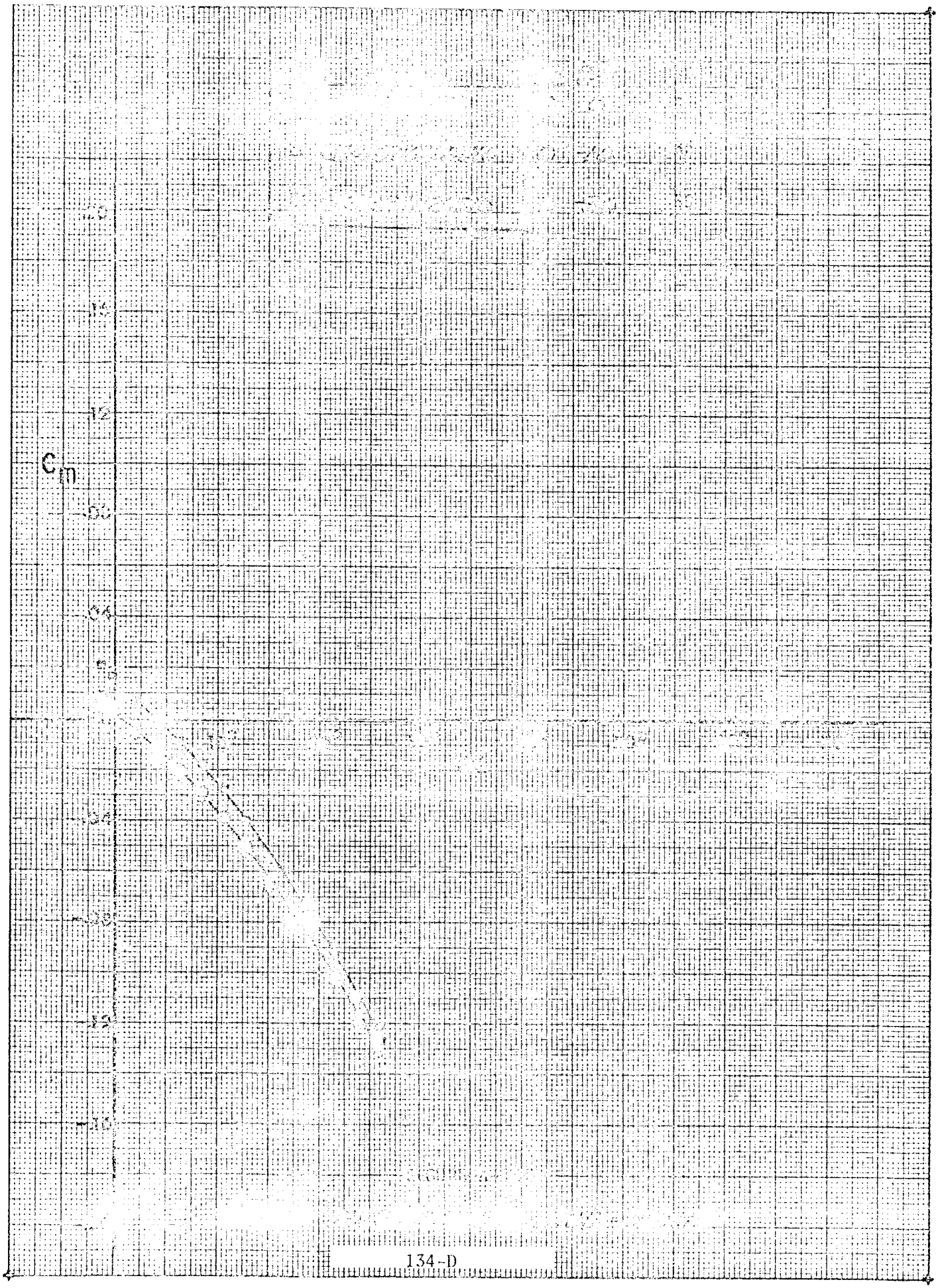
C_m
134-D

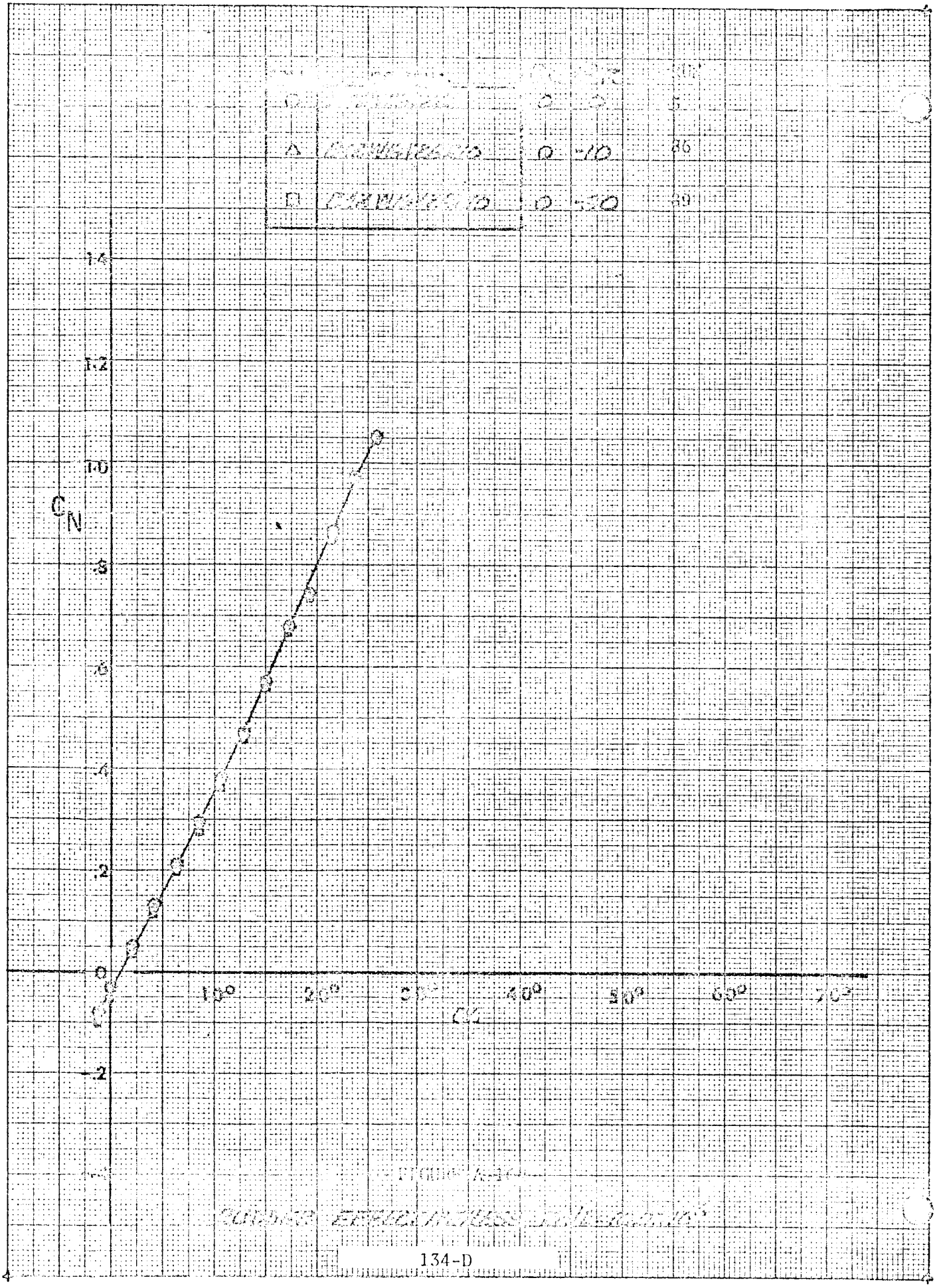

134-D

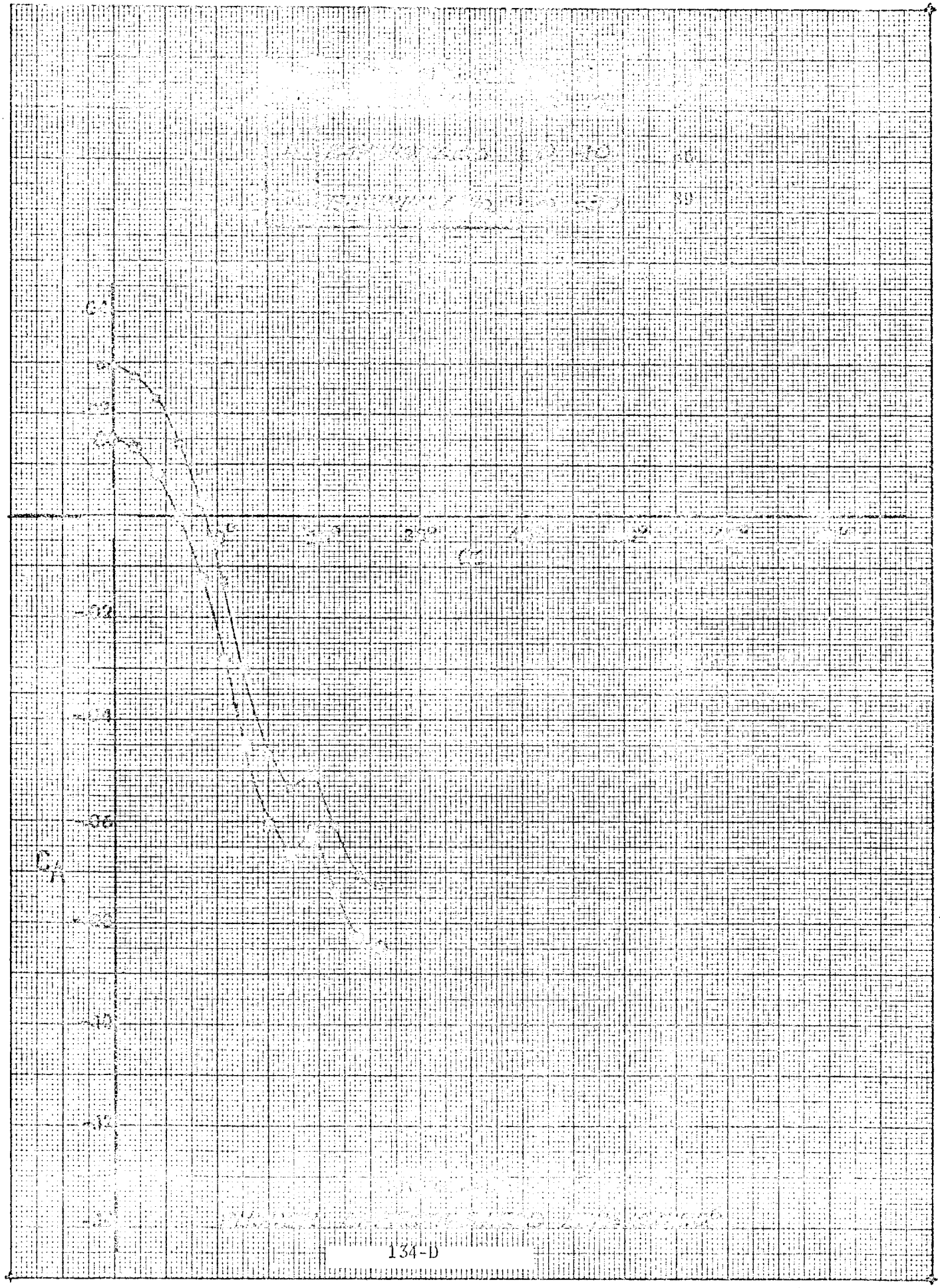

134-D

KEUFFEL & ESSER CO.

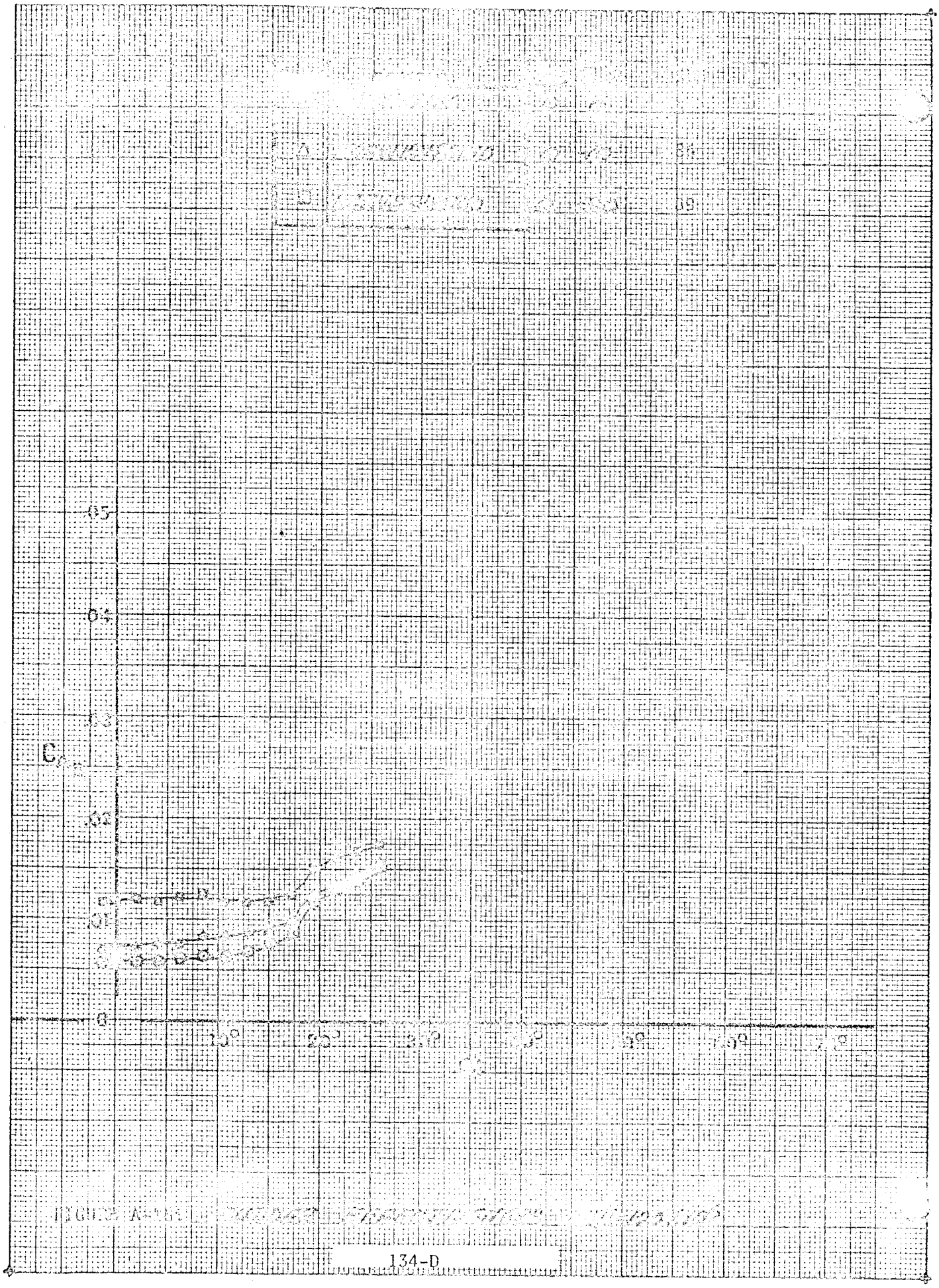

K&E 10 X 10 TO THE CENTIMETER 46 1517
18 X 25 CM. • ALBANENE®
KEUFFEL & ESSER CO.

225

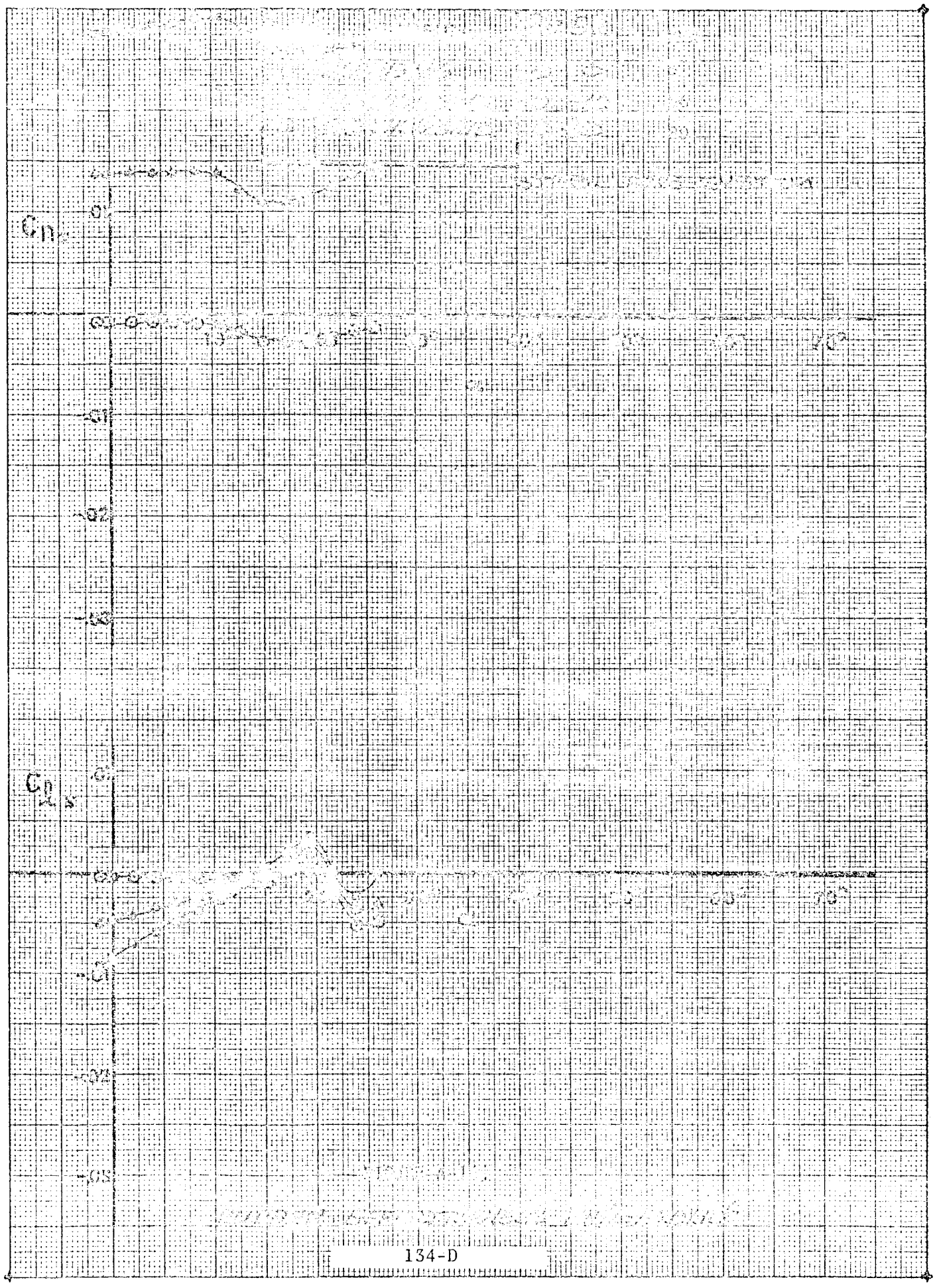

10 X 10 TO THE CENTIMETER 46 1517
18 X 25 CM • ALBANENE
KEUFFEL & ESSER CO.

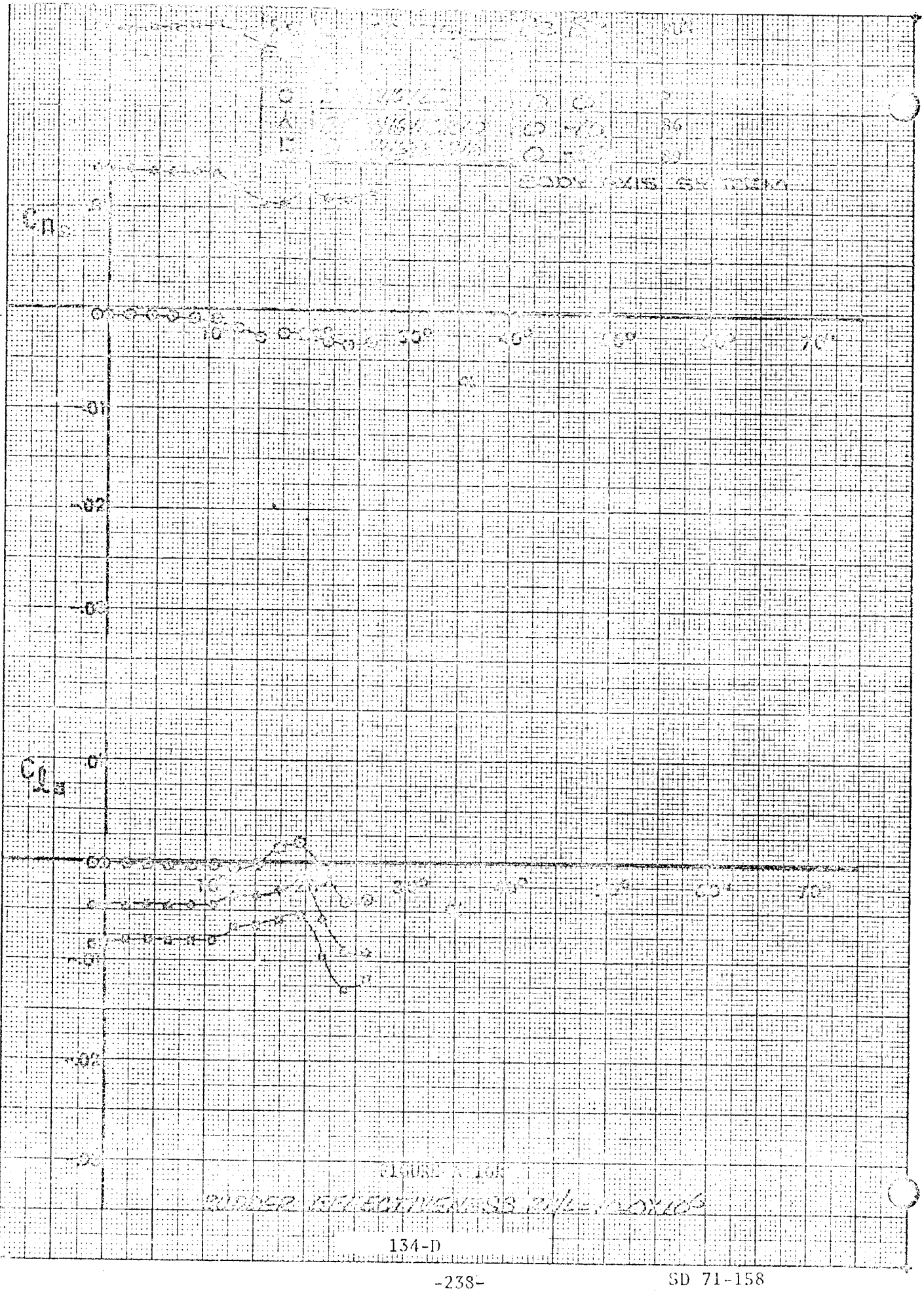

FIGURE [illegible] FOR

BODY REFERENCE AREA [illegible] 10^6

134-D

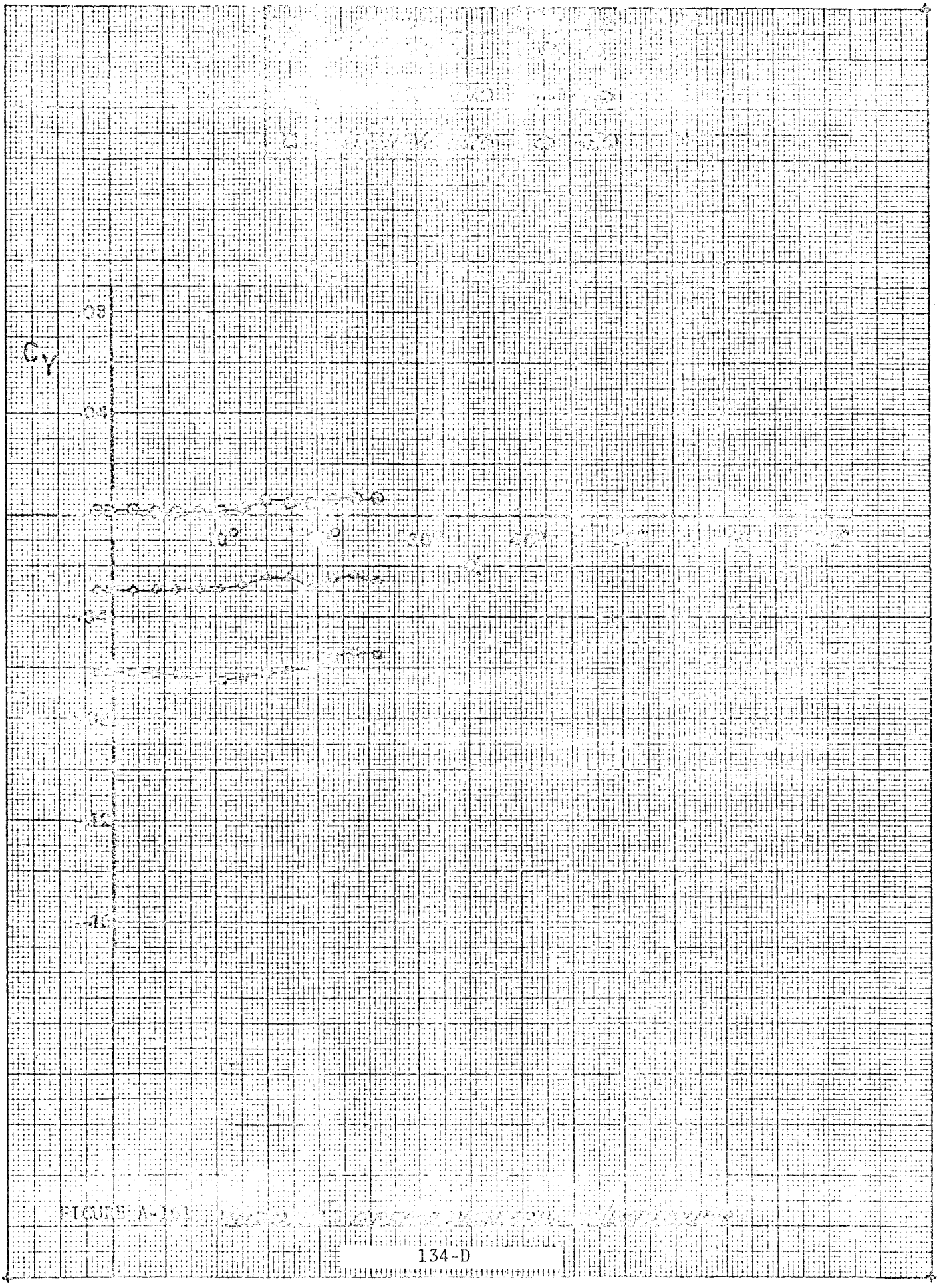

FIGURE A-10

134-D

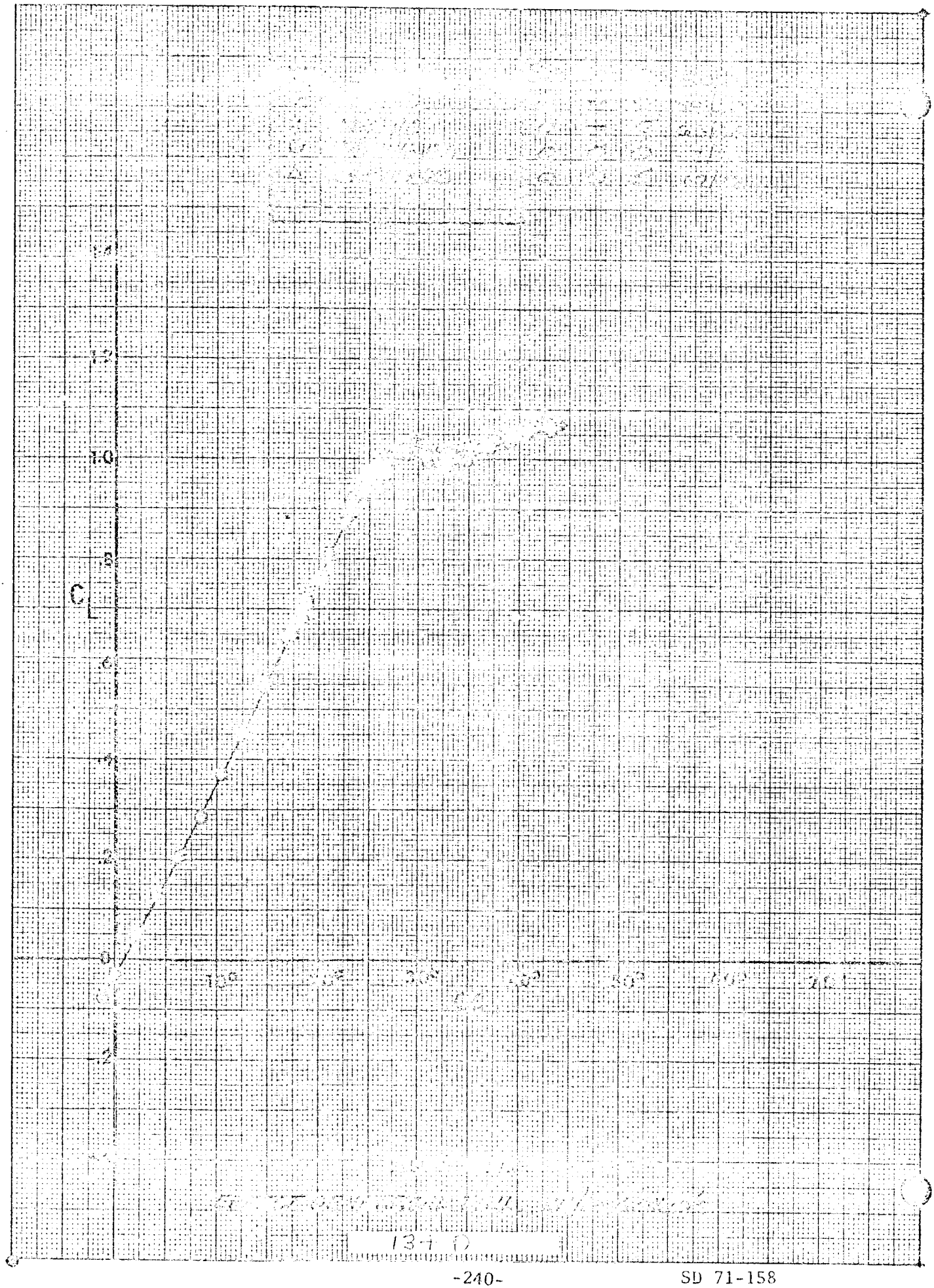

10 X 10 TO THE CENTIMETER 46 1517
18 X 25 CM. • ALBANENE®
KEUFFEL & ESSER CO.

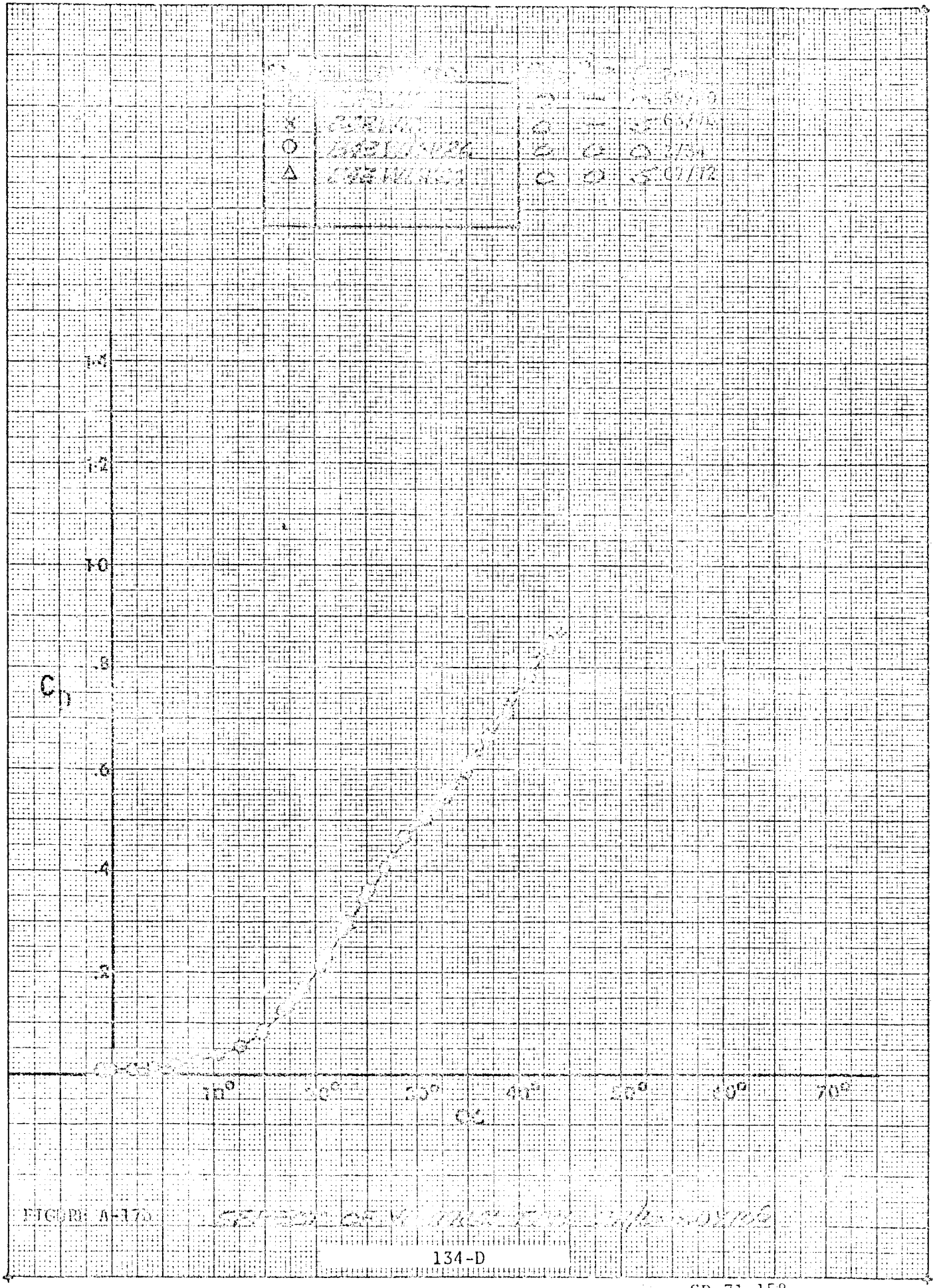

FIGURE A-17

134-D

273

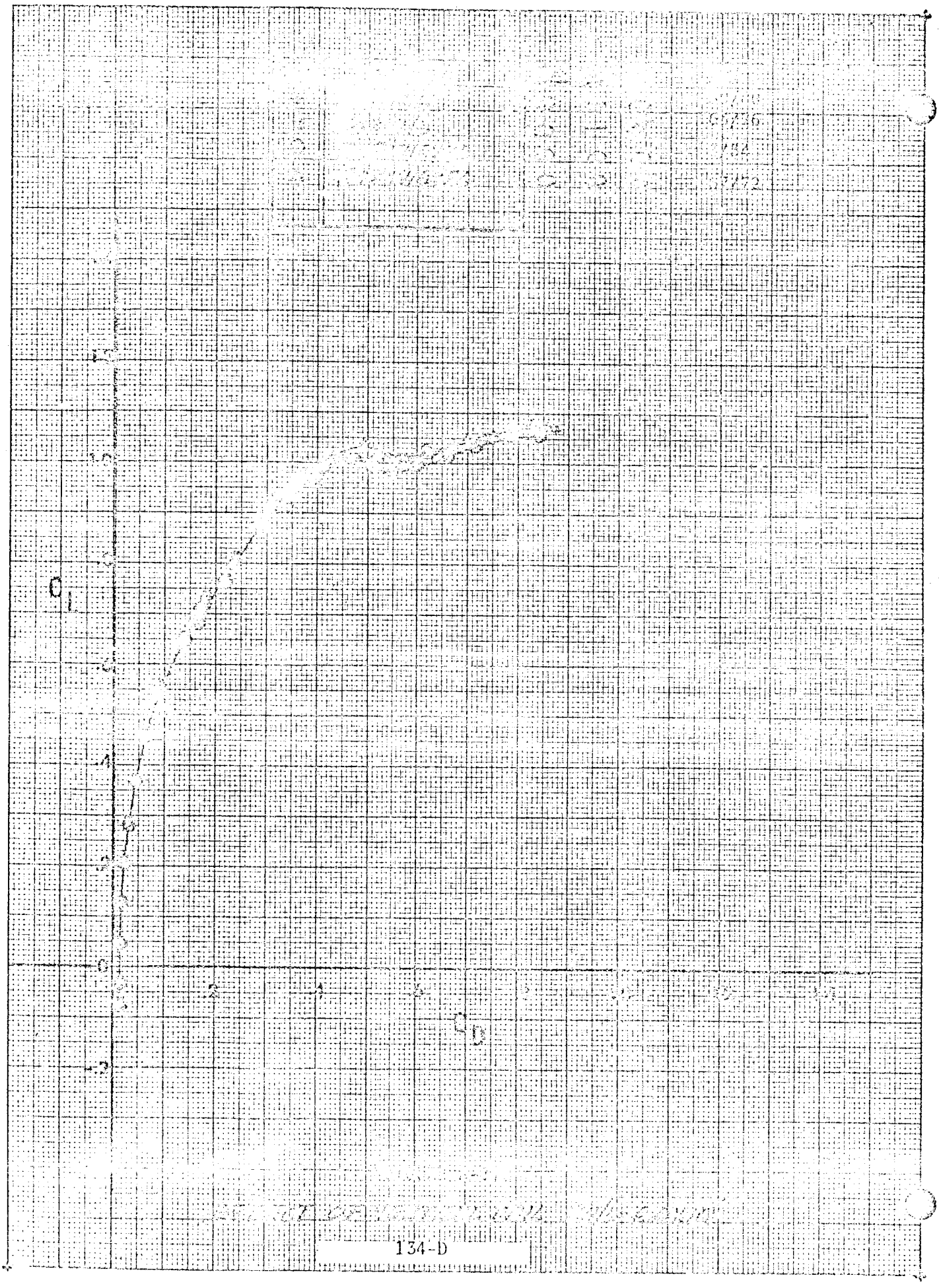

134-D

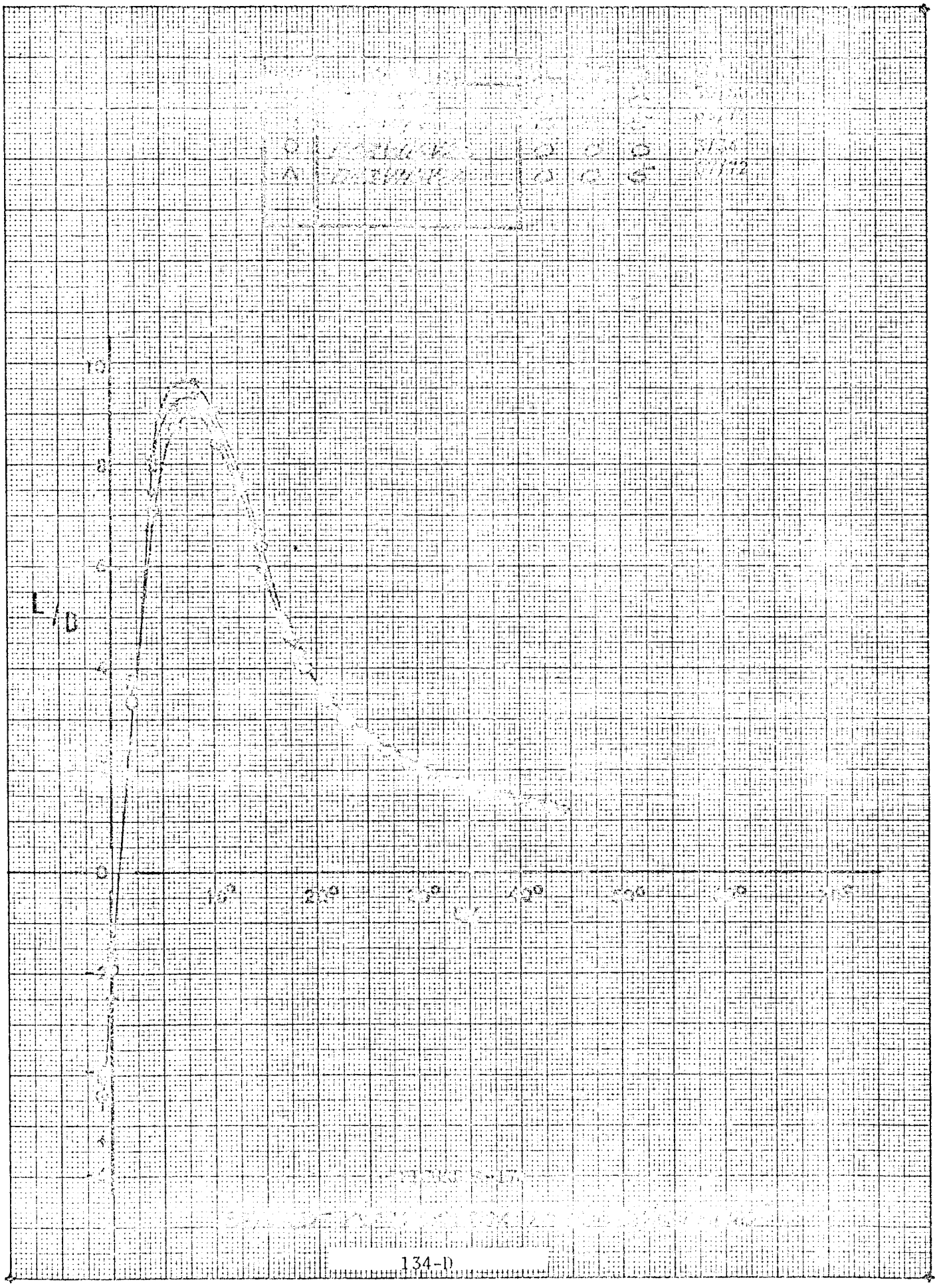

KEUFFEL & ESSER CO.

275

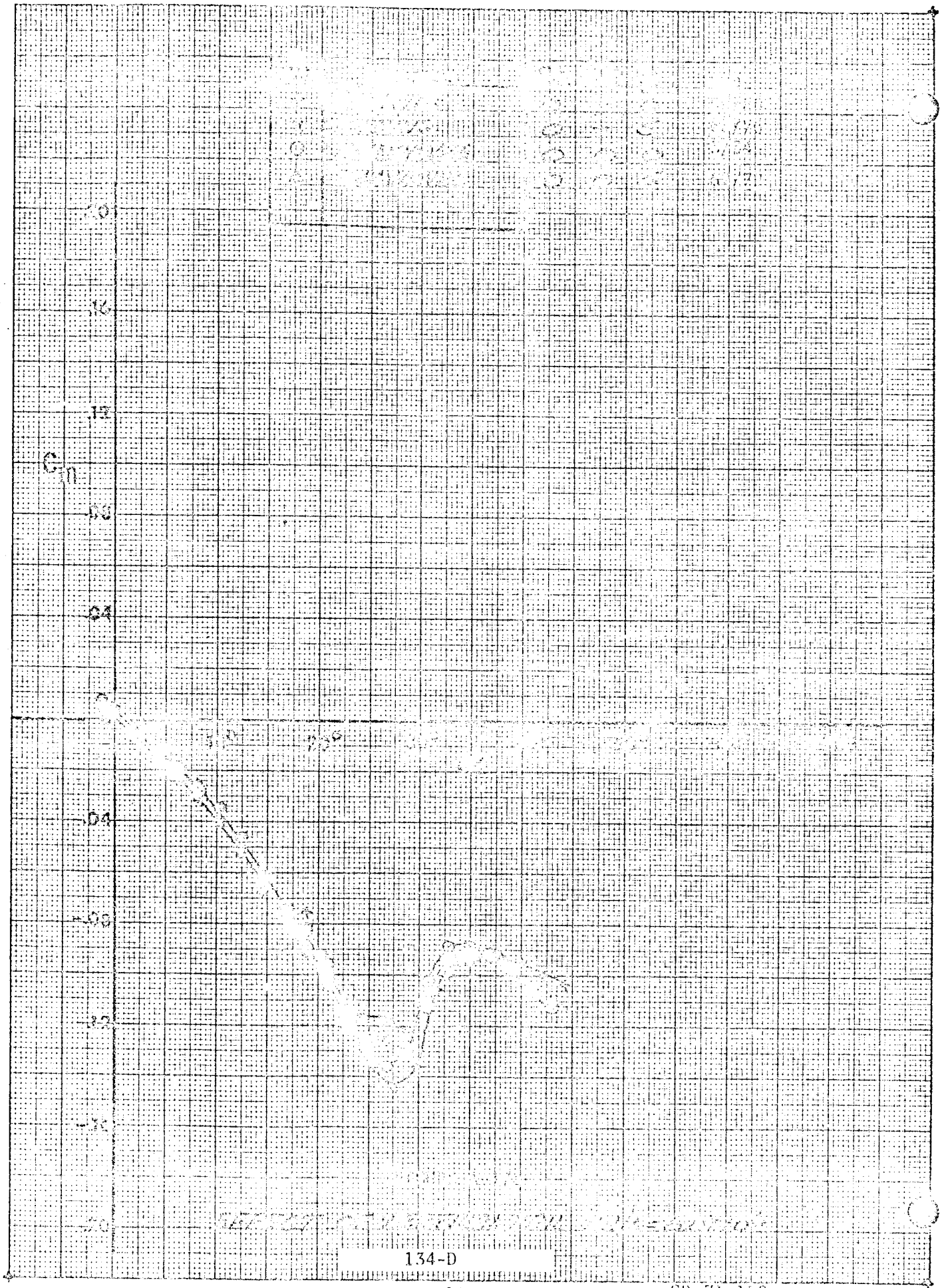

134-D

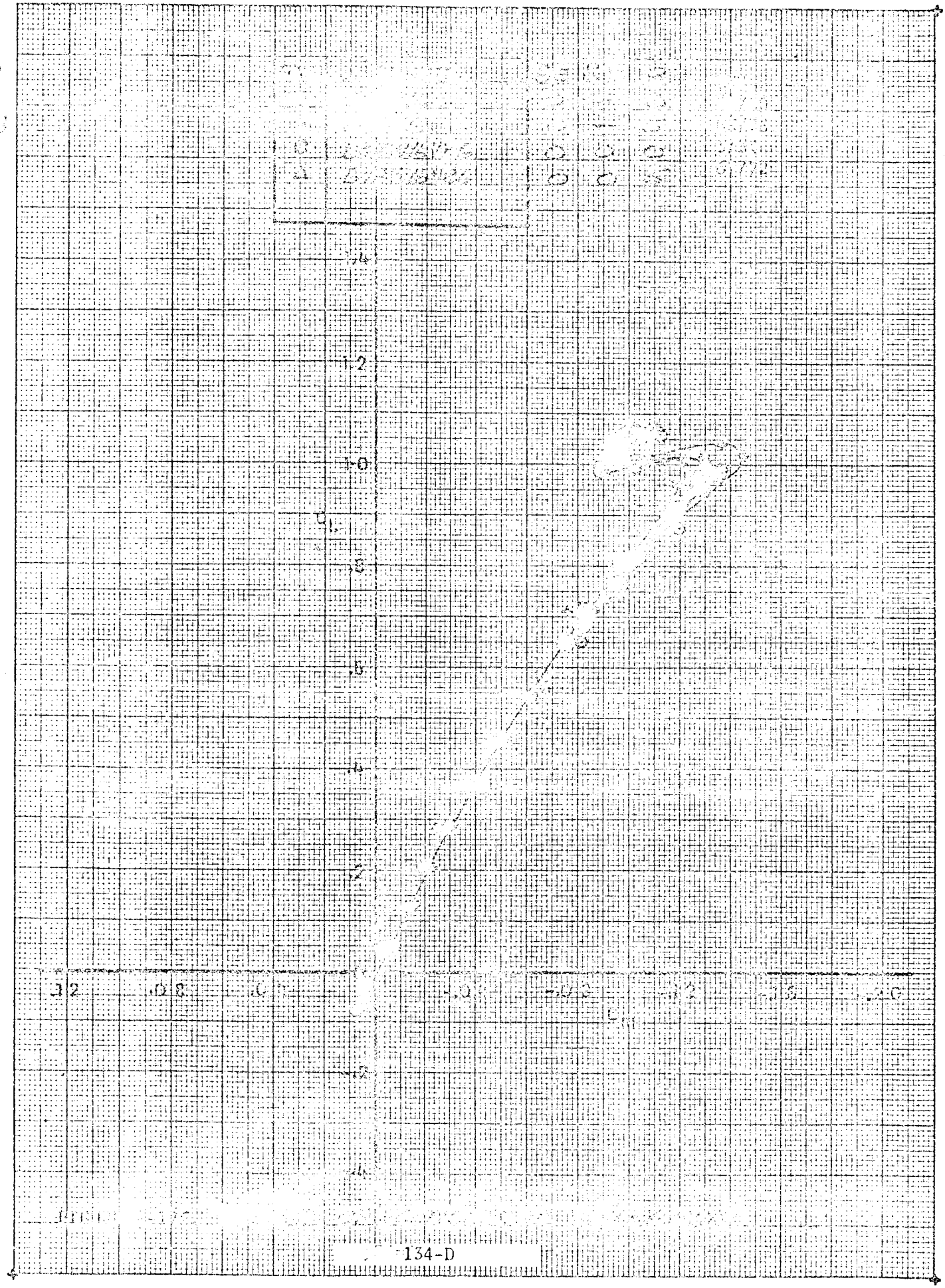

134-D

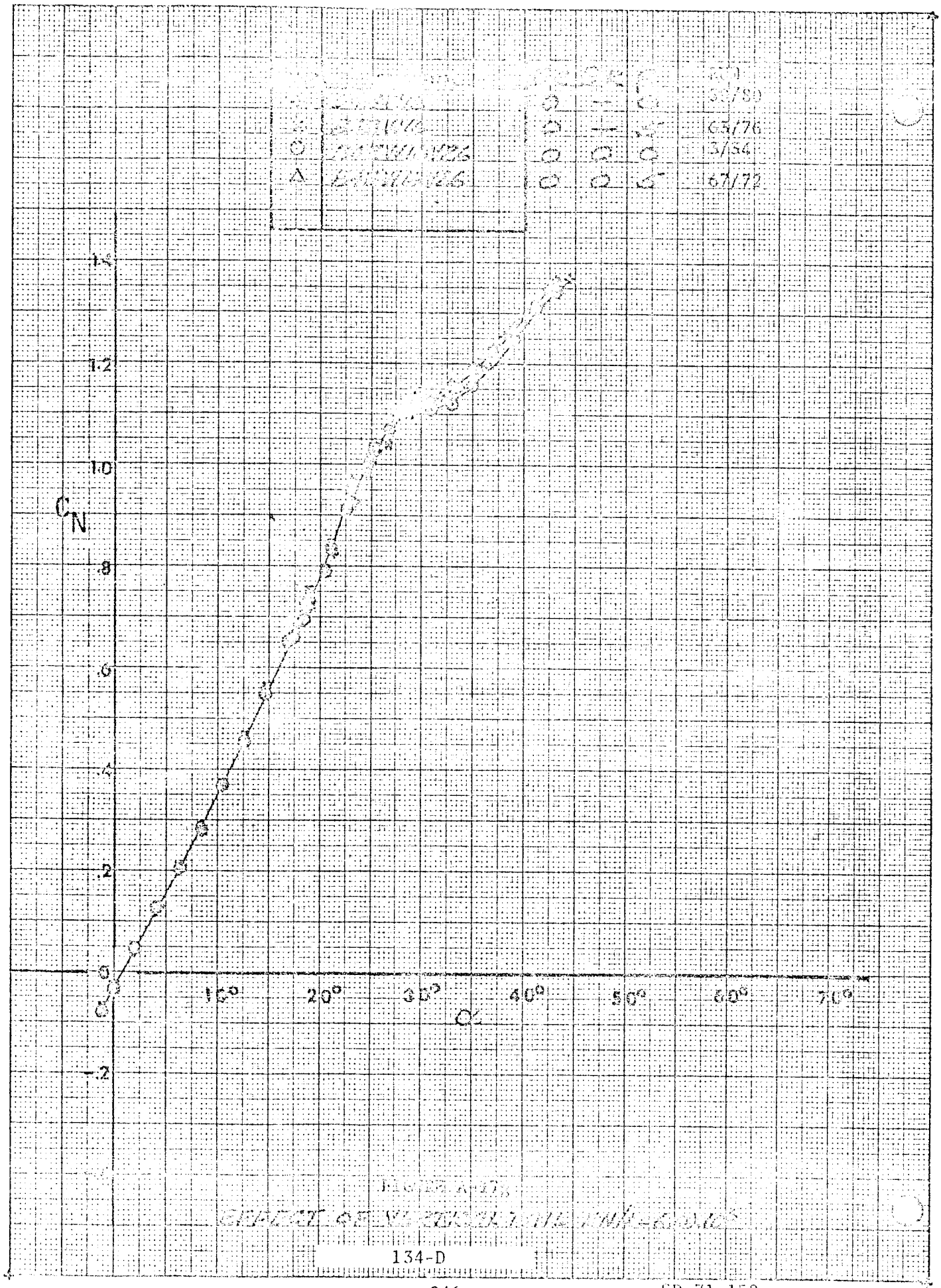
1.4
1.2
1.0
C_N
.8
.6
.4
.2
0
-.2
10°
20°
30°
40°
50°
60°
70°
α
134-D

134-D

KEUFFEL & ESSER CO.

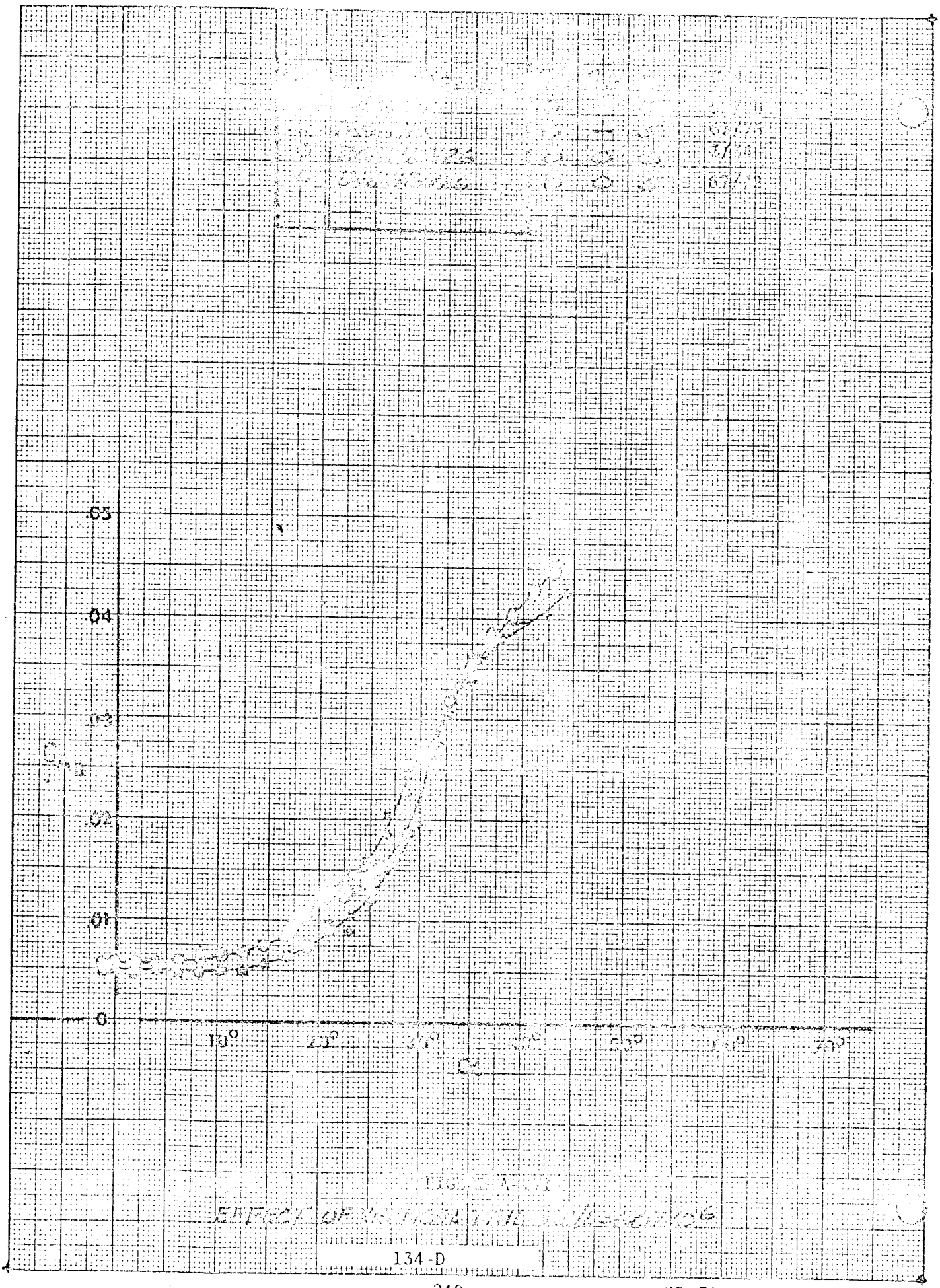

134-D

10 X 10 TO THE CENTIMETER 46 1517
10 X 25 CM. • ALBANENE
KEUFFEL & ESSER CO.

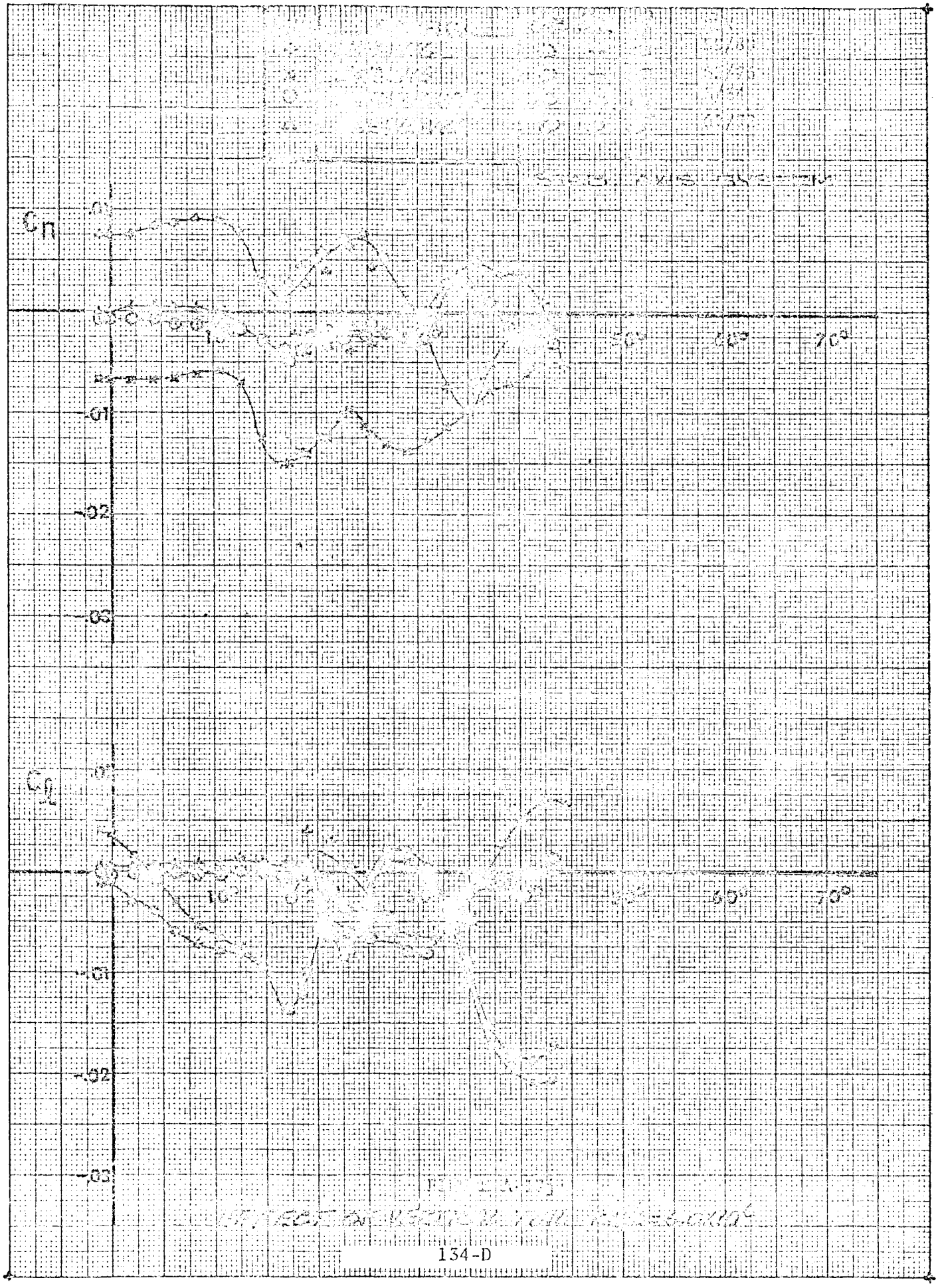

134-D

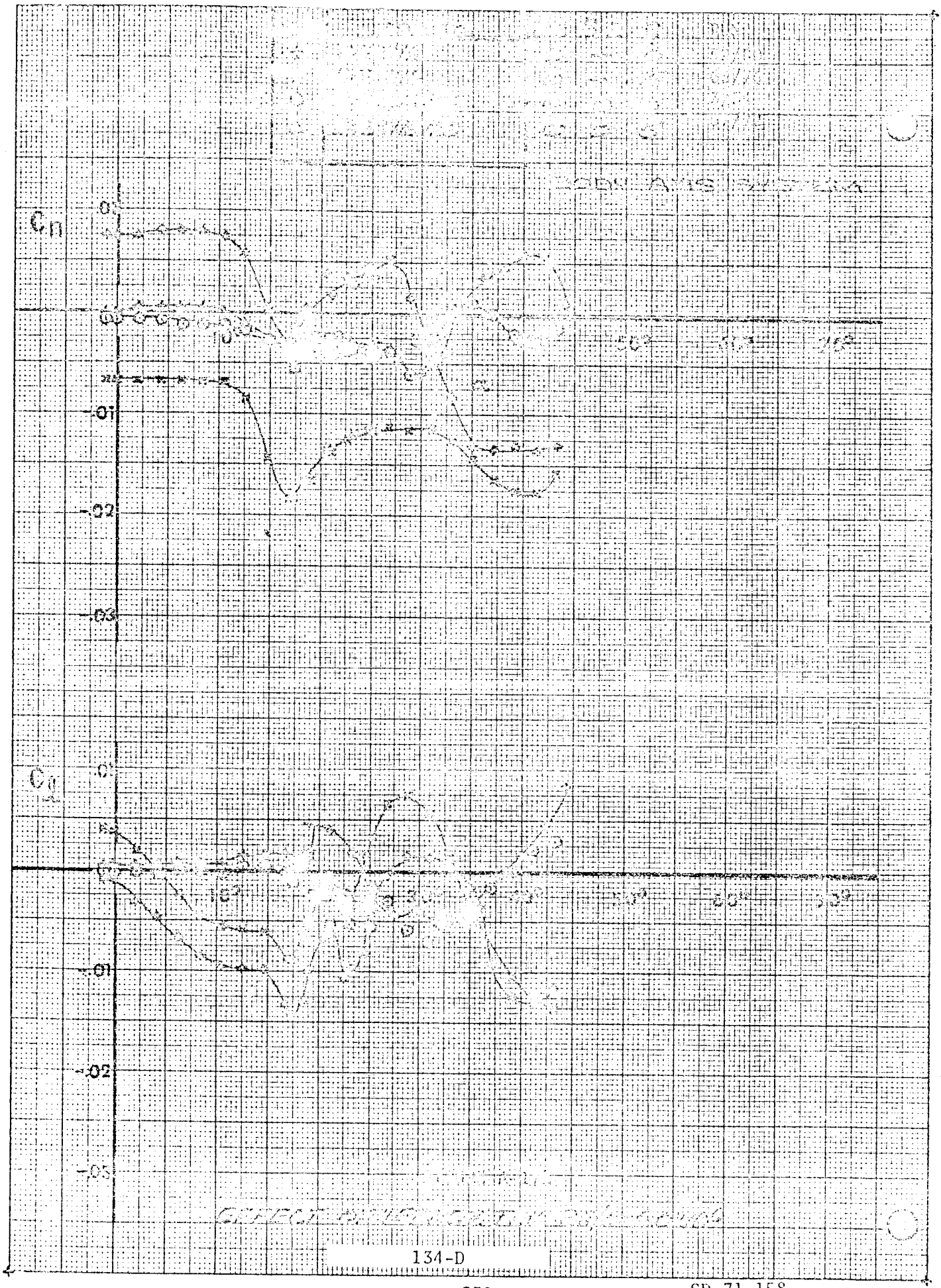

134-D

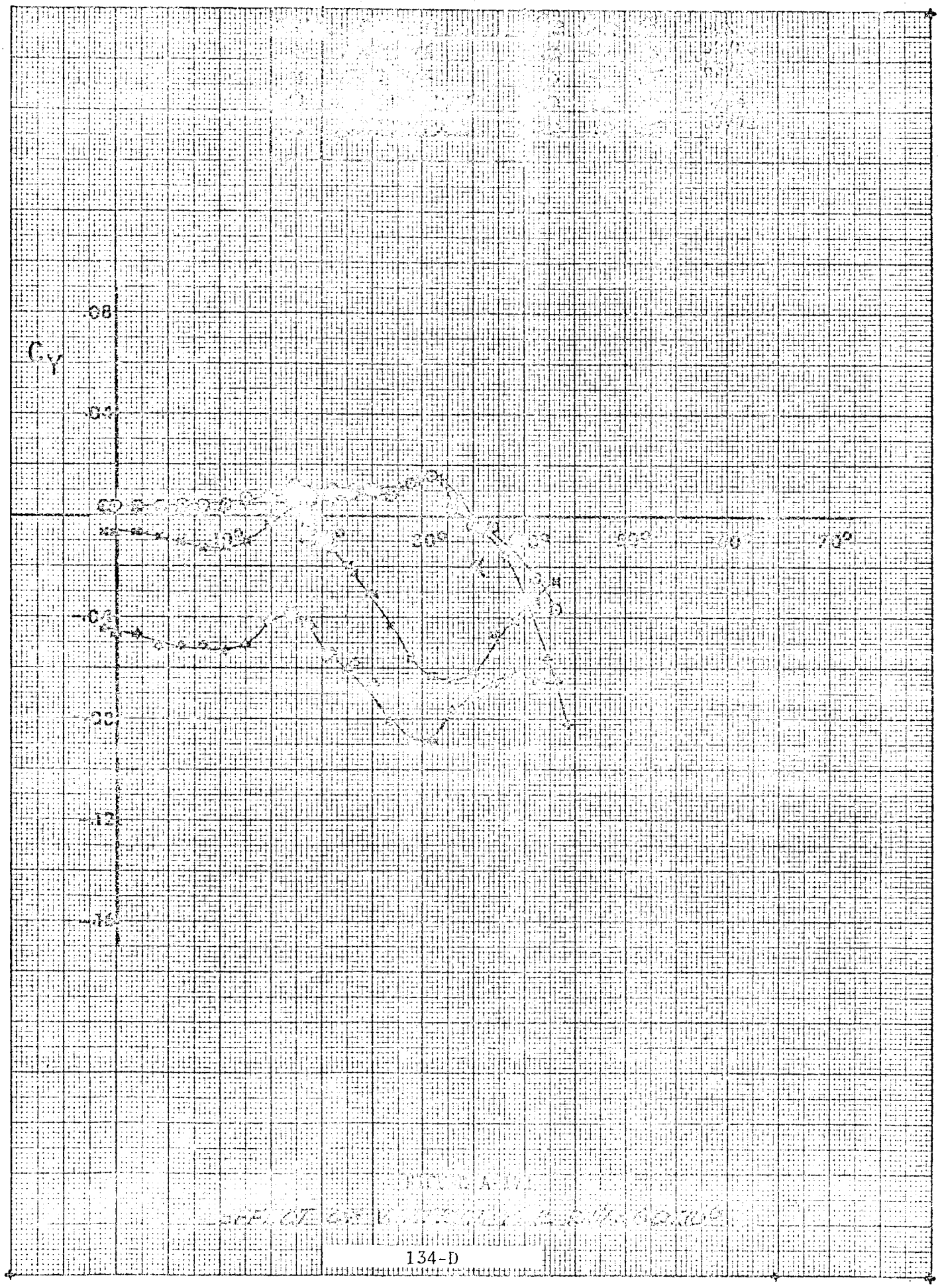

134-D

10 X 25 CM. • ALBANENE
KEUFFEL & ESSER CO.

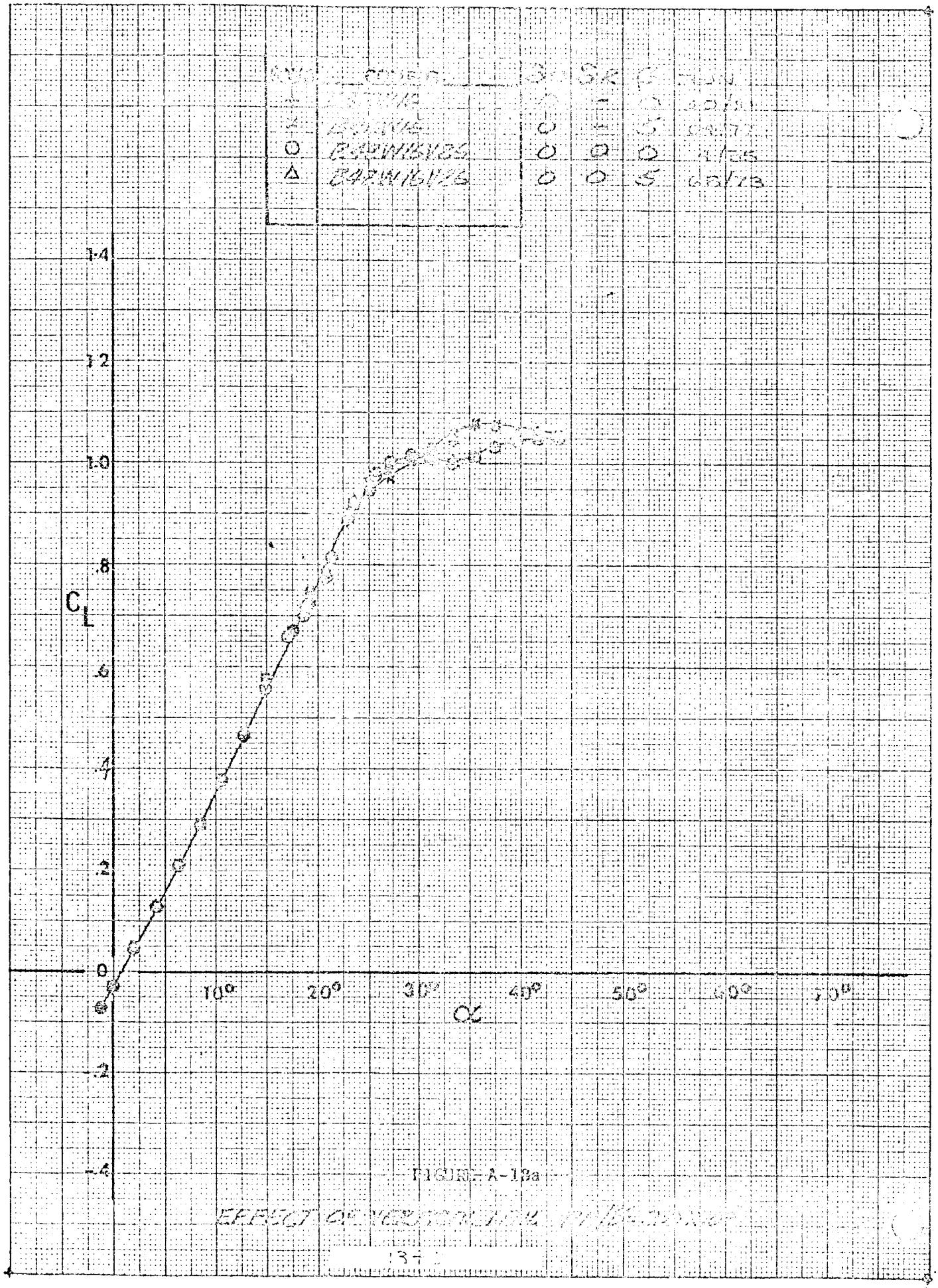

FIGURE A-19a

EFFECT OF VERTICAL TAIL ON LIFT

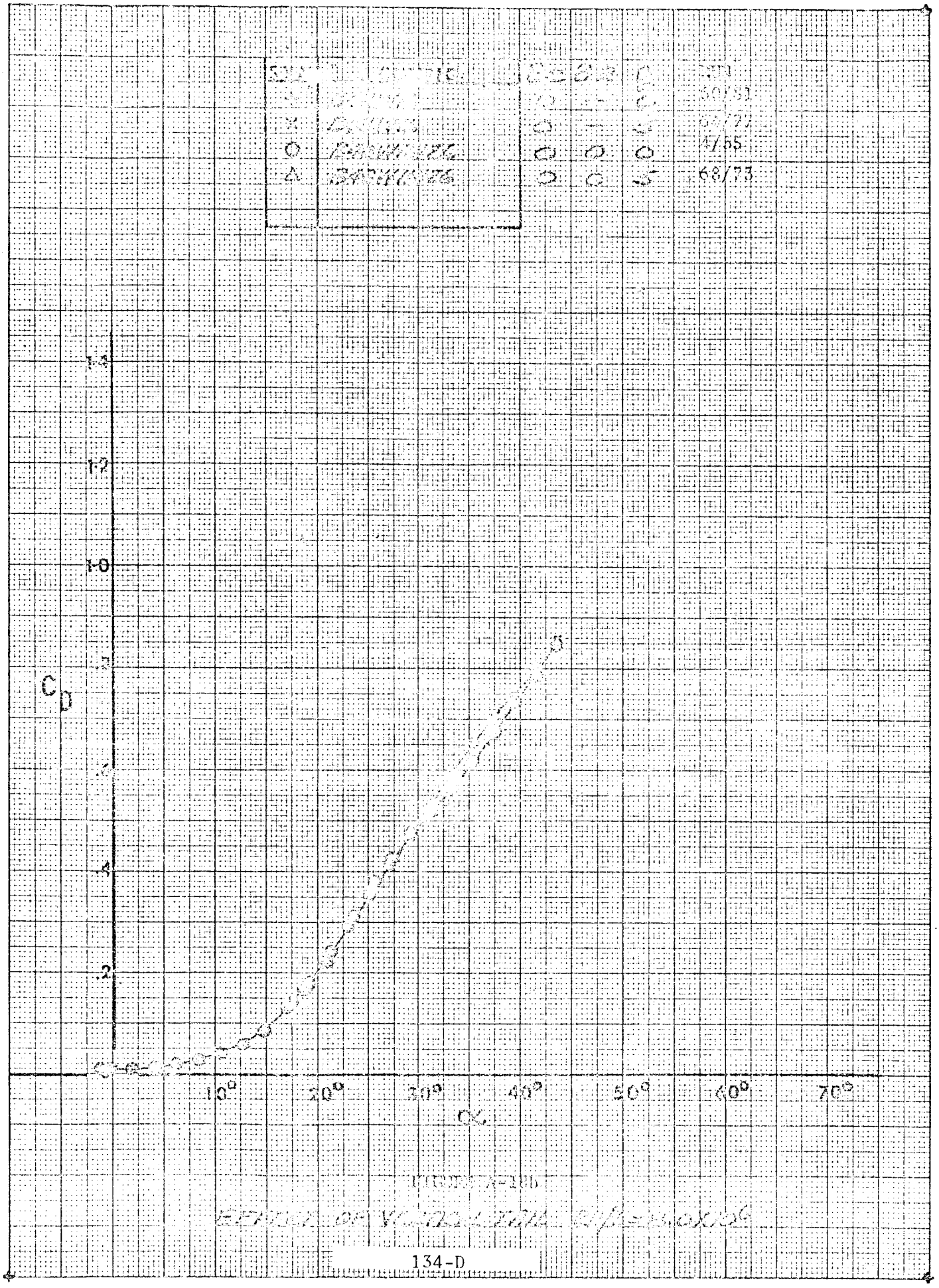

FIGURE X-18b

EFFECT OF VARIABLE [illegible] OXIDE

134-D

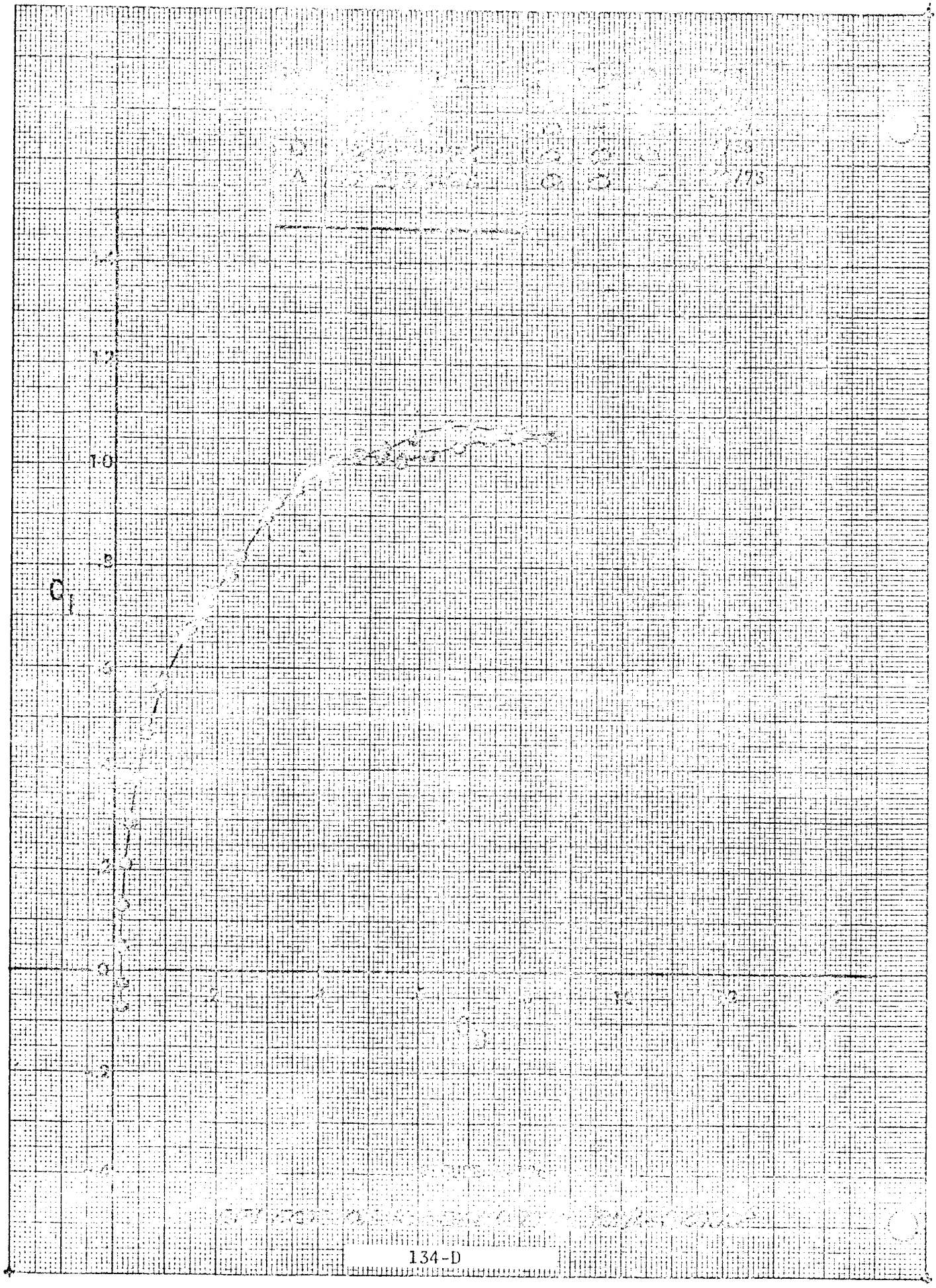

K&E 10 X 10 TO THE CENTIMETER 46 1517
10 X 25 CM • ALBANENE®
KEUFFEL & ESSER CO.

134-D

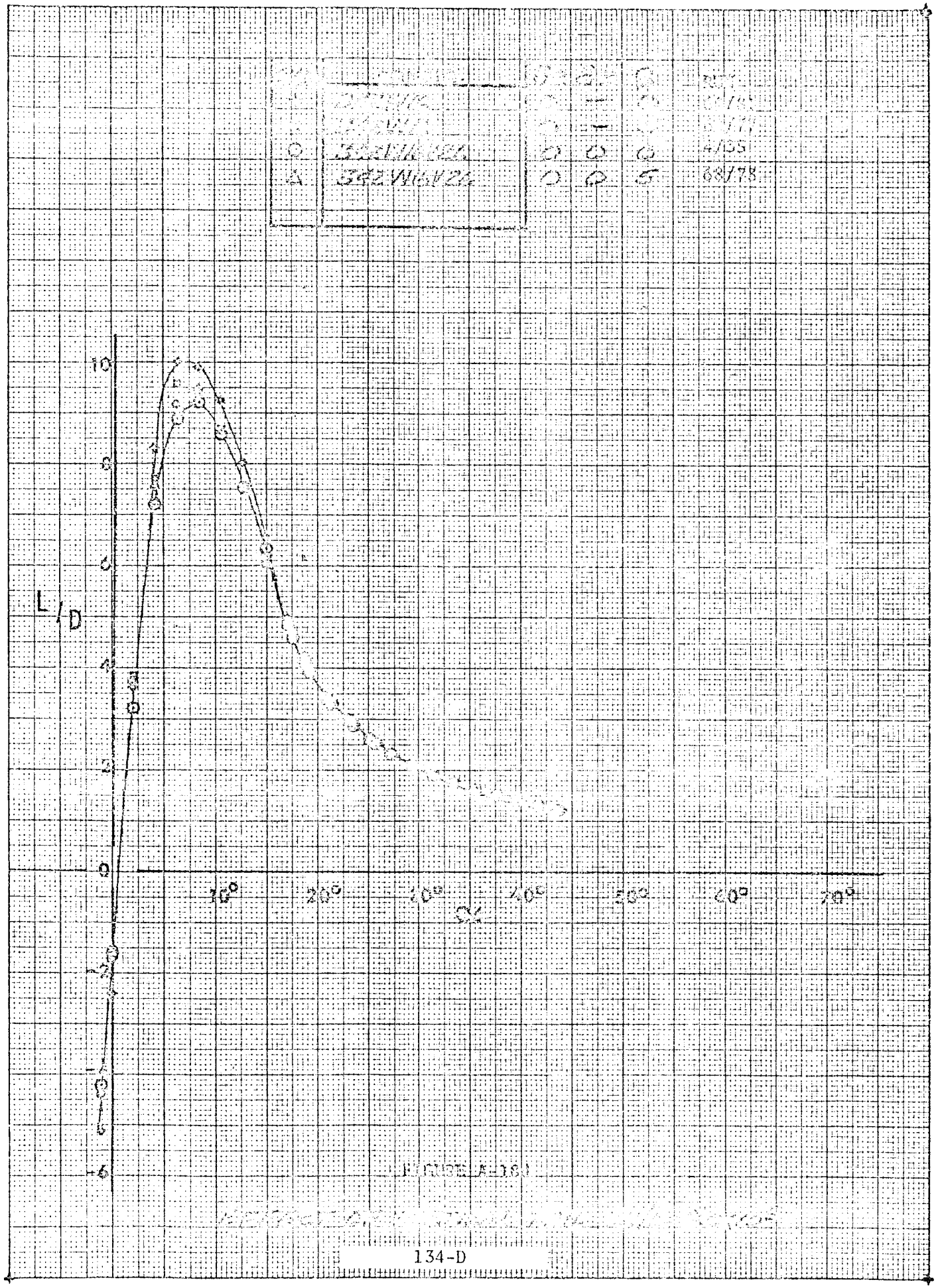

134-D

275

34

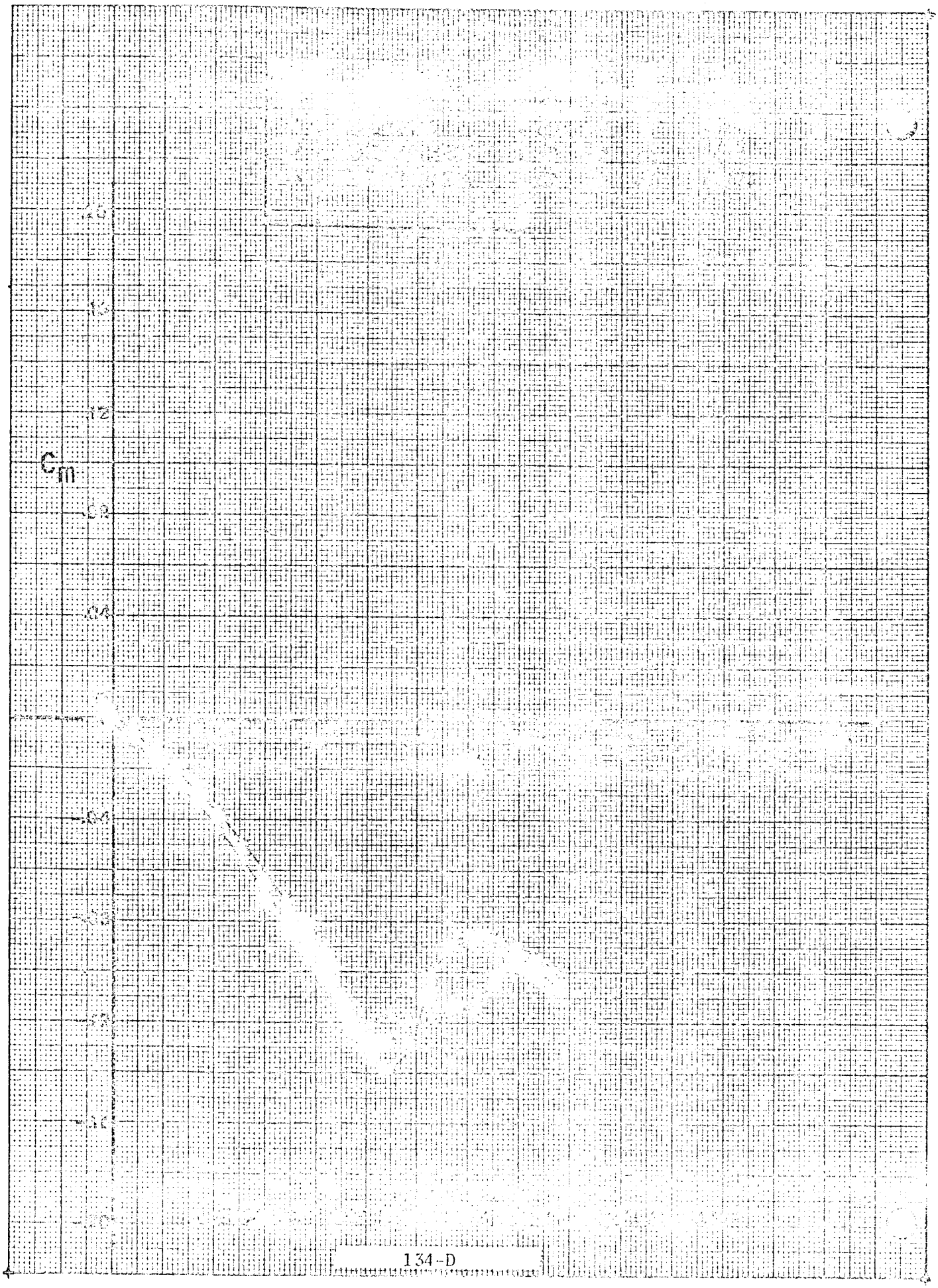
Cm
.15
.10
.05
.00
-.05
-.10
-.15
-.20
-.25
-.30
-.35
-.40
-.45
-.50
-.55
-.60
-.65
-.70
-.75
-.80
-.85
-.90
-.95
-1.00
-1.05
-1.10
-1.15
-1.20
-1.25
-1.30
-1.35
-1.40
-1.45
-1.50
-1.55
-1.60
-1.65
-1.70
-1.75
-1.80
-1.85
-1.90
-1.95
-2.00
-2.05
-2.10
-2.15
-2.20
-2.25
-2.30
-2.35
-2.40
-2.45
-2.50
-2.55
-2.60
-2.65
-2.70
-2.75
-2.80
-2.85
-2.90
-2.95

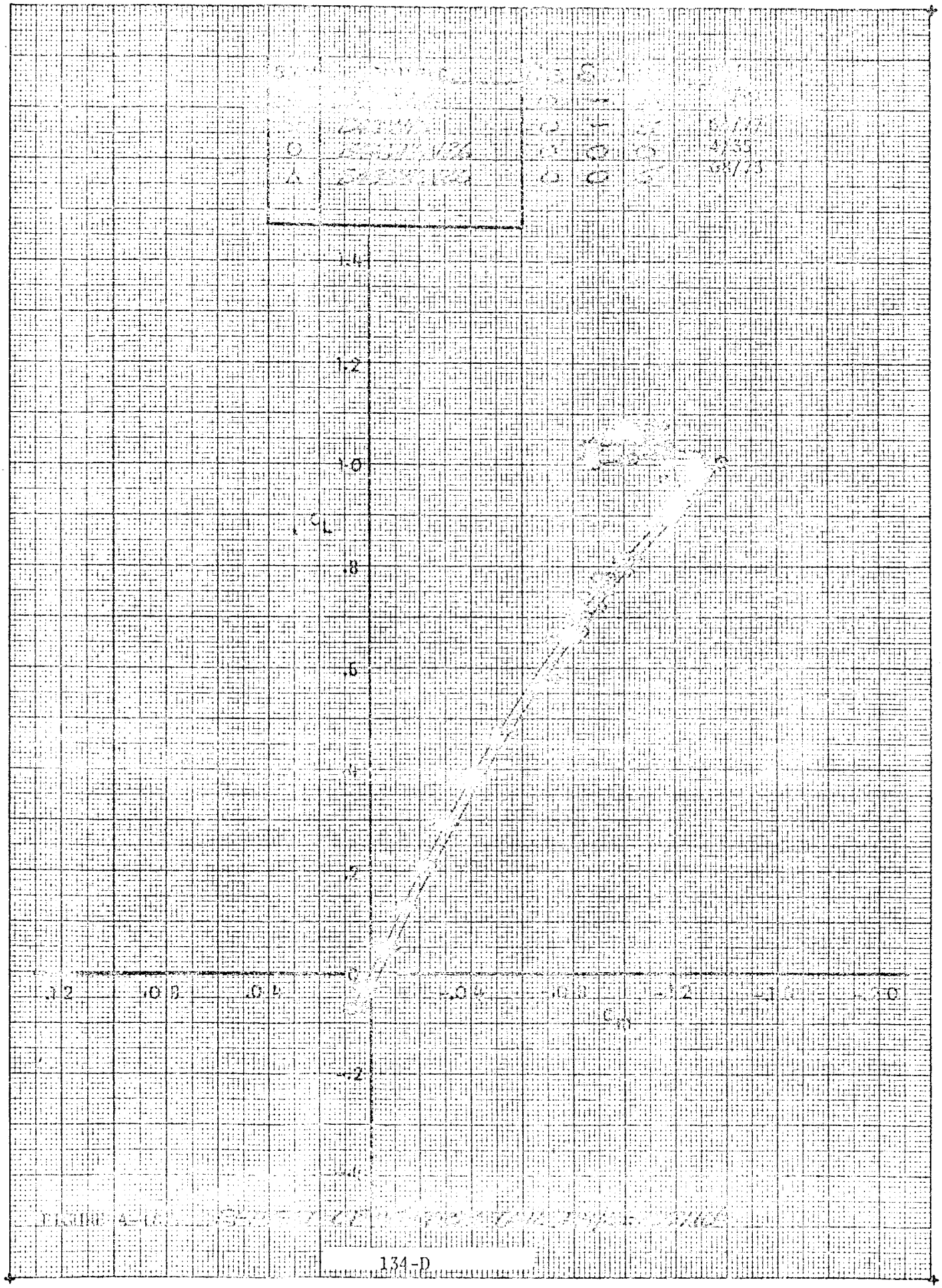
1.4
1.2
1.0
.8
.6
.4
.2
0
-.2
-.4
C_L
C_m
134-D

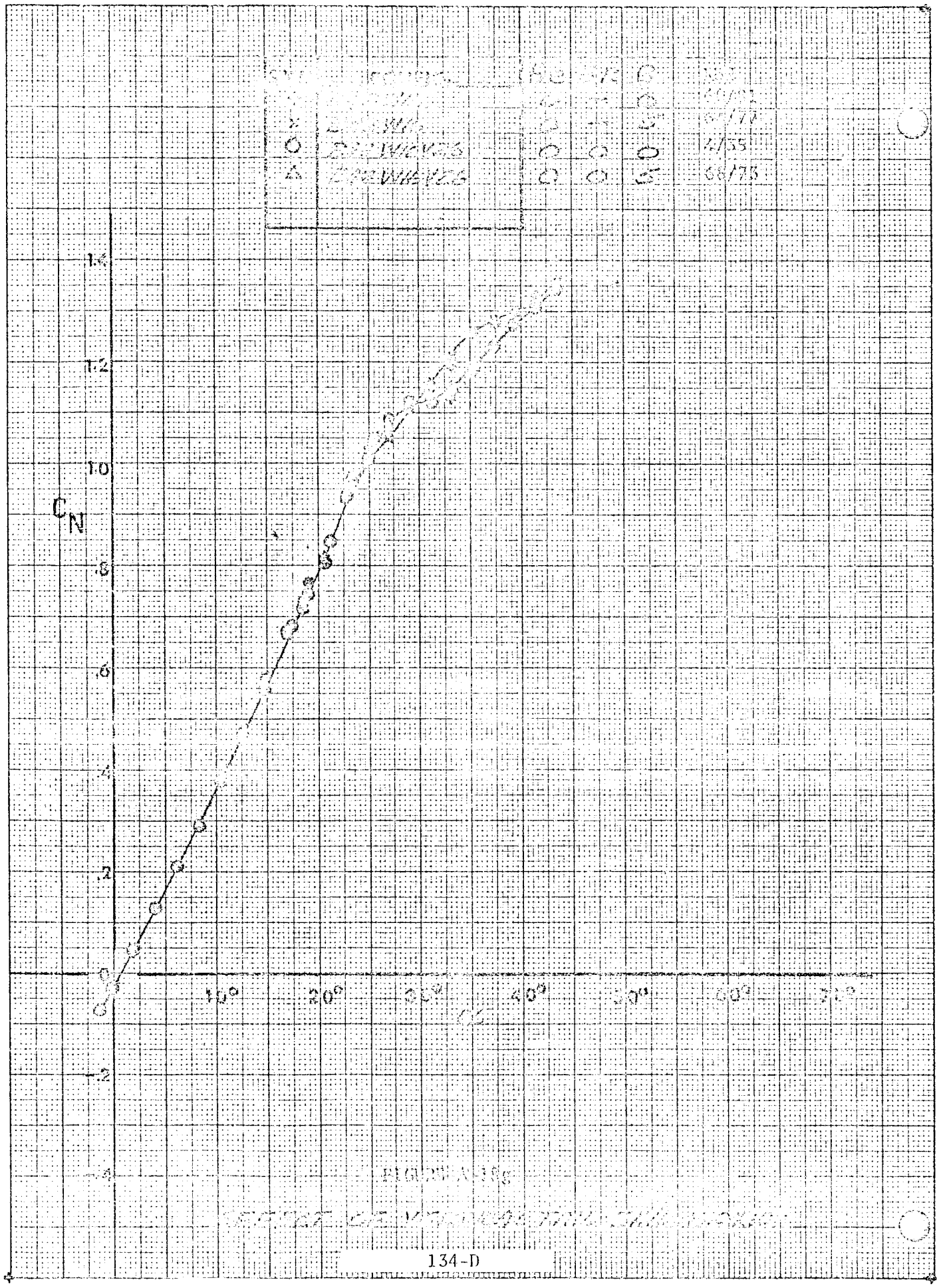

134-D

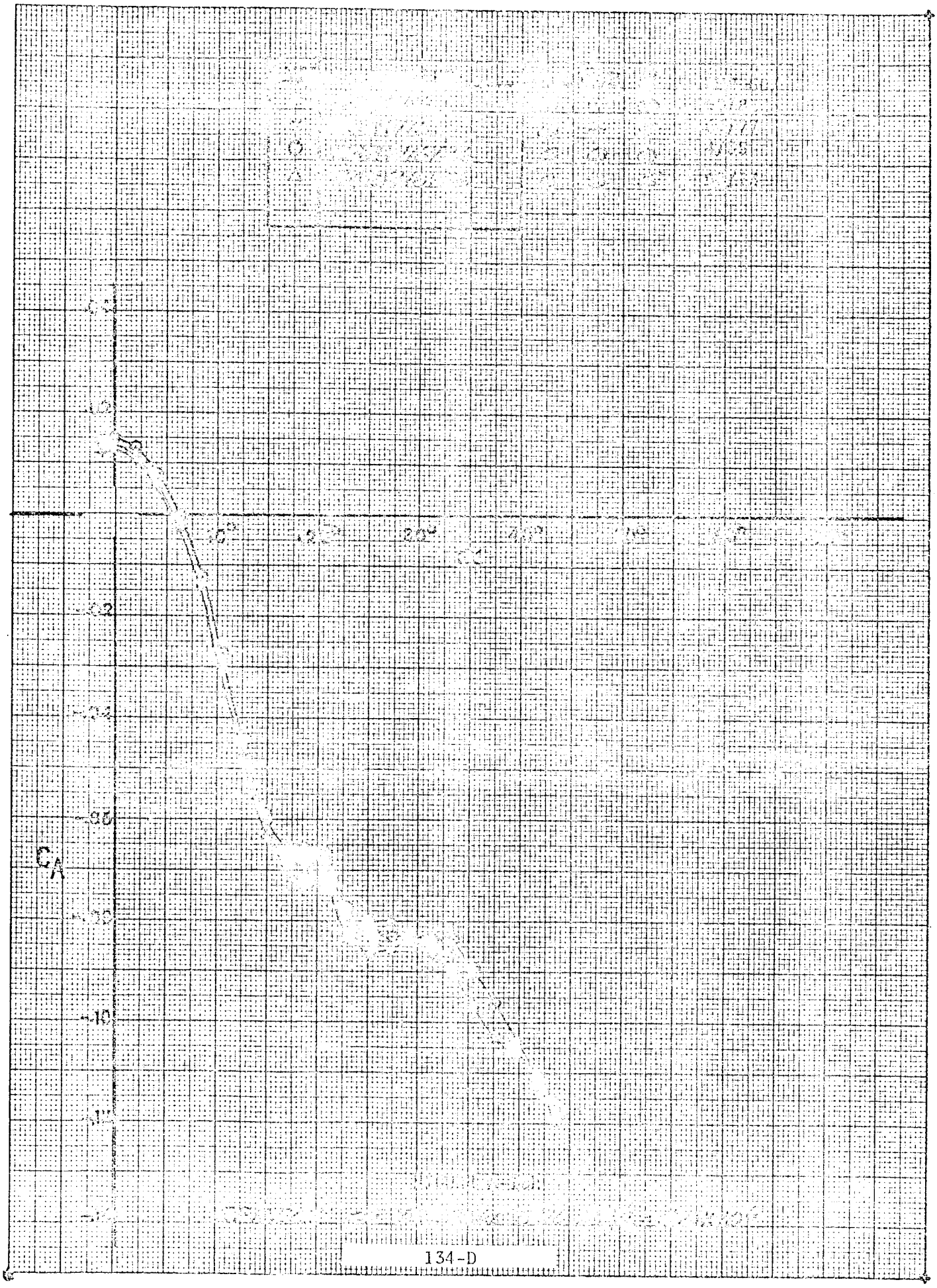

KEUFFEL & ESSER CO.

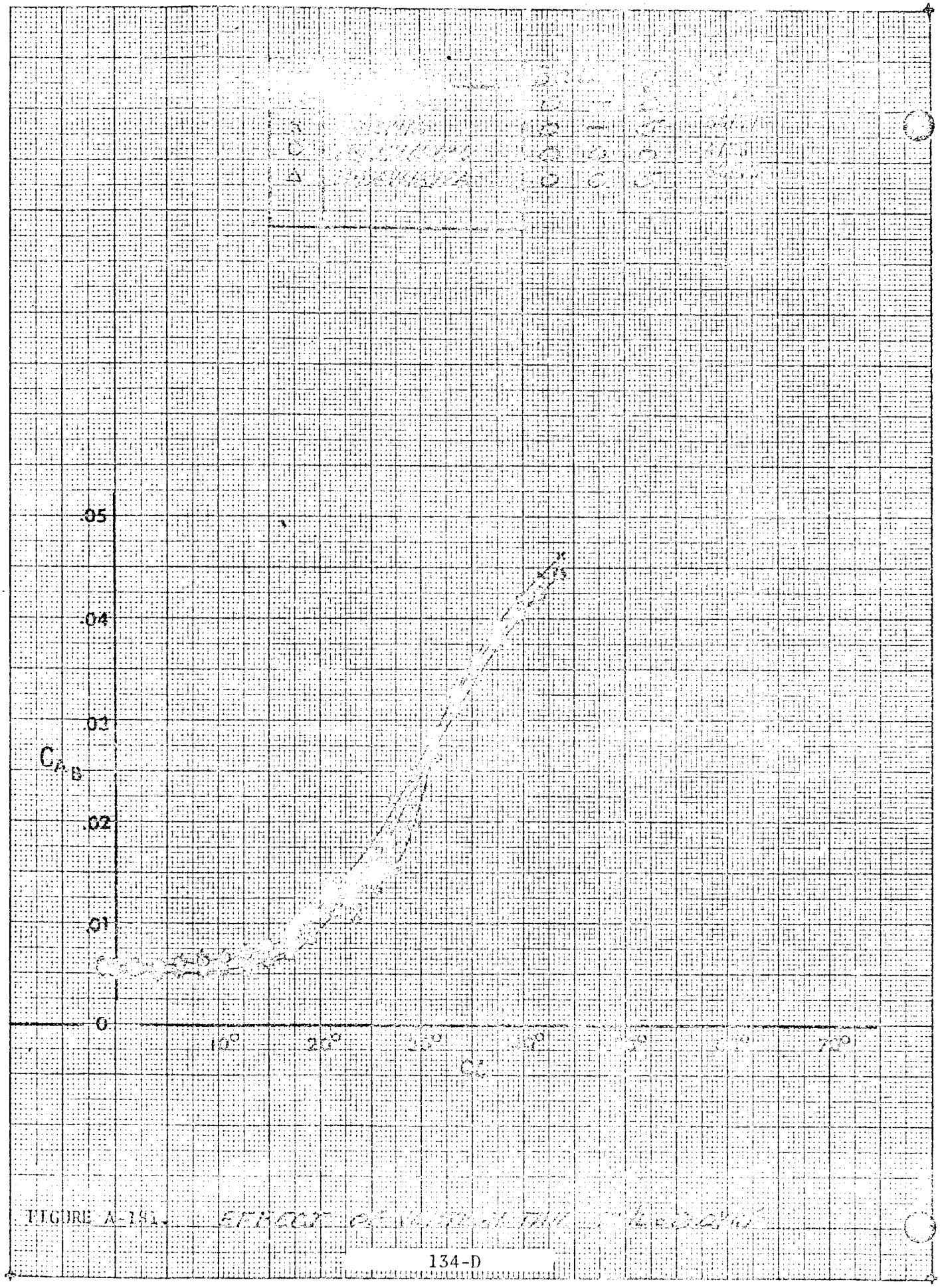

FIGURE A-131. EFFECT OF [illegible]

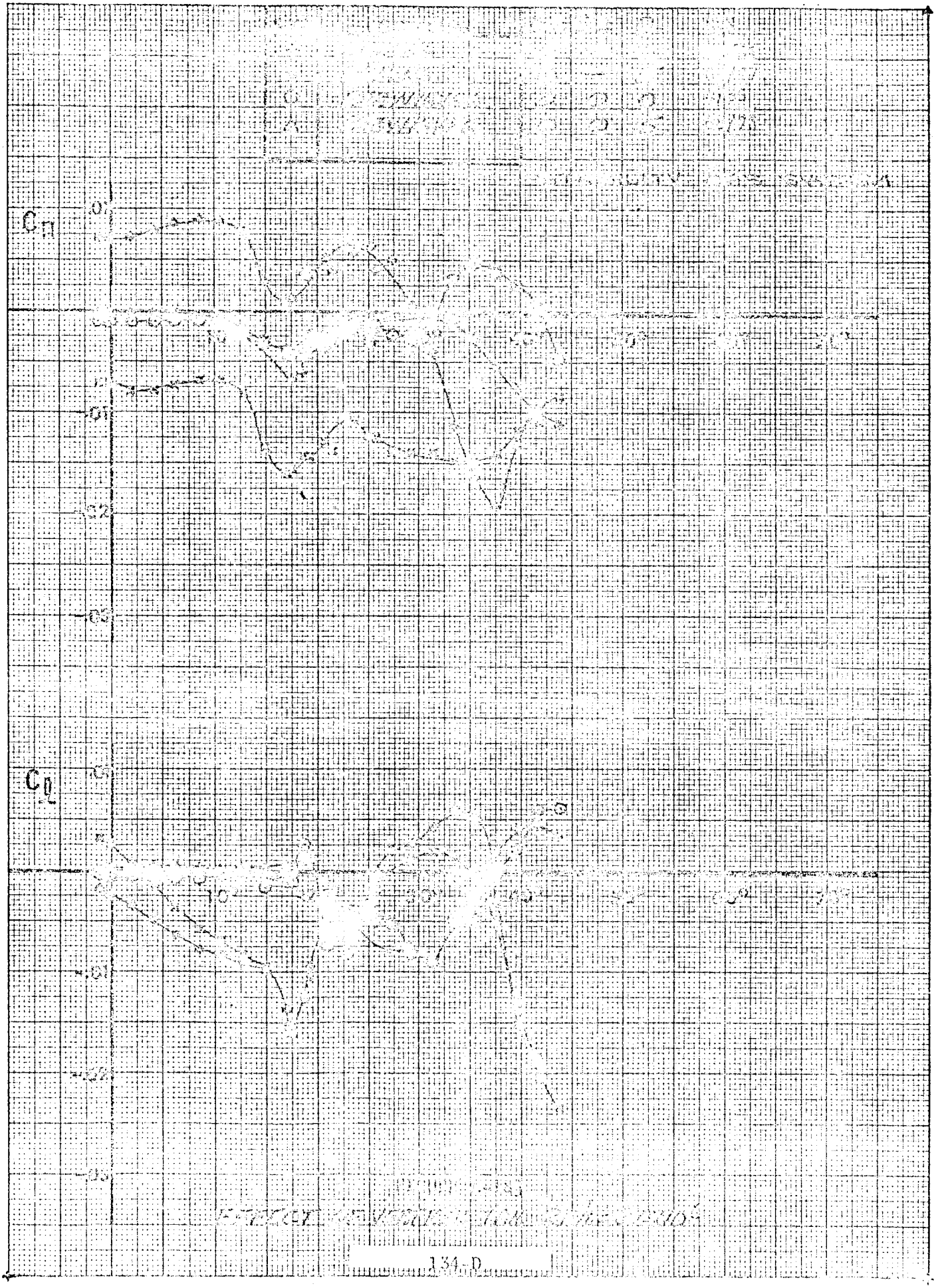

KEUFFEL & ESSER CO.

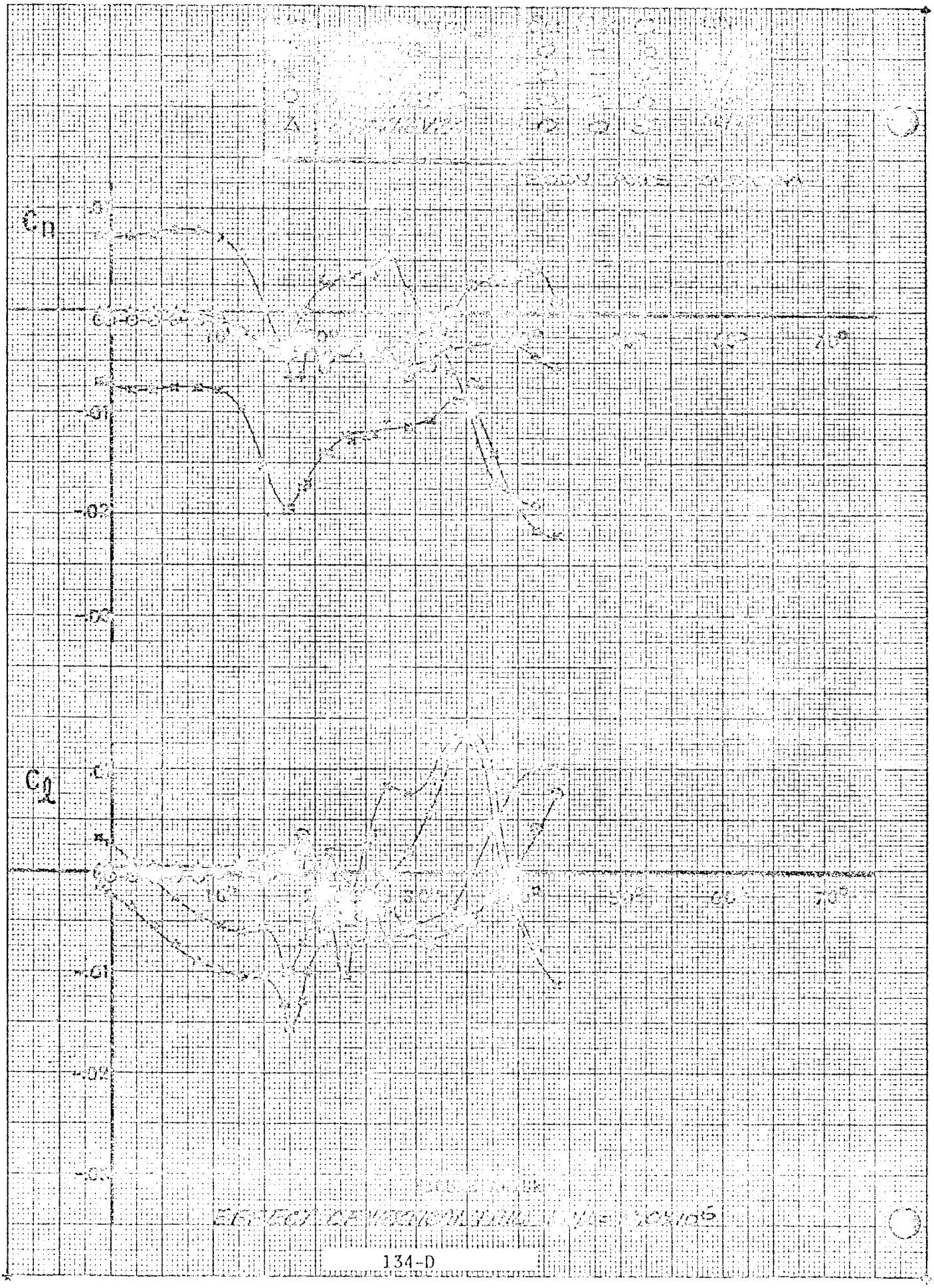

K&E 10 X 10 TO THE CENTIMETER 46 1517
18 X 25 CM. • ALBANENE
KEUFFEL & ESSER CO.

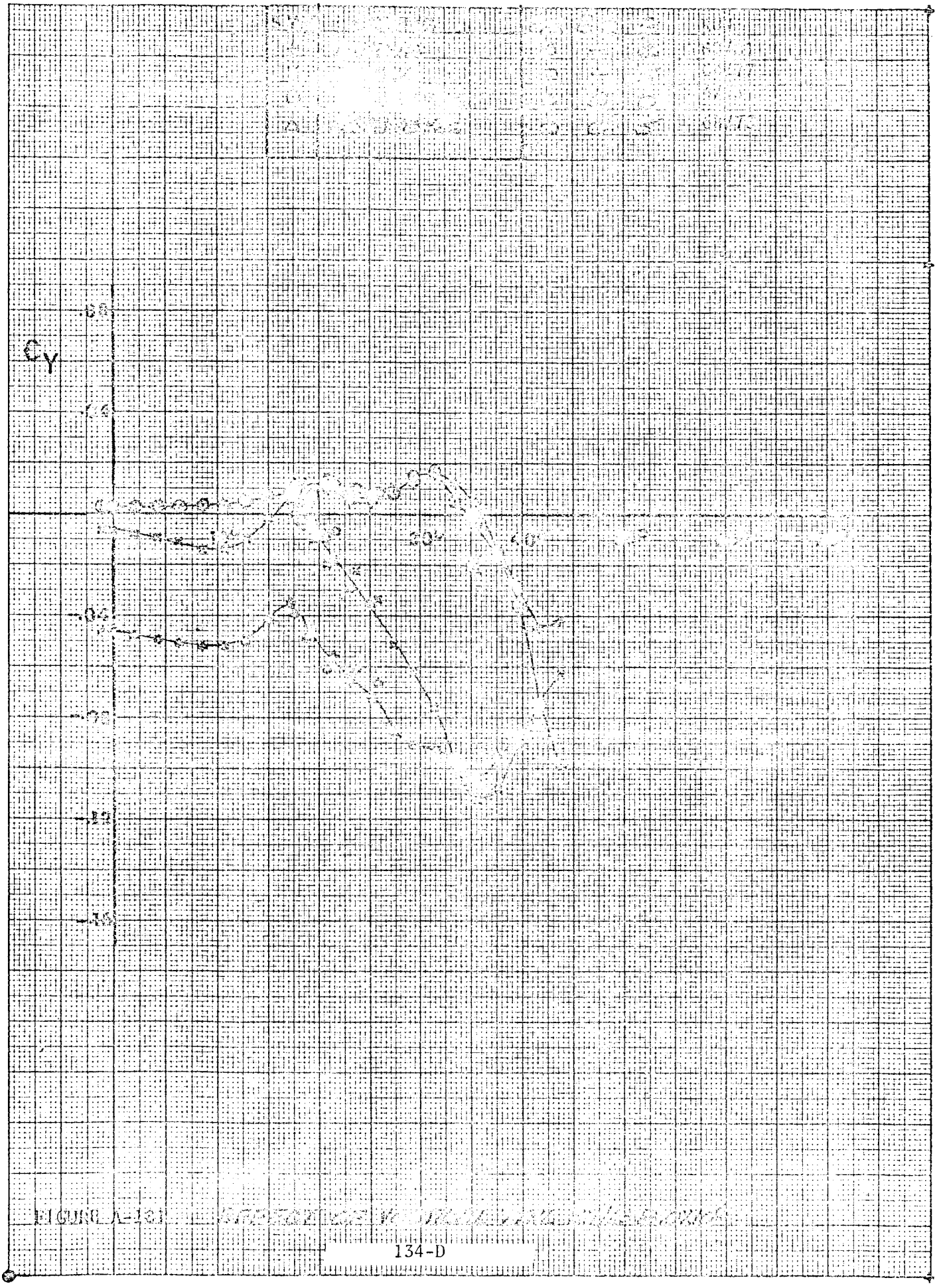
Cy
.06
.04
.02
-.02
-.04
-.06
-.08
-.10
-.12
-.14
-.16
-.18
-.20
-.22
-.24
-.26
-.28
-.30
-.32
-.34
-.36
-.38
-.40
-.42
-.44
-.46
-.48
-.50
-.52
-.54
-.56
-.58
-.60
-.62
-.64
-.66
-.68
-.70
-.72
-.74
-.76
-.78
-.80
-.82
-.84
-.86
-.88
-.90
-.92
-.94
-.96
-.98
-1.00
-1.02
-1.04
-1.06
-1.08
-1.10
-1.12
-1.14
-1.16
-1.18
-1.20
-1.22
-1.24
-1.26
-1.28
-1.30
-1.32
-1.34
-1.36
-1.38
-1.40
-1.42
-1.44
-1.46
-1.48
-1.50
-1.52
-1.54
-1.56
-1.58
-1.60
-1.62
-1.64
-1.66
-1.68
-1.70
-1.72
-1.74
-1.76
-1.78

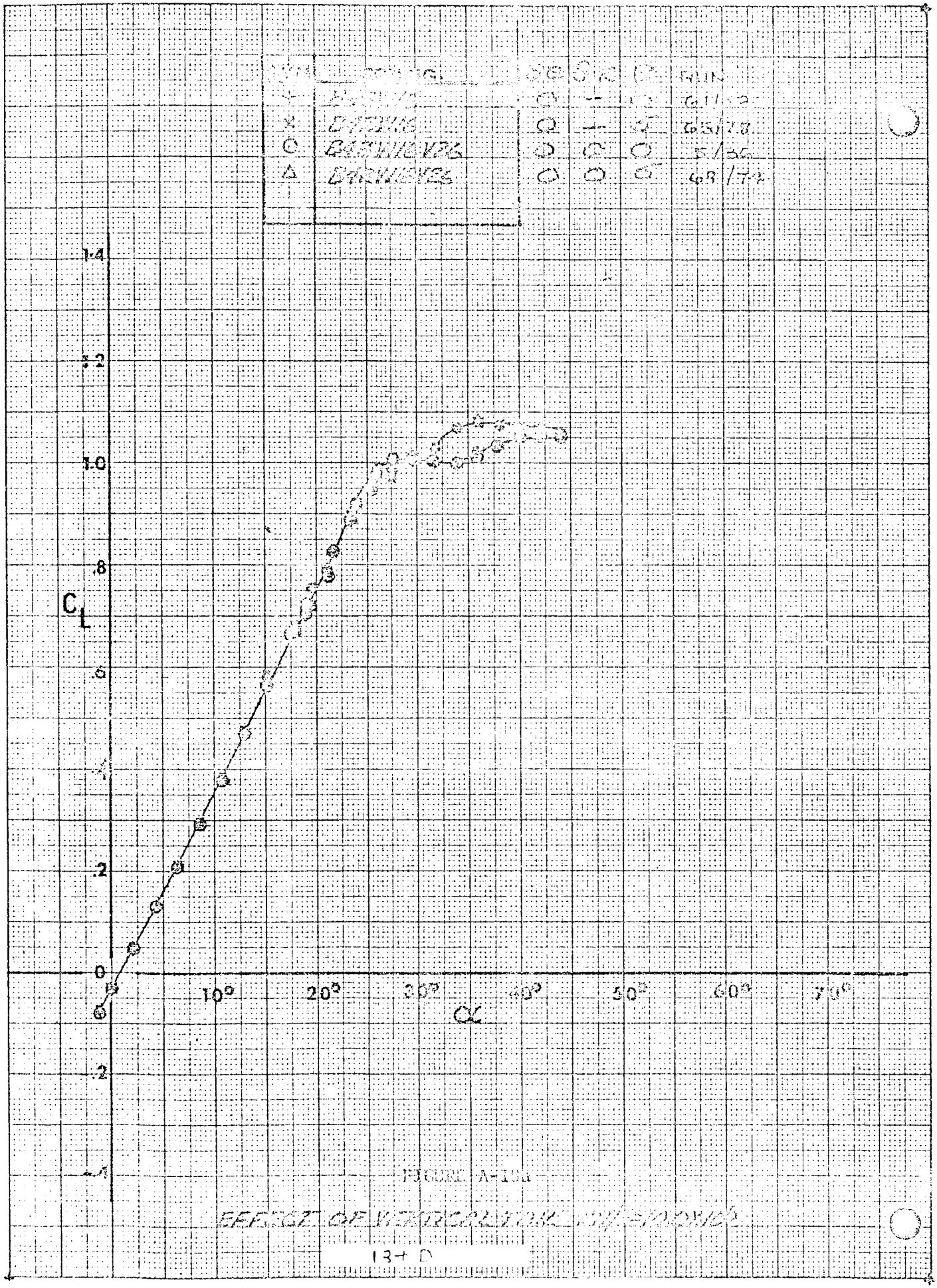

FIGURE A-10a

EFFECT OF HORIZONTAL [illegible]

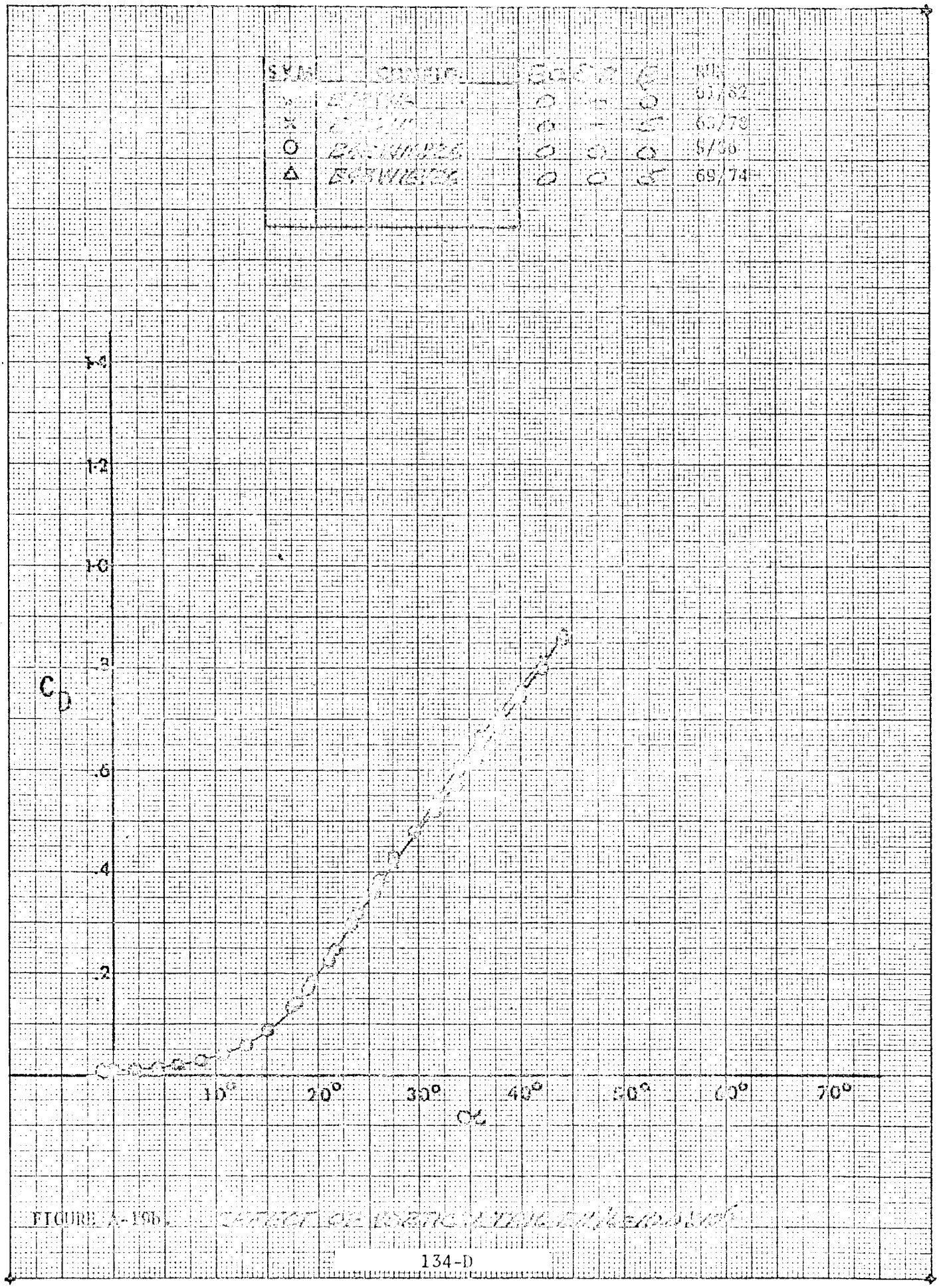

FIGURE A-156. [illegible]

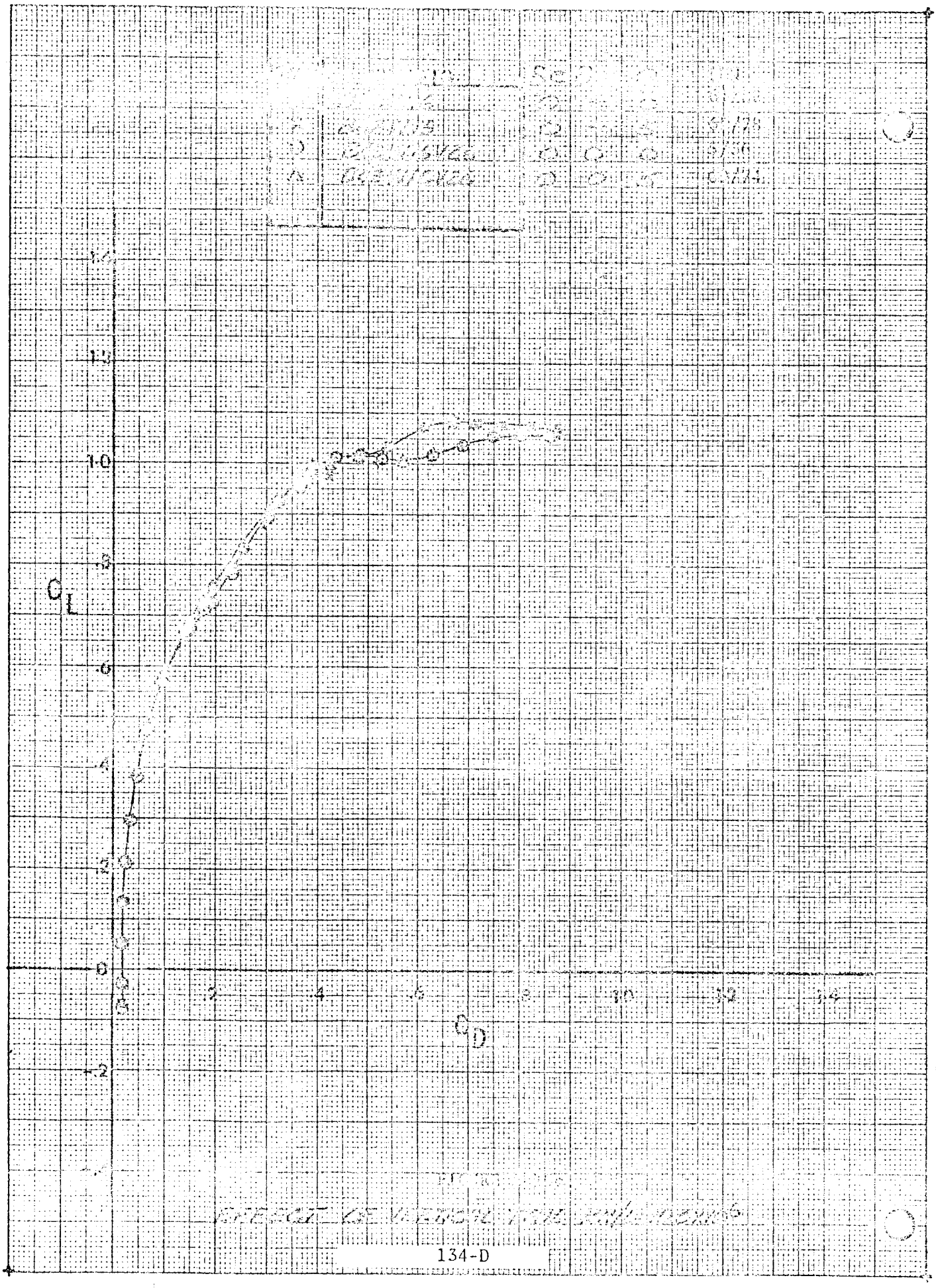

134-D

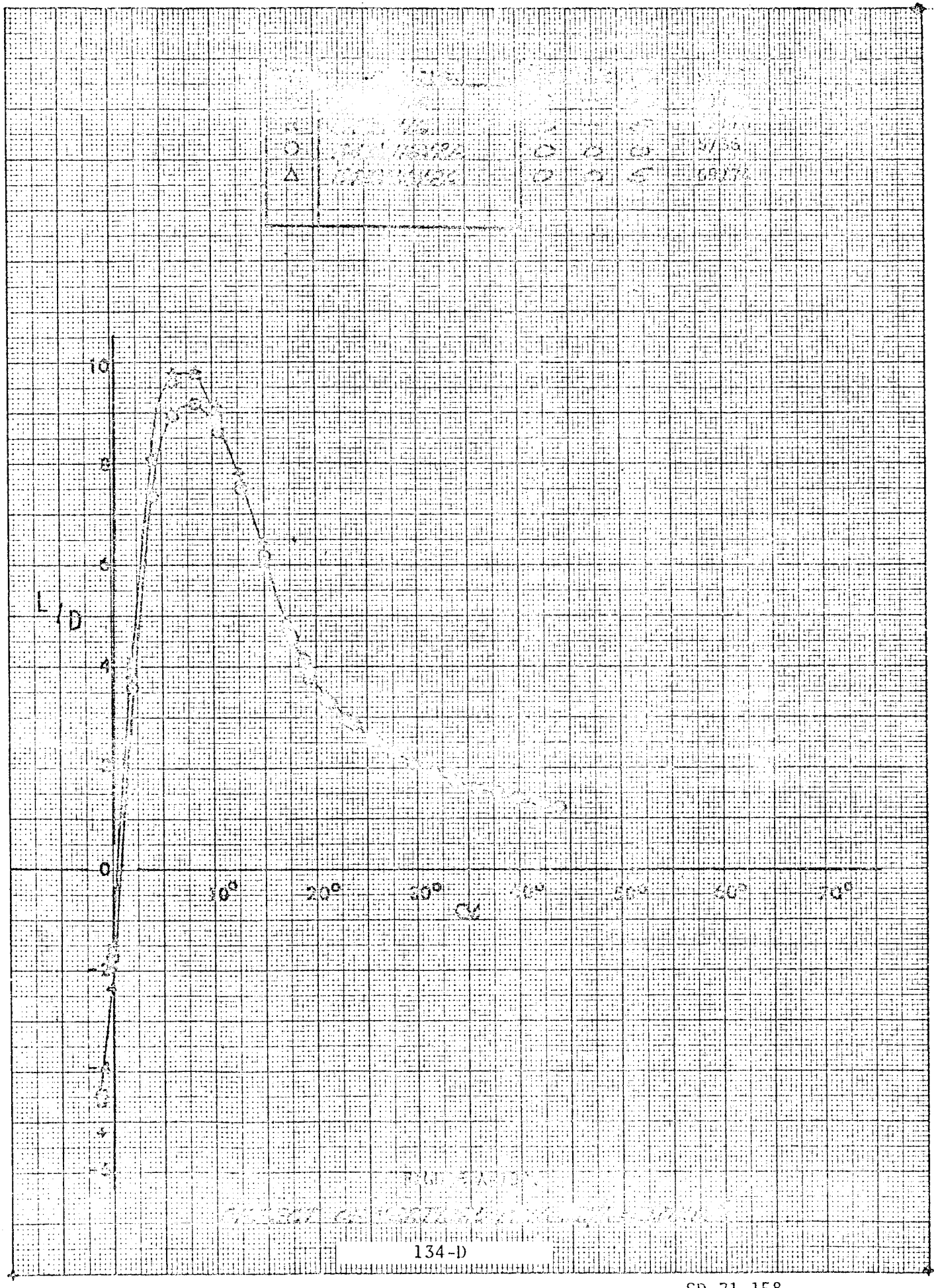

134-D

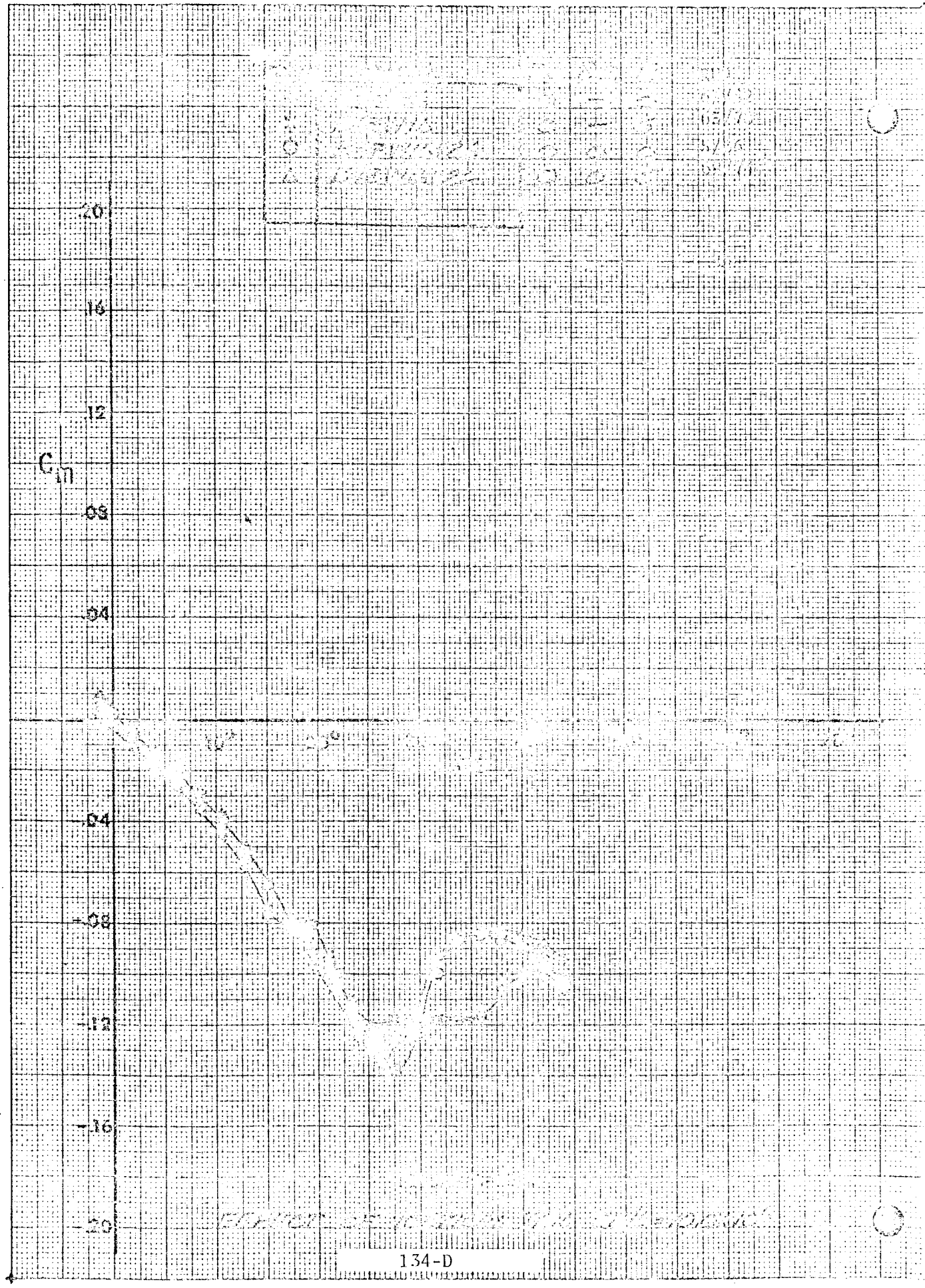

134-D

46 1517
10 X 10 TO THE CENTIMETER
10 X 25 CM. • ALBANENE
KEUFFEL & ESSER CO.

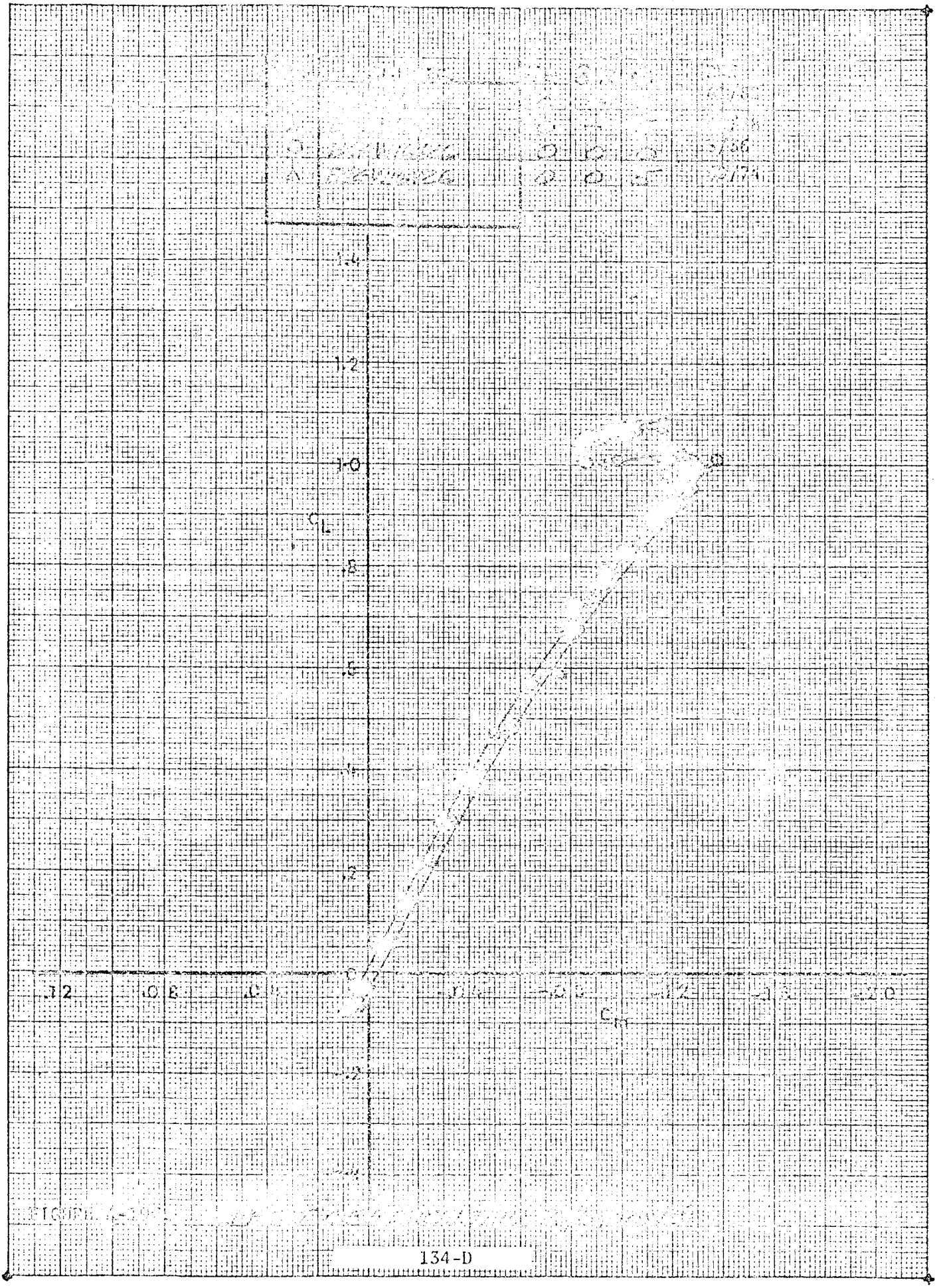

134-D

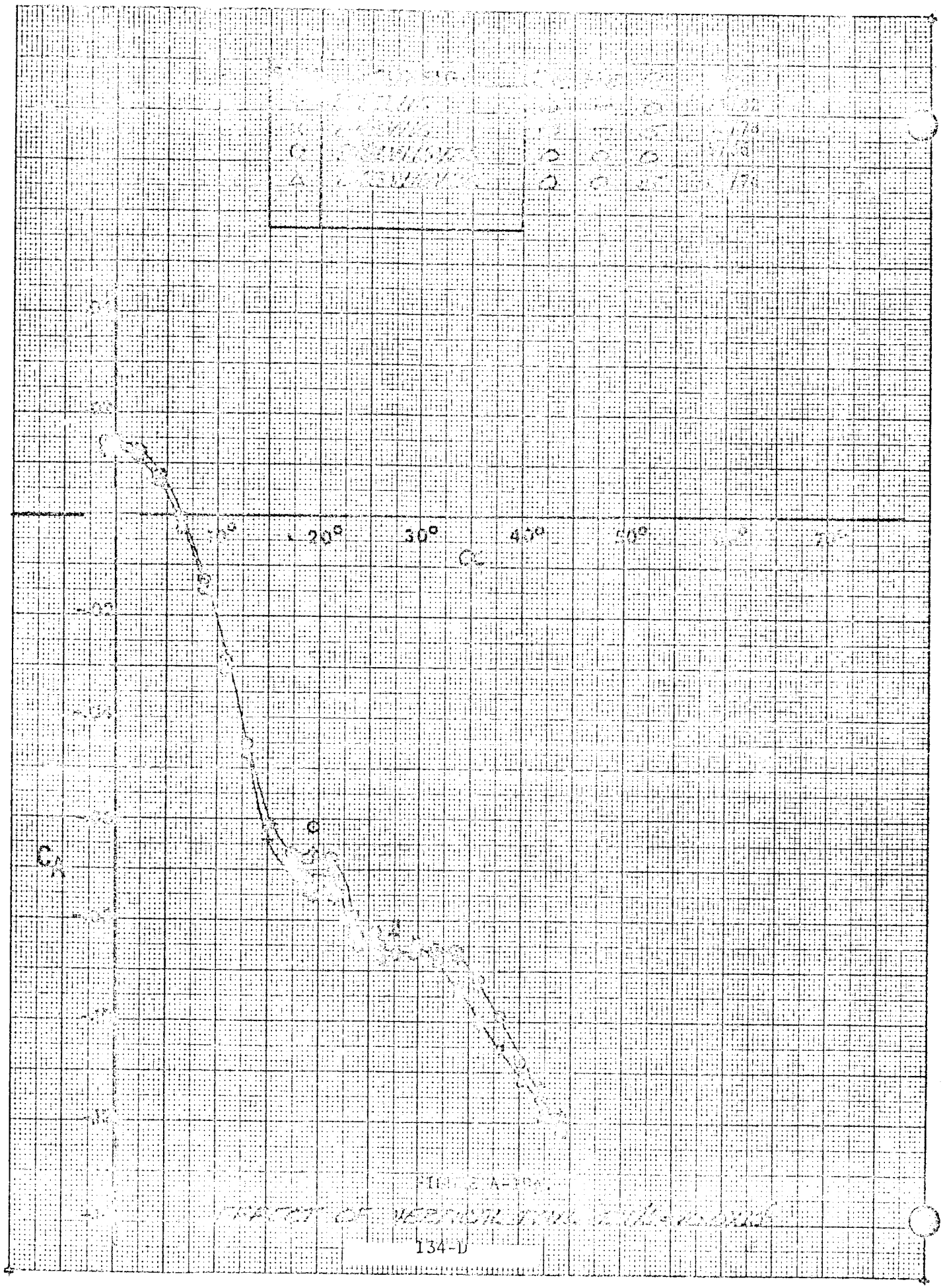

134-D

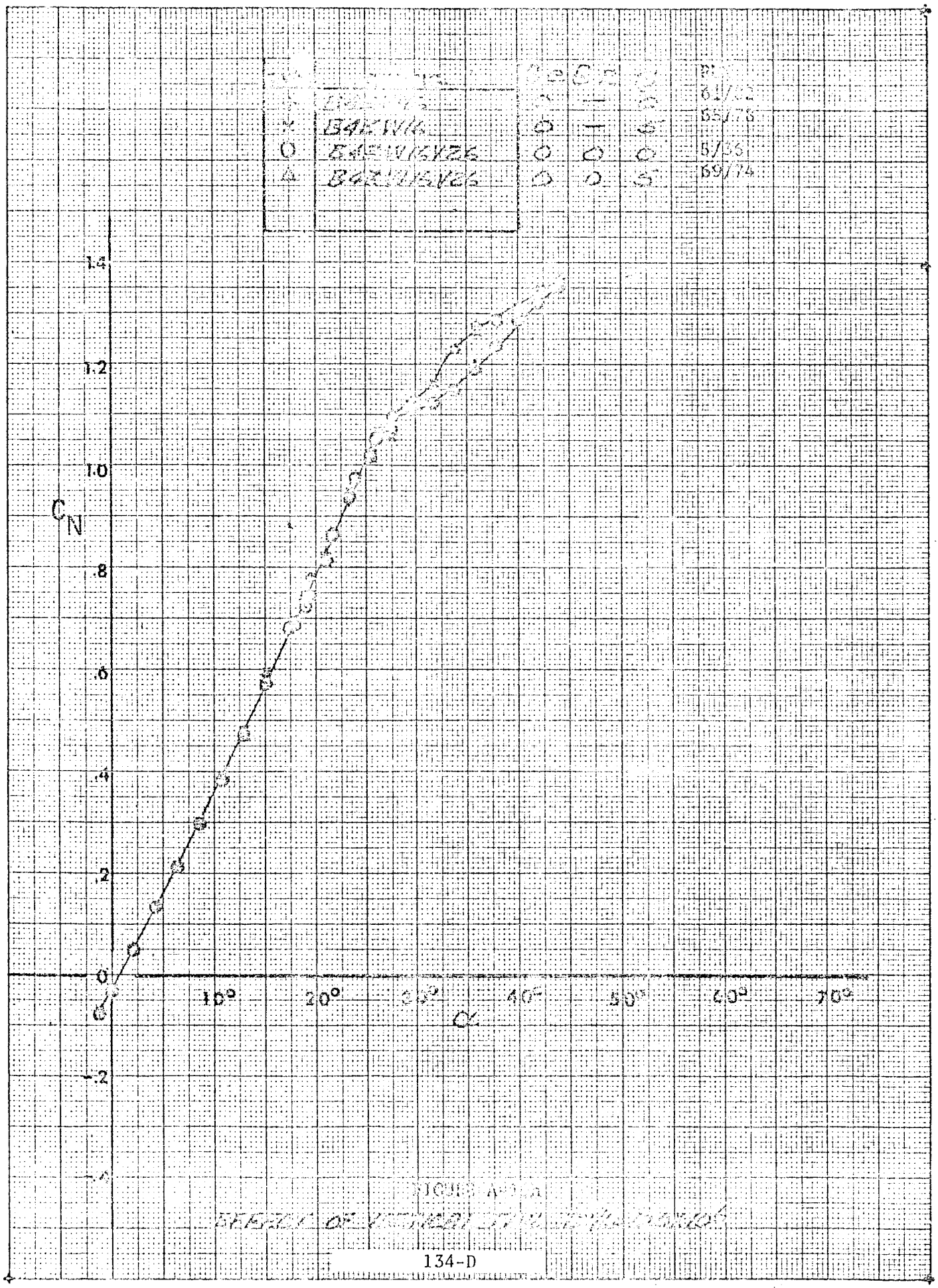
BARWIN
BARWINKES
BARWINKES
1.4
1.2
1.0
C_N
.8
.6
.4
.2
0
-.2
10°
20°
40°
50°
60°
70°
α

134-D

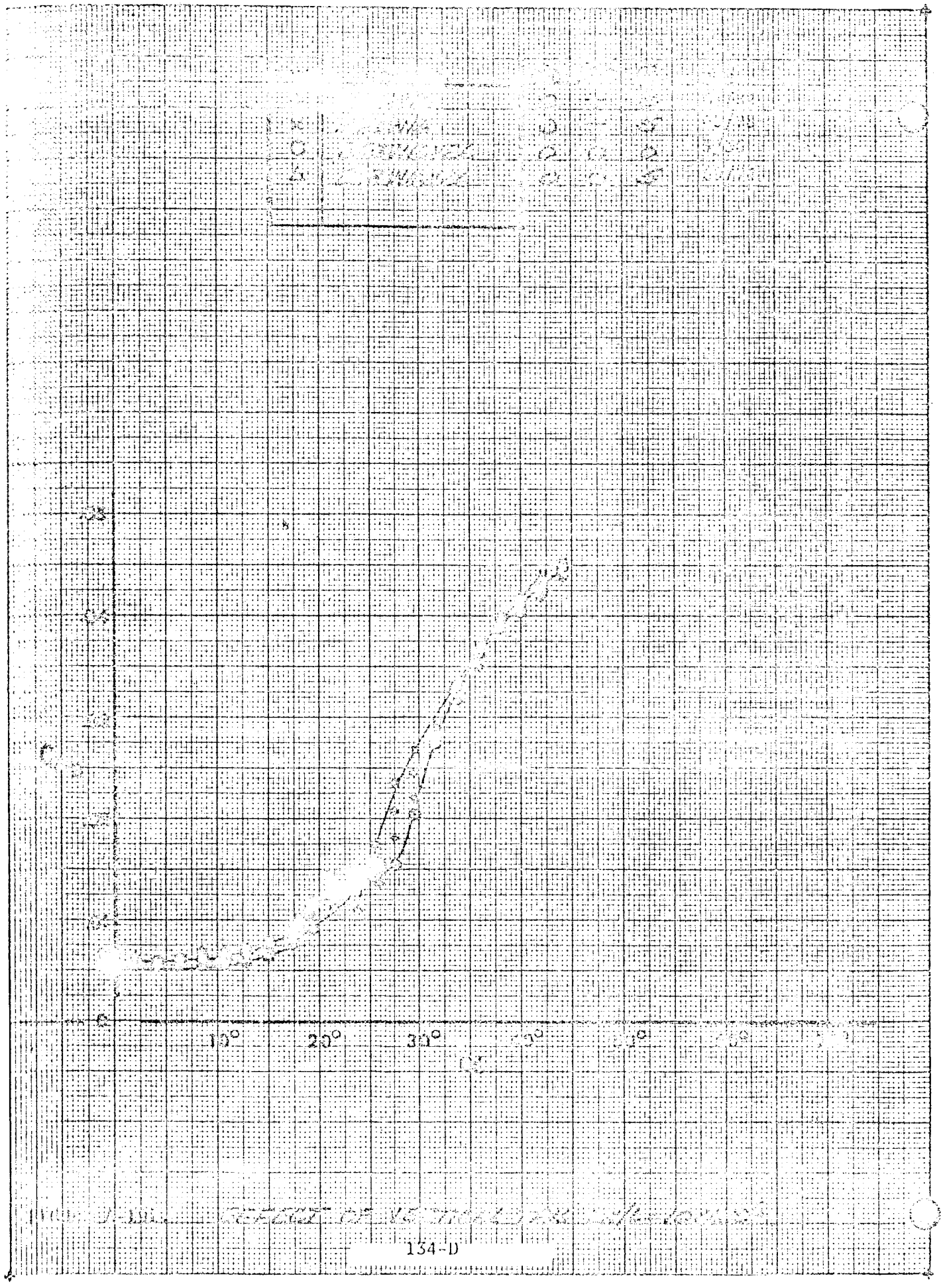

134-D

10 X 10 TO THE CENTIMETER 46 1517
18 X 25 CM. • ALBANENE
KEUFFEL & ESSER CO.

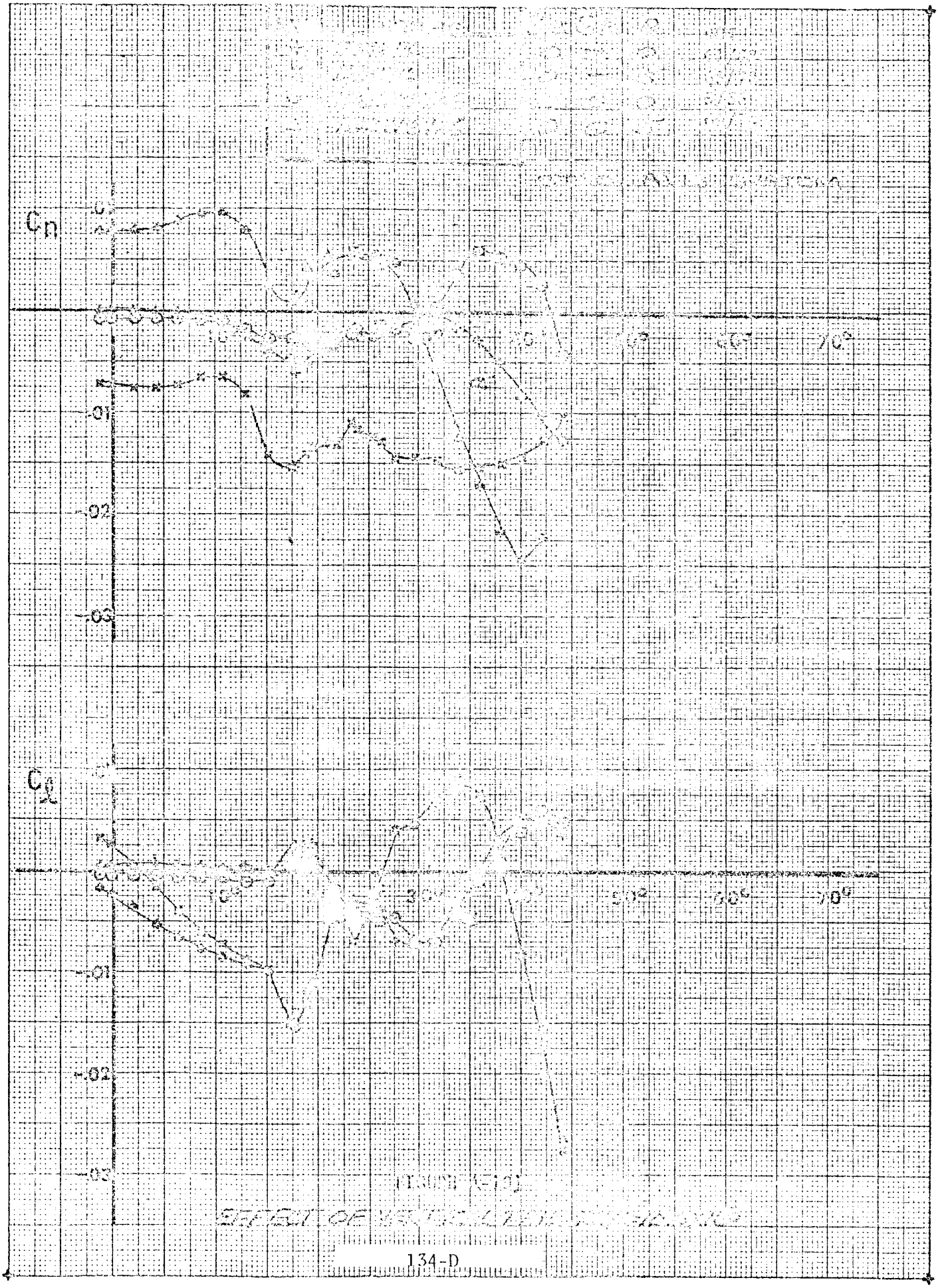

134-D

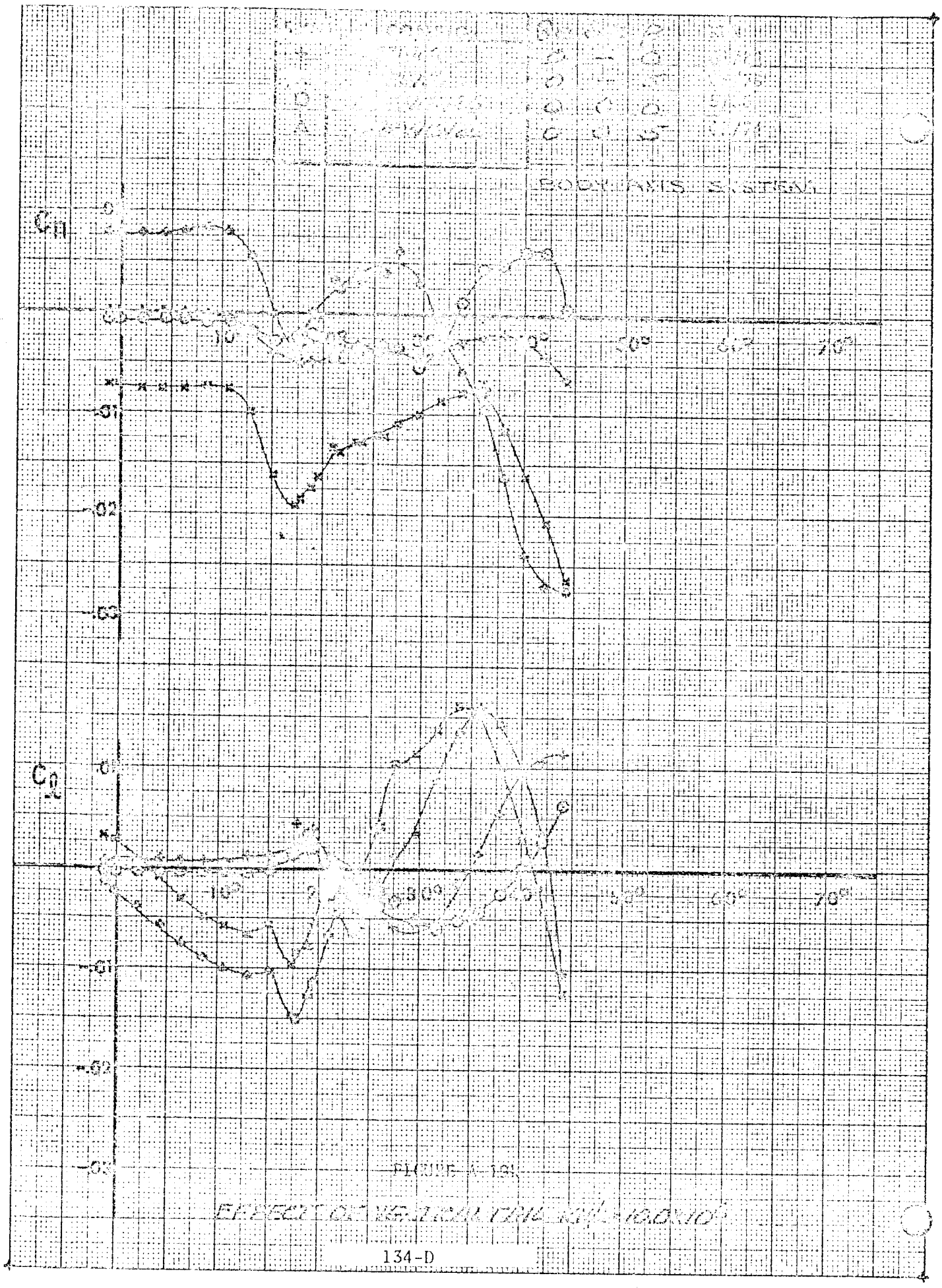

FIGURE A-181

EFFECT OF VERTICAL TAIL RADIUS

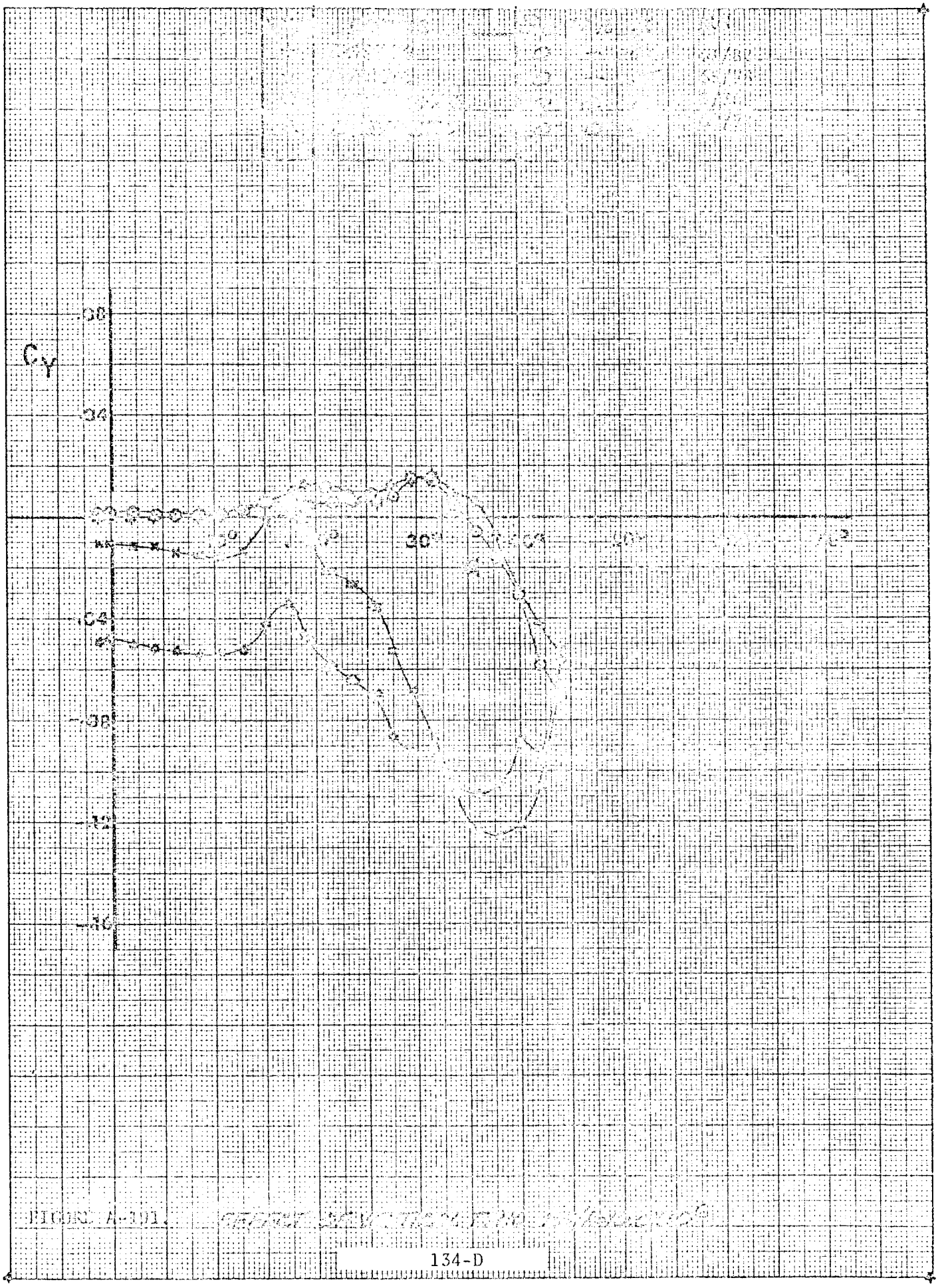

FIGURE A-101. [illegible]

134-D

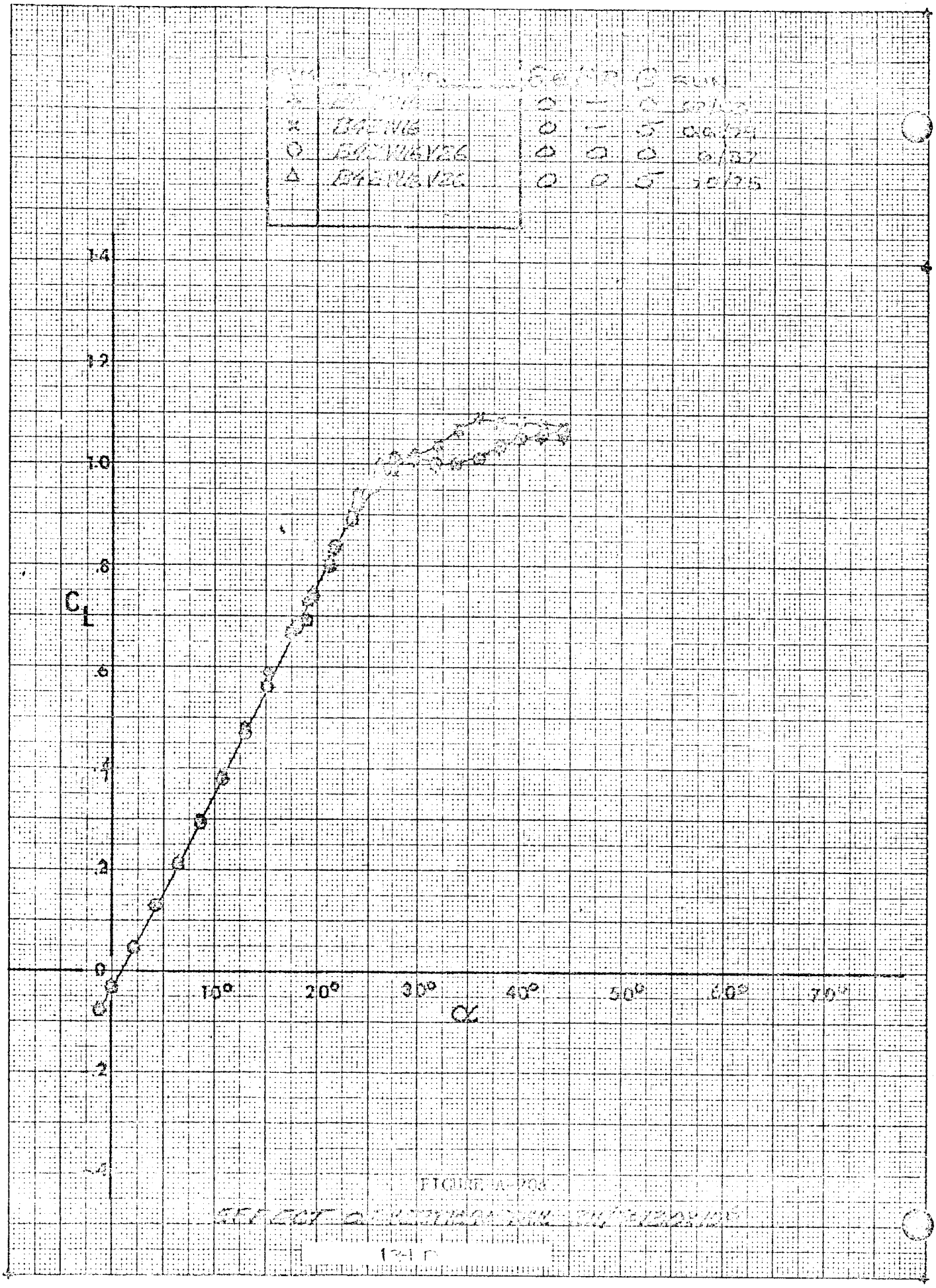

FIGURE A-208

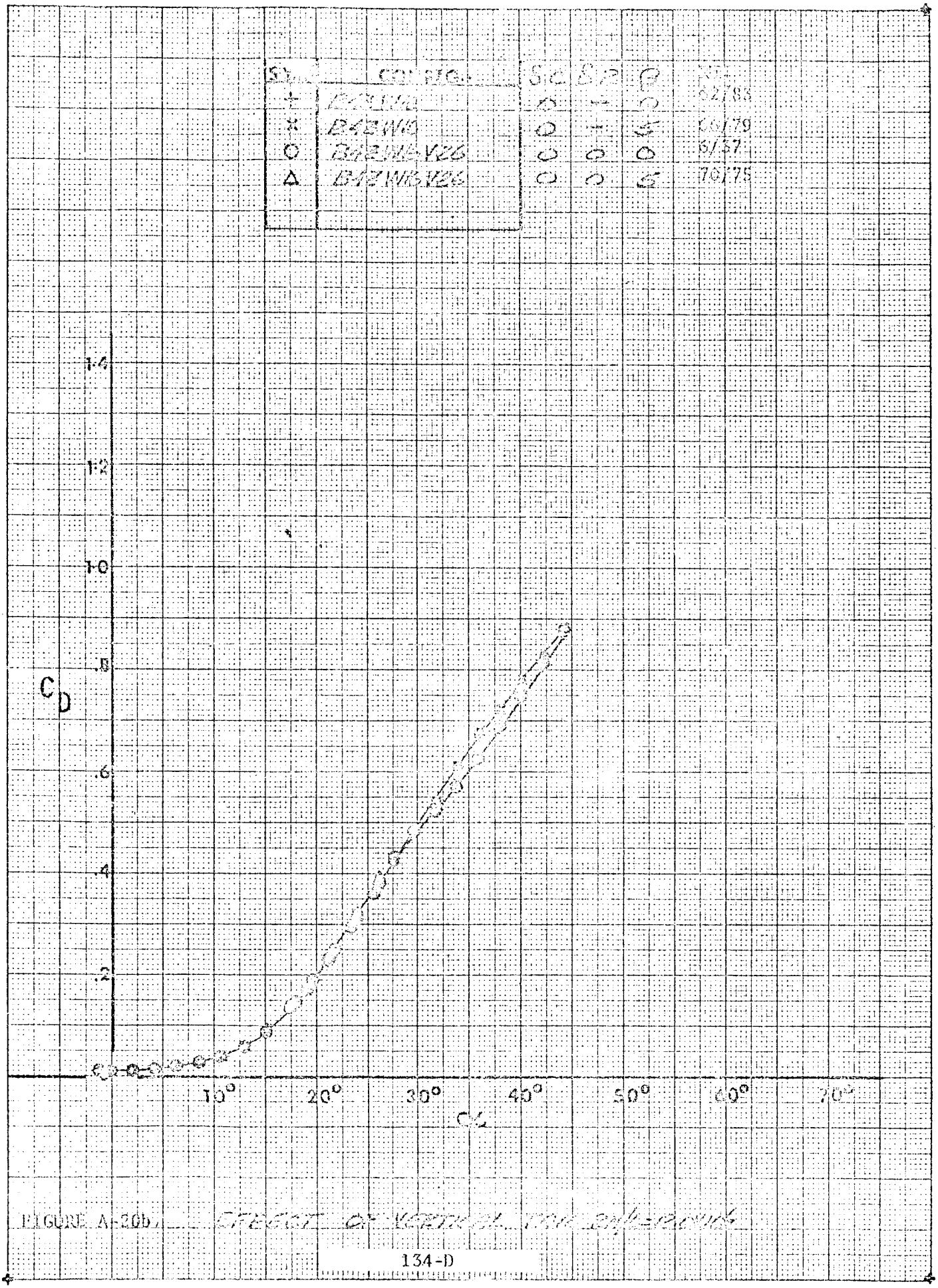

FIGURE A-20b. EFFECT OF VERTICAL TAIL POSITIONING

134-D

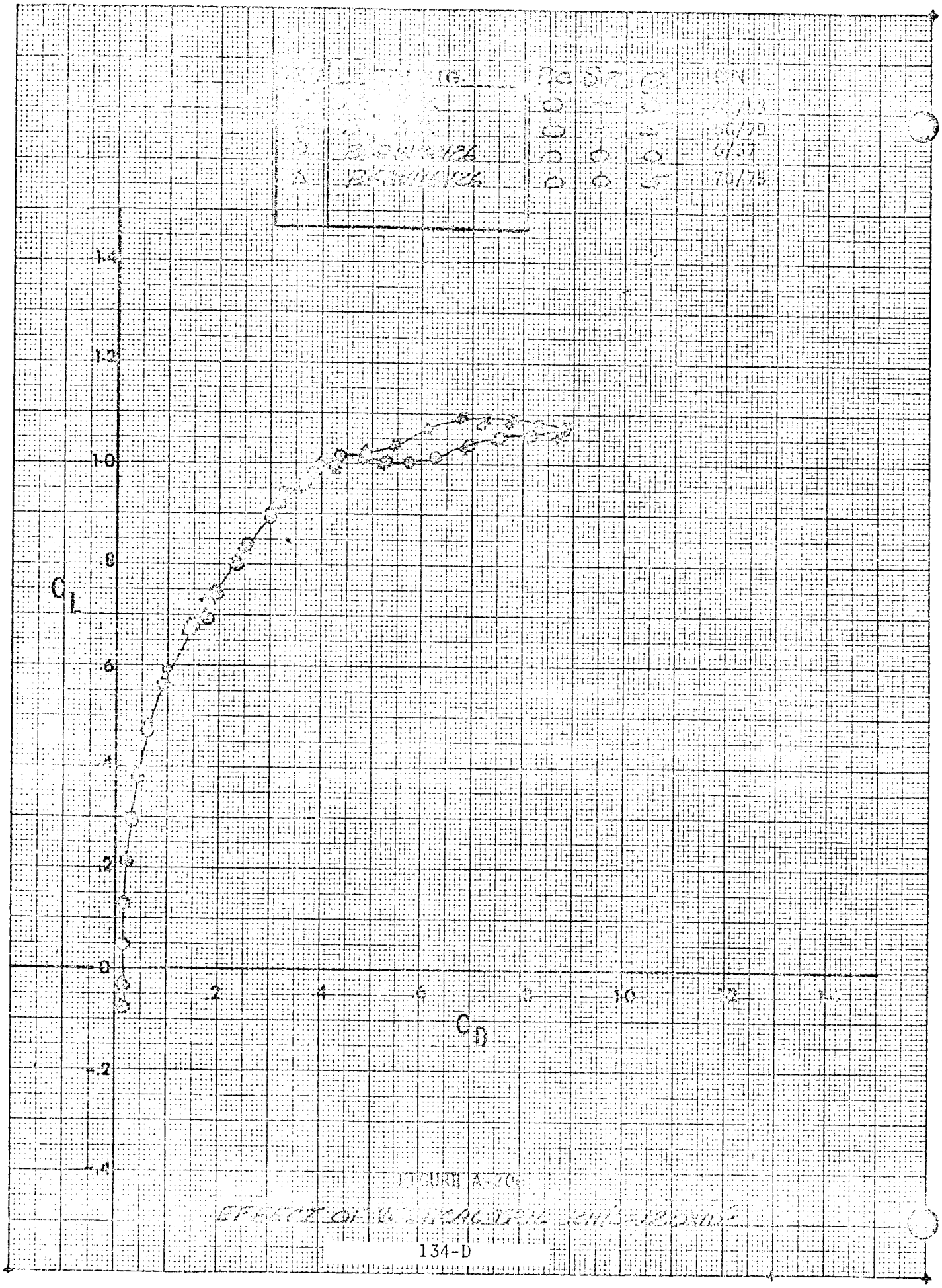

FIGURE A-20

EFFECT OF [illegible] ON [illegible]

134-D

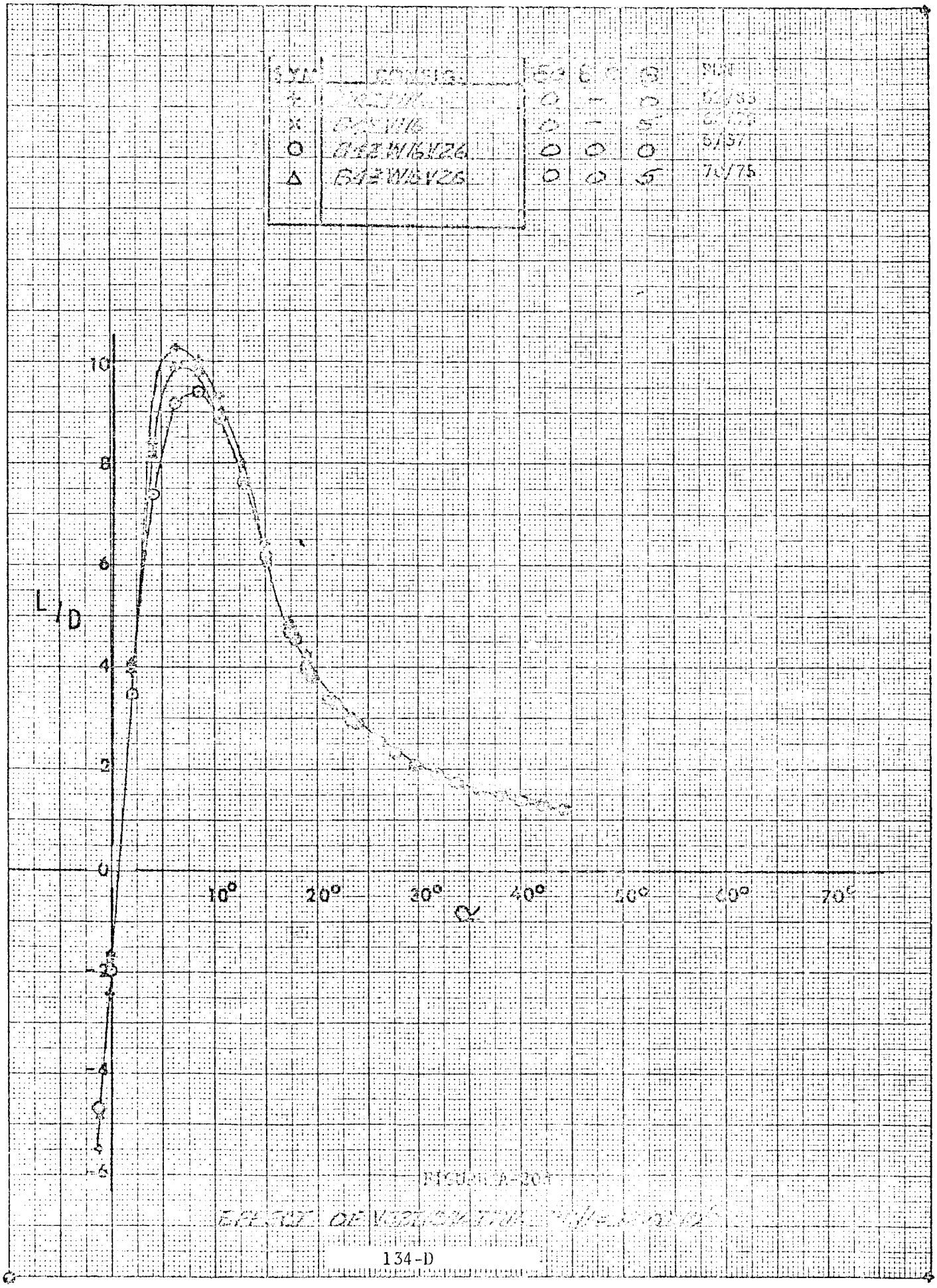

FIGURE A-20

EFFECT OF VISCOSITY [illegible]

134-D

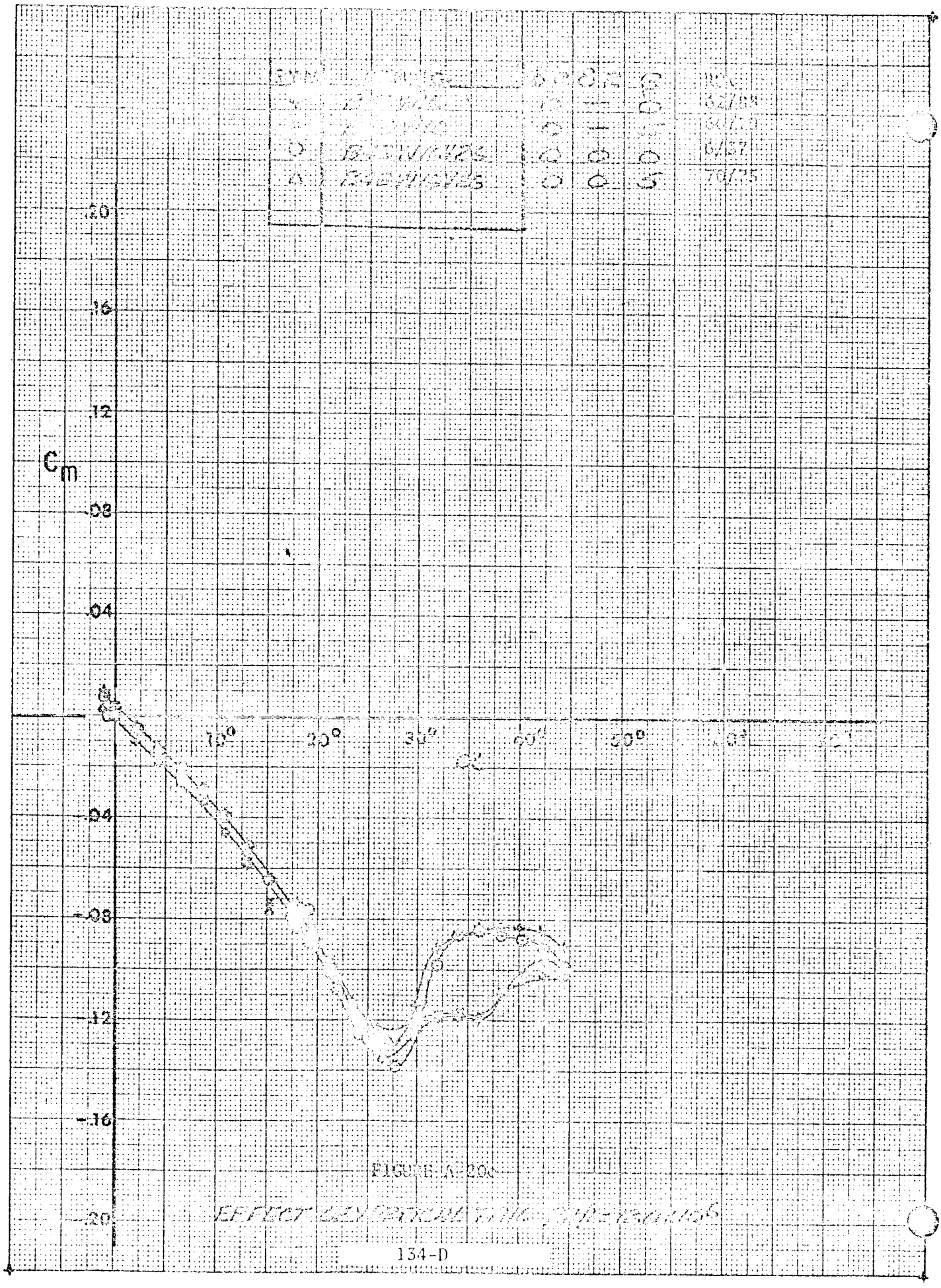

FIGURE A-20c

EFFECT OF PITCH ON [illegible]

134-D

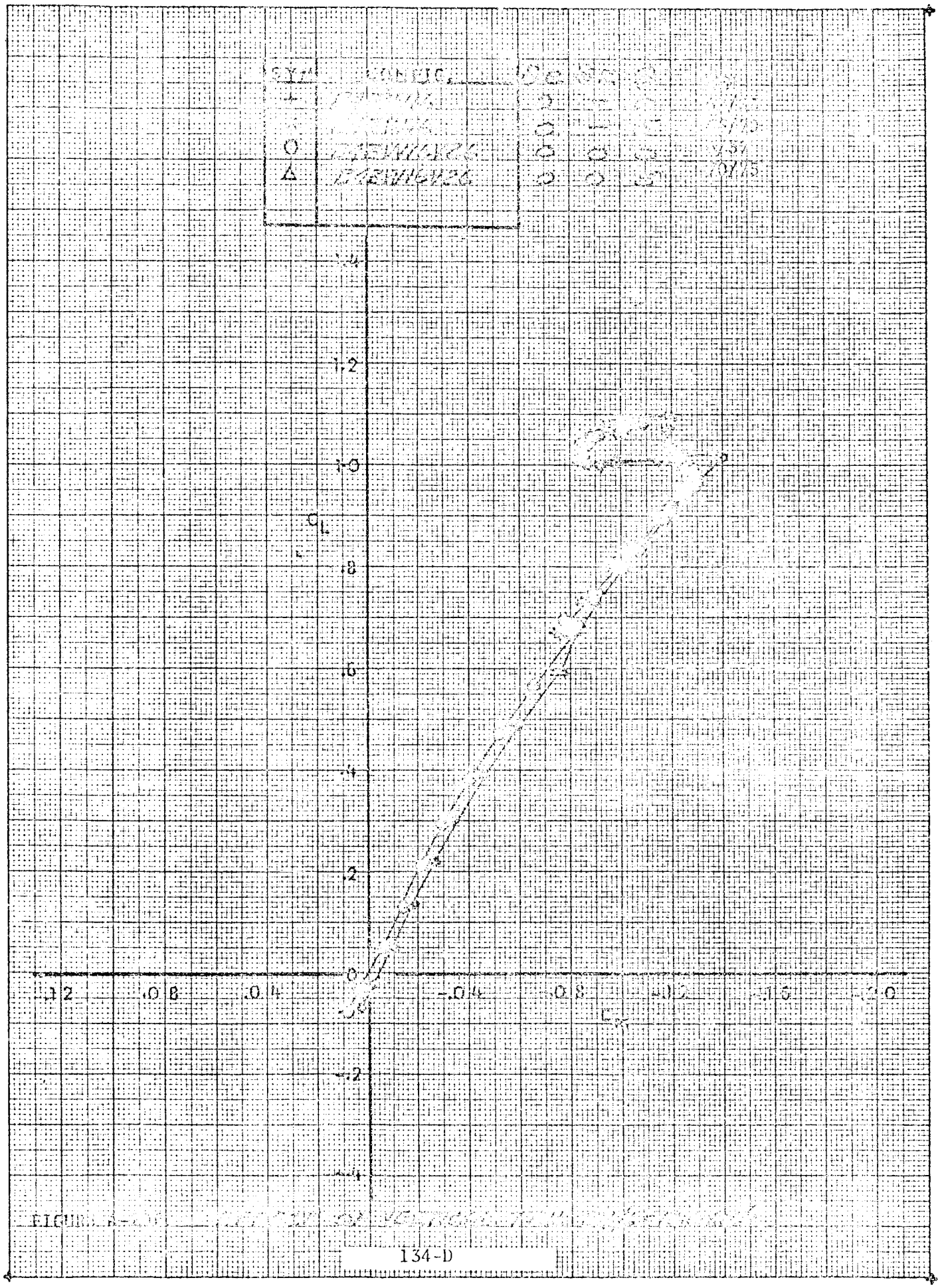

FIGURE [illegible]

134-D

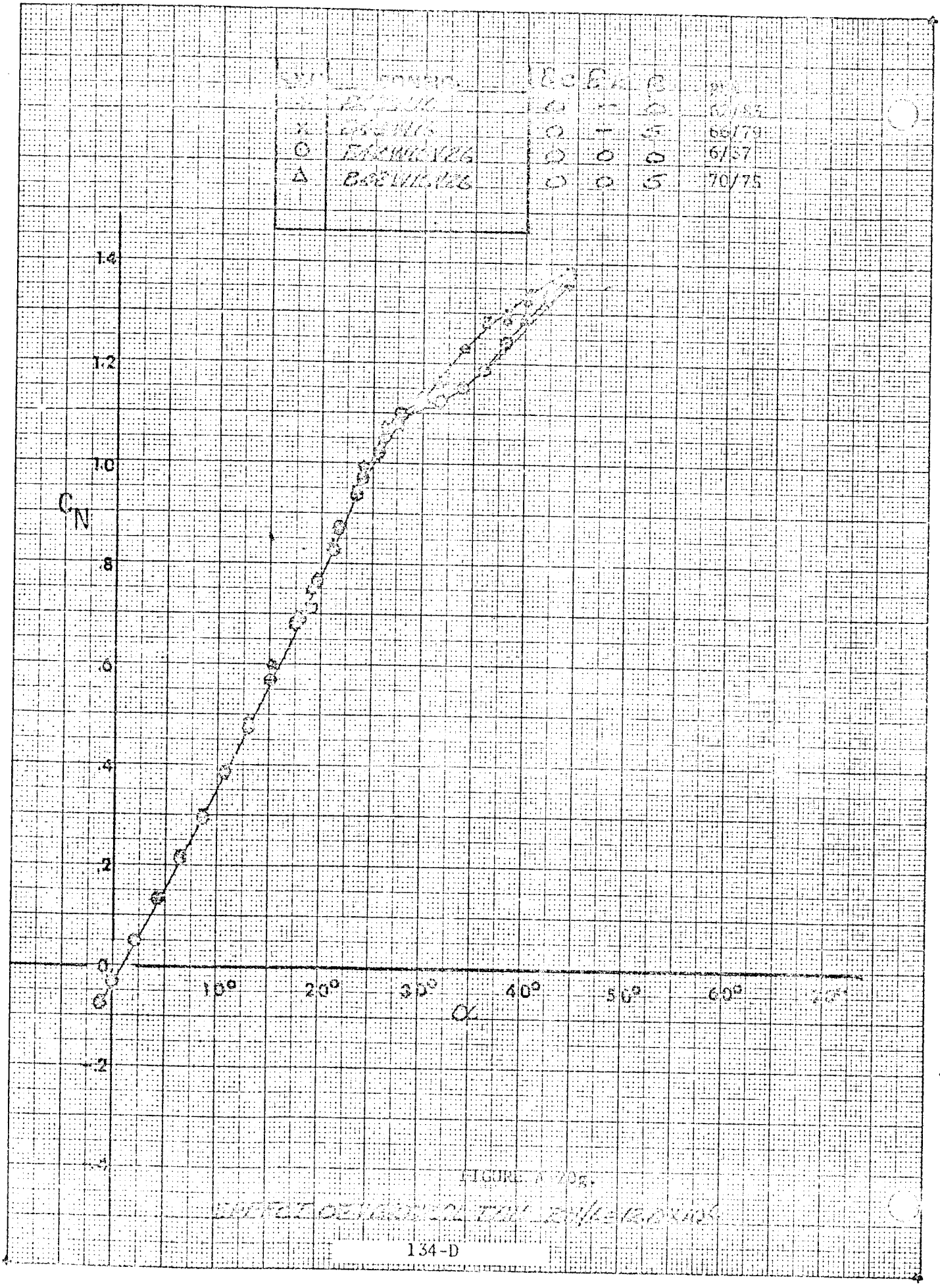

FIGURE A-20e.

[illegible]

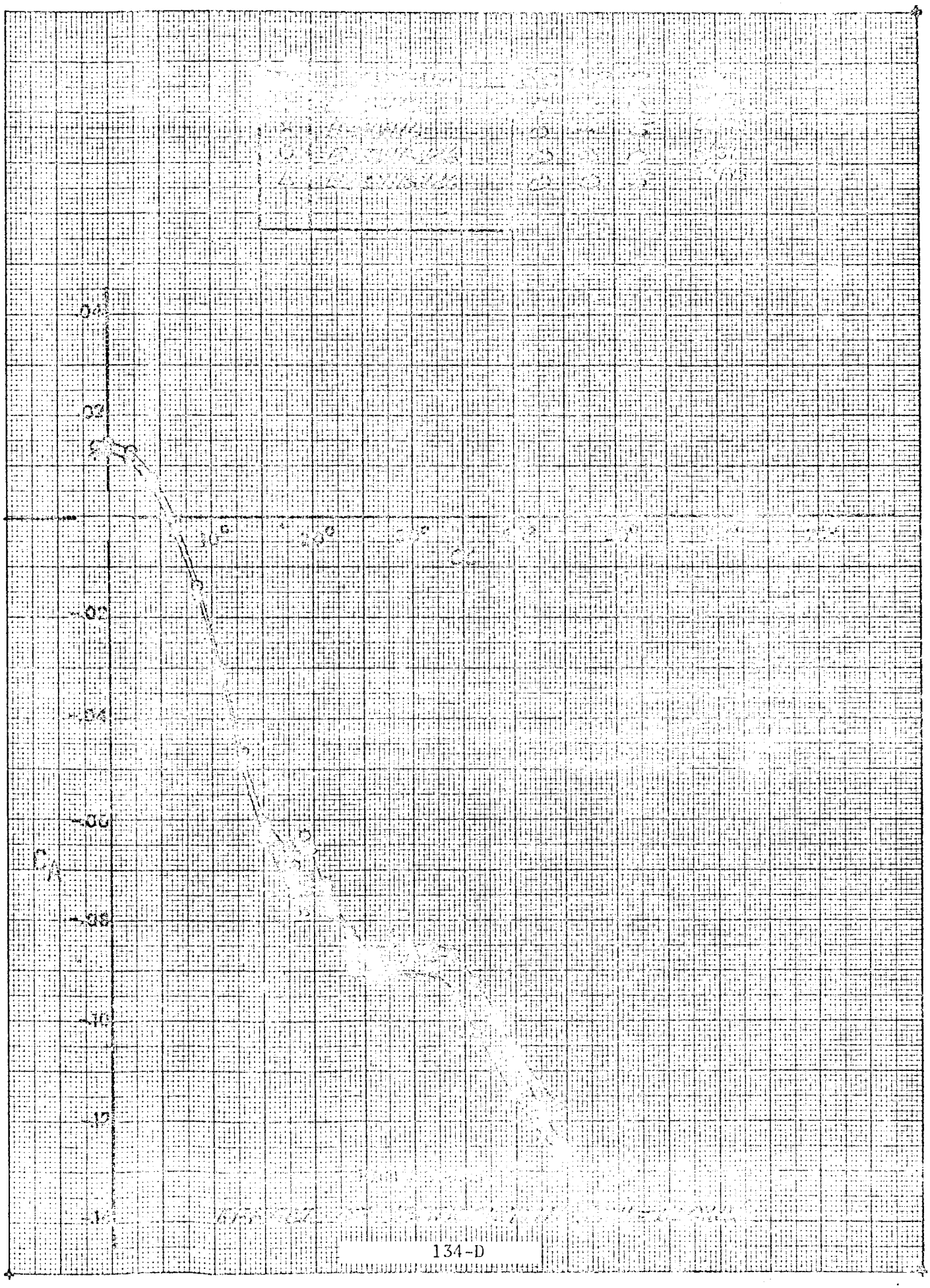

134-D

10 X 10 TO THE CENTIMETER 46 1517
10 X 25 CM. • ALBANENE® MADE IN U.S.A.
KEUFFEL & ESSER CO.

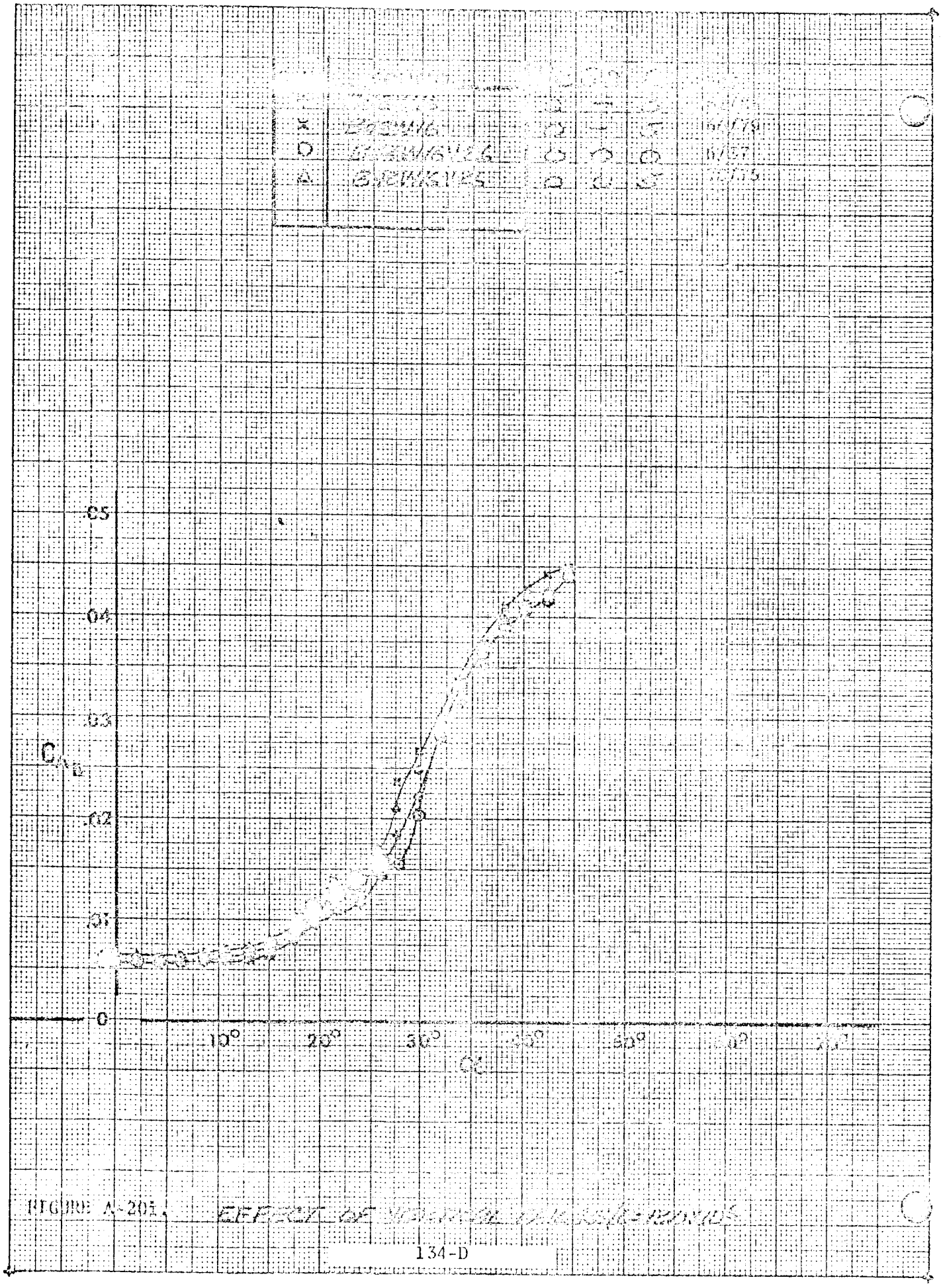

FIGURE A-201. EFFECT OF VORTICES ON DRAG-RAMPS

134-D

10 X 10 TO THE CENTIMETER 46 1517
18 X 25 CM. • ALBANENE
KEUFFEL & ESSER CO.

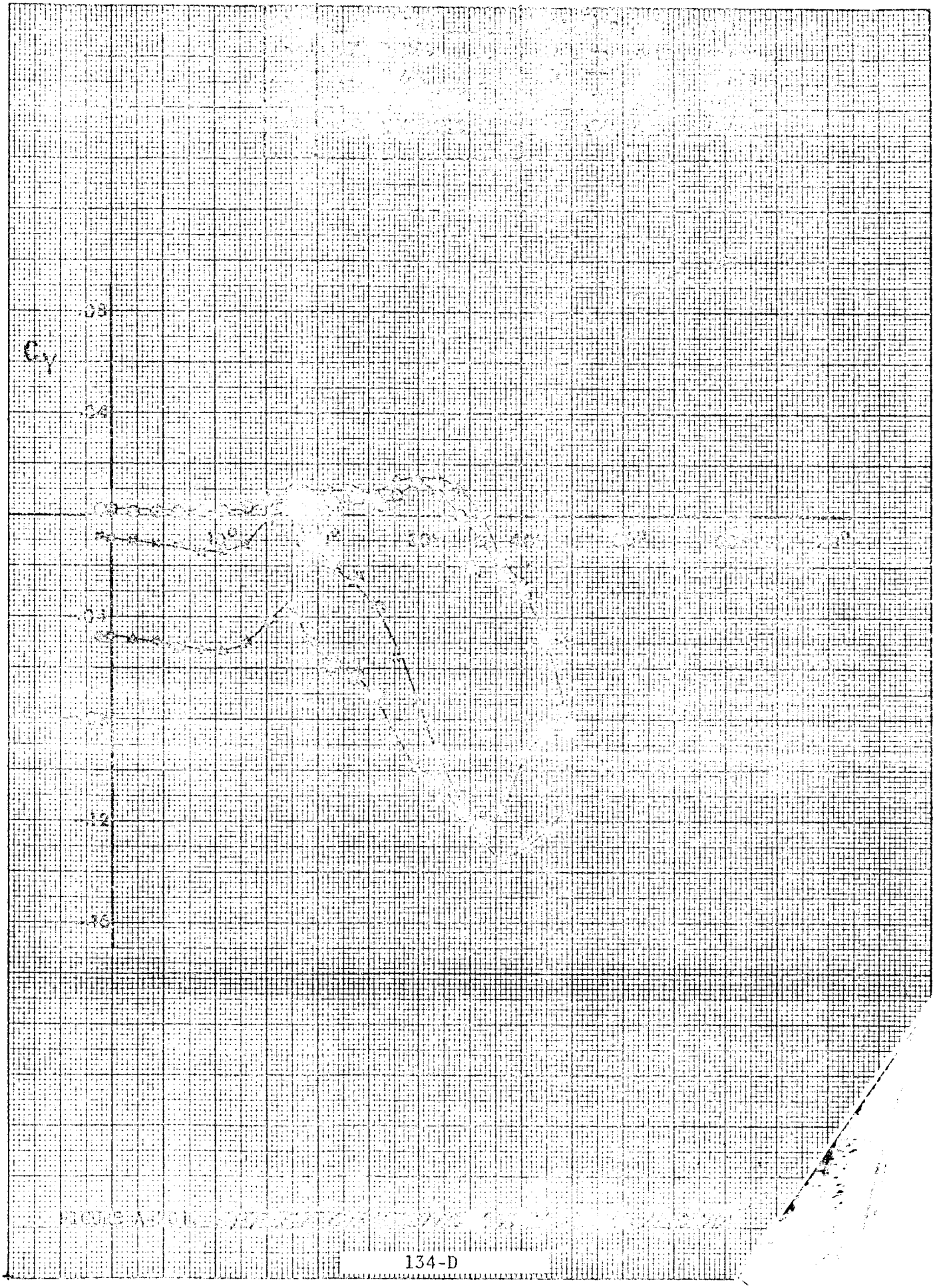

134-D

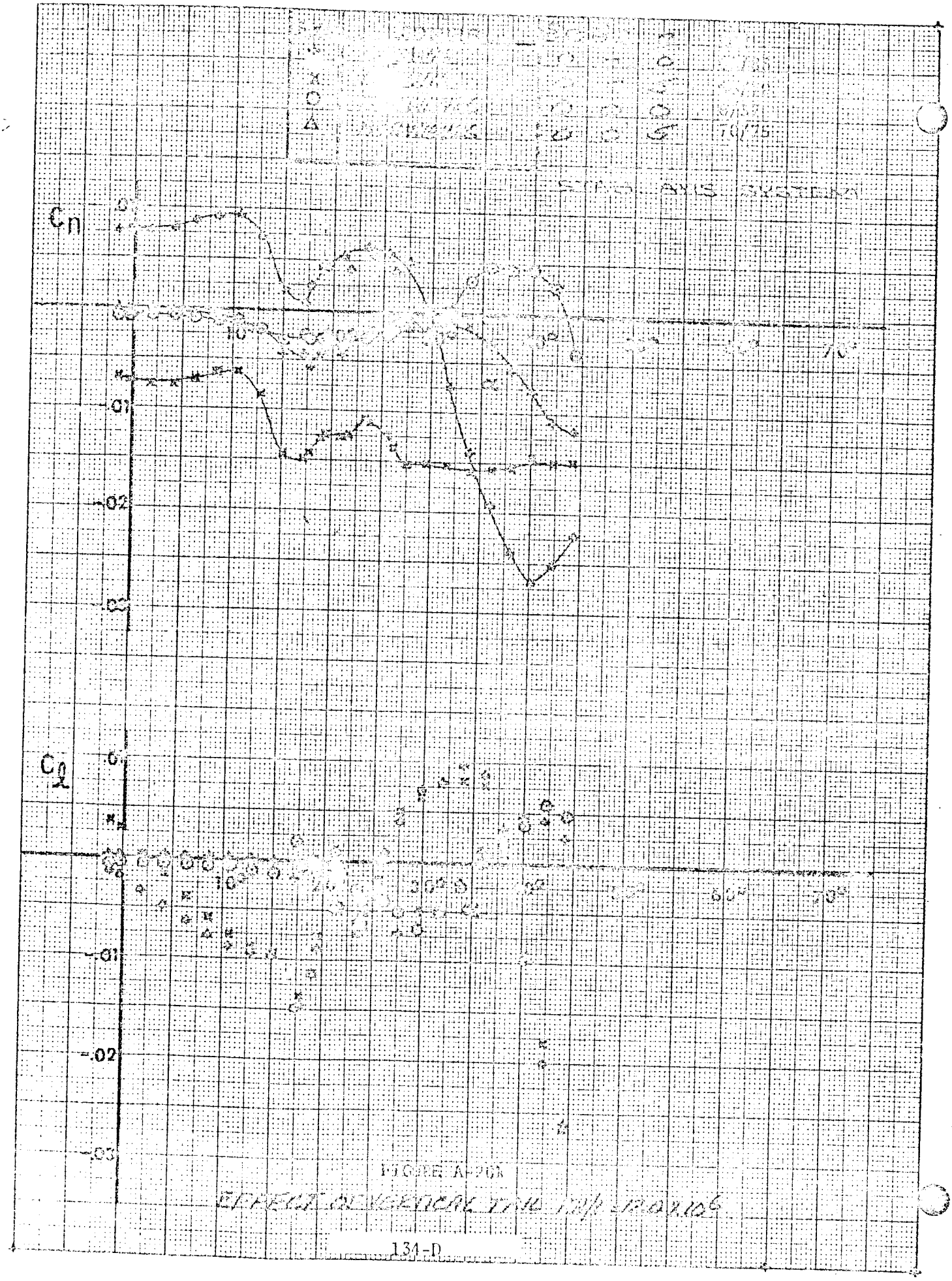

FIGURE A-90B

EFFECT OF VERTICAL TAIL ASPECT RATIOS

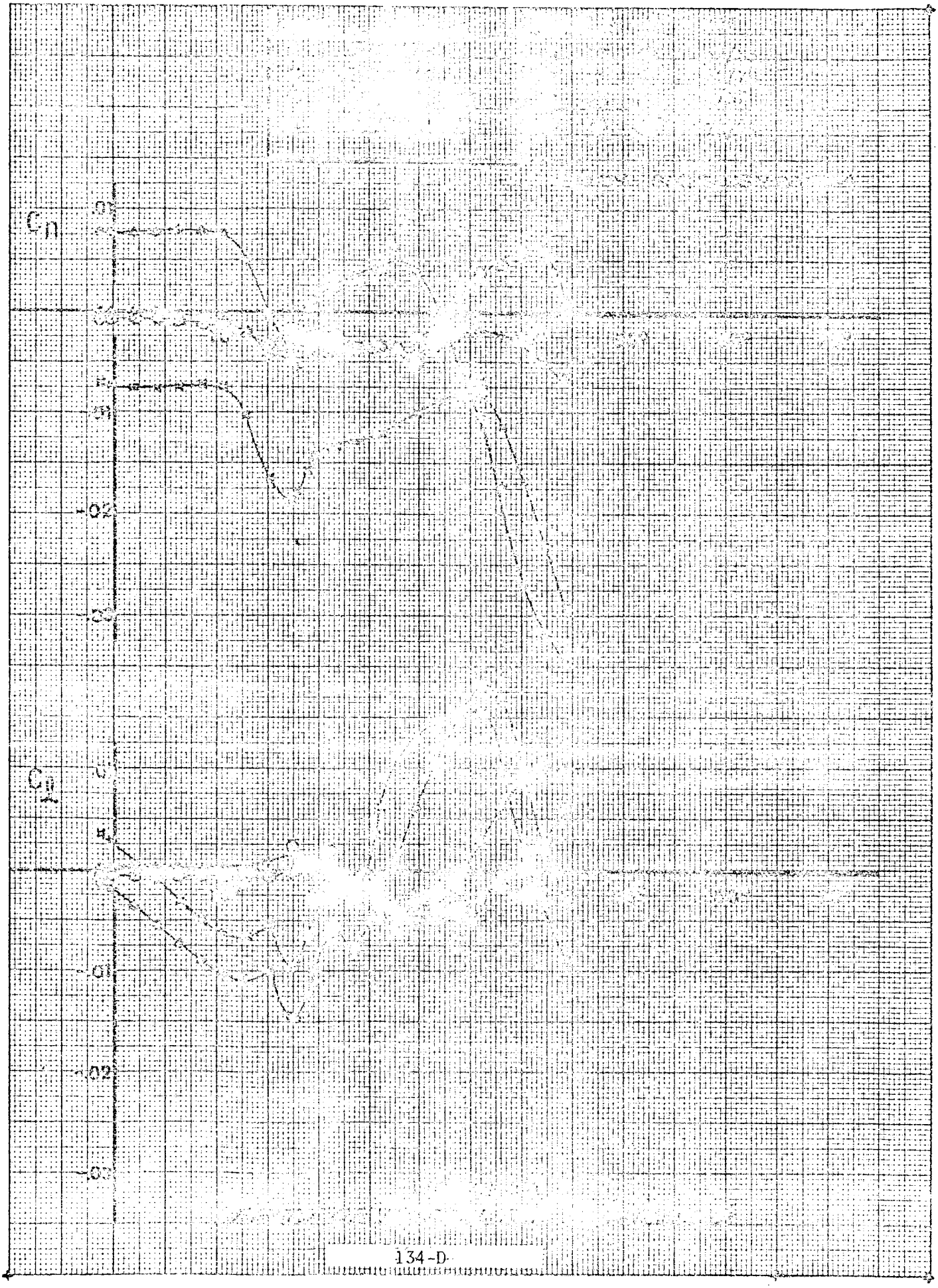
C_n
.02
0
-.02
-.03
C_m
.5
0
-.5
-1.0
-1.5
-2.0
-2.5
-3.0
-3.5
-4.0
-4.5
-5.0
-5.5
-6.0
-6.5
-7.0
-7.5
-8.0
-8.5
-9.0
-9.5
-10.0
-10.5
-11.0
-11.5
-12.0
-12.5
-13.0
-13.5
-14.0
-14.5
-15.0
-15.5
-16.0
-16.5
-17.0
-17.5
-18.0
-18.5
-19.0
-19.5
-20.0
-20.5

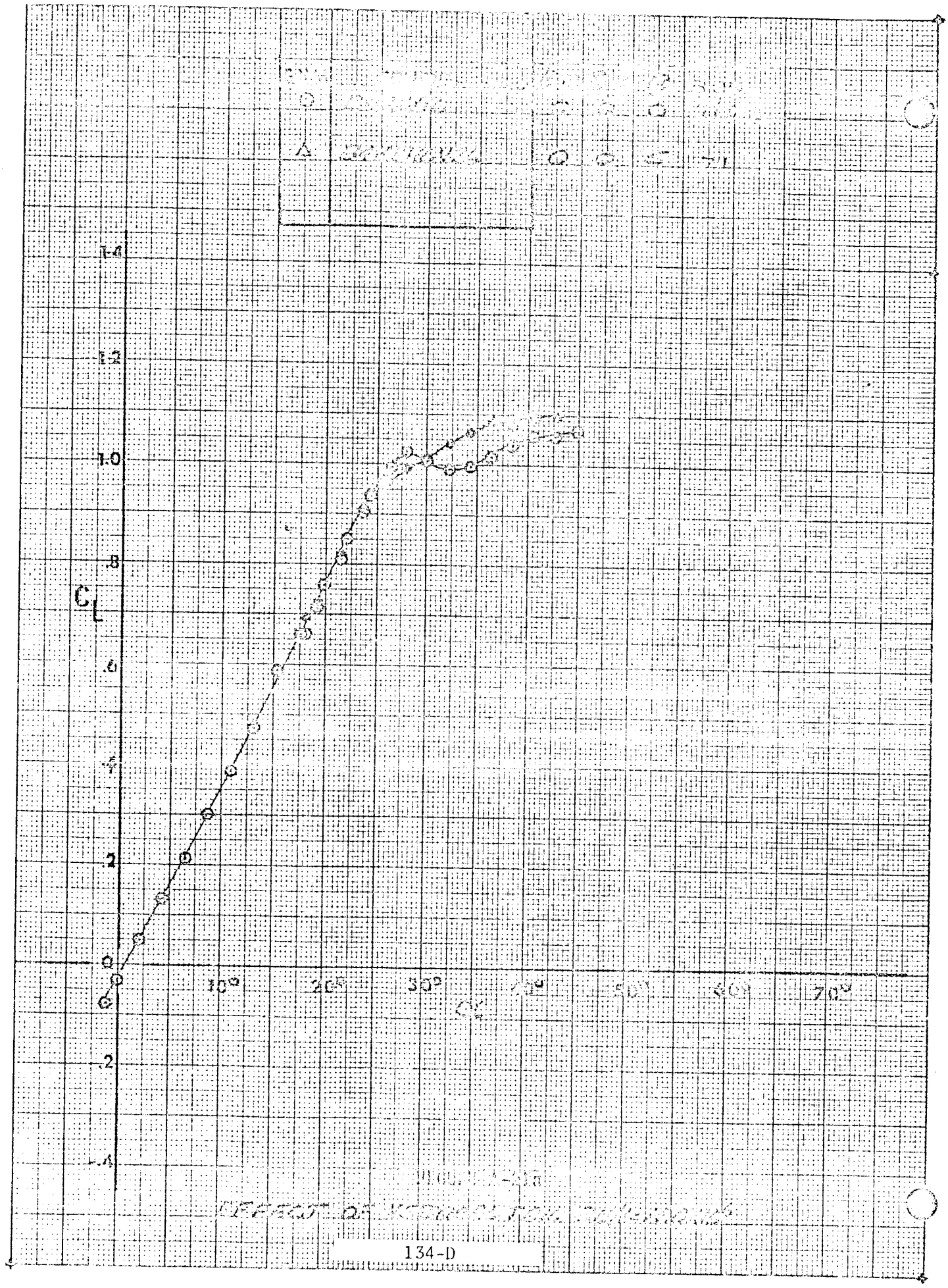

134-D

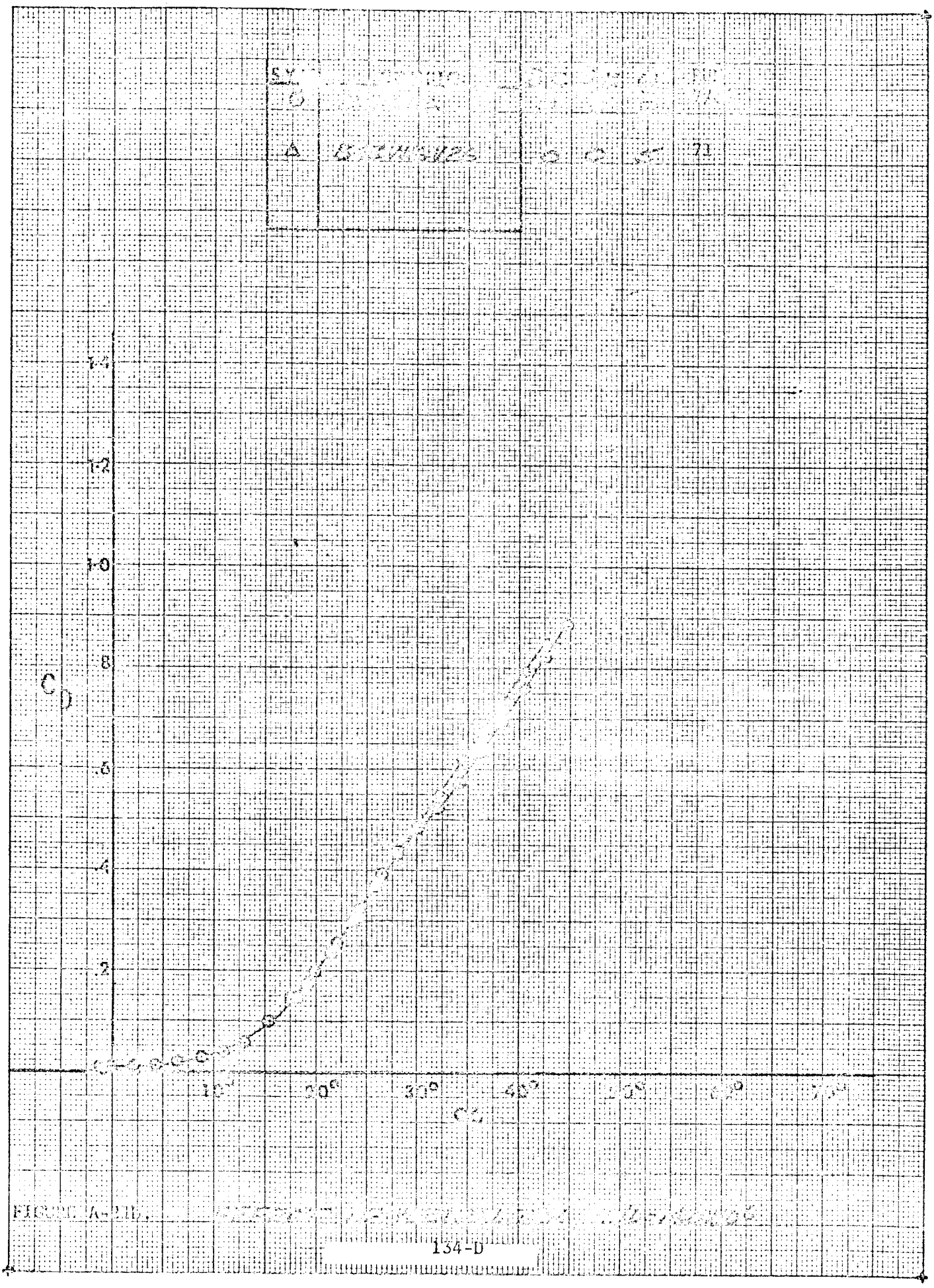

FIGURE A-21b.

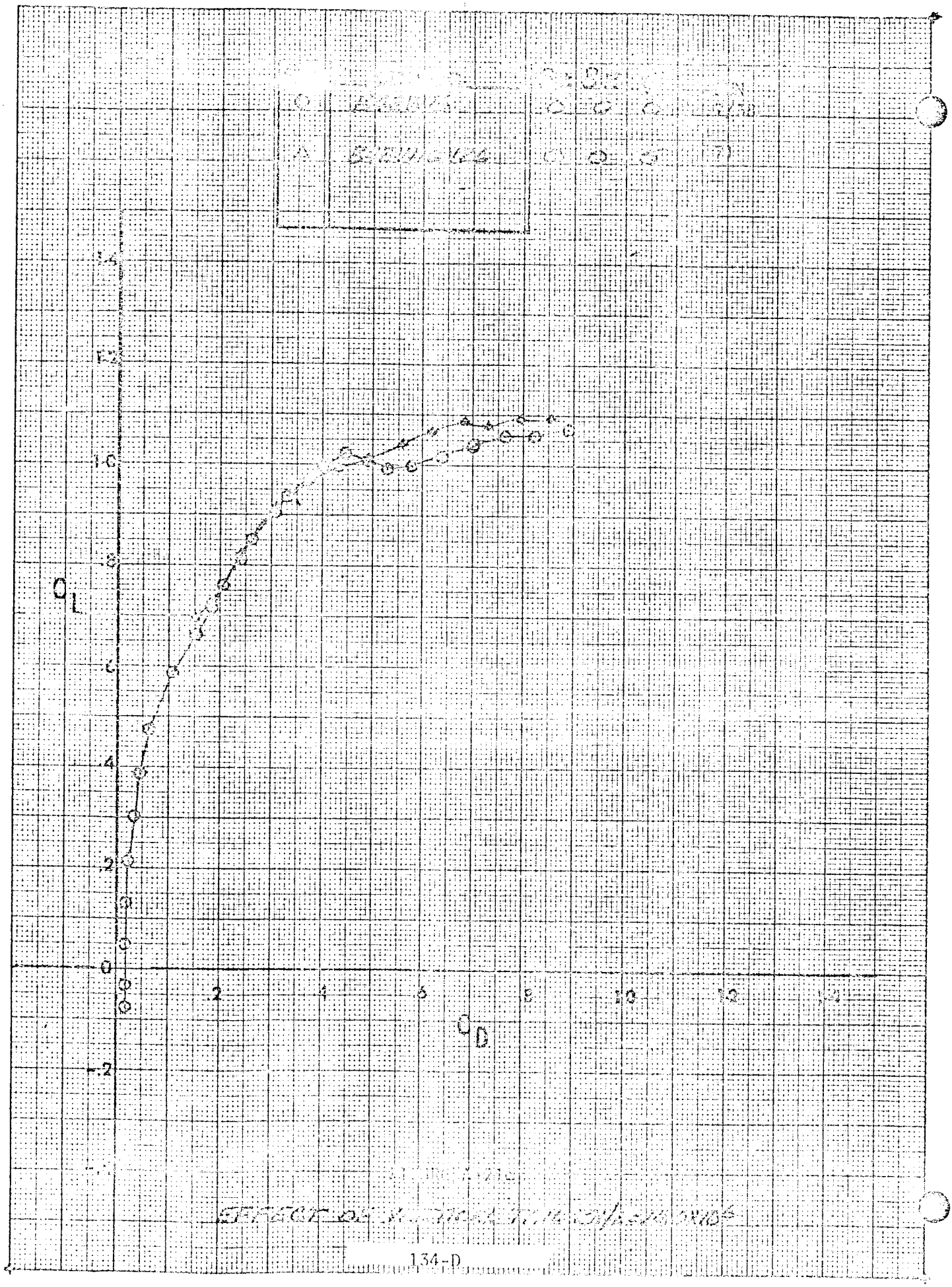
C_L
C_D
.2
.4
.6
.8
1.0
1.2
1.4
0
-.2
2
4
6
8
10
12
14

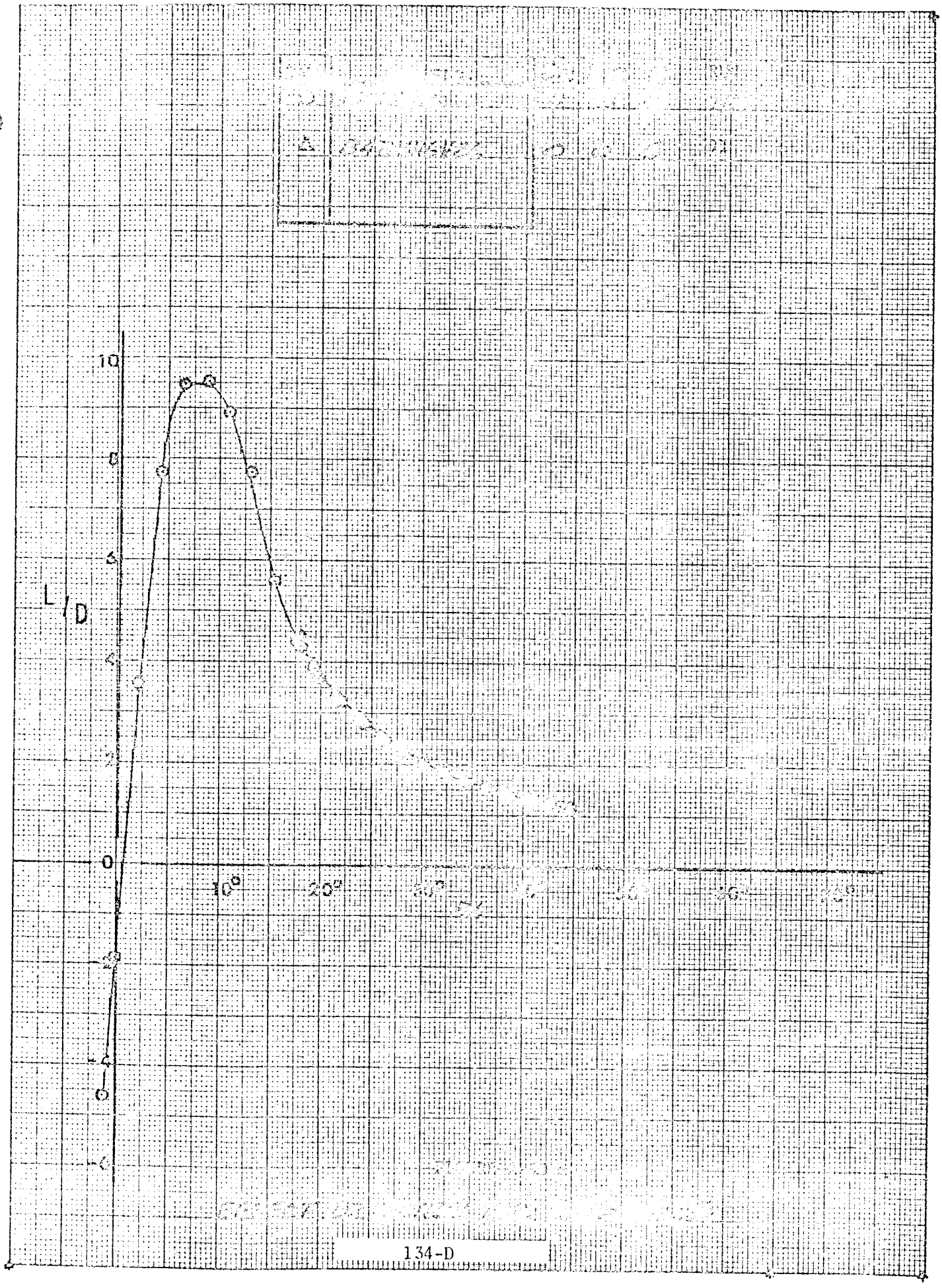

134-D

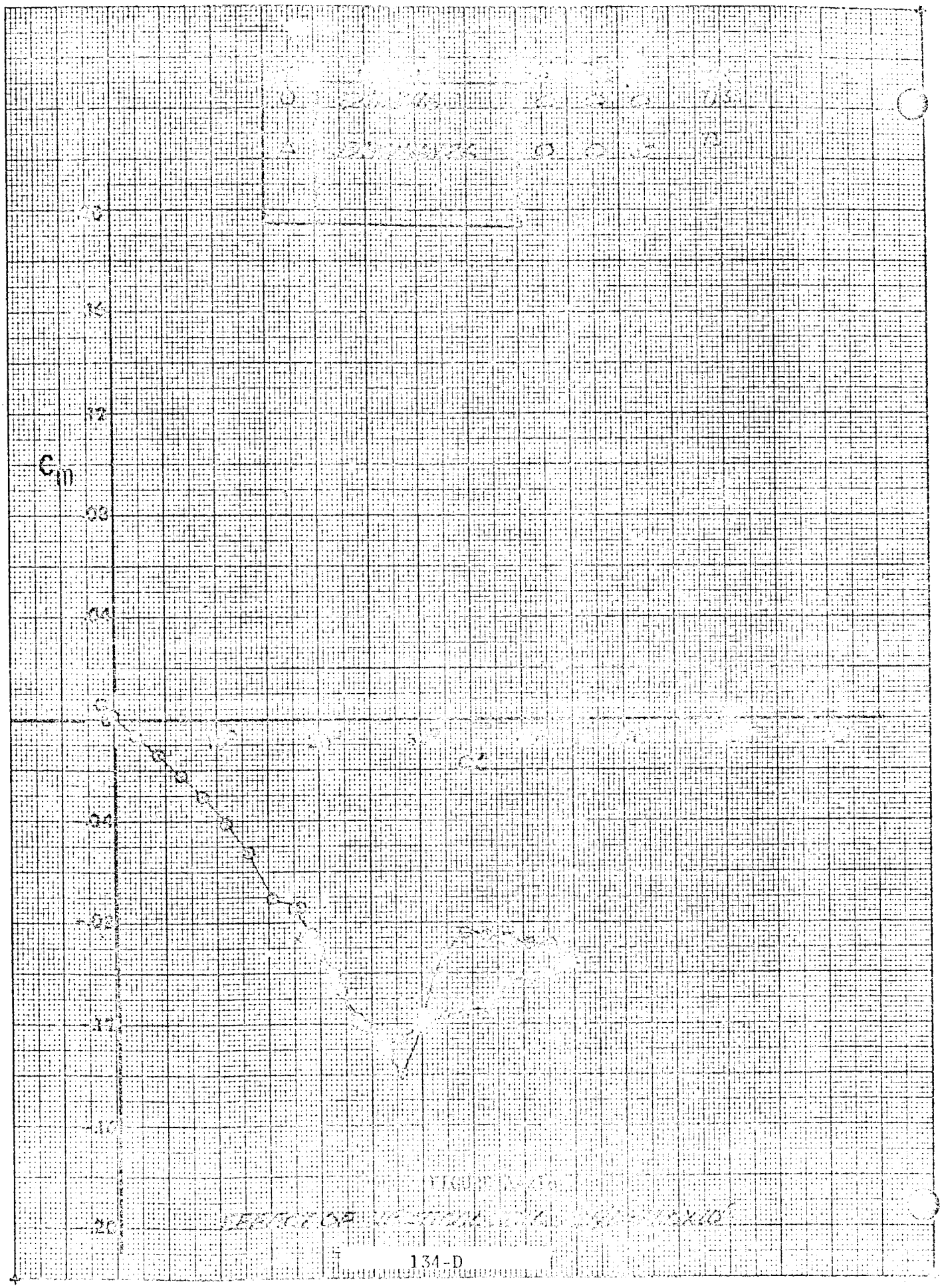

K&E 10 X 10 TO THE CENTIMETER 46 1517
19 X 25 CM. • ALBANENE MADE IN U.S.A.
KEUFFEL & ESSER CO.

260

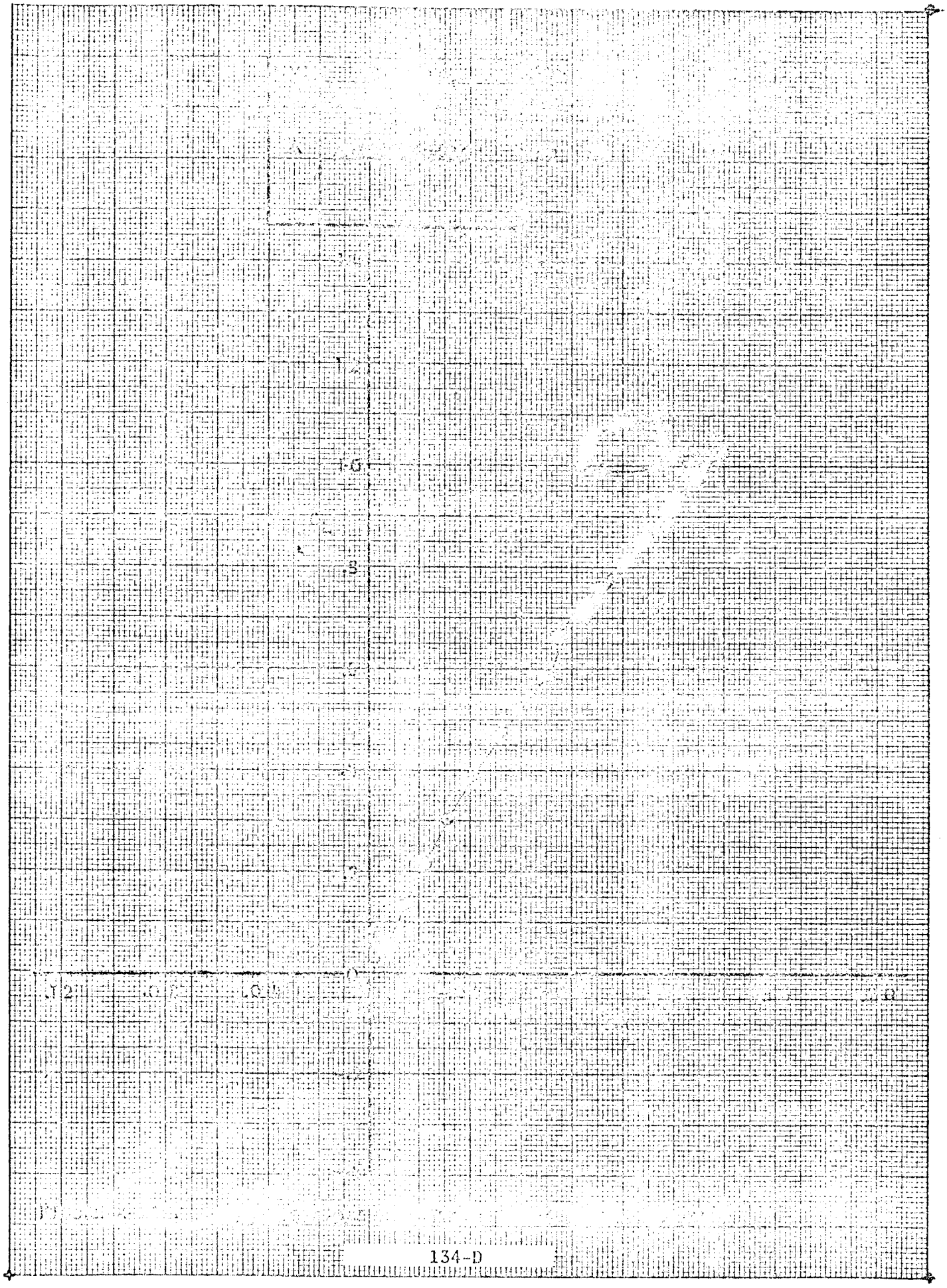
.12
.08
.04
0
.04
.08
.12
.16
.20
.24
.28
.32
.36
.40
.44
.48
.52
.56
.60
.64
.68
.72
.76
.80
.84
.88
.92
.96
1.00
1.04
1.08
1.12
1.16
1.20
1.24
1.28
1.32
1.36
1.40
1.44
1.48
1.52
1.56
1.60
1.64
1.68
1.72
1.76
1.80
1.84
1.88
1.92
1.96
2.00
2.04
2.08
2.12
2.16
2.20
2.24
2.28
2.32
2.36
2.40
2.44
2.48
2.52
2.56

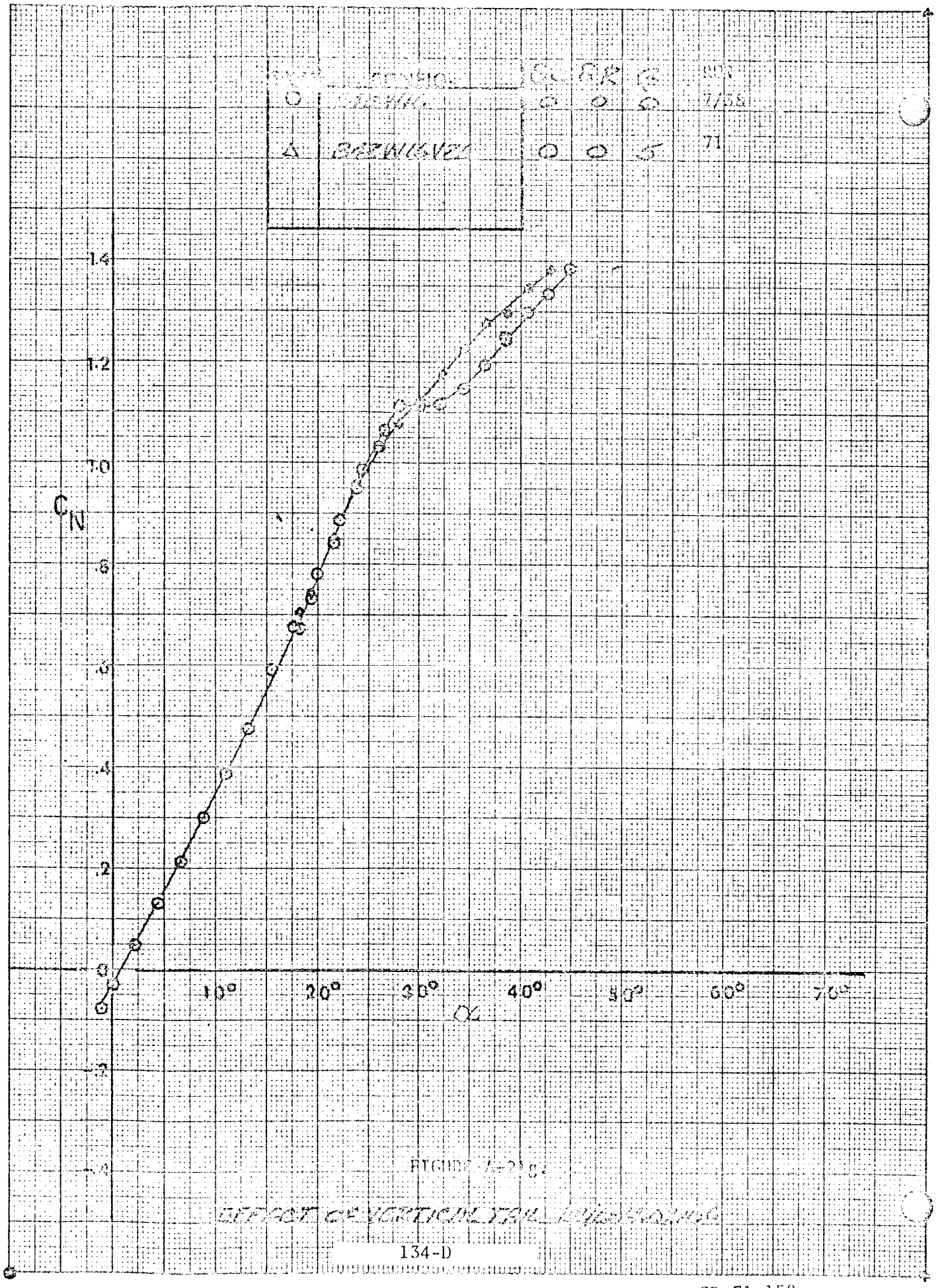

FIGURE A-29 g

EFFECT OF VERTICAL TAIL [illegible]

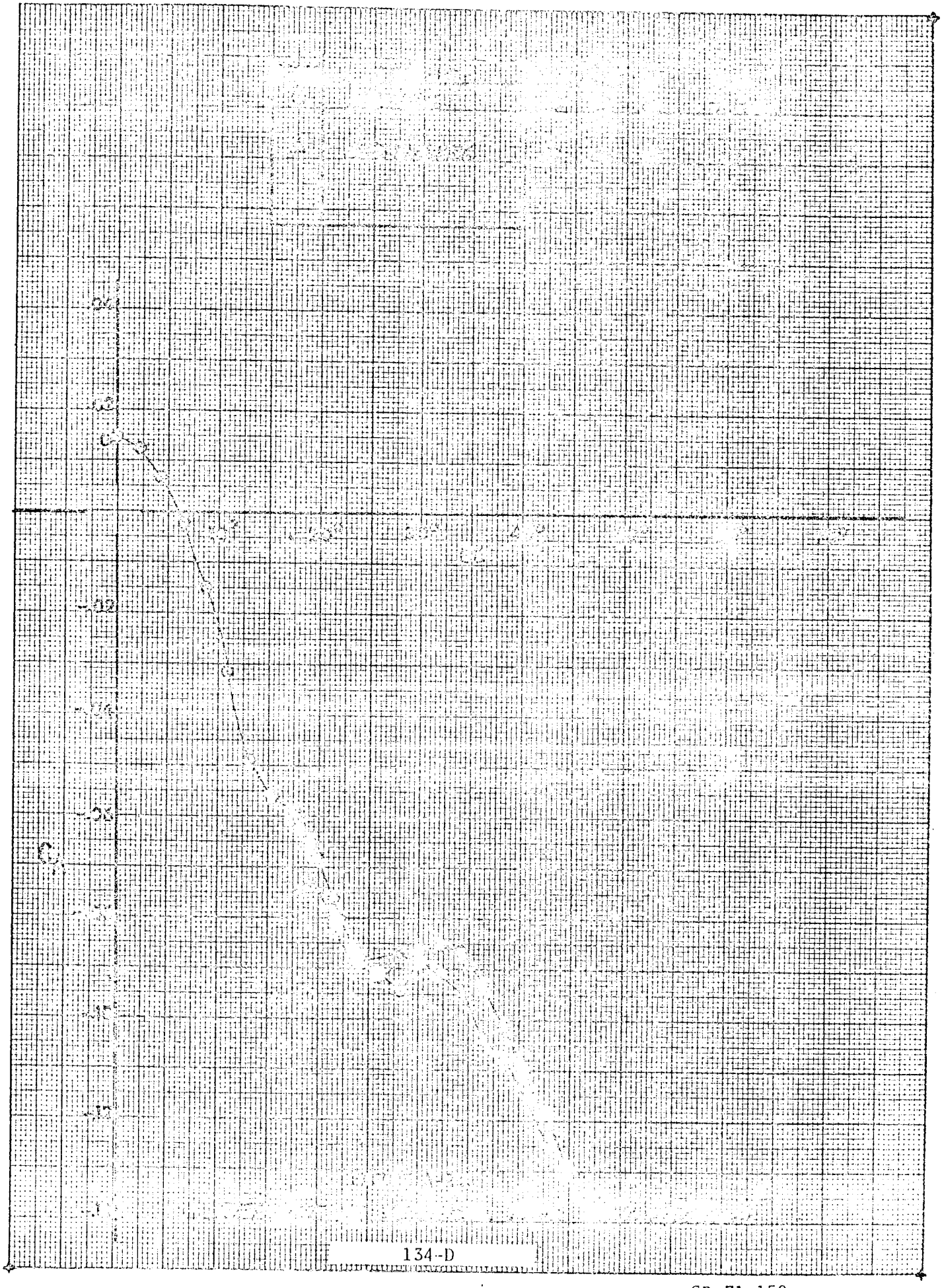

134-D

10 X 10 TO THE CENTIMETER 46 1512
18 X 25 CM. • ALBANENE VISCHIN U.S.A.
KEUFFEL & ESSER CO.

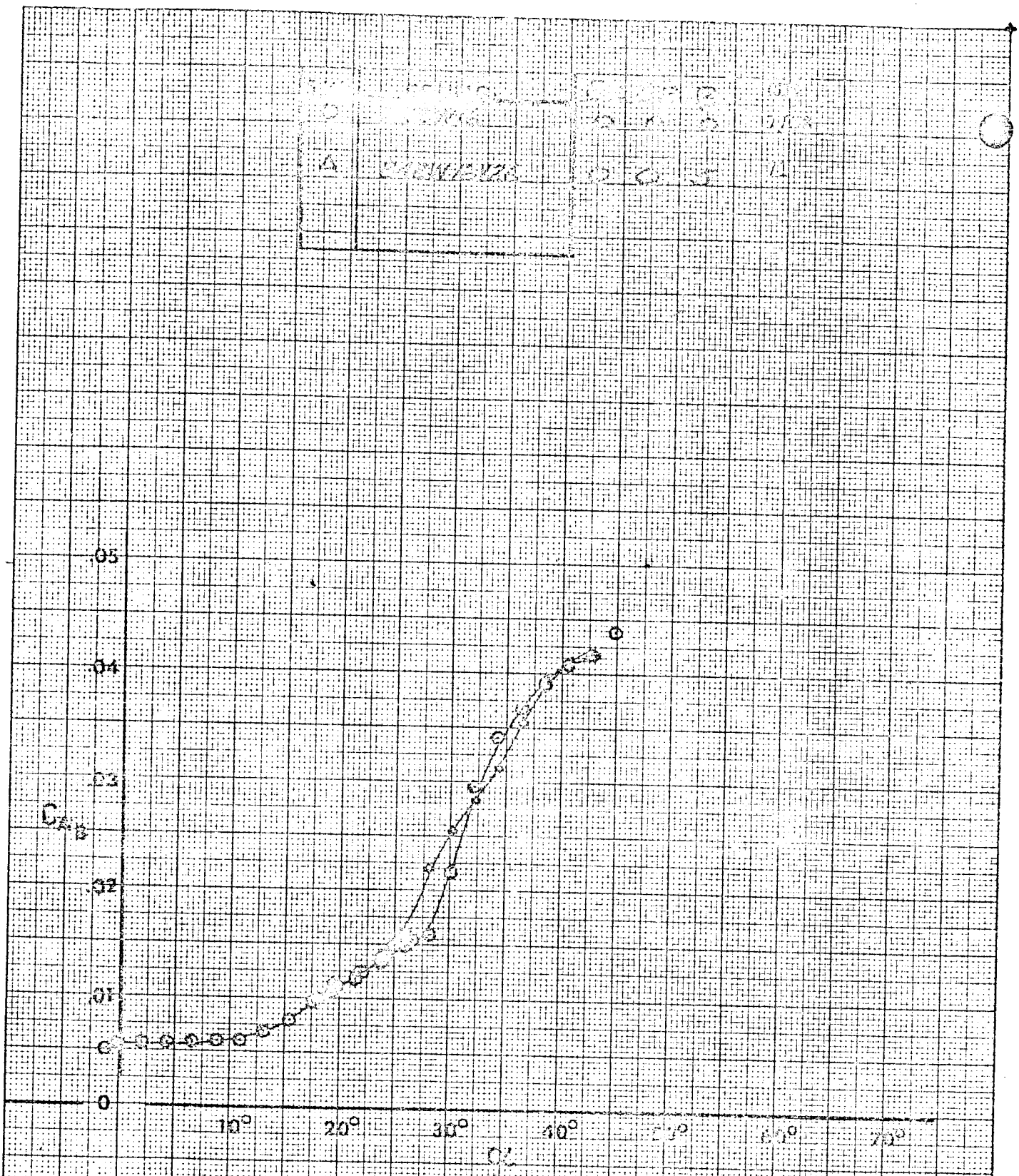

FIGURE A-21j

EFFECT OF [illegible] TAIL [illegible]

134-D

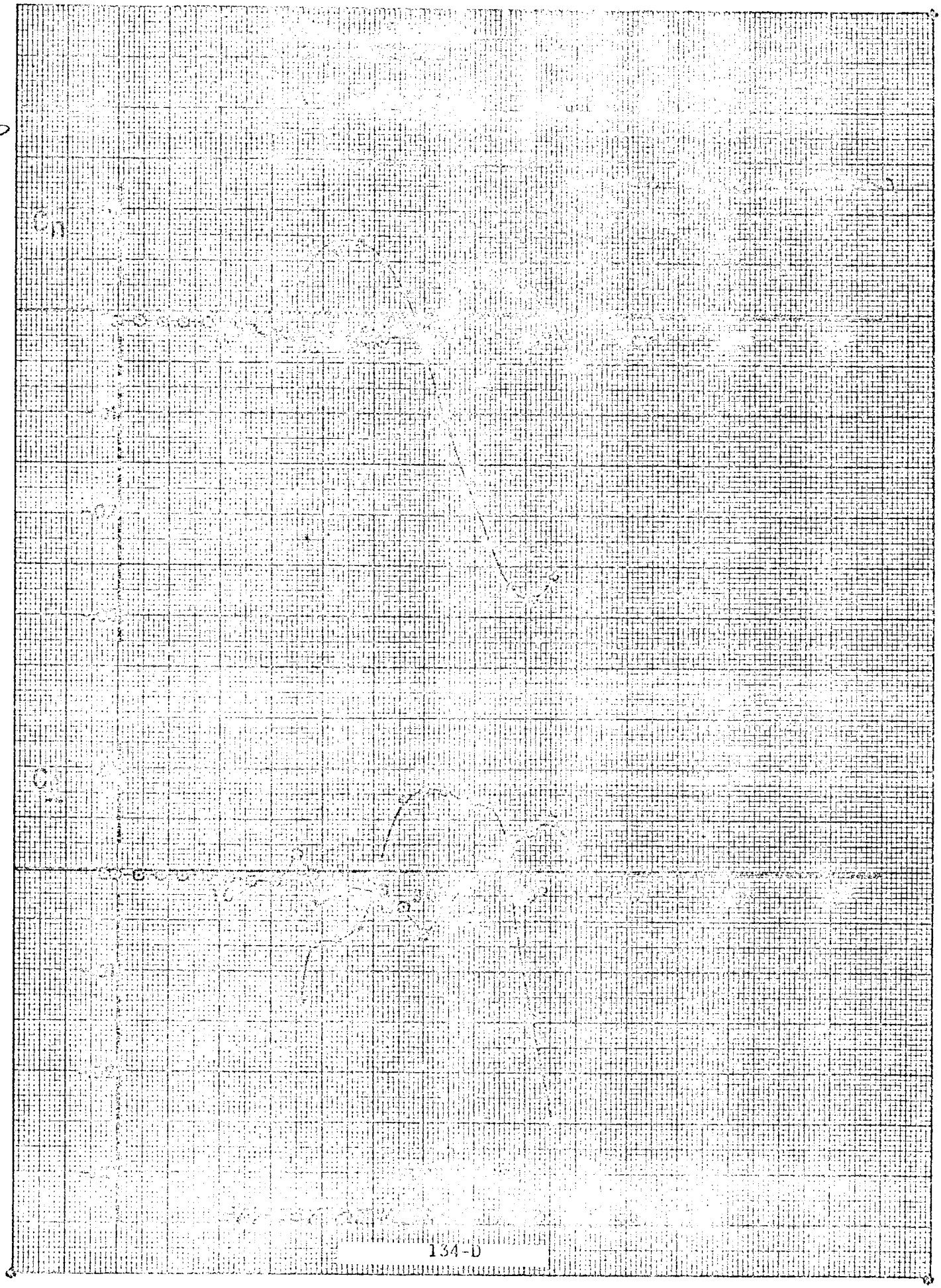

KEUFFEL & ESSER CO.

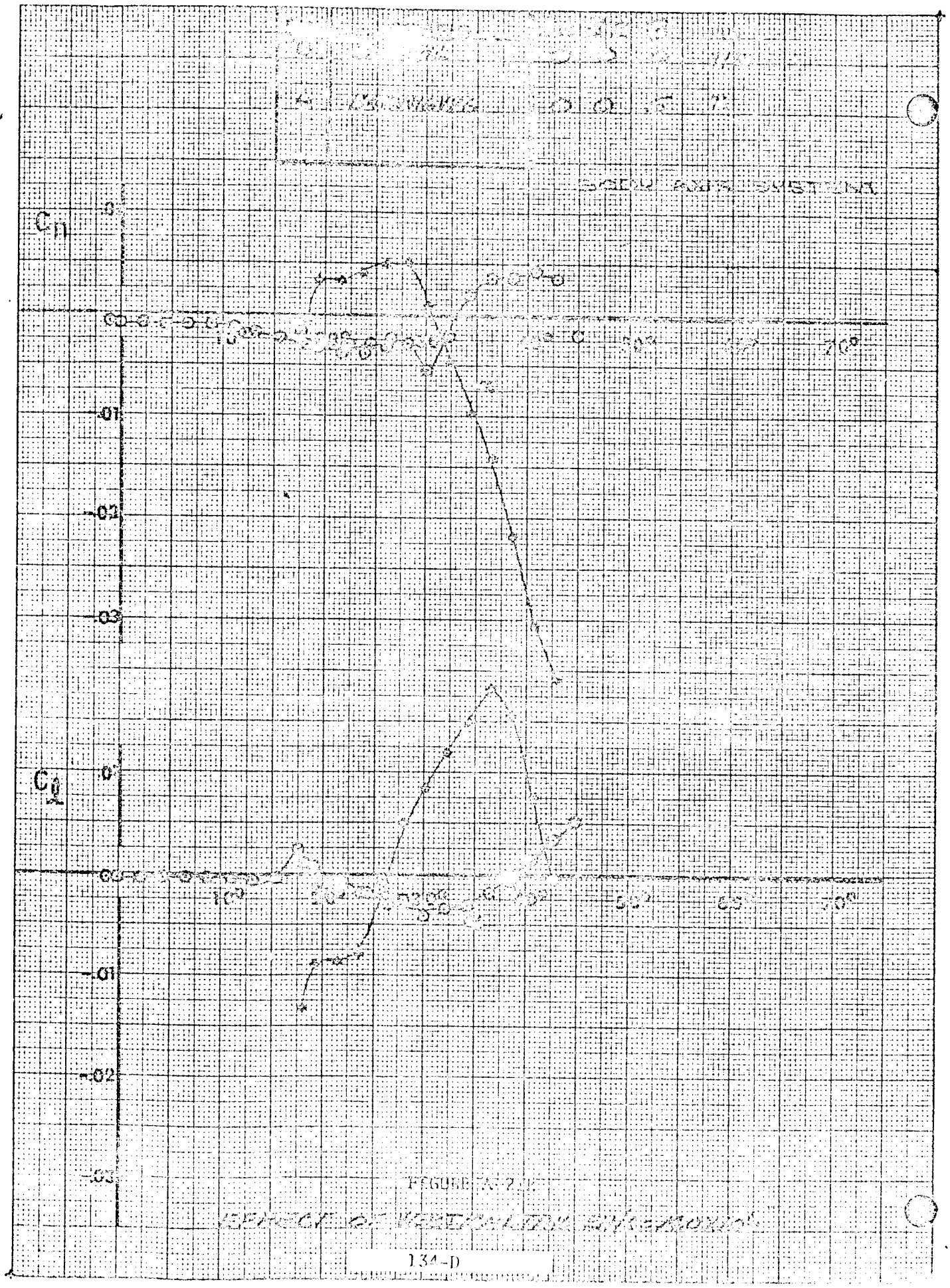

FIGURE A-2.

46 1517
10 X 10 TO THE CENTIMETER
KEUFFEL & ESSER CO.

281

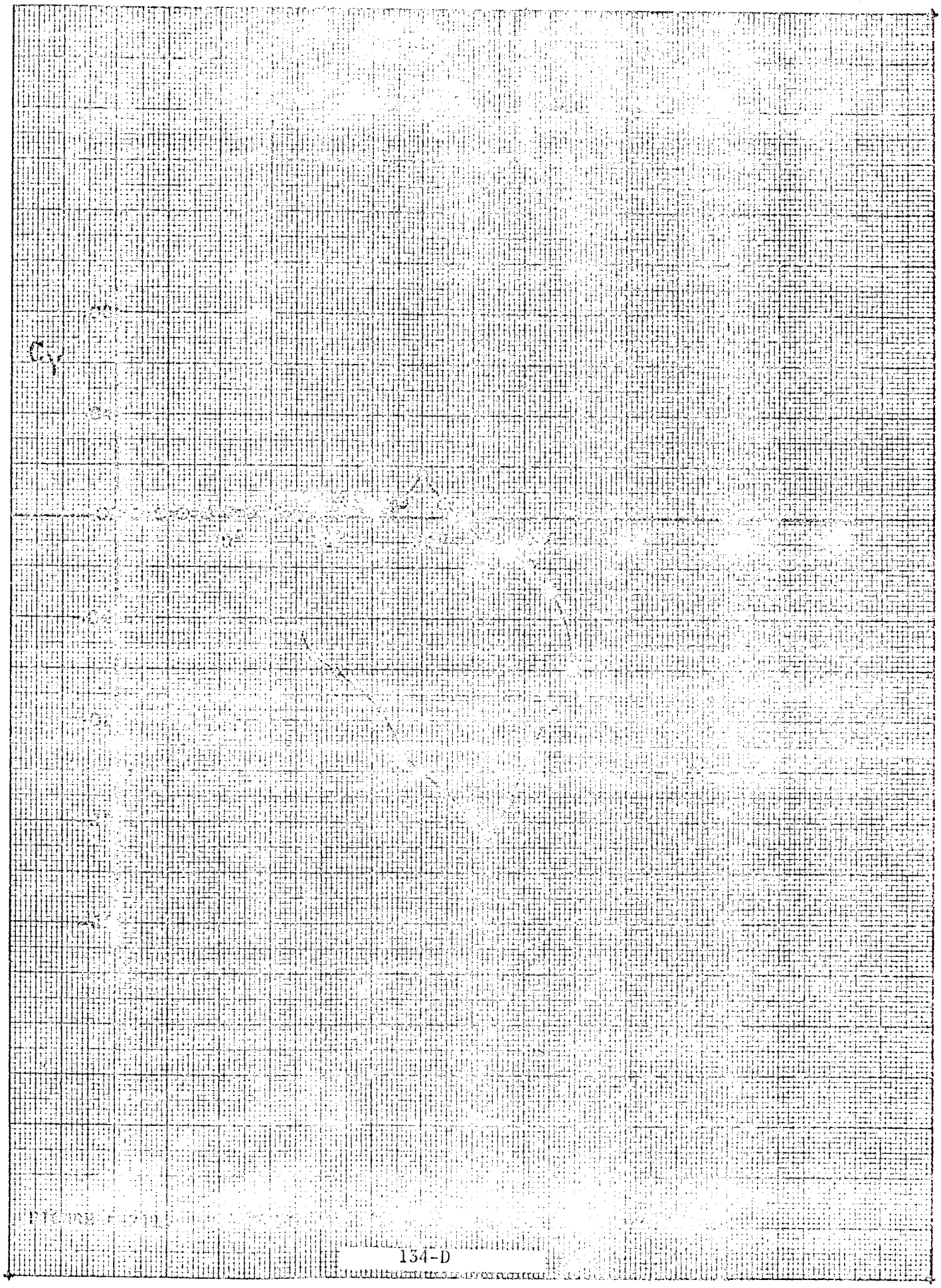

134-D